Design, Simulation and Virtual Testing

# madymo

Model Manual | VERSION 7.7

www.tassinternational.com

# MADYMO Manuals

An overview of the MADYMO solver related manuals is given below. From Acrobat Reader, these manuals can be accessed directly by clicking the manual in the table below. Manuals marked with a star (*) are also provided in hard-copy (major releases only).

| | |
|---|---|
| **Theory Manual** | The theoretical concepts of the MADYMO solver. |
| **Reference Manual*** | Detailed information on how to use the MADYMO solver and how to specify the input. |
| **Model Manual*** | Dummy, Dummy Subsystem and Barrier Models with simple examples. |
| **Human Model Manual** | Human Models and applications that make use of Human Models. |
| **Tyre Model Manual** | Documentation about Tyre Models. |
| **Utilities Manual** | User's guide for MADYMO/Optimiser, MADYMO/Scaler, MADYMO/Dummy Generator, MADYMO/Tank Test Analysis |
| **Folder Manual** | Describes the use of MADYMO/Folder. |
| **Programmer's Manual** | Information about user-defined routines. |
| **Release Notes** | Describes the new features, modifications and bug fixes with respect to the previous release. |
| **Installation Instructions** | Description for the system administrator to install MADYMO. |
| **Coupling Manual** | Description of coupling with ABAQUS, LS-DYNA, PAM CRASH/SAFE and Radioss and the TCP/IP coupling with MATLAB/Simulink. |

TASS International provides extensive and high quality support for its products to help you in utilizing the software most efficiently. TASS International offers extensive hotline support for our software products, MADYMO, PreScan and Delft-Tyre. Our hotline support can be reached over phone as well as via email and will assist you with your questions regarding our different software products. Your requests will be dealt with in a fast and effective manner to support you in the continuation of your work in progress. On the website you will find your local representative with the accompanying support contact details.

# Table of contents

# Preface

This manual contains background information and user instructions for the models included in the MADYMO model database. Tyre Models and Human models are described in the Tyre Model Manual and Human Model Manual respectively. Every other chapter describes models of one specific hardware dummy or barrier. In these chapters also examples are given, in which the models are applied. These examples are included to illustrate the usage of the models. Further examples of MADYMO applications are presented in the Applications Manual.

In this manual, the location of model files is given relative to the *installationdirectory*. The *installationdirectory* can be requested by running the runscript **madymo77 -show**.

This manual will be continually updated and extended as part of the services provided under the MADYMO maintenance agreement and based on the results of research activities at TASS International.

Suggestions from users for improvements in the models are welcome. We also appreciate users sending us their own model application input decks and/or results for possible inclusion in this manual.

# 1 Introduction

This part of the manual describes MADYMO models of crash dummies and subsystems. This chapter gives a generalised description of all these models and forms the basis for the understanding of the models and how to use them. In each of the following chapters, the models available are described.

## 1.1 Model description

This section describes general features of the different types of MADYMO models. It also gives information on application of the models and what models are currently available.

Model specific features are discussed in the model description sections of the following chapters. The sections present the configurations of, respectively, the ellipsoid, the facet and the finite element model. For the latter two, only those parts are described that differ from the ellipsoid model.

### 1.1.1 Model types

Three MADYMO model types are distinguished. These model types are:

1. Ellipsoid models
2. Facet models
3. Finite Element models

The main difference between the model types lies in the modelling techniques applied to represent the geometry and mechanical properties of the modelled components. The geometry of the models is based on contour maps derived from digital surface measurements, technical drawings, or both.

All MADYMO models have a similar basis, consisting of chains of rigid bodies with inertial properties, which are connected by kinematic joints. This basis allows for a general positioning procedure for three model types. Instrumentation is also modelled the same way (with some exceptions) in the three model types. Load cells are modelled by bracket joints at the sensor locations. Accelerometers and displacement transducers are modelled as output defined for points on bodies. The models of dummies include the inertial properties of standard dummy instrumentation in the inertial properties of the related bodies. Inertial properties of optional dummy instrumentation is not included in the models. Also the inertial properties of sensor cables and dummy clothing is not included in the dummy models. If desired, the user could add these properties, although it is noticed from user applications and dummy validations that in general satisfactory results are obtained without such modifications.

Below, the specific features of the three types of models are described.

**ELLIPSOID MODELS**

Ellipsoid models are models that are based fully on MADYMO's rigid body modelling features. The inertial properties of the hardware components are incorporated in the rigid bodies of the model. Their geometry is described by means of ellipsoids, cylinders and planes.

Structural deformation of flexible components is lumped in kinematic joints in combination with dynamic restraint models. Deformation of soft materials (like flesh and skin components in dummies) is represented by force-based contact characteristics defined for the ellipsoids. These characteristics are used to describe contact interactions within the models and between the model and environment.

**FACET MODELS**

Facet models are in principle also multibody models, but compared to the ellipsoid models they benefit from more advanced multibody and also rigid surface FE technology. The inertial properties of the hardware are incorporated in the rigid and deformable bodies of the model.

In facet models the outer surfaces of the model is described with meshes of shell-type, massless contact elements (further referred to as facet surfaces). These facet surfaces are fully connected to rigid bodies and/or deformable bodies. They allow a more accurate geometric representation in comparison with ellipsoids. Although the facet surfaces are defined in FE_MODEL elements, facet models are still multibody models, since no FE solver is used in the simulations. Consequently, they require only a MADYMO multibody solver license and not a MADYMO structural license.

Structural deformation of flexible components such as ribs, is represented by deformable bodies. These deformable bodies enable a more realistic representation of structural deformation than the joints and restraint models used in the ellipsoid models. Deformation of soft materials (flesh and skin components in dummies) is represented by stress-based contact characteristics defined for the facet surfaces. Using these contact characteristics in contact definitions, soft material deformation is represented accurately through the contact interactions within the model and between the model and its environment.

**FINITE ELEMENT MODELS**

In the MADYMO FE models important deformable parts are modelled with finite elements. Inertial properties of components are represented by the inertial properties of both the rigid bodies and the FE meshes. Using these models requires both a MADYMO solver and a MADYMO structural license.

Compared with ellipsoid and facet models, the FE models are able to reproduce accurately not only kinematics and global deformations, but also local deformations of components and flesh/skin/honeycomb materials. The FE meshes are defined with respect to those bodies of the rigid body chain to which they are connected. This enables the FE models to be positioned in the same manner as the ellipsoid and facet model: simply by initialising the positioning joints.

### 1.1.2 What model type to use

Ellipsoid models are the most CPU-time efficient type of models. Therefore, they are particularly suitable for concept, optimisation and extensive parameter sensitivity studies. Their time efficiency has the most benefit in a multibody environment that is modelled similarly by ellipsoids, planes and cylinders. Nevertheless, ellipsoid models can also be used in a facet or FE environment and in coupling with several other FE codes.

Facet models are more realistic and detailed than ellipsoid models, but are still very CPU-time efficient compared to FE models. They include a number of degrees of freedom that is comparable to that of the ellipsoid models. The limited increase in CPU costs are mainly due to the additional evaluations performed in the contact algorithm. Because of their CPU-time efficiency, the facet models are highly suitable for use in optimisation and parameter variation studies. Most benefit is gained from them when the environment is represented in similar or higher level of geometric detail, either by facet surfaces or finite elements.

FE models incorporate a vast amount of degrees of freedom and require a small timestep. As a result of this, they are much less CPU-time efficient than the ellipsoid and facet models. FE Models are recommended for use in the most detailed studies, where local effects of contact interactions and local material deformations are of interest for the user. Compared to ellipsoid and facet models, FE models are less suitable for concept, optimisation and extensive parameter sensitivity studies.

### 1.1.3 Available models and examples

The MADYMO models are split up in six modules: frontal and rear impact dummies, side impact dummies, child dummies, subsystems, and an aviation module. The models available in a certain MADYMO release are listed with their corresponding version numbers in the Release Notes of that release. All dummy and subsystem model files can be found in directory *installationdirectory*/share/dbs/dummies/3d. For many models, examples are provided in which the models are applied. The available examples are also listed in the Release Notes and can be found in the directory *installationdirectory*/share/appl/3d.

Note that model updates and new models are also released in between MADYMO releases. In this case, the models are be released through the download area on the MADYMO website: www.tassinternational.com.

## 1.2 Model validation

MADYMO supplied models are calibrated and validated both on component and full system level. Calibration is performed on an iterative basis: when the full system level validation results are not satisfactory, a step back may be made to component level in order to get results improved. Component level calibration concerns static and dynamic mechanical properties, translated into model parameters such as stiffness and damping for joint-, kelvin- and point restraints, flexible body modes and contact interactions within the components. FE material parameters are generally based on material level test data, but where found necessary they have been adapted during component level calibration. The (contact) interactions between components are calibrated at assembled component and full system level.

Major effort is put into the systematic validation of the models in a loading range that covers all realistic applications. A review of the component and full system test data used for model calibration and validation, is given for each model in the referring chapter. Also examples are given of results of the validation process.

## 1.3 Instructions for model application

### 1.3.1 General

The 'user instructions' sections in this chapter and all following chapters describe how to handle the models. In these sections, information is given that guides the users through implementing models into their own applications.

Each MADYMO model is defined by a single system. This allows for a modular set-up of a MADYMO input deck, where each physical system is represented by a SYSTEM.MODEL element. Loads applied to systems (acceleration fields) and interactions between systems (contact definitions) can be defined outside the systems, while for instance contact interactions between parts of the same system can be defined within the system.

Although modelled as a single system, each MADYMO model is supplied in two files: an include file (⟨name⟩_inc.xml) and a user file (⟨name⟩_usr.xml).

The include file contains the model itself, including features like internal contact interactions and dummy sensor output definitions. It is strongly advised not to modify any parameters in the include files '⟨name⟩_inc.xml', since this may affect the performance of the models. Model include files can be called directly from the MADYMO installation directories.

The user file contains the model system, in which the user interactive model elements are defined and the include file is called. The user-interactive elements are those model elements that may need modification when applying the model. Besides the model's system, the user file contains the required control elements and a reference space system. This makes it a complete MADYMO input deck containing the model defined in its reference position. Figure 1.1 shows the general set-up of a model user file.

Models can be applied in two ways:

1. by building an 'environment' model around the model in the user file. Besides systems representing the 'environment', also applied acceleration fields and contact interactions between model and environment should be included in the user file.

2. by including the model (the SYSTEM.MODEL element in the user file) in an existing 'environment' model input deck. Again, applied acceleration fields and contact interactions between model and environment should be included.

When calling model sensor output signals, or defining loads onto and contact interactions with a model, reference must be made to the model system. This can be done by referring either to the system ID or to the system NAME. When a model is included more than once in an application, the system IDs and NAMEs should be made unique.

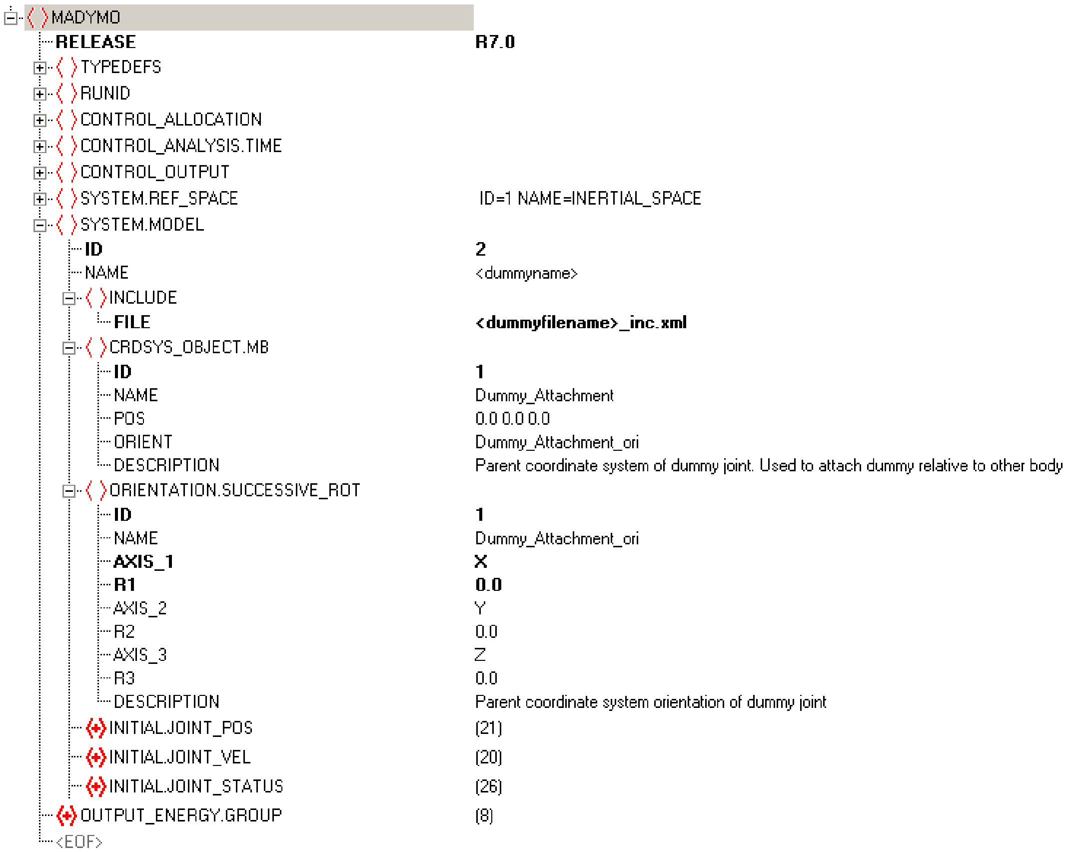


Figure 1.1: Set-up of a model user file input deck.

### 1.3.2 Integration method and timestep

It is recommended for all models to use the Euler time integration method. Each model has a recommended maximum multibody (MB) integration time step. This time step is defined for each model in the CONTROL.ANALYSIS_TIME element in the user file (see Figure 1.1). It is also presented in the user instruction section of the referring chapter in this manual. For the ellipsoid and facet models the recommended maximum MB timesteps lie in the order of 1.0E-04s to 1.0E-05s. In general in FE models the FE components have a predefined variable FE timestep included, which can vary between the recommended maximum MB timestep and a mininum FE time step of 1.0E-06s. The maximum MB timesteps for the FE models are found to vary between 2.0E-05 and 1.0E-06. A maximum MB timestep of 1.0E-06 effectively results in a FE model timestep that is kept constant.

### 1.3.3 Positioning of dummy models

To position a dummy model the INITIAL.JOINT_POS elements have to used. For all the joints needed for positioning a dummy model, the INITIAL.JOINT_POS elements are defined in the dummy model user file (see Figure 1.1). For joints of the types FREE and SPHERICAL the rotational degrees of freedom are to be defined in the related ORIENTATION elements. The defined elements use the successive rotation method. Initial velocities on joint degrees of freedom can be applied in the INITIAL.JOINT_VEL elements. Joints can be locked in the INITIAL.JOINT_STATUS elements.

Positioning and orientation of dummy components (such as arms and legs) can be done by initialising the related positioning joints. Positioning of the complete dummy must be done by initialising the so-called dummy joint (*'Dummy_jnt'*), which is a free joint connecting the H-point of the dummy to its environment.

All joints needed for dummy positioning are listed in the dummy model positioning tables in user instruction sections of the following chapters. In these tables all rotations are referred to with the terms *pitch*, *roll* and *yaw*. Joint degree of freedom translations and rotations are defined according to the direction definitions in Figure 1.2. The directions given in the tables refer to the positive translation and rotation directions. For all joints, the directions are defined with respect to their co-ordinate system orientation when the dummy model is in its reference position.

A dummy model is by default positioned relatively to the (global) reference space co-ordinate system. When a user wishes to position a dummy relative to a body of another system, this can be done by 'attaching' the dummy model to this body. This attachment is made through the dummy joint. The dummy attachment elements are the CRDSYS_OBJECT element named *'Dummy_Attachment'* and the associated orientation element named *'Dummy_Attachment_ori'*.

The reference position defined in the user file represents the dummy in a seated position, where initial deformation due to gravity is not taken into account. This refers particularly to the lumbar spine and neck components, which show some deformation, in terms of compression and bending, in response to gravity. In order to get a dummy model seated in an equilibrium position, the user could follow one of the procedures described below:

1. Position the dummy model just above the seat and perform a pre-simulation in which gravity pulls the dummy into the seat. In this pre-simulation, the user can choose to lock some of the positioning joints of the dummy model. By using OUTPUT_JOINT_DOF for the non-locked positioning joints, the dummy equilibrium position can be read out and included in the INITIAL.JOINT_DOF in the actual simulation to be performed.

2. Position the dummy in the estimated seated position. Then perform a one to five millisecond simulation with only gravity load included, to check if the dummy acceleration peaks remain close to zero level. When this is the case, the dummy can be considered in equilibrium position. If desired, the user can predefine small deformations in e.g. lumbar spine and neck joints to compensate for gravity forces.

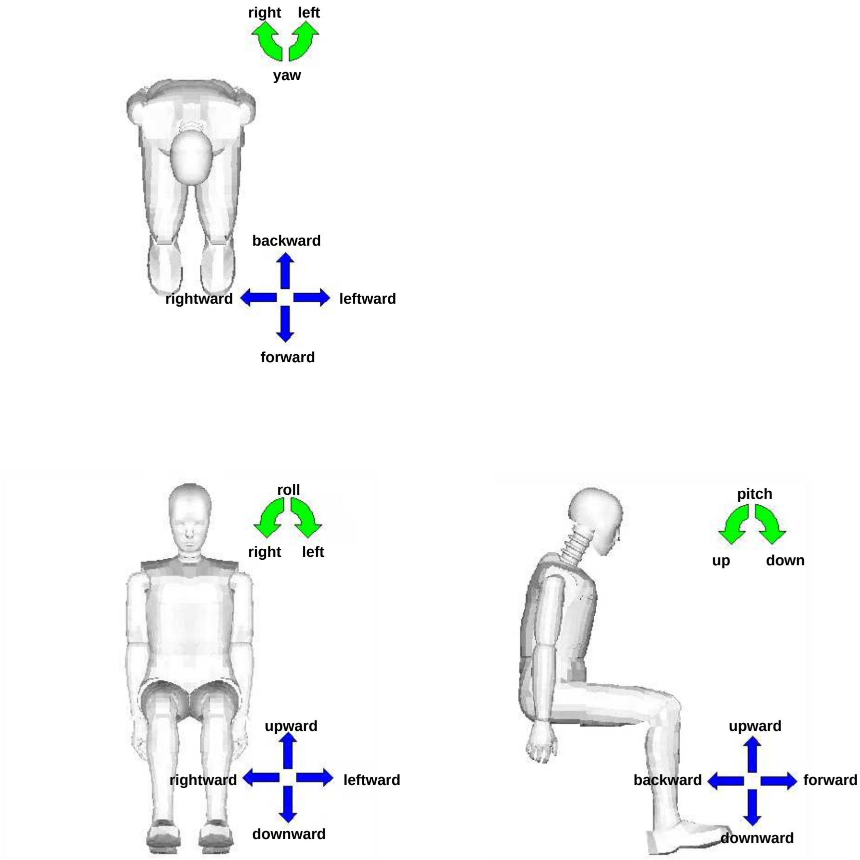


Figure 1.2: Definition of translations and rotations for dummy model positioning joints.

### 1.3.4 Definition of contact interactions

All relevant internal contact interactions inside the hardware tool are predefined in the model. The user has to define the external contact interactions between the model and its environment. To facilitate this, the models have pre-defined contact groups that can be referred to in the external contact definitions. These pre-defined contact groups are available for all relevant components. Model specific information on these contact groups is given in tables in the referring chapters. Friction parameters for external contact definitions will differ from application to application and are therefore not supplied. It is recommended to perform experiments in order to obtain accurate friction parameters. General guidelines for contact definitions between a dummy and its environment are given below.

***Ellipsoid dummy models:***

All contacts defined between an ellipsoid dummy and its environment should use the element CONTACT.FORCE_CHAR. The following guidelines can be defined for contact definitions with ellipsoid models:

1. Contacts defined with a stiff multibody environment or any FE environment should use the contact characteristics of the dummy surface (defined with attribute CONTACT_TYPE).
2. For contact definitions between a dummy and a deformable (padded) multibody environment, combined contact characteristics should be used.
3. In general, the ellipsoid dummy model contact functions are defined such that the EVALUATION option is not needed in contact definitions. Therefore, the attribute EVALUATION_TYPE under CONTACT.MB_MB normally has to be set to NONE for contacts with the ellipsoid dummy models. If in the future, for new and updated ellipsoid dummy models, the contact functions would be defined for use with EVALUATION_TYPE=CONTINUOUS, this will be mentioned explicitly in the "Dummy contacts" section in the related chapter in this manual.

***Facet dummy models:***

Contacts defined between a facet dummy and a facet or FE environment should be defined as elastic contacts, using the element CONTACT_FORCE.CHAR. For facet dummies in contact with a facet or FE environment it is recommended to model the contacting environmental surfaces as closed meshes, to prevent incorrect contacts near surface edges. It is important to always keep the SYMMETRIC option OFF. Also the definition of master surface and slave surface is very important. The following guidelines for selection of master and slave surface are given in decreasing order of priority:

1. It should always be avoided to have surface edges directly in contact. This can often be done by simply extending the mesh at the edge. For those conditions where it is impossible to extend the mesh (like for FE membrane belts) the surface with the edge in contact should be chosen as the slave surface.
2. When nodal penetrations are large in comparison to the surface curvatures, the most significantly curved surface should be the slave surface.
3. When master and slave surface have different mesh densities, the surface with the highest mesh density should be the slave surface.

From MADYMO R6.2.1 onwards, it has been possible to use combined facet to facet surface contacts. In earlier versions of MADYMO, the most compliant surface was typically chosen to define the contact interaction, and the other surface was treated as rigid. If both surfaces were equally compliant, the modeller would then have to use a user-defined contact function, and design a new contact function that combined the stiffness characteristics of the two contact surfaces. In the current MADYMO release, the characteristics of the surfaces can easily be combined using the **"CONTACT_TYPE=COMBINED"** option. Some notes apply: the combined option can only be used with the **"CONTACT_MODEL=STRESS"** option, and the combined option may result in longer simulation times, in particular when the contact characteristics of the surfaces are non-linear. A large hysteresis slope and large damping values will also increase simulation time. If the contact characteristics of the two surfaces are very different, i.e. one surface is clearly much stiffer than the other, it is advised to treat that surface as rigid and use the **"CONTACT_TYPE=MASTER"** or **"CONTACT_TYPE=SLAVE"** options.

When master and slave surfaces are not modelled with similar mesh densities and, following guidelines 1 or 2 above, the master surface turns out to have the more refined mesh, problems may occur when the contact characteristics of the master surface need to be used. In this situation the difference in mesh density would lead to an underestimation of the total contact surface and total contact force. Workarounds for this situation are:

- When possible, adjusting the mesh density of master or slave surface, in order to obtain similar mesh densities.
- Copying the contact characteristics for the master surface onto those for the slave surface, and then use the slave surface contact characteristics. Note that hysteresis is not handled correctly in this situation (important for rebound loading) and the points of application of the friction forces are at the wrong surface (important for sliding movement of the contacting surfaces).
- Scaling up the contact functions manually in order to compensate for the underestimated contact forces.

***FE dummy models:***

Contacts defined between a FE dummy and FE environment should be defined as elastic contacts, using the elements CONTACT_FORCE.PENALTY or CONTACT_FORCE.ADAPTIVE. In these types of contacts, penetration of the contacting surfaces is minimised. Some general guidelines for this type of contact are:

1. If mesh densities are significantly different, the most refined surface should be chosen as the slave surface.
2. If the master surface material is more compliant than the slave surface material, for CONTACT_FORCE.PENALTY the penalty factor defined for the contact should be increased so that penetrations are kept small. It should be increased to a level that ensures converged dummy sensor output signals.
3. If contact is defined between relatively coarse meshes, the SYMMETRIC option may be switched ON in order to avoid master surface nodes penetrating locally through the slave surface elements.

### 1.3.5 Belt positioning

Concerning the choice between conventional and finite element belts, it is recommended to use conventional belts on the ellipsoid dummy models and finite element belts on the facet and finite element dummy models.

Conventional belts are positioned over the dummy through the belt attachment points. For some dummy models, recommended points are predefined as POINT_OBJECT elements in the dummy model user file. However, if considered necessary, the user can modify the positions of these points. The lateral co-ordinates of belt positioning points usually differ from test to test, and should be modified accordingly. Predefined belt attachment points are listed in the user instructions section of the referring chapter. For more information on FE belt positioning, the user is referred to the MADYMO application manual.

### 1.3.6 Application of acceleration fields

Gravity load and other applicable acceleration fields can best be applied to a model on system level, using the element LOAD.SYSTEM_ACC. In applications where a dummy is loaded through interactions with a decelerating environment (e.g. the vehicle interior), it is customary in simulations to apply the inverse acceleration field to the dummy model, rather than decelerating the environment itself. With the actual environment being part of the inertial space, the crash pulse is applied on the dummy only. More information on this is given in the theory manual.

Note that for dummies the reference position defined in the user file does not take into account initial component deformation due to gravity (see also Section 1.3.3).

### 1.3.7 Output definition

Model output signals and injury criteria are predefined for each model in the include file. The sensors included in the dummy models have orientations according to the SAE J211/1 sign convention. Output signals are also filtered according to this convention unless stated otherwise in this manual. In order to avoid problems with filtering of output signals, it is recommended to use an output timestep of 1.0E-04 s (TIME_STEP under CONTROL_OUTPUT).

Output from the sensors belonging to the standard instrumentation of the hardware, is called for in the user file. This is done in the TIME_HISTORY.MB element inside the CONTROL_OUTPUT element (see Figure 1.1). In a COMMENT block all available output signal names, meaning both standard and optional instrumentation, are listed. The user can place these names in the elements inside the TIME_HISTORY.MB element, in order to obtain sensor output from optional instrumentation. To obtain injury criteria output, the injury must be specified in the INJURY_LIST in the CONTROL_OUTPUT element. The required signals to calculate the injury also need to be selected. Model specific information on the output signals and injury criteria is given in tables in the user instructions section of the referring chapter.

From MADYMO V7.3 on, the user has the option to select time-history output signals for conversion to ISO-MME data format (i.e. ISO-TS13499:2003 Road Vehicles - Multimedia data exchange format for impact tests). With the new element TIME_HISTORY_ISO_MME under CONTROL_OUTPUT, the user can define sets of time-history signals in the input deck and assign ISO-MME channel codes to them. For those dummy models that have ISO-MME signal output requests already predefined in their *_usr.xml files, more information is given in the next chapters of this manual in paragraph 'Output' under 'User Instructions'.

# 2 Hybrid III 50th percentile Q Dummy

As a follow-up to the frontal module ellipsoid and facet Hybrid III 50$^{th}$ percentile dummy models the quality (Q) ellipsoid and the quality (Q) facet Hybrid III 50$^{th}$ percentile dummy models have been developed, because of the increasing market need for a more CPU-efficient and user-friendly dummy model with a high quality. The quality of the models is determined by an objective rating method. For more information on this subject, the reader is referred to the quality reports supplied with these models.

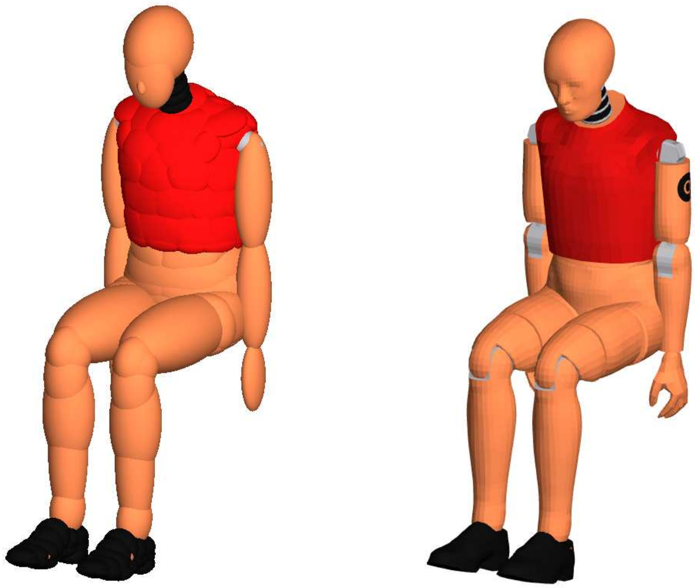

Figure 2.1: Hybrid III 50$^{th}$ percentile ellipsoid Q (left) and facet Q (right) dummy models in the reference position.

## 2.1 Model description

Quality ellipsoid and facet models of the Hybrid III 50$^{th}$ percentile male dummy are available. The input is given in the files:

| | |
|---|---|
| Ellipsoid model: | d_hyb350el_Q_usr.xml<br>d_hyb350el_Q_inc.xml |
| Facet model: | d_hyb350fc_Q_usr.xml<br>d_hyb350fc_Q_inc.xml |

To run these models, the following licenses are required:

| | |
|---|---|
| Ellipsoid model: | MADYMO/Solver (Multibody)<br>MADYMO/Dummy Models/Frontal |
| Facet model: | MADYMO/Solver (Multibody)<br>MADYMO/Dummy Models/Hybrid III |

Figure 2.1 shows the quality ellipsoid and facet model in the reference position. The ellipsoid and facet model consists of 211 bodies including 50 bodies for the jacket and 6 bodies for the left and the right shoe.

**ELLIPSOID MODEL AND FACET MODEL**

The ellipsoid model has the same multibody basis as the facet model. The facet model has been developed on basis of the CAD scanning data while the ellipsoid model gives a very good approximation of the facet model using ellipsoid surfaces.

For the facet model the internal geometry, which is only used for the visualisation, is placed in separate FE-models.

In the next sections the components of the dummy will be described in detail. The description is for both model types the same, since the multibody basis are the same. Only the geometry description differs, ellipsoids or facet surfaces.

To enable energy flow output MB and compound groups are added to the models. In the user files for both models energy output groups are pre-defined (see user instructions). These groups can be used in combination with other energy output groups to evaluate the energy flow of the application.

**Head and neck**

The head has been modelled with a rigid body having three associated ellipsoid surfaces, representing the skull, the face and the nose, for the ellipsoid model. The facet model uses one closed surface. It is connected by a bracket joint to the upper neck load cell.

The neck is composed of four parts: the upper neck load cell, the neck nodding plate, the neck column with cable and the neck bracket. The upper and lower neck load cells are modelled with bracket joints. The nodding joint is a revolute joint combined with a restraint. The neck bracket is modelled with a revolute joint which is locked during the simulation. When the neck bracket joint has not the default value of zero, the lower neck load cell results will not be the same as in the hardware dummy.

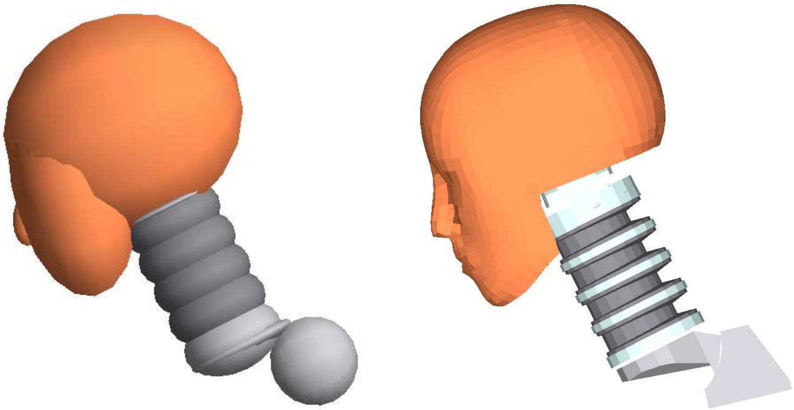

Figure 2.2: Hybrid III $50^{th}$ percentile ellipsoid Q (left) and facet Q (right) head-neck geometry.

The neck column with cable is represented by 6 joints of which four are universal and two are cylindrical joints. Two triple joint restraints are used for the lower and the upper part of the neck. Universal joints are located in the centres of the 4 rubber disks (see Figure 2.3).

The neck parts are coupled with bracket joints, further the neck assembly is coupled with a bracket joint to the thoracic spine.

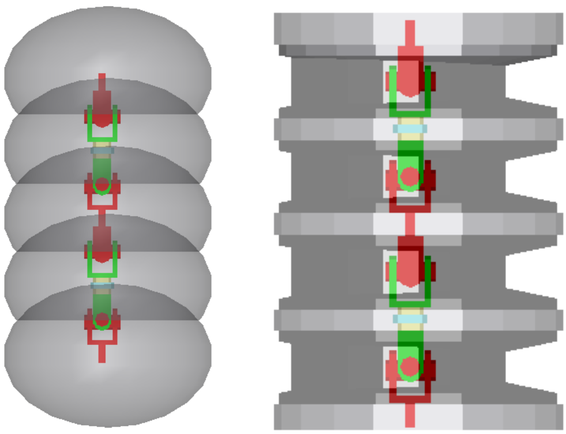

Figure 2.3: Hybrid III $50^{th}$ percentile ellipsoid Q (left) and facet Q (right) neck model.

**Thorax**

The thorax consists in general of the following parts: the spinebox, the ribcage, the clavicles, the bib and the jacket. The thorax is modelled with multiple chains of bodies and joints.

The spinebox has been modelled by means of three bodies, representing the thoracic spine and the lower and upper part of the thoracic load cell, connected with bracket joints. The bracket joint between the thoracic load cell parts represents the load cell itself.

The ribcage has been modelled with 12 chains of bodies and joints forming the six ribs (see Figure 2.4). Another chain models the potentiometer and ends with the sternum body. It uses two revolute joints, representing the potentiometer, a spherical joint and a translational joint modeling the connection from the potentiometer to the sternum. The front of the ribs are connected to the front rib end bodies with universal joints, forming closed loops. The front rib end bodies are connected with point restraints to the sternum. All kinematic joints have joint restraints which give the ribcage its stiffness.

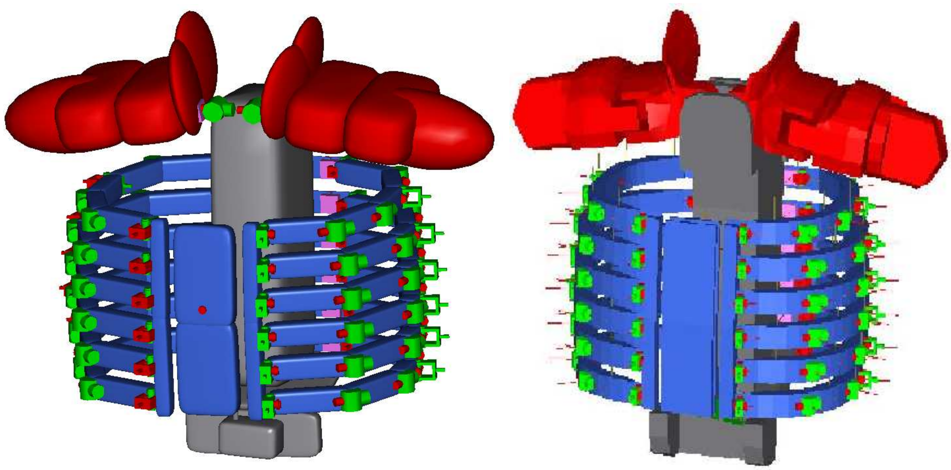

Figure 2.4: Hybrid III 50$^{th}$ percentile ellipsoid Q (left) and facet Q (right) ribcage model.

The clavicles are modelled with eight bodies and eight joints, where two are bracket joints to represent the load cells of the left and right clavicle. Revolute joints are connecting the shoulder yokes to the clavicles and the clavicles to the clavicle load cells. Revolute joints also connecting the clavicle links to the thoracic spine.

The bib has been modelled with a point restraint and a kelvin element. Both elements are connected between the sternum body and the upper neck bracket body. Additionally three point restraints were connected between jacket bodies and left and right clavicle and upper neck bracket bodies.

The jacket is modelled separately with 50 bodies and free joints. The bodies are connected to each other with a lot of point and cardan restraints (see Figure 2.5). The body at the lower back side of the jacket is connected to the thoracic spine by means of a free joint.

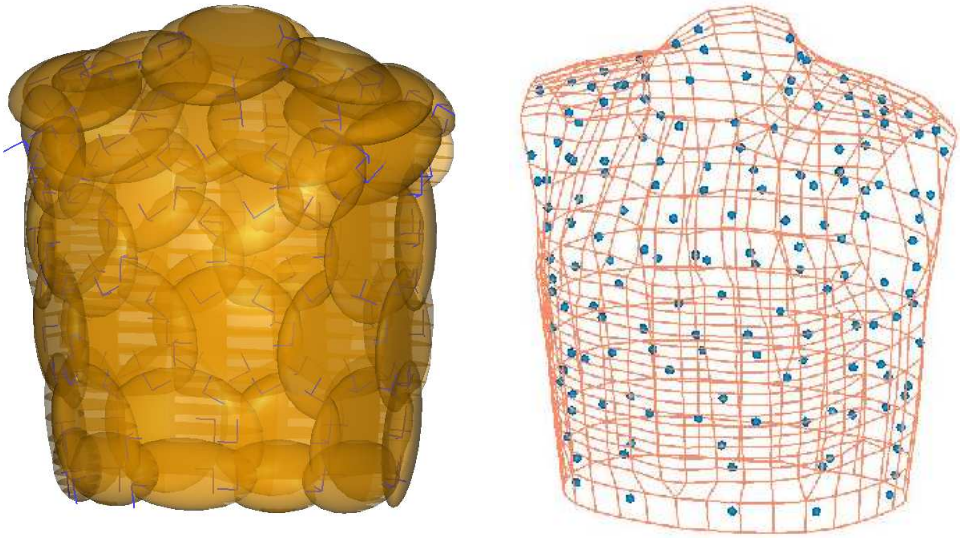

Figure 2.5: Hybrid III 50$^{th}$ percentile ellipsoid Q (left) and facet Q (right) jacket model.

Interaction between jacket and spinebox, ribcage and clavicles is modelled by means of point restraints (see Figure 2.6).

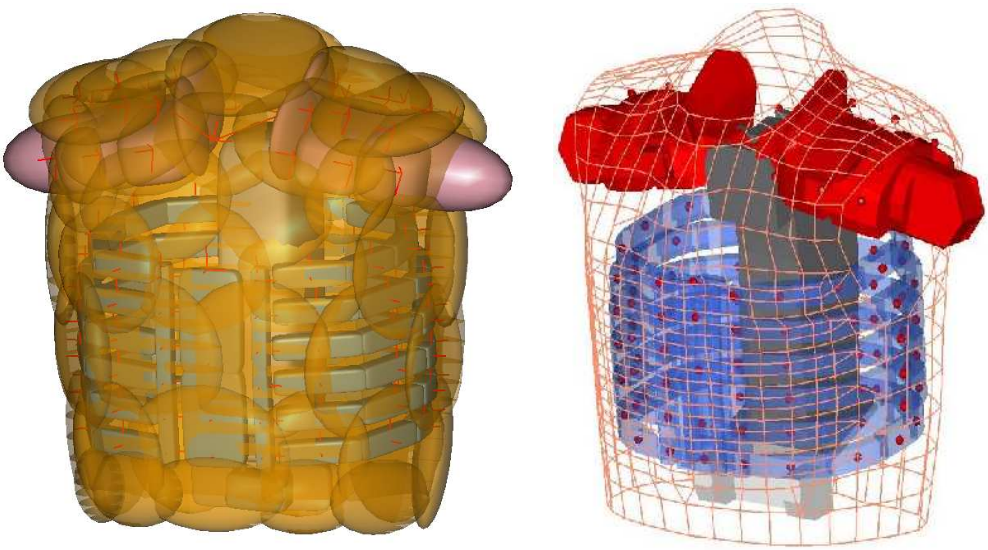

Figure 2.6: Hybrid III 50$^{th}$ percentile ellipsoid Q (left) and facet Q (right) jacket ribcage interaction model.

### Lumbar spine

The lumbar spine assembly consists of the lumbar spine mould with the lumbar load cell. The influence of the lumbar spine cables is lumped in the multibody chain of the lumbar spine mould. The lumbar spine mould is represented with seven bodies. Two bodies and a bracket joint are used for the load cell.

The chain of joints of the lumbar spine mould consists of four universal and three cylindrical joints. Two sets of universal - cylindrical - universal joint sequences make use of a triple joint restraint and the cylindrical joint in the middle has a normal joint restraint (see Figure 2.7). The lumbar spine mould is coupled to the load cell by means of a bracket joint.

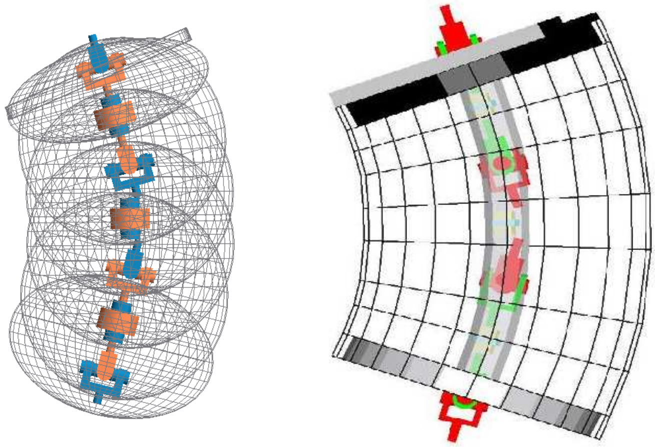

Figure 2.7: Hybrid III 50$^{th}$ percentile ellipsoid Q (left) and facet Q (right) lumbar spine model.

In the complete physical dummy, lumbar spine deformation is not only resisted by the lumbar spine itself but also by contact interactions with ribcage, abdomen and pelvis. These interactions are included in the model in the form of point restraints. For the ellipsoid model these point restraints are attached to the abdomen and connected at the lower side of the abdomen to the pelvis and at the upper side to the lower ribs. For the facet model these point restraints are referred to as "Abdomen vertical compression left/middle/right".

### Abdomen and pelvis

The abdomen has been modelled as a separate body, which is connected to the pelvis by means of a free joint for the ellipsoid and a bracket joint for the facet model.

The abdomen body of the ellipsoid model is associated with six ellipsoid surfaces while the facet model is associated with a closed facet surface. The abdomen body of the ellipsoid model is connected to the surrounding components with point restraints to represent the contact with the pelvis, lumbarspine and lower ribs.

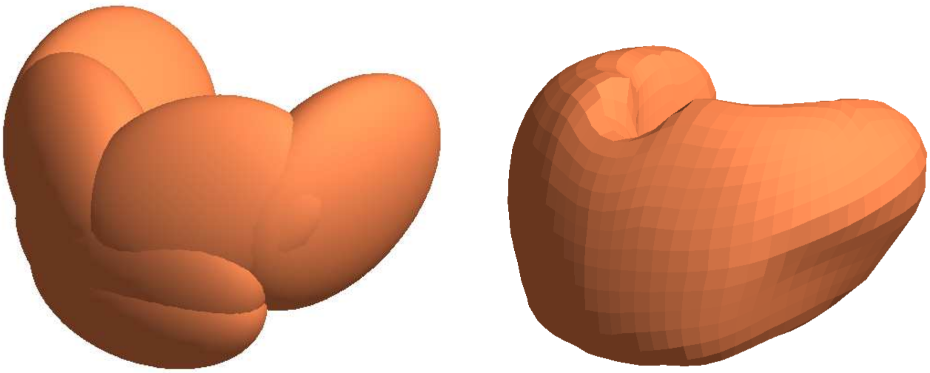

Figure 2.8: Hybrid III $50^{th}$ percentile ellipsoid (left) and facet (right) abdomen model.

The pelvis has been modelled with three bodies and three joints, one free dummy joint and two spherical joints for the hips and are part of the pelvis assembly. Sixdof restraints modelled between the pelvis and the hips models the stiffness of the spherical hip joint and the compression of the femur and pelvis flesh around the femurs. The friction in the hip joints is represented in joint restraints which are located in the user file and can be modified by the user.

The ellipsoid model has 43 ellipsoids to model the skin of the pelvis, 2 ellipsoids represent the pelvis buttocks and 6 ellipsoids the iliac wings.

The facet model has surfaces representing the metal skeleton. The pelvis outer facet surface model is divided into parts which have seven different contact characteristics and variable thicknesses (see Figure 2.9). This is because the proportion of PVC-skin and foam material inside the hardware pelvis is different. The outer and inner PVC-skin is always about 5mm thick and in the PVC-skin the foam filling thickness varies from 1cm up to about 10 cm. Therefore characteristic contact 1 is for material thickness up to 6cm, 2 for thickness from 6cm to 11cm, 3 and 4 for hole edges, 5 for the back hole, 6 for pelvis-abdomen area and 7 for top iliac wings area. Since the abdomen is behind the pelvis skin only the pelvis has been calibrated. This means that the abdomen stiffness is included in the pelvis skin characteristics.

2

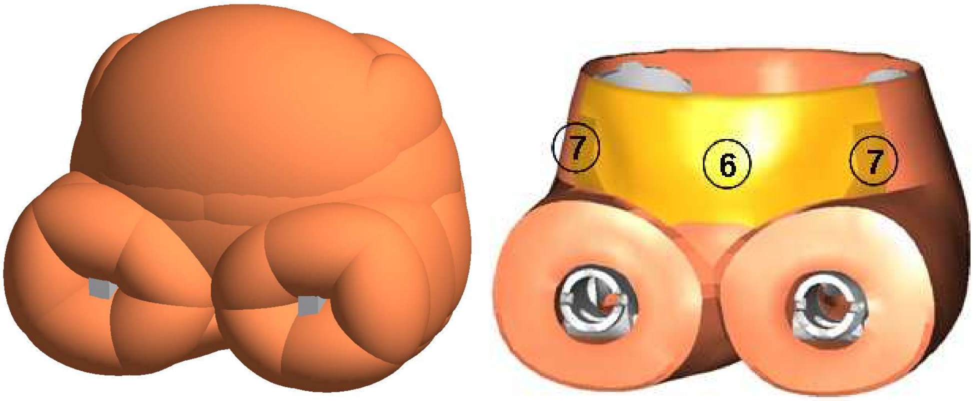


Figure 2.9: Front of pelvis, ellipsoid (left) and facet surface parts (right).

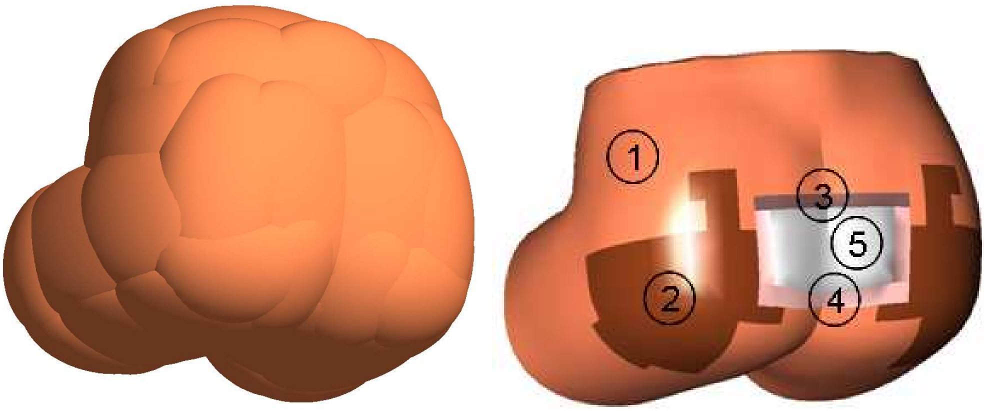


Figure 2.10: Back of pelvis, ellipsoid (left) and facet surface parts (right).

## Arms

The arm consists of the upper arm and the lower arm with the hand. Figure 2.11 shows the model of the arm for both the ellipsoid Q and facet Q models.

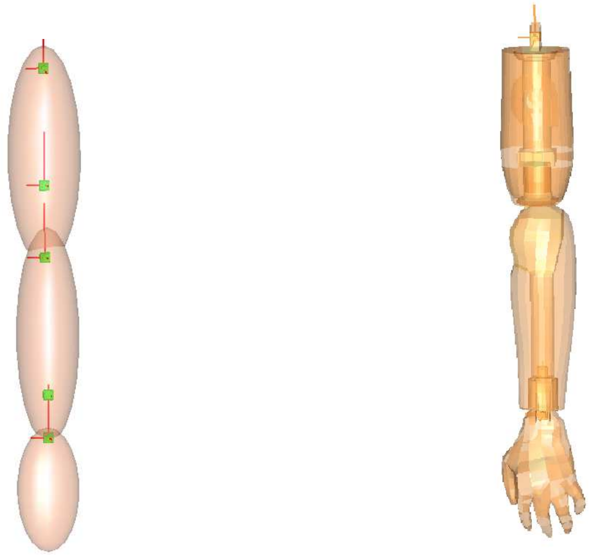

Figure 2.11: Hybrid III 50$^{th}$ percentile ellipsoid Q (left) and facet Q (right) arm model.

The upper arm has been modelled by means of two bodies one for the upper arm and one for the elbow and two revolute joints, one connecting the upper arm to the shoulder and the other one connecting the elbow to the upper arm.

The lower arm has been modelled by means of three bodies for the lower arm, the wrist and the hand and three revolute joints connecting the lower arm to the elbow part of the upper arm, the wrist part to the lower arm and the hand to the wrist part of the lower arm.

### Legs

The femurs have been modelled with five bodies and joints. Four of them are bracket joints, and one is a revolute joint used for the knee. The femur load cells are modelled, using bracket joints, as well as the part of the femurs. The femurs are coupled to the pelvis assembly by means of the bracket joints.

The tibias are modelled with three bodies: one for the upper part, one for the mid part and one for the lower part. Bracket joints are defined for the lower tibia and the upper tibia load cell and connects the lower, mid and upper part of the tibia bodies. A translational joint is used to model the knee slider and connects the tibia to the knee.

Figure 2.12 shows the model of the leg for both the ellipsoid Q and facet Q models.

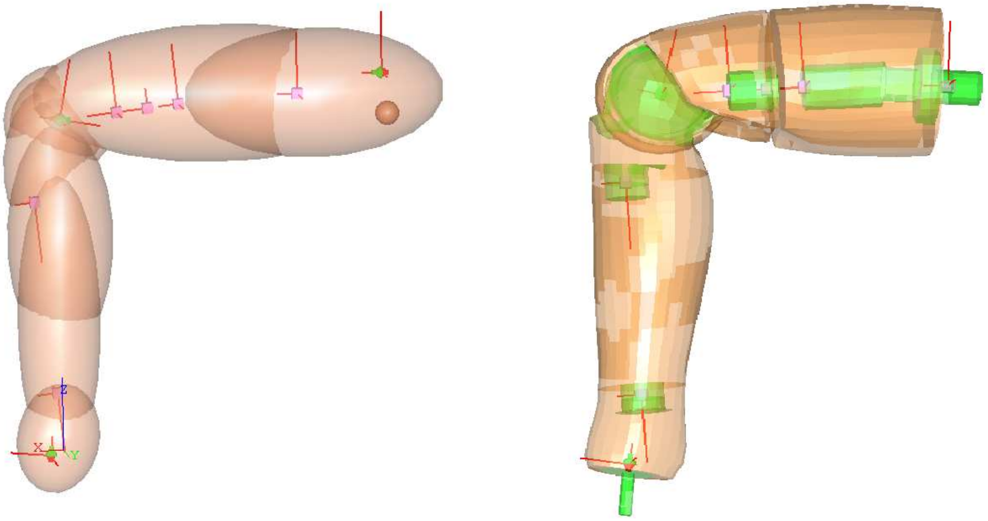

Figure 2.12: Hybrid III 50$^{th}$ percentile ellipsoid Q (left) and facet Q (right) leg model.

### Feet and ankles

The foot has been modelled by means of three bodies one for the foot and two for the toes connected with two revolute joints. A spherical joint connects the foot to the tibia to represent the ankle (see Figure 2.13).

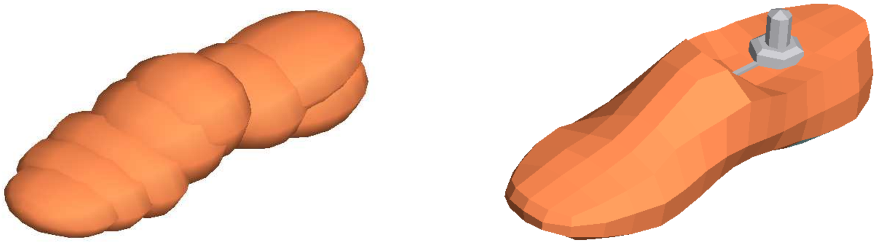

Figure 2.13: Hybrid III 50$^{th}$ percentile ellipsoid Q (left) and facet Q (right) foot model.

### Shoes

The shoes have been implemented as separate components. Each shoe consists of three bodies, two revolute joints and one free joint. The free joint links the shoe to the foot. This joint is restrainted and allows translation and rotation of the foot inside the shoe. The ellipsoid model has four additional point restraints to model the interaction between the foot and the shoe at the toes and heel positions. The toes are made deformable by means of the revolute joints. (see Figure 2.14).

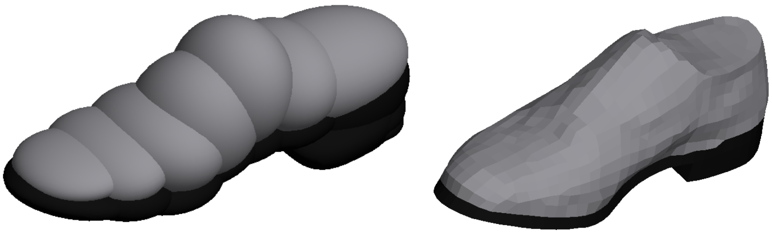

Figure 2.14: Hybrid III $50^{th}$ percentile ellipsoid Q (left) and facet Q (right) shoe model.

## CONTACTS BETWEEN DUMMY COMPONENTS

The contacts between dummy components defined can be found in Table 2.1 for both models.

Table 2.1: Intercomponent contacts for the Hybrid III $50^{th}$ percentile Q models.

| Model type | Contact surface master | slave |
|---|---|---|
| ellipsoid | Jacket_gmb | Head_gmb |
| | Jacket_gmb | ArmL_gmb |
| | Jacket_gmb | ArmR_gmb |
| | FemurKneeL_gmb | ArmLowL_gmb |
| | FemurKneeR_gmb | ArmLowR_gmb |
| | Jacket_gmb | FemurKneeL_gmb |
| | Jacket_gmb | FemurKneeR_gmb |
| | FemurKneeR_gmb | FemurKneeL_gmb |
| | TibiaR_gmb | TibiaL_gmb |
| facet | Jacket_gfe | Head_gfe |
| | Jacket_gfe | ArmUpL_gfe |
| | Jacket_gfe | ArmLowL_gfe |
| | Jacket_gfe | ArmUpR_gfe |
| | Jacket_gfe | ArmLowR_gfe |
| | FemurKneeL_gfe | ArmLowL_gfe |
| | FemurKneeR_gfe | ArmLowR_gfe |
| | Jacket_gfe | FemurKneeL_gfe |
| | Jacket_gfe | FemurKneeR_gfe |
| | FemurKneeR_gfe | FemurKneeL_gfe |
| | TibiaR_gfe | TibiaL_gfe |

## 2.2 User instructions

### Timestep

Table 2.2: Recommended timestep for the Hybrid III 50$^{th}$ percentile Q dummy model.

| Model | timestep (s) |
|---|---|
| Ellipsoid | $\leq 1.0 \cdot 10^{-5}$ |
| Facet | $\leq 1.0 \cdot 10^{-5}$ |

### Dummy positioning

The generic way to position the dummy model is to start with the dummy joint. The dummy joint is located at the H-point of the dummy model and is meant to position the complete model in reference space or relative to another body (e.g. seat). The thorax is next to be positioned by rotating the lumbar spine joints. The easiest way is to divide the total angle between the pelvis and thorax over the lumbar spine joints. An alternative way is to use the Q-HIII Spine Angle Calculator in xMADgic and use the values for joints LumbarMouldPart<1, 3 and 5> and LumbarSpineUp. Older facet Q dummy model versions may have separately modelled spine cables (models v3.0 to v3.3). In this case the spine angle calculator must be used in order to position the cables correctly inside the lumbar mould. A third method is to do a pre-simulation to get the lumbar spine in the desired position and use the joint position output as initial position in the actual simulation. Remember that the lumbar spine is a rubber component and needs external loading to keep it bended.

If necessary the head can be positioned by rotating the neck joints. This can be achieved by dividing the total angle or by a pre-simulation, similar as with the lumbar spine. The legs can then be positioned by rotating the hips, knees and ankles. Finally the arms can be positioned by rotating the shoulder, elbow and wrist joints. It might be possible that the upper arm is initially contacting the jacket resulting in initial accelerations in the thorax. To reduce the initial accelerations the upper arm needs to be rotated more from the jacket.

Table 2.3: Positioning joints of the Hybrid III 50$^{th}$ percentile ellipsoid Q and facet Q dummy models

| Joint Description | Identifier | Degree of freedom[(a)] | | | | | | Comment |
|---|---|---|---|---|---|---|---|---|
| Complete dummy | Dummy_jnt | D1<br>R1 | forward<br>roll right | D2<br>R2 | leftward<br>pitch down | D3<br>R3 | upward<br>yaw left | |
| Neck bracket | NeckBracket_jnt | R1 | pitch down | | | | | (b) |
| Neck element | NeckPivot1_jnt | R1 | pitch up | R2 | roll right | | | (c) |
| | NeckCylinder1_jnt | R1<br>D1 | yaw left<br>upward | | | | | (c) |
| | NeckPivot2_jnt | R1 | roll right | R2 | pitch up | | | (c) |
| | NeckPivot3_jnt | R1 | pitch up | R2 | roll right | | | (c) |
| | NeckCylinder2_jnt | R1<br>D1 | yaw left<br>upward | | | | | (c) |
| | NeckPivot4_jnt | R1 | roll right | R2 | pitch up | | | (c) |

*Continued on the next page*

*Table 2.3 cont.*

| Joint Description | Identifier | Degree of freedom[a] | | | Comment |
|---|---|---|---|---|---|
| Left shoulder | ShoulderYokeL_jnt | R1 pitch down | | | |
| | ShoulderL_jnt | R1 roll right | | | |
| Right shoulder | ShoulderYokeR_jnt | R1 pitch down | | | |
| | ShoulderR_jnt | R1 roll right | | | |
| Left elbow | ElbowPivotL_jnt | R1 yaw left | | | |
| | ElbowL_jnt | R1 pitch down | | | |
| Right elbow | ElbowPivotR_jnt | R1 yaw left | | | |
| | ElbowR_jnt | R1 pitch down | | | |
| Left wrist | WristPivotL_jnt | R1 yaw left | | | |
| | WristL_jnt | R1 roll right | | | |
| Right wrist | WristPivotR_jnt | R1 yaw left | | | |
| | WristR_jnt | R1 roll right | | | |
| Lumbar Spine | LumbarSpineUp_jnt | R1 roll left | R2 pitch down | | [d] |
| | LumbarMouldPart6_jnt | R1 yaw left<br>D1 upward | | | [d] |
| | LumbarMouldPart5_jnt | R1 pitch down | R2 roll left | | [d] |
| | LumbarMouldPart4_jnt | R1 yaw left<br>D1 upward | | | [d] |
| | LumbarMouldPart3_jnt | R1 roll left | R2 pitch down | | [d] |
| | LumbarMouldPart2_jnt | R1 yaw left<br>D1 upward | | | [d] |
| | LumbarMouldPart1_jnt | R1 pitch down | R2 roll left | | [d] |
| Left hip | HipL_jnt | R1 roll right | R2 pitch down | R3 yaw left | |
| Right hip | HipR_jnt | R1 roll right | R2 pitch down | R3 yaw left | |
| Left knee | KneeL_jnt | R1 pitch down | | | |
| Right knee | KneeR_jnt | R1 pitch down | | | |
| Left ankle | AnkleL_jnt | R1 yaw left | R2 roll right | R3 pitch down | |
| Right ankle | AnkleR_jnt | R1 yaw left | R2 roll right | R3 pitch down | |

[a] Positive translation or rotation given in global coordinate system while dummy is in reference position (see Figure 1.2).

[b] The neck bracket angle corresponds directly to that of the physical dummy. If the lower neck load cell is used in the physical dummy, this angle must be zero.

[c] Only for equilibrium state.

[d] In principle only for equilibrium state, however it might be necessary to rotate lumbar joints to position upper torso with neck and head correctly.

## Dummy contacts

Table 2.4: Available groups to define contact between the Hybrid III 50$^{th}$ percentile Q components and environment.

| Contact Description | Identifier$^{(a)(b)}$ | Ellipsoid model$^{(b)}$ | Facet model$^{(b)}$ |
|---|---|---|---|
| Full Dummy | Dummy_ctg | all exterior ellipsoids except the shoes | |
| Head | Head_ctg | Head_ell<br>Face_ell<br>Nose_ell | Elements and nodes |
| Neck | Neck_ctg | NeckPlateLow_ell<br>NeckPlateUp_ell<br>NeckPart⟨$i$⟩_ell,<br>for i=1 to 3 | Elements and nodes |
| Left Upper Arm | ArmUpL_ctg | ArmUpL_ell | Elements and nodes |
| Right Upper Arm | ArmUpR_ctg | ArmUpR_ell | Elements and nodes |
| Left Lower Arm and Hand | ArmLowL_ctg | ArmLowL_ell<br>HandL_ell | Elements and nodes |
| Right Lower Arm and Hand | ArmLowR_ctg | ArmLowR_ell<br>HandR_ell | Elements and nodes |
| Thorax | Thorax_*ctg* | Jacket⟨$i$⟩_ell,<br>for i=01 to 50<br>Jacket99_ell<br>ClavicleL/R_ell<br>ClavicleLinkL/R_ell<br>ShoulderYokeL/R_ell | |
| Jacket | Jacket_ctg | Jacket⟨$i$⟩_ell,<br>for i=01 to 50<br>Jacket99_ell | Elements and nodes |
| Clavicles | Clavicles_ctg | | Elements and nodes |
| Abdomen | Abdomen_ctg | AbdomenLow_ell<br>AbdomenMid_ell<br>AbdomenUpL/R_ell<br>AbdomenL/R_ell | |
| Lumbarspine | LumbarBack_ctg | LumbarSpineLow_ell<br>LumbarSpineUp_ell<br>LumbarMouldPart⟨$i$⟩_ell,<br>for i=1 to 6 | |
| Pelvis | Pelvis_ctg | Pelvis⟨$i$⟩L/R_ell,<br>for i=01 to 20<br>Pelvis⟨$i$⟩_ell,<br>for i=21 to 23<br>PelvisButtockL/R_ell<br>IliacWingLowL/R_ell<br>IliacWingMidL/R_ell<br>IliacWingUpL/R_ell | Elements and nodes |
| | IliacWings_ctg | | Elements and nodes |
| Left Femur and Knee | FemurKneeL_ctg | FemurFleshL_ell<br>KneeFleshL_ell | Elements and nodes |
| Left Femur | FemurL_ctg | FemurFleshL_ell | Elements and nodes |
| Left Knee | KneeL_ctg | KneeFleshL_ell | Elements and nodes |

*Continued on the next page*

*Table 2.4 cont.*

| Contact Description | Identifier[a][b] | Ellipsoid model[b] | Facet model[b] |
|---|---|---|---|
| Right Femur and Knee | FemurKneeR_ctg | FemurFleshR_ell<br>KneeFleshR_ell | Elements and nodes |
| Right Femur | FemurR_ctg | FemurFleshR_ell | Elements and nodes |
| Right Knee | KneeR_ctg | KneeFleshR_ell | Elements and nodes |
| Left Tibia | TibiaL_ctg | TibiaFleshUp⟨$i$⟩L_ell,<br>for i=1 to 2<br>TibiaFleshMid⟨$j$⟩L_ell,<br>for j=1 to 2<br>TibiaFleshLowL_ell | Elements and nodes |
| Right Tibia | TibiaR_ctg | TibiaFleshUp⟨$i$⟩R_ell,<br>for i=1 to 2<br>TibiaFleshMid⟨$j$⟩R_ell,<br>for j=1 to 2<br>TibiaFleshLowR_ell | Elements and nodes |
| Left Foot | FootL_ctg [c] | Toes⟨$i$⟩L_ell,<br>for i=1 to 3<br>FootDorsal⟨$j$⟩L_ell,<br>for j=1 to 2<br>FootBack⟨$k$⟩L_ell,<br>for k=1 to 2<br>HeelL_ell | Elements and nodes |
| Left heel | HeelL_ctg [c] | HeelL_ell | |
| Left toes | ToesL_ctg [c] | Toes⟨$i$⟩L_ell,<br>for i=1 to 3 | |
| Right Foot | FootR_ctg [c] | Toes⟨$i$⟩R_ell,<br>for i=1 to 3<br>FootDorsal⟨$j$⟩R_ell,<br>for j=1 to 2<br>FootBack⟨$k$⟩R_ell,<br>for k=1 to 2<br>HeelR_ell | Elements and nodes |
| Right heel | HeelR_ctg [c] | HeelR_ell | |
| Right toes | ToesR_ctg [c] | Toes⟨$i$⟩R_ell,<br>for i=1 to 3 | |
| Left Shoe | ShoeL_ctg [c] | ShoeBackL_ell<br>ShoeDorsal⟨$i$⟩L_ell,<br>for i=1 to 6<br>ShoeHeel1L/RL_ell<br>ShoeHeel⟨$j$⟩L_ell,<br>for j=2 to 4<br>ShoeSole⟨$k$⟩L/RL_ell,<br>for k=1 to 3<br>ShoeSole⟨$l$⟩L_ell,<br>for l=4 to 6 | Elements and nodes |

*Continued on the next page*

2

*Table 2.4 cont.*

| Contact Description | Identifier[a][b] | Ellipsoid model[b] | Facet model[b] |
|---|---|---|---|
| Right Shoe | ShoeR_ctg [c] | ShoeBackR_ell<br>ShoeDorsal⟨$i$⟩R_ell,<br>for i=1 to 6<br>ShoeHeel1L/RR_ell<br>ShoeHeel⟨$j$⟩R_ell,<br>for j=2 to 4<br>ShoeSole⟨$k$⟩L/RR_ell,<br>for k=1 to 3<br>ShoeSole⟨$l$⟩R_ell,<br>for l=4 to 6 | Elements and nodes |

[a] *ctg*= contact group, for the ellipsoid models ctg is replaced by gmb(group_multibody) and for the facet model ctg is replaced by gfe (group_finite element).

[b] L = Left; R = Right

[c] If the dummy wear shoes only the shoe contact groups should be selected and not those of the feet.

### FE belt positioning and contact definition

In the application manual an example is given on how to position a FE belt on a facet dummy model (see Application manual). FE belts can also be created and repositioned with XMADgic 5.0 and higher.

For the lapbelt to facet Q model contact it is recommended to add besides the normal lapbelt to pelvis contact an extra contact definition (model version 3.1 and higher). This contact is between the iliac wings and the lapbelt with the iliac wings as slave and the option RELEDG to ON. This option prevents the lapbelt, with relatively large elements, to get stuck around an iliac wing.

The recommended contacts between dummy and belts are pre-defined in the user file under the SYSTEM.MODEL Belt_to_Dummy_contacts. The references in FE_MODEL of Shoulder-Belt_gfe and LapBelt_gfe needs to be changed to the proper FE-models to make the contacts work. By default the user file will give two warnings due to the fact that the referred FE-model for the belts is empty.

### MB seat to ellipsoid pelvis contact definition

The contact definition between the ellipsoid pelvis and multi-body seat (CONTACT.MB_MB) need some attention. The stiffness of the seat can be modelled with a multi-body chain, in contact characteristics or with a combination of the two.

When the stiffness of the seat is modelled in the multi-body chain and therefore the contact surfaces are considered to be rigid or very stiff, the characteristics of the pelvis should be used. In this case the contact EVALUATION_TYPE needs to be set to NONE.

When the stiffness of the seat is modelled in the contact characteristics. Meaning the contact surface is considered deformable and the modelled characteristics of the seat will be used. In general the contact EVALUATION_TYPE should be set to CONTINUOUS. This depends on how the characteristics are created.

## Output

From MADYMO V7.3 on ISO-MME output can be generated for the Hybrid III 50$^{th}$ percentile Q dummy models. Output requests for signals in ISO-MME format are pre-defined in the CONTROL_OUTPUT element in the user file.

Table 2.5: Hybrid III 50$^{th}$ percentile Q dummy model output signals.

| Sensor | Identifier | Signal resultant | x | direction[(a)] | y | direction[(a)] | z | direction[(a)] | Filter |
|---|---|---|---|---|---|---|---|---|---|
| Head | | | | | | | | | |
| CG accelerometer[(b)] | HeadCG_acc | ar | a1 | forward | a2 | lateral | a3 | vertical | CFC1000 |
| Neck | | | | | | | | | |
| Upper load cell | NeckUp_lce_F_CFC1000 | fr | f1 | shear | f2 | shear | f3 | axial | CFC1000 |
| | NeckUp_lce_F_CFC600 | fr | f1 | shear | f2 | shear | f3 | axial | CFC600 |
| | NeckUp_lce_T | tr | t1 | roll | t2 | pitch | t3 | yaw | CFC600 |
| Lower load cell | NeckLow_lce_F | fr | f1 | shear | f2 | shear | f3 | axial | CFC1000 |
| | NeckLow_lce_T | tr | t1 | roll | t2 | pitch | t3 | yaw | CFC600 |
| Thorax | | | | | | | | | |
| accelerometer[(a)] | Thorax_acc | ar | a1 | forward | a2 | lateral | a3 | vertical | CFC180 |
| Chest deflection | ChestDeflection_dis | dr | d1 | displacement | | | | | CFC600 |
| | ChestDefl_dis_CFC180 | dr | d1 | displacement | | | | | CFC180 |
| | ChestDeflection_vel_CFC600 | vr | v1 | velocity | | | | | CFC600 |
| | ChestDeflection_vel_CFC180 | vr | v1 | velocity | | | | | CFC180 |
| | ChestDeflection_CFC60_vel | vr | v1 | velocity | | | | | CFC60 |
| Clavicles | ClavicleL_lce_F | fr | f1 | shear | f2 | shear | f3 | axial | CFC1000 |
| | ClavicleR_lce_F | fr | f1 | shear | f2 | shear | f3 | axial | CFC1000 |
| Lumbar Spine | | | | | | | | | |
| Thoracic load cell | Thoracic_lce_F | fr | f1 | shear | f2 | shear | f3 | axial | CFC1000 |
| | Thoracic_lce_T | tr | t1 | roll | t2 | pitch | t3 | yaw | CFC1000 |
| Lumbar load cell | Lumbar_lce_F | fr | f1 | shear | f2 | shear | f3 | axial | CFC1000 |
| | Lumbar_lce_T | tr | t1 | roll | t2 | pitch | t3 | yaw | CFC1000 |
| Pelvis | | | | | | | | | |
| accelerometer[(a)] | Pelvis_acc | ar | a1 | forward | a2 | lateral | a3 | vertical | CFC1000 |
| Femur | | | | | | | | | |
| Left load cell | FemurL_lce_F | fr | f1 | shear | f2 | shear | f3 | axial | CFC600 |
| | FemurL_lce_T | tr | t1 | roll | t2 | pitch | t3 | yaw | CFC600 |
| Right load cell | FemurR_lce_F | fr | f1 | shear | f2 | shear | f3 | axial | CFC600 |
| | FemurR_lce_T | tr | t1 | roll | t2 | pitch | t3 | yaw | CFC600 |
| Knee | | | | | | | | | |
| Left Slider | KneeL_dis | dr | d1 | displ | | | | | CFC180 |
| Right Slider | KneeR_dis | dr | d1 | displ | | | | | CFC180 |
| Tibia | | | | | | | | | |
| Left Upper load cell | TibiaUpL_lce_F | fr | f1 | shear | f2 | shear | f3 | axial | CFC600 |
| | TibiaUpL_lce_T | tr | t1 | roll | t2 | pitch | t3 | yaw | CFC600 |
| Right Upper load cell | TibiaUpR_lce_F | fr | f1 | shear | f2 | shear | f3 | axial | CFC600 |
| | TibiaUpR_lce_T | tr | t1 | roll | t2 | pitch | t3 | yaw | CFC600 |

*Continued on the next page*

2

*Table 2.5 cont.*

| Sensor | Identifier | Signal | | | | | | | Filter |
|---|---|---|---|---|---|---|---|---|---|
| | | resul-tant | x | direc-tion[a] | y | direc-tion[a] | z | direc-tion[a] | |
| Left Lower load cell | TibiaLowL_lce_F | fr | f1 | shear | f2 | shear | f3 | axial | CFC600 |
| | TibiaLowL_lce_T | tr | t1 | roll | t2 | pitch | t3 | yaw | CFC600 |
| Right Lower load cell | TibiaLowR_lce_F | fr | f1 | shear | f2 | shear | f3 | axial | CFC600 |
| | TibiaLowR_lce_T | tr | t1 | roll | t2 | pitch | t3 | yaw | CFC600 |
| Foot | | | | | | | | | |
| Left foot accelerometer[a] | FootL_acc | ar | a1 | forward | a2 | lateral | a3 | vertical | CFC1000 |
| Right foot accelerometer[a] | FootR_acc | ar | a1 | forward | a2 | lateral | a3 | vertical | CFC1000 |

[a] Positive direction given according to SAE J211/1.

[b] The calculated acceleration is corrected in the x-direction for a prescribed fictitious acceleration field to get correct values (see Theory manual).

Table 2.6: Injury criteria defined for the Hybrid III 50$^{th}$ percentile Q dummy models.

| Injury criteria | Identifier | Filter |
|---|---|---|
| Head | | |
| HIC (15) | HIC15_inj | |
| HIC (36) | HIC36_inj | |
| 3ms (cumulative) | H3MS_inj | |
| max Res Acc | HaccRpeak_inj | |
| Neck | | |
| max Tension | NecktensZpeak_inj | |
| max Compression | NeckcompZpeak_inj | |
| MOC | | |
| lateral | MOCx_inj | CFC600 (force and moment) |
| frontal | MOCy_inj | CFC600 (force and moment) |
| | MOCy_CFC1000_inj | CFC1000/CFC600 (force/moment) |
| FNIC | | |
| tension | FNICtension_inj | CFC1000 |
| shear | FNICshear_inj | CFC1000 |
| bending | FNICbending_inj | CFC1000/CFC600 (force/moment) |
| NIJ | | |
| tension-extension | NTE_inj | CFC600 (force and moment) |
| tension-flexion | NTF_inj | CFC600 (force and moment) |
| compression-extension | NCE_inj | CFC600 (force and moment) |
| compression-flexion | NCF_inj | CFC600 (force and moment) |
| tension-extension | NTE_CFC1000_inj | CFC1000/CFC600 (force/moment)[a] |
| tension-flexion | NTF_CFC1000_inj | CFC1000/CFC600 (force/moment)[a] |
| compression-extension | NCE_CFC1000_inj | CFC1000/CFC600 (force/moment)[a] |
| compression-flexion | NCF_CFC1000_inj | CFC1000/CFC600 (force/moment)[a] |
| Thorax | | |
| 3ms (cumulative) | T3MS_inj | |
| 3ms (contiguous) | TCon3MS_inj | |
| Chest Compression | ThCC_inj | CFC180 |
| | ThCC_CFC600_inj | CFC600 |
| max Res Acc | TaccRpeak_inj | |
| CTI | CTI_inj | |

*Continued on the next page*

*Table 2.6 cont.*

| Injury criteria | Identifier | Filter |
|---|---|---|
| VC | VC_inj_CFC180<br>VC_inj_CFC600 | CFC180 (deflection)<br>CFC600 (deflection) |
| Femurs | | |
| FFC | | |
| Left | FFCL_inj | CFC600 |
| Right | FFCR_inj | CFC600 |
| max Left Compression | FemurLcompZpeak_inj | |
| max Right Compression | FemurRcompZpeak_inj | |
| Knees | | |
| Left Compression | kneesliderL_inj | |
| Right Compression | kneesliderR_inj | |
| Tibia | | |
| TI | | |
| Upper Left | TIUpL_inj | CFC600 |
| Upper Right | TIUpR_inj | CFC600 |
| Lower Left | TILowL_inj | CFC600 |
| Lower Right | TILowR_inj | CFC600 |
| Upper Left | TIUpL_adjusted_inj[b] | CFC600 |
| Upper Right | TIUpR_adjusted_inj[b] | CFC600 |
| Lower Left | TILowL_adjusted_inj[b] | CFC600 |
| Lower Right | TILowR_adjusted_inj[b] | CFC600 |
| TCFC | | |
| Upper Left | TCFCUpL_inj | CFC600 |
| Upper Right | TCFCUpR_inj | CFC600 |
| Lower Left | TCFCLowL_inj | CFC600 |
| Lower Right | TCFCLowR_inj | CFC600 |
| Feet | | |
| max Res Acc Left[c] | FootLaccRpeak_inj | |
| max Res Acc Right[c] | FootRaccRpeak_inj | |

[a] NIJ injury output with other filtering than CFC600 will generate a warning in the reprint file in MADYMO release 7.2 and older.
[b] Eccentricity feature is not available in MADYMO release 7.2 and older and will result in wrong values. Feature is available from MADYMO 7.3 on.
[c] The result of the 2-D acceleration vector (in ZX-plane) will be given as the maximum value. In MADYMO release 7.3 and older the result of the 3-D acceleration vector will be given.

# 3 Hybrid III 5th percentile Q Dummy



The Hybrid III 5$^{th}$ percentile small female dummy represents the smallest size in the adult population and has been derived from scaled data from the Hybrid III 50$^{th}$ percentile dummy. Originally developed in 1988, the dummy was upgraded in 1991 to evaluate seat belt submarining, and again in 1997 to improve the dummy's ability to evaluate the aggressiveness of airbags, mainly in "Out-of-Position" (OOP) test conditions. The dummy is also included in FMVSS 208.

As a follow-up to the available standard Hybrid III 5$^{th}$ percentile dummy models, the quality (Q) ellipsoid and the quality (Q) facet Hybrid III 5$^{th}$ percentile dummy models have been developed. This is because of the increasing market need for a more CPU-efficient and user-friendly dummy model with a high quality. The quality of the models is determined by an objective rating method. For more information on this subject, the reader is referred to the quality reports supplied with these models.

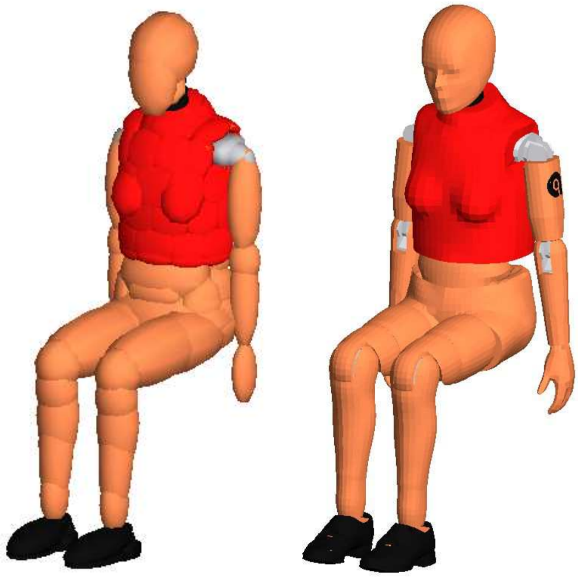

Figure 3.1: Hybrid III 5$^{th}$ percentile ellipsoid Q (left) and facet Q (right) models.

The Q models of the Hybrid III 5$^{th}$ percentile dummy are similar to the Hybrid III 50$^{th}$ percentile Q models. The differences with respect to the Hybrid III 50th percentile Q models are described below. For a description of equivalent parts, please refer to Chapter 2.

## 3.1 Model description

Quality ellipsoid and facet models of the Hybrid III 5$^{th}$ percentile female dummy are available. The input is given in the files:

| | |
|---|---|
| Ellipsoid model: | d_hyb305el_Q_usr.xml<br>d_hyb305el_Q_inc.xml |
| Facet model: | d_hyb305fc_Q_usr.xml<br>d_hyb305fc_Q_inc.xml |

To run these models, the following licenses are required:

| | |
|---|---|
| Ellipsoid Q model : | MADYMO/Solver (Multibody)<br>MADYMO/Dummy Models/Frontal |
| Facet Q model: | MADYMO/Solver (Multibody)<br>MADYMO/Dummy Models/Frontal/HIII 5th Fc Q |

Figure 3.1 shows the models in the reference position. Both models consist of 229 bodies.

### ELLIPSOID AND FACET Q MODELS

The ellipsoid Q model has the same multibody basis as the facet Q model. The facet Q model has been developed on basis on the CAD scanning data combined with the datastructure of the Hybrid III 50$^{th}$ percentile facet Q dummy model while the ellipsoid model represents the very good approximation of the facet Q model using ellipsoid surfaces. This paragraph gives a summarised description of the design of both models.

#### Ellipsoid Q model

The configuration of the ellipsoid Q model of the Hybrid III 5$^{th}$ percentile dummy model is almost identical to the configuration of the ellipsoid Q model of the Hybrid III 50$^{th}$ percentile dummy (see Chapter 2). The thorax has only two extra ellipsoids, describing the 5$^{th}$ percentile female dummy breasts. The feet are modelled somewhat more simply.

#### Facet Q model

The configuration of the facet Q model is almost identical to the configuration of the facet Q model of the Hybrid III 50$^{th}$ percentile dummy (see Chapter 2). The feet are modelled somewhat more simply.

#### Head and neck

The head and the neck of the Hybrid III 5$^{th}$ percentile Q models are modelled in the same way as for the Hybrid III 50$^{th}$ percentile Q models, except that the head has been modelled in more detail with the mounting block to measure the head acceleration as a separate body. The mounting block is connected to the upper neck load cell by means of a bracket joint. For more information about the head and the neck modelling the user is referred to Chapter 2. For more details see Figure 3.2 and Figure 3.3.

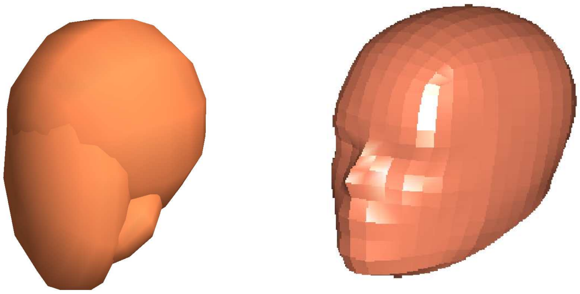

Figure 3.2: Hybrid III 5$^{th}$ percentile ellipsoid Q (left) and facet Q (right) head models.

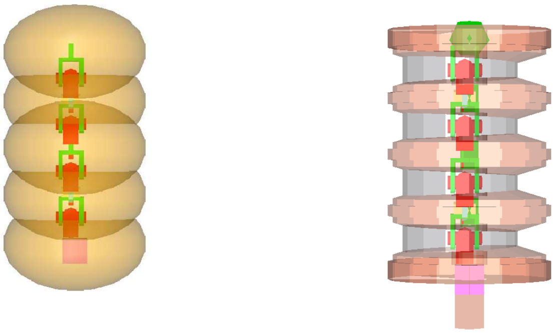

Figure 3.3: Hybrid III 5$^{th}$ percentile ellipsoid Q (left) and facet Q (right) neck models.

**Thorax**

The thorax structure of the Hybrid III 5$^{th}$ percentile Q models is the same as for the 50$^{th}$ percentile Q models. This means that the thorax for both models consists of the spinebox, the ribcage, the clavicles and the jacket. The whole multibody chain has the same structure as for the 50$^{th}$ percentile Q models (see Chapter 2).

The facet thorax model of the Hybrid III 5$^{th}$ percentile differs from the 50$^{th}$ percentile in the sense that the 5$^{th}$ has vertical restraints on the ribcage to model the vertical ribstops. The frontal part of the jacket is modelled with two surfaces: one surface represents the undeformed breasts and is used only for visualisation; another surface, lying slightly behind the outer one, represents the pre-compressed breasts and is used in the contact. Note that an insignificantly small load can result in such a pre-compression of foam and breasts.

The geometry of the ellipsoid Q thorax model is also very accurate; not only the external but also the internal parts are represented with ellipsoids.

See Figure 3.4 for an overview of the ellipsoid and facet Q thorax models.

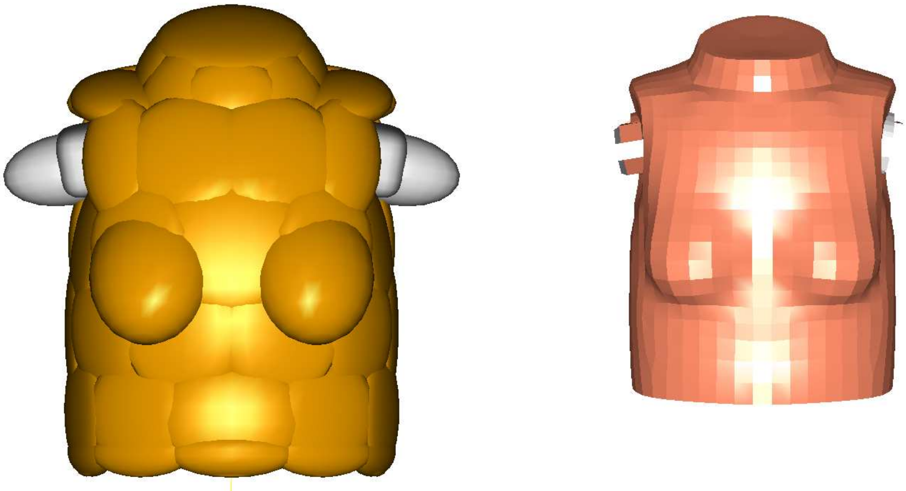

Figure 3.4: Hybrid III 5$^{th}$ percentile ellipsoid Q (left) and facet Q (right) thorax models.

While all of the components now have a detailed facet mesh, the thorax is by far the most complex structure, its stiffness determined not only by its shape and material, but also by the interaction of several independently-moving structures.

### Lumbar spine

The multibody chain of the lumbarspine is the same as for the 50$^{th}$ percentile Q models (see Chapter 2). The chain of the 5$^{th}$ is straight while the chain of the 50$^{th}$ is curved.

The thoracic adaptor is connected to the lumbarmould part of the lumbarspine by means of the bracket joint and is located at the bottom of the lumbarspine.

### Abdomen and pelvis

The abdomen part for both models has been modelled as a separate body. In the ellipsoid model, this is connected to the pelvis by means of a free joint, and the abdomen is retained in place by point restraints modelling the physical restraint of the abdominal cavity. The facet model has a locked translational joint and the stiffness of the abdomen in contact is modelled wholly in the contact characteristics.

Both the ellipsoid and facet Q models require a characteristic based force contact with the lap belt.

For the pelvis part the user is also referred to Chapter 2. For more details see Figure 3.5.

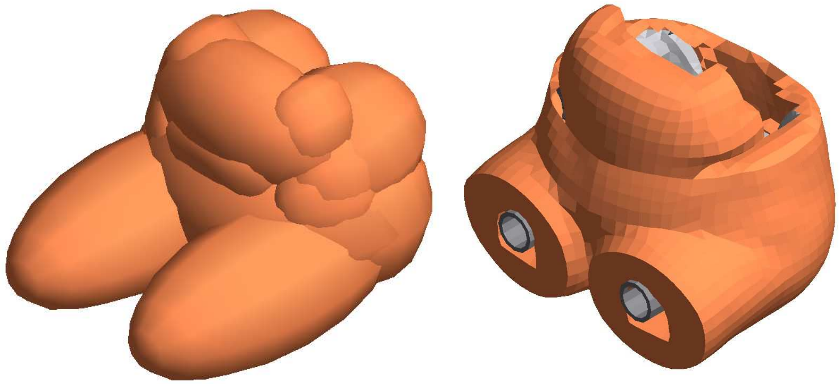

Figure 3.5: Hybrid III 5$^{th}$ percentile ellipsoid Q (left) and facet Q (right) pelvis and abdomen models.

The iliac wing load cells are modelled in the pelvis by means of bracket joints. Part of the outer surface of the pelvis is supported to the iliac wing load cells upper part bodies to ensure a proper load transfer through the load cells.

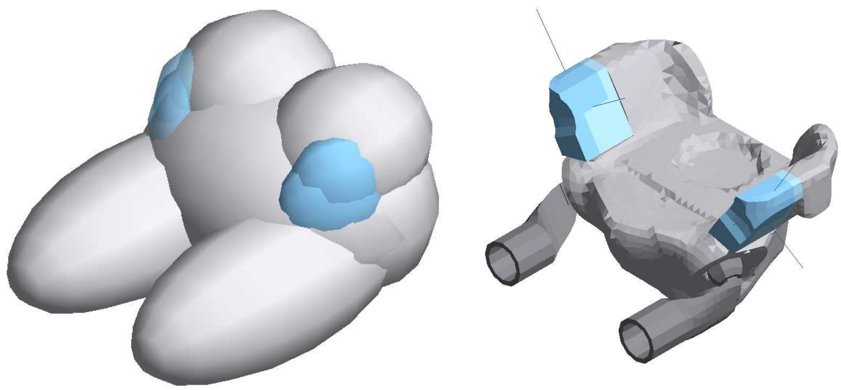

Figure 3.6: Hybrid III 5$^{th}$ percentile ellipsoid Q (left) and facet Q (right) iliac wing load cell models.

**Arms**

The arms of both models are modelled in the same way as for the 50$^{th}$ percentile Q models (see Chapter 2).

For more details see also Figure 3.7.

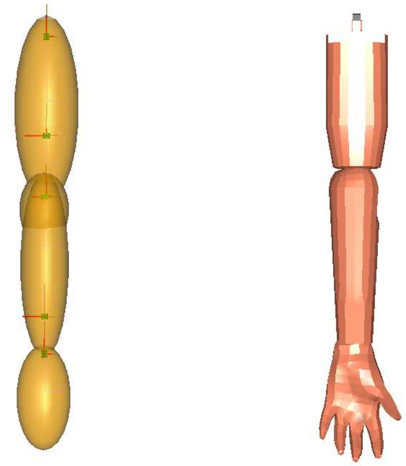

Figure 3.7: Hybrid III 5$^{th}$ percentile ellipsoid Q (left) and facet Q (right) arm models.

**Legs**

The femurs for both models have been modelled with eight bodies and eight joints. Five of them are bracket joints, two are revolute joints and one is a translational joint. Two load cells are modelled as part of the femurs. The femurs of the ellipsoid model have two associated ellipsoid surfaces representing the femur flesh and the knee flesh. The facet model has its corresponding facet surfaces.

The tibias for both models are modelled with ten bodies: three for the upper part, one for the mid part, three for the lower part, and one for the knee-clevis, the ankle-shell and the tibia respectively. They are connected to each other by means of bracket joints. Two load cells for the upper and the lower tibias are included. The tibia of the ellipsoid model has five associated ellipsoid surfaces representing the tibia flesh for the upper (two), the mid (two) and the lower part (one). The tibia of the facet models has corresponding facet surfaces.

Figure 3.8 and Figure 3.9 show the models of the leg for both models.

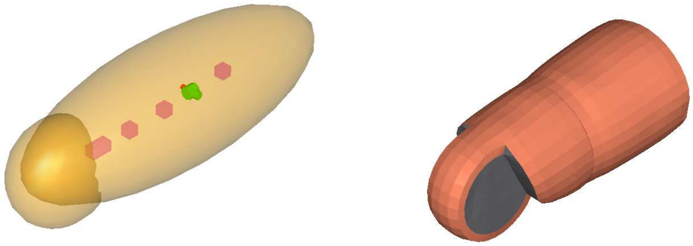

Figure 3.8: Hybrid III 5$^{th}$ percentile ellipsoid Q (left) and facet Q (right) femur models.

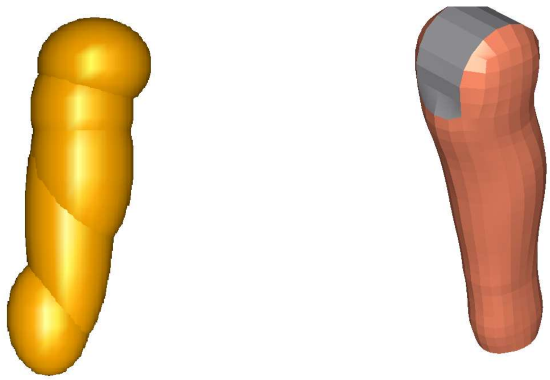

Figure 3.9: Hybrid III 5$^{th}$ percentile ellipsoid Q (left) and facet Q (right) tibia models.

### Feet and ankles

The geometry of the feet is described in detail by three ellipsoids for the ellipsoid Q model and by facet surfaces for the facet Q model. One spherical joint connects the foot body to the tibia (see Figure 3.10).

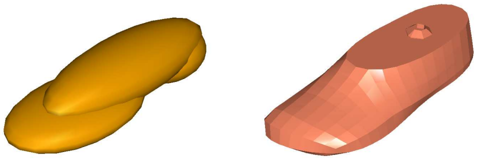

Figure 3.10: Hybrid III 5$^{th}$ percentile ellipsoid Q (left) and facet Q (right) foot models.

### Shoes

The shoes have been implemented as separate components. Each shoe assembly consists of one single rigid body and a free joint that links the shoe to the foot. The shoe is restrained by several point and cardan restraints that allow translation and rotation of the foot inside the shoe (see Figure 3.11).

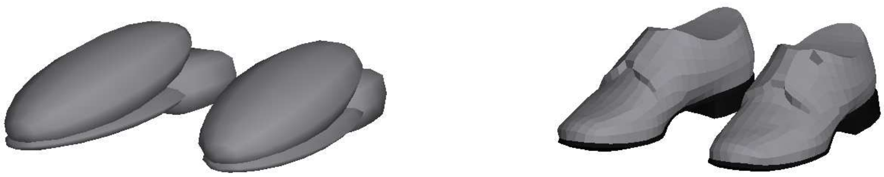

Figure 3.11: Hybrid III 5$^{th}$ percentile ellipsoid Q (left) and facet Q (right) shoes.

## CONTACTS BETWEEN DUMMY COMPONENTS

In both models, contacts are already defined between the head and the thorax, between the thorax and the left and right upper leg, between the left upper leg and the left lower arm, between the right upper leg and the right lower arm, between the left upper leg and the right upper leg and between the left tibia and the right tibia.

Table 3.1: Intercomponent contacts for the Hybrid III 5$^{th}$ percentile Q models.

| Model Type | Contact | Master Surface | Slave Surface |
|---|---|---|---|
| ellipsoid | HeadToJacket_cnt | Jacket_gmb | Head_gmb |
| | ArmLowLToFemurKneeL_cnt | FemurKneeL_gmb | ArmLowL_gmb |
| | ArmLowRToFemurKneeR_cnt | FemurKneeR_gmb | ArmLowR_gmb |

*Continued on the next page*

*Table 3.1 cont.*

| Model Type | Contact | Master Surface | Slave Surface |
|---|---|---|---|
| | AbdomenToSpinebox_cnt | LumbarBack_gmb | Abdomen_gmb |
| | FemurKneeLToThorax_cnt | Jacket_gmb | FemurKneeL_gmb |
| | FemurKneeRToThorax_cnt | Jacket_gmb | FemurKneeR_gmb |
| | FemurKneeLToFemurKneeR_cnt | FemurKneeR_gmb | FemurKneeL_gmb |
| | TibiaLToTibiaR_cnt | TibiaR_gmb | TibiaL_gmb |
| facet | HeadToJacket_cnt | Jacket_gfe | Head_gfe |
| | ArmLowLToFemurKneeL_cnt | FemurKneeL_gfe | ArmLowL_gfe |
| | ArmLowRToFemurKneeR_cnt | FemurKneeR_gfe | ArmLowR_gfe |
| | FemurKneeLToJacket_cnt | Jacket_gfe | FemurKneeL_gfe |
| | FemurKneeRToJacket_cnt | Jacket_gfe | FemurKneeR_gfe |
| | FemurKneeLToFemurKneeR_cnt | FemurKneeR_gfe | FemurKneeL_gfe |
| | TibiaLToTibiaR_cnt | TibiaR_gfe | TibiaL_gfe |

## 3.2 User instructions

### Timestep

Table 3.2: Recommended timestep for the Hybrid III 5$^{th}$ percentile dummy models.

| Model | timestep (s) |
|---|---|
| Ellipsoid | $\leq 1 \cdot 10^{-5}$ |
| Facet | $\leq 1 \cdot 10^{-5}$ |

### Dummy positioning

The ellipsoid and facet Hybrid III 5$^{th}$ percentile Q models can be positioned in the same way as the Hybrid III 50$^{th}$ percentile Q models (see Chapter 2).

Table 3.3: Positioning joints of the Hybrid III 5$^{th}$ percentile dummy models.

| Joint Description | Identifier | Degree of freedom[a] | | | Comment |
|---|---|---|---|---|---|
| Complete dummy | Dummy_jnt | D1 forward<br>R1 roll right | D2 leftward<br>R2 pitch down | D3 upward<br>R3 yaw left | |
| Neck bracket | NeckBracket_jnt | R1 pitch down | | | [b] |
| Neck element | NeckPivot4_jnt | R1 roll right | R2 pitch up | | [c] |
| | NeckCylinder2_jnt | D1 upward | R1 yaw left | | [c] |
| | NeckPivot3_jnt | R1 pitch up | R2 roll right | | [c] |
| | NeckPivot2_jnt | R1 roll right | R2 pitch up | | [c] |
| | NeckCylinder1_jnt | D1 upward | R1 yaw left | | [c] |
| | NeckPivot1_jnt | R1 pitch up | R2 roll right | | [c] |
| Left shoulder | ShoulderYokeL_jnt<br>ShoulderL_jnt | R1 pitch down<br>R1 roll right | | | |
| Right shoulder | ShoulderYokeR_jnt<br>ShoulderR_jnt | R1 pitch down<br>R1 roll right | | | |
| Left elbow | ElbowPivotL_jnt<br>ElbowL_jnt | R1 yaw left<br>R1 pitch down | | | |
| Right elbow | ElbowPivotR_jnt<br>ElbowR_jnt | R1 yaw left<br>R1 pitch down | | | |
| Left wrist | WristPivotL_jnt<br>WristL_jnt | R1 yaw left<br>R1 roll right | | | |
| Right wrist | WristPivotR_jnt<br>WristR_jnt | R1 yaw left<br>R1 roll right | | | |
| Lumbar spine | LumbarFlangeUp_jnt | R1 roll left | R2 pitch down | | [d] |
| | LumbarMouldPart6_jnt | R1 yaw left<br>D1 upward | | | [d] |
| | LumbarMouldPart5_jnt | R1 pitch down | R2 roll left | | [d] |
| | LumbarMouldPart3_jnt | R1 roll left | R2 pitch down | | [d] |
| | LumbarMouldPart2_jnt | R1 yaw left<br>D1 upward | | | [d] |

*Continued on the next page*

*Table 3.3 cont.*

| Joint Description | Identifier | Degree of freedom[a] | | | | | | Comment |
|---|---|---|---|---|---|---|---|---|
| | LumbarMouldPart1_jnt | R1 | pitch down | R2 | roll left | | | [d] |
| Left hip | HipL_jnt | R1 | roll right | R2 | pitch down | R3 | yaw left | |
| Right hip | HipR_jnt | R1 | roll right | R2 | pitch down | R3 | yaw left | |
| Left knee | KneeL_jnt | R1 | pitch down | | | | | |
| Right knee | KneeR_jnt | R1 | pitch down | | | | | |
| Left ankle | AnkleL_jnt | R1 | yaw left | R2 | roll right | R3 | pitch down | |
| Right ankle | AnkleR_jnt | R1 | yaw left | R2 | roll right | R3 | pitch down | |

[a] Positive translation or rotation given in global co-ordinate system while dummy is in reference position (see Figure 1.2).
[b] Angle for the neck bracket is directly to derive from the physical dummy. A lower neck load cell in the physical dummy means a zero angle for the neck bracket.
[c] only for equilibrium state.
[d] In principle only for equilibrium state, however it might be necessary to rotate lumbar joints to position upper torso with neck and head correctly.

## Dummy contacts

Table 3.4: Available groups to define contact between the Hybrid III 5$^{th}$ percentile Q components and environment.

| Contact Description | Identifier[a][b] | Ellipsoid model[b] | Facet model[b] |
|---|---|---|---|
| Full Dummy | Dummy_ctg | all exterior ellipsoids | |
| Head | Head_ctg | Head_ell<br>Face_ell<br>Cheek_ell | Elements and nodes |
| Neck | Neck_ctg | NeckPlateLow_ell<br>NeckPlateUp_ell<br>NeckPart⟨*i*⟩_ell<br>for i=1 to 3 | Elements and nodes |
| Left Upper Arm | ArmUpL_ctg | ArmUpL_ell | Elements and nodes |
| Right Upper Arm | ArmUpR_ctg | ArmUpR_ell | Elements and nodes |
| Left Lower Arm and Hand | ArmLowL_ctg | ArmLowElbowL_ell<br>ArmLowL_ell<br>HandL_ell | Elements and nodes |
| Right Lower Arm and Hand | ArmLowR_ctg | ArmLowElbowR_ell<br>ArmLowR_ell<br>HandR_ell | Elements and nodes |
| Thorax | Thorax_*ctg* | Jacket⟨*i*⟩_ell<br>for i=01 to 50<br>Jacket⟨*i*⟩Low_ell<br>for i=04 to 08<br>Jacket⟨*j*⟩_ell<br>for j=97 to 99<br>ClavicleL/R_ell<br>ClavicleLinkL/R_ell<br>ShoulderYokeL/R_ell | Elements and nodes |

*Continued on the next page*

3

*Table 3.4 cont.*

| Contact Description | Identifier$^{(a)(b)}$ | Ellipsoid model$^{(b)}$ | Facet model$^{(b)}$ |
|---|---|---|---|
| Jacket | Jacket_ctg | Jacket⟨i⟩_ell<br>for i=01 to 50<br>Jacket⟨i⟩Low_ell<br>for i=04 to 08<br>Jacket⟨j⟩_ell<br>for j=97 to 99 | Elements and nodes |
| Clavicles | Clavicles_ctg | ClavicleL/R_ell<br>ClavicleLinkL/R_ell<br>ShoulderYokeL/R_ell | Elements and nodes |
| Lumbar Spine | LumbarBack_ctg | LumbarSpineLow_ell<br>LumbarSpineUp_ell<br>LumbarMouldPart⟨i⟩_ell<br>for i=1 to 3<br>LumbarMouldPart⟨j⟩_ell<br>for j=5 to 6 | |
| Abdomen | Abdomen_ctg | AbdomenL/R_ell<br>AbdomenLow_ell<br>AbdomenMid_ell | Elements and nodes |
| Pelvis | Pelvis_ctg | PelvisFemurL/R_ell<br>Pelvis_ell<br>Pelvisbone_ell<br>PelvisBottomL/R_ell<br>PelvisUpL/R_ell<br>pelvis_LCL/R_ell<br>pelvisIliacL/R_ell | Elements and nodes |
| Iliac Wings | IliacWings_ctg | | Elements and nodes |
| Left Femur and Knee | FemurKneeL_ctg | FemurFleshL_ell<br>KneeFleshL_ell | Elements and nodes |
| Left Femur | FemurL_ctg | FemurFleshL_ell | |
| Left Knee | KneeL_ctg | KneeFleshL_ell | |
| Right Femur and Knee | FemurKneeR_ctg | FemurFleshR_ell<br>KneeFleshR_ell | Elements and nodes |
| Right Femur | FemurR_ctg | FemurFleshR_ell | |
| Right Knee | KneeR_ctg | KneeFleshR_ell | |
| Left Tibia | TibiaL_ctg | TibiaFleshUp⟨i⟩L_ell,<br>for i=1 to 2<br>TibiaFleshMid⟨j⟩L_ell,<br>for j=1 to 2<br>TibiaFleshLowL_ell | Elements and nodes |
| Right Tibia | TibiaR_ctg | TibiaFleshUp⟨i⟩R_ell,<br>for i=1 to 2<br>TibiaFleshMid⟨j⟩R_ell,<br>for j=1 to 2<br>TibiaFleshLowR_ell | Elements and nodes |
| Left Foot | FootL_ctg $^{(c)}$ | FootL_ell<br>ToesL_ell<br>HeelL_ell | Elements and nodes |
| Left heel | HeelL_ctg $^{(c)}$ | HeelL_ell | |
| Left toes | ToesL_ctg $^{(c)}$ | ToesL_ell | |

*Continued on the next page*

*Table 3.4 cont.*

| Contact Description | Identifier[a][b] | Ellipsoid model[b] | Facet model[b] |
|---|---|---|---|
| Right Foot | FootR_ctg [c] | FootR_ell<br>ToesR_ell<br>HeelR_ell | Elements and nodes |
| Right heel | HeelR_ctg [c] | HeelR_ell | |
| Right toes | ToesR_ctg [c] | ToesR_ell | |
| Left Shoe | ShoeL_ctg [c] | ShoeSoleL_ell<br>ShoeHeelL_ell<br>ShoeFrontL_ell | Elements and nodes |
| Right Shoe | ShoeR_ctg [c] | ShoeSoleR_ell<br>ShoeHeelR_ell<br>ShoeFrontR_ell | Elements and nodes |

[a] *ctg*= contact group, for the ellipsoid models ctg is replaced by gmb(group_multibody) and for the facet model ctg is replaced by gfe (group_finite element).

[b] L = Left; R = Right

[c] If the dummy wear shoes only the shoe contact groups should be selected and not those of the feet.

FE belts can be created and (re)positioned with the belt fitting tool of XMADgic (version 5.0 and higher).

The recommended contacts between dummy and belts are pre-defined in the user file under the SYSTEM.MODEL Belt_to_Dummy_contacts. From model version 2.0 of the ellipsoid model the lateral orthotropic friction values recommended for the contact between lap belt and the pelvis and abdomen are different to the standard modelling recommendations: 0.65 instead of 0.5. This is based on experimental validation of the interaction.

The references in FE_MODEL of ShoulderBelt_gfe and LapBelt_gfe need to be changed to the proper FE-models to make the contacts work. By default the user file will give two warnings due to the fact that the referred FE-model for the belts is empty.

### Output

From MADYMO V7.3 on ISO-MME output can be generated for the Hybrid III 5$^{th}$ percentile Q dummy models. Output requests for signals in ISO-MME format are pre-defined in the CONTROL_OUTPUT element in the user file.

The output signals for the Hybrid III 5$^{th}$ percentile Q models are almost the same as for the Hybrid III 50$^{th}$ percentile Q models. See Table 3.5 for a complete overview of those output signals.

Table 3.5: Hybrid III 5$^{th}$ percentile output signals.

| Sensor | Identifier | Signal | | | | | | | Filter |
|---|---|---|---|---|---|---|---|---|---|
| | | resultant | x | direction[a] | y | direction[a] | z | direction[a] | |
| Head CG accelerometer[b] | HeadCG_acc | ar | a1 | forward | a2 | lateral | a3 | vertical | CFC1000 |

*Continued on the next page*

*Table 3.5 cont.*

| Sensor | Identifier | Signal | | | | | | | Filter |
|---|---|---|---|---|---|---|---|---|---|
| | | resultant | x | direction[a] | y | direction[a] | z | direction[a] | |
| Neck | | | | | | | | | |
| Upper load cell | NeckUp_lce_F_CFC1000 | fr | f1 | shear | f2 | shear | f3 | axial | CFC1000 |
| | NeckUp_lce_F_CFC600 | fr | f1 | shear | f2 | shear | f3 | axial | CFC600 |
| | NeckUp_lce_T | tr | t1 | roll | t2 | pitch | t3 | yaw | CFC600 |
| Lower load cell | NeckLow_lce_F | fr | f1 | shear | f2 | shear | f3 | axial | CFC1000 |
| | NeckLow_lce_T | tr | t1 | roll | t2 | pitch | t3 | yaw | CFC600 |
| Thorax | | | | | | | | | |
| accelerometer[b] | Thorax_acc | ar | a1 | forward | a2 | lateral | a3 | vertical | CFC180 |
| Chest deflection | ChestDeflection_dis | dr | d1 | displacement | | | | | CFC600 |
| | ChestDefl_dis_CFC180 | dr | d1 | displacement | | | | | CFC180 |
| | ChestDeflection_vel_CFC600 | vr | v1 | velocity | | | | | CFC600 |
| | ChestDeflection_vel_CFC180 | vr | v1 | velocity | | | | | CFC180 |
| Sternum | SternumUp_acc | ar | a1 | forward | a2 | lateral | a3 | vertical | CFC1000 |
| accelerometer[b] | SternumLow_acc | ar | a1 | forward | a2 | lateral | a3 | vertical | CFC1000 |
| | SternumMid_acc | ar | a1 | forward | a2 | lateral | a3 | vertical | CFC1000 |
| Lumbar Spine | | | | | | | | | |
| Thoracic load cell | Thoracic_lce_F | fr | f1 | shear | f2 | shear | f3 | axial | CFC1000 |
| | Thoracic_lce_T | tr | t1 | roll | t2 | pitch | t3 | yaw | CFC1000 |
| Lumbar load cell | Lumbar_lce_F | fr | f1 | shear | f2 | shear | f3 | axial | CFC1000 |
| | Lumbar_lce_T | tr | t1 | roll | t2 | pitch | t3 | yaw | CFC1000 |
| Pelvis | | | | | | | | | |
| Accelerometer[b] | Pelvis_acc | ar | a1 | forward | a2 | lateral | a3 | vertical | CFC1000 |
| Left iliac wing load cell | IliacL_lce_F | | f1 | forward | | | | | CFC600 |
| | IliacL_lce_T | | | | t2 | pitch | | | CFC600 |
| Right iliac wing load cell | IliacR_lce_F | | f1 | forward | | | | | CFC600 |
| | IliacR_lce_T | | | | t2 | pitch | | | CFC600 |
| Femur | | | | | | | | | |
| Left load cell | FemurL_lce_F | fr | f1 | shear | f2 | shear | f3 | axial | CFC600 |
| | FemurL_lce_T | tr | t1 | roll | t2 | pitch | t3 | yaw | CFC600 |
| Right load cell | FemurR_lce_F | fr | f1 | shear | f2 | shear | f3 | axial | CFC600 |
| | FemurR_lce_T | tr | t1 | roll | t2 | pitch | t3 | yaw | CFC600 |
| Knee | | | | | | | | | |
| Left Slider | KneeL_dis | dr | d1 | displ | | | | | CFC180 |
| Right Slider | KneeR_dis | dr | d1 | displ | | | | | CFC180 |
| Tibia | | | | | | | | | |
| Left Upper load cell | TibiaUpL_lce_F | fr | f1 | shear | f2 | shear | f3 | axial | CFC600 |
| | TibiaUpL_lce_T | tr | t1 | roll | t2 | pitch | t3 | yaw | CFC600 |
| Right Upper load cell | TibiaUpR_lce_F | fr | f1 | shear | f2 | shear | f3 | axial | CFC600 |
| | TibiaUpR_lce_T | tr | t1 | roll | t2 | pitch | t3 | yaw | CFC600 |
| Left Lower load cell | TibiaLowL_lce_F | fr | f1 | shear | f2 | shear | f3 | axial | CFC600 |
| | TibiaLowL_lce_T | tr | t1 | roll | t2 | pitch | t3 | yaw | CFC600 |
| Right Lower load cell | TibiaLowR_lce_F | fr | f1 | shear | f2 | shear | f3 | axial | CFC600 |
| | TibiaLowR_lce_T | tr | t1 | roll | t2 | pitch | t3 | yaw | CFC600 |

[a] Positive direction given according to SAE J211/1.

[b] The calculated acceleration is corrected in the x-, y- and z-directions for a prescribed fictitious acceleration field to get correct values (see Theory manual).

### Injury

The injury criteria selected for the Hybrid III 5$^{th}$ percentile component models are almost the same as for the Hybrid III 50$^{th}$ percentile Q models. See Table 3.6 for a complete overview of those criteria.

Table 3.6: Injury criteria defined for the Hybrid III 5$^{th}$ percentile .

| Injury criteria | Identifier | Filter |
|---|---|---|
| Head | | |
| HIC (15) | HIC15_inj | |
| HIC (36) | HIC36_inj | |
| 3ms (cumulative) | H3MS_inj | |
| max Res Acc | HaccRpeak_inj | |
| Neck | | |
| MOC | | |
| lateral | MOCx_inj | CFC600 (force and moment) |
| frontal | MOCy_inj | CFC600 (force and moment) |
| FNIC | | |
| tension | FNICtension_inj | CFC1000 |
| shear | FNICshear_inj | CFC1000 |
| bending | FNICbending_inj | CFC1000/CFC600 (force/moment) |
| NIJ | | |
| tension-extension | NTE_inj | CFC600 (force and moment) |
| tension-flexion | NTF_inj | CFC600 (force and moment) |
| compression-extension | NCE_inj | CFC600 (force and moment) |
| compression-flexion | NCF_inj | CFC600 (force and moment) |
| tension-extension | NTE_OOP_inj | CFC600 (force and moment) |
| tension-flexion | NTF_OOP_inj | CFC600 (force and moment) |
| compression-extension | NCE_OOP_inj | CFC600 (force and moment) |
| compression-flexion | NCF_OOP_inj | CFC600 (force and moment) |
| Thorax | | |
| 3ms (cumulative) | T3MS_inj | |
| 3ms (contiguous) | TCon3MS_inj | |
| Chest Compression | ThCC_inj | CFC180 |
| CTI | CTI_inj | |
| VC | VC_inj_CFC180 | CFC180 (deflection) |
| | VC_inj_CFC600 | CFC600 (deflection) |
| Femurs | | |
| FFC | | |
| Left | FFCL_inj | CFC600 |
| Right | FFCR_inj | CFC600 |
| max Left Compression | FemurLcompZpeak_inj | |
| max Right Compression | FemurLcompZpeak_inj | |
| Knees | | |
| Left Compression | kneesliderL_inj | CFC180 |
| Right Compression | kneesliderR_inj | CFC180 |
| Tibia | | |
| TI | | |
| Upper Left | TIUpL_inj | CFC600 |
| Upper Right | TIUpR_inj | CFC600 |
| Lower Left | TILowL_inj | CFC600 |
| Lower Right | TILowR_inj | CFC600 |

*Continued on the next page*

*Table 3.6 cont.*

| Injury criteria | Identifier | Filter |
|---|---|---|
| TCFC | | |
| Upper Left | TCFCUpL_inj | CFC600 |
| Upper Right | TCFCUpR_inj | CFC600 |
| Lower Left | TCFCLowL_inj | CFC600 |
| Lower Right | TCFCLowR_inj | CFC600 |

# 4 Hybrid III 95th percentile Q Dummy



The Hybrid III $95^{th}$ percentile male dummy stands for the largest size in the adult population and has been derived from scaled data from the Hybrid III $50^{th}$ percentile dummy. The dummy has recently been included in FMVSS 208.

As a follow-up to the available standard Hybrid III 95th percentile dummy models, the quality (Q) ellipsoid and the quality (Q) facet Hybrid III 95th percentile dummy models have been developed. This is because of the increasing market need for a more CPU-efficient and user-friendly dummy model with a high quality. The quality of the models is determined by an objective rating method. For more information on this subject, the reader is referred to the quality reports supplied with these models.

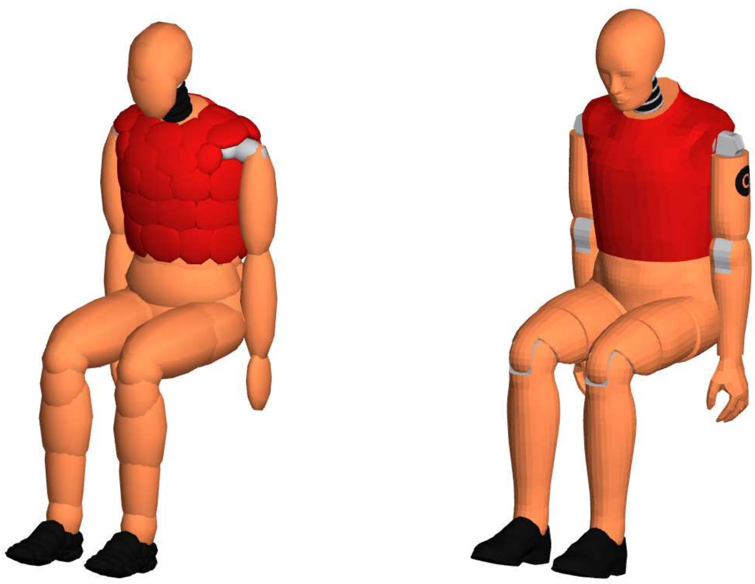

Figure 4.1: Hybrid III $95^{th}$ percentile Q dummy model; ellipsoid model (left) and facet model (right).

## 4.1 Model description



The ellipsoid Q model of the Hybrid III 95th percentile dummy is derived from scaling the Hybrid III 50th percentile ellipsoid Q model version 1.0. The facet Q model of the Hybrid III 95th percentile dummy is derived from scaling the Hybrid III 50th percentile facet Q model version 4.0.

Quality ellipsoid and facet models of the Hybrid III 95$^{th}$ percentile dummy are available. The input is given in the files:

| | |
|---|---|
| Ellipsoid model: | d_hyb395el_Q_usr.xml<br>d_hyb395el_Q_inc.xml |
| Facet model: | d_hyb395fc_Q_usr.xml<br>d_hyb395fc_Q_inc.xml |

To run these models, the following licenses are required:

| | |
|---|---|
| Ellipsoid Q model: | MADYMO/Solver (Multibody)<br>MADYMO/Dummy Models/Frontal |
| Facet Q model: | MADYMO/Solver (Multibody)<br>MADYMO/Dummy Models/Frontal/HIII 95th Fc Q |

Figure 4.1 shows the models in the reference position. Both models consist of 211 bodies including 50 bodies for the jacket and 6 bodies for the left and the right shoe.

**ELLIPSOID AND FACET Q MODELS**

The ellipsoid Q model has the same multibody structure as the facet Q model. The facet Q model has been developed on basis of scaling the Hybrid III 50$^{th}$ percentile facet Q model and checked against CAD scanning data while the ellipsoid model represents the very good approximation of the facet Q model using ellipsoid surfaces. This paragraph gives a summarised description of the design of both models.

**Head and neck**

The head has been modelled with a rigid body having two associated ellipsoid surfaces, representing the skull and the face, for the ellipsoid model. The facet model uses one closed surface. It is connected by a bracket joint to the upper neck load cell.

The neck is composed of four parts: the upper neck load cell, the neck nodding plate, the neck column with cable and the neck bracket. The upper and lower neck load cells are modelled with bracket joints. The nodding joint is a revolute joint combined with a restraint. The neck bracket is modelled with a revolute joint which is locked during the simulation. When the neck bracket joint has not the default value of zero, the lower neck load cell results will not be the same as in the hardware dummy.

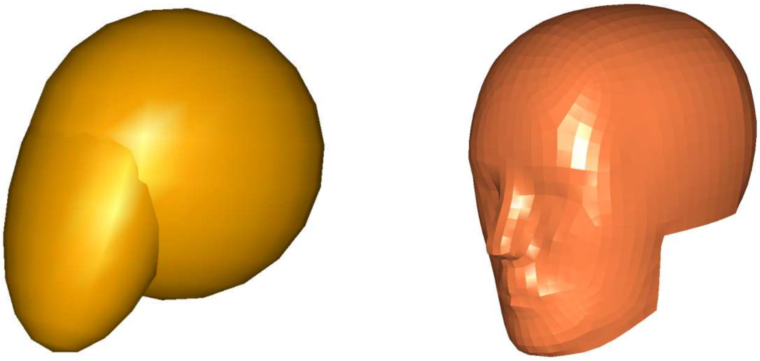

Figure 4.2: Hybrid III 95$^{th}$ percentile ellipsoid Q (left) and facet Q (right) head models.

The neck column with cable is represented by 6 joints of which four are universal and two are cylindrical joints. Two triple joint restraints are used for the lower and the upper part of the neck. Universal joints are located in the centres of the 4 rubber disks (see Figure 4.3).

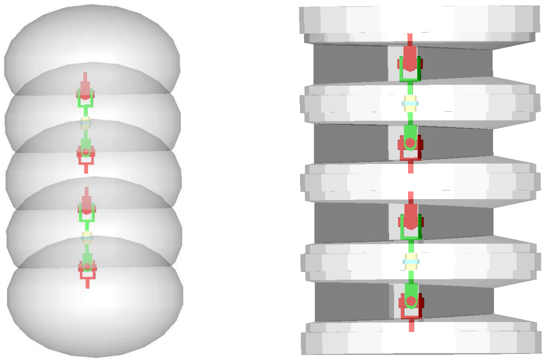

Figure 4.3: Hybrid III 95$^{th}$ percentile ellipsoid Q (left) and facet Q (right) neck models.

**Thorax**

The thorax consists in general of the following parts: the spinebox, the ribcage, the clavicles and the jacket. The thorax is modelled with multiple chains of bodies and joints.

The spinebox has been modelled by means of three bodies, representing the thoracic spine and the lower and upper part of the thoracic load cell, connected with bracket joints. The bracket joint between the thoracic load cell parts represents the load cell itself.

The ribcage has been modelled with 12 chains of bodies and joints forming the six ribs (see Figure 4.4). Another chain models the potentiometer and ends with the sternum body. It uses two revolute joints, representing the potentiometer, a spherical joint and a translational joint modeling the connection from the potentiometer to the sternum. The front of the ribs are connected to the front rib end bodies with universal joints, forming closed loops. The front rib end bodies are connected with point restraints to the sternum. All kinematic joints have joint restraints which give the ribcage its stiffness.

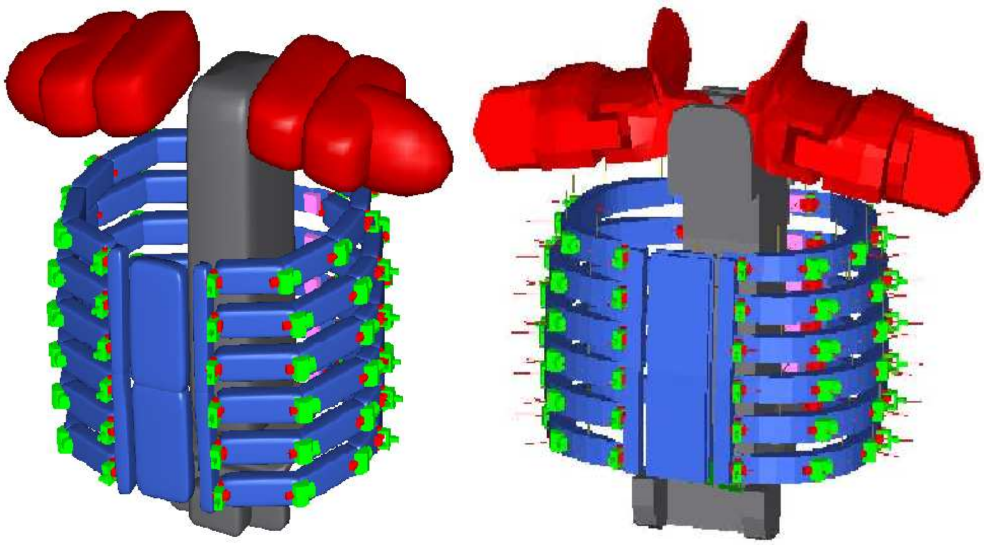

Figure 4.4: Hybrid III 95$^{th}$ percentile ellipsoid Q (left) and facet Q (right) ribcage model.

The clavicles are modelled with eight bodies and eight joints, where two are bracket joints to represent the load cells of the left and right clavicle. Revolute joints are connecting the shoulder yokes to the clavicles and the clavicles to the clavicle load cells. revolute joints also connecting the clavicle links to the thoracic spine.

The jacket is modelled separately with 50 bodies and free joints. The bodies are connected to each other with a lot of point and cardan restraints (see Figure 4.5). The body at the lower back side of the jacket is connected to the thoracic spine by means of a free joint.

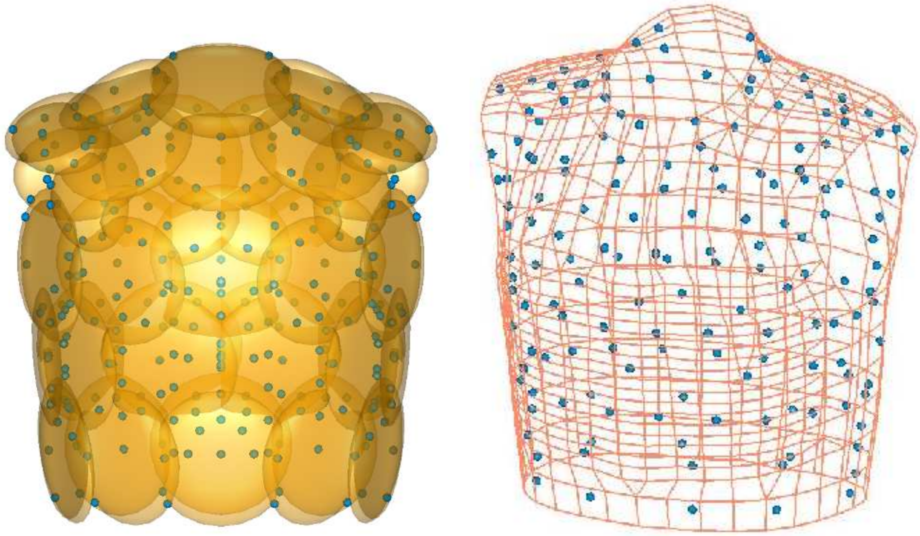

Figure 4.5: Hybrid III 95$^{th}$ percentile ellipsoid Q (left) and facet Q (right) jacket model.

Interaction between jacket and ribcage is modelled by means of point restraints (see Figure 4.6).

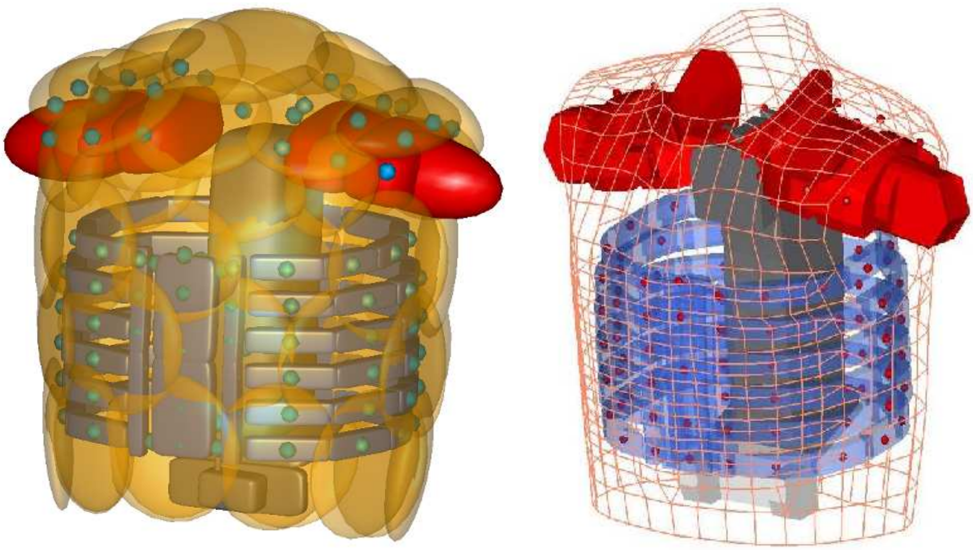

Figure 4.6: Hybrid III 95$^{th}$ percentile ellipsoid Q (left) and facet Q (right) jacket ribcage interaction model.

### Lumbar spine

The lumbar spine assembly consists of the lumbar spine mould with the lumbar load cell. The influence of the lumbar spine cables is lumped in the multibody chain of the lumbar spine mould. The lumbar spine mould is represented with seven bodies. Two bodies and a bracket joint are used for the load cell.

The chain of joints of the lumbar spine mould consists of four universal and three cylindrical joints. Two sets of universal - cylindrical - universal joint sequences make use of a triple joint restraint and the cylindrical joint in the middle has a normal joint restraint (see Figure 4.7). The lumbar spine mould is coupled to the load cell by means of a bracket joint.

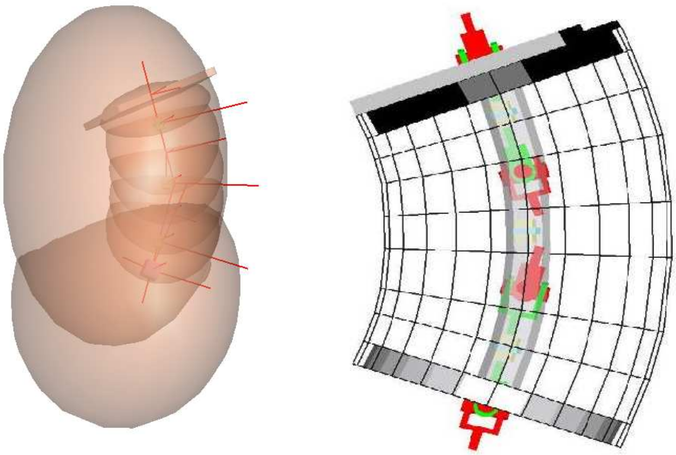

Figure 4.7: Hybrid III 95$^{th}$ percentile ellipsoid Q (left) and facet Q (right) lumbar spine model.

In the complete physical dummy, lumbar spine deformation is not only resisted by the lumbar spine itself but also by contact interactions with ribcage, abdomen and pelvis. These interactions are included in the model in the form of point restraints. These point restraints are referred to as "Abdomen vertical compression left/middle/right".

The ellipsoid model has two large ellipsoids attached to the lower and upper part of the lumbar spine representing the lower and upper lumbar spine region at the back of the dummy model.

### Abdomen and pelvis

The abdomen has been modelled as a separate body, which is connected to the pelvis by means of a bracket joint.

For the ellipsoid model the abdomen body is associated with two ellipsoid surfaces, for the lower and upper part, while the facet model is associated with facet surfaces. The ellipsoid pelvis is made of 6 ellipsoids of which two are used to model the pelvis buttock. The iliac wings are modelled separately with 4 ellipsoids (see Figure 4.8).

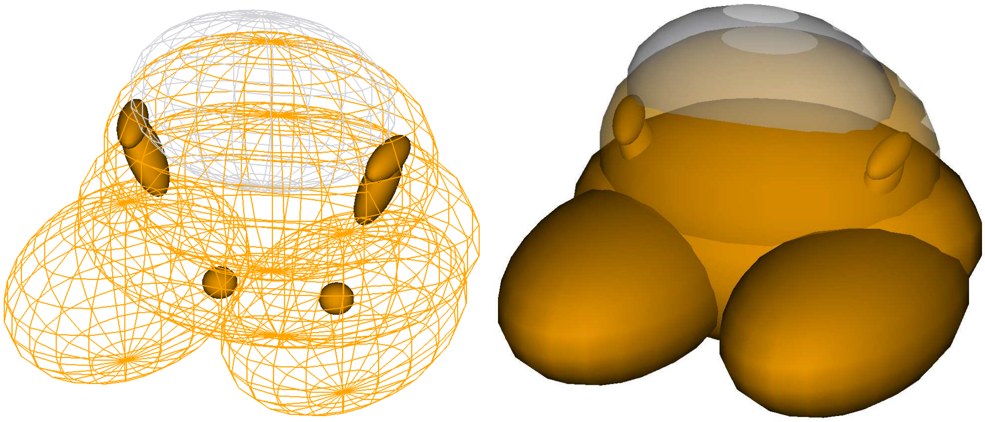

Figure 4.8: Pelvis ellipsoid surface parts.

The facet model has surfaces representing the metal skeleton. The pelvis outer facet surface model is divided into parts which have seven different contact characteristics and variable thicknesses (see Figure 4.9). This is because the proportion of PVC-skin and foam material inside the hardware pelvis is different. The outer and inner PVC skin is always about 5mm thick and in the PVC skin the foam filling thickness varies from 1cm up to about 10 cm. Therefore characteristic contact 1 is for material thickness up to 6cm, 2 for thickness from 6cm to 11cm, 3 and 4 for hole edges, 5 for the back hole, 6 for pelvis-abdomen area and 7 for top iliac wings area. Since the abdomen is behind the pelvis skin only the pelvis has been calibrated. This means that the abdomen stiffness is included in the pelvis skin characteristics.

Figure 4.9: Pelvis facet surface parts.

The pelvis has been modelled with three bodies and three joints, one free dummy joint and two spherical joints for the hips and are part of the pelvis assembly. Sixdof restraints modelled between the pelvis and the hips models the stiffness of the spherical hip joint and the compression of the femur and pelvis flesh around the femurs. The friction in the hip joints is represented in joint restraints which are located in the user file and can be modified by the user.

**Arms**

The arm consists of the upper arm and the lower arm with the hand.

Figure 4.10 shows the model of the arm for both the ellipsoid Q and facet Q models.

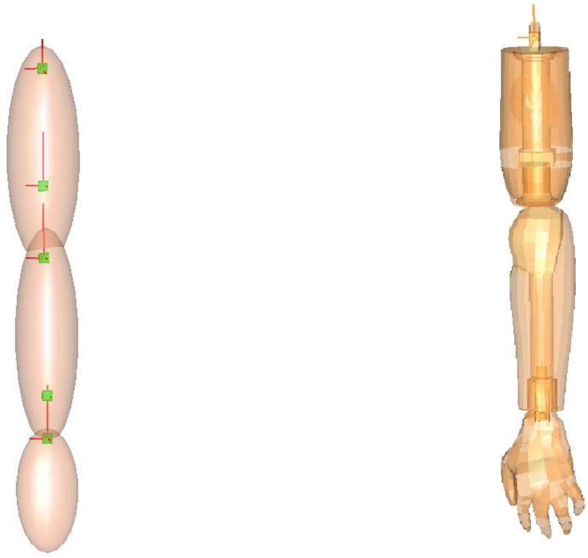

Figure 4.10: Hybrid III $95^{th}$ percentile ellipsoid Q (left) and facet Q (right) arm model.

The upper arm has been modelled by means of two bodies one for the upper arm and one for the elbow and two revolute joints, one connecting the upper arm to the shoulder and the other one connecting the elbow to the upper arm.

The lower arm has been modelled by means of three bodies for the lower arm, the wrist and the hand and three revolute joints connecting the lower arm to the elbow part of the upper arm, the wrist part to the lower arm and the hand to the wrist part of the lower arm.

**Legs**

The femurs have been modelled with five bodies and joints. Four of them are bracket joints, and one is a revolute joint used for the knee. The femur load cells are modelled, using bracket joints, as well as the part of the femurs. The femurs are coupled to the pelvis assembly by means of the bracket joints.

The tibias are modelled with three bodies: one for the upper part, one for the mid part and one for the lower part. Bracket joints are defined for the lower tibia and the upper tibia load cell and connects the lower, mid and upper part of the tibia bodies. A translational joint is used to model the knee slider and connects the tibia to the knee.

Figure 4.11 shows the model of the leg for both the ellipsoid Q and facet Q models.

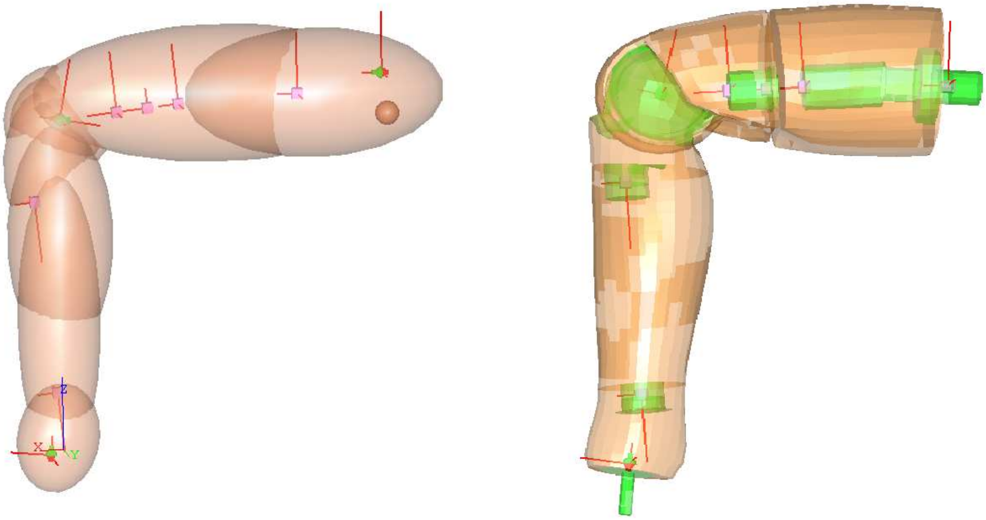

Figure 4.11: Hybrid III 95$^{th}$ percentile ellipsoid Q (left) and facet Q (right) leg model.

### Feet and ankles

The foot has been modelled by means of three bodies one for the foot and two for the toes connected with two revolute joints. A spherical joint connects the foot to the tibia to represent the ankle (see Figure 4.12).

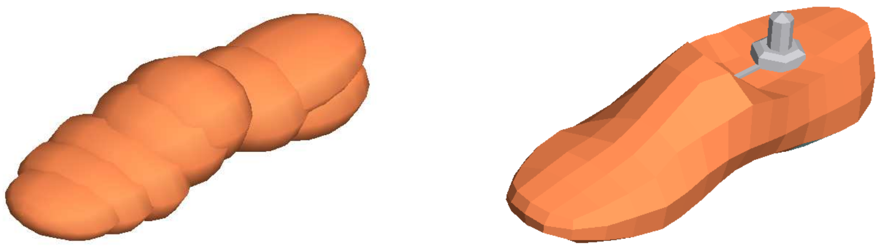

Figure 4.12: Hybrid III 95$^{th}$ percentile ellipsoid Q (left) and facet Q (right) foot model.

### Shoes

The shoes of both models are the same as for the 50$^{th}$ percentile Q models size 11XW that meet military specification MIL-S-13192P.

The shoes have been modelled as separate components. Each shoe consists of three bodies, two revolute joints and one free joint. The free joint links the shoe to the foot. This joint is restrainted and allows translation and rotation of the foot inside the shoe. The toes are made deformable by means of the revolute joints. (see Figure 4.13).

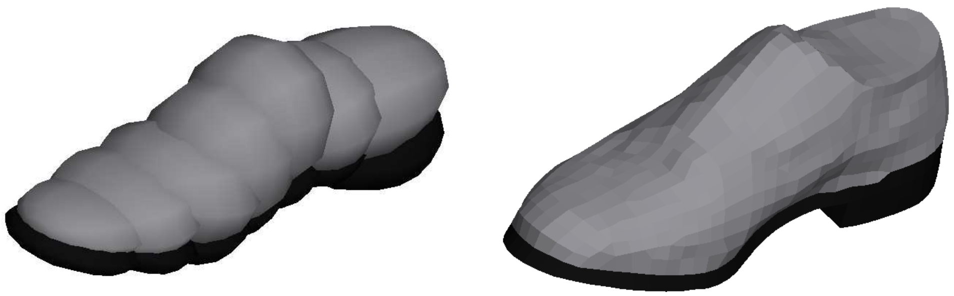

Figure 4.13: Hybrid III 95$^{th}$ percentile ellipsoid Q (left) and facet Q (right) shoe model.

## CONTACTS BETWEEN DUMMY COMPONENTS

The contacts between dummy components defined can be found in Table 4.1 for both models.

Table 4.1: Intercomponent contacts for the Hybrid III 95$^{th}$ percentile Q models.

| **Model type** | **Contact surface** master | slave |
|---|---|---|
| ellipsoid | Jacket_gmb | Head_gmb |
| | Jacket_gmb | FemurKneeL_gmb |
| | Jacket_gmb | FemurKneeR_gmb |
| | FemurKneeR_gmb | FemurKneeL_gmb |
| | Head_gmb | ArmUpL_gmb |
| | Head_gmb | ArmUpR_gmb |
| | ArmLowR_gmb | ArmLowL_gmb |
| | Head_gmb | ArmLowL_gmb |
| | Head_gmb | ArmLowR_gmb |
| | FemurKneeL_gmb | ArmLowL_gmb |
| | FemurKneeR_gmb | ArmLowR_gmb |
| | TibiaL_gmb | ArmLowL_gmb |
| | TibiaR_gmb | ArmLowR_gmb |
| | TibiaR_gmb | TibiaL_gmb |
| | ShoeR_gmb | ShoeL_gmb |
| facet | Jacket_gfe | Head_gfe |
| | Jacket_gfe | FemurKneeL_gfe |
| | Jacket_gfe | FemurKneeR_gfe |
| | FemurKneeR_gfe | FemurKneeL_gfe |
| | Head_gfe | ArmUpL_gfe |
| | Head_gfe | ArmUpR_gfe |
| | ArmLowR_gfe | ArmLowL_gfe |

*Continued on the next page*

*Table 4.1 cont.*

| **Model type** | **Contact surface** | |
|---|---|---|
| | **master** | **slave** |
| | Head_gfe | ArmLowL_gfe |
| | Head_gfe | ArmLowR_gfe |
| | FemurKneeL_gfe | ArmLowL_gfe |
| | FemurKneeR_gfe | ArmLowR_gfe |
| | TibiaL_gfe | ArmLowL_gfe |
| | TibiaR_gfe | ArmLowR_gfe |
| | TibiaR_gfe | TibiaL_gfe |
| | ShoeR_gfe | ShoeL_gfe |

4

## 4.2 User instructions

### Timestep

Table 4.2: Recommended timestep for the Hybrid III 95th percentile dummy models.

| Model | timestep (s) |
|---|---|
| Ellipsoid | $\leq 1 \cdot 10^{-5}$ |
| Facet | $\leq 1 \cdot 10^{-5}$ |

### Dummy positioning

Table 4.3: Positioning joints of the Hybrid III 95th percentile ellipsoid Q and facet Q dummy models

| Joint Description | Identifier | Degree of freedom[(a)] | | | | | | Comment |
|---|---|---|---|---|---|---|---|---|
| Complete dummy | Dummy_jnt | D1<br>R1 | forward<br>roll right | D2<br>R2 | leftward<br>pitch down | D3<br>R3 | upward<br>yaw left | |
| Neck bracket | NeckBracket_jnt | R1 | pitch down | | | | | (b) |
| Neck element | NeckPivot1_jnt | R1 | pitch up | R2 | roll right | | | (c) |
| | NeckCylinder1_jnt | R1<br>D1 | yaw left<br>upward | | | | | (c) |
| | NeckPivot2_jnt | R1 | roll right | R2 | pitch up | | | (c) |
| | NeckPivot3_jnt | R1 | pitch up | R2 | roll right | | | (c) |
| | NeckCylinder2_jnt | R1<br>D1 | yaw left<br>upward | | | | | (c) |
| | NeckPivot4_jnt | R1 | roll right | R2 | pitch up | | | (c) |
| Left shoulder | ShoulderYokeL_jnt | R1 | pitch down | | | | | |
| | ShoulderL_jnt | R1 | roll right | | | | | |
| Right shoulder | ShoulderYokeR_jnt | R1 | pitch down | | | | | |
| | ShoulderR_jnt | R1 | rol right | | | | | |
| Left elbow | ElbowPivotL_jnt | R1 | yaw left | | | | | |
| | ElbowL_jnt | R1 | pitch down | | | | | |
| Right elbow | ElbowPivotR_jnt | R1 | yaw left | | | | | |
| | ElbowR_jnt | R1 | pitch down | | | | | |
| Left wrist | WristPivotL_jnt | R1 | yaw left | | | | | |
| | WristL_jnt | R1 | roll right | | | | | |
| Right wrist | WristPivotR_jnt | R1 | yaw left | | | | | |
| | WristR_jnt | R1 | roll right | | | | | |
| Lumbar Spine | LumbarSpineUp_jnt | R1 | roll left | R2 | pitch down | | | (d) |
| | LumbarMouldPart6_jnt | R1<br>D1 | yaw left<br>upward | | | | | (d) |
| | LumbarMouldPart5_jnt | R1 | pitch down | R2 | roll left | | | (d) |
| | LumbarMouldPart4_jnt | R1<br>D1 | yaw left<br>upward | | | | | (d) |
| | LumbarMouldPart3_jnt | R1 | roll left | R2 | pitch down | | | (d) |
| | LumbarMouldPart2_jnt | R1<br>D1 | yaw left<br>upward | | | | | (d) |

*Continued on the next page*

*Table 4.3 cont.*

| Joint Description | Identifier | Degree of freedom[a] | | | | | | Comment |
|---|---|---|---|---|---|---|---|---|
| | LumbarMouldPart1_jnt | R1 | pitch down | R2 | roll left | | | [d] |
| Left hip | HipL_jnt | R1 | roll right | R2 | pitch down | R3 | yaw left | |
| Right hip | HipR_jnt | R1 | roll right | R2 | pitch down | R3 | yaw left | |
| Left knee | KneeL_jnt | R1 | pitch down | | | | | |
| Right knee | KneeR_jnt | R1 | pitch down | | | | | |
| Left ankle | AnkleL_jnt | R1 | yaw left | R2 | roll right | R3 | pitch down | |
| Right ankle | AnkleR_jnt | R1 | yaw left | R2 | roll right | R3 | pitch down | |

[a] Positive translation or rotation given in global coordinate system while dummy is in reference position (see Figure 1.2).

[b] The neck bracket angle corresponds directly to that of the physical dummy. If the lower neck load cell is used in the physical dummy, this angle must be zero.

[c] Only for equilibrium state.

[d] In principle only for equilibrium state, however it might be necessary to rotate lumbar joints to position upper torso with neck and head correctly.

4

## Dummy contacts

Table 4.4: Available groups to define contact between the Hybrid III 95$^{th}$ percentile Q components and environment.

| Contact Description | Identifier$^{(a)(b)}$ | Ellipsoid model$^{(b)}$ | Facet model$^{(b)}$ |
|---|---|---|---|
| Head | Head_ctg | Head_ell<br>Face_ell | Elements and nodes |
| Neck | Neck_ctg | NeckPlateLow_ell<br>NeckPlateUp_ell<br>NeckPart$\langle i \rangle$_ell<br>for i=1 to 3 | Elements and nodes |
| Left Upper Arm | ArmUpL_ctg | ArmUpL_ell | Elements and nodes |
| Right Upper Arm | ArmUpR_ctg | ArmUpR_ell | Elements and nodes |
| Left Lower Arm and Hand | ArmLowL_ctg | ArmLowL_ell<br>HandL_ell | Elements and nodes |
| Right Lower Arm and Hand | ArmLowR_ctg | ArmLowR_ell<br>HandR_ell | Elements and nodes |
| Thorax | Thorax_*ctg* | Jacket$\langle i \rangle$_ell<br>for i=01 to 50<br>Jacket$\langle j \rangle$_ell<br>for j=97 to 99<br>ClavicleL/R_ell<br>ClavicleLinkL/R_ell<br>ShoulderYokeL/R_ell | |
| Jacket | Jacket_ctg | Jacket$\langle i \rangle$_ell<br>for i=01 to 50<br>Jacket$\langle j \rangle$_ell<br>for j=97 to 99 | Elements and nodes |
| Clavicles | Clavicles_ctg | ClavicleL/R_ell<br>ClavicleLinkL/R_ell<br>ShoulderYokeL/R_ell | Elements and nodes |
| Abdomen | Abdomen_ctg | AbdomenLow_ell<br>AbdomenMid_ell | Elements and nodes |
| Pelvis | Pelvis_ctg | Pelvis_ell<br>PelvisFront_ell<br>PelvisFemurL/R_ell<br>PelvisButtockL/R_ell<br>IliacWingL/R_ell<br>IliacWingUpL/R_ell | Elements and nodes |
| | IliacWings_ctg | | Elements and nodes |
| Left Femur and Knee | FemurKneeL_ctg | FemurFleshL_ell<br>KneeFleshL_ell | Elements and nodes |
| Left Femur | FemurL_ctg | FemurFleshL_ell | Elements and nodes |
| Left Knee | KneeL_ctg | KneeFleshL_ell | Elements and nodes |
| Right Femur and Knee | FemurKneeR_ctg | FemurFleshR_ell<br>KneeFleshR_ell | Elements and nodes |
| Right Femur | FemurR_ctg | FemurFleshR_ell | Elements and nodes |
| Right Knee | KneeR_ctg | KneeFleshR_ell | Elements and nodes |

*Continued on the next page*

*Table 4.4 cont.*

| Contact Description | Identifier$^{(a)(b)}$ | Ellipsoid model$^{(b)}$ | Facet model$^{(b)}$ |
|---|---|---|---|
| Left Tibia | TibiaL_ctg | TibiaFleshUp⟨*i*⟩L_ell, for i=1 to 2 TibiaFleshMid⟨*j*⟩L_ell, for j=1 to 2 TibiaFleshLowL_ell | Elements and nodes |
| Right Tibia | TibiaR_ctg | TibiaFleshUp⟨*i*⟩R_ell, for i=1 to 2 TibiaFleshMid⟨*j*⟩R_ell, for j=1 to 2 TibiaFleshLowR_ell | Elements and nodes |
| Left Foot | FootL_ctg $^{(c)}$ | Toes⟨*i*⟩L_ell, for i=1 to 3 FootDorsal⟨*j*⟩L_ell, for j=1 to 2 FootBack⟨*k*⟩L_ell, for k=1 to 2 HeelL_ell | Elements and nodes |
| Left heel | HeelL_ctg $^{(c)}$ | HeelL_ell | |
| Left toes | ToesL_ctg $^{(c)}$ | Toes⟨*i*⟩L_ell, for i=1 to 3 | |
| Right Foot | FootR_ctg $^{(c)}$ | Toes⟨*i*⟩R_ell, for i=1 to 3 FootDorsal⟨*j*⟩R_ell, for j=1 to 2 FootBack⟨*k*⟩R_ell, for k=1 to 2 HeelR_ell | Elements and nodes |
| Right heel | HeelR_ctg $^{(c)}$ | HeelR_ell | |
| Right toes | ToesR_ctg $^{(c)}$ | Toes⟨*i*⟩R_ell, for i=1 to 3 | |
| Left Shoe | ShoeL_ctg $^{(c)}$ | ShoeBackL_ell ShoeDorsal⟨*i*⟩L_ell, for i=1 to 6 ShoeHeelL_ell ShoeSole⟨*j*⟩L_ell, for j=1 to 6 | Elements and nodes |
| Right Shoe | ShoeR_ctg $^{(c)}$ | ShoeBackR_ell ShoeDorsal⟨*i*⟩R_ell, for i=1 to 6 ShoeHeelR_ell ShoeSole⟨*j*⟩R_ell, for j=1 to 6 | Elements and nodes |

$^{(a)}$ *ctg*= contact group, for the ellipsoid models ctg is replaced by gmb(group_multibody) and for the facet model ctg is replaced by gfe (group_finite element).
$^{(b)}$ L = Left; R = Right
$^{(c)}$ If the dummy wear shoes only the shoe contact groups should be selected and not those of the feet.

### FE belt positioning and contact definition

In the application manual an example is given on how to position a FE belt on a facet dummy model (see Application manual). FE belts can also be created and repositioned with XMADgic 5.0 and higher.

For the lapbelt to facet Q model contact it is recommended to add besides the normal lapbelt to pelvis contact an extra contact definition. This contact is between the iliac wings and the lapbelt with the iliac wings as slave and the option RELEDG to ON. This option prevents the lapbelt, with relatively large elements, to get stuck around an iliac wing.

The recommended contacts between dummy and belts are pre-defined in the user file under the SYSTEM.MODEL Belt_to_Dummy_contacts. The references in FE_MODEL of Shoulder-Belt_gfe and LapBelt_gfe needs to be changed to the proper FE-models to make the contacts work. By default the user file will give two warnings due to the fact that the referred FE-model for the belts is empty.

### Output

From MADYMO V7.3 on ISO-MME output can be generated for the Hybrid III 95th percentile Q dummy models. Output requests for signals in ISO-MME format are pre-defined in the CONTROL_OUTPUT element in the user file.

The output options for the Hybrid III 95$^{th}$ percentile are the same as those of the hybrid III 50$^{th}$ percentile dummies from which they were derived. See Table 4.5 for a complete overview of those signals.

Table 4.5: Hybrid III 95$^{th}$ percentile Q dummy model output signals.

| Sensor | Identifier | Signal resul-tant | x | direc-tion[(a)] | y | direc-tion[(a)] | z | direc-tion[(a)] | Filter |
|---|---|---|---|---|---|---|---|---|---|
| Head | | | | | | | | | |
| CG accelerometer[(b)] | HeadCG_acc | ar | a1 | forward | a2 | lateral | a3 | vertical | CFC1000 |
| Neck | | | | | | | | | |
| Upper load cell | NeckUp_lce_F_CFC1000 | fr | f1 | shear | f2 | shear | f3 | axial | CFC1000 |
| | NeckUp_lce_F_CFC600 | fr | f1 | shear | f2 | shear | f3 | axial | CFC600 |
| | NeckUp_lce_T | tr | t1 | roll | t2 | pitch | t3 | yaw | CFC600 |
| Lower load cell | NeckLow_lce_F | fr | f1 | shear | f2 | shear | f3 | axial | CFC1000 |
| | NeckLow_lce_T | tr | t1 | roll | t2 | pitch | t3 | yaw | CFC600 |
| Thorax | | | | | | | | | |
| accelerometer[(a)] | Thorax_acc | ar | a1 | forward | a2 | lateral | a3 | vertical | CFC180 |
| Chest deflection | ChestDeflection_dis | dr | d1 | displace-ment | | | | | CFC600 |
| | ChestDefl_dis_ CFC180 | dr | d1 | displace-ment | | | | | CFC180 |
| | ChestDeflection_vel_ CFC600 | vr | v1 | velocity | | | | | CFC600 |
| | ChestDeflection_vel_ CFC180 | vr | v1 | velocity | | | | | CFC180 |
| Clavicles[(c)] | ClavicleL_lce_F | fr | f1 | shear | f2 | shear | f3 | axial | CFC1000 |
| | ClavicleR_lce_F | fr | f1 | shear | f2 | shear | f3 | axial | CFC1000 |
| Lumbar Spine | | | | | | | | | |
| Thoracic load cell | Thoracic_lce_F | fr | f1 | shear | f2 | shear | f3 | axial | CFC1000 |
| | Thoracic_lce_T | tr | t1 | roll | t2 | pitch | t3 | yaw | CFC1000 |
| Lumbar load cell | Lumbar_lce_F | fr | f1 | shear | f2 | shear | f3 | axial | CFC1000 |
| | Lumbar_lce_T | tr | t1 | roll | t2 | pitch | t3 | yaw | CFC1000 |

*Continued on the next page*

*Table 4.5 cont.*

| Sensor | Identifier | Signal | | | | | | | Filter |
|---|---|---|---|---|---|---|---|---|---|
| | | resultant | x | direction[a] | y | direction[a] | z | direction[a] | |
| Pelvis | | | | | | | | | |
| Accelerometer[a] | Pelvis_acc | ar | a1 | forward | a2 | lateral | a3 | vertical | CFC1000 |
| Femur | | | | | | | | | |
| Left load cell | FemurL_lce_F | fr | f1 | shear | f2 | shear | f3 | axial | CFC600 |
| | FemurL_lce_T | tr | t1 | roll | t2 | pitch | t3 | yaw | CFC600 |
| Right load cell | FemurR_lce_F | fr | f1 | shear | f2 | shear | f3 | axial | CFC600 |
| | FemurR_lce_T | tr | t1 | roll | t2 | pitch | t3 | yaw | CFC600 |
| Knee | | | | | | | | | |
| Left Slider | KneeL_dis | dr | d1 | displ | | | | | none |
| Right Slider | KneeR_dis | dr | d1 | displ | | | | | none |
| Tibia | | | | | | | | | |
| Left Upper load cell | TibiaUpL_lce_F | fr | f1 | shear | f2 | shear | f3 | axial | CFC600 |
| | TibiaUpL_lce_T | tr | t1 | roll | t2 | pitch | t3 | yaw | CFC600 |
| Right Upper load cell | TibiaUpR_lce_F | fr | f1 | shear | f2 | shear | f3 | axial | CFC600 |
| | TibiaUpR_lce_T | tr | t1 | roll | t2 | pitch | t3 | yaw | CFC600 |
| Left Lower load cell | TibiaLowL_lce_F | fr | f1 | shear | f2 | shear | f3 | axial | CFC600 |
| | TibiaLowL_lce_T | tr | t1 | roll | t2 | pitch | t3 | yaw | CFC600 |
| Right Lower load cell | TibiaLowR_lce_F | fr | f1 | shear | f2 | shear | f3 | axial | CFC600 |
| | TibiaLowR_lce_T | tr | t1 | roll | t2 | pitch | t3 | yaw | CFC600 |

[a] Positive direction given according to SAE J211/1.

[b] The calculated acceleration is corrected in the x-direction for a prescribed fictitious acceleration field to get correct values (see Theory manual).

[c] The physical Hybrid III 95$^{th}$ percentile dummy do not have clavicle load cells. The fact that the clavicle load cells are available in this model is because it is a scaled version of the Hybrid III 50$^{th}$ percentile dummy model.

## Injury criteria

Table 4.6: Injury criteria defined for the Hybrid III 95$^{th}$ percentile Q dummy models.

| Injury criteria | Identifier | Filter |
|---|---|---|
| Head | | |
| HIC (15) | HIC15_inj | |
| HIC (36) | HIC36_inj | |
| 3ms (cumulative) | H3MS_inj | |
| max Res Acc | HaccRpeak_inj | |
| Neck | | |
| max Tension | NecktensZpeak_inj | |
| max Compression | NeckcompZpeak_inj | |
| MOC | | |
| lateral | | |
| frontal | MOCx_inj | CFC600 (force and moment) |
| | MOCy_inj | CFC600 (force and moment) |
| FNIC | | |
| tension | FNICtension_inj | CFC1000 |
| shear | FNICshear_inj | CFC1000 |
| bending | FNICbending_inj | CFC1000/CFC600 (force/moment) |

*Continued on the next page*

*Table 4.6 cont.*

| Injury criteria | Identifier | Filter |
|---|---|---|
| NIJ | | |
| tension-extension | NTE_inj | CFC600 (force and moment) |
| tension-flexion | NTF_inj | CFC600 (force and moment) |
| compression-extension | NCE_inj | CFC600 (force and moment) |
| compression-flexion | NCF_inj | CFC600 (force and moment) |
| Thorax | | |
| 3ms (cumulative) | T3MS_inj | |
| 3ms (contiguous) | TCon3MS_inj | |
| Chest Compression | ThCC_inj | CFC180 |
| | ThCC_CFC600_inj | CFC600 |
| max Res Acc | TaccRpeak_inj | |
| CTI | CTI_inj | |
| VC | VC_inj_CFC180 | CFC180 (deflection) |
| | VC_inj_CFC600 | CFC600 (deflection) |
| Femurs | | |
| FFC | | |
| Left | FFCL_inj | CFC600 |
| Right | FFCR_inj | CFC600 |
| max Left Compression | FemurLcompZpeak_inj | |
| max Right Compression | FemurRcompZpeak_inj | |
| Knees | | |
| Left Compression | kneesliderL_inj | |
| Right Compression | kneesliderR_inj | |
| Tibia | | |
| TI | | |
| Upper Left | TIUpL_inj | CFC600 |
| Upper Right | TIUpR_inj | CFC600 |
| Lower Left | TILowL_inj | CFC600 |
| Lower Right | TILowR_inj | CFC600 |
| TCFC | | |
| Upper Left | TCFCUpL_inj | CFC600 |
| Upper Right | TCFCUpR_inj | CFC600 |
| Lower Left | TCFCLowL_inj | CFC600 |
| Lower Right | TCFCLowR_inj | CFC600 |

# 5 Standing Hybrid III 50th percentile Dummy



The standard Hybrid III 50$^{th}$ percentile dummy has been developed for seated automotive applications. The standing Hybrid III contains some adapted parts and thereby has a wider range of application including standing. There is however, no well-defined application for the physical standing dummy. The design of the dummy has also not been based on specific biofidelity requirements like for testing pedestrian accidents.

The model is based on the standard Hybrid III 50$^{th}$ percentile model. The differences with respect to standard Hybrid III 50$^{th}$ percentile ellipsoid model are described below. For a description of those parts equivalent to the standard Hybrid III 50$^{th}$ percentile is referred to Chapter 36.

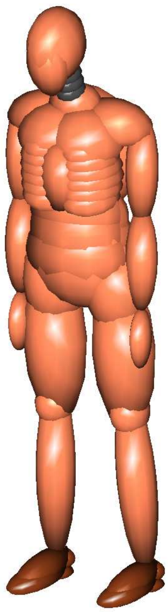

Figure 5.1: Ellipsoid standing Hybrid III 50$^{th}$ percentile dummy model.

5

## 5.1 Model description

An ellipsoid model of the standing Hybrid III dummy $50^{th}$ percentile is available. The input is given in the file:

| | |
|---|---|
| Ellipsoid model: | d_shb350el_usr.xml<br>d_shb350el_inc.xml |

To run the model, the following licenses are required:

| | |
|---|---|
| Ellipsoid model: | MADYMO/Solver (Multibody)<br>MADYMO/Dummy Models/Frontal |

Figure 5.1 shows the model in the reference position. The ellipsoid model consists of 35 bodies.

**ELLIPSOID MODEL**

Almost all parts of the standing Hybrid III dummy $50^{th}$ percentile are equal to the parts of the ellipsoid model of the Hybrid III dummy $50^{th}$ percentile as described in Chapter 36. The only exceptions are the lumbar spine, abdomen, pelvis. legs, ankles and feet as described below.

**Lumbar Spine**

The standing Hybrid III has a straight lumbar spine while the standard Hybrid III has a curved lumbar spine. The model geometry and inertia were adapted for this modification, but the protected lumbar spine deformation resistance model was not modified.

**Abdomen**

The geometry and inertia of the abdomen is adapted with respect to the standard Hybrid III and the model is adapted accordingly.

**Pelvis**

The geometry and inertia of the pelvis, is adapted. The hip joints of the standing Hybrid III have a large free range of motion similar to the human range of motion. The range of motion of the standing dummy was measured and implemented. The joint frictions in hips have been implemented using Coulomb friction in RESTRAINT.JOINT and have been set to rather high values needed for standing.

**Legs**

The geometry and inertia of the upper legs were adapted. The joint frictions in knees have been implemented using Coulomb friction in RESTRAINT.JOINT and have been set to rather high values needed for standing.

**Ankles and feet**

The model of ankles and feet are based on the ankles that allow 30 degrees dorsiflexion. The joint frictions in ankles have been implemented using Coulomb friction in RESTRAINT.JOINT and have been set to rather high values needed for standing.

## CONTACTS BETWEEN DUMMY COMPONENTS

For the ellipsoid model contact is defined between the head and thorax.

5

## 5.2 Model validation

The tests for the validation of the model are described in Table 5.1.

Table 5.1: Component tests for Hybrid III 50$^{th}$ percentile dummy model.

| Component | Test description | specifications | | Model Ellipsoid |
|---|---|---|---|---|
| Neck | Static forward bending | Range | +57/-80° | x |
| | Static lateral bending | | +57/-57° | x |
| | Static torsion | | +45/-45° | x |
| | Dynamic forward bending | Sled test | 7g, 15g | x |
| | | | 7, 9.5, 13.5 m/s (with contact on forehead or chin) | x |
| | Dynamic rearward bending | Sled test | 7g | x |
| | Dynamic lateral bending | Sled test | 7g | x |
| Clavicles | Static downward | Range | +5/-5° | x |
| | Static forward | | +12/-12° | x |
| Shoulders, Elbows & Wrists | Static all implemented loading/ unloading functions | Complete range of motion | | x |
| | Dynamic shoulder adduction | Velocity | 3.5, 4.5, 6.5 m/s | x |
| | Dynamic shoulder flexion/ extension | | 3.5, 4.5, 6.5 m/s | x |
| Thorax | Static sternum loading | Force | 3.0kN at 5mm/s | x |
| | Static rib loading | | 3.5kN at 3, 5mm/s | x |
| | Static oblique rib loading | | 2.4kN at 4mm/s | x |
| | Static vertical loading | | 0.5kN at 2mm/s | x |
| | Dynamic sternum loading | Mass & velocity | 9kg & 5.5m/s | x |
| | | | 43kg & 2.5m/s | x |
| | Dynamic rib loading | Mass & velocity | 9kg & 5.5m/s | x |
| | | | 43kg & 2.5m/s | x |
| | Dynamic large plate loading | Mass & velocity | 9kg & 5.5m/s | x |
| Abdomen | Dynamic lap belt loading | | | |
| Lumbar spine | Static forward bending | Range | +57/-45° | x |
| | Static lateral bending | | +34/-34° | x |
| | Static torsion | | +57/-57° | x |
| | Static forward shear | | +0.25/-0.25 m displacement | x |
| | Static lateral shear | | +0.25/-0.25 m displacement | x |
| | Static elongation/ compression | | +0.005/-0.022m displacement | x |
| | Dynamic forward bending | Pendulum-test: velocity & mass of impactor | 6 m/s & 3.8 kg | x |
| | Dynamic rearward bending | | 6 m/s & 3.8 kg | x |
| | Dynamic forward shear | | 6 m/s & 3.8 kg | x |
| | Dynamic torsion | | 6 m/s & 3.8 +2.85 kg | x |
| | Dynamic compression | | 6 m/s & 3.8 kg | x |

*Continued on the next page*

*Table 5.1 cont.*

| **Component** | **Test** description | specifications | | **Model** Ellipsoid |
|---|---|---|---|---|
| Hip joints | Static flexion | Range | +50/-50° | x |
| | Static abduction | | +20/-20° | x |
| | Static exo/endo-rotation | | | |
| | Dynamic flexion | Sled test: velocity | 6, 10, 20 & 30 m/s | x |
| Knees & Ankles | Equal to Shoulders, Elbows & Wrists in this table | | | |
| Ankle, Foot & Shoe | Dynamic compression | mass & velocity | 10 kg, 7.5 m/s | x |
| | Dynamic dorsiflection | | 9.75 kg, 3-8.5 m/s | x |
| | Dynamic inversion | | 9.75 kg, 4-8.5 m/s | x |
| Surface compliance | Static lower torso – flat plate | | | x |
| | Static thorax foam jacket – flat plate | | | x |
| | Dynamic lower torso – flat plate | mass & velocity | 20.15 kg, 1.7, 3.5, 5 m/s | x |
| | Dynamic thorax jacket – flat plate | | 20.15 kg, 2.1, 3.5, 5.5 m/s | x |
| | Dynamic thorax jacket-sphere | | 6 kg, 2, 3.8 m/s | x |

## 5.3 User instructions

### Timestep

Table 5.2: Recommended timestep for the Hybrid III 50th percentile standing dummy model.

| Model | timestep (s) |
|---|---|
| Ellipsoid | $\leq 2 \cdot 10^{-4}$ |

### Dummy positioning

When the dummy model is in the reference position, it is approximately in equilibrium with gravity on a rigid horizontal surface when contact is defined with the shoes. Additional supports of the upper torso may be implemented to fully stabilise the dummy.

### Notes

Joint friction values can be adjusted in the model if required.

# 6 Hybrid III 50th dummy with THOR-LX legs

The THOR-LX leg is a retrofit design lower leg for the Hybrid-III dummy family that replaces the standard lower leg and foot. THOR-LX was commissioned by the National Transportation Biomechanics Research Center (NTBRC) of the NHTSA Research and Development Office. The design is based on the leg used in the THOR ATD, but has been modified for compatibility with the standard Hybrid-III dummy. The THOR-LX dummy attaches to the Hybrid-III knee. The THOR dummy has been developed by GESAC Inc. A description of THOR-LX, and more background information can be found on the NHTSA website (www.nhtsa.gov).

The MADYMO model of THOR-LX contains all features and functionality of the hardware leg. All outputs from load cells and accelerometers are defined.

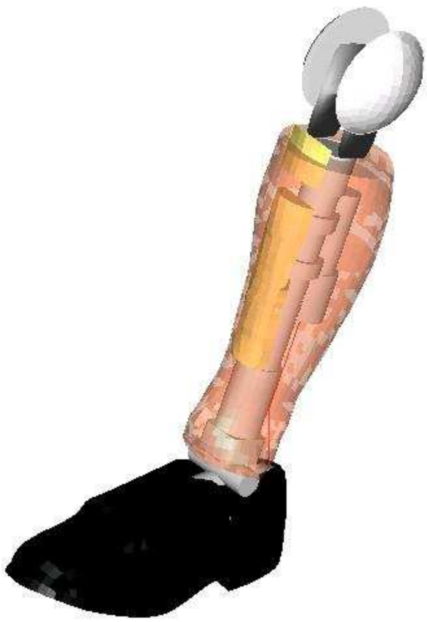

Figure 6.1: THOR-LX leg (left side).

## 6.1 Model description

The THOR-LX leg is available as a facet model, as a part of the standard Hybrid-III model. The input is given in files:

| | | |
|---|---|---|
| Facet model: | d_hyb350fc_thorlx_usr.xml | (user file) |
| | d_hyb350fc_thorlx_inc.xml | (model file) |

To run the model, the following licenses are required:

| | |
|---|---|
| Facet model: | MADYMO/Solver (Multibody) |
| | MADYMO/Dummy Models/Frontal |

**FACET MODEL**

The facet model has been created by 3D-scanning the surfaces of the foot, the shoe, and the leg skin. Foot and shoe are separate bodies, each with a facet surface description and contact characteristics. The model follows the hardware leg closely, and includes all the ankle joints, the Achilles tendon, the compliant tibia element, the knee bumper and the tibia guard.

**CONTACTS BETWEEN DUMMY COMPONENTS**

Contacts are defined between the shoe and the foot of the THOR-LX leg. Forces that are applied to the sole and heel of the shoe are transmitted through the foot to the lower leg.

## 6.2 Model validation

The THOR-LX model has been developed for use with the Hybrid-III in frontal impacts. The model has been developed and validated with data from component tests. The components tests were set up to:

- Determine joint characteristics and response to loading ;
- Determine compliant tibia characteristics and response to loading ;
- Determine leg skin stiffness (impact response) at several points along the length of the lower leg.

The data required was acquired through two types of tests:

- Impactor tests to the foot and heel, with and without the shoe ;
- Impactor tests to the leg skin at various points along the length of the lower leg.

An example of a test of the first category is shown in the figure below: in the test the foot and lower leg are loaded by a circular impactor.

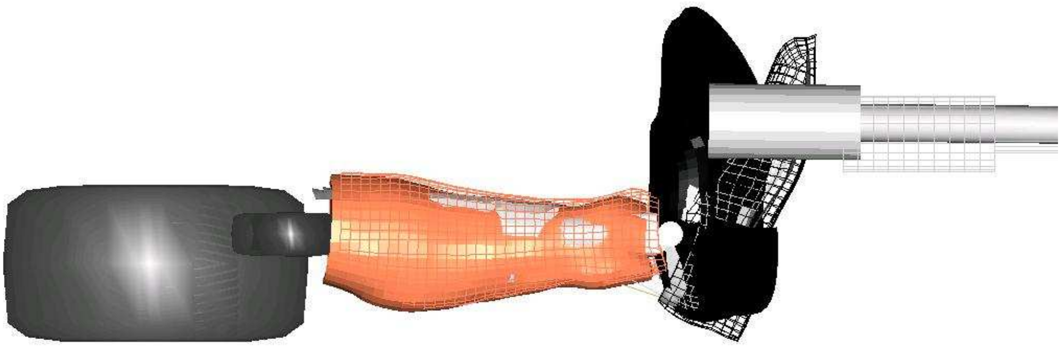

Figure 6.2: 5 m/s dorsi-flexion test. Initial position shown in wireframe.

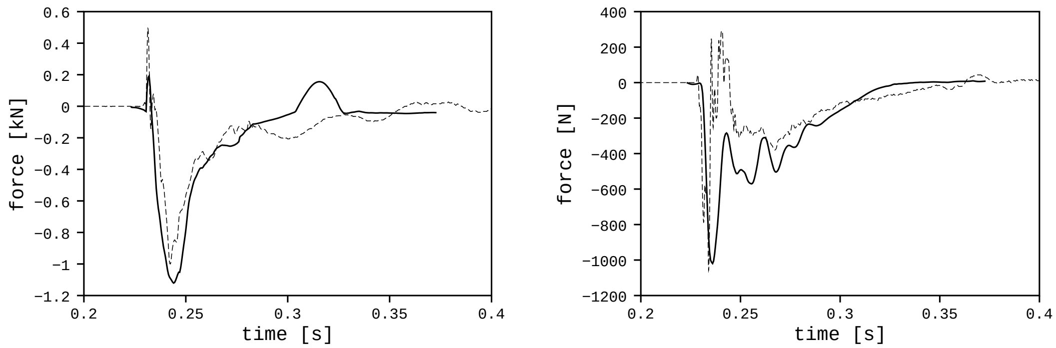


Figure 6.3: Upper tibia load cell X (left) and Z force; simulation (———), experiment (— — —).

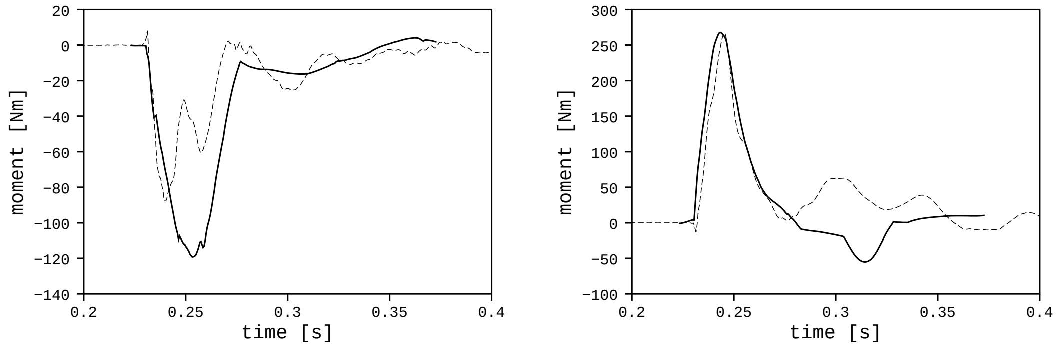


Figure 6.4: Upper tibia load cell X-moment (left) and Y-moment (right) ; simulation(———), experiment (— — —).

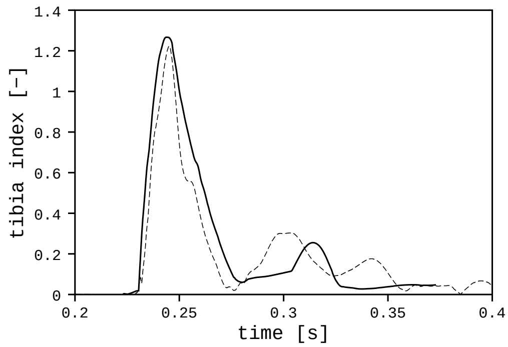


Figure 6.5: Upper tibia index (TI); simulation (———), experiment (— — —).

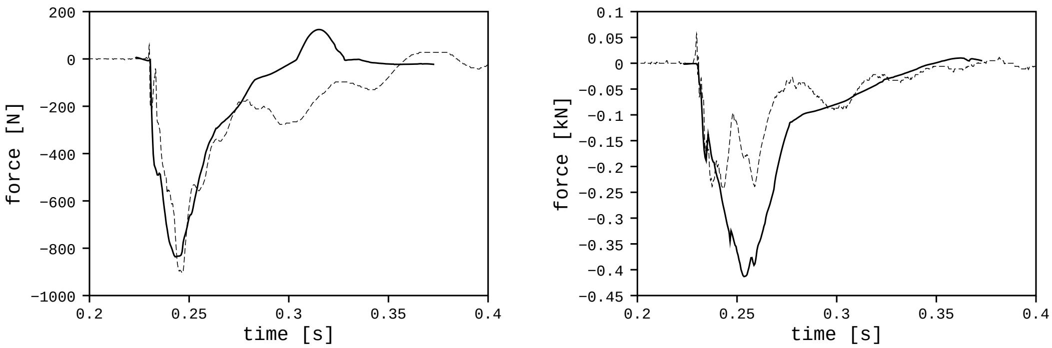


Figure 6.6: Lower tibia load cell X-force (left) and Y-force (right) ; simulation (———), experiment (– – –).

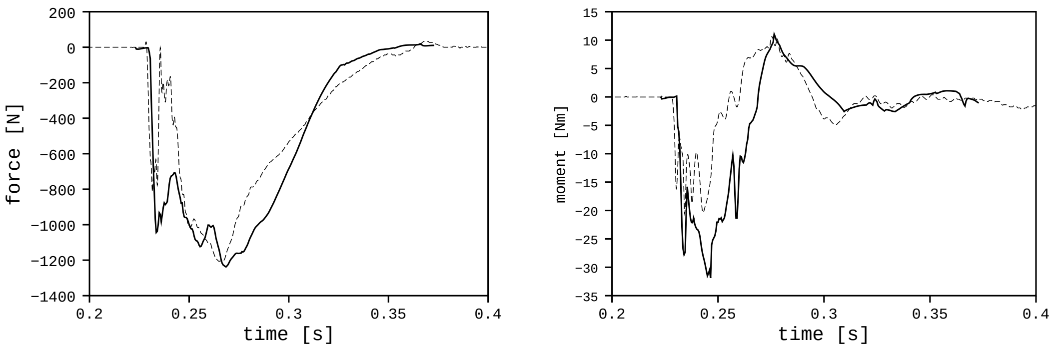


Figure 6.7: Lower tibia load cell Z-force (left) and X-moment (right).

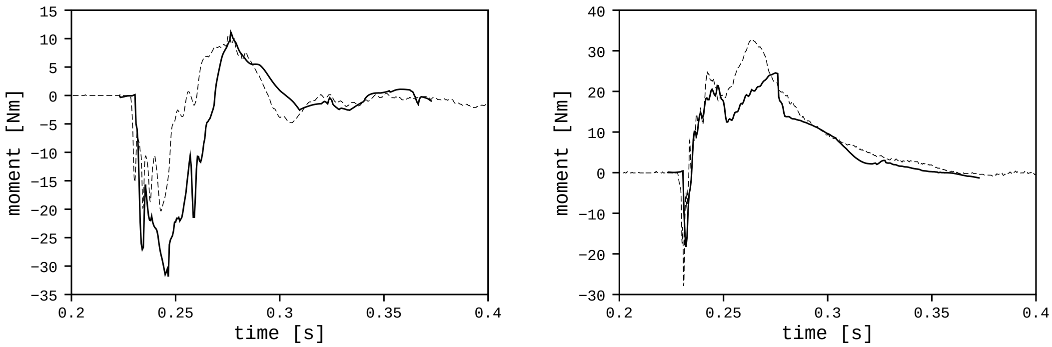


Figure 6.8: Ankle X-moment (left) and Y-moment (right).

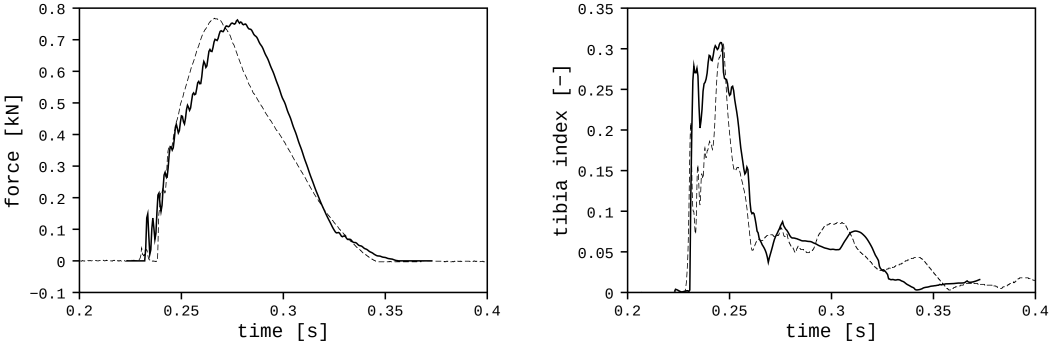


Figure 6.9: Achilles cable Z-force (left) and lower tibia index TI (right).

The second series shows the response of the upper tibia to impactor loading. The velocity of the impactor is 4 m/s.

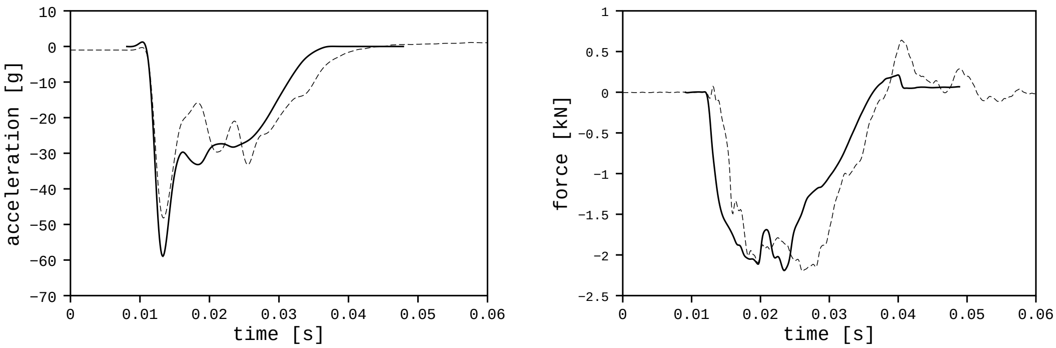


Figure 6.10: Impactor deceleration (left) and upper femur Z-force (axial loading, right) ; simulation (———), experiment (— — —).

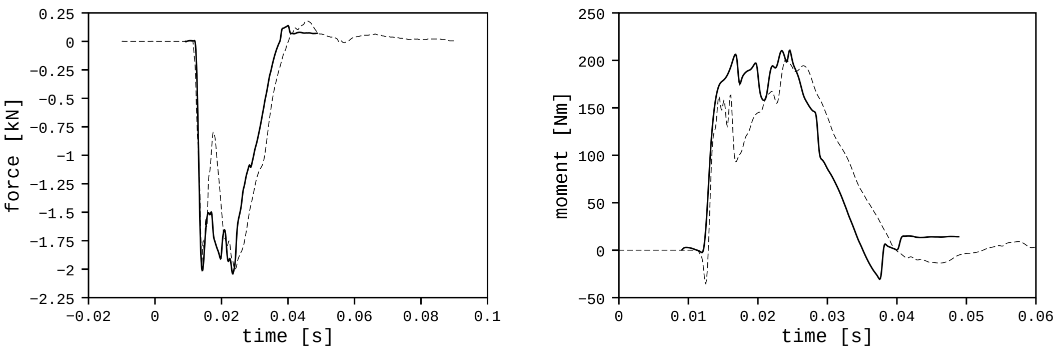


Figure 6.11: Upper tibia X-force (left) and upper tibia Y-moment (right) ; simulation (———), experiment (— — —).

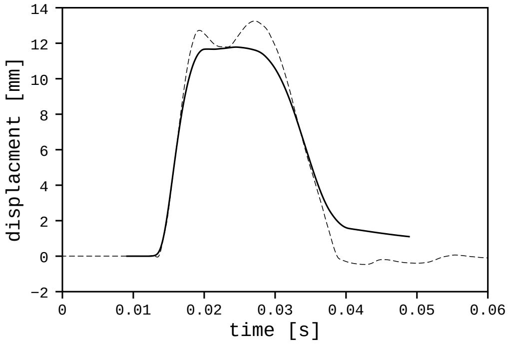


Figure 6.12: Knee slider displacement ; simulation (———), experiment (– – –).

## 6.3 User instructions

### Timestep

Table 6.1: Recommended timestep for the THOR-LX model.

| Model | timestep (s) |
|---|---|
| Facet | $\leq 5 \cdot 10^{-5}$ |

### Dummy positioning

Table 6.2: Positioning joints of the Hybrid III 50th percentile dummy model with THOR-LX legs.

| Joint Description | Identifier | Degree of freedom$^{(a)}$ | | | | | | Comment |
|---|---|---|---|---|---|---|---|---|
| Dummy | Dummy_jnt | D1 | forward | D2 | leftward | D3 | upward | Dummy position |
| Neck bracket | NeckBracket_jnt | R1 | pitch down | | | | | $^{(b)}$ |
| Neck element | NeckPivot$\langle i \rangle$_jnt, for i=1 to 4 $^{(c)}$ | R1 | roll right | R2 | pitch down | R3 | yaw left | only for equilibrium state |
| Left clavicle | ClavicleL_jnt | R1 | roll right | R2 | yaw left | | | only for equilibrium state |
| Right clavicle | ClavicleR_jnt | R1 | roll right | R2 | yaw left | | | |
| Left shoulder | ShoulderL_jnt | R1 | pitch down | R2 | roll right | | | |
| Right shoulder | ShoulderR_jnt | R1 | pitch down | R2 | roll right | | | |
| Left elbow | ElbowL_jnt | R1 | yaw left | R2 | pitch down | | | |
| Right elbow | ElbowR_jnt | R1 | yaw left | R2 | pitch down | | | |
| Left wrist | WristL_jnt | R1 | yaw left | R2 | roll right | | | |
| Right wrist | WristR_jnt | R1 | yaw left | R2 | roll right | | | |
| Lumbar spine | LumbarSpine_jnt | R1<br>D1 | roll right<br>forward | R2<br>D2 | pitch down<br>leftward | R3<br>D3 | yaw left<br>upward | only for equilibrium state |
| Left hip | HipL_jnt | R1 | roll left | R2 | pitch down | R3 | yaw left | |
| Right hip | HipR_jnt | R1 | roll left | R2 | pitch down | R3 | yaw left | |
| Left knee | KneeL_jnt | R2<br>D1 | pitch down<br>compression | | | | | <br>always zero |
| Right knee | KneeR_jnt | R2<br>D1 | pitch down<br>compression | | | | | <br>always zero |

*Continued on the next page*

*Table 6.2 cont.*

| Joint Description | Identifier | Degree of freedom[a] | | Comment |
|---|---|---|---|---|
| Left ankle | Ankle_torsionL _jnt | R1 | yaw left | |
| | Ankle_flexionL _jnt | R1 | pitch up | |
| | Ankle_versionL _jnt | R1 | roll right | |
| Right ankle | Ankle_torsionR _jnt | R1 | yaw left | |
| | Ankle_flexionR _jnt | R1 | pitch up | |
| | Ankle_versionR _jnt | R1 | roll right | |

[a] Positive translation or rotation given in global co-ordinate system while dummy is in reference position (see Figure 6.1)
[b] Angle for the neck bracket is directly to derive from the physical dummy. A lower neck load cell in the physical dummy means a zero angle for the neck bracket.
[c] Part⟨i⟩: numbered from bottom to top / rear to front / right to left.

## Dummy contacts

The contacts groups of the Hybrid-III model with THOR-LX legs are identical to those of the standard Hybrid-III 50th percentile dummy, with exception of the tibia and the foot/shoe. The new contact groups for these parts only are given in table 6.3 below. All other contacts are defined in the chapter 'Hybrid-III 50$^{th}$ percentile dummy', under 'Dummy contacts'.

Table 6.3: Available modified groups to define contact between the Hybrid III 50$^{th}$ percentile dummy with THOR-LX legs and the environment.

| Contact description | Identifier [a][b] |
|---|---|
| Left Tibia | TibiaUpL_gfe<br>TibiaMidL_gfe<br>TibiaLowL_gfe |
| Right Tibia | TibiaUpR_gfe<br>TibiaMidR_gfe<br>TibiaLowR_gfe |
| Left Shoe | OuterShoeL_gfe<br>OuterSoleL_gfe<br>OuterHeelL_gfe |
| Right Shoe | OuterShoeR_gfe<br>OuterSoleR_gfe<br>OuterHeelR_gfe |

[a] *ctg*= contact group, for all ellipsoid models ctg is replaced by gmb(group_multibody).
[b] L=Left; R=Right.

## Output

Table 6.4: Hybrid III $50^{th}$ percentile with THOR-LX legs output signals.

| Sensor | Identifier | Signal | | | | | | | Filter |
|---|---|---|---|---|---|---|---|---|---|
| | | resultant | x | direction[a] | y | direction[a] | z | direction[a] | |
| Head | | | | | | | | | |
| CG accelerometer[b] | HeadCG_acc | ar | a1 | forward | a2 | lateral | a3 | vertical | CFC1000 |
| Neck | | | | | | | | | |
| Upper load cell | NeckUp_lce_F_CFC1000 | fr | f1 | shear | f2 | shear | f3 | axial | CFC1000 |
| | NeckUp_lce_F_CFC600 | fr | f1 | shear | f2 | shear | f3 | axial | CFC600 |
| | NeckUp_lce_T | tr | t1 | roll | t2 | pitch | t3 | yaw | CFC600 |
| Lower load cell | NeckLow_lce_F_CFC1000 | fr | f1 | shear | f2 | shear | f3 | axial | CFC1000 |
| | NeckLow_lce_F_CFC600 | fr | f1 | shear | f2 | shear | f3 | axial | CFC600 |
| | NeckLow_lce_T | tr | t1 | roll | t2 | pitch | t3 | yaw | CFC600 |
| Thorax | | | | | | | | | |
| accelerometer | Thorax_acc | ar | a1 | forward | a2 | lateral | a3 | vertical | CFC180 |
| deflection | ChestDeflection_dis | dr | d1 | displacement | | | | | CFC600 |
| Chest | ChestDefl_dis_CFC180 | dr | d1 | displacement | | | | | CFC180 |
| | ChestDeflection_vel_CFC600 | vr | v1 | velocity | | | | | CFC600 |
| Sternum | | | | | | | | | |
| accelerometer | Sternum_acc | ar | a1 | forward | a2 | lateral | a3 | vertical | CFC1000 |
| Upper Spine | | | | | | | | | |
| accelerometer | UpperSpineT1_acc | ar | a1 | forward | a2 | lateral | a3 | vertical | CFC180 |
| Lower Spine | | | | | | | | | |
| accelerometer | LowerSpineT12_acc | ar | a1 | forward | a2 | lateral | a3 | vertical | CFC180 |
| Lumbar Spine | | | | | | | | | |
| Upper load cell | LumbarSpineUp_lce_F | fr | f1 | shear | f2 | shear | f3 | axial | CFC1000 |
| | LumbarSpineUp_lce_T | tr | t1 | roll | t2 | pitch | t3 | yaw | CFC1000 |
| Lower load cell | LumbarSpineLow_lce_F | fr | f1 | shear | f2 | shear | f3 | axial | CFC1000 |
| | LumbarSpineLow_lce_T | tr | t1 | roll | t2 | pitch | t3 | yaw | CFC1000 |
| Pelvis | | | | | | | | | |
| Accelerometer | Pelvis_acc | ar | a1 | forward | a2 | lateral | a3 | vertical | CFC1000 |
| Femur | | | | | | | | | |
| Left load cell | FemurL_lce_F | fr | f1 | shear | f2 | shear | f3 | axial | CFC600 |
| | FemurL_lce_T | tr | t1 | roll | t2 | pitch | t3 | yaw | CFC600 |
| Right load cell | FemurR_lce_F | fr | f1 | shear | f2 | shear | f3 | axial | CFC600 |
| | FemurR_lce_T | tr | t1 | roll | t2 | pitch | t3 | yaw | CFC600 |
| Tibia | | | | | | | | | |
| Left Upper load cell | TibiaUpL_lce_F | fr | f1 | shear | f2 | shear | | | CFC600 |
| | TibiaUpL_lce_T | tr | t1 | roll | t2 | pitch | | | CFC600 |
| Right Upper load cell | TibiaUpR_lce_F | fr | f1 | shear | f2 | shear | | | CFC600 |
| | TibiaUpR_lce_T | tr | t1 | roll | t2 | pitch | | | CFC600 |
| Left Lower load cell | TibiaLowL_lce_F | fr | f1 | shear | f2 | shear | f3 | axial | CFC600 |
| | TibiaLowL_lce_T | tr | t1 | roll | t2 | pitch | | | CFC600 |

*Continued on the next page*

*Table 6.4 cont.*

| Sensor | Identifier | Signal | | | | | | | Filter |
|---|---|---|---|---|---|---|---|---|---|
| | | resultant | x | direction(a) | y | direction(a) | z | direction(a) | |
| Right Lower load cell | TibiaLowR_lce_F | fr | f1 | shear | f2 | shear | f3 | axial | CFC600 |
| | TibiaLowR_lce_T | tr | t1 | roll | t2 | pitch | | | CFC600 |
| Accelerometers | TibiaL_x_acc | | a1 | forward | | | | | |
| | TibiaL_y_acc | | | | a1 | lateral | | | |
| | Foot_L_xyz_acc | ar | a1 | forward | a2 | lateral | a3 | vertical | |
| | TibiaR_x_acc | | a1 | forward | | | | | |
| | TibiaR_y_acc | | | | a2 | lateral | | | |
| | Foot_R_xyz_acc | ar | a1 | forward | a2 | lateral | a3 | vertical | |

(a) Positive direction given according to SAE J211/1.

(b) The calculated acceleration is corrected in the x direction for a prescribed fictitious acceleration field to get correct values (see Theory manual).

## Injury Criteria

Table 6.5: Injury criteria defined for the Hybrid III 50th percentile with THOR-LX legs.

| Injury criteria | Identifier | Filter |
|---|---|---|
| TI | | |
| Upper left | TILUp_inj | CFC600 |
| Upper right | TIRUp_inj | CFC600 |
| Lower left | TILLow_inj | CFC600 |
| Lower right | TIRLow_inj | CFC600 |
| TCFC | | |
| Upper left | TCFCLUp_inj | CFC600 |
| Upper right | TCFCRUp_inj | CFC600 |
| Lower left | TCFCLLow_inj | CFC600 |
| Lower right | TCFCRLow_inj | CFC600 |
| Neck | | |
| FNIC | | |
| tension | FNICtension_inj | CFC1000 |
| shear | FNICshear_inj | CFC1000 |
| bending | FNICbending_inj | CFC1000 |
| NIJ | | |
| tension-extension | NTE_inj | CFC600 (force)<br>CFC600 (moment) |
| tension-flexion | NTF_inj | CFC600 (force)<br>CFC600 (moment) |
| compression-extension | NCE_inj | CFC600 (force)<br>CFC600 (moment) |
| compression-flexion | NCF_inj | CFC600 (force)<br>CFC600 (moment) |

*Continued on the next page*

*Table 6.5 cont.*

| Injury criteria | Identifier | Filter |
|---|---|---|
| NIJ lower neck | | |
| tension-extension | NTELow_inj | CFC600 (force) |
| | | CFC600 (moment) |
| tension-flexion | NTFLow_inj | CFC600 (force) |
| | | CFC600 (moment) |
| compression-extension | NCELow_inj | CFC600 (force) |
| | | CFC600 (moment) |
| compression-flexion | NCFLow_inj | CFC600 (force) |
| | | CFC600 (moment) |
| Thorax | | |
| 3ms | T3MS_inj | |
| VC | VC_inj_CFC180 | CFC180 |
| | VC_inj_CFC600 | CFC600 (deflection) |
| Femurs | | |
| FFC | | |
| Left | FFCL_inj | CFC600 |
| Right | FFCR_inj | CFC600 |
| Tibia | | |
| TI | | |
| Upper left | TIUpL_inj | CFC600 |
| Upper right | TIUpR_inj | CFC600 |
| Lower Left | TILowL_inj | CFC600 |
| Lower right | TILowR_inj | CFC600 |
| TCFC | | |
| Upper left | TCFCUpL_inj | CFC600 |
| Upper right | TCFCUpR_inj | CFC600 |
| Lower Left | TCFCLowL_inj | CFC600 |
| Lower right | TCFCLowR_inj | CFC600 |

# 7 Hybrid II standard Part 572 Dummy

In 1973, the 50$^{th}$ percentile standard Part 572 (Hybrid II) dummy was the first dummy to be mandated by NHTSA for use in testing automotive restraint systems to meet Federal Motor Vehicle Safety Standards (FMVSS) 208. Nowadays, the dummy is used mainly in non-automotive applications, in particular for aircraft seat certification according to FAA/JAA regulations.

The 50$^{th}$ percentile standard Part 572 (Hybrid II) dummy is available as an ellipsoid model with improved facet parts.



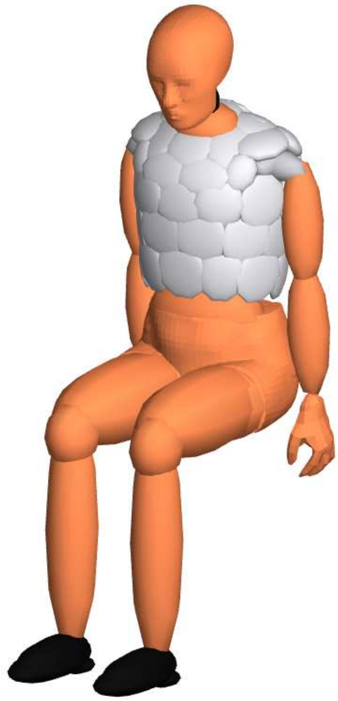

Figure 7.1: Ellipsoid Hybrid II 50$^{th}$ percentile standard Part 572 dummy model.

7

## 7.1 Model description

The user can find the input for the Hybrid II 50$^{th}$ percentile standard Part 572 dummy model in the following files:

| | |
|---|---|
| Ellipsoid model: | d_p57250el_usr.xml<br>d_p57250el_inc.xml |

To run the model, the following license combination is required:

| | |
|---|---|
| Ellipsoid model: | MADYMO/Solver (Multibody)<br>MADYMO/Dummy Models/Hybrid II |

Figure 7.1 shows the model in the reference position. The ellipsoid model consists of 183 bodies.

**ELLIPSOID MODEL**

The neck model uses flexion-torsion restraints to represent bending and torsion.

The ribcage is modelled with a chain of bodies and joints with appropriate restraints. The jacket surface is represented by 50 ellipsoids, its mass is distributed over 50 bodies and its stiffness is modelled through point and cardan restraints. The interaction between ribcage and jacket is also modelled with point and cardan restraints. The ribcage and jacket are shown in Figure 7.2 .

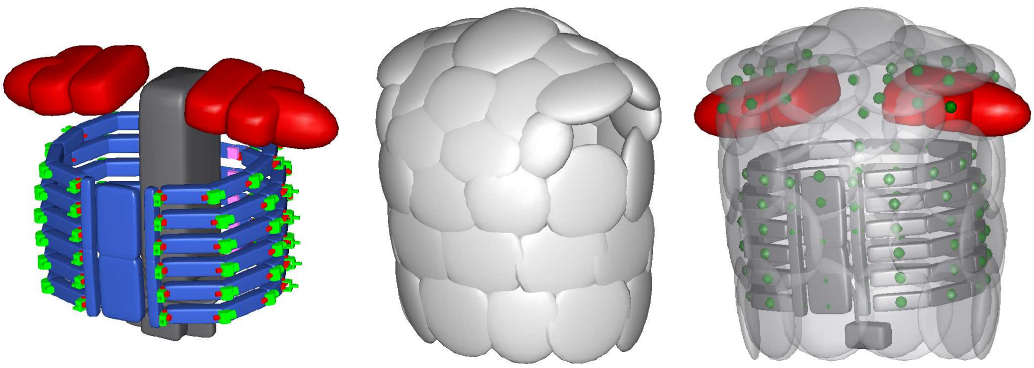

Figure 7.2: Hybrid II 50$^{th}$ percentile standard Part 572 thorax (ribcage and jacket) model.

The lumbar spine is modelled with a succession of 4 universal and two cylindrical joints, combined with two triple joint restraints (see Figure 7.3).

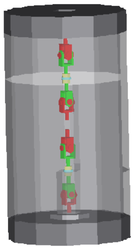

Figure 7.3: Hybrid II 50$^{th}$ percentile standard Part 572 spine model.

The pelvis combines ellipsoid and facet surfaces for optimal contact interactions with the environment (Figure 7.4). The bottom part of the pelvis uses ellipsoids for seat contact, the front part uses facet surfaces for lap belt contact. A more detailed description of the contact groups is given in the paragraph "Dummy contacts".

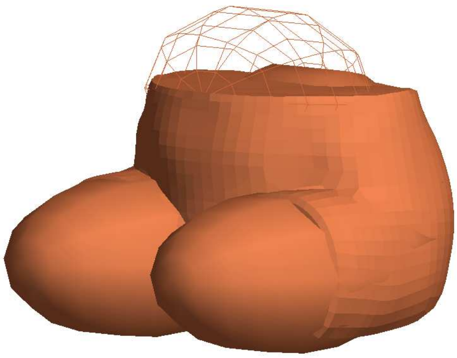

Figure 7.4: Hybrid II 50$^{th}$ percentile standard Part 572 pelvis model.

The data for the dimensions of the ellipsoids have been determined from technical drawings available at TASS International. The masses of the different components of the models have been checked against the specifications of dummies available from dummy hardware manufacturers.

## CONTACTS BETWEEN DUMMY COMPONENTS

Contact is defined between the following components:

Table 7.1: Intercomponent contacts for the Hybrid II 50$^{th}$ percentile standard Part 572 dummy model.

| Model Type | Contact | Master Surface | Slave Surface |
|---|---|---|---|
| ellipsoid | ThoraxHead_con | Jacket_gmb | Head_gfe |
| | Head_tibiaL_con | TibiaL_gmb | Head_gfe |
| | Head_tibiaR_con | TibiaR_gmb | Head_gfe |
| | HandL_ShoeL_con | ShoeL_gmb | HandL_gfe |
| | HandR_ShoeR_con | ShoeR_gmb | HandR_gfe |
| | HandL_FemurL_con | FemurKneeL_gmb | HandL_gfe |
| | HandR_FemurR_con | FemurKneeR_gmb | HandR_gfe |
| | Thorax_FemurL_con | FemurL_gmb | Thorax_gmb |
| | Thorax_FemurR_con | FemurR_gmb | Thorax_gmb |

7

## 7.2 Model validation

The Part 572 model is developed and validated for frontal loading (automotive applications) and vertical loading (aircraft applications[1]). The performed component and full dummy tests are given below in Table 7.2 and Table 7.3.

Table 7.2: Component tests for the Hybrid II 50th percentile dummy model.

| Component | Test Description | Specifications | Model Ell |
|---|---|---|---|
| Head | Repeated drop tests | Certification | x |
| Neck | Repeated pendulum tests | Certification, 4.14 - 4.25m/s | x |
| Thorax | Repeated impact tests | Certification, low velocity 4.2 - 4.34m/s | x |
| | | Certification, high velocity 6.58 - 6.74m/s | x |
| Lumbar Spine | Axial loading test | Low velocity 4.19m/s | x |
| | | High velocity 7.95m/s | x |
| | Repeated pendulum tests | Without spine cable, 0.52 - 2.3m/s | x |
| | | With spine cable, 0.54 - 2.29m/s | x |
| Knee | Repeated impact tests | 2.1m/s | x |

Table 7.3: Full tests for the Hybrid II 50th percentile dummy model.

| Test Description | Specifications | Model Ell |
|---|---|---|
| Repeated dynamic sled tests | 2-point belt, 0 degrees | x |
| Repeated dynamic sled tests | 2-point belt, 60 degrees | x |
| Repeated dynamic sled tests | 3-point belt, 0 degrees | x |
| Repeated dynamic sled tests | 4-point belt, 0 degrees | x |

[1]Manning J.E., Happee R., "Validation of the MADYMO Hybrid II and Hybrid III 50th percentile models in vertical impacts", Presented at Specialists' Meeting: Models for aircrew safety assessment: uses, limitations and requirements. Ohio USA, 26–28 October, 1998.

## 7.3 User instructions

### Timestep

Table 7.4: Recommended timestep for the Hybrid II 50th percentile model.

| Model | timestep (s) |
|---|---|
| Ellipsoid | $\leq 5 \cdot 10^{-6}$ |

The recommended timestep for the Hybrid II 50th percentile model is smaller than for other comparable ellipsoid models, due to the detailed lumbar spine model.

### Memory Allocation

Table 7.5: Recommended memory allocation values for the Hybrid II 50th percentile model.

| Type | Allocation |
|---|---|
| I_SIZE | $2 \cdot 10^6$ |
| R_SIZE | $2 \cdot 10^6$ |
| C_SIZE | $2 \cdot 10^5$ |

The recommended allocation values are higher than the default values due to the higher number of bodies and ellipsoids.

### Dummy positioning

Table 7.6: Positioning joints of the Hybrid II 50th percentile model

| Joint Description | Identifier | Degree of freedom[a] | | | | | | Comment |
|---|---|---|---|---|---|---|---|---|
| Dummy | Dummy_jnt | D1<br>R1 | forward<br>roll right | D2<br>R2 | leftward<br>pitch down | D3<br>R3 | upward<br>yaw left | |
| Neck bracket | NeckBracket_jnt | R1 | pitch down | | | | | [b] |
| Upper neck joint | NeckPivotUp_jnt | R1 | roll right | R2 | pitch down | R3 | yaw left | [c] |
| Lower neck joint | NeckPivotUp_jnt | R1 | roll right | R2 | pitch down | R3 | yaw left | [c] |
| Left shoulder | ShoulderL_jnt | R1 | pitch down | R2 | roll right | | | |
| Right shoulder | ShoulderL_jnt | R1 | pitch down | R2 | roll right | | | |
| Left elbow | ElbowL_jnt | R1 | yaw left | R2 | pitch down | | | |
| Right elbow | ElbowR_jnt | R1 | yaw left | R2 | pitch down | | | |

*Continued on the next page*

*Table 7.6 cont.*

| Joint Description | Identifier | Degree of freedom[a] | | | Comment |
|---|---|---|---|---|---|
| Left wrist | WristL_jnt | R1 yaw left | R2 roll right | | |
| Right wrist | WristR_jnt | R1 yaw left | R2 roll right | | |
| Lumbar Spine | LumbarFlangeUp_jnt | R1 roll left | R2 pitch down | | [c] |
| | LumbarMouldPart6_jnt | R1 yaw left<br>D1 upward | | | [c] |
| | LumbarMouldPart5_jnt | R1 pitch down | R2 roll left | | [c] |
| | LumbarMouldPart3_jnt | R1 roll left | R2 pitch down | | [c] |
| | LumbarMouldPart2_jnt | R1 yaw left<br>D1 upward | | | [c] |
| | LumbarMouldPart1_jnt | R1 pitch down | R2 roll left | | [c] |
| Left hip | HipL_jnt | R1 roll right | R2 pitch down | R3 yaw left | |
| Right hip | HipR_jnt | R1 roll right | R2 pitch down | R3 yaw left | |
| Left knee | KneeL_jnt | R1 pitch down | | | |
| Right knee | KneeR_jnt | R1 pitch down | | | |
| Left ankle | AnkleL_jnt | R1 pitch down | | | |
| Right ankle | AnkleR_jnt | R1 pitch down | | | |

[a] Positive translation or rotation given in global co-ordinate system while dummy is in reference position (see Figure 1.2).
[b] Angle for the neck bracket is directly derived from the physical dummy.
[c] Only for equilibrium state.

## Dummy contacts

Table 7.7: Contact groups for the Hybrid II 50$^{th}$ percentile dummy model.

| Contact Description | Identifier[a] | Surfaces involved[a] | Comment |
|---|---|---|---|
| Head | Head_gfe | Elements and nodes | |
| Neck | Neck_gmb | NeckNoddingPlate_ell<br>Neck_ell | |
| Left Upper Arm | ArmUpL_gmb | ArmUpL_ell | |
| Right Upper Arm | ArmUpR_gmb | ArmUpR_ell | |
| Left Lower Arm | ArmLowL_gmb | ArmLowL_ell | |
| Right Lower Arm | ArmLowR_gmb | ArmLowR_ell | |
| Left Hand | HandL_gfe | Elements and nodes | |
| Right Hand | HandR_gfe | Elements and nodes | |

*Continued on the next page*

7

*Table 7.7 cont.*

| Contact Description | Identifier[a] | Surfaces involved[a] | Comment |
|---|---|---|---|
| Clavicles and Shoulders | Clavicles_gmb | ClavicleL/R_ell<br>ClavicleLinkL/R_ell<br>ShoulderYokeL/R_ell | |
| Jacket | Jacket_gmb | Jacket⟨$i$⟩_ell<br>for i=01 to 50<br>Jacket99_ell<br>Collar_ell | |
| Thorax | Thorax_gmb | Jacket⟨$i$⟩_ell<br>for i=01 to 50<br>Jacket99_ell<br>Collar_ell<br>ClavicleL/R_ell<br>ClavicleLinkL/R_ell<br>ShoulderYokeL/R_ell | Jacket_gmb +<br>Clavicles_gmb |
| Abdomen | Abdomen_gmb | AbdomenMid_ell | |
| Pelvis | Pelvis_gmb | Pelvis_ell<br>PelvisUp_ell<br>PelvisFemurR/L_ell<br>PelvisButtockL/R_ell | for seat contact |
| | Pelvis_gfe | Elements and nodes | for FE lap belt contact |
| Left Femur and Knee | FemurKneeL_gmb | FemurL_ell<br>KneeL_ell | |
| Right Femur and Knee | FemurKneeR_gmb | FemurR_ell<br>KneeR_ell | |
| Left Femur | FemurL_gmb | FemurL_ell | for seat contact |
| | FemurLapBeltL_gmb | FemurLapBeltL_ell | for FE lap belt contact |
| Right Femur | FemurR_gmb | FemurR_ell | for seat contact |
| | FemurLapBeltR_gmb | FemurLapBeltR_ell | for FE lap belt contact |
| Left Knee | KneeL_gmb | KneeL_ell | |
| Right Knee | KneeR_gmb | KneeR_ell | |
| Left Tibia | TibiaL_gmb | TibiaL_ell | |
| Right Tibia | TibiaR_gmb | TibiaR_ell | |
| Left Foot | FootL_gmb | FootL_ell | |
| Right Foot | FootR_gmb | FootR_ell | |
| Left Shoe | ShoeL_gmb | ShoeSoleL_ell<br>ShoeHeelL_ell | |
| Right Shoe | ShoeR_gmb | ShoeSoleR_ell<br>ShoeHeelR_ell | |

[a] L=Left, R=Right

### Use of conventional belts

Table 7.8 is a sequential list of the proposed points of attachment for a conventional belt to the ellipsoid dummy model. These are valid for a left hand side positioned belt; for a right hand side belt, replace LHS with RHS and switch the pelvis order.

Table 7.8: Belt attachment points defined for the Hybrid II 50$^{th}$ percentile model.

| Attachment point | |
|---|---|
| **point 1 (POINT_REF_1)** | **point 2 (POINT_REF_2)** |
| defined by user (D-ring) | ClavicleLHS_pnt |
| ClavicleLHS_pnt | RibsLowLHS_pnt |
| RibsLowLHS_pnt | defined by user (buckle) |
| defined by user (buckle) | PelvisR_pnt |
| PelvisL_pnt | defined by user |

### Use of FE belts

In many applications of this dummy, a FE belt can be used instead of a conventional belt. During loading conditions with a significant vertical component, slip of the belt over the dummy is relevant, and the most convenient way to take this aspect into account is to use a FE belt.

In the application manual an example is given on how to position a FE belt on a facet dummy model (see Application manual). A similar procedure can be applied to position a FE belt on an ellipsoid dummy model. The MADYMO XMADgic editor can also be used to automatically design FE belt systems.

When FE belts are used the dummy-belt contacts should be defined as described in Table 7.9. In the user file of the dummy model, those contact definitions are also available in a DISABLE block so that the user can easily use them in his own application.

Table 7.9: Contact definition for the Hybrid II 50$^{th}$ percentile dummy - FE belt interactions.

| Contact Description | Master Group(s) | Slave group | Remarks |
|---|---|---|---|
| Shoulder Belt to Dummy | Neck_gmb<br>Thorax_gmb<br>ArmUpL_gmb<br>ArmUpR_gmb<br>Abdomen_gmb | ShoulderBelt_gfe | Use orthotropic friction<br>Longitudinal friction 0.3<br>Lateral friction 0.4 |
| Lap Belt to Abdomen | Abdomen_gmb | LapBelt_gfe | Friction 0.3 |
| Lap Belt to Pelvis | Pelvis_gfe | LapBelt_gfe | Use orthotropic friction<br>Longitudinal friction 0.3<br>Lateral friction 1.0 |
| Lap Belt to Femurs | FemurLapBeltL_gmb<br>FemurLapBeltR_gmb | LapBelt_gfe | Friction 0.3 |

7

## Output

Table 7.10: Output signals for the Hybrid II 50$^{th}$ percentile dummy model.

| Sensor | Identifier | Signal resultant | x | direction[a] | y | direction[a] | z | direction[a] | Filter |
|---|---|---|---|---|---|---|---|---|---|
| Head | | | | | | | | | |
| CG acceleration[b] | HeadCG_acc | ar | a1 | forward | a2 | lateral | a3 | vertical | CFC1000 |
| CG position | HeadCG_pos | dr | d1 | forward | d2 | leftward | d3 | upward | CFC600 |
| Neck | | | | | | | | | |
| Upper load cell | NeckUp_lce_F | fr | f1 | shear | f2 | shear | f3 | axial | CFC1000 |
| | NeckUp_lce_T | tr | t1 | roll | t2 | pitch | t3 | yaw | CFC600 |
| Lower load cell | NeckLow_lce_F | fr | f1 | shear | f2 | shear | f3 | axial | CFC1000 |
| | NeckLow_lce_T | tr | t1 | roll | t2 | pitch | t3 | yaw | CFC600 |
| Thorax | | | | | | | | | |
| Acceleration[b] | Thorax_acc | ar | a1 | forward | a2 | lateral | a3 | vertical | CFC180 |
| Chest deflection | ChestDeflection_dis | dr | d1 | displacement | | | | | CFC600 |
| | ChestDefl_dis_CFC180 | dr | d1 | displacement | | | | | CFC180 |
| Lumbar Spine | | | | | | | | | |
| Lower load cell | LumbarSpineLow_lce_F | fr | f1 | shear | f2 | shear | f3 | axial | CFC1000 |
| | LumbarSpineLow_lce_T | tr | t1 | roll | t2 | pitch | t3 | yaw | CFC1000 |
| Pelvis | | | | | | | | | |
| Acceleration[b] | Pelvis_acc | ar | a1 | forward | a2 | lateral | a3 | vertical | CFC1000 |
| Position | Pelvis_pos | dr | d1 | forward | d2 | leftward | d3 | upward | CFC600 |
| Femur | | | | | | | | | |
| Left load cell | FemurL_lce_F | fr | f1 | shear | f2 | shear | f3 | axial | CFC600 |
| | FemurL_lce_T | tr | t1 | roll | t2 | pitch | t3 | yaw | CFC600 |
| Right load cell | FemurR_lce_F | fr | f1 | shear | f2 | shear | f3 | axial | CFC600 |
| | FemurR_lce_T | tr | t1 | roll | t2 | pitch | t3 | yaw | CFC600 |
| Knee | | | | | | | | | |
| Position | | | | | | | | | |
| Left | KneeL_pos | dr | d1 | forward | d2 | leftward | d3 | upward | CFC600 |
| Right | KneeR_pos | dr | d1 | forward | d2 | leftward | d3 | upward | CFC600 |
| Tibia | | | | | | | | | |
| Left Upper load cell | TibiaUpL_lce_F | fr | f1 | shear | f2 | shear | f3 | axial | CFC600 |
| | TibiaUpL_lce_T | tr | t1 | roll | t2 | pitch | t3 | yaw | CFC600 |
| Right Upper load cell | TibiaUpR_lce_F | fr | f1 | shear | f2 | shear | f3 | axial | CFC600 |
| | TibiaUpR_lce_T | tr | t1 | roll | t2 | pitch | t3 | yaw | CFC600 |
| Left Lower load cell | TibiaLowL_lce_F | fr | f1 | shear | f2 | shear | f3 | axial | CFC600 |
| | TibiaLowL_lce_T | tr | t1 | roll | t2 | pitch | t3 | yaw | CFC600 |
| Right Lower load cell | TibiaLowR_lce_F | fr | f1 | shear | f2 | shear | f3 | axial | CFC600 |
| | TibiaLowR_lce_T | tr | t1 | roll | t2 | pitch | t3 | yaw | CFC600 |

[a] Positive direction given according to SAE J211/1.

[b] The calculated acceleration is corrected in the x direction for a prescribed fictitious acceleration field to get correct

values (see Theory manual).

## Injury

Table 7.11: Injury criteria defined for the Hybrid II 50$^{th}$ percentile dummy model.

| Injury criteria | Identifier | Filter |
|---|---|---|
| Head | | |
| HIC(no window) | HIC_inj | CFC1000 |
| HIC (15ms) | HIC15_inj | CFC1000 |
| HIC (36ms) | HIC36_inj | CFC1000 |
| HIC (50ms) | HIC50_inj | CFC1000 |
| Thorax | | |
| 3ms (cumulative) | T3MS_inj | CFC180 |
| 3ms (contiguous) | TCon3MS_inj | CFC180 |
| Femurs | | |
| FFC | | |
| Left | FFCL_inj | CFC600 |
| Right | FFCR_inj | CFC600 |



## Position Markers

For comparison of kinematic data, markers have been defined at the locations of the head centre of gravity, the pelvis H-point, and the left and right knees. The displacement of these locations can be determined relative to a reference point named **Disp_Ref_point**, which is to be defined in the main application XML file. See the dummy model user file for the definitions of these points.

## Notes

Hardware calibration procedures prescribe that "Limb joints are set at 1 G, barely restraining the weight of the limb when it is extended horizontally" (CFR part 572 subpart B, paragraph 11). Static hip joint friction is estimated to be about 56.1 Nm to comply with the hardware calibration procedures. However, a friction much below 56.1 Nm is often applied in real dummies. **A default friction of 12.8 Nm is defined in the model**. These values can be adjusted in the model if required. Note that the frictions settings in the joints can have a significant influence on the dummy model response, so it is important to check this setting with the settings of the actual dummy used, or to be used, in the experiment.

## 7.4 Example: sled test with two-point FE belt restraint

This example features the Hybrid II 50$^{th}$ percentile dummy in a sitting position on a sled with rigid seat, restrained by a two-point FE harness. The dummy is subjected to a crash pulse with a peak acceleration of 16 G and duration of 170 ms. This example is meant to help the user in correct usage of the dummy model, particularly on positioning and contact definitions. The input of the model is given in the file:

Ellipsoid model: e_p57250el.xml

The model set-up is illustrated in Figure 7.5. The example uses a FE harness. The harness has been positioned using the XMADGIC Belt fit preprocessor.

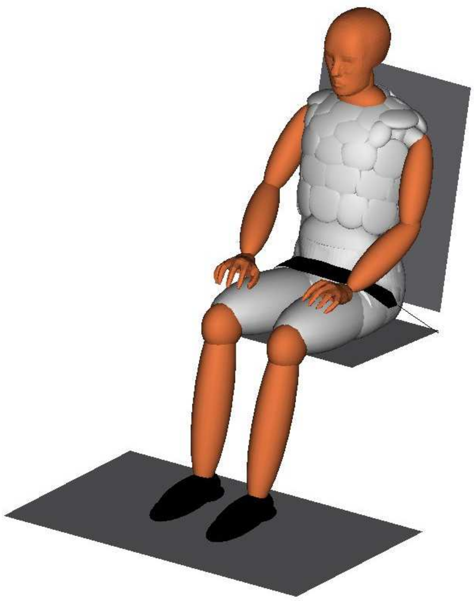

Figure 7.5: Two-point lap belt test set-up for the Hybrid II 50th percentile ellipsoid model.

**Results**

For a complete overview of the results the reader is referred to the Quality Report.

# 8 Hybrid III 50 FAA Dummy

The Hybrid III 50$^{th}$ percentile FAA dummy is a Hybrid III 50$^{th}$ percentile male based dummy used for the development and certification of aircraft seats. The dummy is allowed by the Federal Aviation Administration (FAA) as an alternative to the Hybrid II dummy in dynamic aircraft seat test regulations FAR/JAR 23, 25, 27 and 29 Section 562. The main difference between the standard Hybrid III and the Hybrid FAA is the lumbar spine, that is capable of a more realistic response in severe vertical loading. The major improvement of the Hybrid III 50$^{th}$ FAA over the Hybrid II dummy is the extended instrumentation, in particular in the thorax, neck, and leg regions.



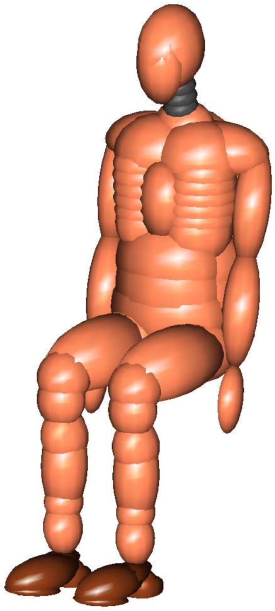

Figure 8.1: Hybrid III 50$^{th}$ FAA ellipsoid dummy model in reference position.

## 8.1 Model description

An ellipsoid model of the Hybrid III 50$^{th}$ FAA dummy is available. The input is given in the files:

| | |
|---|---|
| Ellipsoid mode | d_hyb350faael_usr.xml<br>d_hyb350faael_inc.xml |

To run the model, the following licenses are required:

| | |
|---|---|
| Ellipsoid model: | MADYMO/Solver (Multibody)<br>MADYMO/Aviation |

Figure 8.1 shows the model in reference position. The ellipsoid model consists of 49 bodies. The inertia properties in the model include the standard instrumentation consisting of the sternum deflection sensor and the acceleration sensors of the lower torso, the upper torso and the head. The inertia of the clothes is not included in the model.

**ELLIPSOID MODEL**

The model is based on the standard Hybrid III 50$^{th}$ percentile model. The differences with respect to the standard Hybrid III 50$^{th}$ percentile ellipsoid model are described below. For a description of those parts equivalent to the standard Hybrid III 50$^{th}$ percentile is referred to "ELLIPSOID MODEL" on page 416.

**Thorax/Ribs and sternum**

The chest flesh is a Hybrid II part. The chest flesh is modelled similar to the Hybrid III 50$^{th}$ percentile male dummy ellipsoid model, but the size, location and contact characteristics of the ellipsoids have been adjusted.

**Lumbar spine**

The lumbar spine is a Hybrid II part. The lumbar spine model is quite detailed, with representations of both the straight rubber column as well as the internal steel cable. The rubber colum is a series of bodies connected by free joints which are limited in their range of motion by protected joint resistance models. The division into mutiple bodies connected by free joints has been done in order to allow a realistic deformation of the lumbar spine in different loading modes. The protected joint resistance model describes the lumbar spine compliance in the model. The relations between rotations (bending and torsion) and displacements (compression, elongation and shear) are specified in the protected model. The mass and inertia properties of the actual lumbar spine have been divided over the lumbar spine bodies. The upper spine body is connected to the upper torso by means of a bracket joint, similarly the lower spine body is connected to the lower torso. These bracket joints allow for the output of constraint loads at the upper and lower lumbar spine loadcells. The detail in the model ensures that loads and forces at both ends of the lumbar spine are measured correctly.

In the complete physical dummy, lumbar spine deformation is not only resisted by the lumbar spine itself but also by contact interaction of the rib cage, the abdomen and the lower torso. This interaction is included in the models with three point-restraints. These point-restraints are referred to as "AbdomenVertL/M/R".

### Abdomen

The abdomen is a standard Hybrid II part. The abdomen has been modelled as a separate body, which is connected to the lower torso with a translational joint. This body is included to describe the combined deformation of the abdomen and the lower torso flesh in response to lap belt loading. A modified Hybrid III FAA exists, in which the abdomen has a cut-away to make place for the Hybrid III chest deflection potentiometer. The Hybrid III 50$^{th}$ FAA ellipsoid model also represents the modified hardware dummy.

### Pelvis

Two additional ellipsoids have been added to the pelvis. These represent the inferior points on the metal pelvis bone casting of the Hybrid-III pelvis and can be used to model contact between the pelvis bone and the seat if the pelvis flesh is fully compressed.

### Legs, ankles and feet

The legs, ankles and feet are Hybrid II components, but the lower legs and feet are Hybrid III. The model is identical to the ellipsoid Hybrid III 50$^{th}$ percentile dummy, but inertia and dimensions have been modified to represent Hybrid II legs instead.

## CONTACTS BETWEEN DUMMY COMPONENTS

In the model contacts are defined between the head and thorax, the thorax and left and right upper leg, between the upper legs and between lower arms and upper legs.

8

## 8.2 Model validation

The validation of model components that have been taken from the Hybrid III 50$^{th}$ percentile male dummy ellipsoid model, is described in "Model validation" on page 78. In this chapter only Hybrid III 50$^{th}$ FAA specific validation is described.

### Component tests

The component tests used for development of the Hybrid III 50$^{th}$ FAA specific components are summarised below. Validation results of the thorax are shown in Figure 8.2.

Table 8.1: Component tests performed for Hybrid III 50th FAA specific components.

| Component | Test description | specifications | | Model Ellipsoid |
|---|---|---|---|---|
| Thorax | Pendulum impact | mass<br>velocity | 23.4 kg,<br>3.97 m/s | x |
| | | | 23.4 kg,<br>6.68 m/s | x |

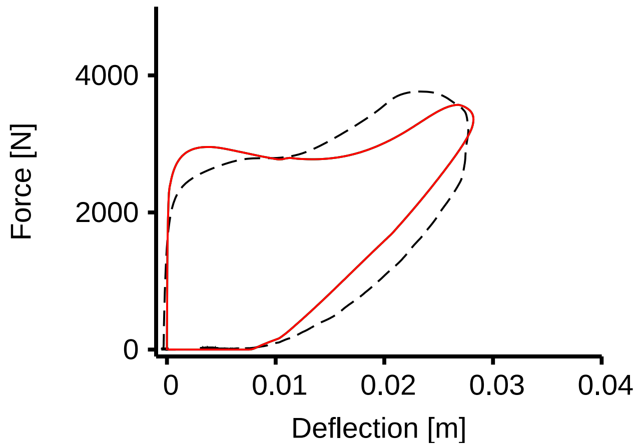


Figure 8.2: Results of thorax pendulum impact validation, experiment (— — —) and simulation (———).

### Full dummy tests

The tests with the complete dummy used for development and validation of the models are summarised in Table 8.2. A sled test is shown in the example (See section 8.4 "Example: sled test with FE harness restraint" on page 116.). The result of the sled test example is shown in Figure 8.3.

Table 8.2: Full dummy tests for Hybrid III 50th FAA models.

| **Test** | | **Model** |
|---|---|---|
| **description** | **specification** | **Ellipsoid** |
| | **max acc., duration** | |
| Horizontal (0° ) sled test with belted dummy on rigid seat | 18 G, 142 ms | x |
| Vertical (90° ) sled test with belted dummy on rigid seat | 30 G, 62 ms | x |
| Oblique (60° ) sled test with belted dummy on rigid seat | 30 G, 62 ms | x |



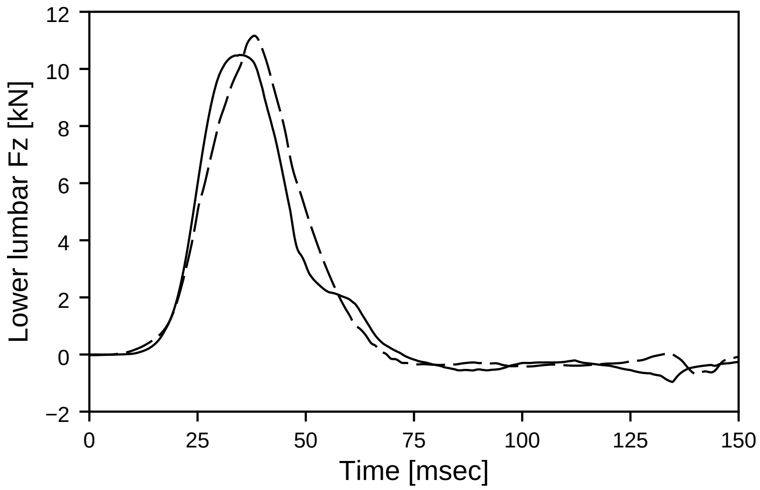


Figure 8.3: Results of lower lumber spine vertical load during full dummy 60 degree oblique sled test on rigid seat; experiment (— — —), simulation (———).

### Range of validity of the model

Multi-directional component tests were used to develop models of all kinematic joints, the neck and the lumbar spine.

8

## 8.3 User instructions

### Timestep

Table 8.3: Recommended timestep for the Hybrid III 50th percentile FAA dummy model.

| Model | timestep (s) |
|---|---|
| Ellipsoid | $\leq 5.0 \cdot 10^{-6}$ |

### Dummy positioning

Table 8.4: Positioning joints of the Hybrid III 50th percentile FAA dummy.

| Joint Description | Identifier | Degree of freedom$^{(a)}$ | | | | | | Comment |
|---|---|---|---|---|---|---|---|---|
| Dummy | Dummy_jnt | D1 | forward | D2 | leftward | D3 | upward | Dummy position |
| Neck bracket | NeckBracket_jnt | R1 | pitch down | | | | | $^{(b)}$ |
| Neck element | NeckPivot⟨i⟩_jnt, for i=1 to 4 $^{(c)}$ | R1 | roll right | R2 | pitch down | R3 | yaw left | only for equilibrium state |
| Left clavicle | ClavicleL_jnt | R1 | roll right | R2 | yaw left | | | only for equilibrium state |
| Right clavicle | ClavicleR_jnt | R1 | roll right | R2 | yaw left | | | |
| Left shoulder | ShoulderL_jnt | R1 | pitch down | R2 | roll right | | | |
| Right shoulder | ShoulderR_jnt | R1 | pitch down | R2 | roll right | | | |
| Left elbow | ElbowL_jnt | R1 | yaw left | R2 | pitch down | | | |
| Right elbow | ElbowR_jnt | R1 | yaw left | R2 | pitch down | | | |
| Left wrist | WristL_jnt | R1 | yaw left | R2 | roll right | | | |
| Right wrist | WristR_jnt | R1 | yaw left | R2 | roll right | | | |
| Lumbar spine | SpineMouldPivot ⟨i⟩ _jnt (1-5) SpineCablePivot ⟨i⟩ _jnt (1-5) SpineCableBall_ jnt $^{(d)}$ | R1 | roll right | R2 | pitch down | R3 | yaw left | only for equilibrium state |
| Left hip | HipL_jnt | R1 | roll left | R2 | pitch down | R3 | yaw left | |
| Right hip | HipR_jnt | R1 | roll left | R2 | pitch down | R3 | yaw left | |
| Left knee | KneeL_jnt | R2 | pitch down | | | | | |
| | | D1 | compression | | | | | always zero |
| Right knee | KneeR_jnt | R2 | pitch down | | | | | |
| | | D1 | compression | | | | | always zero |
| Left ankle | AnkleL_jnt | R1 | yaw right | R2 | roll left | R3 | pitch down | |

*Continued on the next page*

*Table 8.4 cont.*

| Joint Description | Identifier | Degree of freedom[a] | | | | | | Comment |
|---|---|---|---|---|---|---|---|---|
| Right ankle | AnkleR_jnt | R1 | yaw right | R2 | roll left | R3 | pitch down | |

[a] Positive translation or rotation given in global co-ordinate system while dummy is in reference position (see Figure 8.1)
[b] Angle for the neck bracket is directly to derive from the physical dummy. A lower neck load cell in the physical dummy means a zero angle for the neck bracket.
[c] Part⟨i⟩: numbered from bottom to top / rear to front / right to left.
[d] All SpineMouldPivot_jnt angles should be identical, and no more than 0.05 rad. The SpineCablePivot_jnt and SpineCableBall_jnt angles should be set at 5/6 (83.3%) of the SpineMouldPivot_jnt angles.



## Dummy contacts

Table 8.5: Contact groups for the Hybrid III $50^{th}$ percentile FAA dummy.

| Contact Description | Identifier [a] [b] | Ellipsoid model [b] [c] |
|---|---|---|
| Head | Head_*ctg* | Head_ell<br>Face_ell |
| Neck | Neck_*ctg* | NeckNoddingPlate_ell<br>NeckPart⟨*i*⟩_ell,<br>for i=1 to 5 |
| Left Upper Arm | ArmUpL_*ctg* | ArmUpL_ell |
| Right Upper Arm | ArmUpR_*ctg* | ArmUpR_ell |
| Left Lower Arm and Hand | ArmLowL_*ctg* | ArmLowL_ell HandL_ell |
| Right Lower Arm and Hand | ArmLowR_*ctg* | ArmLowR_ell HandR_ell |
| Shoulders | Shoulders_ctg | Collar_ell<br>ShoulderL/R_ell |
| Thorax | Thorax_*ctg* | ChestUpL/R_ell<br>RibPart⟨*i*⟩L/R_ell,<br>for i=1 to 6<br>Sternum_ell<br>ThoracicBackPlate_ell |
| Ribcage | Ribcage_*ctg* | ChestUpL/R_ell<br>RibPart⟨*i*⟩L/R_ell,<br>for i=1 to 6<br>Sternum_ell |
| Abdomen | Abdomen_*ctg* | AbdomenLow_ell<br>AbdomenMid_ell<br>AbdomenUp_ell |
| Pelvis | Pelvis_*ctg* | Pelvis_ell<br>HipL/R_ell<br>PelvisButtockL/R |

*Continued on the next page*

8

*Table 8.5 cont.*

| Contact Description | Identifier [a] [b] | Ellipsoid model [b] [c] |
|---|---|---|
| Left Femur | FemurL_*ctg* | FemurL_ell |
| Left Knee | KneeL_*ctg* | KneeL_ell |
| Right Femur | FemurR_*ctg* | FemurR_ell |
| Right Knee | KneeR_*ctg* | KneeR_ell |
| Left Femur and Knee | FemurKneeL_*ctg* | FemurL_ell KneeL_ell |
| Right Femur and Knee | FemurKneeR_*ctg* | FemurR_ell KneeR_ell |
| Left Tibia | TibiaL_*ctg* | TibiaPart⟨*i*⟩L_ell, for i=1 to 5 |
| Right Tibia | TibiaR_*ctg* | TibiaPart⟨*i*⟩R_ell, for i=1 to 5 |
| Left Shoe | ShoeL_*ctg* | ShoeSoleL_ell ShoeHeelL_ell ShoeFrontL_ell |
| Right Shoe | ShoeR_*ctg* | ShoeSoleR_ell ShoeHeelR_ell ShoeFrontR_ell |

[a] *ctg*= contact group, for all ellipsoid models *ctg* is replaced by gmb(group_multibody).
[b] L=Left; R=Right.
[c] Part ⟨i⟩: numbered from bottom to top / rear to front / right to left.

## Conventional belt positioning

For the usual applications of this dummy, it is recommended to use a FE belt instead of a conventional belt. During loading conditions with a significant vertical component, slip of the belt over the dummy is relevant, and the most convenient way to take this aspect into account is to use a FE belt. If, e.g. for reasons of calculation speed, a conventional belt is needed, the belt must be attached directly to the dummy. For this purpose the attachment points given below in Table 8.6 can be used.

Table 8.6: Proposed attachment points on the ellipsoid model for the conventional belt for left hand side position in sequential order.[a]

| Attachment point | |
|---|---|
| **point 1 (POINT_REF_1)** | **point 2 (POINT_REF_2)** |
| defined by user (D-ring) | ClavicleLHS_pnt |
| ClavicleLHS_pnt | RibsUpLHS_pnt |
| RibsUpLHS_pnt | RibsLowLHS_pnt |
| RibsLowLHS_pnt | defined by user (buckle) |
| defined by user (buckle) | AbdomenInsertR_pnt |
| AbdomenInsertL_pnt | defined by user |

[(a)] For a Right Hand Side (RHS) belt, replace LHS (Left Hand Side) by RHS and switch the order of the AbdomenInsert point.

### FE belt positioning

An example is given in the application manual on how to position a FE belt on a facet dummy model (see Application manual). A similar procedure can be applied to position a FE belt on an ellipsoid dummy model.

Note: If a FE belt is used with an ellipsoid dummy, the contact group Ribcage_gmb must be used, and *not* the Thorax_gmb or Dummy_gmb contact groups. The reason for this is that for large deformations of the abdomen or thorax, the FE belt may contact the lumbar spine or thoracic spine ellipsoids. These ellipsoids are only intended for contacts between the dummy and the seat and are not supposed to come in contact with the belts.



### Output

Table 8.7: Output signals for Hybrid III 50th percentile FAA dummy.

| Sensor | Identifier | Signal | | | | | | | Filter |
|---|---|---|---|---|---|---|---|---|---|
| | | resultant | x | direction[(a)] | y | direction[(a)] | z | direction[(a)] | |
| Head | | | | | | | | | |
| CG accelerometer [(b)] | HeadCG_acc | ar | a1 | forward | a2 | lateral | a3 | vertical | CFC1000 |
| Neck | | | | | | | | | |
| Upper load cell | NeckUp_lce_F_CFC1000 | fr | f1 | shear | f2 | shear | f3 | axial | CFC1000 |
| | NeckUp_lce_F_CFC600 | fr | f1 | shear | f2 | shear | f3 | axial | CFC600 |
| | NeckUp_lce_T | tr | t1 | roll | t2 | pitch | t3 | yaw | CFC600 |
| Lower load cell | NeckLow_lce_F_CFC1000 | fr | f1 | shear | f2 | shear | f3 | axial | CFC1000 |
| | NeckLow_lce_F_CFC600 | fr | f1 | shear | f2 | shear | f3 | axial | CFC600 |
| | NeckLow_lce_T | tr | t1 | roll | t2 | pitch | t3 | yaw | CFC600 |
| Thorax | | | | | | | | | |
| accelerometer | Thorax_acc | ar | a1 | forward | a2 | lateral | a3 | vertical | CFC180 |
| deflection | ChestDeflection_dis | dr | d1 | displacement | | | | | CFC600 |
| Chest | ChestDefl_dis_CFC180 | dr | d1 | displacement | | | | | CFC180 |
| | ChestDeflection_vel_ CFC600 | vr | v1 | velocity | | | | | CFC600 |
| Sternum accelerometer | Sternum_acc | ar | a1 | forward | a2 | lateral | a3 | vertical | CFC1000 |
| Upper Spine accelerometer | UpperSpineT1_acc | ar | a1 | forward | a2 | lateral | a3 | vertical | CFC180 |
| Lower Spine accelerometer | LowerSpineT12_acc | ar | a1 | forward | a2 | lateral | a3 | vertical | CFC180 |
| Lumbar Spine | | | | | | | | | |
| Upper load cell | LumbarSpineUp_lce_F | fr | f1 | shear | f2 | shear | f3 | axial | CFC1000 |
| | LumbarSpineUp_lce_T | tr | t1 | roll | t2 | pitch | t3 | yaw | CFC1000 |

*Continued on the next page*

*Table 8.7 cont.*

| Sensor | Identifier | Signal resultant | x | direction[a] | y | direction[a] | z | direction[a] | Filter |
|---|---|---|---|---|---|---|---|---|---|
| Lower load cell | LumbarSpineLow_lce_F | fr | f1 | shear | f2 | shear | f3 | axial | CFC1000 |
| | LumbarSpineLow_lce_T | tr | t1 | roll | t2 | pitch | t3 | yaw | CFC1000 |
| Pelvis | | | | | | | | | |
| Accelerometer[b] | Pelvis_acc | ar | a1 | forward | a2 | lateral | a3 | vertical | CFC1000 |
| Femur | | | | | | | | | |
| Left load cell | FemurL_lce_F | fr | f1 | shear | f2 | shear | f3 | axial | CFC600 |
| | FemurL_lce_T | tr | t1 | roll | t2 | pitch | t3 | yaw | CFC600 |
| Right load cell | FemurR_lce_F | fr | f1 | shear | f2 | shear | f3 | axial | CFC600 |
| | FemurR_lce_T | tr | t1 | roll | t2 | pitch | t3 | yaw | CFC600 |
| Tibia | | | | | | | | | |
| Left Upper load cell | TibiaUpL_lce_F | fr | f1 | shear | f2 | shear | | | CFC600 |
| | TibiaUpL_lce_T | tr | t11 | roll | t2 | pitch | | | CFC600 |
| Right Upper load cell | TibiaUpR_lce_F | fr | f1 | shear | f2 | shear | | | CFC600 |
| | TibiaUpR_lce_T | tr | t1 | roll | t2 | pitch | | | CFC600 |
| Left Lower load cell | TibiaLowL_lce_F | fr | f1 | shear | f2 | shear | f3 | axial | CFC600 |
| | TibiaLowL_lce_T | tr | t1 | roll | t2 | pitch | | | CFC600 |
| Right Lower load cell | TibiaLowR_lce_F | fr | f1 | shear | f2 | shear | f3 | axial | CFC600 |
| | TibiaLowR_lce_T | tr | t1 | roll | t2 | pitch | | | CFC600 |

[a] Positive direction given according to SAE J211/1.

[b] The calculated acceleration is corrected in the x direction for a prescribed fictitious acceleration field to get correct values (see Theory manual).

Table 8.8: Injury criteria defined for the Hybrid III 50$^{th}$ percentile FAA dummy.

| Injury criteria | Identifier | Filter |
|---|---|---|
| Head | | |
| HIC (15) | HIC15_inj | |
| HIC(36) | HIC36_inj | |
| HIC(50) | HIC50_inj | |
| Neck | | |
| FNIC | | |
| tension | FNICtension_inj | CFC1000 |
| shear | FNICshear_inj | CFC1000 |
| bending | FNICbending_inj | CFC1000 |
| NIJ | | |
| tension-extension | NTE_inj | CFC600 (force)<br>CFC600 (moment) |
| tension-flexion | NTF_inj | CFC600 (force)<br>CFC600 (moment) |
| compression-extension | NCE_inj | CFC600 (force)<br>CFC600 (moment) |
| compression-flexion | NCF_inj | CFC600 (force)<br>CFC600 (moment) |

*Continued on the next page*

*Table 8.8 cont.*

| Injury criteria | Identifier | Filter |
|---|---|---|
| NIJ lower neck | | |
| tension-extension | NTELow_inj | CFC600 (force)<br>CFC600 (moment) |
| tension-flexion | NTFLow_inj | CFC600 (force)<br>CFC600 (moment) |
| compression-extension | NCELow_inj | CFC600 (force)<br>CFC600 (moment) |
| compression-flexion | NCFLow_inj | CFC600 (force)<br>CFC600 (moment) |
| Thorax | | |
| 3ms | T3MS_inj | |
| VC | VC_inj_CFC180 VC_inj_CFC600 | CFC180<br>CFC600 (deflection) |
| Femurs | | |
| FFC | | |
| Left | FFCL_inj | CFC600 |
| Right | FFCR_inj | CFC600 |
| Tibia | | |
| TI | | |
| Upper left | TIUpL_inj | CFC600 |
| Upper right | TIUpR_inj | CFC600 |
| Lower Left | TILowL_inj | CFC600 |
| Lower right | TILowR_inj | CFC600 |
| TCFC | | |
| Upper left | TCFCUpL_inj | CFC600 |
| Upper right | TCFCUpR_inj | CFC600 |
| Lower Left | TCFCLowL_inj | CFC600 |
| Lower right | TCFCLowR_inj | CFC600 |

### Position Markers

For comparison of kinematic data, markers have been defined at the locations of the head centre of gravity, the pelvis Hpoint, and the left and right knees. The displacement of these locations can be determined relative to a reference point named **Disp_Ref_point**, which is to be defined in the main application XML file. See the dummy model USR file for the definitions of these points.

### Notes

Hardware calibration procedures describe that "Limb joints are set at 1 G, barely restraining the weight of the limb when it is extended horizontally" (CFR part 572 subpart E). Static hip joint friction is estimated to be about 56.1 Nm to comply with the hardware calibration procedures. However, a friction much below 56.1 Nm is often applied in real dummies. **A default friction of 12.8Nm is defined in the model**. These values can be adjusted in the model if required.Note that the frictions settings in the joints can have a significant influence on the dummy model response, so it is important to check this setting with the settings of the actual dummy used, or to be used, in the experiment.

It should be noted that shoes of different designs are on the market. The user may adapt the shoe model to specific shoes applied in experiments.

8

## 8.4 Example: sled test with FE harness restraint

This example features the Hybrid III $50^{th}$ percentile FAA dummy in a sitting position on a sled, restrained by a FE harness. The dummy is subjected to a severe crash pulse with a peak acceleration of 30 G and a duration of 62 ms. The direction of impact is 60° from below. The input of the model is given in the file:

Ellipsoid model: e_hyb350faael.xml

This file is available upon request. The model set-up of the ellipsoid model is illustrated in Figure 8.4. The example uses a FE harness. The harness has been positioned using the XMADGIC preprocessor, by creating a new FE belt model for each of the four belts.

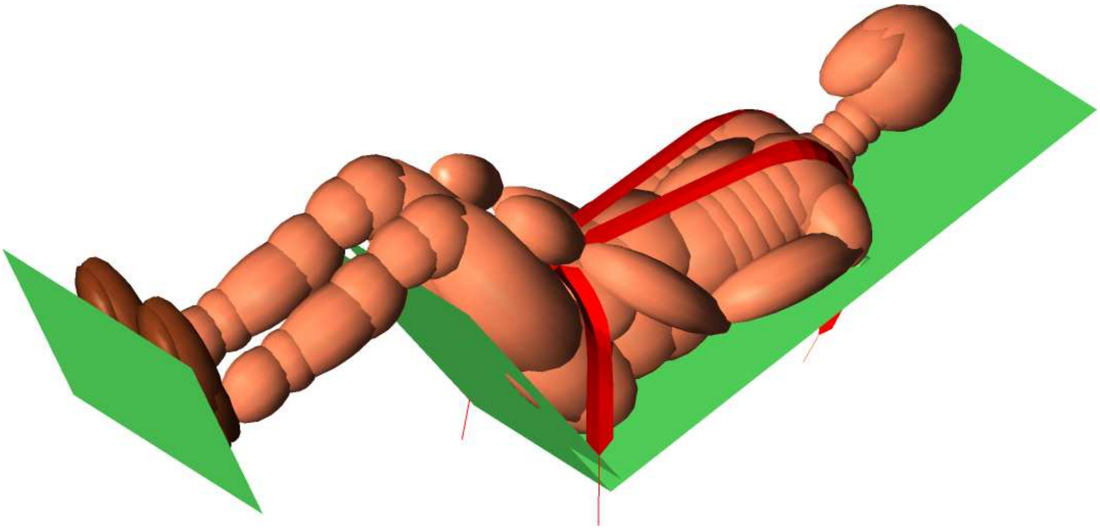

Figure 8.4: Model set-up for the Hybrid III 50th percentile FAA ellipsoid model.

**Environment**

The test environment consists of a rigid seat and a foot plane mounted on a rigid sled. The dummy is placed in a 60° backwards reclined seating position. The applied pulse is horizontal, which is 60° from below with respect to the dummy coordinate system. The test environment is modelled with planes.

**Harness system**

The finite element harness system is attached to the sled by means of single conventional belt system segments.

**Contact interactions**

The dummy interacts with the rigid seat, the foot plane and the belts. The contact interactions defined are listed in Table 8.9. Kinematic contacts are defined between the dummy and all harness parts.

Table 8.9: Contact interactions between dummy and sled for the ellipsoid model.

| **Model type** | **contact surface** | |
|---|---|---|
| | **Master** | **Slave** |
| ellipsoid | SeatPan_gmb | Pelvis_gmb |
| | SeatPan_gmb | FemurKneeL_gmb |
| | SeatPan_gmb | FemurKneeR_gmb |
| | SeatBack_gmb | Pelvis_gmb |
| | SeatBack_gmb | Thorax_gmb |
| | FootRest_gmb | ShoeL_gmb |
| | FootRest_gmb | ShoeR_gmb |

### Results

Though the test is severe, good results are seen for the example. The lower lumbar spine axial force is shown in Figure 8.3 on page 109. In this loading direction the harness without retractors is not very effective in keeping the dummy on the seat.

# 9 THOR 50th percentile Dummy

The National Highway Traffic Safety Agency (NHTSA) in the US has invested significant resources into the research and development of a successor to the Hybrid-III ATD, with the aim of improving the biofidelic occupant response prediction when interacting with advanced restraint systems. The successor dummy has been developed in several stages, and the current designation is the THOR Metric.

The THOR represents a 50$^{th}$ percentile adult male, and is extensively instrumented to capture in detail the loading to the neck, thorax and legs of an occupant as are currently assessed, while also measuring injuries to new areas such as the face and abdomen of the dummy.



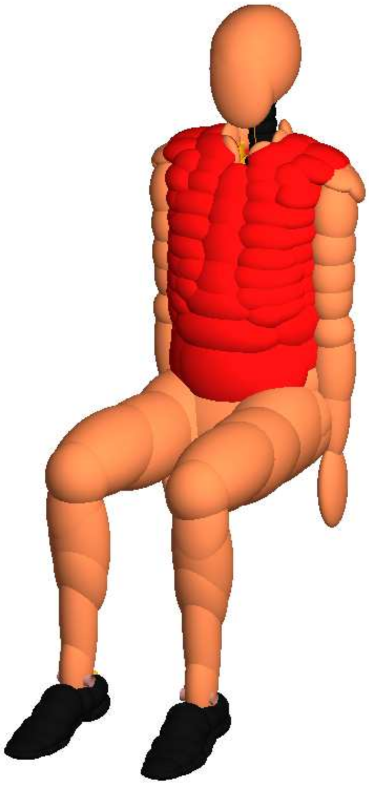

Figure 9.1: THOR 50th percentile (THOR-50M) ellipsoid model

## 9.1 Model description

An ellipsoid model of the THOR-50M dummy is available. The input is given in the files:

| | |
|---|---|
| Ellipsoid model: | d_thor50el_usr.xml<br>d_thor50el_inc.xml |

To run this model, the following licenses are required:

| | |
|---|---|
| Ellipsoid model : | MADYMO/Solver (Multibody)<br>MADYMO/Dummy Models/Frontal/THOR |



Figure 9.1 shows the model in the reference position.

**ELLIPSOID MODEL**

The ellipsoid model was developed based on CAD data and drawing packages released by the NHTSA in September 2015. To this date those documents are still subject to a Request For Comments and pending a Final Decision Notice. This paragraph gives a summarised description of the design of the MADYMO ellipsoid model according to the revision provided by the NHTSA in September 2015.

**Head and neck**

The head is modelled with several contact surfaces for the skull and the face so that the contact loads are measured accurately at the load cells. The head casting is attached to the head/neck mounting platform which supports the front and rear neck cable housings and connects to the upper neck.

The head/neck mounting platform meets the neck at the occipital condyle joint, modelled with a revolute joint. Below that, the neck column is represented by a series of free joints with six-degree-of-freedom restraints applied. This allows the neck to respond omnidirectionally. The neck cables are modelled using multibody belt elements. See Figure 9.2 for the model of the head/neck assembly and the overlay with the CAD data provided by the NHTSA in September 2015.

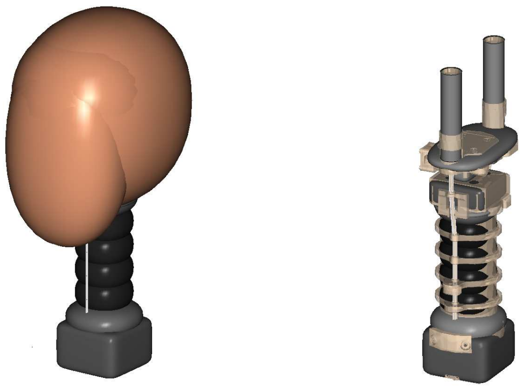

Figure 9.2: THOR-50M ellipsoid head and neck assembly

## Upper and lower torso

The core of the thorax architecture consists of a central spinal column with two flexible joints, one each at the thoracic and lumbar regions. The thoracic joint is modelled with a six-degree-of-freedom restraint, while the lumbar flexion joint is modelled using a triple joint restraint to capture the kinematic behaviour of a thick beam. The ribs are connected flexibly to the thoracic spine and are modelled as flexible components using a succession of universal and revolute joints. See Figure 9.3 for the model of the ribcage and the overlay with the CAD data provided by the NHTSA in September 2015.

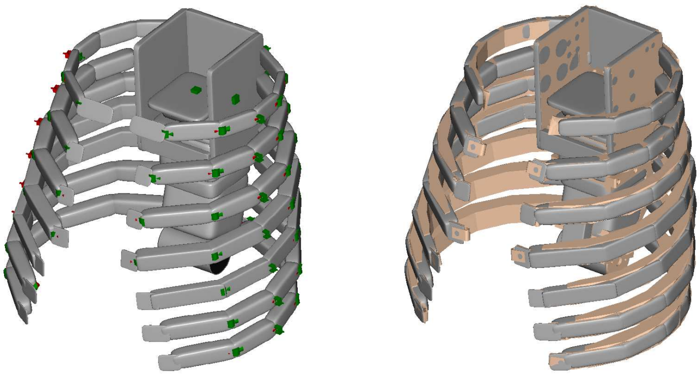

Figure 9.3: THOR-50M ellipsoid ribcage assembly

The posture settings for the dummy are set using DEFINE elements in a GROUP_DEFINE under the SYSTEM.MODEL THOR_50th_sys. Using these, the dummy's posture can be set as erect, normal, slouch or super-slouch.

The ellipsoid model of the THOR-50M includes the SD3 shoulder design. The multi body chain of the SD3 shoulder assembly forms a closed loop between the thoracic spine block and the sternum at the front. It is made of a succession of rigid bodies with universal and revolute joints, completed with joint restraints. See Figure 9.4 for the model of the SD3 shoulder and the overlay with the CAD data provided by the NHTSA in September 2015.

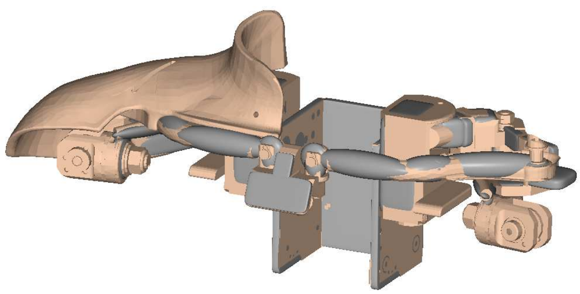

Figure 9.4: THOR-50M ellipsoid SD3 shoulder assembly

The upper and lower abdomen components are modelled as compressible bodies, through both a compliant contact characteristic and the possibility to move relative to the surrounding dummy parts. Both abdomen components are connected to the spine with free joints but kept in place and interacting with other components by means of restraints.

The IR-TRACC sensors that measure rib and abdominal deformation are modelled explicitly and have surfaces assigned to aid visualisation.

The jacket surface is modelled by describing the contact surface with ellipsoids supported directly on the bodies of the substructure. See Figure 9.5 for an overview of the complete thorax model including jacket.

Figure 9.5: THOR-50M ellipsoid thorax

The deformability of the pelvis is entirely captured in the contact stiffness definitions applied to the ellipsoids. The pelvis model also includes iliac wing and acetabular load cells. See Figure 9.6 for the model of the pelvis and the overlay with the CAD data provided by the NHTSA in September 2015.

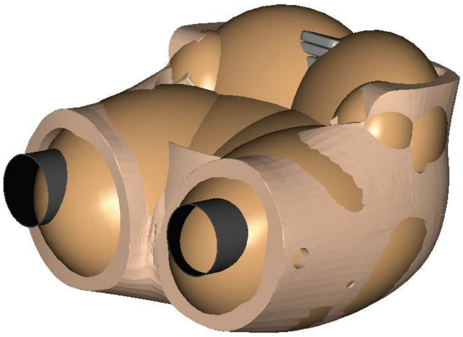

Figure 9.6: THOR-50M ellipsoid pelvis



**Arms**

The arms are modelled as a succession of rigid bodies with single revolute joints in between that represent the different distinct motions of the shoulder, elbow and wrist articulations. The load cell present in the upper arm is also modelled. See Figure 9.7 for the model of the arm and the overlay with the CAD data provided by the NHTSA in September 2015.

Figure 9.7: THOR-50M ellipsoid arm

**Legs**

The femur of the THOR dummy has a compliant section in order to make leg load measurements more biofidelic. This is simulated in the model with a translational joint having a representative restraint stiffness. The femoral load cell is also modelled.

According to the drawing package and CAD data provided by the NHTSA in September 2015, the lower legs of the THOR-50M resemble the lower legs of the THOR-LX and present a moulded foot with separate shoe. The neutral position of the ankle shows 15 degrees plantarflexion. See Figure 9.8 for the model of the lower and upper leg and the overlay with the CAD data provided by the NHTSA in September 2015.

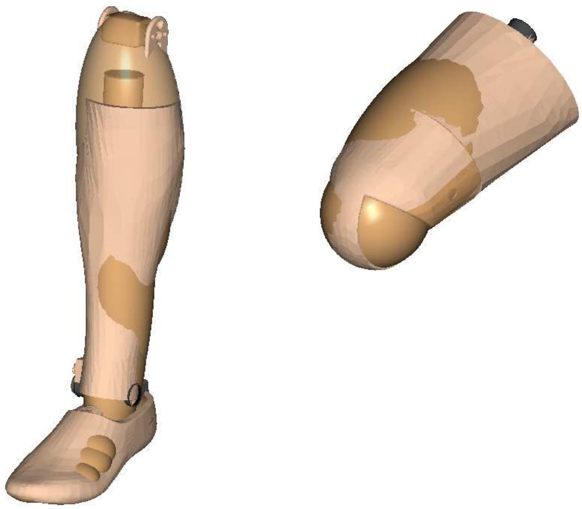

Figure 9.8: THOR-50M ellipsoid lower and upper leg

## CONTACTS BETWEEN DUMMY COMPONENTS

The pre-defined contacts between dummy components can be found in table Table 9.1.

Table 9.1: Intercomponent contacts for the THOR-50M ellipsoid model

| Model Type | Contact | Master Surface | Slave Surface |
|---|---|---|---|
| Ellipsoid | HeadToJacket_cnt | Jacket_gmb | Head_gmb |
| | ArmLToJacket_cnt | Jacket_gmb | ArmL_gmb |
| | ArmRToJacket_cnt | Jacket_gmb | ArmR_gmb |
| | ArmLowLToArmLowR_cnt | ArmLowR_gmb | ArmLowL_gmb |
| | ArmLowLToFemurKneeL_cnt | FemurKneeL_gmb | ArmLowL_gmb |
| | ArmLowLToPelvis_cnt | Pelvis_gmb | ArmLowL_gmb |
| | ArmLowRToFemurKneeR_cnt | FemurKneeR_gmb | ArmLowR_gmb |
| | ArmLowRToPelvis_cnt | Pelvis_gmb | ArmLowR_gmb |
| | Rib4LToRib5L_cnt | Rib4L_gmb | Rib5L_gmb |
| | Rib4RToRib5R_cnt | Rib4R_gmb | Rib5R_gmb |
| | FemurKneeLToFemurKneeR_cnt | FemurKneeR_gmb | FemurKneeL_gmb |
| | FemurKneeLToJacket_cnt | Jacket_gmb | FemurKneeL_gmb |
| | FemurKneeRToJacket_cnt | Jacket_gmb | FemurKneeR_gmb |
| | TibiaLToTibiaR_cnt | TibiaR_gmb | TibiaL_gmb |
| | TibiaLToKneeR_cnt | KneeR_gmb | TibiaL_gmb |
| | TibiaRToKneeL_cnt | KneeL_gmb | TibiaR_gmb |
| | ShoeLToShoeR_cnt | ShoeR_gmb | ShoeL_gmb |
| | ShoeLToTibiaR_cnt | TibiaR_gmb | ShoeL_gmb |
| | ShoeRToTibiaL_cnt | TibiaL_gmb | ShoeR_gmb |
| | CollarToNeck_cnt | Collar[L I R]_gmb | Neck_gmb |
| | HeadToArmL_cnt | Head_gmb | ArmL_gmb |
| | HeadToArmR_cnt | Head_gmb | ArmR_gmb |
| | ShoeLToShoeR_cnt | ShoeR_gmb | ShoeL_gmb |

## 9.2 User instructions

### Timestep

Table 9.2: Recommended timestep for the THOR-50M dummy model.

| Model | timestep (s) |
|---|---|
| Ellipsoid | $\leq 1 \cdot 10^{-5}$ |

### Dummy positioning

Table 9.3: Positioning joints of the THOR-50M dummy model.

| Joint Description | Identifier | Degree of freedom[a] | | | Comment |
|---|---|---|---|---|---|
| Complete dummy | Dummy_jnt | D1 forward<br>R1 roll right | D2 leftward<br>R2 pitch down | D3 upward<br>R3 yaw left | |
| Neck element | NeckOC_jnt | R1 pitch down | | | [b] |
| | NeckPivot1_jnt | D1 forward<br>R1 roll right | D2 leftward<br>R2 pitch down | D3 upward<br>R3 yaw left | [b] |
| | NeckPivot2_jnt | D1 forward<br>R1 roll right | D2 leftward<br>R2 pitch down | D3 upward<br>R3 yaw left | [b] |
| | NeckPivot3_jnt | D1 forward<br>R1 roll right | D2 leftward<br>R2 pitch down | D3 upward<br>R3 yaw left | [b] |
| | NeckPivot4_jnt | D1 forward<br>R1 roll right | D2 leftward<br>R2 pitch down | D3 upward<br>R3 yaw left | [b] |
| | NeckPivot5_jnt | D1 forward<br>R1 roll right | D2 leftward<br>R2 pitch down | D3 upward<br>R3 yaw left | [b] |
| Left shoulder | ShoulderYokeL_jnt<br>ShoulderL_jnt | R1 pitch down<br>R1 roll right | | | |
| Right shoulder | ShoulderYokeR_jnt<br>ShoulderR_jnt | R1 pitch down<br>R1 roll right | | | |
| Left elbow | ElbowPivotL_jnt<br>ElbowL_jnt | R1 yaw left<br>R1 pitch down | | | |
| Right elbow | ElbowPivotR_jnt<br>ElbowR_jnt | R1 yaw left<br>R1 pitch down | | | |
| Left wrist | WristPivotL_jnt<br>WristL_jnt | R1 yaw left<br>R1 roll right | | | |
| Right wrist | WristPivotR_jnt<br>WristR_jnt | R1 yaw left<br>R1 roll right | | | |
| Thoracic Spine | ThoracicSpineFlex_jnt | D1 forward<br>R1 roll right | D2 leftward<br>R2 pitch down | D3 upward<br>R3 yaw left | [b] |
| Lumbar spine | LumbarSpineUp_jnt | R1 roll right | R2 pitch up | | [b] |
| | LumbarSpineMid_jnt | R1 yaw left<br>D1 upward | | | [b] |
| | LumbarSpineLow_jnt | R1 pitch up | R2 roll right | | [b] |
| Left hip | HipL_jnt | R1 roll right | R2 pitch down | R3 yaw left | |

*Continued on the next page*

*Table 9.3 cont.*

| Joint Description | Identifier | Degree of freedom[a] | | | | | | Comment |
|---|---|---|---|---|---|---|---|---|
| Right hip | HipR_jnt | R1 | roll right | R2 | pitch down | R3 | yaw left | |
| Left knee | KneeL_jnt | R1 | pitch down | | | | | |
| Right knee | KneeR_jnt | R1 | pitch down | | | | | |
| Left ankle | AnkleTorsionL_jnt | R1 | yaw left | | | | | |
| | AnkleFlexionL_jnt | R1 | pitch up | | | | | [c] |
| | AnkleVersionL_jnt | R1 | roll right | | | | | |
| | AchillesPistonL_jnt | D1 | upwards | | | | | [c] |
| Right ankle | AnkleTorsionR_jnt | R1 | yaw left | | | | | |
| | AnkleFlexionR_jnt | R1 | pitch up | | | | | [c] |
| | AnkleVersionR_jnt | R1 | roll right | | | | | |
| | AchillesPistonR_jnt | D1 | upwards | | | | | [c] |

[a] Positive translation or rotation given in global co-ordinate system while dummy is in reference position (see Figure 1.2).
[b] In principle only for equilibrium state, however it might be necessary to rotate joints to position the dummy correctly.
[c] The left and right ankle flexion joints are prepositioned using the DEFINE element "AnkleFlexion[L|R]Angle", and the left and right Achilles piston joints are adjusted automatically using a mathematical formula. See description in the user file.

9

### Neck and Spine positioning

The THOR-50M dummy has two pitch changing mechanisms in the spine which allow it to be seated in different postures. The pitches are altered using the DEFINE elements "SpineLow-PitchAngle" and "NeckPitchAngle". These elements accept the value of the pitch settings in degrees, rounded (as in the hardware mechanisms) to discrete values in multiples of 3.

SpineLowPitchAngle has predefined positions corresponding to the four basic seated postures for the THOR-50M, described below:

Table 9.4: Lower spine angles for predefined postures in the THOR-50M .

| Posture | Angle (deg.) |
|---|---|
| Erect | -9 |
| Neutral | 0 |
| Slouch | 9 |
| Super Slouch | 12 |

The *Slouch* posture is the standard seated position analogous to that of the Hybrid-III 50$^{th}$ percentile dummy.

9

### Dummy contacts

Table 9.5: Available groups to define contact between the THOR-50M components and environment.

| Contact zone | Contact group[a] | Comment |
|---|---|---|
| Full Dummy | Dummy_gmb | |
| Head | Head_gmb | |
| Neck | Neck_gmb | |
| Left Arm | ArmL_gmb<br>ArmUpL_gmb<br>ArmLowL_gmb | |
| Right Arm | ArmR_gmb<br>ArmUpR_gmb<br>ArmLowR_gmb | |
| Jacket | Jacket_gmb | |
| Left Shoulder | ShoulderL_gmb<br>CollarL_gmb | |
| Right Shoulder | ShoulderR_gmb<br>CollarR_gmb | |
| Pelvis | Pelvis_gmb | |
| Left Upper Leg | FemurKneeL_gmb<br>FemurL_gmb<br>KneeL_gmb | |
| Right Upper Leg | FemurKneeR_gmb<br>FemurR_gmb<br>KneeR_gmb | |
| Left Lower Leg | TibiaL_gmb<br>FootL_gmb<br>HeelL_gmb<br>ToesL_gmb | |
| Right Lower Leg | TibiaR_gmb<br>FootR_gmb<br>HeelR_gmb<br>ToesR_gmb | |
| Left Shoe | ShoeL_gmb | |
| Right Shoe | ShoeR_gmb | |

[a] L = Left; R = Right

The recommended contacts between dummy and belts are pre-defined in the user file under the SYSTEM.MODEL Belt_to_Dummy_contacts. The references in FE_MODEL of Shoulder-Belt_gfe and LapBelt_gfe needs to be changed to the proper FE-models to make the contacts work. By default the user file will give two warnings due to the fact that the referred FE-model for the belts is empty.

9

## Output

Table 9.6: THOR-50M output signals.

| Sensor | Identifier | Signal | | | | | | |
|---|---|---|---|---|---|---|---|---|
| | | resul-tant | x | direction[(a)] | y | direc-tion[(a)] | z | direc-tion[(a)] |
| Head | | | | | | | | |
| accelerometers[(b)] | HeadCG_CFC1000_acc | ar | a1 | frontal | a2 | lateral | a3 | vertical |
| | HeadTop_CFC1000_acc | | a1 | frontal | a2 | lateral | | |
| | HeadRear_CFC1000_acc | | | | a2 | lateral | a3 | vertical |
| | HeadLeft_CFC1000_acc | | a1 | frontal | | | a3 | vertical |
| ARS | Head_CFC60_avl | avr | av1 | roll | av2 | pitch | av3 | yaw |
| Face load cells | FaceEyeL_CFC600_lce_F | | f1 | compression | | | | |
| | FaceEyeR_CFC600_lce_F | | f1 | compression | | | | |
| | FaceCheekL_CFC600_lce_F | | f1 | compression | | | | |
| | FaceCheekR_CFC600_lce_F | | f1 | compression | | | | |
| | FaceChin_CFC600_lce_F | | f1 | compression | | | | |
| Neck | | | | | | | | |
| Upper load cell | NeckUp_CFC1000_lce_F | fr | f1 | shear | f2 | shear | f3 | axial |
| | NeckUp_CFC600_lce_F | fr | f1 | shear | f2 | shear | f3 | axial |
| | NeckUp_CFC600_lce_T | tr | t1 | roll | t2 | pitch | t3 | yaw |
| Neck OC | NeckOC_CFC180_ang | | phi | pitch | | | | |
| Lower load cell | NeckLow_CFC1000_lce_F | fr | f1 | shear | f2 | shear | f3 | axial |
| | NeckLow_CFC600_lce_T | tr | t1 | roll | t2 | pitch | t3 | yaw |
| Neck spring load cells | NeckFrontSpring_CFC1000_lce_F | | | | | | f3 | axial |
| | NeckRearSpring_CFC1000_lce_F | | | | | | f3 | axial |
| | NeckFrontSpring_CFC600_lce_F | | | | | | f3 | axial |
| | NeckRearSpring_CFC600_lce_F | | | | | | f3 | axial |
| Arms | | | | | | | | |
| Upper load cell | ArmUpL_CFC600_lce_F | fr | f1 | shear | f2 | shear | f3 | axial |
| | ArmUpL_CFC600_lce_T | tr | t1 | roll | t2 | pitch | t3 | yaw |
| | ArmUpR_CFC600_lce_F | fr | f1 | shear | f2 | shear | f3 | axial |
| | ArmUpR_CFC600_lce_T | tr | t1 | roll | t2 | pitch | t3 | yaw |
| Upper Thorax | | | | | | | | |
| Clavicles | ClavicleInL_CFC1000_lce_F | | f1 | shear | | | f3 | shear |
| | ClavicleOutL_CFC1000_lce_F | | f1 | shear | | | f3 | shear |
| | ClavicleInR_CFC1000_lce_F | | f1 | shear | | | f3 | shear |
| | ClavicleOutR_CFC1000_lce_F | | f1 | shear | | | f3 | shear |
| accelerometers[(b)] | SternumMid_CFC1000_acc | ar | a1 | frontal | a2 | lateral | a3 | vertical |
| | Thorax_CFC180_acc | ar | a1 | frontal | a2 | lateral | a3 | vertical |
| | T1_CFC180_acc | ar | a1 | frontal | a2 | lateral | a3 | vertical |
| | T12_CFC180_acc | ar | a1 | frontal | a2 | lateral | a3 | vertical |
| T4 ARS | Thorax_CFC60_avl | avr | av1 | roll | av2 | pitch | av3 | yaw |

*Continued on the next page*

*Table 9.6 cont.*

| Sensor | Identifier | Signal | | | | | | |
|---|---|---|---|---|---|---|---|---|
| | | resul-tant | x | direction[a] | y | direc-tion[a] | z | direc-tion[a] |
| Chest deflection | ChestDeflectionLowL_CFC180_dis | dr | d1 | frontal | d2 | lateral | d3 | vertical |
| | ChestDeflectionLowL_CFC600_dis | dr | d1 | frontal | d2 | lateral | d3 | vertical |
| | ChestDeflectionLowR_CFC180_dis | dr | d1 | frontal | d2 | lateral | d3 | vertical |
| | ChestDeflectionLowR_CFC600_dis | dr | d1 | frontal | d2 | lateral | d3 | vertical |
| | ChestDeflectionUpL_CFC180_dis | dr | d1 | frontal | d2 | lateral | d3 | vertical |
| | ChestDeflectionUpL_CFC600_dis | dr | d1 | frontal | d2 | lateral | d3 | vertical |
| | ChestDeflectionUpR_CFC180_dis | dr | d1 | frontal | d2 | lateral | d3 | vertical |
| | ChestDeflectionUpR_CFC600_dis | dr | d1 | frontal | d2 | lateral | d3 | vertical |
| | ThxIrTraccLowLLength_CFC180_pos | dr | | | | | | |
| | ThxIrTraccLowLLength_CFC600_pos | dr | | | | | | |
| | ThxIrTraccLowRLength_CFC180_pos | dr | | | | | | |
| | ThxIrTraccLowRLength_CFC600_pos | dr | | | | | | |
| | ThxIrTraccUpLLength_CFC180_pos | dr | | | | | | |
| | ThxIrTraccUpLLength_CFC600_pos | dr | | | | | | |
| | ThxIrTraccUpRLength_CFC180_pos | dr | | | | | | |
| | ThxIrTraccUpRLength_CFC600_pos | dr | | | | | | |
| | ThxIrTraccLowLAngleY_CFC180_res | | phi | pitch | | | | |
| | ThxIrTraccLowLAngleZ_CFC180_res | | phi | yaw | | | | |
| | ThxIrTraccLowRAngleY_CFC180_res | | phi | pitch | | | | |
| | ThxIrTraccLowRAngleZ_CFC180_res | | phi | yaw | | | | |
| | ThxIrTraccUpLAngleY_CFC180_res | | phi | pitch | | | | |
| | ThxIrTraccUpLAngleZ_CFC180_res | | phi | yaw | | | | |
| | ThxIrTraccUpRAngleY_CFC180_res | | phi | pitch | | | | |
| | ThxIrTraccUpRAngleZ_CFC180_res | | phi | yaw | | | | |
| Thorax load cells | T12_CFC600_lce_F | fr | f1 | shear | f2 | shear | f3 | axial |
| | T12_CFC600_lce_T | tr | t1 | roll | t2 | pitch | t3 | yaw |
| | T12_CFC180_lce_F | fr | f1 | shear | f2 | shear | f3 | axial |
| | T12_CFC180_lce_T | tr | t1 | roll | t2 | pitch | t3 | yaw |
| Abdomen | | | | | | | | |
| accelerometers[b] | AbdomenUp_CFC1000_acc | | a1 | frontal | | | | |
| | AbdomenUp_CFC180_acc | | a1 | frontal | | | | |
| Abdomen deflection | AbdIrTraccLLength_CFC180_pos | dr | | | | | | |
| | AbdIrTraccRLength_CFC180_pos | dr | | | | | | |
| | AbdomenDeflectionL_CFC180_dis | dr | d1 | frontal | d2 | lateral | d3 | vertical |
| | AbdomenDeflectionR_CFC180_dis | dr | d1 | frontal | d2 | lateral | d3 | vertical |
| | AbdomenDeflectionL_CFC600_dis | dr | d1 | frontal | d2 | lateral | d3 | vertical |
| | AbdomenDeflectionR_CFC600_dis | dr | d1 | frontal | d2 | lateral | d3 | vertical |
| | AbdIrTraccLAngleY_CFC180_res | | phi | pitch | | | | |
| | AbdIrTraccLAngleZ_CFC180_res | | phi | yaw | | | | |
| | AbdIrTraccRAngleY_CFC180_res | | phi | pitch | | | | |
| | AbdIrTraccRAngleZ_CFC180_res | | phi | yaw | | | | |
| Pelvis | | | | | | | | |
| accelerometers[b] | Pelvis_CFC1000_acc | ar | a1 | frontal | a2 | lateral | a3 | vertical |
| ARS | Pelvis_CFC60_avl | avr | av1 | roll | av2 | pitch | av3 | yaw |
| Acetabular load cells[c] | AcetabularL_CFC600_lce_F | fr | f1 | shear | f2 | axial | f3 | shear |
| | AcetabularR_CFC600_lce_F | fr | f1 | shear | f2 | axial | f3 | shear |
| Iliac wing load cells | IliacL_CFC600_lce_F | | f1 | axial | | | | |
| | IliacR_CFC600_lce_F | | f1 | axial | | | | |
| | IliacL_CFC600_lce_T | | | | t2 | pitch | | |
| | IliacR_CFC600_lce_T | | | | t2 | pitch | | |

*Continued on the next page*

*Table 9.6 cont.*

| Sensor | Identifier | Signal | | | | | | |
|---|---|---|---|---|---|---|---|---|
| | | resul-tant | x | direction[a] | y | direc-tion[a] | z | direc-tion[a] |
| Femur | | | | | | | | |
| load cells | FemurL_CFC600_lce_F | fr | f1 | shear | f2 | shear | f3 | axial |
| | FemurR_CFC600_lce_F | fr | f1 | shear | f2 | shear | f3 | axial |
| | FemurL_CFC600_lce_T | tr | t1 | yaw | t2 | pitch | t3 | roll |
| | FemurR_CFC600_lce_T | tr | t1 | yaw | t2 | pitch | t3 | roll |
| | FemurL_CFC180_lce_F | fr | f1 | shear | f2 | shear | f3 | axial |
| | FemurR_CFC180_lce_F | fr | f1 | shear | f2 | shear | f3 | axial |
| | FemurL_CFC180_lce_T | tr | t1 | yaw | t2 | pitch | t3 | roll |
| | FemurR_CFC180_lce_T | tr | t1 | yaw | t2 | pitch | t3 | roll |
| Knee | | | | | | | | |
| Sliders | KneeL_CFC180_dis | | d1 | displacement | | | | |
| | KneeR_CFC180_dis | | d1 | displacement | | | | |
| Tibia | | | | | | | | |
| accelerometers[b] | TibiaFrontalL_CFC1000_acc | | a1 | frontal | | | | |
| | TibiaFrontalR_CFC1000_acc | | a1 | frontal | | | | |
| | TibiaLateralL_CFC1000_acc | | | | a2 | lateral | | |
| | TibiaLateralR_CFC1000_acc | | | | a2 | lateral | | |
| load cells | | | | | | | | |
| | TibiaUpL_CFC600_lce_F | fr | f1 | shear | f2 | shear | f3 | axial |
| | TibiaUpR_CFC600_lce_F | fr | f1 | shear | f2 | shear | f3 | axial |
| | TibiaUpL_CFC600_lce_T | tr | t1 | roll | t2 | pitch | t3 | yaw |
| | TibiaUpR_CFC600_lce_T | tr | t1 | roll | t2 | pitch | t3 | yaw |
| | TibiaLowL_CFC600_lce_F | fr | f1 | shear | f2 | shear | f3 | axial |
| | TibiaLowR_CFC600_lce_F | fr | f1 | shear | f2 | shear | f3 | axial |
| | TibiaLowL_CFC600_lce_T | tr | t1 | roll | t2 | pitch | t3 | yaw |
| | TibiaLowR_CFC600_lce_T | tr | t1 | roll | t2 | pitch | t3 | yaw |
| | AchillesL_CFC600_lce_F | | | | | | f3 | axial |
| | AchillesR_CFC600_lce_F | | | | | | f3 | axial |
| Ankle position | AnkleFlexionL_CFC180_ang | | phi | pitch | | | | |
| | AnkleFlexionR_CFC180_ang | | phi | pitch | | | | |
| | AnkleTorsionL_CFC180_ang | | phi | yaw | | | | |
| | AnkleTorsionR_CFC180_ang | | phi | yaw | | | | |
| | AnkleVersionL_CFC180_ang | | phi | roll | | | | |
| | AnkleVersionR_CFC180_ang | | phi | roll | | | | |
| Foot | | | | | | | | |
| accelerometers[b] | FootL_CFC1000_acc | ar | a1 | frontal | a2 | lateral | a3 | vertical |
| | FootR_CFC1000_acc | ar | a1 | frontal | a2 | lateral | a3 | vertical |

[a] Positive direction given according to SAE J211/1.

[b] The calculated acceleration is corrected in the x-, y- and z-directions for a prescribed fictitious acceleration field to get correct values (see Theory manual).

[c] The left acetabulum load cell output is defined according to the drawing SA572-S128; the polarity is conform to the SAE J211/1 RIGHT SIDE ONLY.

Additionally, output requests for signals in ISO-MME format are pre-defined in the CONTROL_OUTPUT element in the dummy model user file.

### Injury

The injury criteria selected for the THOR-50M component can be found in Table 9.7.

Table 9.7: Injury criteria defined for the THOR-50M.

| Injury criteria | Identifier | Filter |
|---|---|---|
| Head | | |
| HIC 15ms | HIC15_inj | CFC1000 |
| BrIC | BrIC_inj | CFC60 |
| Neck | | |
| NIJ | | CFC600 |
| tension-extension | NTE_inj | CFC600 |
| tension-flexion | NTF_inj | CFC600 |
| compression-extension | NCE_inj | CFC600 |
| compression-flexion | NCF_inj | CFC600 |
| Thorax | | |
| Peak deflection | ChestDeflectionUpLpeakR_CFC180_inj | CFC180 |
| | ChestDeflectionUpRpeakR_CFC180_inj | CFC180 |
| | ChestDeflectionLowLpeakR_CFC180_inj | CFC180 |
| | ChestDeflectionLowRpeakR_CFC180_inj | CFC180 |
| MTIC | MTIC_inj | CFC180 |
| Abdomen | | |
| Peak deflection | AbdomenDeflectionLpeakX_CFC600_inj | CFC600 |
| | AbdomenDeflectionRpeakX_CFC600_inj | CFC600 |
| Abdomen Compression | AbdomenCompression_inj | CFC600 |
| Acetabula | | |
| Peak load | AcetabulumLpeakFrcR_CFC600_inj | CFC600 |
| | AcetabulumRpeakFrcR_CFC600_inj | CFC600 |
| Femurs | | |
| Peak load | FemurLpeakFrcZ_CFC600_inj | CFC600 |
| | FemurLpeakFrcZ_CFC600_inj | CFC600 |
| Tibias | | |
| Peak load | TibiaUpLpeakFrcZ_CFC600_inj | CFC600 |
| | TibiaUpLpeakMomRxy_CFC600_inj | CFC600 |
| | TibiaLowLpeakFrcZ_CFC600_inj | CFC600 |
| | TibiaLowLpeakMomRxy_CFC600_inj | CFC600 |
| | TibiaUpRpeakFrcZ_CFC600_inj | CFC600 |
| | TibiaUpRpeakMomRxy_CFC600_inj | CFC600 |
| | TibiaLowRpeakFrcZ_CFC600_inj | CFC600 |
| | TibiaLowRpeakMomRxy_CFC600_inj | CFC600 |

# 10 BioRID II Rear Impact Q Dummy

The BioRID II (see Figure 10.1) is the production version of a rear impact dummy developed by Chalmers University of Technology, that has been produced to meet the need for more biofidelic dummy response to rear impact events than can be obtained using a standard Hybrid III dummy.

While largely based on the Hybrid III 50$^{th}$ percentile dummy, the BioRID II has a hinged-segment spine design, with each of the 24 vertebrae explicitly represented. Stiffening springs and dampers are fitted to model the effect of the neck muscles, and the thoracic spine and torso are more flexible than that of the Hybrid III.



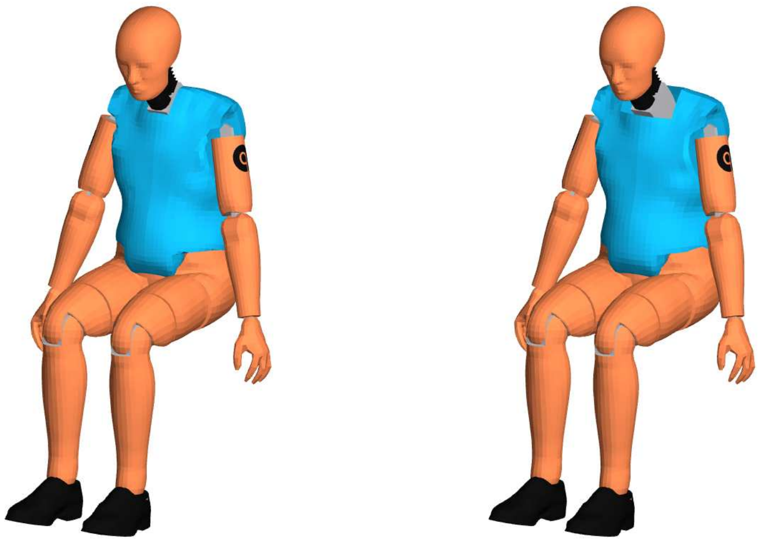

Figure 10.1: Facet (left) and FE (right) Q models of the BioRID II dummy.

## 10.1 Model description

Facet and FE models developed by MADYMO are available. The input is given in the files:

| | |
|---|---|
| Facet model: | d_biorid2fc_usr.xml<br>d_biorid2fc_inc.xml |
| FE model: | d_biorid2fe_usr.xml<br>d_biorid2fe_inc.xml |

To run these models, the following licenses are required:

| | |
|---|---|
| Facet model: | MADYMO/Solver (Multibody)<br>MADYMO/Dummy Models/BioRID_Facet |
| FE model: | MADYMO/Solver (Multibody)<br>MADYMO/Solver (FEM)<br>MADYMO/Dummy Models/BioRID_FE |

Figure 10.1 shows the models in the reference position. The facet model consists of 96 rigid bodies and the FE model of 80.

**FACET AND FE MODELS**

**Head and Neck**

The head is modelled with a rigid body having a facet surface of the head attached. It is connected by a bracket joint to the upper neck load cell, which in turn is connected to the nodding plate.

Each of the seven cervical vertebrae are represented by a rigid body with a facet vertebra associated. The bodies are connected in series by revolute joints; the first and seventh vertebrae are connected by revolute joints to the nodding plate and first thoracic vertebra, respectively.

Muscle substitutes and dampers are also modelled in the neck and upper thoracic spine, using belt elements to represent the wires. These are attached to springs and dampers as appropriate, and feed through the neck to the nodding plate. These have a significant influence on the kinematics of the head.

**Thorax and Lumbar spine**

As with the neck, each of the twelve thoracic- and five lumbar vertebrae are modelled as individual rigid bodies, connected in series by revolute joints. The vertebrae are represented explicitly with facet surfaces; in the facet model this is for visualisation purposes, while in the FE model the interaction between vertebrae and jacket is explicitly modelled with a contact interaction. The fifth lumbar vertebra is connected to the sacral block via a revolute joint; this in turn is connected to the pelvis with a bracket joint.

The first thoracic vertebra is modelled as two bodies joined by a bracket joint, allowing measurements to be taken from the lower neck load cell.

Each clavicle is attached to the first thoracic body with a free joint and in the case of the facet model, restrained with a SIXDOF restraint that captures the stiffness of the jacket. The clavicles are attached to the adjacent upper arms.

The jacket and the water cavity are modelled explicitly in the FE model, nodes of the jacket corresponding to the position of the spin pins are supported on the relevant spine bodies. The facet model divides the jacket into layers, each of which is assigned to the relevant pinning vertebra. The mass of each layer of the jacket is modelled as a rigid body, attached to its parent vertebra by a planar joint - allowing no out-of-plane lateral movement relative to the spine. Each body is then restrained to its vertebra with a joint restraint and to adjacent bodies using kelvin restraints. The band of facet surface appropriate to the mass is supported on the rigid body.

**Pelvis**

The pelvis is a modified version of the Hybrid-III 50$^{th}$ percentile pelvis; the geometry of the upper edge is adjusted to take account of the jacket and the range of motion of the hips is slightly different, as the hardware pelvis has been adapted. The flexion-extension stiffness values are therefore different to those in the Hybrid-III.



**Head, Arms and Legs**

The head, arms and legs of the dummies are identical to the Hybrid-III 50$^{th}$ percentile facet model, as these components of the hardware dummy are also identical.

## CONTACTS BETWEEN DUMMY COMPONENTS

Contact is defined between the chin and the neck, the left and right lower arms, between the lower arms and the femurs, between the lower arms and the pelvis, between the left and right femurs and between the left and right shoes.

## 10.2 Model validation

The facet and FE models were developed co-operatively with Denton ATD Inc, the makers of the hardware dummy. Component tests were carried out and the model was validated against the standard thorax calibration test, as described in the BioRID User's Manual. This is a test comprising the spine, jacket and head mounted on a sled, which is then given an impulse. The performed component and full dummy tests are given below in Table 10.1 and Table 10.2.

Table 10.1: Component tests for BioRID II dummy models.

| Component | Test | | Model | |
|---|---|---|---|---|
| | description | specifications | Facet | FE |
| Spinal column with head | BioRID II without jacket, springs or damper T6-sacral block rigid | Pendulum heights 1.27m and 1.4m and pendulum velocity 4.25m/s | x | x |
| Spinal column with head | BioRID II without jacket or damper T6-sacral block rigid | Pendulum heights 1.27m and 1.4m and pendulum velocity 4.25m/s | x | x |
| Spinal column with head | BioRID II without jacket T6-sacral block rigid | Pendulum heights 1.27m and 1.4m and pendulum velocity 4.25m/s | x | x |
| Spinal column with head | BioRID II without jacket T12-sacral block rigid | Pendulum velocity 4.25m/s | x | x |
| Spinal column with head | BioRID II without jacket | Pendulum heights 1.27m and 1.4m and pendulum velocity 4.25m/s | x | x |
| Pelvis stiffness tests | Impactor tests against the pelvis | Varying speeds and positions | x | x |
| Full torso | BioRID II with jacket | Pendulum height: 1.9m | x | x |

Table 10.2: Full dummy sled tests for BioRID II dummy models.

| Test description | Test specification | | Model | |
|---|---|---|---|---|
| | Peak acc. | Delta V | Facet | FE |
| Sled test, dummy on facet seat | 10g | 16 km/h | x | x |
| Sled test, dummy on facet seat | 10g | 16 km/h | x | x |
| Sled test, dummy on facet seat | 10g | 16 km/h | x | x |

### Range of Validity of the Models

As the spines are modelled in both dummy models using revolute joints, it will not respond biofidelically to lateral loads and should only be used to investigate longitudinal and vertical aspects of rear impact dynamics.

## 10.3 User instructions

### Timestep

Table 10.3: Recommended timestep for the BioRID II dummy model.

| Model | timestep (s) |
|---|---|
| Facet | $\leq 1.0 \cdot 10^{-5}$ |
| FE | $\leq 1.0 \cdot 10^{-6}$ |



### Dummy positioning

Table 10.4: Positioning joints of the BioRID II dummy model.

| Joint Description | Identifier | Degree of freedom [a] | | | | | | Comment |
|---|---|---|---|---|---|---|---|---|
| Complete dummy | Dummy_jnt | R1<br>D1 | roll right<br>forward | R2<br>D2 | pitch down<br>leftward | R3<br>D3 | yaw left<br>upward | |
| Left shoulder | ShoulderL_jnt | R1 | pitch down | R2 | roll right | | | |
| Right shoulder | ShoulderR_jnt | R1 | pitch down | R2 | roll right | | | |
| Left elbow pivot | ElbowPivotL_jnt | R1 | yaw left | | | | | |
| Right elbow pivot | ElbowPivotR_jnt | R1 | yaw left | | | | | |
| Left elbow | ElbowL_jnt | R1 | pitch down | | | | | |
| Right elbow | ElbowR_jnt | R1 | pitch down | | | | | |
| Left wrist pivot | WristPivotL_jnt | R1 | yaw left | | | | | |
| Right wrist pivot | WristPivotR_jnt | R1 | yaw left | | | | | |
| Left wrist | WristL_jnt | R1 | roll right | | | | | |
| Right wrist | WristR_jnt | R1 | roll right | | | | | |
| Left hip | HipL_jnt | R1 | pitch down | R2 | roll left | R3 | yaw left | |
| Right hip | HipR_jnt | R1 | pitch down | R2 | roll left | R3 | yaw left | |
| Left knee | KneeL_jnt | R1 | pitch down | | | | | |
| Right knee | KneeR_jnt | R1 | pitch down | | | | | |
| Left ankle | AnkleL_jnt | R1 | yaw left | R2 | roll right | R3 | pitch down | |
| Right ankle | AnkleR_jnt | R1 | yaw left | R2 | roll right | R3 | pitch down | |

[a] Positive values given in global co-ordinate system while dummy is in reference position (see Figure 1.2 and Figure 10.1)

To position the spine initially, a pre-simulation is strongly recommended. Giving directly initial angles to the spine joints can lead to instabilities.

### Dummy contacts

Table 10.5: Available groups to define contact between the BioRID II components and environment.

| Contact Description | Identifier | Facet/FE model |
|---|---|---|
| Head | Head_gfe | Elements and nodes |
| Neck | Neck_gfe | Elements and nodes |
| Neck | NeckToChincnt_gfe | Elements and nodes |
| Left Arm | ArmUpL_gfe<br>ArmLowL_gfe | Elements and nodes<br>Elements and nodes |
| Right Arm | ArmUpR_gfe<br>ArmLowL_gfe | Elements and nodes<br>Elements and nodes |
| Jacket | Jacket_gfe | Elements and nodes |
| Pelvis | Pelvis_gfe | Elements and nodes |
| Left Femur and Knee | FemurKneeL_gfe | Elements and nodes |
| Right Femur and Knee | FemurKneeR_gfe | Elements and nodes |
| Left Tibia | TibiaL_gfe | Elements and nodes |
| Right Tibia | TibiaR_gfe | Elements and nodes |
| Left Shoe | ShoeL_gfe | Elements and nodes |
| Right Shoe | ShoeR_gfe | Elements and nodes |

## Output

From MADYMO V7.3 on ISO-MME output can be generated for the BioRID II Q dummy model. Output requests for signals in ISO-MME format are pre-defined in the CONTROL_OUTPUT element in the user file.

Signal zero-ing is available in the user file for NeckUp_FrcZ and NeckLowLCAxial_inj to correct for initial signal offsets.

Table 10.6: BioRID II output signals.

| Sensor | Identifier | Signal resultant | x | direction[(a)] | y | direction[(a)] | z | direction[(a)] | Filter |
|---|---|---|---|---|---|---|---|---|---|
| Head | | | | | | | | | |
| displacement | Head_dis | dr | d1 | forward | d2 | lateral | d3 | vertical | CFC600 |
| relative to T1 | HeadT1Disp_dis | dr | d1 | forward | d2 | lateral | d3 | vertical | CFC1000 |
| velocity | Head_vel | vr | d1 | forward | v2 | lateral | v3 | vertical | CFC1000 |
| acceleration [(b)] | Head_acc | ar | a1 | forward | a2 | lateral | a3 | vertical | CFC1000 |
| acc. for RNIC calculation | HeadRNIC_acc | ar | a1 | forward | a2 | lateral | a3 | vertical | CFC180 |
| | HeadRNICCFC60_acc | ar | a1 | forward | a2 | lateral | a3 | vertical | CFC60 |
| angular velocity | HeadVel_ang | vr | r1 | roll | r2 | pitch | r3 | yaw | CFC1000 |
| angular acceleration | HeadAcc_ang | ar | r1 | roll | r2 | pitch | r3 | yaw | CFC1000 |
| Neck | | | | | | | | | |
| acceleration [(b)] | C4_acc | ar | a1 | forward | a2 | lateral | a3 | vertical | CFC180 |
| Cervical load cells | NeckUp_lce_F_CFC1000 | fr | f1 | shear | f2 | shear | f3 | axial | CFC1000 |
| | NeckUp_lce_F_CFC600 | fr | f1 | shear | fe | shear | f3 | axial | CFC600 |
| | NeckUp_lce_T | tr | t1 | roll | t2 | pitch | t3 | yaw | CFC600 |
| | NeckLow_lce_F | fr | f1 | shear | f2 | shear | f3 | axial | CFC1000 |
| | NeckLow_lce_F_ CFC600 | | | | | | | | |
| | NeckLow_lce_T | fr | f1 | shear | f2 | shear | f3 | axial | CFC600 |
| | | fr | f1 | roll | f2 | pitch | f3 | yaw | CFC600 |
| 1st Thoracic Vertebra | | | | | | | | | |
| displacement | T1_dis | dr | d1 | forward | d2 | lateral | d3 | vertical | CFC600 |
| relative to H-Point | T1HPointDisp_dis | dr | d1 | forward | d2 | lateral | d3 | vertical | CFC600 |
| velocity | T1_vel | vr | v1 | forward | v2 | lateral | v3 | vertical | CFC1000 |
| acceleration [(b)] | T1_acc | ar | a1 | forward | a2 | lateral | a3 | vertical | CFC180 |
| | T1Reverse_acc | ar | a1 | forward | a2 | lateral | a3 | vertical | CFC180 |
| | T1CFC1000_acc | ar | a1 | forward | a2 | lateral | a3 | vertical | CFC1000 |
| | T1CFC60_acc | ar | a1 | forward | a2 | lateral | a3 | vertical | CFC60 |
| angular velocity | T1Vel_ang | vr | r1 | roll | r2 | pitch | r3 | yaw | CFC1000 |
| angular acceleration | T1Acc_ang | ar | r1 | roll | r2 | pitch | r3 | yaw | CFC1000 |
| 8th Thoracic Vertebra | | | | | | | | | |

*Continued on the next page*

*Table 10.6 cont.*

| Sensor | Identifier | Signal resul-tant | x | direc-tion[(a)] | y | direc-tion[(a)] | z | direc-tion[(a)] | Filter |
|---|---|---|---|---|---|---|---|---|---|
| acceleration[(b)] | T8_acc | ar | a1 | forward | a2 | lateral | a3 | vertical | CFC180 |
| 1st Lumbar Vertebra | | | | | | | | | |
| acceleration | L1_acc | ar | a1 | forward | a2 | lateral | a3 | vertical | CFC180 |
| H-Point | | | | | | | | | |
| displacement | HPoint_dis | dr | d1 | forward | d2 | lateral | d3 | vertical | CFC600 |
| velocity | HPoint_vel | vr | v1 | forward | v2 | lateral | v3 | vertical | CFC1000 |
| acceleration[(b)] | HPoint_acc | ar | a1 | forward | a2 | lateral | a3 | vertical | CFC1000 |
| angular velocity | HPointVel_ang | vr | r1 | roll | r2 | pitch | r3 | yaw | CFC1000 |
| angular acceleration | HPointAcc_ang | ar | r1 | roll | r2 | pitch | r3 | yaw | CFC1000 |

10

[(a)] Positive direction given according to SAE J211/1.
[(b)] The acceleration is corrected in the x direction for a prescribed fictitious acceleration field (see Theory manual). In the case of T1 acceleration, the original BioRID design used a reverse orientation, while most current SAE-based work uses the standard forward-positive convention. The original output option is given as T1Reverse_acc.

Table 10.7: Injury criteria defined for the BioRID II.

| Injury criteria | Identifier | Filter |
|---|---|---|
| Head | | |
| HIC(15) | HIC15_inj | CFC1000 |
| HIC(36) | HIC36_inj | CFC1000 |
| Neck | | |
| Rear NIC | RearNIC_inj | CFC180 |
| | RearNICCFC60_inj | CFC60 |
| NIJ | NTE_inj | CFC600 |
| | NTF_inj | CFC600 |
| | NCE_inj | CFC600 |
| | NCF_inj | CFC600 |
| FNIC | FNICshear_inj | CFC1000 |
| | FNICbending_inj | CFC1000/CFC600(F/T) |
| | FNICtension_inj | CFC600 |
| NKM | NEA_inj | CFC600 |
| | NEP_inj | CFC600 |
| | NFA_inj | CFC600 |
| | NFP_inj | CFC600 |

The legs are also modelled as instrumented components with output and injury criteria defined, but because leg injury investigations are not common in BioRID testing, the user is referred to Chapter 2 for the description of the related output and injury criteria.

# 11 ES-2 and ES-2re Q Side Impact Dummies

Following the increased market demand for dummy models that are CPU-efficient as well as accurate in response, the quality (Q) ellipsoid and the quality (Q) facet models of the ES-2 and ES-2re dummies were developed. The ES-2 and ES-2re dummies are used in regulatory and consumer test protocols for side impact injury assessment of an occupant that anthropometrically corresponds to a mid-sized (50th percentile) male adult.

The final design of the ES-2 dummy was adopted in Europe for the EuroNCAP and ECE R95 test protocols in 2003 and 2004 respectively. Shortly after, in 2006, the US agency NHTSA finally approved the ES-2re (the ES-2 with modified rib unit) to be used for the US occupant safety test protocols FMVSS 214 and eventually USNCAP MY 2011, thus globally replacing its predecessors EUROSID-1 and US-SID.

The models represent both ES-2 and ES-2re versions of the hardware dummy. The models were completely rebuilt and their design significantly differs from the former ES-2 ellipsoid and facet models. Both models were extensively calibrated and validated using numerous component and full dummy impact tests.



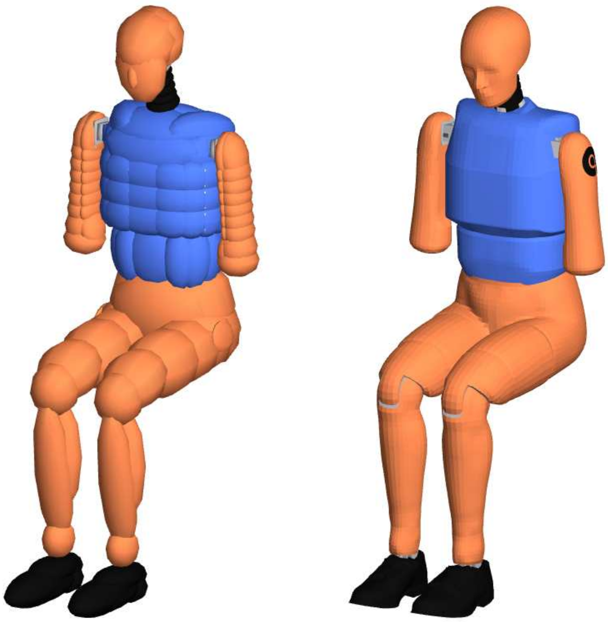

Figure 11.1: ES-2(re) ellipsoid Q (left) and facet Q (right) models in the reference position.

## 11.1 Model description

The quality rated ellipsoid and facet models of the ES-2 and ES-2re dummies are available. The input is given in the files:

| | |
|---|---|
| Ellipsoid models: | d_es2lhel_Q_usr.xml + d_es2lhel_Q_inc.xml<br>d_es2rhel_Q_usr.xml + d_es2rhel_Q_inc.xml<br>d_es2relhel_Q_usr.xml + d_es2relhel_Q_inc.xml<br>d_es2rerhel_Q_usr.xml + d_es2rerhel_Q_inc.xml |
| Facet models: | d_es2lhfc_Q_usr.xml + d_es2lhfc_Q_inc.xml<br>d_es2rhfc_Q_usr.xml + d_es2rhfc_Q_inc.xml<br>d_es2relhfc_Q_usr.xml + d_es2relhfc_Q_inc.xml<br>d_es2rerhfc_Q_usr.xml + d_es2rerhfc_Q_inc.xml |

11

To run these models, the following licenses are required:

| | |
|---|---|
| Ellipsoid model: | MADYMO/Solver (Multibody)<br>MADYMO/Dummy Models/Side |
| Facet model: | MADYMO/Solver (Multibody)<br>MADYMO/Dummy Models/Side/ES2(re) Fc Q |

Figure 11.1 shows the ES-2 (re) ellipsoid and facet Q models in the reference position.

The ellipsoid and facet models consist of 202 bodies each (217 in RE version), 29 joint restraints, 176 other kinematic restraints (188 in RE version) and has 35 MADYMO outputs and 61 injury criteria initially predefined, thus covering all possible hardware dummy instrumentation available and injury criteria required by testing assessment protocols relevant for ES-2 and ES-2re dummies.

### ELLIPSOID MODEL AND FACET MODEL

The ES-2 (re) Q models were rebuilt completely with respect to the former ellipsoid and facet models. Both ellipsoid Q and facet Q model types are based on the same multibody skeleton design. Separate models of each type are available for left hand drive and right hand drive versions of the dummy.

The external and internal geometry of the facet model is represented by facet surfaces, derived from the latest official technical drawings and/or 3D laser scans of the ES-2 (re) hardware dummy. In general, an element size of approximately 10 mm is used. All parts have contact compliance characteristics included in their NULL materials. Masses, centres of gravity and moments of inertia are determined on the basis of hardware component mass measurements and geometric representation of the components in 3D CAD drawings. The geometry, both external and internal, of the ellipsoid dummy is fully represented with ellipsoid surfaces that closely approximate the detailed geometry of the facet model.

Dummy load cells are modelled with two separate rigid bodies connected to each other and to neighbouring bodies by bracket joints. The central bracket joint represents the point of measurement, from which the load cell signal output is derived. All dummy sub-assemblies are modelled as separate entities and are connected to each other by bracket "interface" joints at the locations where the hardware sub-assemblies are connected with screws. The following paragraphs give an overview of the model design per dummy sub-assembly.

The level of validation of the ES-2 (re) ellipsoid and facet Q models (in terms of simulation signal correlation with hardware test signals) was determined using an objective rating method and is more extensively described in the model quality report.

### Head and neck

For the head, facet or ellipsoid surfaces (depending on the model type) representing the head skin, skull and skull cap, the upper neck load cell and the head accelerometer mount are included. Bodies included represent the upper neck load cell, the accelerometer with mounting block, and the head assembly of skull, skull cap, skin and skin cap.

In the neck column, facet surfaces representing the neck mould and the top and bottom plates are included. The openings between plates and mould are closed in the facet surface model to avoid potential contact problems with belt/airbags. The neck column is modelled with six bodies. Two of these represent the top and bottom plate; the four bodies in between together represent the rubber neck mould. Restraints on spherical joints represent the compliance of the deforming neck buffers. The compliance of the rubber neck mould is represented with restraints on free joints in between the neck mould bodies. The neck bracket is modelled with a lower neck load cell included. The geometry of the neck bracket and load cell is represented with facet or ellipsoid surfaces. The ES-2 head-neck models are shown in the Figure 11.2.



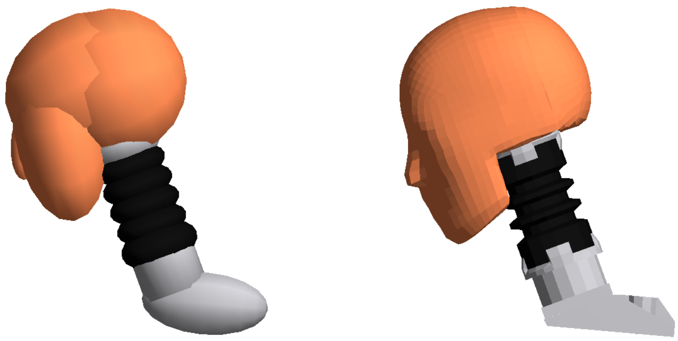

Figure 11.2: The ES-2 ellipsoid Q (left) and facet Q (right) head-neck assemblies.

### Shoulder box and clavicles

The shoulder assembly is modelled in detail to allow an accurate representation of the clavicle range of motion inside the clavicle box. Facet or ellipsoid surfaces representing the clavicle box components, end stop blocks, U-block and U-spring, clavicle cams, shoulder load cells and elastic cords and holder, allow for a realistic visualisation of the shoulder response during side impact loading. The U-spring bending compliance is modelled in detail by multiple revolute joints with restraints. The clavicle cam compliance (bending and torsion) is also represented, using a spherical joint with a restraint located in the reduced thickness region of the cam.

The clavicle cam motion inside the shoulder box is restrained by point restraints (interactions with U-spring) as well as an internal contact definition (interactions with end stop blocks and sides of shoulder box). The elastic cords are modelled as belt segments. The interaction between the cords and outside shoulder box is represented by point restraints. The geometry of the shoulder box internal design is shown in the Figure 11.3.



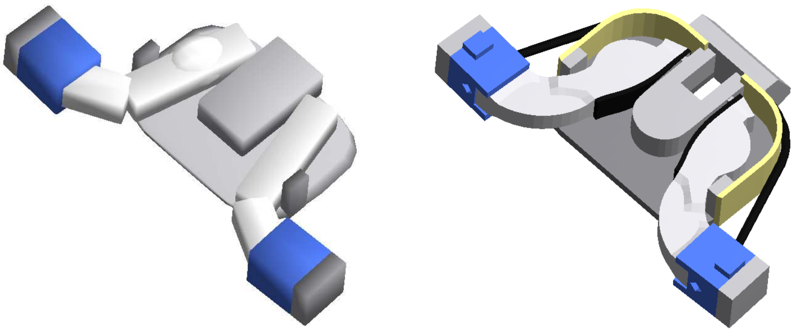

Figure 11.3: Internal shoulder design of ellipsoid Q (left) and facet Q (right) models.

**Arms**

The arms are modelled with chains of rigid bodies connected by spherical joints and restraints, representing the arm bending torsion compliance. The top body of the arm can also move with respect to the arm pivot plate body. This represents the shoulder "flesh" (Hyperlast) and arm strip deformation directly around the shoulder pivot. The upper and lower region of the arms have different contact characteristics, representing the Hyperlast and PU foam filled segments of the arms. The arm facet surface has a varying element thickness, depending on the depth of the arm mould from skin to internal plastic arm strip. Figure 11.4 shows the arm ellipsoid and facet models.

Figure 11.4: The ellipsoid Q (left) and facet Q (right) models of the arm assembly.

### 11.1.1 Thorax – ES-2

The thorax consists of the spinebox with T12 load cell adaptor, the backplate assembly and the three rib modules. All component geometry is represented with facet or ellipsoid surfaces. Rigid bodies are included for the T12 load cell, the spinebox, the backplate load cell and the backplate itself. Each rib module includes 19 bodies; 13 of these form the rib steel strip with its foam padding. The other six bodies represent parts of the guiding and damper module inside the rib arc. Rib steel bending stiffness is modelled with revolute joints with restraints. The damper and the various springs in the rib guiding system are all represented by kelvin restraints. The end stops in the damper and guiding system are included in the restraints applied on translation joints. The geometries of the single rib unit and the complete thorax assembly for both type of models are shown in the Figure 11.5 and Figure 11.6 respectively.



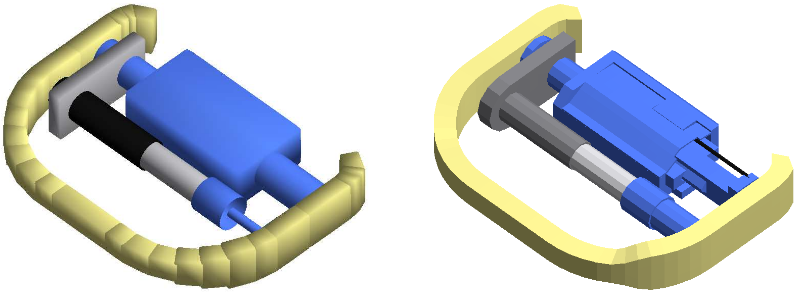

Figure 11.5: Single rib unit of the ellipsoid Q (left) and facet Q (right) models.

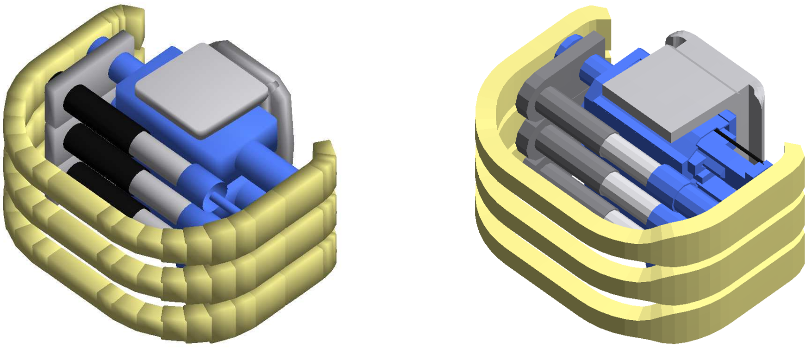

Figure 11.6: Thorax assembly of the ellipsoid Q (left) and facet Q (right) models.

### 11.1.2 Thorax – ES-2re

The thorax model for the ES-2re (ES-2 dummy with rib extensions) is identical to the standard ES-2 thorax model, except for the rear end rib steel on the impact side (where the rib extensions are attached) and the modified backplate assembly with rib extension guiding. The rib extension consists of four extra rib steel bodies connected by revolute joints and is connected to the impact side rib steel end by a bracket joint.

The modified backplate assembly consists of the backplate load cell, rib extension guide casting with needle roller bearings and a cover plate. All these parts are represented by either the facet or ellipsoid surfaces. Rigid bodies represent the rib extension guide with cover and the needle rollers. The guidance of the rib extensions on the needle rollers and the contacts with the rib extension guide and cover are modelled with point restraints.



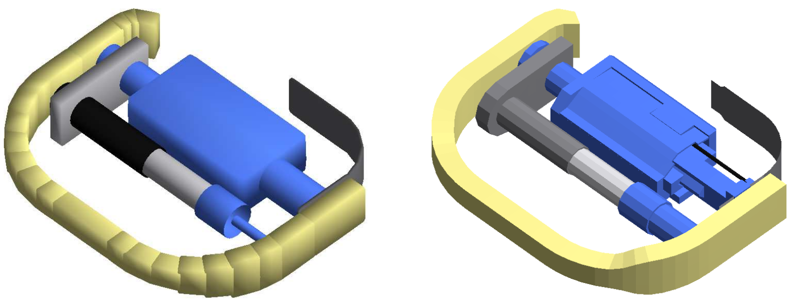

Figure 11.7: Single rib unit of the ellipsoid Q (left) and facet Q (right) RE models.

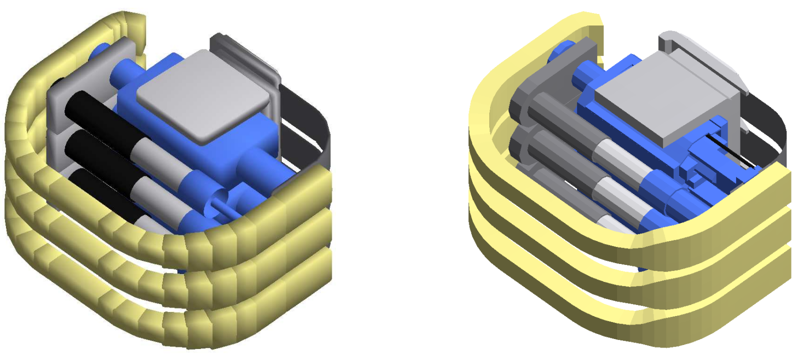

Figure 11.8: Thorax assembly of the ellipsoid Q (left) and facet Q (right) RE models.

### 11.1.3 Lumbar spine and abdomen

The lumbar spine mould is modelled with rigid bodies connected with free joints and sixdof restraints. The cable is also modelled as a rigid body chain. Spherical joints with sixdof restraints connect the cable bodies. The spine cable ball body is connected to the spine mould bottom plate body with spherical joint. At the top side of the lumbar spine, the cable shaft body is connected to the mould top plate with a point restraint and a flexion-torsion restraint. Kelvin restraints are used to model the interaction of the cable with the inside of the central opening in the mould. The lumbar mould geometry is represented with either facet or ellipsoid surfaces connected per region to the adjacent rigid bodies. In the facet model type, the geometrical representation of the cable was also included. The lumbar ellipsoid and facet models are presented in the Figure 11.9.

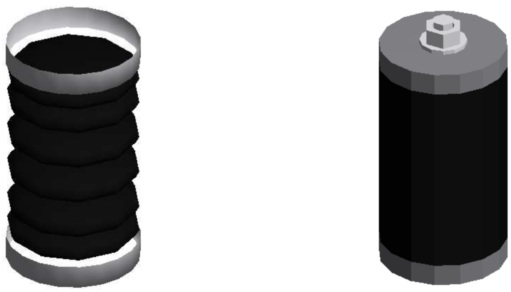

Figure 11.9: Lumbar geometries of the ellipsoid Q (left) and facet Q (right) models.

The abdomen assembly Figure 11.11 consists of the T12 load cell adaptor, the abdomen drum, the cover plate, three load cell replacements (non-impact side), three load cells (impact side) and the abdomen mould. All the components are represented by separate rigid bodies. The mould is modelled as a chain of eleven bodies connected by translation joints with restraints to allow shearing of the different mould segments when loaded. The mould body chain is connected to the drum body with a free joint.

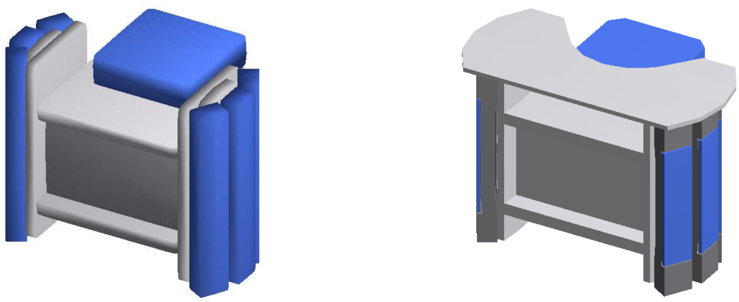

Figure 11.10: The abdomen drum ellipsoid Q (left) and facet Q (right) models.

The contact load paths between the drum and the mould are modelled with point restraints between mould segment bodies on one hand and the load cell (replacement) bodies on the other. Three point restraints transfer the load from the mould to each load cell. The upper and lower point restraints transfer the loads on the bottom and top ends, which are not sensed by the load cell sensor. The middle point restraint transfers the load going through the sensor in the central section of the load cell. The mould compliance is represented mainly by the outside mould contact characteristics.

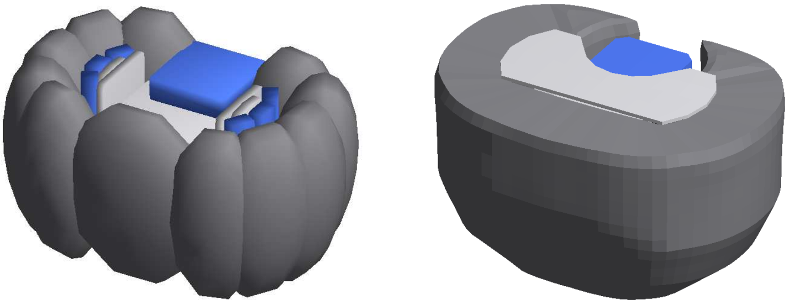

Figure 11.11: The Abdomen ellipsoid Q (left) and facet Q (right) models.

**Pelvis**

The pelvis assembly is modelled with 18 rigid bodies. The sacrum block, iliac wing, transducer bushing and pubic load cell bodies together form a closed body chain with revolute joints that deform in reaction to pelvis side impact loading. Another part of the iliac wing deformation is modelled with a translation joint with a restraint between sacrum block and iliac wings. The bodies representing the left and right side of the pelvis flesh are connected to the iliac wing bodies.

The hip pivot pins, H-point backplates and H-point foam plugs are represented by separate rigid body chains connected to the iliac wings, allowing realistic load paths through pelvis flesh and H-point foam plugs. The upper femur shaft bodies are connected to the hip pivot pin bodies through spherical joints, representing the physical hip pivots. Cardan restraints represent the soft hip rotation end stops, the contact between femur shafts and pelvis flesh and the pelvis to femur flesh contact. The internal structure of pelvis models is shown in the Figure 11.12.

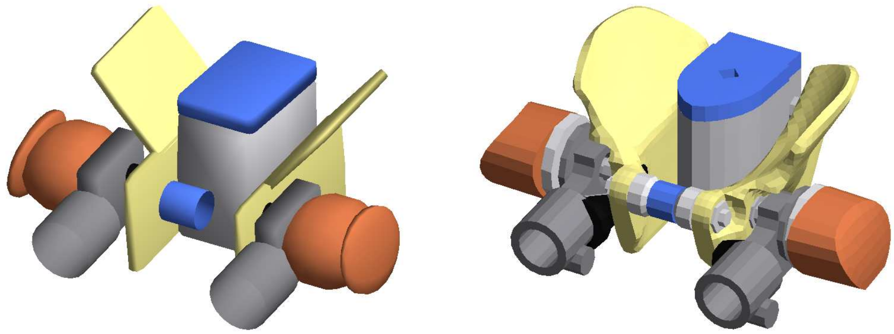

Figure 11.12: The ellipsoid Q (left) and facet Q (right) models of the pelvis assembly internal parts



All pelvis components are represented geometrically with either ellipsoid or facet surfaces. The pelvis facet flesh surface is closed at the top and front (femur openings) and has a varying element thickness representing the differences in foam-skin thickness. In this way a single contact characteristic can be used for modelling the pelvis flesh compliance. The H-point foam plugs have their own contact characteristic. The complete pelvis model is shown in the Figure 11.13.

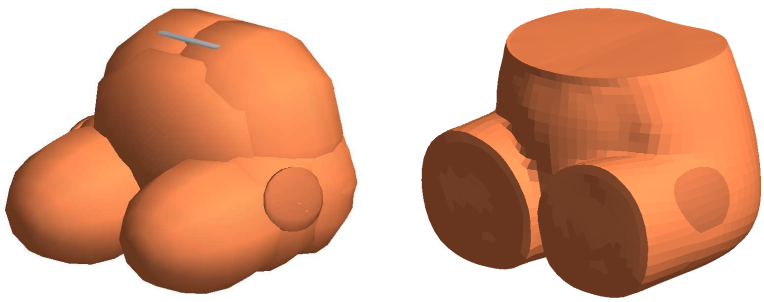

Figure 11.13: The ellipsoid Q (left) and facet Q (right) models of the complete pelvis assembly.

**Legs and feet**

The leg model includes separate rigid bodies for the femur steel, femur load cell, knee steel, thigh flesh, knee flesh, tibia steel, ankle steel, tibia flesh, foot assembly and shoe. The femur steel is connected to the pelvis (upper femur shaft) by a revolute joint with a restraint that includes the end stops limiting the rotation range of the femur steel in the shafts. The thigh flesh is connected to the femur steel by a revolute joint with restraint allowing the flesh to rotate around the femur steel. The knee pivot is modelled with a revolute joint. The ankle steel can rotate with respect to the tibia steel (with end stops modelled in a restraint). The ankle pivot itself is represented by a revolute joint. The shoe is connected to the foot with a free joint and a sixdof restraint.

The femur and knee flesh meshes in the facet model are connected with closing elements to make a closed outer flesh contact surface. Also the outer tibia flesh surface mesh and the shoe mesh are closed to prevent contact problems.



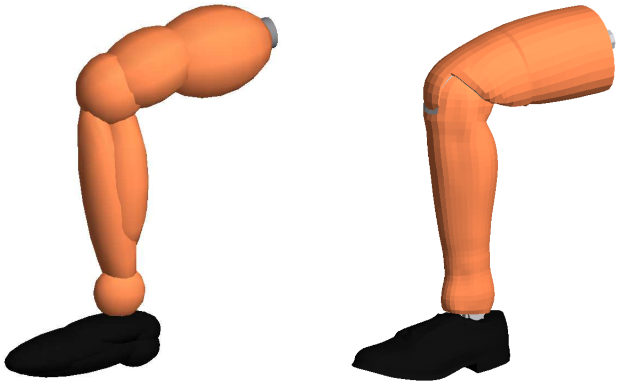

Figure 11.14: The ellipsoid Q (left) and facet Q (right) models of the complete leg assembly.

**Jacket**

The jacket of the facet model is represented with four closed facet surfaces covering shoulder region, ribs, abdomen & spine, back plate & clavicle box. This ensures continuity of jacket surface contact stiffness and thus higher robustness of the model. Each closed surface is locally supported to the various underlying component rigid bodies. In this way the contact forces applied to the jacket are realistically divided over the dummy components underneath. The sleeves and the parts over the pelvis are not included in the jacket model. The jacket mass is included by using a non-zero density in the null materials defined for the different jacket regions.

In the ellipsoid model the suit is represented with a number of ellipsoid surfaces supported to the underlying bodies, covering shoulder, rib cage, abdomen and back plate regions, similarly to the facet model. This ensures the same external loads distribution in both facet and ellipsoid models.

In the facet model each jacket FE part, has its own contact characteristic, corresponding to the compliance of the underlying dummy parts. Where the jacket covers stiff structural parts, the compliance of the jacket material itself is defined in the contact characteristic. For the parts that cover the openings in between dummy components, a very compliant contact characteristic is used.

The ES-2re jacket model insignificantly differs from the standard ES-2 jacket in both ellipsoid and facet models, due to the presence of the rib extensions and modified back plate assembly in the ES-2re model.

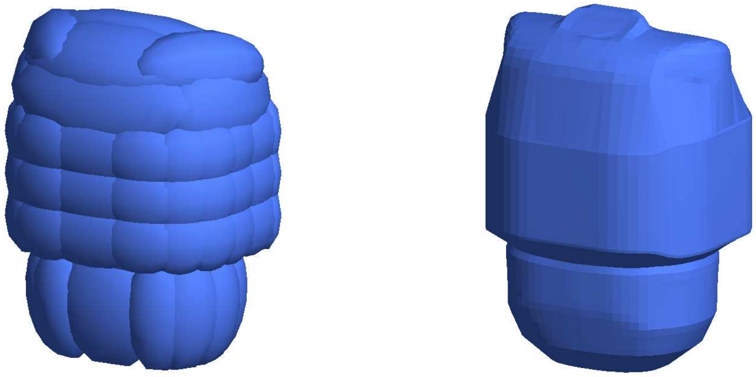

Figure 11.15: The ellipsoid Q (left) and facet Q (right) models of the ES-2 jacket.



**CONTACTS BETWEEN DUMMY COMPONENTS**

Inter-component contacts in both dummy model types were defined between the left and right arm, between the arms and the jacket and between the left and right leg and shoe. The interaction between pelvis and abdomen flesh is represented with point restraints instead of a contact definition.

## 11.2 Model validation

The dummy models have been developed and validated for side impact loading using tests listed below. For detailed information on the model validation the reader is referred to the quality report supplied with the dummy models.

### Component tests

The component tests used for development and validation of the ellipsoid and facet models are summarised in the Table 11.1. The full overview of the validation results can be found in the quality report.

Table 11.1: Component tests for the ES-2(re) ellipsoid Q and facet Q models.

| **Component** | **Test** | | | **Model** | |
|---|---|---|---|---|---|
| | **description** | **specification** | | **ES-2** | **ES-2re** |
| Head | Certification drop | height | 0.2 m | x | x |
| Neck | Certification pendulum | velocity | 3.4 m/s | x | x |
| Arm | Guided, 2.95 kg, upper arm compression | velocity | 2.0 m/s | x | x |
| | Guided, 2.95 kg, lower arm compression | velocity | 2.0 m/s | x | x |
| | Guided, 2.95 kg, lower arm bending | velocity | 2.0 m/s | x | x |
| Rib up | Certification drop, 7.8 kg | velocity | 2.0, 3.0, 4.0 m/s | x | x |
| Rib mid | Certification drop, 7.8 kg | velocity | 2.0, 3.0, 4.0 m/s | x | x |
| Rib low | Certification drop, 7.8 kg | velocity | 2.0, 3.0, 4.0 m/s | x | x |
| Lumbar spine | Certification pendulum | velocity | 6.1 m/s | x | x |
| Abdomen | Drop, 8.0 kg, 0 deg | velocity | 2.3, 3.3, 4.9 m/s | x | x |
| | Guided, 7.7 kg, 0 deg | velocity | 5.4, 8.8 m/s | x | x |
| | Guided, 10.6 kg, 0 deg | velocity | 6.2 m/s | x | x |
| Pelvis | Guided, 19.6 kg, square, 5 deg rear | velocity | 3.0, 4.4, 6.0 m/s | x | x |
| | Guided, 19.6 kg, square, 20 deg rear | velocity | 4.5 m/s | x | x |
| | Guided, 19.8 kg, cylinder horiz., 5 deg rear | velocity | 4.5 m/s | x | x |
| | Guided, 19.8 kg, cylinder vert., 5 deg rear | velocity | 4.5 m/s | x | x |
| Pelvis + legs | Guided, 19.6 kg, square, 5 deg rear, at pelvis | velocity | 4.5 m/s | x | x |
| | Guided, 19.6 kg, square, 5 deg rear, at pelvis and leg | velocity | 4.5 m/s | x | x |

### Full dummy tests

The tests with the complete dummy used for development and validation of the ellipsoid and facet models are summarised in the Table 11.2. The validation results on the full dummy level can also be found in the quality report supplied with the dummy models.

Table 11.2: Full dummy tests for the ES-2(re) ellipsoid Q and facet Q models.

| **Test** | | | **Model** | |
|---|---|---|---|---|
| **description** | **specification** | | **ES-2** | **ES-2re** |
| Certification shoulder, pendulum | velocity | 4.3 m/s | x | x |
| Certification abdomen, pendulum | velocity | 4.0 m/s | x | x |
| Certification pelvis, pendulum | velocity | 4.3 m/s | x | x |
| Sled, side padded plates, rigid seat | velocity | 7.7, 9.7 m/s | x | |

**Range of validity of the model**

The ellipsoid and facet dummy models were validated in side impact loading conditions.

## 11.3 User instructions

### Timestep

Table 11.3: Recommended timestep for the ES-2(re) ellipsoid and facet Q models.

| Model | timestep (s) |
|---|---|
| Ellipsoid | $\leq 1.0 \cdot 10^{-5}$ |
| Facet | $\leq 1.0 \cdot 10^{-5}$ |

### Dummy positioning



The basic way to position the ES-2 Q models is to use the dummy joint. The dummy joint is located on the so called H-point of the dummy. In practise however, another point is measured to check the correct position of the dummy in the seat. This point is called the Hm-point or H-point of the H-point manikin (Chapter 34).

The ES-2 Q models have an extra body and translational joint to facilitate the positioning using the Hm-point of the dummy. The INITIAL.JOINT_POS for the HPointLocation_jnt needs to be enabled and the value for D1 must be 0.021 to use the Hm-point for positioning the dummy model. When the D1 value is set to 0.0 the H-point of the dummy is used for positioning. It should be noted that NO vertical shift of 5mm between Hm-point and H-point is taken into account. This is because for the Hm-point markings on the ES-2 hardware dummy this vertical shift relative to the dummy H-point is also not applied, as it is assumed to be compensated by the pelvis foam compression.

Table 11.4: Positioning joints for the ES-2(re) ellipsoid and facet Q models.

| Joint Description | Identifier | Degree of freedom[(a)] | | | | | | Comment |
|---|---|---|---|---|---|---|---|---|
| Complete dummy | Dummy_jnt[(b)] | D1 | forward | D2 | leftward | D3 | upward | |
| | | R1 | roll right | R2 | pitch down | R3 | yaw left | |
| | HPointLocation_jnt[(b)] | D1 | forward | | | | | either 0 or 0.021 |
| Neck OC | Neck OC_jnt | R1 | yaw left | R2 | pitch down | R3 | roll left | equilibrium[(c)] |
| Neck mould | NeckMouldPivot ⟨i⟩_jnt, | D1 | upward | D2 | leftward | D3 | rearward | equilibrium[(c)] |
| | for i=1 to 3 | R1 | yaw left | R2 | pitch down | R3 | roll left | |
| Neck T1 | NeckT1_jnt | R1 | yaw left | R2 | pitch down | R3 | roll left | |
| Left shoulder | ShoulderL_jnt | R1 | pitch up | | | | | either 0° , |
| Right shoulder | ShoulderR_jnt | R1 | pitch up | | | | | 40° or 90° |
| Spine mould | SpineMouldPivot⟨i⟩_jnt, | D1 | upward | D2 | leftward | D3 | rearward | equilibrium[(d)] |
| | for i=1 to 5 | R1 | yaw left | R2 | pitch down | R3 | roll left | |
| Spine cable | SpineCablePivot⟨i⟩_jnt, | R1 | yaw left | R2 | pitch down | R3 | roll left | equilibrium[(e)] |
| | for i=1 to 5 | | | | | | | |
| Left hip | HipL_jnt | R1 | pitch down | R2 | roll left | R3 | yaw left | |
| Right hip | HipR_jnt | R1 | pitch down | R2 | roll left | R3 | yaw left | |

*Continued on the next page*

*Table 11.4 cont.*

| Joint Description | Identifier | Degree of freedom[(a)] | Comment |
|---|---|---|---|
| Left knee | KneeL_jnt | R1 pitch down | |
| Right knee | KneeR_jnt | R1 pitch down | |
| Left ankle | AnkleL_jnt | R1 pitch down | |
| Right ankle | AnkleR_jnt | R1 pitch down | |

[(a)] Positive translation or rotation given in global coordinate system, with dummy in reference position (see Figure 11.1).

[(b)] The complete dummy can be positioned relative to the H-point (use 0.0) or the Hm-point (use 0.021) (see also text Dummy positioning).

[(c)] Can be adjusted for equilibrum state only

[(d)] (D1, D2, D3, R1, R3 for equilibrum state only. R2 can be used to bend the dummy forward or backward.

[(e)] (R1, R3 for equilibrum state only. R2 can be used to bend the dummy forward or backward.



### Dummy contacts

When defining the contacts between the dummy model and its environment, only the contact groups defined in the Table 11.5 for the ellipsoid model and in the Table 11.6 need to be used; no contacts should be defined with the dummy components underneath the jacket surface.

In general, the dummy surface (ellipsoid or facet) should be chosen as the master group in contact definitions. This is also the way in which the contacts were defined in the dummy model validation test suite. With the dummy facet surfaces chosen as master group in the contact definitions, the user will avoid problems with edges in the master surfaces because the dummy contact surfaces are all closed. Furthermore, with the dummy surfaces as master the direction of the contact forces and torques is always controlled by the dummy model. As an exception to this guideline, the dummy surfaces can best be chosen as slave group in contacts between the dummy and a facet seat.

When meshing FE or facet surfaces that will be in contact with the facet dummy, an element size of 15 mm or smaller is the optimal choice. This element size has also been used in the models of the facet dummy model validation test suite.

Table 11.5: Predefined groups to define contact between the ES-2(re) ellipsoid Q models components and their interacting environment.

| Contact Description | Identifier[(a)] | Ellipsoid Q models |
|---|---|---|
| Head | Head_gmb | head skin ellipsoids |
| Neck | Neck_gmb | neck mould ellipsoids |
| Left Arm | ArmL_gmb | left arm flesh ellipsoids |
| Right Arm | ArmR_gmb | right arm flesh ellipsoids |
| Pelvis | Pelvis_gmb | pelvis flesh and H-point foam ellipsoids |
| Left upper leg | FemurKneeL_gmb | left femur and knee flesh ellipsoids |
| Right upper leg | FemurKneeR_gmb | right femur and knee flesh ellipsoids |

*Continued on the next page*

*Table 11.5 cont.*

| Contact Description | Identifier[a] | Ellipsoid Q models |
|---|---|---|
| Left lower leg<br>Right lower leg | TibiaL_gmb<br>TibiaR_gmb | left tibia flesh ellipsoids<br>right tibia flesh ellipsoids |
| Left Shoe<br>Right Shoe | ShoeL_gmb<br>ShoeR_gmb | left shoe ellipsoids<br>right shoe ellipsoids |
| Jacket | Jacket_gmb | jacket ellipsoids covering thoracic and abdomen regions |

[a] L=Left; R=Right.

Table 11.6: Predefined groups to define contact between the ES-2(re) facet Q models components and their interacting environment.

| Contact Description | Identifier[a] | Facet Q models |
|---|---|---|
| Head | Head_gfe | closed outer head skin surface |
| Neck | Neck_gfe | closed neck mould and interface plates surface |
| Left Arm<br>Right Arm | ArmL_gfe<br>ArmR_gfe | closed left arm flesh surface<br>closed left arm flesh surface |
| Pelvis | Pelvis_gfe | closed outer pelvis flesh and H-point foam surface |
| Left upper leg<br>Right upper leg | FemurKneeL_gfe<br>FemurKneeR_gfe | closed left outer femur and knee flesh surface<br>closed right outer femur and knee flesh surface |
| Left lower leg<br>Right lower leg | TibiaL_gfe<br>TibiaR_gfe | closed left outer tibia flesh surface<br>closed right outer tibia flesh surface |
| Left Shoe<br>Right Shoe | ShoeL_gfe<br>ShoeR_gfe | closed left outer shoe surface<br>closed right outer shoe surface |
| Jacket | Jacket_gfe | closed jacket surface |

[a] L=Left; R=Right.

### Output

From MADYMO V7.3 on, ISO-MME output can be generated for the ES-2(re) Q dummy models. Output requests for signals in ISO-MME format are predefined in the CONTROL_OUTPUT element in the user file.

In the Table 11.7 all predefined output definitions for the ES-2(re) models are listed. Note that the output signal filtering in the Q models is adopted from the EuroNCAP Side Impact and the Pole Impact protocols where applicable. All signal descriptions given below are valid for both right hand side and left hand side dummy models.

Table 11.7: Predefined output signals for the ES-2(re) ellipsoid Q and facet Q models.

| Sensor | Identifier | Signal | | | | | | | Filter |
|---|---|---|---|---|---|---|---|---|---|
| | | resul-tant | x | direc-tion[a] | y | direc-tion[a] | z | direc-tion[a] | |
| Head | | | | | | | | | |
| CG accel. | HeadCG_acc | ar | a1 | forward | a2 | right | a3 | down | CFC1000 |
| Neck | | | | | | | | | |
| Upper LC | NeckUp_lce_F | | f1 | shear | f2 | shear | f3 | axial | CFC1000 |
| | NeckUp_lce_T | | t1 | roll | t2 | pitch | t3 | yaw | CFC600 |
| Lower LC | NeckLow_lce_F | | f1 | shear | f2 | shear | f3 | axial | CFC1000 |
| | NeckLow_lce_T | | t1 | roll | t2 | pitch | t3 | yaw | CFC600 |
| Shoulder | | | | | | | | | |
| Left LC | ShoulderL_lce_F | | f1 | shear | f2 | shear | f3 | axial | CFC600 |
| Right LC | ShoulderR_lce_F | | f1 | shear | f2 | shear | f3 | axial | CFC600 |
| Left accel. | ShoulderL_acc | ar | a1 | forward | a2 | right | a3 | down | CFC180 |
| Right accel. | ShoulderR_acc | ar | a1 | forward | | right | a3 | down | CFC180 |
| T1 accel. | T1_acc | ar | a1 | forward | | right | a3 | down | CFC180 |
| Thorax | | | | | | | | | |
| Rib displ.[b] | | | | | | | | | |
| Up | RibUp_dis | | | | d2 | lateral | | | CFC180 |
| | RibUp_dvl | dr | | | | | | | |
| Mid | RibMid_dis | | | | d2 | lateral | | | CFC180 |
| | RibMid_dvl | dr | | | | | | | |
| Low | RibLow_dis | | | | d2 | lateral | | | CFC180 |
| | RibLow_dvl | dr | | | | | | | |
| Rib accel. | | | | | | | | | |
| Up | RibUp_acc | ar | a1 | forward | a2 | right | a3 | down | CFC180 |
| Mid | RibMid_acc | ar | a1 | forward | a2 | right | a3 | down | CFC180 |
| Low | RibLow_acc | ar | a1 | forward | a2 | right | a3 | down | CFC180 |
| T12 accel. | T12_acc | ar | a1 | forward | a2 | right | a3 | down | CFC180 |
| T12 LC | T12_lce_F | | f1 | shear | f2 | shear | | | CFC600 |
| | T12_lce_T | | t1 | roll | t2 | pitch | | | CFC600 |
| Backplate | BackPlate_lce_F | | f1 | axial | f2 | shear | | | CFC600 |
| LC | BackPlate_lce_T | | | | t2 | pitch | t3 | yaw | CFC600 |
| Abdomen[c] | | | | | | | | | |
| Front LC (L) | AbdomenLFront_lce_F | | | | f2 | axial | | | CFC600 |
| Mid LC (L) | AbdomenLMid_lce_F | | | | f2 | axial | | | CFC600 |
| Rear LC (L) | AbdomenLRear_lce_F | | | | f2 | axial | | | CFC600 |
| Front LC (R) | AbdomenRFront_lce_F | | | | f2 | axial | | | CFC600 |
| Mid LC (R) | AbdomenRMid_lce_F | | | | f2 | axial | | | CFC600 |
| Rear LC (R) | AbdomenRRear_lce_F | | | | f2 | axial | | | CFC600 |
| Pelvis | | | | | | | | | |
| Pelvis accel. | Pelvis_acc | ar | a1 | forward | a2 | right | a3 | down | CFC180 |
| Lumbar LC | Lumbar_lce_F | | f1 | shear | f2 | shear | f3 | axial | CFC600 |
| | Lumbar_lce_T | | t1 | roll | t2 | pitch | t3 | yaw | CFC600 |
| Pubic LC | Pubic_lce_F | | | | f2 | axial | | | CFC600 |
| Femur | | | | | | | | | |
| Left LC | FemurL_lce_F | | f1 | shear | f2 | shear | f3 | axial | CFC600 |
| | FemurL_lce_T | | t1 | roll | t2 | pitch | t3 | yaw | CFC600 |

*Continued on the next page*

*Table 11.7 cont.*

| Sensor | Identifier | Signal | | | | | | | Filter |
|---|---|---|---|---|---|---|---|---|---|
| | | resul-tant | x | direc-tion[a] | y | direc-tion[a] | z | direc-tion[a] | |
| Right LC | FemurR_lce_F | | f1 | shear | f2 | shear | f3 | axial | CFC600 |
| | FemurR_lce_T | | t1 | roll | t2 | pitch | t3 | yaw | CFC600 |

[a] Positive direction given according to SAE J211/1.
[b] The "_dvl" output produces resultant rib displacements and velocities; which are used to calculate the rib VC criteria.
[c] Left side load cell output (L) defined only for the left hand side model; right side load cell output (R) defined only for the right hand side model.

In the Table 11.8 all predefined injury criteria for the ES-2(re) ellipsoid Q and facet Q models are listed.

11

Table 11.8: Predefined injury criteria for the ES-2(re) ellipsoid Q and facet Q models.

| Injury criteria | Identifier | Filter |
|---|---|---|
| Head | | |
| HIC (36) | HIC36_inj | CFC1000 |
| 3ms cumulative exceedence | H3ms_inj | CFC1000 |
| Thorax | | |
| Upper rib compression | RibUpRDC_inj | CFC180 |
| Middle rib compression | RibMidRDC_inj | CFC180 |
| Lower rib compression | RibLowRDC_inj | CFC180 |
| Upper rib VC | RibUpVC_inj | CFC180 |
| Middle rib VC | RibMidVC_inj | CFC180 |
| Lower rib VC | RibLowVC_inj | CFC180 |
| Backplate Force[a] | BackPlate_Fy_inj | CFC600 |
| T12 Force[a] | T12_Fy_inj | CFC600 |
| T12 Moment[a] | T12_Mx_inj | CFC600 |
| Abdomen | | |
| Abdomen Peak Force | APF_inj | CFC600 |
| Pelvis | | |
| Pubic Symphysis Peak Force | PSPF_inj | CFC600 |

[a] Side impact Modifiers for the EuroNCAP Protocol rating

# 12 WorldSID 50th percentile Q Dummy

Following the increased market demand for dummy models that are CPU-efficient as well as accurate in response, quality (Q) models of the WorldSID side impact dummies were developed. The 50th percentile WorldSID dummy is a side impact dummy that was developed with the aim of creating a globally acceptable model with robust biofidelity and extensive injury monitoring capabilities.

The quality of the models, in terms of response correlation with validation test signals, have been determined by an objective rating method. For more information on this subject, the user is referred to the model quality report, which is supplied together with the special license needed to use these models.



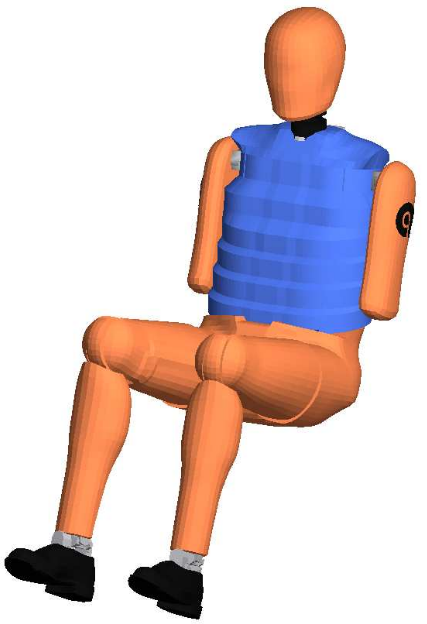

Figure 12.1: The WorldSID 50th percentile facet Q dummy model.

## 12.1 Model description

Left- and right-hand side quality rated facet models of the WorldSID are available. The input is given in the files:

| | | |
|---|---|---|
| Facet model: | Left-hand side: | d_ws50lhfc_Q_usr.xml |
| | | d_ws50lhfc_Q_inc.xml |
| | Right-hand side: | d_ws50rhfc_Q_usr.xml |
| | | d_ws50rhfc_Q_inc.xml |

To run this model, the following licenses are required:

| | |
|---|---|
| Facet model: | MADYMO/Solver (Multibody) |
| | MADYMO/Dummy Models/Side/WS50 Fc Q |

Figure 12.1 shows the WorldSID facet Q model in the reference position. The model consists of 643 bodies.



**FACET MODEL**

The geometry is represented by facet surfaces based on technical drawings and/or 3D laser scans the hardware dummy. In general, an element size of approximately 10 mm is used. Facet parts relevant to user contact definitions have contact compliance characteristics included in their NULL materials. Masses, centres of gravity and moments of inertia were applied or calculated on the basis of hardware component mass measurements and 3D CAD drawings.

All load cells are modelled with two separate rigid bodies connected to each other and to neighbouring bodies by bracket joints. The central bracket joint is the one from which the load cell output is derived. All dummy sub-assemblies are modelled as separate entities and are connected to each other by bracket "interface" joints at the locations where the hardware sub-assemblies are connected with screws. The remainder of this section gives an overview of the model design of the different dummy sub-assemblies.

**Head and neck**

For the head, facet surfaces representing the head skin and the face represent the contact surfaces. Internal surfaces are included for visualisation purposes.

For the neck column, facet surfaces representing the neck mould and the top and bottom plates are included. The openings between plates and mould are closed to avoid potential contact problems with belt/airbags. The neck column is modelled with six bodies. Two of these represent the top and bottom plate; the four bodies in between together representing the rubber neck mould. Restraints on spherical joints represent the compliance of the deforming neck buffers. The compliance of the rubber neck mould is represented with restraints on free joints in between the neck mould bodies.

The neck bracket is modelled with a lower neck load cell included. Geometry of the bracket and load cell is represented by facet surfaces. Bodies represent the head, the upper and lower neck load cells, the neck mould, and the lower neck bracket that attaches to the spinebox.

**Arms**

The arms are modelled as chains of seven rigid bodies connected by revolute joints and restraints, representing the arm bending compliance. The upper and central regions of the arm have a contact stiffness representative of the shoulder "flesh" (Hyperlast). The lower region of the arm has a different contact characteristics, representing the PU foam-filled lower end of the arm.

**Thorax**

The thorax consists of the spinebox with onboard data collection, a shoulder rib assembly by which the spinebox is connected to the arms, three thoracic ribs and two abdominal ribs. All component geometry is represented with facet surfaces. Rigid bodies are included for the spinebox, the battery and the battery mounting bracket. The T4 and T12 accelerometers are attached rigidly to the spinebox.

Each rib module includes 21 bodies; 11 of these form the inner band of the rib, the other 10 bodies represent the rib outer band. The bending stiffnesses of the two bands are modelled with revolute joints with restraints. The rib-spinebox connections are all represented by point restraints. The IR-TRACC assembly is not included geometrically but is included in the body chain. The rib response data is extracted from the acceleration and relative displacement output definitions included in the model.



The thorax is enclosed by a facet jacket, that closes the contact surfaces and has a contact characteristic representative of the jacket padding.

In the right-hand side dummy the battery and battery mounting bracket as well as the IR-TRACC assembly have been reflected about the xz-plane.

**Lumbar spine**

The lumbar spine mould is modelled as a universal, a cylindrical and a universal joint in series. A triple joint restraint is used on the three joints to define the stiffness of the spinebox relative to the hips. A bracket joint is used to represent the lumbar load cell.

**Pelvis**

The pelvis assembly is modelled with thirty rigid bodies in total. The represent amongst others the sacrum, the pubic load cell, the sacro-iliac load cells, the the iliac wings and the femur ball-socket joint. The pelvis flesh is split up over nine different bodies allowing inclussion of the different load paths from flesh to inner structural parts. The loop of bodies of the internal pelvis structure is closed by point- and flexion-torsion restraints representing the pubic buffers. The upper femurs are connected to their respective iliac sockets through spherical joints, representing the physical hip pivots.

The contact stiffness defined for the pelvis is that of Hyperlast material, as for the arms.

**Legs and feet**

The left and right leg model include separate rigid bodies for the femur neck load cell, femur load cell, knee, femur flesh, knee flesh, upper and lower tibia load cells, ankle steel, tibia flesh, foot assembly and the foot. The hip joint is a spherical joint with a cardan restraint applied. The thigh flesh is connected to the femur steel by a bracket joint. The knee pivot is modelled with a revolute joint. The ankle pivot is also represented by a revolute joint. Joint friction is included in the different revolute joints.

## CONTACTS BETWEEN DUMMY COMPONENTS

Inter-component contacts have been defined between the head and the thorax, the head and the arms, the arms and the jacket and between the left and right leg.

## 12.2 Model validation

The dummy model has been developed and validated for side impact loading using the tests listed below. For detailed information on the model validation the reader is referred to the quality report supplied with the dummy model.

### Component tests

The component tests used for development and validation of the model are summarised in Table 12.1. The component level validation results can be found in the quality report supplied with the dummy models.

Table 12.1: Component tests for the WorldSID facet Q model.

| Component | Test description | specification | | Model Facet Q |
|---|---|---|---|---|
| Head | Lateral drop tests | drop height/angle | 150 mm/35° | x |
| | | | 200mm/35° | x |
| | | | 200mm/10° | x |
| Neck | Pendulum swing tests | velocity | 2.5 m/s | x |
| | | | 3.4 m/s | x |
| | | | 4.0 m/s | x |

### Full dummy tests

The tests with the complete dummy used for development and validation of the model are summarised in Table 12.2. The validation results at full dummy level can also be found in the quality report supplied with the dummy models.

Table 12.2: Full dummy tests for the WorldSID facet Q models.

| Test description | specification | | Model Facet Q |
|---|---|---|---|
| Pendulum shoulder test | velocity | 3.0m/s<br>4.3m/s<br>5.0m/s | x<br>x<br>x |
| Pendulum thorax test | velocity | 3.0m/s<br>4.3m/s<br>5.0m/s | x<br>x<br>x |
| Pendulum arm test | velocity | 5.0m/s<br>6.7m/s | x<br>x |

*Continued on the next page*

*Table 12.2 cont.*

| Test | | | Model |
|---|---|---|---|
| description | specification | | Facet Q |
| Pendulum abdomen test | velocity | 3.0m/s<br>4.3m/s<br>5.0m/s | x<br>x<br>x |
| Pendulum pelvis test | velocity | 5.0m/s<br>6.7m/s | x<br>x |
| Pendulum pelvis test, forward offset | velocity | 5.0m/s<br>6.7m/s | x<br>x |
| Pendulum pelvis test, rear offset | velocity | 5.0m/s<br>6.7m/s | x<br>x |
| Pendulum femur test | velocity | 5.0m/s<br>6.7m/s | x<br>x |
| Sled test with arm | offsets/velocity | 0-50-50/4.7m/s | x |
| Sled test without arm | offsets/velocity | 0-50-50/4.7m/s | x |
| Sled test without arm | offsets/velocity | 0-50-50/7.1m/s | x |
| Sled test without arm, dummy turned 10° | offsets/velocity | 0-50-50/4.7m/s | x |
| Sled test with arm | offsets/velocity | 50-0-0/4. m/s | x |
| Sled test without arm | offsets/velocity | 50-0-0/4.7m/s | x |
| Sled test without arm, pelvis impact | offsets/velocity | – – 0 /4.0m/s | x |
| Sled test without arm, pelvis impact | offsets/velocity | – – 0 /4.7m/s | x |
| Sled test without arm, pelvis impact | offsets/velocity | – – 0 /7.1m/s | x |
| Sled test without arm, thorax impact | offsets/velocity | 0 – – /4.0m/s | x |

## Range of validity of the model

The dummy model has been validated for side impact loading conditions.

## 12.3 User instructions

### Timestep

Table 12.3: Recommended timestep for the WorldSID Q model.

| Model | timestep (s) |
|---|---|
| Facet | $\leq 1.0 \cdot 10^{-5}$ |

### Dummy positioning

Table 12.4: Positioning joints for the WorldSID Q model.

| Joint Description | Identifier | Degree of freedom[a] | | | | | |
|---|---|---|---|---|---|---|---|
| Complete dummy | Dummy_jnt | D1 | forward | D2 | leftward | D3 | upward |
| | | R1 | roll right | R2 | pitch down[b] | R3 | yaw left |
| Neck bracket | NeckBracket_jnt | R1 | pitch down | | | | |
| Left shoulder | ShoulderL_jnt | R1 | pitch up | | | | |
| Right shoulder | ShoulderR_jnt | R1 | pitch up | | | | |
| Left shoulder clevis | ShoulderLClevis_jnt | R1 | roll right | | | | |
| Right shoulder clevis | ShoulderRClevis_jnt | R1 | roll left | | | | |
| Lumbar spine | LumbarMouldPart3_jnt [c] | R1 | roll left | R2 | pitch down | | |
| | LumbarMouldPart2_jnt [c] | R1 | yaw left | | | | |
| | | D1 | upward | | | | |
| | LumbarMouldPart1_jnt [c] | R1 | pitch down | R2 | roll left | | |
| Left hip | HipL_jnt | R1 | pitch down | R2 | roll left | R3 | yaw left |
| Right hip | HipR_jnt | R1 | pitch down | R2 | roll left | R3 | yaw left |
| Left knee | KneeL_jnt | R1 | pitch down | | | | |
| Right knee | KneeR_jnt | R1 | pitch down | | | | |
| Left ankle | | | | | | | |
| Up | AnkleUpL_jnt | R1 | yaw left | | | | |
| Mid | AnkleMidL_jnt | R1 | pitch down | | | | |
| Low | AnkleLowL_jnt | R1 | roll right | | | | |
| Right ankle | | | | | | | |
| Up | AnkleUpR_jnt | R1 | yaw left | | | | |
| Mid | AnkleMidR_jnt | R1 | pitch down | | | | |
| Low | AnkleLowR_jnt | R1 | roll right | | | | |

[a] Positive translation or rotation given in global coordinate system, with dummy in reference position (see Figure 12.1).

[b] The pitch angle of the INITIAL.JOINT_POS element in the usr-file is predefined such that the H-point tool would be oriented 45° below horizontal, the pelvis tilt sensor Y-angle reading would be 14.5° and the top of the lower neck bracket has a downward pitch angle of 0.5°.

[c] In principle only for equilibrium state, however it might be necessary to rotate lumbar joints to position upper torso with neck and head correctly.

12

### Dummy contacts

When defining contacts between the dummy model and its environment, only the contact groups defined in Table 12.5 need to be used; no contacts should be defined with the dummy components underneath the outer facet surfaces.

In general, the dummy surface should be chosen as the master group in contact definitions. This is also the way in which the contacts have been defined in the dummy model validation test suite. With the dummy surfaces chosen as master group in the contact definitions, the user will avoid problems with edges in the master surfaces because the dummy contact surfaces are all closed. Furthermore, with the dummy surfaces as master the direction of the contact forces and torques is always controlled by the dummy model. As an exception to this guideline, the dummy surface can best be chosen as the slave group when the dummy is placed on a flat rigid seat or bench with initial contact.

For the environmental structures that contact the dummy, meshes with an element size of about 10–15 mm or smaller are recommended. This element size was also used in the models of the dummy model validation test suite.

Table 12.5: Predefined groups to define contact between the WorldSID Q model components and their environment.

| Contact Description | Identifier[a] | Facet Q models |
|---|---|---|
| Head | Head_gfe | closed outer head skin surface |
| Neck | Neck_gfe | closed neck mould and interface plates surface |
| Neck bracket | NeckBracket_gfe | closed bracket and lower neck load cell surfaces |
| Jacket | Jacket_gfe | closed jacket surface |
| Left arm<br>Right arm | ArmL_gfe<br>ArmR_gfe | closed left arm flesh surface<br>closed right arm flesh surface |
| Pelvis | Pelvis_gfe | closed outer pelvis |
| Left upper leg<br>Right upper leg | FemurKneeL_gfe<br>FemurKneeR_gfe | closed left outer femur and knee flesh surface<br>closed right outer femur and knee flesh surface |
| Left lower leg<br>Right lower leg | TibiaL_gfe<br>TibiaR_gfe | closed left outer tibia flesh surface<br>closed right outer tibia flesh surface |
| Left shoe<br>Right shoe | ShoeL_gfe<br>ShoeR_gfe | closed left outer shoe mould surface<br>closed right outer shoe mould surface |

### Output

In Table 12.6 all predefined output definitions for the WorldSID Q model are listed. Note that the output signal filtering is taken from SAE standards. For the rib displacements the output signals with extension _dis should be used. The output signals with extension _dvl are to be used for generating the VC injury output only. ISO-MME output can also be generated for the WorldSID 50th percentile Q dummy models. Output requests for signals in ISO-MME format are pre-defined in the CONTROL_OUTPUT element in the user file.

Table 12.6: Predefined output signals for the WorldSID Q model.

| **Sensor** | **Identifier** | **Signal** | | | | | | | **Filter** |
|---|---|---|---|---|---|---|---|---|---|
| | | **resul-tant** | **x** | **direc-tion**[(a)] | **y** | **direc-tion**[(a)] | **z** | **direc-tion**[(a)] | |
| Head | | | | | | | | | |
| CG accel. | HeadCG_acc | ar | a1 | forward | a2 | right | a3 | down | CFC1000 |
| CG ang. acc | HeadCG_aac | ar | a1 | roll | a2 | pitch | a3 | yaw | CFC1000 |
| Neck | | | | | | | | | |
| Upper LC | NeckUp_lce_F | | f1 | shear | f2 | shear | f3 | axial | CFC1000 |
| | NeckUp_lce_T | | t1 | roll | t2 | pitch | t3 | yaw | CFC600 |
| Lower LC | NeckLow_lce_F | | f1 | shear | f2 | shear | f3 | axial | CFC1000 |
| | NeckLow_lce_T | | t1 | roll | t2 | pitch | t3 | yaw | CFC600 |
| Shoulder | | | | | | | | | |
| Left LC | ShoulderL_lce_F | | f1 | rearward | f2 | leftward | f3 | upward | CFC600 |
| Right LC | ShoulderR_lce_F | | f1 | rear-ward | f2 | right-ward | f3 | down-ward | CFC600 |
| Left accel. | ShoulderRibL_acc | ar | a1 | forward | a2 | right | a3 | down | CFC600 |
| Right accel. | ShoulderRibR_acc | ar | a1 | forward | a2 | right | a3 | down | CFC600 |
| T1 accel. | T1_acc | ar | a1 | forward | a2 | right | a3 | down | CFC180 |
| Displacement | ShoulderRibR/L_dis | dr | | | d2 | lateral | | | CFC600 |
| | ShoulderRibR/L_dvl | dr | | | | | | | CFC180 |
| Thorax | | | | | | | | | |
| Rib | | | | | | | | | |
| Thorax 1 | ThoracicRib1R/L_dis | dr | | | d2 | lateral | | | CFC600 |
| | ThoracicRib1R/L_dvl | dr | | | | | | | CFC180 |
| | ThoracicRib1R/L_acc | ar | a1 | forward | a2 | right | a3 | down | CFC1000 |
| Thorax 2 | ThoracicRib2R/L_dis | dr | | | d2 | lateral | | | CFC600 |
| | ThoracicRib2R/L_dvl | dr | | | | | | | CFC180 |
| | ThoracicRib2R/L_acc | ar | a1 | forward | a2 | right | a3 | down | CFC1000 |
| Thorax 3 | ThoracicRib3R/L_dis | dr | | | d2 | lateral | | | CFC600 |
| | ThoracicRib3R/L_dvl | dr | | | | | | | CFC180 |
| | ThoracicRib3R/L_acc | ar | a1 | forward | a2 | right | a3 | down | CFC1000 |
| T4 accel. | T4_acc | ar | a1 | forward | a2 | right | a3 | down | CFC180 |
| T12 accel. | T12_acc | ar | a1 | forward | a2 | right | a3 | down | CFC180 |
| T4 ang. accel. | T4 aac | ar | a1 | roll | a2 | pitch | a3 | yaw | CFC600 |
| Abdomen | | | | | | | | | |
| Rib | | | | | | | | | |
| Abd. 1 | AbdominalRib1R/L_dis | dr | | | d2 | lateral | | | CFC600 |
| | AbdominalRib1R/L_dvl | dr | | | | | | | CFC180 |
| | AbdominalRib1R/L_acc | ar | a1 | forward | a2 | right | a3 | down | CFC1000 |
| Abd. 2 | AbdominalRib2R/L_dis | dr | | | d2 | lateral | | | CFC600 |
| | AbdominalRib2R/L_dvl | dr | | | | | | | CFC180 |
| | AbdominalRib2R/L_acc | ar | a1 | forward | a2 | right | a3 | down | CFC1000 |
| Pelvis | | | | | | | | | |
| Pelvis accel. | Pelvis_acc | ar | a1 | forward | a2 | right | a3 | down | CFC1000 |
| Lumbar LC | Lumbar_lce_F | | f1 | shear | f2 | shear | f3 | axial | CFC1000 |
| | Lumbar_lce_T | | t1 | roll | t2 | pitch | t3 | yaw | CFC1000 |
| Pubic LC | Pubic_lce_F | | f1 | shear | f2 | axial | f3 | shear | CFC1000 |
| | Pubic_lce_T | | t1 | roll | t2 | torsion | t3 | yaw | CFC1000 |

*Continued on the next page*

12

*Table 12.6 cont.*

| Sensor | Identifier | Signal resultant | x | direction[a] | y | direction[a] | z | direction[a] | Filter |
|---|---|---|---|---|---|---|---|---|---|
| Sacroiliac LC | SacroiliacLCR/L_lce_F | | f1 | shear | f2 | axial | f3 | shear | CFC1000 |
| | SacroiliacLCR/L_lce_T | | t1 | roll | t2 | torsion | t3 | yaw | CFC1000 |
| Femur | | | | | | | | | |
| Left neck LC | FemurNeckL_lce_F | | f1 | shear | f2 | shear | f3 | axial | CFC600 |
| | FemurNeckL_lce_T | | t1 | yaw | t2 | pitch | t3 | roll | CFC600 |
| Left LC | FemurL_lce_F | | f1 | shear | f2 | shear | f3 | axial | CFC600 |
| | FemurL_lce_T | | t1 | roll | t2 | pitch | t3 | yaw | CFC600 |
| Right neck LC | FemurNeckR_lce_F | | f1 | shear | f2 | shear | f3 | axial | CFC600 |
| | FemurNeckR_lce_T | | t1 | yaw | t2 | pitch | t3 | roll | CFC600 |
| Right LC | FemurR_lce_F | | f1 | shear | f2 | shear | f3 | axial | CFC600 |
| | FemurR_lce_T | | t1 | roll | t2 | pitch | t3 | yaw | CFC600 |
| Knee | | | | | | | | | |
| Left Knee rot. | KneeL_pos | | r1 | pitch | | | | | CFC180 |
| Right Knee rot. | KneeR_pos | | r1 | pitch | | | | | CFC180 |
| Ankle | | | | | | | | | |
| Left Ankle rot. | AnkleUpL_pos | | r1 | yaw | | | | | CFC180 |
| | AnkleMidL_pos | | r1 | pitch | | | | | CFC180 |
| | AnkleLowL_pos | | r1 | roll | | | | | CFC180 |
| Right Ankle rot. | AnkleUpR_pos | | r1 | yaw | | | | | CFC180 |
| | AnkleMidR_pos | | r1 | pitch | | | | | CFC180 |
| | AnkleLowR_pos | | r1 | roll | | | | | CFC180 |

[a] Positive direction given according to SAE J211/1.

In Table 12.7 all predefined injury criteria for the WorldSID Q model are listed. Injury criteria that are actually peak levels of single output signals are not explicitly defined in the models, since these peak levels are already printed in the peak files.

Table 12.7: Predefined injury criteria for the WorldSID Q model.

| Injury criteria | Identifier | Filter |
|---|---|---|
| Head | | |
| HIC (36) | HIC36_inj | CFC1000 |
| 3ms cumulative exceedence | H3ms_inj | CFC1000 |
| Thorax | | |
| VC | ShoulderRibR/LVC_inj | CFC180 |
| | ThoracicRib1R/LVC_inj | CFC180 |
| | ThoracicRib2R/LVC_inj | CFC180 |
| | ThoracicRib3R/LVC_inj | CFC180 |
| Abdomen | | |
| VC | AbdominalRib1R/LVC_inj | CFC180 |
| | AbdominalRib2R/LVC_inj | CFC180 |

# 13 US DoT-SID Side Impact Dummy

The US DoT-SID is a side impact dummy that was originally adapted from the Hybrid II 50th percentile male test dummy. This dummy is prescribed for side impact testing following the former US regulation FMVSS214.

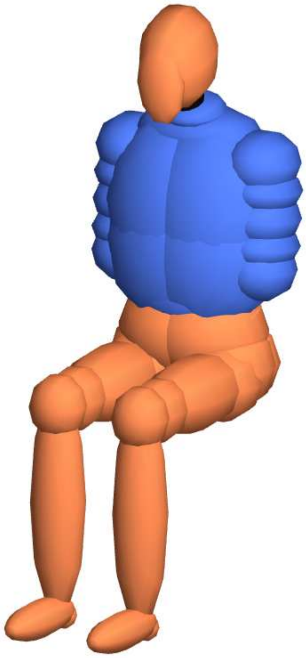

Figure 13.1: US DoT-SID ellipsoid dummy model in reference position.

## 13.1 Model description

Left and right hand side ellipsoid models of the US DoT-SID dummy are available. The models are provided in the following files:

| | | |
|---|---|---|
| Ellipsoid model: | Left Hand Side: | d_usslhel_usr.xml |
| | | d_usslhel_inc.xml |
| | Right Hand Side: | d_ussrhel_usr.xml |
| | | d_ussrhel_inc.xml |

To run these models, the following licenses are required:

| | |
|---|---|
| Ellipsoid model: | MADYMO/Solver (Multibody) |
| | MADYMO/Dummy Models/Side |

Figure 13.1 shows the ellipsoid model in the reference position.



**DUMMY MODEL**

**Head and Neck**

The neck is represented by a rigid body that is connected to the spine box and head bodies by spherical joints: the lower neck joint and upper neck joint. Static and dynamic neck behaviour is represented by flexion-torsion restraints between thorax and neck and head and neck. A single ellipsoid represents the neck geometry. The head is modelled by a rigid body and two ellipsoids representing skull and face.

**Thorax, jacket and arms**

The spine box is represented by a rigid body and a fourth order hyper-ellipsoid. Another fourth order hyper-ellipsoid represents the rubber bump stop attached to the spine box and a second order ellipsoid represents the shoulder foam.

The ribcage is subdivided into a sternum body and ten rib segment bodies (five on each side). The ribcage segment bodies are connected by revolute joints having stiffness and damping characteristics that represent ribcage bending behaviour. Part of the jacket mass is included in the ribcage model by dividing it over the ribcage bodies. The characteristics of the joints linking the rib segment bodies were derived from thorax component tests. The influence of the poly-urethane rib damping material on the bending stiffness has been included by a damping function.

To model the canvas hinge that connects the ribcage to the spine box, four pairs of point-restraints and four kelvin elements are used. On either side of the spine box a pair of point restraints and a kelvin element are modelled both at the top and the bottom of the hinge. Connecting the spine box body to the left and right back side ribcage bodies, these point restraints and kelvin elements represent bending, compression and vertical shear of the hinge.

The damper unit (shock absorber) is modelled by two bodies, damper and damper rod end, connected by a translational joint with complex, non-linear stiffness and damping characteristics. Component tests were used to determine the characteristics of the (protected) damper joint characteristics. These characteristics are calibrated using damper component tests. The damper body connects to the spine box by a spherical joint. The damper rod end body connects to the left lateral ribcage segment body by a revolute joint.

The left and right arm foam blocks are represented each by five arm segment bodies. The three central arm segment bodies are connected to the lateral ribcage segment bodies by translational joints. Similar translational joints connect the upper and lower arm bodies to the central arm bodies. The three central arm bodies are interconnected by point restraints with characteristics identical to those of the translational joints. The characteristics of the joints and point restraints connecting the arm segment bodies represent the arm foam and jacket deformation when (part of) the arm is impacted. The load paths from upper arm to the upper thoracic spine and from lower arm via abdomen to lower thoracic spine are represented by two pairs of point restraints. A small part of the arm compression is incorporated in the elastic contact characteristics of the arm ellipsoids. The arm characteristics are calibrated using (thorax/arm/jacket) assembly and full dummy dynamic impact tests. The jacket geometry is represented by the ten arm ellipsoids and eight ellipsoids attached to the spine box body.

**Lumbar spine**

To obtain a model for the lumbar spine a combination of a free joint and a (protected) six-dof joint restraint is used and a kelvin element was included to model the spine cable. The six-dof restraint describes the lumbar spine characteristics for (combined) bending, shear, compression and torsion. The joint is positioned centrally between the lumbar spine connection plates. The mass and inertia properties of the actual lumbar spine have been divided over the upper and lower spine bodies. The upper and lower lumbar spine bodies are connected to the spine box and pelvis body by means of bracket joints. Some effects of the contact interactions between jacket, abdomen and pelvis are included in the model by adjustment of the parameters of the protected six-dof restraint model.



**Pelvis and abdomen**

The pelvis is modelled as a rigid body with ten ellipsoids attached. Both the left and right side of the pelvis geometry are modelled with five ellipsoids; one of them representing the iliac wing. The left and right iliac wing ellipsoids are included to model the stiff contact interactions between environment and the upper lateral pelvis region. The contact characteristics for the ellipsoid represent the compliance of the pelvis.

During abdomen impacts on the US DoT-SID dummy, loads are transferred from jacket and lower arm foam onto the abdomen and then from abdomen onto the spine. In the model, the load transfer through the abdomen is not explicitly modelled. Instead, this load transfer is incorporated in the model by means of the point restraints that directly connect the lower arm bodies to the spine box body (see thorax, jacket and arms section). The abdomen is represented visually by an ellipsoid attached to the upper lumbar spine body. The inertia properties of the abdomen are incorporated in the pelvis body.

**Legs and Feet**

Each leg consists of three bodies: the femur, knee and tibia body. The legs are connected to the pelvis by the hip joints, which are universal joints. Femur and knee bodies are connected by revolute joints. These joints allow sideward rotation ("yaw") halfway in the upper legs, as in the hardware dummy. The revolute joints between knee and tibia bodies enable knee rotation in the model. Each leg has four ellipsoids, two for the upper leg, one for the knee and one for the lower leg. Foot bodies are connected to the tibia bodies by revolute ankle joints. The foot geometry is modelled by a foot and a heel ellipsoid. Contact characteristics for the ellipsoid represent the compliance of the leg flesh and feet.

## CONTACTS BETWEEN DUMMY COMPONENTS

Contact is defined between the left and right leg.

## 13.2 Model validation

The dummy models are developed and validated using component tests and tests on the complete dummy.

### Component tests

The component tests used for development and validation of the models are summarised in Table 13.1.

Table 13.1: Component tests for US DoT-SID dummy model.

| Component | Test description | specification | |
|---|---|---|---|
| Neck | Static flexion/extension<br>Static lateral flexion/extension<br>Static oblique flexion/extension<br>Static torsion | | |
| Damper | Dynamic impact | mass+velocity | 4.7 kg, 3.1 m/s<br>4.7 kg, 4.0 m/s<br>4.7 kg, 6.1 m/s |
| Thorax | Static compression:<br>- free ribcage<br>- fixed ribcage<br>Static chest deflection | | |
| | Dynamic impact | mass+velocity | 9.9 kg, 3.5 m/s<br>9.9 kg, 4.5 m/s<br>9.9 kg, 6.5 m/s<br>9.9 kg, 4.0 m/s<br>9.9 kg, 6.0 m/s<br>20.75 kg, 4.3 m/s<br>20.75 kg, 8.1 m/s<br>20.75 kg, 10.3 m/s |
| Arm & Jacket | Dynamic impact | mass+velocity | 9.9 kg, 1.1 m/s<br>9.9 kg, 2.2 m/s<br>9.9 kg, 3.5 m/s |
| Upper Torso Assembly (thorax, arms and jacket) | Static chest deflection | | |
| | Dynamic impact | mass+velocity | 9.9 kg, 4.0m/s<br>9.9 kg, 6.0 m/s<br>9.9 kg, 8.0 m/s |
| Lumbar Spine | Static flexion/extension<br>Static torsion<br>Static compression/extension<br>Static shear | | |
| | Dynamic pendulum test | mass+velocity | 9.9 kg, 6.9 m/s |
| | Oblique dynamic pendulum | mass+velocity | 9.9 kg, 4.7 m/s |
| Pelvis | Static compression | | |
| | Dynamic impact | mass+velocity | 9.9 kg, 3.5 m/s<br>9.9 kg, 4.5 m/s |

*Continued on the next page*

*Table 13.1 cont.*

| Component | Test description | specification |
|---|---|---|
| Upper leg | Hip joint:<br>static flexion/extension<br>static adduction/abduction<br>Femur joint:<br>static adduction/ abduction | |

### Full dummy tests

A series of side impact tests involving the three main areas of interest in side impact, i.e. pelvis, thorax and abdomen, have been used to validate the behaviour of the complete dummy model. These tests are listed in Table 13.2.

Table 13.2: Full dummy tests for US DoT-SID dummy model.



| Test description | specification | |
|---|---|---|
| Full side impact, thorax, abdomen and pelvis plates aligned (0/0/0) | mass+velocity | 35.9 kg, 6.4 m/s |
| Staggered impact, thorax and abdomen plate leading 50 mm (50/50/0) | mass+velocity | 37.6 kg, 6.4 m/s |
| Staggered impact, pelvis plate leading 50 mm (0/0/50) | mass+velocity | 36.8 kg, 6.4 m/s |
| Staggered impact, thorax plate leading 50 mm (50/0/0) | mass+velocity | 36.0 kg, 4.4 m/s<br>36.0 kg, 6.3 m/s |
| Staggered impact, abdomen plate leading 100 mm (0/100/0) | mass+velocity | 36.5 kg, 4.3 m/s<br>36.5 kg, 6.2 m/s |
| Guided head impact | mass+velocity | 28.5 kg, 4.7 m/s |
| Guided pelvis impact | mass+velocity | 31.5 kg, 6.8 m/s |
| Pendulum impact | lower arm region<br>abdomen region | 3 velocities<br>3 velocities |
| Staggered impact sled test | several configurations with padded impactor | v>10 m/s |
| Thorax certification test | mass+velocity | 23.4 kg, 4.6 m/s |

## 13.3 User instructions

### Timestep

Table 13.3: Recommended timestep for the US DoT-SID dummy model.

| Model | timestep (s) |
|---|---|
| Ellipsoid | $\leq 1.0 \cdot 10^{-4}$ |

### Dummy positioning

Table 13.4: Positioning joints of the US-DoT SID dummy model.

| Joint Description | Identifier | Degree of freedom [a] | | | | | | Comment |
|---|---|---|---|---|---|---|---|---|
| Complete dummy | Dummy_jnt | R1 | roll right | R2 | pitch down | R3 | yaw left | |
| | | D1 | forward | D2 | leftward | D3 | upward | |
| Lumbar spine | LumbarSpine_jnt | R1 | yaw left | R2 | pitch down | R3 | roll left | |
| | | D1 | upward | D2 | leftward | D3 | backward | |
| Left hip | HipL_jnt | R1 | yaw left | R2 | pitch down | | | |
| Right hip | HipR_jnt | R1 | yaw left | R2 | pitch down | | | |
| Left knee | KneeL_jnt | R1 | pitch down | | | | | |
| Right knee | KneeR_jnt | R1 | pitch down | | | | | |
| Left ankle | AnkleL_jnt | R1 | pitch down | | | | | |
| Right ankle | AnkleR_jnt | R1 | pitch down | | | | | |

[a] Positive translation or rotation given in global co-ordinate system while dummy is in reference position (see Figure 1.2)

### Dummy contacts

In Table 13.5 the groups available for defining contacts between the dummy model components and environment are listed. No jacket contact characteristics are defined. The ellipsoid jacket group should not be used in the contact definitions between dummy and impacting (vehicle) structures. When defining contacts between the ellipsoid dummy and a seat, the Jacket, Pelvis and both FemurKnee groups should be used. For contacts between jacket and seat, the user can either use the seat characteristics or define combined seat-jacket contact characteristics.

Table 13.5: Available groups to define contact between the US DoT-SID model components and environment.

| Contact Description | Identifier[a],[b] | Ellipsoid model[b],[c] |
|---|---|---|
| Head[d] | Head_*ctg* | Head_ell |

*Continued on the next page*

Table 13.5 *cont.*

| **Contact Description** | **Identifier**[a],[b] | **Ellipsoid model**[b],[c] |
|---|---|---|
| Left Arm | ArmL_*ctg* | ArmPart⟨i⟩L_ell, for i=1 to 5 [a] |
| Right Arm | ArmR_*ctg* | ArmPart⟨i⟩R_ell, for i=1 to 5 [a] |
| Jacket | Jacket_*ctg* | JacketShoulderRear_ell<br>JacketBodyUpL/R_ell<br>JacketBodyLowL/R_ell |
| Pelvis | Pelvis_*ctg* | PelvisRearLowL/R_ell<br>PelvisMidLowL/R_ell<br>PelvisFrontLowL/R_ell<br>PelvisMidUpL/R_ell<br>PelvisIliacWingL/R_ell |
| Left Femur and Knee | FemurKneeL_*ctg* | FemurUpL_ell<br>FemurLowL_ell<br>KneeL_ell |
| Right Femur and Knee | FemurKneeR_*ctg* | FemurUpR_ell<br>FemurLowR_ell<br>KneeR_ell |
| Left Tibia | TibiaL_*ctg* | TibiaL_ell |
| Right Tibia | TibiaR_*ctg* | TibiaR_ell |
| Left Shoe | ShoeL_*ctg* | FootL_ell<br>HeelL_ell |
| Right Shoe | ShoeR_*ctg* | FootR_ell<br>HeelR_ell |

[a] *ctg*= contact group, for the ellipsoid models ctg is replaced by gmb(group_multibody) and for the FE model by gfe (group_finite element).

[b] L=Left; R=Right.

[c] Part⟨i⟩: numbered from bottom to top / rear to front / right to left.



## Output

Table 13.6: US DoT-SID output signals.

| **Sensor** | **Identifier** | **Signal** resultant | x | direction[a] | y | direction[a] | z | direction[a] | **Filter** |
|---|---|---|---|---|---|---|---|---|---|
| Head | | | | | | | | | |
| accelerometers | HeadCG_acc | ar | a1 | forward | a2 | lateral | a3 | vertical | CFC1000 |
| Thorax | | | | | | | | | |
| accelerometers | ThoraxSpineUp_acc | | a1 | forward | a2 | lateral | a3 | vertical | FIR100 |
| | ThoraxSpineLow_acc | | a1 | forward | a2 | lateral | a3 | vertical | FIR100 |
| | RibUp_acc | | | | | lateral | | | FIR100 |
| | RibLow_acc | | | | | lateral | | | FIR100 |
| potentiometer | ChestDeflection_dis | | | | d2 | displacement | | | CFC600 |
| Pelvis | | | | | | | | | |

*Continued on the next page*

*Table 13.6 cont.*

| Sensor | Identifier | Signal | | | | | | | Filter |
|---|---|---|---|---|---|---|---|---|---|
| | | resul-tant | x | direc-tion[a] | y | direc-tion[a] | z | direc-tion[a] | |
| accelerometers | Pelvis_acc | | a1 | forward | a2 | lateral | a3 | vertical | FIR100 |

[a] Positive direction given according to SAE J211/1.

Table 13.7: Injury criteria defined for the US DoT-SID.

| Injury criteria | Identifier | Filter |
|---|---|---|
| Head | | |
| HIC (36) | HIC36_inj | CFC1000 |
| Thorax | | |
| TTI | TTI_inj | FIR100 |

13

# 14 SID-H3 Side Impact Dummy

The SID-H3 dummy is identical to the US DoT-SID dummy with exception of the neck and the head. These two components are adopted from the Hybrid III 50$^{th}$ percentile dummy. The SID-H3 dummy is used in US regulations for protection against lateral pole impact (FMVSS 201).

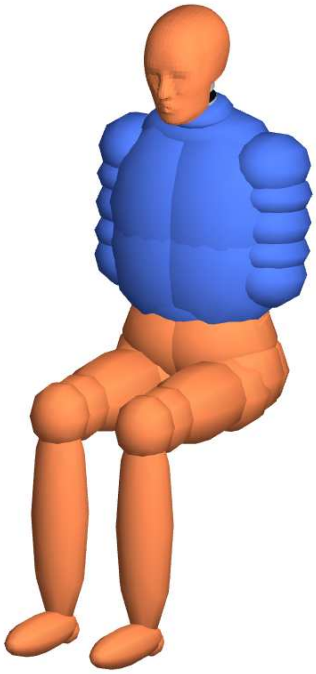

Figure 14.1: Ellipsoid model of SID-H3 dummy.

## 14.1 Model description

Ellipsoid models of the SID-H3 Side Impact Dummy are available. The input is given in the files:

| | | |
|---|---|---|
| Ellipsoid model: | Left hand side: | d_sidh3lhel_usr.xml |
| | | d_sidh3lhel_inc.xml |
| | Right hand side: | d_sidh3rhel_usr.xml |
| | | d_sidh3rhel_inc.xml |

To run these models, the following licenses are required:

| | |
|---|---|
| Ellipsoid models: | MADYMO/Solver (Multibody) |
| | MADYMO/Dummy Models/Side |

Figure 14.1 shows the model in the reference position.

### ELLIPSOID MODEL

Following the hardware, the torso and extremities of the SID-H3 dummy model are adopted from the US DoT-SID dummy model (Chapter 13) and the neck and head are adopted from the Hybrid III 50$^{th}$ percentile dummy model (Chapter 36). The US DoTSID components are represented as ellipsoids models; the head and neck are represented as facet models. The position and orientation of the head-neck assembly is modified with respect to the US DoT-SID head-neck assembly in such a way that it corresponds with the differences in geometry of the SID-H3 and US DoT-SID neck brackets.

14

### CONTACTS BETWEEN DUMMY COMPONENTS

Contact is defined between the left and right leg.

## 14.2 Model validation

No additional validation has been done for the SID-H3 dummy model other than those applicable for the US DOTSID dummy model (see Section 13.2) and the Hybrid III 50$^{th}$ percentile dummy model (see Section 5.2).

14

## 14.3 User instructions

### Timestep

Table 14.1: Recommended timestep for the SID-H3 dummy model.

| Model | timestep (s) |
|---|---|
| Ellipsoid | $\leq 1.0 \cdot 10^{-4}$ |

### Dummy positioning

Table 14.2: Positioning joints of the SID-H3 dummy model.

| Joint Description | Identifier | Degree of freedom [a] | | | | | | Comment |
|---|---|---|---|---|---|---|---|---|
| Complete dummy | Dummy_jnt | R1<br>D1 | roll right<br>forward | R2<br>D2 | pitch down<br>leftward | R3<br>D3 | yaw left<br>upward | |
| Neck element | NeckPivot⟨i⟩_jnt, for i=1 to 4 [b] | R1 | roll right | R2 | pitch down | R3 | yaw left | only for equilibrium state |
| Lumbar spine | LumbarSpine_jnt | R1<br>D1 | yaw left<br>upward | R2<br>D2 | pitch down<br>leftward | R3<br>D3 | roll left<br>backward | |
| Left hip | HipL_jnt | R1 | yaw left | R2 | pitch down | | | |
| Right hip | HipR_jnt | R1 | yaw left | R2 | pitch down | | | |
| Left knee | KneeL_jnt | R1 | pitch down | | | | | |
| Right knee | KneeR_jnt | R1 | pitch down | | | | | |
| Left ankle | AnkleL_jnt | R1 | pitch down | | | | | |
| Right ankle | AnkleR_jnt | R1 | pitch down | | | | | |

[a] Positive translation or rotation given in global co-ordinate system while the dummy is in reference position.
[b] Part⟨i⟩: numbered from bottom to top.

### Output

Table 14.3: SID-H3 output signals.

| Sensor | Identifier | Signal | | | | | | | Filter |
|---|---|---|---|---|---|---|---|---|---|
| | | resul-tant | x | direc-tion[a] | y | direc-tion[a] | z | direc-tion[a] | |
| Head | | | | | | | | | |
| accelerometers | HeadCG_acc | ar | a1 | forward | a2 | lateral | a3 | vertical | CFC1000 |
| Neck | | | | | | | | | |
| Upper load cell | NeckUp_lce_F | fr | f1 | shear | f2 | shear | f3 | axial | CFC1000 |
| | NeckUp_lce_T | tr | t1 | roll | t2 | pitch | t3 | yaw | CFC600 |
| Thorax | | | | | | | | | |
| accelerometers | TopSpine_acc | | a1 | forward | a2 | lateral | a3 | vertical | FIR100 |
| | BottomSpine_acc | | a1 | forward | a2 | lateral | a3 | vertical | FIR100 |
| | RibUp_acc | | | | | lateral | | | FIR100 |
| | RibLow_acc | | | | | lateral | | | FIR100 |
| potentiometer | ChestDeflection_dis | | | | d2 | displace-ment | | | CFC600 |
| Pelvis | | | | | | | | | |
| accelerometers | Pelvis_acc | | a1 | forward | a2 | lateral | a3 | vertical | FIR100 |

[a] Positive direction given according to SAE J211/1.

Table 14.4: Injury criteria defined for the SID-H3 components.

| Injury criteria | Identifier | Filter |
|---|---|---|
| Head | | |
| HIC (36) | HIC36_inj | CFC1000 |
| Thorax | | |
| TTI | TTI_inj | FIR100 |

14

# 15 SID-IIs Side Impact Dummy

The SID-IIs has the anthropometry of adolescents (12 to 14 years old) or smallest adults and is particularly used to evaluate active automotive side impact protection systems, such as side airbags. SID-IIs was developed by the Occupant Safety Research Partnership (OSRP) of the USCAR program.

A complete airbag interaction arm including the hand, the lower and upper arms, was also designed.[1]

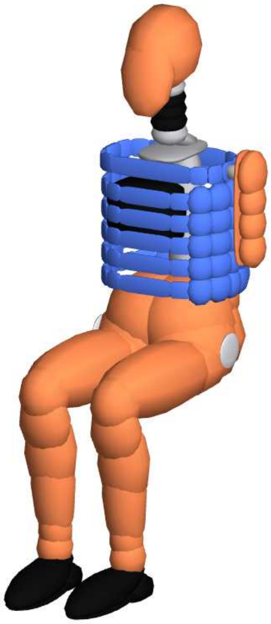

Figure 15.1: SID-IIs ellipsoid dummy model in reference position



[1]R.A. Denton Inc., "model 4380 Enhanced Airbag Interaction Arm for Hybrid III 5$^{th}$ precentile and SID-IIs ATD's", 23/02/2000.

## 15.1 Model description

The ellipsoid model of the standard SID-IIs dummy is available. The input is given in the files:

| | |
|---|---|
| Ellipsoid model: | d_sid2sel_usr.xml + d_sid2sel_inc.xml |

Figure 15.1 shows the SID-IIs ellipsoid model in its reference position.

The ellipsoid models of the SID-IIs with the airbag interaction arm are also available. The left hand side and right hand side model exist. The input is given in the files:

| | |
|---|---|
| Ellipsoid model: | d_sid2slharmel_usr.xml + d_sid2slharmel_inc.xml<br>d_sid2srharmel_usr.xml + d_sid2srharmel_inc.xml |

To run these models, the following licenses are required:

| | |
|---|---|
| Ellipsoid models: | MADYMO/Solver (Multibody)<br>MADYMO/Dummy Models/Side |

**ELLIPSOID MODEL**



The model comprises 46 rigid bodies and 47 joints.

**Head and Neck**

The head and neck of the SID-IIs are modelled the same way as for the Hybrid III 50$^{th}$ percentile (see paragraph 36.1). The neck is represented by 5 kinematic joints located in the centres of the 4 rubber disks and on the rotation axis of the nodding joint (OC). The rubber disks are represented by spherical joints and the nodding joint by a revolute joint.

**Shoulder**

The design of the shoulder rib is the same as the thoracic and abdomens ribs, except that, the shoulder rib is larger. A linear potentiometer is used to measure the shoulder deflection. A shoulder load cell is placed on the impact side of the dummy to measure arm $F_x$ and $F_z$ loads as well as shoulder lateral ($F_y$) loads.

The arm is connected to the shoulder rib via two revolute joints. The first joint represents the arm adjustment, which can rotate the arm back or forward. The second is the arm clevis, which is used to rotate the arm into a horizontal or vertical position. Another body, fixed to the shoulder rib body by a bracket joint, acts as the shoulder load cell.

A chain of hyper ellipsoids are used to describe the shoulder rib, but these are only used for visualisation, since it is assumed that the shoulder rib will never make contact with an airbag or the vehicle structure. A hyper ellipsoid (referred to as "ArmPivot_ell") is placed between the arm and shoulder rib to describe the shoulder yoke (again for visual detailing).

**Arm (standard)**

The stub arm is constructed with a foam block, covered by a vinyl skin. This is mounted onto a steel support plate. A rubber torus is inserted into a cut-out in the foam centre line of the shoulder rib. Apart from the deformation of the foam and shoulder plug, the arm is prevented from bending or twisting by the steel support plate.

The arm is represented with a single rigid body. A total of five ellipsoids are used to define the deforming parts of the arm. Three ellipsoids were used to represent the arm foam, one ellipsoid for the shoulder plug area and one ellipsoid for the support plate. The properties of the arm foam and shoulder plug ellipsoids were derived by component test. The loading functions derived are distinctive of foam material behaviour. The region of penetration between 0 and approximately 15 mm describes the phase where the cells in the foam undergo collapse. Immediately after, the force increases significantly with penetration, to reflect the foam becoming very stiff as it condenses.

**Airbag interaction Arm**

This arm is especially designed to measure the arm interaction during airbag testing. The arm is significantly different from the usual SID-IIs arm, as it represents a complete arm including upper arm, lower arm, and hand. It provides the capability to measure accelerations, loads (moment and forces), and rotations at several places.

The Airbag Interaction Arm model is made with 6 rigid bodies. The clavicle pivot joint is identical to the normal SID-IIs. Elbow and wrist joint have been implemented, with the correct ranges of motion, including a soft stop. The ability of the upper arm to rotate around the z-axis, has been modelled in the elbow joint using a universal joint, the wrist is modelled with a revolute joint.



The upper arm and the lower arm load cells (3 forces + 3 moments each), as well as the elbow load cell (2 moments), are available in the model. The upper and lower arm acceleration outputs are available.

The arm geometry is represented by ellipsoids connected to the corresponding bodies. The ellipsoids shape, the inertia values, and the joint stiffness are derived from the Hybrid III $5^{th}$ percentile arm.

**Thorax and abdomen**

The SID-IIs thorax and abdomen consist of five individual ribs that are mounted onto the spine box. The upper torso is divided into three thoracic ribs and two lower abdominal ribs. The thoracic and abdomen ribs are separately coupled with a flexible polyurethane elastomeric material. EnsoliteTM foam is attached to a jacket (worn by the dummy) on the struck side of the ribs. The lateral deflection of each rib is measured using linear potentiometers, while the rib acceleration is measured with accelerometers placed at the impacted side of the ribs.

The ribs are guided by rib stops on the front and rear of the upper torso. This allows the ribs to deflect mainly in the lateral direction. The five ribs are modelled as single rigid bodies, which are connected to the spine box body using translational joints. Damping in the ribs, provided by damping material inserted on the inside of the steel strip, is approximated with a viscous damping. Kelvin elements with non-linear stiffness are used to describe the polyurethane bibs, which restricts the relative motion between each of the thoracic and abdomen ribs.

The rib surface consists of a chain of regular-ellipsoids and hyper-ellipsoids. On the struck side, five ellipsoids (segments 6–10 in the ellipsoid chain) on each of the rib bodies describe the EnsoliteTM foam. The dimensions of these ellipsoids are such that they accurately describe the thickness of the jacket and foam.

### Lumbar spine

The lumbar spine of the SID-IIs is modelled the same way as for the Hybrid III 50$^{th}$ percentile (see paragraph 36.1).

### Pelvis

The SID-IIs pelvis is designed with a special linkage system to allow greater adduction (in ward movement) of the femurs. The linkage system consists of two thick femur-mounting plates fixed to each side of the pelvic bone. The left and right femur shafts are attached to the femur mount plates at the hip location. The Pubic Symphysis Load Cell is fixed to the end of the femur mount plates by two screws on each of the load cell.

The pelvis is described by a closed chain of rigid bodies. The body "Pelvis_bod" represents the non-deforming components of the pelvic assembly. The bodies "FemurMountPlateL_bod" and "FemurMountPlateR_bod" are the left and right side femur mount plates. The femurs ("FemurL_bod" and "FemurR_bod") are connect to these bodies through the hip joints. The bodies "PubicSymphysisL_bod" and "PubicSymphysisR_bod" represent the left and right parts of the pubic symphysis load transducer. The inward bending of the femur plates is approximated by revolute joints located at the pelvic bone attachment points. A closing joint between the bodies "PubicSymphysisL_bod" and "PubicSymphysisR_bod" is used to measure the Pubic Symphysis Force (PSF). The iliac wings are represented by two bodies ("IliacWingL_bod" and "IliacWingR_bod") connected to each side the pelvis body through bracket joints that represent the iliac wing load cells. The acetabulum load cells are represented by two bodies ("AcetabulumLCL_bod" and "AcetabulumLCR_bod") connected through bracket joints that supply the load cell output. Laterally attached to these bodies are bodies representing the Pelvis plug bodies. Ellipsoids represent the plug geometry and their stiff contact characteristics allow loads transmitted from environment through the pelvis plugs to the acetabulum load cells. Pelvis plug compression stiffness is represented by joint restraints imposed on the translational joints connecting the pelvis plug bodies to the actabulum bodies.

The compression of the flesh is modelled with four ellipsoids on each side of the pelvis. This allows different contact stiffness functions of each ellipsoid to represent the local stiffness of the pelvis in that area. The ellispoids are connected to different internal pelvis bodies in order to generate the correct internal load paths in the pelvis.Also the iliac wings are represented with ellipsoids.

### Legs

Each SID-IIs leg is modelled with one femur body, one knee body, three tibia bodies, one foot body and one shoe body. The femur surface consists of one ellipsoid as well as the knee surface, the tibia surface consists of five ellipsoids, the foot surface consists of three ellipsoids as well as the shoe surface. Spherical joints are used to model the rotations at the hips and ankles, while a revolute-translational joint is used for the knee rotation and compression. Bracket joints are also used in the femur and in the upper and lower tibia parts, so that leg load cell output and injuries can be determined. A free joint completed with multidirectional restraints connects the shoe to the foot body.

### CONTACTS BETWEEN DUMMY COMPONENTS

For the ellipsoid model contacts are defined between inner arm plate and ribs and between the legs.

## 15.2 Model validation

The SID-IIs model is developed and validated using tests as described below.

### Component tests

The component tests are summarised in Table 15.1.

Table 15.1: Component tests for SID-IIs dummy model.

| Component<br>c | Test<br>description | specification | | Model<br>Ellipsoid |
|---|---|---|---|---|
| Arm (standard) | Lateral shoulder plug impact with flat round, 100mm impactor | mass, velocity | 7.70 kg, 2.6 m/s<br>7.70 kg, 3.8 m/s<br>7.70 kg, 4.9 m/s | x<br>x<br>x |
| | Lateral arm flesh impact with flat round, 100mm impactor | mass, velocity | 7.70 kg, 2.3 m/s<br>7.70 kg, 3.9 m/s<br>7.70 kg, 5.1 m/s | x<br>x<br>x |
| Upper Torso | Lateral thorax rib impact with flat round, 150mm impactor | mass, velocity | 14.35 kg, 2.7 m/s<br>14.35 kg, 3.9 m/s<br>8.35 kg, 6.4 m/s | x<br>x<br>x |
| | Lateral thorax rib impact with flat round, 75mm impactor | mass, velocity | 13.85 kg, 3.2 m/s<br>13.85 kg, 4.2 m/s | x<br>x |
| | 20° rear oblique thorax rib impact with flat round, 150mm impactor | mass, velocity | 14.35 kg, 4.1 m/s<br>8.35 kg, 6.1 m/s | x<br>x |
| | 15° forward oblique thorax rib impact with flat round, 150mm impactor | mass, velocity | 14.35 kg, 4.1 m/s<br>14.35 kg, 6.1 m/s | x<br>x |
| | Lateral abdomen rib impact with flat round, 150mm impactor | mass, velocity | 14.35 kg, 2.2 m/s<br>8.35 kg, 5.1 m/s | x<br>x |
| | Lateral abdomen rib impact with flat round, 75mm impactor | mass, velocity | 13.85 kg, 2.3 m/s<br>7.85 kg, 5.1 m/s | x<br>x |
| | Lateral shoulder rib impact with flat round, 100mm impactor | mass, velocity | 13.70 kg, 2.8 m/s<br>13.70 kg, 4.3 m/s<br>13.70 kg, 4.8 m/s<br>7.70 kg, 3.9 m/s<br>7.70 kg, 5.0 m/s | x<br>x<br>x<br>x<br>x |
| Pelvis | Lateral pelvis impact with flat round, 150mm impactor | mass, velocity | 14.35 kg, 2.6 m/s<br>14.35 kg, 4.3 m/s<br>14.35 kg, 4.7 m/s<br>8.35 kg, 6.2 m/s | x<br>x<br>x<br>x |
| | 20° rear oblique pelvis impact with flat round, 150mm impactor | mass, velocity | 14.35 kg, 4.6 m/s | x |
| | 19° forward oblique pelvis impact with flat round, 150mm impactor | mass, velocity | 14.35 kg, 4.3 m/s | x |

### Full dummy tests

The tests with the complete dummy are summarised in Table 15.2. The (c) indicates that the specific test configuaration equals a dummy certification test. One of the thorax calibration tests is described in Section 15.4.

Table 15.2: Full dummy tests for SID-IIs dummy model.

| Test cdescription | specification | | Model Ellipsoid |
|---|---|---|---|
| Shoulder certification test + variants | velocity, angle | 4.5 m/s, 0° (c)<br>5.4 m/s, 0°<br>6.7 m/s, 0° | x<br>x<br>x |
| Thorax with arm certification test + variant | velocity, angle | 4.3 m/s, 0°<br>6.7 m/s, 0° (c) | x<br>x |
| Thorax without arm certification test + variants | velocity, angle | 4.3 m/s, 0° (c)<br>4.3 m/s, +20°<br>4.3 m/s, -20°<br>6.7 m/s, 0° | x<br>x<br>x<br>x |
| Abdomen certification test | velocity, angle | 4.5 m/s, 0° (c) | x |
| Pelvis certifiaction tests + variants | velocity, angle | 6.7 m/s, 0° (c)<br>7.0 m/s, 0° | x<br>x |
| Series of 18 hydraulic sledtests with various side face padding configurations. | | | x |
| Series of 6 hydraulic sledtests with various side face padding configurations. | | | x |

15

## 15.3 User instructions

### Timestep

Table 15.3: Recommended timestep for the SID-IIs dummy model.

| Model | timestep (s) |
|---|---|
| Ellipsoid | $\leq 2.5 \cdot 10^{-6}$ |

### Dummy positioning

Table 15.4: Positioning joints of the SID-IIs dummy model.

| Joint Description | Identifier | Degree of freedom[a] | | | | | | Comment |
|---|---|---|---|---|---|---|---|---|
| Complete dummy | Dummy_jnt | R1<br>D1 | roll right<br>forward | R2<br>D2 | pitch down<br>leftward | R3<br>D3 | yaw left<br>upward | |
| Lumbar spine | LumbarSpine_jnt | R1<br>D1 | yaw left<br>upward | R2<br>D2 | pitch down<br>leftward | R3<br>D3 | roll left<br>rearward | only used for equilibrium state |
| Neck bracket | NeckBracket_jnt | R1 | pitch down | | | | | always locked |
| Neck element | NeckPivot⟨i⟩_jnt, for i=1 to 4 [b]<br>NeckOC_jnt | R1<br>R1 | roll right<br>pitch down | R2 | pitch down | R3 | yaw left | only used for equilibrium state |
| Arm rotation | ArmPositioning_jnt | R1 | pitch down | | | | | always locked |
| Dummy lhs - rhs switch[c] | ThoraxSpineBox_jnt | R1 | yaw left | | | | | always locked |
| Left elbow[d]<br>Right elbow[e] | ElbowL_jnt<br>ElbowR_jnt | R1<br>R1 | yaw left<br>yaw left | R2<br>R2 | pitch down<br>pitch down | | | |
| Left wrist[d]<br>Right wrist[e] | WristL_jnt<br>WristR_jnt | R1<br>R1 | pitch down<br>pitch down | | | | | |
| Left hip<br>Right hip | HipL_jnt<br>HipR_jnt | R1<br>R1 | roll left<br>roll left | R2<br>R2 | pitch down<br>pitch down | R3<br>R3 | yaw left<br>yaw left | |
| Left knee | KneeL_jnt | R2 | pitch down | D1 | compression | | | D1 always zero |
| Right knee | KneeR_jnt | R2 | pitch down | D1 | compression | | | D1 always zero |
| Left ankle<br>Right ankle | AnkleL_jnt<br>AnkleR_jnt | R1<br>R1 | yaw right<br>yaw right | R2<br>R2 | roll left<br>roll left | R3<br>R3 | pitch down<br>pitch down | |

[a] Positive translation or rotation given in global co-ordinate system while the dummy is in reference position.
[b] Name ⟨i⟩: numbered from bottom to top / rear to front/ right to left.

[c] Change the value of this joint from 0 to 3.14159 to convert the default left hand side standard SID-IIs model to a right hand side model.
[d] Used only in the left hand side model of the SID-IIs with airbag interaction arm.
[e] Used only in the right hand side model of the SID-IIs with airbag interaction arm.

### Dummy contacts

In Table 15.5 the groups available for defining contacts between the dummy model components and environment are listed.

Table 15.5: Predefined groups to define contact between the SID-IIs Q model components and their interacting environment.

| Contact Description | Identifier[a] | Ellipsoid model[a][b] |
|---|---|---|
| Head | Head_gmb | Head_ell<br>Face_ell |
| Upper arm | ArmUp_gmb | ArmUp_ell<br>ArmMid_ell<br>ArmLow_ell<br>Shoulder_ell |
| Thorax | Thorax_gmb | RibThoraxLow⟨i⟩_ell, i=1 to 15<br>RibThoraxMid⟨i⟩_ell, i=1 to 15<br>RibThoraxUp⟨i⟩_ell, i=1 to 15 |
| Abdomen | Abdomen_gmb | RibAbdomenLow⟨i⟩_ell, i=1 to 15<br>RibAbdomenUp⟨i⟩_ell, i=1 to 15 |
| Pelvis | PelvisSeat_gmb[c] | PelvisRearL/R_ell<br>PelvisMidL/R_ell<br>PelvisUpL/R_ell<br>PelvisFrontL/R_ell |
| Pelvis | PelvisSide_gmb[d] | PelvisRearL/R_ell<br>PelvisUpL/R_ell<br>PelvisFrontL/R_ell<br>PelvisPlugL/R_ell<br>IliacWingL/R_ell |
| Left femur and knee | FemurKneeL_gmb | FemurL_ell<br>KneeL_ell |
| Right femur and knee | FemurKneeR_gmb | FemurR_ell<br>KneeR_ell |
| Left tibia | TibiaL_gmb | TibiaPart⟨i⟩L_ell, i=1 to 5 |
| Right tibia | TibiaR_gmb | TibiaPart⟨i⟩R_ell, i=1 to 5 |
| Left shoe | ShoeL_gmb | ShoeSoleL_ell<br>ShoeHeelL_ell<br>ShoeFrontL_ell |
| Right shoe | ShoeR_gmb | ShoeSoleR_ell<br>ShoeHeelR_ell<br>ShoeFrontR_ell |

[a] L=Left; R=Right.

(b) Part⟨i⟩: numbered from bottom to top / rear to front / right to left.
(c) To be used for contact definitions with the seat.
(d) To be used for contact definitions with the impacting side structure, e.g. vehicle door.

## Output

Table 15.6: SID-IIs output signals.

| Sensor | Identifier | Signals | | | | | | | Filter |
|---|---|---|---|---|---|---|---|---|---|
| | | resul-tant | x | direc-tion[a] | y | direc-tion[a] | z | direc-tion[a] | |
| Head | | | | | | | | | |
| CG accelero-meter | HeadCG_acc | ar | a1 | forward | a2 | lateral | a3 | vertical | CFC1000 |
| Neck | | | | | | | | | |
| Upper load cell | NeckUp_lce_F_CFC600 | | f1 | shear | f2 | shear | f3 | axial | CFC600 |
| | NeckUp_lce_F_CFC1000 | | f1 | shear | f2 | shear | f3 | axial | CFC1000 |
| | NeckUp_lce_T | | t1 | roll | t2 | pitch | t3 | jaw | CFC600 |
| Lower load cell | NeckLow_lce_F | | f1 | shear | f2 | shear | f3 | axial | CFC1000 |
| | NeckLow_lce_T | | t1 | roll | t2 | pitch | t3 | jaw | CFC600 |
| Arm[b] | | | | | | | | | |
| Upper arm load cell | ArmUp_lce_F | | f1 | shear | f2 | shear | f3 | axial | CFC600 |
| | ArmUp_lce_T | | t1 | roll | t2 | pitch | t3 | jaw | CFC600 |
| Elbow load cell | Elbow_lce_F | | f1 | shear | f2 | shear | f3 | axial | CFC600 |
| | Elbow_lce_T | | t1 | roll | t2 | pitch | t3 | jaw | CFC600 |
| Lower arm load cell | ArmLow_lce_F | | f1 | shear | f2 | shear | f3 | axial | CFC600 |
| | ArmLow_lce_T | | t1 | roll | t2 | pitch | t3 | jaw | CFC600 |
| Shoulder | | | | | | | | | |
| load cell | Shoulder_lce_F | | f1 | shear | f2 | axial | f3 | shear | CFC1000 |
| Upper Torso accelero-meters | | | | | | | | | |
| Thorax T1 | ThoraxT1_acc_FIR100 | ar | a1 | forward | a2 | lateral | a3 | vertical | FIR100 |
| | ThoraxT1_acc_CFC1000 | ar | a1 | forward | a2 | lateral | a3 | vertical | CFC1000 |
| Thorax T4 | ThoraxT4_acc_FIR100 | ar | a1 | forward | a2 | lateral | a3 | vertical | FIR100 |
| | ThoraxT4_acc_CFC1000 | ar | a1 | forward | a2 | lateral | a3 | vertical | CFC1000 |
| Thorax T12 | ThoraxT12_acc_FIR100 | ar | a1 | forward | a2 | lateral | a3 | vertical | FIR100 |
| | ThoraxT12_acc_CFC1000 | ar | a1 | forward | a2 | lateral | a3 | vertical | CFC1000 |
| Shoulder rib | RibShoulder_acc_FIR100 | ar | a1 | forward | a2 | lateral | a3 | vertical | FIR100 |
| | RibShoulder_acc_CFC1000 | ar | a1 | forward | a2 | lateral | a3 | vertical | CFC1000 |
| Up thor. rib | RibThoraxUp_acc_FIR100 | ar | a1 | forward | a2 | lateral | a3 | vertical | FIR100 |
| | RibThoraxUp_acc_CFC1000 | ar | a1 | forward | a2 | lateral | a3 | vertical | CFC1000 |
| Mid thor. rib | RibThoraxMid_acc_FIR100 | ar | a1 | forward | a2 | lateral | a3 | vertical | FIR100 |
| | RibThoraxMid_acc_CFC1000 | ar | a1 | forward | a2 | lateral | a3 | vertical | CFC1000 |
| Low thor. rib | RibThoraxLow_acc_FIR100 | ar | a1 | forward | a2 | lateral | a3 | vertical | FIR100 |
| | RibThoraxLow_acc_CFC1000 | ar | a1 | forward | a2 | lateral | a3 | vertical | CFC1000 |
| Up abd. rib | RibAbdomenUp_acc_FIR100 | ar | a1 | forward | a2 | lateral | a3 | vertical | FIR100 |
| | RibAbdomenUp_acc_ CFC1000 | ar | a1 | forward | a2 | lateral | a3 | vertical | CFC1000 |
| Low abd. rib | RibAbdomenLow_acc_FIR100 | ar | a1 | forward | a2 | lateral | a3 | vertical | FIR100 |
| | RibAbdomenLow_acc_ CFC1000 | ar | a1 | forward | a2 | lateral | a3 | vertical | CFC1000 |

*Continued on the next page*



15

*Table 15.6 cont.*

| Sensor | Identifier | Signals | | | | | | | Filter |
|---|---|---|---|---|---|---|---|---|---|
| | | resul-tant | x | direc-tion[a] | y | direc-tion[a] | z | direc-tion[a] | |
| Upper Torso potentio-meters | | | | | | | | | |
| Shoulder rib | RibShoulder_dis | | d1 | displ. | | | | | CFC180 |
| Up thor. rib | RibThoraxUp_dis | | d1 | displ. | | | | | CFC180 |
| Mid thor. rib | RibThoraxMid_dis | | d1 | displ. | | | | | CFC180 |
| Low thor.rib | RibThoraxLow_dis | | d1 | displ. | | | | | CFC180 |
| Up abd. rib | RibAbdomenUp_dis | | d1 | displ. | | | | | CFC180 |
| Low abd. rib | RibAbdomenLow_dis | | d1 | displ. | | | | | CFC180 |
| load cells | | | | | | | | | |
| Shoulder | Shoulder_lce_F | | f1 | shear | f2 | axial | f3 | shear | CFC1000 |
| Lumbar Spine | | | | | | | | | |
| Low load cell | LumbarSpineLow_lce_F | | f1 | shear | f2 | shear | f3 | axial | CFC1000 |
| | LumbarSpineLow_lce_T | | t1 | roll | t2 | pitch | t3 | jaw | CFC600 |
| Pelvis | | | | | | | | | |
| accelero-meter | Pelvis_acc_FIR100 | ar | a1 | forward | a2 | lateral | a3 | vertical | FIR100 |
| | Pelvis_acc_CFC1000 | ar | a1 | forward | a2 | lateral | a3 | vertical | CFC1000 |
| load cells | | | | | | | | | |
| Pubic | PubicSymphysis_lce_F | | | | f2 | axial | | | CFC1000 |
| Aceta-bulum | AcetabulumL_lce_F | | | | f2 | axial | | | CFC1000 |
| | AcetabulumR_lce_F | | | | f2 | axial | | | CFC1000 |
| Iliac | IliacWingL_lce_F | | | | f2 | axial | | | CFC1000 |
| | IliacWingR_lce_F | | | | f2 | axial | | | CFC1000 |
| Femur | | | | | | | | | |
| Left load cell | FemurL_lce_F | | f1 | shear | f2 | shear | f3 | axial | CFC600 |
| | FemurL_lce_T | | t1 | roll | t2 | pitch | t3 | yaw | CFC600 |
| Right load cell | FemurR_lce_F | | f1 | shear | f2 | shear | f3 | axial | CFC600 |
| | FemurR_lce_T | | t1 | roll | t2 | pitch | t3 | yaw | CFC600 |
| Tibia | | | | | | | | | |
| Left upper load cell | TibiaUpL_lce_F | | f1 | shear | f2 | shear | f3 | axial | CFC600 |
| | TibiaUpL_lce_T | | t1 | roll | t2 | pitch | t3 | yaw | CFC600 |
| Right upper load cell | TibiaUpR_lce_F | | f1 | shear | f2 | shear | f3 | axial | CFC600 |
| | TibiaUpR_lce_T | | t1 | roll | t2 | pitch | t3 | yaw | CFC600 |
| Left lower load cell | TibiaLowL_lce_F | | f1 | shear | f2 | shear | f3 | axial | CFC600 |
| | TibiaLowL_lce_T | | t1 | roll | t2 | pitch | t3 | yaw | CFC600 |
| Right lower load cell | TibiaLowR_lce_F | | f1 | shear | f2 | shear | f3 | axial | CFC600 |
| | TibiaLowL_lce_T | | t1 | roll | t2 | pitch | t3 | yaw | CFC600 |

[a] Positive direction given according to SAE J211/1.
[b] Only available for the left and right hand side SID-IIs ellipsoid model with the airbag interaction arm.

Table 15.7: Injury criteria defined for the SID-IIs.

| Injury criteria | Identifier | Filter |
|---|---|---|
| Head | | |
| HIC (15) | HIC15_inj | CFC1000 |
| HIC (36) | HIC36_inj | CFC1000 |
| Neck | | |
| NIJ | | |
| tension-extension | NTE_inj | CFC1000 (force)<br>CFC600 (moment) |
| tension-flexion | NTF_inj | CFC1000 (force)<br>CFC600 (moment) |
| compression-extension | NCE_inj | CFC1000 (force)<br>CFC600 (moment) |
| compression-flexion | NCF_inj | CFC1000 (force)<br>CFC600 (moment) |
| Thorax | | |
| VC | | |
| upper thorax rib | VCRibThoraxUp_inj | CFC180 |
| mid thorax rib | VCRibThoraxMid_inj | CFC180 |
| lower thorax rib | VCRibThoraxLow_inj | CFC180 |
| upper abdomen rib | VCRibAbdomenUp_inj | CFC180 |
| lower abdomen rib | VCRibAbdomenLow_inj | CFC180 |
| Pelvis | | |
| CIAPF | CIAPF_inj | CFC600 |

15

## 15.4 Example: Thorax certification test

This example features the SID-IIs ellipsoid dummy model applied in a standard thorax certification test. The input is given in the files:

| | |
|---|---|
| Ellipsoid model : | e_sid2sel.xml |
| | d_sid2sel_inc.xml |

The model set-up is illustrated in Figure 15.2.

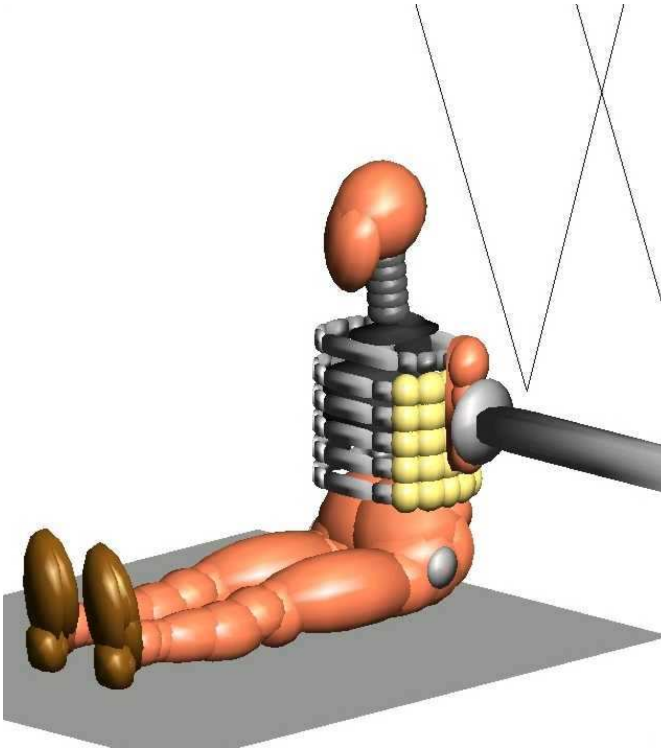

Figure 15.2: SID-IIs thorax certification test set-up.

**Environment**

In the thorax certification set-up, the probe centre strikes the arm with a velocity of 6.74 m/s at the position of the middle thoracic rib. The impactor mass is 14 kg and the diameter of the impactor face is 152 mm.

**Contact Interactions**

Contact with the rigid seat plane is defined between the pelvis, femurs, tibias and left and right shoes. Contact between the impactor and the arm and shoulder plug ellipsoids is defined. The seat is a low friction surface, therefore the co-efficients of friction are set to zero.

A co-efficient of friction of 0.4 is used between the impactor and the dummy. The damping coefficient (DAMP_COEF) is set to 100 Ns/m .

### Results

The simulation results are compared with the experimental results as shown in Figure 15.3 to Figure 15.6.

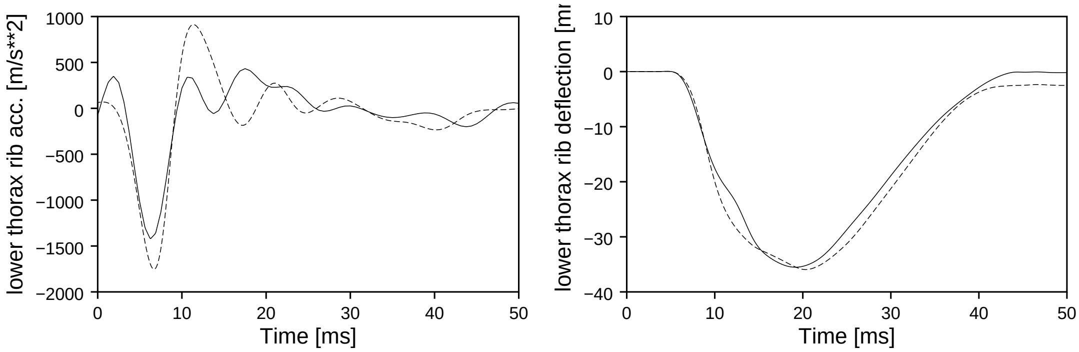


Figure 15.3: Validation results: Lower thorax rib acceleration (left) and deflection (right); experiment (– – –), simulation (———).



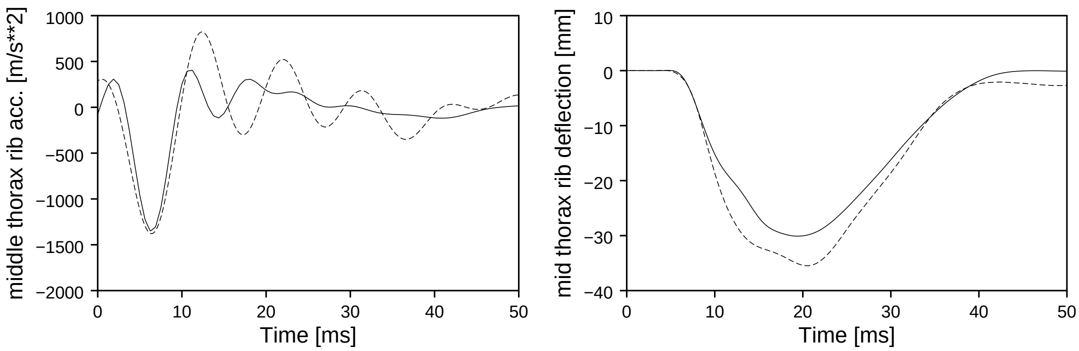


Figure 15.4: Validation results: Middle thorax rib acceleration (left) and deflection (right); experiment (– – –), simulation (———).

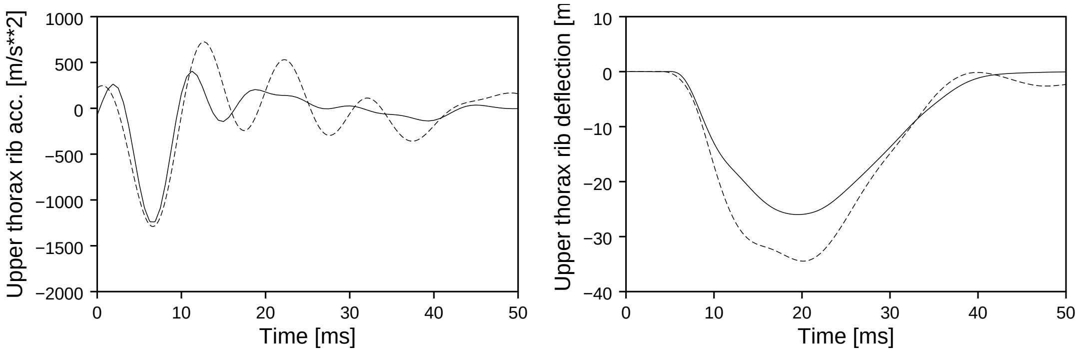


Figure 15.5: Validation results: Upper thorax rib acceleration (left) and deflection (right); experiment (— — —), simulation (———).

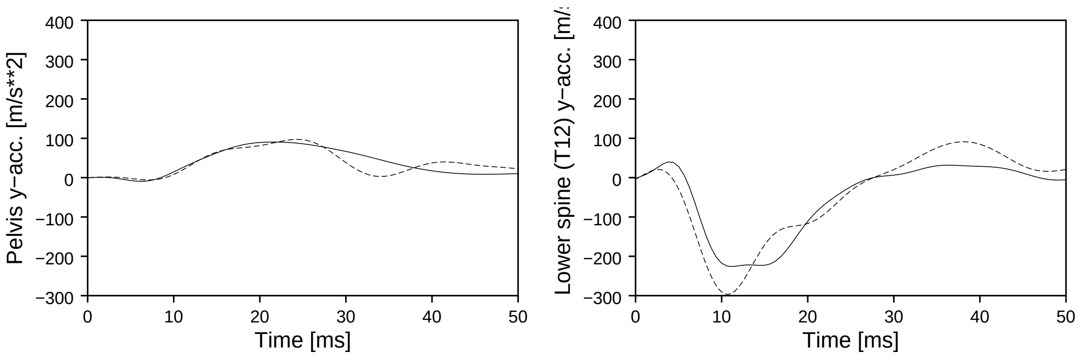


Figure 15.6: Validation results: Pelvis acceleration (left) and Lower spine (T12) acceleration (right); experiment (— — —), simulation (———).

# 16 SID-IIs Q Side Impact Dummy

Following the increased market demand for dummy models that are CPU-efficient as well as accurate in response, quality rated (Q) models of the SID-IIs side impact dummies were developed. The SID-IIs dummy is used in regulatory and consumer test protocols for side impact injury assessment of an occupant that anthropometrically corresponds to a small adult or a 12 to 14-year old adolescent.

The development of the second-generation small sized dummy, referred to as the SID-IIs, was started in 1994 within the USCAR program. The design of the dummy recently evolved to build level D, was adopted in the US occupant safety test protocols FMVSS 214 and USNCAP (MY 2011) and is planned for adoption in the IIHS test protocol.

The models represent the SID-IIs build level D version of the hardware dummy and were extensively calibrated and validated using numerous component and full dummy impact tests. Before the release, the models were also evaluated on the application level throughout all test protocols in which the dummy is used (FMVSS 214, USNCAP, IIHS).

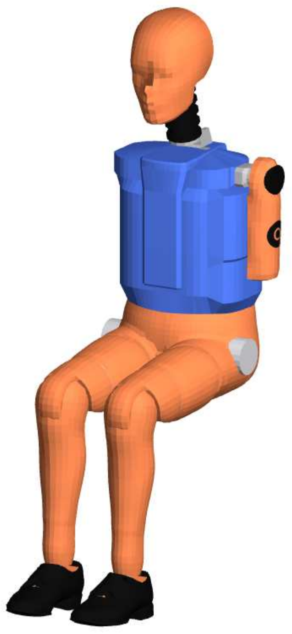

Figure 16.1: SID-IIs facet Q dummy model in reference position.

## 16.1 Model description

Quality rated facet models of the SID-IIs dummy are available. The input is given in the following files:

| | |
|---|---|
| Facet models: | d_sid2slhfc_Q_usr.xml + d_sid2slhfc_Q_inc.xml<br>d_sid2srhfc_Q_usr.xml + d_sid2srhfc_Q_inc.xml |

To run these models, the following licenses are required:

| | |
|---|---|
| Facet model: | MADYMO/Solver (Multibody)<br>MADYMO/Dummy Models/Side/SID-IIs Fc Q |

Figure 16.1 shows the SID-IIs facet Q model in its reference position.

The model consists of 358 bodies, 166 joint restraints, 86 other kinematic restraints and has 81 MADYMO outputs and 119 injury criteria initially predefined, thus covering all possible hardware dummy instrumentation available and injury criteria required by testing assessment protocols relevant for SID-IIs.

**FACET MODEL**

The SID-IIs Q model was developed and calibrated fully from scratch, using SID-IIs BL-D documentation and measurements on the hardware dummy itself and also on performance specifications. Separate models are available for left hand drive and right hand drive versions of the dummy. All external and internal geometry is represented by facet surfaces, derived from the latest official technical drawings and/or 3D laser scans of moulded parts of the SID-IIs hardware dummy. In general, an element size of approximately 10 mm is used. All facet parts have contact compliance characteristics included in their NULL materials. Masses, centres of gravity and moments of inertia are determined based on hardware component mass measurements and geometric representation of the components in 3D CAD documentation.



Dummy load cells are modelled with two separate rigid bodies connected to each other and to neighbouring bodies by bracket joints. The central bracket joint represents the point of measurement, from which the load cell signal output is derived. All dummy sub-assemblies are modelled as separate entities and are connected to each other by bracket "interface" joints at the locations where the hardware sub-assemblies are connected with screws. The following paragraphs give an overview of the model design per dummy sub-assembly.

The level of validation of the SID-IIs Q models (in terms of simulation signal correlation with hardware test signals) was determined using an objective rating method and is more extensively described in the model quality report.

**Head and neck**

For the head, facet surfaces representing head vinyl skin, skull and skull cap, upper neck load cell and head accelerometer mount are included. The rigid bodies included represent the upper neck load cell, accelerometer with mounting block, and head assembly consisting of skull, skull cap, skin and skin cap.

In the neck column, facet surfaces representing the upper nodding plate and neck column are included. The neck assembly is modelled with eight bodies, one at the top representing the nodding plate and the other seven comprising the neck column. The hardware neck consists of five metal discs built in the rubber mould column and its compliance in the model is represented with kinematic restraints on six joints (four universal and two cylindrical) in between the bodies of intervertebral discs. This design allows to accurately represent all possible neck deformation modes: bending, tension-compression and torsion. The neck bracket, connecting neck column with spinebox, is modelled with lower neck load cell included. The SID-IIs head-neck model is shown in Figure 16.2.

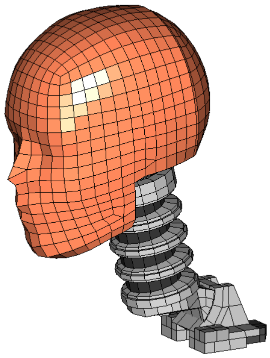

Figure 16.2: Complete head-neck assembly.



**Arm**

The arm is modelled with two rigid bodies representing the rubber plug and the assembly of moulded inner tube and arm flesh. The compliance of the arm flesh and arm plug is modelled with two separate contact characteristics. The arm facet surface has a varying element thickness, directly related to the thickness of the arm mould from the outer surface to the inner steel tube. Figure 16.3 shows the arm model.

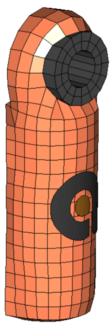

Figure 16.3: Arm assembly of the left hand side dummy model (with TASS International logo).

**Thorax**

The thorax of the dummy consists of the spinebox assembly, shoulder assembly, one set of three thoracic rib modules and one set of two abdominal rib modules.

Within the spinebox assembly there are rigid bodies representing the steel spinebox with rigidly attached neck mounting block, shoulder rib mount, clavicle, rib stoppers, rib padding and potentiometer frames. All component geometry is represented with facet surfaces. Both rib stops and rib padding have contact characteristics defined to replicate the compliance of the urethane covers when interacting with ribs. The spinebox assembly is shown in Figure 16.4.

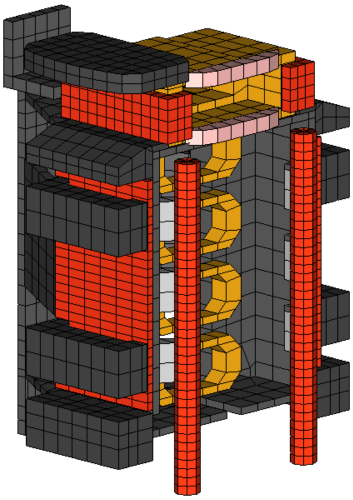

Figure 16.4: Spinebox assembly.

The shoulder assembly includes 31 bodies, 27 of which form the rib band and the other four represent the potentiometer module. The bending stiffness of the rib band is modelled with body-joint chains with joint restraints. The stiffness characteristics defined for the joint restraints ensure appropriate rib deformation and energy dissipation. The rib to shoulder rib mount connection is modelled with point restraints representing the screw connection. On the outer surface of the rib band there is a rigidly fixed 3-axis shoulder load cell and the shoulder yoke, through which the arm assembly connects to the thorax.

The designs of the thoracic and abdominal rib modules are very similar. The only difference is in the rib damping material on the inside of the steel rib bands, which is longer in abdominal ribs. Each of the rib modules is composed of 27 bodies belonging to the rib band, four to the potentiometer and one representing rib stiffener. Similarly to the shoulder rib, body-joint chains with joint restraints and appropriate stiffness and damping characteristics are used to ensure realistic rib deformation. The joint restraint characteristics are adjusted such that also the effect of different damping material length between thorax and abdomen ribs is properly represented.

Each of the six rib modules is equipped with the accelerometers and a potentiometer, represented as acceleration and relative displacement output definitions predefined in the model. All three rib type modules are shown in Figure 16.5.

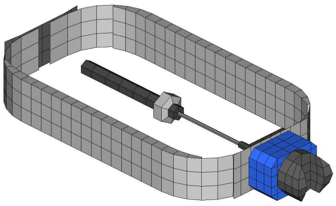

Figure 16.5: Shoulder rib with shoulder load cell and shoulder yoke assembly (left), thoracic rib module (centre) and abdominal rib module (right).

The modules described above, form together the thorax assembly as shown in Figure 16.6. At the impact side, the three thoracic ribs are interconnected through an elastic urethane bib. In the model, this elastic interaction between the ribs is represented with ten kelvin elements with calibrated stiffness characteristics. The same modelling solution is applied to represent the bib connecting the two abdominal ribs.

On top of the urethane bibs, the two sets of ribs are covered with two foam pads. These thorax and abdomen pads have a different thickness. In the models their compliance is represented with a contact characteristic. The pas thickness is represented through the element thickness in the foam pad facet surfaces. The foam pads consist of one surface, of which sections are supported to different rigid bodies, thus also representing foam pad shear and bending deformation.



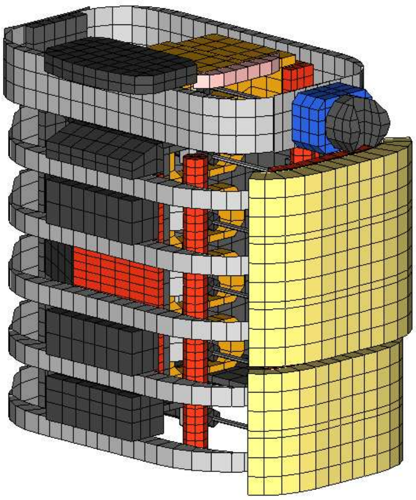

Figure 16.6: Complete thorax assembly with rib pads

#### Lumbar spine

The lumbar spine assembly is modelled with five rigid bodies forming the lumbar column and two bodies representing the upper lumbar plate to which the spinebox is rigidly fixed. The compliance of the spine in bending, torsion and tension deformation modes is realized by four free joints with corresponding four sixdof joint restraints. Additionally, the steel inner cable is modelled with a belt with four segments connecting the adjacent bodies and thus ensuring appropriate extension stiffness. The lumbar mould geometry is represented with facet surfaces connected per region to the adjacent rigid bodies. The lumbar spine column model with lumbar mount plate is shown in Figure 16.7.

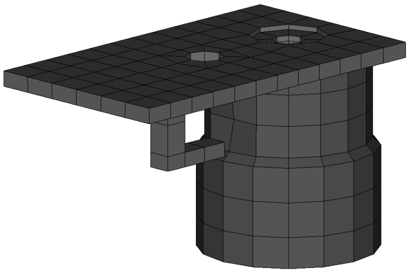

Figure 16.7: Lumbar spine column with lumbar mount plate



#### Pelvis

The pelvis assembly is modelled with 31 rigid bodies. They represent among others the pelvic bone, femur mount plates, pubic symphysis, acetabula, plugs, femurs, iliac wings and pelvis flesh parts distributed appropriately to ensure realistic load transfer between the environment and pelvis internal sensors. The pelvic bone, femur mount plates and pubic load cell bodies together form a closed body chain with revolute joints that deform in reaction to pelvis side impact loading. The upper femur bodies are connected to the femur holding shaft bodies through spherical joints, representing the physical hip pivots. Sixdof restraints represent the hip rotation end stops, the contact between femur shafts and pelvis flesh and the pelvis to femur flesh contact.

Within the pelvis, there are six load cells: acetabulum (left and right), iliac crest (left and right), pubic and lumbar. All are incorporated in separate body chains that represent the actual load paths and thus ensure realistic load transfer from the pelvis flesh.

All pelvis components are represented geometrically with facet surfaces. The pelvis flesh surface is closed at the top and front (femur openings) and has a varying element thickness representing the differences in flesh (foam-skin) thickness. In this way a single contact characteristic is used for representing the pelvis flesh compliance. The pelvis plugs have their own contact characteristic. The model is shown in Figure 16.8.

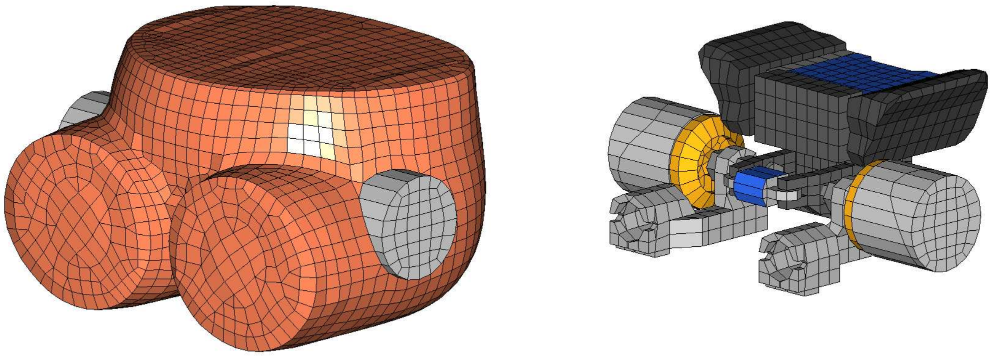

Figure 16.8: Complete pelvis assembly (left) and inner pelvis structure (right).

### Legs

The left and right leg model include 18 bodies each, representing the femur shaft, femur load cell, knee cap, knee clevis, tibia upper and lower load cells, tibia, ankle shell, foot, shoe, and the leg flesh parts covering the leg steel skeleton for realistic mass distribution. The thigh flesh is connected to the femur steel by a revolute joint with joint restraint allowing some flesh rotation around the femur steel. The knee pivot is modelled with a revolute joint with joint restrain applied representing end stops and joint friction. The ankle pivot is modelled with a spherical joint with two joint restraints applied ensuring realistic range of rotation and joint friction respectively. The shoe is connected to the foot with a free joint and with cardan and point restraints replication the foot to shoe elastic interaction.



The leg load cell sensors are located in upper leg (6-channel femur load cell) and in lower leg (upper and lower tibia 4-channel load cells). The leg flesh geometry is split and appropriately supported to the underlying bodies, to ensure the transfer of realistic amount of external loading to the corresponding load cells along the leg.

All components are represented geometrically with facet surfaces. The openings in femur, tibia and foot meshes are closed with additional facet surface elements, thus forming continuous contact surfaces and preventing potential contact problems near sharp surface edges. The leg model is shown in Figure 16.9.

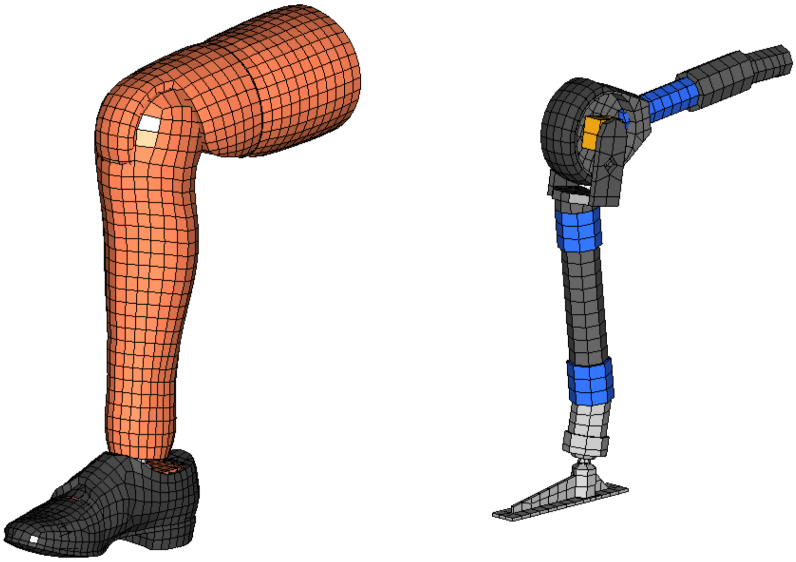

Figure 16.9: Complete leg assembly with and without fleshes (right leg shown).



**Jacket**

The jacket is modelled with two closed facet surfaces, one covering the rigid parts of spine, clavicle and neck mount bloc region, and the other enclosing the deformable rib cage. This ensures continuity of jacket surface contact stiffness and thus higher robustness of the model. Each closed surface is locally supported to the various underlying component rigid bodies. In this way the contact forces applied to the jacket are realistically divided over the dummy components underneath. The jacket mass is included by using a non-zero density in the null materials defined for the different jacket regions.

On the impact side, where the jacket covers the underlying rib foam pads, there are 25 kelvin restraints defined with appropriate tension characteristics, replicating the shear resistance of the foam pads and transferring it to the adjacent rib end bodies of thoracic and abdominal rib sets.

Jacket compliance is represented with a single contact characteristic. Its compressive stiffness varies throughout the surface due to different element thicknesses defined for different jacket regions, depending on the presence, stiffness and thickness of underlying structures. In the regions that cover stiff structural parts, the actual jacket thickness is defined, the regions with soft materials or voids underneath, have larger thicknesses defined to compensate for the additional overall compliance. The jacket model is shown in Figure 16.10.

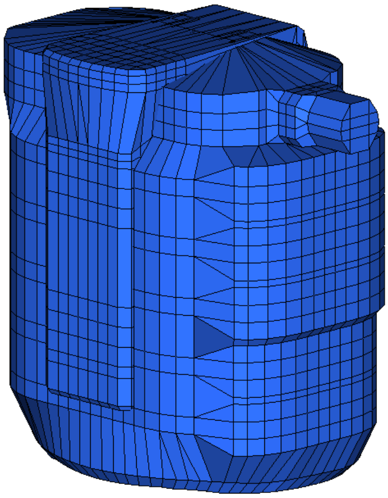

Figure 16.10: Jacket model

**CONTACTS BETWEEN DUMMY COMPONENTS**

Inter-component contacts have been defined between the arm and the jacket and between the left and right legs and shoes.

Within the thorax internal contacts are defined between the ribs and rib stops and pads. These contact definitions are ensuring realistic bottoming out of the ribs, in case excessive rib deformation occurs.

## 16.2 Model validation

The dummy models have been developed and validated for side impact loading using tests listed below. For detailed information on the model validation the reader is referred to the model quality report.

### Component tests

The component tests used for development and validation of the model are summarised in Table 16.1. The component level validation results can be found in the model quality report.

Table 16.1: Component tests for the SID-IIs facet Q model.

| **Component** c | **Test** **description** | **specification** | | **Model** **SID-IIs** |
|---|---|---|---|---|
| Head | Cerification drop | height | 0.2m | x |
| | Drop, 20 deg side | height | 0.15m, 0.2m, 0.3m | x |
| | Drop, 45 deg side | height | 0.15m, 0.2m, 0.3m | x |
| Neck | Certification pendulum | velocity | 5.6 m/s | x |
| | Sled, lateral bending | acc. pulse | low, high | x |
| Arm | Drop, 7.0 kg , at plug centre | velocity | 3.0, 4.0, 5.2 m/s | x |
| | Drop, 7.0 kg , at arm flesh | velocity | 3.6, 4.3, 5.2 m/s | x |
| Rib shoulder | Pendulum, 5.0 kg, 0 deg | velocity | 4.0, 5.0, 6.0 m/s | x |
| | Pendulum, 5.0 kg, 17 deg oblique | velocity | 3.0, 4.0, 5.0 m/s | x |
| Rib thorax | Pendulum, 3.0 kg, 0 deg | velocity | 4.0, 5.0 m/s | x |
| | Pendulum, 3.0 kg, 17 deg oblique | velocity | 3.0, 4.0 m/s | x |
| Rib abdomen | Pendulum, 3.0 kg, 0 deg | velocity | 4.0, 5.0 m/s | x |
| | Pendulum, 3.0 kg, 17 deg oblique | velocity | 3.0, 4.0 m/s | x |
| Rib thx. set | Pendulum, 15.2 kg, 0 deg | velocity | 2.0, 3.0, 4.0 m/s | x |
| | Pendulum, 15.2 kg, 17 deg oblique | velocity | 2.0, 3.0, 3.5 m/s | x |
| Rib abd. set | Pendulum, 7.0 kg, 0 deg | velocity | 3.0, 4.0, 5.0 m/s | x |
| | Pendulum, 7.0 kg, 17 deg oblique | velocity | 3.0, 4.0 m/s | x |
| Thorax | Pendulum, at low thx rib, 14.0 kg, 0 deg | velocity | 2.0, 3.0, 4.0 m/s | x |
| | Pendulum, at low thx rib, 14.0 kg, 17 deg oblique | velocity | 2.0, 3.0, 4.0 m/s | x |
| Thorax & arm | Pendulum, at arm plug, 14.0 kg, | velocity | 2.0, 3.0, 4.0 m/s | x |
| | Pendulum, at arm flesh, 14.0 kg, | velocity | 2.5, 3.5, 4.4 m/s | x |
| Lumbar | Sled, bending, 0 deg | acc. pulse | low, mid, high | x |
| | Sled, bending, 15 deg | acc. pulse | low, mid, high | x |
| | Sled, bending, 30 deg | acc. pulse | low, mid, high | x |
| Pelvis | Drop, 7.0 kg, 0 deg | velocity | 3.0, 4.0, 5.0 m/s | x |
| | Drop, 7.0 kg, 20 deg rear oblique | velocity | 3.0, 4.0, 5.0 m/s | x |
| | Drop, 7.0 kg, 40 deg rear oblique | velocity | 3.0, 4.0, 5.0 m/s | x |
| | Drop, 14.0 kg, 0 deg large impactor | velocity | 3.0, 4.0, 5.0 m/s | x |

*Continued on the next page*

*Table 16.1 cont.*

| Component c | Test description | specification | | Model SID-IIs |
|---|---|---|---|---|
| | Pendulum, 8.0 kg, 0 deg iliac only | velocity | 3.0, 4.0, 5.0 m/s | x |
| Pelvis & leg | Pendulum, at femur flesh, 7.0 kg | velocity | 2.0 m/s | x |
| | Pendulum, at pelvis-leg connection, 7.0 kg | velocity | 2.0 m/s | x |
| | Pendulum, at pelvis plug, 7.0 kg | velocity | 2.0 m/s | x |
| Leg upper | Drop, at femur flesh, 7.0 kg | velocity | 3.0, 4.0, 5.0 m/s | x |
| | Drop, at knee flesh, 3.0 kg | velocity | 3.0, 4.0, 5.0 m/s | x |
| Leg lower | Drop, at up tibia flesh, 3.0 kg | velocity | 3.0, 4.0 m/s | x |
| | Drop, at mid tibia flesh, 3.0 kg | velocity | 3.0, 4.0 m/s | x |
| | Drop, at low tibia flesh, 3.0 kg | velocity | 3.0, 4.0 m/s | x |

### Full dummy tests

The tests with the complete dummy used for development and validation of the model are summarised in Table 16.2. The validation results at full dummy level can also be found in the model quality report.

Table 16.2: Full dummy tests for the SID-IIs facet Q models.

| Test cdescription | specification | | Model SID-IIs |
|---|---|---|---|
| Certification shoulder, pendulum, 14.0 kg | velocity | 4.3 m/s | x |
| Certification thorax without arm, pendulum, 14.0 kg | velocity | 4.3 m/s | x |
| Certification thorax with arm, pendulum, 14.0 kg | velocity | 6.7 m/s | x |
| Certification abdomen, pendulum, 14.0 kg | velocity | 4.3 m/s | x |
| Certification pelvis acetabulum, pendulum, 14.0 kg | velocity | 6.7 m/s | x |
| Certification pelvis iliac, pendulum, 14.0 kg | velocity | 4.3 m/s | x |
| Biofidelity pendulum, at pelvis plug, 10.1 kg | velocity | 6.0, 10.0 m/s | x |
| Biofidelity drop, on rigid plates | height | 0.5m, 1.0m | x |
| Heidelberg sled, side rigid plates | velocity | 6.7 m/s | x |

### Range of validity of the model

The dummy model has been validated for side impact loading conditions.

## 16.3 User instructions

### Timestep

Table 16.3: Recommended timestep for the SID-IIs Q model.

| Model | timestep |
|---|---|
| Facet | $\leq 1.0 \cdot 10^{-5}$ |

### Dummy positioning

Table 16.4: Positioning joints for the SID-IIs Q model.

| Joint Description | Identifier | Degree of freedom[a] | | | | | | Comment |
|---|---|---|---|---|---|---|---|---|
| Complete dummy | Dummy_jnt | D1 | forward | D2 | leftward | D3 | upward | |
| | | R1 | roll right | R2 | pitch down | R3 | yaw left | |
| Neck OC | NeckOC_jnt | R1 | pitch down | | | | | equilibrum[b] |
| Neck column | NeckPivot1_jnt | R1 | pitch down | R2 | roll left | | | equilibrum[b] |
| | NeckCylinder1_jnt | D1 | upward | R1 | yaw left | | | |
| | NeckPivot2_jnt | R1 | roll left | R2 | pitch down | | | |
| | NeckPivot3_jnt | R1 | pitch down | R2 | roll left | | | |
| | NeckCylinder2_jnt | D1 | upward | R1 | yaw left | | | |
| | NeckPivot4_jnt | R1 | roll left | R2 | pitch down | | | |
| Neck positioning | NeckBracket_jnt | R1 | pitch down | | | | | [d] |
| Arm positioning | Shoulder_jnt | R1 | pitch up | | | | | [e] |
| Arm abduction | ArmClevis_jnt | R1 | roll right | | | | | [f] |
| Lumbar spine | Lumbar(..)Pivot⟨i⟩_jnt | D1 | upward | D2 | leftward | D3 | rearward | equilibrum[c] |
| | for i=1 to 4 | R1 | yaw left | R2 | pitch down | R3 | roll left | |
| Hip left | HipL_jnt | R1 | pitch down | R2 | roll left | R3 | yaw left | |
| Hip right | HipR_jnt | R1 | pitch down | R2 | roll left | R3 | yaw left | |
| Knee left | KneeL_jnt | R1 | pitch down | | | | | |
| Knee right | KneeR_jnt | R1 | pitch down | | | | | |
| Ankle left | AnkleL_jnt | R1 | pitch down | R2 | yaw right | R3 | roll left | |
| Ankle right | AnkleR_jnt | R1 | pitch down | R2 | yaw right | R3 | roll left | |

[a] Positive translation or rotation given in global coordinate system, with dummy in reference position (see Figure 16.1).

[b] Can be adjusted for equilibrum state only

[c] (D1, D2, D3, R1, R3 for equilibrum state only. R2 can be used to bend the dummy forward or backward.

[d] (Can be adjusted in hardware only when lower neck load cell is not built in; fixed neutral position represented by 0.0 [rad] in model. Range: +0.1440, -0.1440 [rad]; Graduation: 0.0360 [rad].

[e] Adjustable range: +3.1416, -3.1416 [rad] with graduation: 0.7854 [rad]

[e] Adjustable only to reproduce correct arm first contact with trim from video data

### Dummy contacts

When defining contacts between the dummy model and its environment, only the contact groups defined in Table 16.5 need to be used; no contacts should be defined with the dummy components underneath the jacket surface.

In general, the dummy surface should be chosen as the master group in contact definitions. This is also the way in which the contacts were defined in the dummy model validation test set. With the dummy surfaces chosen as master group in the contact definitions, the user will avoid problems with edges in the master surfaces because the dummy contact surfaces are all closed. Furthermore, with the dummy surfaces as master the direction of the contact forces and torques is always controlled by the dummy model. As an exception to this rule, the dummy surfaces can best be chosen as slave group in contacts between the dummy and a facet surface seat.

When meshing FE or facet surfaces that will be in contact with the dummy, an element size of 10 to 15 mm is the optimal choice. This element size was also used in the models of the dummy model validation test set.

Table 16.5: Predefined groups to define contact between the SID-IIs Q model components and their interacting environment.

| Contact Description | Identifier[a] | Facet model |
|---|---|---|
| Head | Head_gfe | closed outer head skin surface |
| Neck | Neck_gfe | closed neck column |
| Jacket | Jacket_gfe | closed jacket surface |
| Arm | Arm_gfe | closed arm surface |
| Pelvis | Pelvis_gfe | closed pelvis flesh and plugs surface |
| Leg upper left | FemurKneeL_gfe | closed left femur and knee surface |
| Leg upper right | FemurKneeR_gfe | closed right femur and knee surface |
| Leg lower left | TibiaL_gfe | closed left tibia surface |
| Leg lower right | TibiaR_gfe | closed right tibia surface |
| Foot left | FootL_gfe | closed left foot surface |
| Foot right | FootR_gfe | closed right foot surface |
| Shoe left | ShoeL_gfe | closed left shoe surface |
| Shoe right | ShoeR_gfe | closed right shoe surface |

[a] L=Left; R=Right.

### Output

From MADYMO V7.3 on, ISO-MME output can be generated for the SID-IIs Q dummy models. Output requests for signals in ISO-MME format are predefined in the CONTROL_OUTPUT element in the user file.

In Table 16.6 all predefined output definitions for the SID-IIs Q model are listed. Note, that for certain signal output definitions more than one filtering is applied. This is due to the fact



16

that some testing protocol specifications require different filtering than those defined by SAE standards. These signals are indicated with the identifier name extension e.g. '_CFC180', thus specifying the filtering used. The outputs with SAE standard filtering used, have no identifier name extension. All signal descriptions given below are valid for both right hand side and left hand side dummy models.

Table 16.6: Predefined output signals for the SID-IIs Q model.

| Sensor | Identifier | Signal | | | | | | | Filter |
|---|---|---|---|---|---|---|---|---|---|
| | | resul-tant | x | direc-tion[(a)] | y | direc-tion[(a)] | z | direc-tion[(a)] | |
| Head | | | | | | | | | |
| CG accel. | HeadCG_acc | ar | a1 | forward | a2 | right | a3 | down | CFC1000 |
| Neck | | | | | | | | | |
| Upper LC | NeckUp_lce_F | | f1 | shear | f2 | shear | f3 | axial | CFC1000 |
| | NeckUp_lce_F_CFC600 | | f1 | shear | f2 | shear | f3 | axial | CFC600 |
| | NeckUp_lce_T | | t1 | roll | t2 | pitch | t3 | yaw | CFC600 |
| Lower LC | NeckLow_lce_F | | f1 | shear | f2 | shear | f3 | axial | CFC1000 |
| | NeckLow_lce_T | | t1 | roll | t2 | pitch | t3 | yaw | CFC600 |
| Shoulder | | | | | | | | | |
| Rib displ. | RibShoulder_dis | | | | r2 | lateral | | | CFC600 |
| | RibShoulder_dis_CFC180 | | | | r2 | lateral | | | CFC180 |
| | RibShoulder_dvl | dr | | | | | | | CFC600 |
| | RibShoulder_dvl_CFC180 | dr | | | | | | | CFC180 |
| Accel. | Shoulder_acc | ar | a1 | forward | a2 | right | a3 | down | CFC1000 |
| | Shoulder_acc_CFC180 | ar | a1 | forward | a2 | right | a3 | down | CFC180 |
| LC | Shoulder_lce_F | | f1 | shear | f2 | axial | f3 | shear | CFC600 |
| | Shoulder_lce_F_CFC1000 | | f1 | shear | f2 | axial | f3 | shear | CFC1000 |
| Arm | | | | | | | | | |
| Accel. | ArmUp_acc | ar | a1 | forward | a2 | right | a3 | down | CFC600 |
| | ArmLow_acc | ar | a1 | forward | a2 | right | a3 | down | CFC600 |
| Thorax | | | | | | | | | |
| Rib displ. | | | | | | | | | |
| Up | RibThoraxUp_dis | | | | r2 | lateral | | | CFC600 |
| | RibThoraxUp_dis_CFC180 | | | | r2 | lateral | | | CFC180 |
| | RibThoraxUp_dvl | dr | | | | | | | CFC600 |
| | RibThoraxUp_dvl_CFC180 | dr | | | | | | | CFC180 |
| Mid | RibThoraxMid_dis | | | | r2 | lateral | | | CFC600 |
| | RibThoraxMid_dis_CFC180 | | | | r2 | lateral | | | CFC180 |
| | RibThoraxMid_dvl | dr | | | | | | | CFC600 |
| | RibThoraxMid_dvl_CFC180 | dr | | | | | | | CFC180 |
| Low | RibThoraxLow_dis | | | | r2 | lateral | | | CFC600 |
| | RibThoraxLow_dis_CFC180 | | | | r2 | lateral | | | CFC180 |
| | RibThoraxLow_dvl | dr | | | | | | | CFC600 |
| | RibThoraxLow_dvl_CFC180 | dr | | | | | | | CFC180 |
| Rib accel. | | | | | | | | | |
| Up | RibThoraxUp_acc | ar | a1 | forward | a2 | right | a3 | down | CFC1000 |
| | RibThoraxUp_acc_CFC180 | ar | a1 | forward | a2 | right | a3 | down | CFC180 |
| Mid | RibThoraxMid_acc | ar | a1 | forward | a2 | right | a3 | down | CFC1000 |
| | RibThoraxMid_acc_CFC180 | ar | a1 | forward | a2 | right | a3 | down | CFC180 |

*Continued on the next page*

*Table 16.6 cont.*

| Sensor | Identifier | Signal resultant | x | direction[a] | y | direction[a] | z | direction[a] | Filter |
|---|---|---|---|---|---|---|---|---|---|
| Low | RibThoraxLow_acc | ar | a1 | forward | a2 | right | a3 | down | CFC1000 |
| | RibThoraxLow_acc_CFC180 | ar | a1 | forward | a2 | right | a3 | down | CFC180 |
| Abdomen | | | | | | | | | |
| Rib displ. | | | | | | | | | |
| Up | RibAbdomenUp_dis | | | | r2 | lateral | | | CFC600 |
| | RibAbdomenUp_dis_CFC180 | | | | r2 | lateral | | | CFC180 |
| | RibAbdomenUp_dvl | dr | | | | | | | CFC600 |
| | RibAbdomenUp_dvl_CFC180 | dr | | | | | | | CFC180 |
| Low | RibAbdomenLow_dis | | | | r2 | lateral | | | CFC600 |
| | RibAbdomenLow_dis_CFC180 | | | | r2 | lateral | | | CFC180 |
| | RibAbdomenLow_dvl | | | | | | | | |
| | RibAbdomenLow_dvl_CFC180 | dr | | | | | | | CFC600 |
| | | dr | | | | | | | CFC180 |
| Rib accel. | | | | | | | | | |
| Up | RibAbdomenUp_acc | ar | a1 | forward | a2 | right | a3 | down | CFC1000 |
| | RibAbdomenUp_acc_CFC180 | ar | a1 | forward | a2 | right | a3 | down | CFC180 |
| Low | RibAbdomenLow_acc | ar | a1 | forward | a2 | right | a3 | down | CFC1000 |
| | RibAbdomenLow_acc_CFC180 | ar | a1 | forward | a2 | right | a3 | down | CFC180 |
| Spinebox | | | | | | | | | |
| Accel. | T1_acc | ar | a1 | forward | a2 | right | a3 | down | CFC180 |
| | T1_acc_CFC1000 | ar | a1 | forward | a2 | right | a3 | down | CFC1000 |
| | T4_acc | ar | a1 | forward | a2 | right | a3 | down | CFC180 |
| | T4_acc_CFC1000 | ar | a1 | forward | a2 | right | a3 | down | CFC1000 |
| | OppRibThxMid_acc | ar | a1 | forward | a2 | right | a3 | down | CFC1000 |
| | OppRibThxLow_acc | ar | a1 | forward | a2 | right | a3 | down | CFC1000 |
| | T12_acc | ar | a1 | forward | a2 | right | a3 | down | CFC180 |
| | T12_acc_CFC1000 | ar | a1 | forward | a2 | right | a3 | down | CFC1000 |
| | OppRibThxLow_acc | ar | a1 | forward | a2 | right | a3 | down | CFC1000 |
| Pelvis [c] | | | | | | | | | |
| Pelvis accel. | Pelvis_acc | ar | a1 | forward | a2 | right | a3 | down | CFC1000 |
| | Pelvis_acc_CFC180 | ar | a1 | forward | a2 | right | a3 | down | CFC180 |
| Acetabulum LC (L) | AcetabulumL_lce_F | | | | f2 | axial | | | CFC600 |
| | AcetabulumL_lce_F_CFC1000 | | | | f2 | axial | | | CFC1000 |
| Acetabulum LC (R) | AcetabulumR_lce_F | | | | f2 | axial | | | CFC600 |
| | AcetabulumR_lce_F_CFC1000 | | | | f2 | axial | | | CFC1000 |
| Iliac LC (L) | IliacCrestL_lce_F | | | | f2 | axial | | | CFC600 |
| | IliacCrestL_lce_F_CFC1000 | | | | f2 | axial | | | CFC1000 |
| Iliac LC (R) | IliacCrestR_lce_F | | | | f2 | axial | | | CFC600 |
| | IliacCrestR_lce_F_CFC1000 | | | | f2 | axial | | | CFC1000 |
| Lumbar LC | Lumbar_lce_F | | f1 | shear | f2 | shear | f3 | axial | CFC600 |
| | Lumbar_lce_T | | t1 | roll | t2 | pitch | t3 | yaw | CFC600 |
| Pubic LC | Pubic_lce_F | | | | f2 | axial | | | CFC600 |
| | Pubic_lce_F_CFC1000 | | | | f2 | axial | | | CFC1000 |
| Femur | | | | | | | | | |
| Left LC | FemurL_lce_F | | f1 | shear | f2 | shear | f3 | axial | CFC600 |
| | FemurL_lce_T | | t1 | roll | t2 | pitch | t3 | yaw | CFC600 |
| Right LC | FemurR_lce_F | | f1 | shear | f2 | shear | f3 | axial | CFC600 |
| | FemurR_lce_T | | t1 | roll | t2 | pitch | t3 | yaw | CFC600 |

*Continued on the next page*

*Table 16.6 cont.*

| Sensor | Identifier | Signal resul-tant | x | direc-tion[a] | y | direc-tion[a] | z | direc-tion[a] | Filter |
|---|---|---|---|---|---|---|---|---|---|
| Tibia | | | | | | | | | |
| Left Upper | TibiaUpL_lce_F | | f1 | shear | f2 | shear | f3 | axial | CFC600 |
| LC | TibiaUpL_lce_T | | t1 | roll | t2 | pitch | t3 | yaw | CFC600 |
| Right Upper | TibiaUpR_lce_F | | f1 | shear | f2 | shear | f3 | axial | CFC600 |
| LC | TibiaUpR_lce_T | | t1 | roll | t2 | pitch | t3 | yaw | CFC600 |
| Left Lower | TibiaLowL_lce_F | | f1 | shear | f2 | shear | f3 | axial | CFC600 |
| LC | TibiaLowL_lce_T | | t1 | roll | t2 | pitch | t3 | yaw | CFC600 |
| Right Lower | TibiaLowR_lce_F | | f1 | shear | f2 | shear | f3 | axial | CFC600 |
| LC | TibiaLowR_lce_T | | t1 | roll | t2 | pitch | t3 | yaw | CFC600 |

(a) Positive direction of accelerations given according to SAE J211/1.
(b) The "_dvl" output produces resultant rib displacements and velocities that are used to calculate the rib VC criteria.
(c) L=Left; R=Right.

In Table 16.7 all predefined injury criteria for the SID-IIs Q model are listed.

Table 16.7: Predefined injury criteria for the SID-IIs Q model.

| Injury criteria | Identifier | Filter |
|---|---|---|
| Head | | |
| HIC (15) | HIC15_inj | CFC1000 |
| HIC (36) | HIC36_inj | CFC1000 |
| Neck | | |
| MOC | | |
| lateral | MOCx_inj | CFC600 |
| FNIC | | |
| tension | FNICtension_inj | CFC1000 |
| shear | FNICshear_inj | CFC1000 |
| bending | FNICbending_inj | CFC600 |
| NIJ | | |
| tension-extension | NTE_inj | CFC600[a] |
| tension-flexion | NTF_inj | CFC600[a] |
| compression-extension | NCE_inj | CFC600[a] |
| compression-flexion | NCF_inj | CFC600[a] |
| Peak Force | | |
| Neck Up Tension | NeckUpTensionPF_inj | CFC1000 |
| Neck Up Compression | NeckUpCompressionPF_inj | CFC1000 |
| Shoulder | | |
| Rib compression | RibShoulderRDS_inj | CFC600 |
| | RibShoulderRDS_inj_CFC180 | CFC180 |
| Rib VC | RibShoulderVC_inj | CFC600 |
| | RibShoulderVC_inj_CFC180 | CFC180 |
| Thorax | | |
| Rib compression | RibThoraxUpRDS_inj | CFC600 |
| | RibThoraxUpRDS_inj_CFC180 | CFC180 |
| | RibThoraxMidRDS_inj | CFC600 |
| | RibThoraxMidRDS_inj_CFC180 | CFC180 |
| | RibThoraxLowRDS_inj | CFC600 |
| | RibThoraxLowRDS_inj_CFC180 | CFC180 |

*Continued on the next page*

*Table 16.7 cont.*

| Injury criteria | Identifier | Filter |
|---|---|---|
| Rib VC | RibThoraxUpVC_inj | CFC600 |
| | RibThoraxUpVC_inj_CFC180 | CFC180 |
| | RibThoraxMidVC_inj | CFC600 |
| | RibThoraxMidVC_inj_CFC180 | CFC180 |
| | RibThoraxLowVC_inj | CFC600 |
| | RibThoraxLowVC_inj_CFC180 | CFC180 |
| Abdomen | | |
| Rib compression | RibAbdomenUpRDS_inj | CFC600 |
| | RibAbdomenUpRDS_inj_CFC180 | CFC180 |
| | RibAbdomenLowRDS_inj | CFC600 |
| | RibAbdomenLowRDS_inj_CFC180 | CFC180 |
| Rib VC | RibAbdomenUpVC_inj | CFC600 |
| | RibAbdomenUpVC_inj_CFC180 | CFC180 |
| | RibAbdomenLowVC_inj | CFC600 |
| | RibAbdomenLowVC_inj_CFC180 | CFC180 |
| Pelvis | | |
| Acetabulum Peak Force | AcetabulumLPF_inj | CFC600 |
| | AcetabulumLPF_inj_CFC1000 | CFC1000 |
| | AcetabulumRPF_inj | CFC600 |
| | AcetabulumRPF_inj_CFC1000 | CFC1000 |
| Iliac Crest Peak Force | IliacCrestLPF_inj | CFC600 |
| | IliacCrestLPF_inj_CFC1000 | CFC1000 |
| | IliacCrestRPF_inj | CFC600 |
| | IliacCrestRPF_inj_CFC1000 | CFC1000 |
| Combined Iliac and Acetabulum Peak Force | CombinedIliacAcetLPF_inj | CFC600 |
| | CombinedIliacAcetLPF_inj_CFC1000 | CFC1000 |
| | CombinedIliacAcetRPF_inj | CFC600 |
| | CombinedIliacAcetRPF_inj_CFC1000 | CFC1000 |
| Femur[(b)] | | |
| 3ms Force | | |
| Anterior-Posterior | FemurLowLForceAP_inj | CFC600 |
| | FemurLowRForceAP_inj | CFC600 |
| Lateral-Medial | FemurLowLForceLM_inj | CFC600 |
| | FemurLowRForceLM_inj | CFC600 |
| 3ms Moment | | |
| Anterior-Posterior | FemurLowLMomentAP_inj | CFC600 |
| | FemurLowRMomentAP_inj | CFC600 |
| Lateral-Medial | FemurLowLMomentLM_inj | CFC600 |
| | FemurLowRMomentLM_inj | CFC600 |
| Tibia | | |
| TI | | |
| Upper tibia | TIUpL_inj | CFC600 |
| | TIUpR_inj | CFC600 |
| Lower Tibia | TILowL_inj | CFC600 |
| | TILowR_inj | CFC600 |
| TCFC | | |
| Upper tibia | TCFCUpL_inj | CFC600 |
| | TCFCUpR_inj | CFC600 |
| Lower Tibia | TCFCLowL_inj | CFC600 |
| | TCFCLowR_inj | CFC600 |

[(a)] For both force and torque signals

[(b)] Available only as of MADYMO Release R7.2

16

# 17 MATD Dummy

The Motorcycle Anthropometric Test Device, MATD for short, was developed by an international group in the 1990's. The work of ISO TC22/SC22/WG22 resulted in the specifications for a test protocol for evaluating the crashes of motorcycles against automobiles and the specifications for the tools to use in this crash test. The MATD dummy, specified in part 3 of the ISO 13232 document, is based on the Hybrid-III frontal impact dummy - the standard for frontal impacts in the past 30 years. ISO 13232 specifies a number of changes to this dummy to make the dummy suitable for motorcycle crashes. The most important features of the dummy are:

- A modified head, that is compatible with motorcycle helmets;
- A newly designed neck, that allows the dummy to be put in a number of different motorcycle positions, while keeping the head in an up-right position;
- The use of the Hybrid-III sit-stand pelvis, which allows positioning of the dummy on the motorcycle;
- Dummy hands that allow wrapping around the handlebars;
- Frangible upper legs, lower legs, and knees;
- A frangible abdomen;
- An on-board dummy data acquisition system located in a modified spine box.



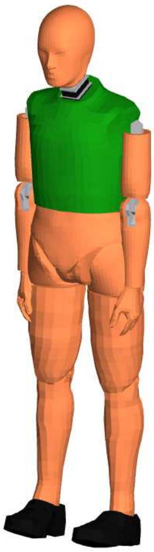

Figure 17.1: MATD model in reference position.

## 17.1 Model description

The MATD is available as a facet model only. The input is given in files:

| | |
|---|---|
| d_matd50fc_inc.xml | MATD facet model include file |
| d_matd50fc_usr.xml | MATD model user file |

**FACET MODEL**

The basis for the MATD model is the Hybrid-III model that has been developed by TASS International. ISO 13232 was used to identify which parts of the Hybrid-III model could serve as the basis of the corresponding MATD part, and which parts of the MATD model required a new component model.

The facet description of the exterior surfaces has been created by 3D-scanning the surfaces of the head, the abdomen, the hands, and the pelvis. A number of facets, which includes the thorax, the upper and lower arms, the upper and lower legs, as well as the foot/shoe are identical to the Hybrid-III versions.

**Head**

The head is modelled with a single rigid body, of which the surface is described with facets. The surface is closed to prevent intrusion of airbags. This was done as an alternative to modelling the neck shroud of the dummy. The neck shroud of the MATD is a padded nylon covering for the neck, which is zippered to the head skin, and which does not have a defined shape. Because the neck can be placed in a number of initial positions, it is not possible to use facet surfaces to describe the neck shroud. Therefore, the lower surface of the head has been closed.



**Neck**

The neck is modelled with a number of bodies and visually represented with facets. At the top, the neck connects to the head through the OC joint. Directly below is the neck slider that allows considerable forward and limited rearward motion of the OC joint relative to the neck (shear). The rubber elements of the neck are modelled with spherical joints. At the middle of the neck and at the base are adjustable revolute joints that can be used to position the head in the required initial position. The initial neck position is determined by the orientation of the motorcycle dummy on the motorcycle (leaning forward or backward).

**Thorax**

The thorax of the MATD dummy is very similar to that of the Hybrid-III facet model, which is also described in the Madymo Users manual. The main difference between the MATD version and the Hybrid-III version is in the dimensions of the thoracic spine box, the interface with the (straight) lumbar spine, and the use of four string potentiometers to measure the deflection of the sternum relative to the spine box. The thorax model of the MATD/Hybrid-III has four deformation modes that allow both frontal and lateral impacts.

ISO 13232 does not contain detailed requirements for the dimensions of the thoracic spine box. That has been done in order to prevent putting restrictions on the design of the in-dummy data acquisition unit. The shape of the MATD facet model thoracic spine box is therefore the sane as that of the standard Hybrid-III spine box model.

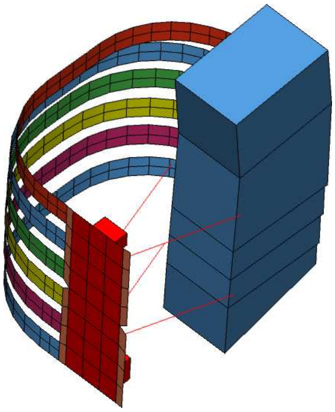

Figure 17.2: Cross-section view of the MATD thoracic spine, ribs, and string potentiometers.

### Lumbar Spine

The MATD uses a straight lumbar spine with an internal steel cable. This has been modelled with two bodies, connected by a spherical joint, and a Kelvin element as a representation of the inner cable.

### Abdomen

The MATD uses a frangible abdomen, based on an abdomen developed by General Motors for the Hybrid-III dummy. The material used for the abdomen is a brittle foam, which is inspected after the test for deformation. Since the abdomen lies recessed within the pelvis skin, loads are transferred to the abdomen through the upper frontal section of the pelvis skin. The skin has been divided into three sections to allow for frontal and oblique impacts to the abdomen. Three additional bodies have been created to model the deformation:

InnerAbdomenMiddle_bod, InnerAbdomenRight_bod and InnerAbdomenLeft_bod.

These bodies are located on the inner surface of the pelvis and are connected to the pelvis by means of three translational joints. The translation of these bodies with respect to the pelvis body takes place in a horizontal plane (global xy) in a direction perpendicular to the outer surface of the abdominal insert. This allows the user to determine maximum deformation of the abdomen from the simulation output files. (.jps).

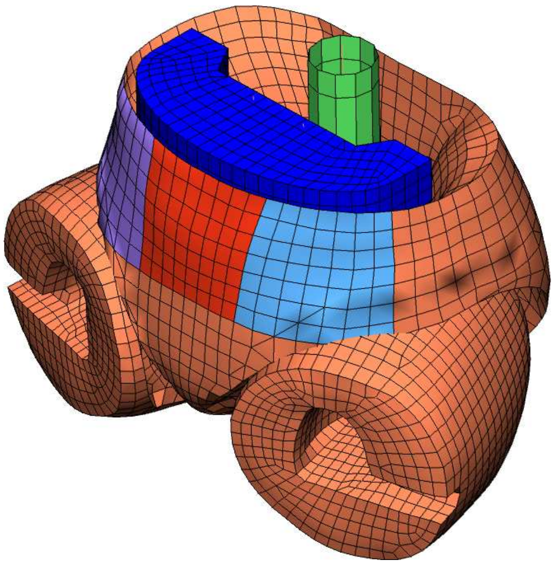

Figure 17.3: Abdomen and pelvis skin showing the abdomen loading paths.



**Pelvis**

The MATD dummy uses the Hybrid-III sit-stand pelvis. This pelvis uses separate flesh moulds for the pelvis and the right and left upper femurs. Consequently, the hip joints of the sit-stand pelvis have a far greater range of motion than the standard Hybrid-III pelvis joints. The MATD model uses three separate detailed meshes to represent the three parts of the pelvis. The definition of the joints is different than for the corresponding joints in the standard Hybrid-III model. This is to prevent joint gimbal locking. This is described in the section “dummy positioning”.

**Legs**

On the outside, the legs and knees of the MATD model resemble the Hybrid-III legs and knees closely. The facets of the upper legs have been modified to allow proper interfacing with the sit-stand pelvis. On the inside, the MATD model has representations of the frangible bones in the upper and lower leg, and of the frangible joints (2) in the knees. The requirements of ISO 13232 part 3 have been used to describe the characteristics of the frangible joints, i.e. at which force and/or torque levels the parts fail. Initially the joints are locked, but when the thresholds levels are exceeded, the joints are unlocked and allow unrestricted motion. The steel cables have been modelled to prevent separation of the legs after fracture.

**Feet**

The foot geometry is represented by ellipsoids while facet surfaces describe the outer geometry of the shoes.

**Hands**

The hand of the MATD dummy consists of an articulated metal skeleton, covered with a plastic. Each finger and the thumb can be put in an initial position. This gives the hands sufficient flexibility to wrap it around the handlebars of the motorcycle. In the MATD model, the fingers have been divided into two sections, the upper part of the four fingers and the lower part of the four fingers. The thumb is attached with a single joint to the hand.

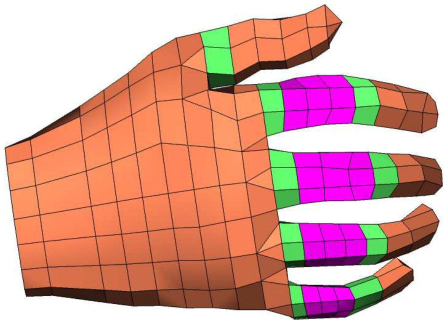

Figure 17.4: MATD right hand showing the articulated fingers.

## CONTACTS BETWEEN DUMMY COMPONENTS

The following dummy to dummy contacts have been defined:

- Head to thorax
- Thorax to left and right upper leg
- Left and right upper legs
- Left and right lower legs
- Arms to thorax
- Left arm to right arm

## 17.2 User instructions

General instructions for the use of the Hybrid-III dummy can be found in the Madymo Database Manual. The instructions for the MATD are very similar, with exceptions for the hands, the neck, and the pelvis.

### Timestep

Table 17.1: Recommended timestep for the MATD dummy model.

| Model | timestep (s) |
|---|---|
| Facet | $\leq 0.5 \cdot 10^{-4}$ |

### Dummy positioning

Table 17.2: Positioning joints of the MATD dummy model.

| Joint Description | Identifier | Degree of freedom[a] | | | | | | Comment |
|---|---|---|---|---|---|---|---|---|
| Complete dummy | Dummy_jnt | D1<br>R1 | forward<br>roll right | D2<br>R2 | leftward<br>pitch down | D3<br>R3 | upward<br>yaw left | |
| Neck bracket | NeckBracket_jnt | R1 | pitch down | | | | | [b] |
| Neck middle Adjustment | NeckMiddle adjustment_jnt | Q1 | pitch down | | | | | [c] |
| Neck element | NeckPivot$\langle i \rangle$_jnt, for i=1 to 4 [d] | R1 | roll right | R2 | pitch down | R3 | yaw left | only for equilibrium state |
| Left shoulder | ShoulderL_jnt | R1 | pitch down | R2 | roll right | | | |
| Right shoulder | ShoulderR_jnt | R1 | pitch down | R2 | roll right | | | |
| Left elbow | ElbowL_jnt<br>ElbowPivotL_jnt | R1<br>R1 | pitch down<br>yaw left | | | | | |
| Right elbow | ElbowR_jnt<br>ElbowPivotR_jnt | R1<br>R1 | pitch down<br>yaw left | | | | | |
| Left wrist | WristL_jnt<br>WristPivotL_jnt | R1<br>R1 | yaw left<br>roll right | | | | | |
| Right wrist | WristR_jnt<br>WristPivotR_jnt | R1<br>R1 | yaw left<br>roll right | | | | | |
| Left fingers (up) | FingersUpL_jnt | Q1 | pitch down | | | | | |
| Right fingers (up) | FingerUpR_jnt | Q1 | pitch down | | | | | |
| Left fingers (low) | FingersLowL_jnt | Q1 | pitch down | | | | | |
| Right fingers (low) | FingersLowR_jnt | Q1 | pitch down | | | | | |
| Left thumb | ThumbL_jnt | Q1 | pitch down | | | | | |
| Right thumb | ThumbR_jnt | Q1 | pitch down | | | | | |

*Continued on the next page*

*Table 17.2 cont.*

| Joint Description | Identifier | Degree of freedom[a] | | | | | | Comment |
|---|---|---|---|---|---|---|---|---|
| Lumbar spine | LumbarSpine_jnt | R1 | yaw left | R2 | pitch down | R3 | roll left | only for equilibrium state |
| | | D1 | upward | D2 | leftward | D3 | rearward | |
| Left hip | HipL_jnt | R1 | pitch down | R2 | roll right | R3 | yaw left | |
| Right hip | HipR_jnt | R1 | pitch down | R2 | roll right | R3 | yaw left | |
| Left knee | KneeL_jnt | R2 | pitch down | | | | | |
| | | D1 | compression | | | | | always zero |
| Right knee | KneeR_jnt | R2 | pitch down | | | | | |
| | | D1 | compression | | | | | always zero |
| Left ankle | AnkleL_jnt | R1 | yaw left | R2 | roll right | R3 | pitch down | |
| Right ankle | AnkleR_jnt | R1 | yaw left | R2 | roll right | R3 | pitch down | |

[a] Positive translation or rotation given in global co-ordinate system while dummy is in reference position.
[b] Angle for the neck bracket is directly to derive from the physical dummy. A lower neck load cell in the physical dummy means a zero angle for the neck bracket.
[c] Adjust to put the head in a horizontal position, as described in ISO 13232.
[d] Part⟨*i*⟩: numbered from bottom to top / rear to front / right to left.

## Dummy contacts

17

Table 17.3: Available groups to define contact between the MATD components and environment.

| Contact Description | Identifier[a] | Facet model |
|---|---|---|
| Head | Head_gfe | Elements and nodes [b] |
| Neck | Neck_gfe | Elements and nodes |
| Left Upper Arm | ArmUpL_gfe | Elements and nodes |
| Right Upper Arm | ArmUpR_gfe | Elements and nodes |
| Left Lower Arm and Hand | ArmLowL_gfe | Elements and nodes |
| Right Lower Arm and Hand | ArmLowR_gfe | Elements and nodes |
| Thorax | Thorax_gfe | Elements and nodes |
| Pelvis | Pelvis_gfe | Elements and nodes |
| Left Femur and Knee | FemurKneeL_gfe | Elements and nodes |
| Right Femur and Knee | FemurKneeR_gfe | Elements and nodes |
| Left Tibia | TibiaL_gfe | Elements and nodes |
| Right Tibia | TibiaR_gfe | Elements and nodes |
| Left Foot | FootL_gfe | Elements and nodes |
| Right Foot | FootR_gfe | Elements and nodes |
| Left Shoe | ShoeL_gfe | Elements and nodes |
| Right Shoe | ShoeR_gfe | Elements and nodes |

[a] L=Left; R=Right.
[b] ISO 13232 requires the use of a helmet.
[c] Part $\langle i \rangle$ : numbered from bottom to top / rear to front / right to left.

## Output

Table 17.4: MATD output signals.

| Sensor | Identifier | Signal | | | | | | | Filter |
|---|---|---|---|---|---|---|---|---|---|
| | | resul-tant | x | direction | y | direc-tion | z | direc-tion | |
| Head | | | | | | | | | |
| CG accelero-meter[a] | HeadCG_acc | ar | a1 | forward | a2 | lateral | a3 | vertical | CFC1000 |
| CG angular[b] | HeadCG_angacc | ar | a1 | roll | a2 | pitch | a3 | yaw | CFC1000 |
| 9-accel. | | | | | | | | | |
| a1_x | a1_x [c] | | a1 | forward | | | | | CFC1000 |
| a2_x | a2_x [c] | | a1 | forward | | | | | CFC1000 |
| a3_x | a3_x [c] | | a1 | forward | | | | | CFC1000 |
| a4_y | a4_y [d] | | | | a2 | lateral | | | CFC1000 |
| a5_y | a5_y [d] | | | | a2 | lateral | | | CFC1000 |
| a6_y | a6_y [d] | | | | a2 | lateral | | | CFC1000 |
| a7_z | a7_z [e] | | | | | | a3 | vertical | CFC1000 |
| a8_z | a8_z [e] | | | | | | a3 | vertical | CFC1000 |
| a9_z | a9_z [e] | | | | | | a3 | vertical | CFC1000 |
| Neck | | | | | | | | | |
| Upper load cell | NeckUp_lce_F | fr | f1 | shear | f2 | shear | f3 | axial | CFC1000<br>CFC600 |
| | NeckUp_lce_T | tr | t1 | roll | t2 | pitch | t3 | yaw | CFC600 |
| Lower load cell[f] | NeckLow_lce_F | fr | f1 | shear | f2 | shear | f3 | axial | CFC1000 |
| | NeckLow_lce_T | tr | t1 | roll | t2 | pitch | t3 | yaw | CFC600 |
| Thorax | | | | | | | | | |
| accelero-meter[a,g] | Thorax_acc | ar | a1 | forward | a2 | lateral | a3 | vertical | CFC180 |
| deflection | ChestDeflectionLUp_dis | dr | | displ. | | | | | CFC180 |
| Chest [h] | ChestDeflectionLLow_ dis | dr | | displ. | | | | | CFC180 |
| | ChestDeflectionRUp_dis | | | | | | | | |
| | ChestDeflectionRLow_ dis | dr | | displ. | | | | | CFC180 |
| | | dr | | displ. | | | | | CFC180 |
| Lumbar Spine | | | | | | | | | |
| Lower load cell | LumbarSpineLow_lce_F | fr | f1 | shear | f2 | shear | f3 | axial | CFC1000 |
| | LumbarSpineLow_lce_T | tr | t1 | roll | t2 | pitch | t3 | yaw | CFC1000 |
| Abdomen | | | | | | | | | |
| Intrusion[i] | | | | | | | | | |
| Middle | MiddleAb_disp | dr | d1 | inwards | | | | | |
| Left | LeftAb_displ | dr | d1 | inwards | | | | | |
| Right | RightAb_displ | dr | d1 | inwards | | | | | |
| Pelvis | | | | | | | | | |

*Continued on the next page*

*Table 17.4 cont.*

| Sensor | Identifier | Signal resultant | x | direction | y | direction | z | direction | Filter |
|---|---|---|---|---|---|---|---|---|---|
| Accelerometer [a] | Pelvis_acc | ar | a1 | forward | a2 | lateral | a3 | vertical | CFC1000 |
| Femur | | | | | | | | | |
| Left load cell | FemurL_lce_F | fr | f1 | shear | f2 | shear | f3 | axial | CFC600 |
| | FemurL_lce_T | tr | t1 | roll | t2 | pitch | t3 | yaw | CFC600 |
| Right load cell | FemurR_lce_F | fr | f1 | shear | f2 | shear | f3 | axial | CFC600 |
| | FemurR_lce_T | tr | t1 | roll | t2 | pitch | t3 | yaw | CFC600 |
| Femure failure [j] | event | | | | | | | | |
| Knee Failure [j] | event | | | | | | | | |
| Tibia | | | | | | | | | |
| Left Upper load cell | TibiaUpL_lce_F | fr | f1 | shear | f2 | shear | | | CFC600 |
| | TibiaUpL_lce_T | tr | t1 | roll | t2 | pitch | | | CFC600 |
| Right Upper load cell | TibiaUpR_lce_F | fr | f1 | shear | f2 | shear | | | CFC600 |
| | TibiaUpR_lce_T | tr | t1 | roll | t2 | pitch | | | CFC600 |
| Left Lower load cell | TibiaLowL_lce_F | fr | f1 | shear | f2 | shear | f3 | axial | CFC600 |
| | TibiaLowL_lce_T | tr | t1 | roll | t2 | pitch | | | CFC600 |
| Right Lower load cell | TibiaLowR_lce_F | fr | f1 | shear | f2 | shear | f3 | axial | CFC600 |
| | TibiaLowR_lce_T | tr | t1 | roll | t2 | pitch | | | CFC600 |
| Tibia Failure | event | | | | | | | | |



[a] The calculated acceleration is corrected in the x direction for a prescribed fictitious acceleration field to get correct values (see Theory manual).

[b] The MATD does not have an angular accelerometer installed at the CG. Instead, it uses the 9-accelerometer array device. The HeadCG_angacc output is a more convenient way to determine angular acceleration at the CG. However, outputs for both methods are provided.

[c] MADYMO provides outputs from tr-axial accelerometers only. To extract information for the 9-accelerometer calculations, only the X-component of this signal is required. To aid in this, the sensor identification is appended with _x.

[d] 9-accelerometer array sensor output. Use Y-component only.

[e] 9-accelerometer array sensor output. Use Z-component only.

[f] The MATD dummy does not have a lower neck load cell, but output is provided at the point where the Hybrid-III dummy optionally has a load cell for comparison purposes.

[g] ISO 13232 does not specify an accelerometer at this location, because of lack of biofidelity in this area. Sensor output is provided for comparison purposes.

[h] Four string potentiometers are used to determine the upper and lower chest deflection. A formula is given in ISO 13232, part 5, for the upper sternum:

$$D_{y,us} = frac(I_{uL} + \Delta I_{uL})^2 + (I_{uR} + \Delta I_{uR})^2 2 \cdot W_{L,R}$$

$$D_{x,us} = [(I_{uR} + \Delta I_{uR})^2 - (\frac{W_{L,R}}{2} - D_{y,us})^2]^{0.5} - d_{us}$$

$$c_{us,norm} = 100\frac{-D_{x,us}}{187.5}$$

Where:
$D_{y,us}$ is the upper sternum deflection in the y direction, in millimeters;
$I_{uL}$ is the cable length of the upper left string pot, in millimeters;
$\Delta I_{uL}$ is the change in cable length of the upper left string pot (positive is longer), in millimeters;
$I_{uR}$ is the cable length of the upper right string pot, in millimeters;

$\Delta l_{uR}$ is the change in cable length of the upper right string pot (positive is longer), in millimeters

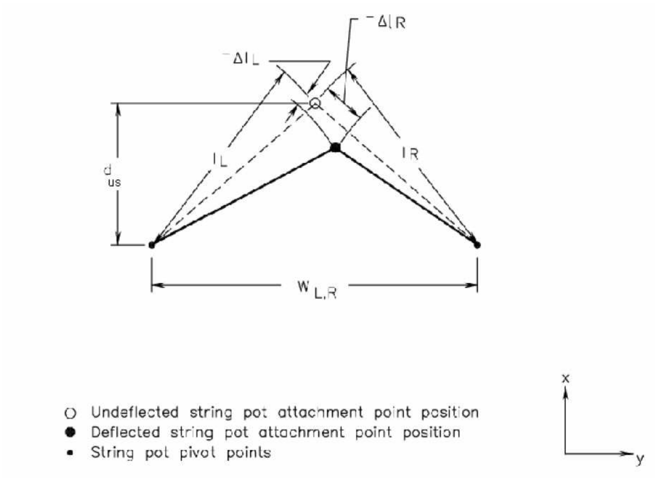


Figure 17.5:

For the MADYMO model the following values for $W_{L,R}$ and $D_{us}$ are used:
$W_{L,R} = 69.5mm$
$D_{us} = 111.8mm$
[i] Residual abdominal penetration is determined by reading the peak values of the 3 joint outputs defined between the abdomen and the pelvis.
[j] The failure of the frangible part is written to the control output file.

17

## Injury Criteria

The following injury criteria can be read directly from the simulation output files. Some criteria cannot be calculated directly by the Madymo solver.

Table 17.5: MATD injury criteria that can be read from output files.

| Injury criterion | Identifier | Filter |
|---|---|---|
| Head | | |
| HIC(15) | HIC15_inj | [a] |
| Abdomen | | |
| Maximum residual compression | MiddleAb_displ<br>LeftAb_displ<br>RightAb_displ | Can be read from the joint position output files |
| Legs | | |
| Frangible parts: Knee, Femur, Tibia | KneeValgusL<br>KneeValgusR | Femur and Tibia failure events can be read from the reprint file. Time of knee failure must be read from the control file. |

[a] ISO 13232 part 5 specifies that the HIC should only be calculated in intervals in which head contact according

to ISO Technical Report TR 12351 is detected. The Madymo HIC implementation does not take head contact into consideration.

Other criteria defined in ISO 13232 can be calculated by the user using the Madymo solver output.

Table 17.6: MATD output that must be calculated by user using MADYMO output.

| **Injury Criteria** | **ISO Reference** | **Madymo Input** |
|---|---|---|
| Head | | |
| GAMBIT | part 5, section 5.1.2 | resultant head acceleration, HeadCG_acc<br>resultant head angular acceleration, HEADCG_angacc |
| Thorax | | |
| upper sternum compression | part 5, section 5.1.4 | upper left string, ChestDeflectionLUp_dis, upper right string, ChestDeflectionRUp_dis |
| lower sternum compression | part 5, section 5.1.4 | lower left string, ChestDeflectionLLow_dis, lower right string, ChestDeflectionRLow_dis |
| upper sternum velocity | part 5, section 5.1.5 | use calculated compression defined in 5.1.4 |
| lower sternum velocity | part 5, section 5.1.5 | use calculated compression defined in 5.1.4 |
| upper sternum VC | part 5, section 5.1.5 | use compression from 5.1.4 and velocity from 5.1.5 |
| lower sternum VC | part 5, section 5.1.5 | use compression from 5.1.4 and velocity from 5.1.5 |

# 18 MATD Dummy Helmet

The MATD helmet model has been developed for exclusive use with the MATD facet model. The model describes the helmet recommended in ISO 13232 for use with the MATD dummy in motorcycle impact testing.

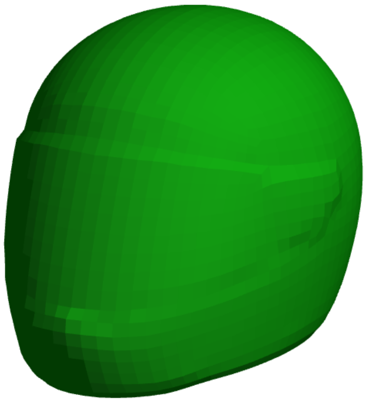

Figure 18.1: MATD dummy helmet model (external surface).

## 18.1 Model description

The MATD helmet model is available as a facet model only. The input is given in files:

| | |
|---|---|
| d_matd_helmet_inc.xml | MATD facet model include file |
| d_matd_helmet_usr.xml | MATD model user file |

The helmet model consists of an external shell and an internal shell, that are attached to a single helmet body. The shape of the helmet, both on the outside and inside, was measured with a 3D scanner.

The outside shell is a single surface that has an opening at the base. It uses a single characteristic to describe the interaction between the helmet and the environment. On the inside, a contact surface between the head and the helmet is described by a shell mesh that has been divided into 6 sections: front, top, rear, left, right, and chin. Each section has a distinct contact characteristic. A shell surface is positioned on the inside of the chin section of the helmet to allow interaction between the chin of the MATD dummy and the helmet. The model uses an FE belt to model the helmet strap. This strap prevents the helmet being pushed off from the head when the helmet is loaded.

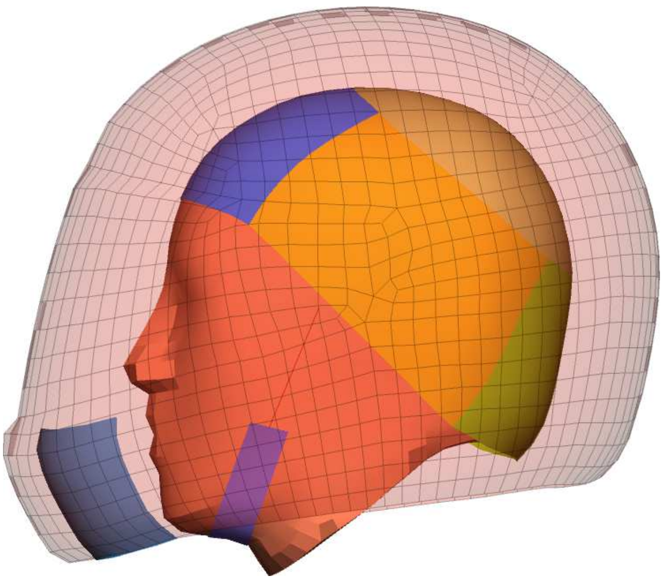

Figure 18.2: View of the inside of the MATD helmet model, showing the chin contact area, the chin strap, and the 5-section inner helmet contact surface.

## 18.2 User instructions

Since the helmet model is intended for exclusive use with the MATD facet model, these instructions describe how to attach the helmet model to the MATD model only.

**Timestep**

Table 18.1: Recommended timestep for the MATD helmet model.

| Model | timestep (s) |
|---|---|
| Facet | $\leq 0.5 \cdot 10^{-4}$ |

**Dummy positioning**

The centres of the MATD head and the MATD helmet model should coincide. The helmet is positioned on the MATD head using a free joint between inertial space and the helmet body (helmet_bod). If the position and orientation of the helmet body is identical to that of the MATD head body, the MATD head and helmet models will be perfectly aligned. This means that in order to set the position of the helmet model, the position and orientation of the MATD head relative to inertial space must be determined, for example by performing a pre-simulation and extracting the position information from the simulation output.

**Contact between the MATD dummy and the MATD head**

The contact between the dummy and the head are defined by two CONTACT.FE_FE definitions: one for the inner helmet surface and one for the chin strap. The contact method is CONTACT_METHOD.NODE_TO_SURFACE_INTERSECT and the CONTACT_TYPE can be set to COMBINED in order to use the deformation characteristics of both the inner helmet surface and the MATD head skin. Friction between the MATD head and the helmet inner surface must be defined in order to prevent the helmet sliding off the head. A friction value of 0.1 is recommended. The inner helmet contact group is **inner_helmet_gfe**.



If the helmet body is positioned correctly relative to the MATD head body, the FE chin strap should automatically be in the correct position relative to the chin of the MATD dummy head. The interaction between the chin and the strap is defined by a FE to FE contact, using the head as master and the strap as slave. The contact uses a gap with a thickness of 5.0E-03 and a friction function that has a recommended constant value of 0.2. The helmet strap contact group is **chinstrap_gfe**.

**External Contacts**

External contacts are described using contact group **outer_helmet_gfe**. Contact types can either be MASTER, SLAVE, or COMBINED, depending on the type of surface the helmet comes in contact with.

**Contact Characteristic Scaling**

The internal and external contact characteristics have been defined using data from a series of drop tests. Different impact locations and impact velocities were used in the tests. The helmet model is validated for all impact directions. It is possible to change the standard values of the loading functions and the damping by using function modifiers (FUNC_MOD) in the model user file. However, only small changes to the standard functions are recommended.

**Output**

The MATD helmet model does not produce any output. The use of the helmet will have an effect on the MATD dummy model head output (head acceleration, HIC).

# 19 Hybrid III 6-year-old Child Dummy

The Hybrid III 6 Year Old (6YO) dummy is used to evaluate the aggressiveness of deploying side and frontal airbags to an out-of position 6-year-old child. Originally developed in 1993 and upgraded in 1997, the dummy is included in the FMVSS 208 and is the recommended dummy to represent a 6-year-old child in all ISO "Out-of-Position" test procedures.

Two MADYMO models of the Hybrid III 6YO dummy are available: an ellipsoid model and a finite element model.

The Hybrid III 6YO ellipsoid model is based on the standard Hybrid III 50$^{th}$ percentile ellipsoid model. Differences between both can be found below in the description of the Hybrid III 6YO ellipsoid model. For those parts equivalent to the standard Hybrid III 50th percentile ellipsoid model the user is referred to Chapter 36.

The Hybrid III 6YO finite element model is based on the Hybrid III 6YO ellipsoid model. Differences between both can be found below in the description of the Hybrid III 6YO finite element model.

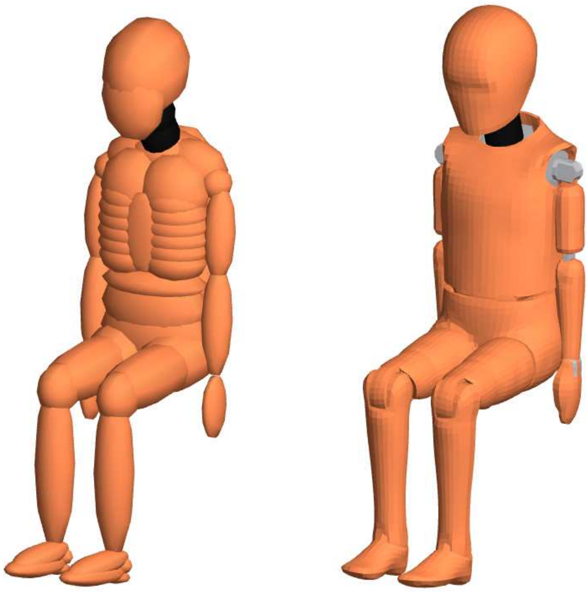

Figure 19.1: Hybrid III 6-year-old dummy models: ellipsoid (left) and finite element (right).

## 19.1 Model description

An ellipsoid model and a finite element model of the Hybrid III 6YO dummy are available. The corresponding input is given in the following files:

| | |
|---|---|
| Ellipsoid model: | d_hyb36yel_inc.xml<br>d_hyb36yel_usr.xml |
| Finite element model: | d_hyb36yfe_inc.xml<br>d_hyb36yfe_usr.xml |

To run these models, the following licenses are required:

| | |
|---|---|
| Ellipsoid model: | MADYMO/Solver (Multibody)<br>MADYMO/Dummy Models/Child |
| Finite element model: | MADYMO/Solver (Multibody)<br>MADYMO/Solver (FEM)<br>MADYMO/Dummy Models/Child |

Figure 19.1 shows both models in the reference position. The ellipsoid model consists of 28 bodies and 51 ellipsoid surfaces. The finite element model consists of a multi-body skeleton of 38 bodies and of an accurate mesh representation of all the components.

**ELLIPSOID MODEL**

Almost all parts of the Hybrid III 6-year-old dummy are scaled from the ellipsoid model of the Hybrid III 50$^{th}$ percentile dummy as described in Section 36.1. The only exceptions are the neck and the lumbar spine as described below.

19

**Neck**

A three-pivot neck model has been implemented. The middle pivot is a revolute-translational joint and the others are spherical joints. The stiffness of the Hybrid III neck depends on the bending direction. For large bending angles, the bending stiffness is strongly non-linear. To take this into account, a direction-dependent non-linear bending stiffness was defined for the neck using protected joint resistance models. The middle joint includes a translational DOF to describe neck elongation and compression. The head-neck model parameters were determined by using isolated neck sled test results and isolated head-neck impact test results.

**Lumbar spine**

To obtain a model of the lumbar spine a combination of a free joint and a protected joint resistance model is used. This protected joint resistance model describes the lumbar spine compliance. The joint location has been chosen in the middle between the connection plates of the lumbar spine. The mass and inertia properties of the actual lumbar spine have been divided over both spine bodies. The upper spine body is connected to the upper torso by means of a bracket joint, similarly the lower spine body is connected to the lower torso.

Like for the Hybrid III adult dummies, upper thorax-pelvis bending is not resisted by the lumbar spine only but also by contact of the rib cage, the abdomen and the lower torso. This interaction is included in the models by two point-restraints. These point-restraints are referred to as "Abdomen vertical left/right". It must be noted that frontal abdomen compression is included separately in the models.

## FINITE ELEMENT MODEL

The Hybrid III 6YO finite element dummy model has the same basic multi-body chain as the ellipsoid model. Some bodies have also been added to represent the complex reality of the Hybrid III 6YO hardware dummy. The neck and the legs are modelled with facet surfaces and their multi-body chains are the same as for the ellipsoid model. The lumbar spine kinematics is also the same as for the ellipsoid model.

### Head

The head skull and skin of the Hybrid III 6YO dummy model are supported on one single body. The skull is modelled with facet elements and is covered with a layer of solid finite elements representing the compliant skin. For airbag to head contact a special head contact group is defined with a closed head surface. This prevents the airbag from getting stuk inside the head especially in OOP simulations.

### Thorax

The multi-body structure of the Hybrid III 6YO finite element thorax is almost the same as for the ellipsoid model. The potentiometer branch has been added for chest deflection measurement and the clavicle assemblies have been split up into two different bodies and revolution joints in order to match the real Hybrid III 6YO hardware dummy.

The compliant ribs are modelled with shell elements with one layer of solid elements at the inner side representing the damping material. The rib stiffeners are modelled with shell elements and rigid material while the thoracic spine assembly, the clavicles, the potentiometer assembly and the rib stops are modelled with solid elements and rigid material. Finally, the compliant bib is modelled with shell elements and extra solid elements on the shoulders to represent the foam pads of the hardware dummy.



The back of the ribs is supported at some nodes on the thoracic spine. The front of the ribs is connected to the sternum assembly and to the bib by means of some rigid elements.

### Jacket

The very compliant jacket of the Hybrid III 6YO dummy is modelled with solid elements. It is not supported to any rigid body and is free to move in all directions, only restricted in its motion by contacts with other dummy components. The thorax assembly and the jacket are shown on Figure 19.2.

Figure 19.2: Hybrid III 6-year-old finite element thorax + jacket.

**Abdomen**

The compliant abdomen of the Hybrid III 6YO dummy has been modelled using tetrahedron elements and is not supported on any rigid body. On the contrary it is free to move in any direction inside the pelvis cavity and is restricted only by internal contacts with surrounding dummy components.

**Pelvis**

The pelvis of the Hybrid III 6YO dummy is modelled as a single piece with facet elements. The internal metal parts are not represented.



**Arms**

The arms of the Hybrid III 6YO dummy are modelled with facet surfaces.The multi-body chain that constitutes the kinematics of the arms has been completed with 3 bodies per arm to match the complex hardware dummy. The shoulder yoke has its own body and is linked to the clavicle by a revolution joint. On the same way, the upper arm is linked to the shoulder yoke, the elbow yoke to the upper arm, the lower arm to the elbow yoke, the wrist yoke to the lower arm and the hand to the wrist yoke. From the shoulder to the hand, there are thus per arm 6 bodies and 6 revolution joints.

## CONTACTS BETWEEN DUMMY COMPONENTS

For the ellipsoid model contact is defined between head and thorax.

For the finite element model all contacts between dummy inner components are already defined (mostly in the thorax and abdomen regions). For interactions between external dummy components, the pre-defined contacts are given in Table 19.1.

Table 19.1: Pre-defined contact interactions between external dummy components in the Hybrid III 6-year-old finite element model.

| Contact Description | Groups involved in the contact | |
|---|---|---|
| Left leg with right leg | Left femur + tibia + foot | Right femur + tibia + foot |
| Left arm with right arm | Left upper arm + lower arm + hand | Right upper arm + lower arm + hand |
| Left arm with pelvis | Left lower arm + hand | Pelvis |
| Right arm with pelvis | Right lower arm + hand | Pelvis |
| Left arm with leg | Left lower arm + hand | Left femur |
| Right arm with leg | Right lower arm + hand | Right femur |
| Left arm with jacket | Left lower arm + hand | Jacket |
| Right arm with jacket | Right lower arm + hand | Jacket |
| Head with jacket | Head | Jacket |
| Neck with jacket | Neck | Jacket |

In the finite element model, contact between upper arms and jacket should be defined when there is no initial penetration detected in the start configuration, otherwise this can lead to problems during the simulation. The same applies for the contact between jacket and pelvis.

## 19.2 Model validation

The Hybrid III 6 year old dummy models are developed and validated for frontal (OOP) loading using component tests and full dummy tests as described below. Although the ellipsoid model is not validated for side impact loading acceptable results have been obtained by some users for this condition as well. For both ellipsoid and finite element models parameters that are expected to have only little influence on OOP results are obtained by scaling down the Hybrid III 50$^{th}$ percentile dummy model (see Chapter 36).

### Component tests

Test programs were carried out for the thorax, the head and the neck, because those parts are considered to be the most important for OOP applications. The initial conditions in the impact tests were chosen such that the dynamic behaviour of the dummy components is comparable to the one of a full dummy in full-scale OOP tests. The component tests used for the development of both ellipsoid and finite element models are summarised in Table 19.2. Validation results are given in Figure 19.3 to Figure 19.5.

Table 19.2: Component tests for Hybrid III 6YO dummy models.

| Component | Test description | specifications | | Model Ellipsoid | Model FE |
|---|---|---|---|---|---|
| Neck | Head and neck on sled | Extension: | 13-20g; 4-7 m/s | x | x |
| | | Flexion: | 18g; 7.5 m/s | x | (a) |
| Neck+Head | Rigid impacts on head, bottom of neck supported | impact mass | 3.4 kg | x | x |
| | | velocity | 3.4-6 m/s | x | x |
| | | impact locations | - horizontal on forehead | x | x |
| | | | - horizontal on nose | x | x |
| | | | - horizontal on mouth | x | x |
| | | | - uppercut on chin | x | |
| | | | - downward on forehead | x | |
| | | | - oblique/lateral on cheek | x | |
| | | | - oblique/lateral on temple | | x |
| Clavicles | | Scaled from Hybrid III 50$^{th}$ percentile dummy model | | | |
| Shoulders | | Scaled from Hybrid III 50$^{th}$ percentile dummy model | | | |
| Elbows | | Scaled from Hybrid III 50$^{th}$ percentile dummy model | | | |
| Wrists | | Scaled from Hybrid III 50$^{th}$ percentile dummy model | | | |
| Thorax | Rigid impacts on isolated ribcage (ribs + sternum + thoracic spine) | Impactor mass | 4.25 & 4.5kg | x | x |
| | | Impact locations: | -frontal on whole sternum | x | x |
| | | | -frontal on upper sternum | x | x |
| | | | -ribcage | x | |
| | | | -oblique on ribcage sidel | | x |
| | | Impact velocity: | 2.7-5.8 m/s | x | x |
| | | Impact variations: | -with and without jacket | x | x |
| | | | -impactor size and shape | x | x |
| | | | -frontal and oblique loading | x | x |

*Continued on the next page*

19

*Table 19.2 cont.*

| Component | Test description | specifications | Model Ellipsoid | FE |
|---|---|---|---|---|
| Abdomen Insert | | Scaled from Hybrid III 50th percentile dummy model | | |
| Lumbar Spine | | Scaled from Hybrid III 3YO percentile dummy model | | |
| Hip joints | | Scaled from Hybrid III 50th percentile dummy model | | |
| Knees | | Scaled from Hybrid III 50th percentile dummy model | | |
| Ankles | | Scaled from Hybrid III 50th percentile dummy model | | |
| Surface compliance | | Calibrated using component tests or scaled from Hybrid III 50th percentile dummy model | | |

[a] Due to contacts between the head-neck assembly and the environment during the experimental sled test it was decided not to use this test for the validation of the Hybrid III 6YO head neck FE model.

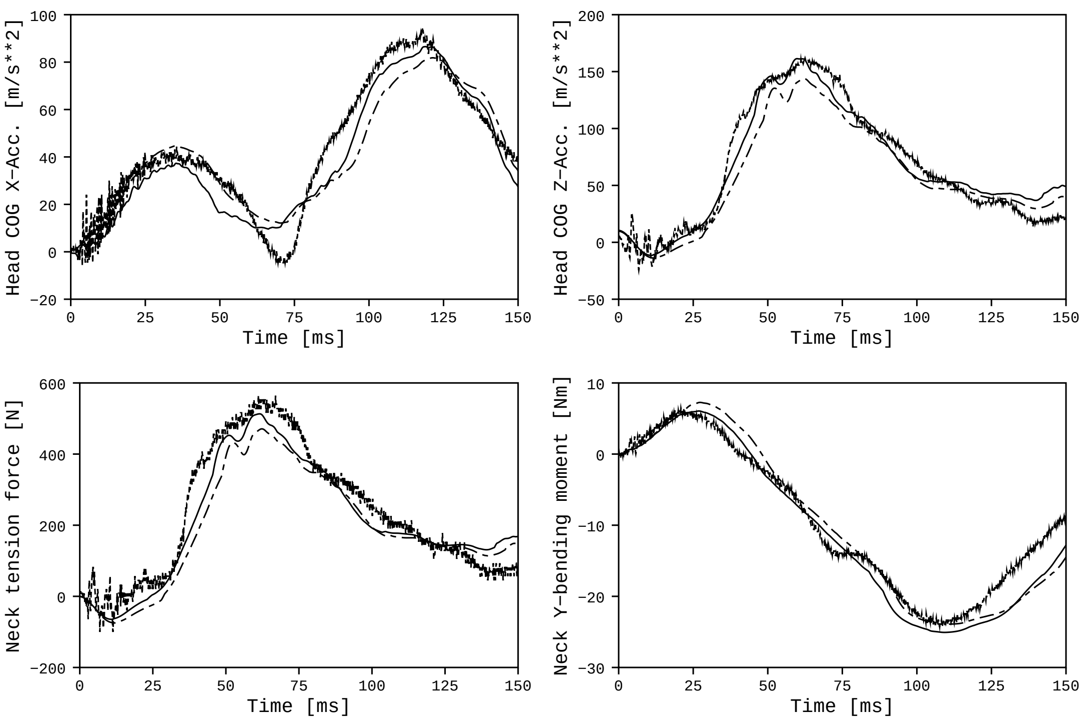


Figure 19.3: Validation results of the Hybrid III 6YO head-neck sled test (extension, 13.3g, 5.36m/s); experiment (— — —), ellipsoid model (—·—), FE model (———).

19

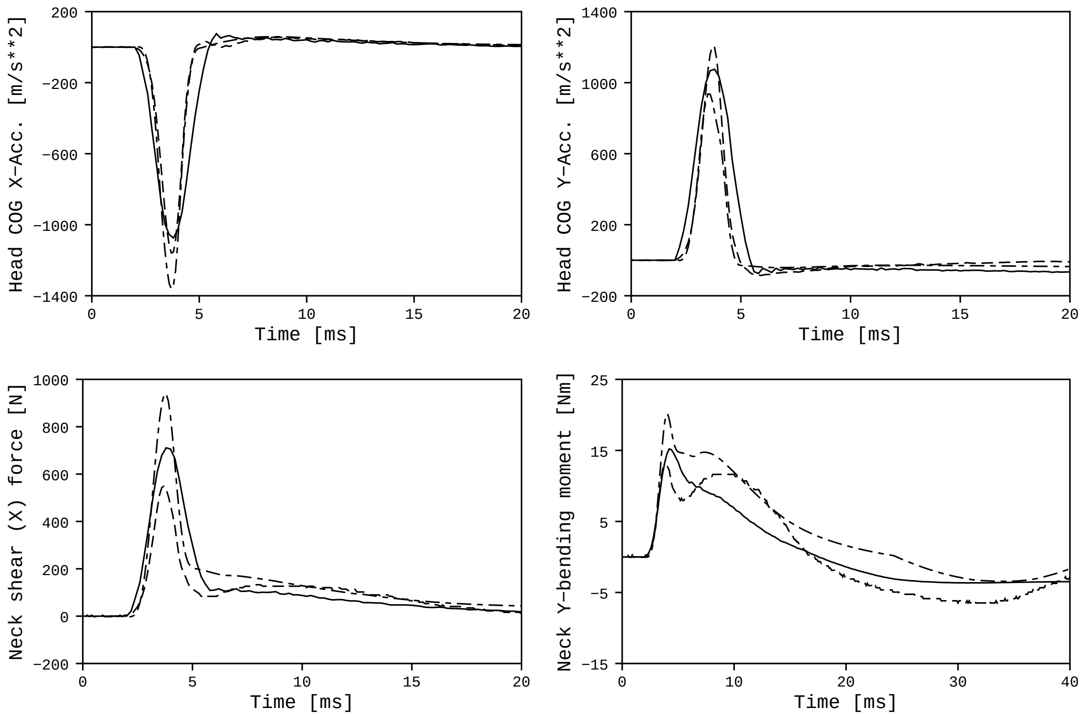


Figure 19.4: Validation results of the Hybrid III 6YO head-neck impact test (oblique impact on left temple, 3.4m/s); experiment (— — —), ellipsoid model (—·—), FE model (———).



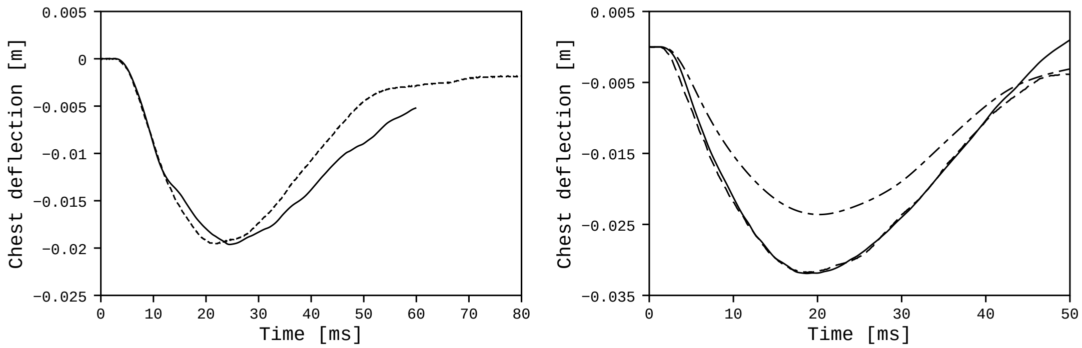


Figure 19.5: Validation results of the hybrid III 6YO thorax impact tests; Left: without jacket, small impactor, frontal impact on sternum, 2.74m/s. Right: with jacket, large impactor, frontal impact on sternum, 3.73m/s. Experiment (— — —), ellipsoid model (—·—), FE model (———).

### Full dummy tests

The tests with the complete Hybrid III 6YO dummy used for development and validation of the models are summarised in Table 19.3. In addition to those tests, several OOP applications done by users made a further validation of the ellipsoid and finite element Hybrid III 6YO dummy models possible.

Table 19.3: Full dummy tests for Hybrid III 6-year-old dummy model.

| **Test Description** | **Test Specifications** | | **Model Ellipsoid** | **FE** |
|---|---|---|---|---|
| Thorax certification pendulum test | | | x | |
| Rigid seat frontal sled test | Belt type<br>Sled velocity | -complete FE belt system<br>-13.4 m/s | x | x[a] |
| Out-of-Position airbag test | | | x | x[a] |

[a] The Hybrid III 6YO FE model was validated based on global motion, robustness and stability criteria. No quantitative comparison with experimental data was done.

## 19.3 User instructions

### Timestep

Table 19.4: Recommended timestep for the Hybrid III 6YO dummy models.

| Model | timestep (s) |
|---|---|
| Ellipsoid | $\leq 2.5 \cdot 10^{-5}$ |
| Finite Element | $\leq 1.0 \cdot 10^{-6}$ |

### Dummy positioning

Table 19.5: Positioning joints of the Hybrid III 6YO dummy models.

| Joint Description | Identifier[(a)] | Degree of freedom[(b)] | | | | | | Comment |
|---|---|---|---|---|---|---|---|---|
| Complete dummy | Dummy_jnt | R1<br>D1 | roll right<br>forward | R2<br>D2 | pitch down<br>leftward | R3<br>D3 | yaw left<br>upward | |
| Neck element | NeckPivotLow_jnt<br>NeckPivotMid_jnt<br>NeckPivotUp_jnt | R1<br>R2<br>R1 | roll right<br>pitch down<br>roll right | R2<br>D1<br>R2 | pitch down<br>downward<br>pitch down | R3<br><br>R3 | yaw left<br><br>yaw left | only for equilibrium state |
| Left shoulder | ShoulderL_jnt | R1 | pitch down | R2 | roll right | | | only for ell. |
| | ShoulderYokeL_jnt | R1 | pitch down | | | | | only for FE |
| | ShoulderL_jnt | R1 | roll right | | | | | only for FE |
| Right shoulder | ShoulderR_jnt | R1 | pitch down | R2 | roll right | | | only for ell. |
| | ShoulderYokeR_jnt | R1 | pitch down | | | | | only for FE |
| | ShoulderR_jnt | R1 | roll right | | | | | only for FE |
| Left elbow | ElbowL_jnt | R1 | yaw left | R2 | pitch down | | | only for ell. |
| | ElbowL_jnt | R1 | yaw left | | | | | only for FE |
| | ArmLowL_jnt | R1 | pitch down | | | | | only for FE |
| Right elbow | ElbowR_jnt | R1 | yaw left | R2 | pitch down | | | only for ell. |
| | ElbowR_jnt | R1 | yaw left | | | | | only for FE |
| | ArmLowR_jnt | R1 | pitch down | | | | | only for FE |
| Left wrist | WristL_jnt | R1 | yaw left | R2 | roll right | | | only for ell. |
| | WristL_jnt | R1 | yaw left | | | | | only for FE |
| | HandL_jnt | R1 | roll right | | | | | only for FE |
| Right wrist | WristR_jnt | R1 | yaw left | R2 | roll right | | | only for ell. |
| | WristR_jnt | R1 | yaw left | | | | | only for FE |
| | HandR_jnt | R1 | roll right | | | | | only for FE |
| Lumbar spine[(c)] | LumbarSpine_jnt | R1<br>D1 | yaw left<br>upward | R2<br>D2 | pitch down<br>leftward | R3<br>D3 | roll left<br>rearward | only for equilibrium state |
| Left hip | HipL_jnt | R1 | pitch down | R2 | roll left | R3 | yaw left | |

*Continued on the next page*

*Table 19.5 cont.*

| Joint Description | Identifier[a] | Degree of freedom[b] | | | | | | Comment |
|---|---|---|---|---|---|---|---|---|
| Right hip | HipR_jnt | R1 | pitch down | R2 | roll left | R3 | yaw left | |
| Left knee | KneeL_jnt | R1 | pitch down | | | | | |
| Right knee | KneeR_jnt | R1 | pitch down | | | | | |
| Left ankle | AnkleL_jnt | R1 | always zero | R2 | always zero | R3 | pitch down | |
| Right ankle | AnkleR_jnt | R1 | always zero | R2 | always zero | R3 | pitch down | |

(a) L=Left; R=Right

(b) Positive translation or rotation given in global co-ordinate system while dummy is in reference position (see Figure 1.2)

(c) Be very careful while changing the initial position of the lumbar spine joint in the finite element model. Some initial positions can cause initial penetrations between the pelvis and the jacket and between the components inside the thorax.

(d) The initial (zero) position of the arms causes intersections in the contacts between the arms and jacket/pelvis. For that the default (arm) joint orientations needs to be adjusted if contact is needed.

### Dummy contacts

Table 19.6: Available groups to define contact between the Hybrid III 6-year-old model components and the environment.

| Contact Group Description | Identifier[a] [b] | Ellipsoid model Surfaces involved | FE model Elements involved |
|---|---|---|---|
| Head | Head_*ctg* | Head_ell[c]<br>Face_ell[c] | Elements and nodes |
| | HeadAirbag_*ctg* | N/A | Elements and nodes[d] |
| Neck | Neck_*ctg* | NeckUp_ell[c]<br>NeckLow_ell[c] | Elements and nodes[e] |
| Thorax | Thorax_*ctg* | Collar_ell<br>ChestUpL/R_ell<br>ClavicleL/R_ell[c]<br>RibPart⟨*i*⟩L/R_ell<br>(for i=1 to 6 [c])<br>Sternum_ell [c]<br>ThoracicBackPlate_ell<br>LumbarSpineLow_ell<br>LumbarSpineUp_ell | N/A |
| Jacket | Jacket_*ctg* | N/A | Elements and nodes of the outside thorax |
| Abdomen | Abdomen_*ctg* | AbdomenLow_ell[c]<br>AbdomenMid_ell[c]<br>AbdomenUp_ell[c] | N/A |
| Pelvis | Pelvis_*ctg* | Pelvis_ell[c]<br>HipL/R_ell[c] | Elements and nodes[e] |
| Left upper arm | ArmUpL_*ctg* | ArmUpL_ell<br>ShoulderL_ell | Elements and nodes |

*Continued on the next page*

*Table 19.6 cont.*

| Contact Group Description | Identifier[(a)] [(b)] | Ellipsoid model Surfaces involved | FE model Elements involved |
|---|---|---|---|
| Right upper arm | ArmUpR_*ctg* | ArmUpR_ell<br>ShoulderR_ell | Elements and nodes |
| Left lower arm only | ArmLowL_*ctg* | N/A | Elements and nodes |
| Right lower arm only | ArmLowR_*ctg* | N/A | Elements and nodes |
| Left hand | HandL_*ctg* | N/A | Elements and nodes |
| Right hand | HandR_*ctg* | N/A | Elements and nodes |
| Left lower arm and left hand | ArmLowL_*ctg* | ArmLowL_ell<br>HandL_ell | N/A |
| Right lower arm and right hand | ArmLowR_*ctg* | ArmLowR_ell<br>HandR_ell | N/A |
| Left arm | ArmL_*ctg*<br>(= ArmUpL_*ctg*<br>+ ArmLowL_*ctg*<br>+ HandL_ctg) | N/A | Elements and nodes of the whole left arm |
| Right arm | ArmR_*ctg*<br>(= ArmUpR_*ctg*<br>+ ArmLowR_*ctg*<br>+ HandR_*ctg*) | N/A | Elements and nodes of the whole right arm |
| Left femur and left knee | FemurKneeL_*ctg* | FemurL_ell [(c)]<br>KneeL_ell [(c)] | Elements and nodes [(e)] |
| Right femur and right knee | FemurKneeR_*ctg* | FemurR_ell[(c)]<br>KneeR_ell[(c)] | Elements and nodes[(e)] |
| Left femur | FemurL_*ctg* | FemurL_ell | N/A |
| Right femur | FemurR_*ctg* | FemurR_ell | |
| Left knee | KneeL_*ctg* | KneeL_ell | N/A |
| Right knee | KneeR_*ctg* | KneeR_ell | |
| Left tibia | TibiaL_*ctg* | TibiaL_ell[(c)] | Elements and nodes[(e)] |
| Right tibia | TibiaR_*ctg* | TibiaR_ell[(c)] | Elements and nodes[(e)] |
| Left shoe | ShoeL_*ctg* | ShoeHeelL_ell[(c)]<br>ShoeL_ell[(c)] | N/A |
| Right shoe | ShoeR_*ctg* | ShoeHeelR_ell[(c)]<br>ShoeR_ell[(c)] | N/A |
| Left foot | FootL_*ctg* | N/A | Elements and nodes[(e)] |
| Right foot | FootR_*ctg* | N/A | Elements and nodes[(e)] |
| Left leg | LegL_*ctg*<br>(=FemurKneeL_*ctg*<br>+ TibiaL_*ctg*<br>+ FootL_*ctg*) | N/A | Elements and nodes of the whole left leg |
| Right leg | LegR_*ctg*<br>(=FemurKneeR_*ctg*<br>+ TibiaR_*ctg*<br>+ FootR_*ctg*) | N/A | Elements and nodes of the whole right leg |

[(a)] *ctg* = contactgroup, ctg is replaced by gmb (group Multibody) or gfe (group FE) respectively.

[b] L=Left; R=Right.
[c] Elastic contact characteristics are predefined for the ellipsoid model.
[d] Recommended for Head to Airbag FE FE contact
[e] Elastic contact characteristics are predefined for the finite element model.

## Output

All available Hybrid III 6YO dummy output signals are shown in table 19.7. ISO-MME output can also be generated for the Hybrid III 6YO dummy. Output requests for signals in ISO-MME format are pre-defined in the CONTROL_OUTPUT element in the user file.

Table 19.7: Hybrid III 6YO output signals.

| Sensor | Identifier | Signal resultant | x | direction[a] | y | direction[a] | z | direction[a] | Filter |
|---|---|---|---|---|---|---|---|---|---|
| Head | | | | | | | | | |
| CG accelerometer | HeadCG_acc | ar | a1 | forward | a2 | lateral | a3 | vertical | CFC1000 |
| Neck | | | | | | | | | |
| upper load cell | NeckUp_lce_F_CFC1000 | fr | f1 | shear | f2 | shear | f3 | axial | CFC1000 |
| | NeckUp_lce_F_CFC600 | fr | f1 | shear | f2 | shear | f3 | axial | CFC600 |
| | NeckUp_lce_T | tr | t1 | roll | t2 | pitch | t3 | yaw | CFC600 |
| lower load cell | NeckLow_lce_F | fr | f1 | shear | f2 | shear | f3 | axial | CFC1000 |
| | NeckLow_lce_T | tr | t1 | roll | t2 | pitch | t3 | yaw | CFC600 |
| Thorax | | | | | | | | | |
| accelerometers[a] | ThoraxT1_acc | ar | a1 | forward | a2 | lateral | a3 | vertical | CFC180 |
| | ThoraxT4_acc | ar | a1 | forward | a2 | lateral | a3 | vertical | CFC180 |
| | ThoraxUp_acc | ar | a1 | forward | a2 | lateral | a3 | vertical | CFC180 |
| | ThoraxLow_acc | ar | a1 | forward | a2 | lateral | a3 | vertical | CFC180 |
| chest deflection | ChestDeflection_dis | dr | d1 | displacement | | | | | CFC600 |
| | ChestDefl_dis_CFC180 | dr | d1 | displacement | | | | | CFC180 |
| | ChestDeflection_vel_CFC600 | vr | v1 | velocity | | | | | CFC600 |
| sternum accelerometer | SternumUp_acc | ar | a1 | forward | | | | | CFC1000 |
| | SternumLow_acc | ar | a1 | forward | | | | | CFC1000 |
| Lumbar Spine | | | | | | | | | |
| lower load cell | LumbarSpineLow_lce_F | fr | f1 | shear | f2 | shear | f3 | axial | CFC1000 |
| | LumbarSpineLow_lce_T | tr | t1 | roll | t2 | pitch | t3 | yaw | CFC1000 |
| Pelvis accelerometer | Pelvis_acc | ar | a1 | forward | a2 | lateral | a3 | vertical | CFC1000 |
| Femur | | | | | | | | | |
| left load cell | FemurL_lce_F | fr | f1 | shear | f2 | shear | f3 | axial | CFC600 |
| | FemurL_lce_T | tr | t1 | roll | t2 | pitch | t3 | yaw | CFC600 |
| right load cell | FemurR_lce_F | fr | f1 | shear | f2 | shear | f3 | axial | CFC600 |
| | FemurR_lce_T | tr | t1 | roll | t2 | pitch | t3 | yaw | CFC600 |

[a] Positive direction given according to SAE J211/1.

Table 19.8: Injury criteria defined for the Hybrid III 6YO.

| Injury criteria | Identifier | Filter |
|---|---|---|
| Head | | |
| HIC (15) | HIC15_inj | CFC1000 |
| HIC (36) | HIC36_inj | CFC1000 |
| Neck | | |
| FNIC | | |
| tension | FNICtension_inj | CFC1000 (force) CFC1000 |
| shear | FNICshear_inj | (force) CFC1000 (force) CFC600 |
| bending | FNICbending_inj | (moment) |
| NIJ | | |
| tension-extension | NTE_inj | CFC600 (force)<br>CFC600 (moment) |
| tension-flexion | NTF_inj | CFC600 (force)<br>CFC600 (moment) |
| compression-extension | NCE_inj | CFC600 (force)<br>CFC600 (moment) |
| compression-flexion | NCF_inj | CFC600 (force)<br>CFC600 (moment) |
| Thorax | | |
| 3ms | T3MS_inj | CFC180 |
| CTI | CTI_inj | CFC180 (acceleration)<br>CFC600 (deflection) |
| VC | VC_inj_CFC180 | CFC180 |
| | VC_inj_CFC600 | CFC600 |
| Chest Deflection | ChestDef_CFC180_inj | CFC180 |
| Femur | | |
| FFC | | |
| Left | FFCL_inj | CFC600 |
| Right | FFCR_inj | CFC600 |

# 20 Hybrid III 3-year-old Child Dummy

The Hybrid III 3-year-old (3YO) dummy is used to evaluate aggressiveness of deploying side and frontal airbags to an out-of-position child of 3 years old. The dummy has recently been included in FMVSS 208 and is the recommended dummy to represent a 3 years old child in the ISO "Out-of-Position" test procedures.

The ellipsoid model is based on the standard Hybrid III 50$^{th}$ percentile model. The differences with respect to the standard Hybrid III 50$^{th}$ percentile ellipsoid model are described below. For a description of those parts equivalent to the standard Hybrid III 50$^{th}$ percentile is referred to Chapter 36.

The finite element model is based on the Hybrid III 3YO ellipsoid model. The differences are described below.

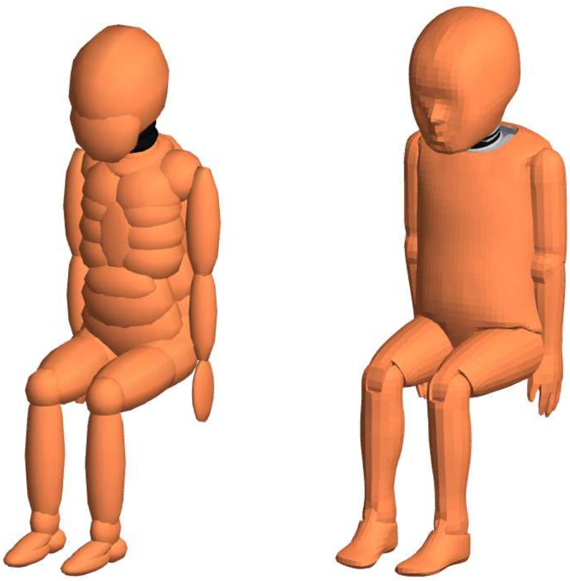

Figure 20.1: Hybrid III 3-year-old dummy models; ellipsoid (left) and finite element (right).

20

## 20.1 Model description

An ellipsoid and a finite element model of the Hybrid III 3-year-old dummy are available. The input is given in the files:

| | |
|---|---|
| Ellipsoid model: | d_hyb33yel_inc.xml<br>d_hyb33yel_usr.xml |
| Finite element model: | d_hyb33yfe_inc.xml<br>d_hyb33yfe_usr.xml |

To run these models, the following licenses are required:

| | |
|---|---|
| Ellipsoid model: | MADYMO/Solver (Multibody)<br>MADYMO/Dummy Models/Child |
| Finite element model: | MADYMO/Solver (Multibody)<br>MADYMO/Solver (FEM)<br>MADYMO/Dummy Models/Child |

Figure 20.1 shows both models in the reference position. The ellipsoid model consists of 28 bodies and the finite element model has a multi-body skeleton containing 41 bodies.

#### ELLIPSOID MODEL

Almost all parts of the Hybrid III 3-year-old dummy are scaled from the ellipsoid model of the Hybrid III 50$^{th}$ percentile dummy as described in Section 36.1. The only exceptions are Thorax/Ribs and sternum as described below. The neck and the lumbar spine are similar to the Hybrid III 6-year-old dummy as described in Section 19.1.

#### Thorax/Ribs and sternum

20

See Section 36.1. For the 3YO, a protected joint resistance model is used to model rib x-displacement. The sternum stop, which limits the sternum to spine box displacement, is modelled by two separate point-restraints.

#### FINITE ELEMENT MODEL

The finite element model has the same multibody basis as the ellipsoid model. this paragraph describes the differences in the finite element model with respect to the ellipsoid model. The neck column and the lumbar spine are modelled the same as in the ellipsoid model. The head, arms and the legs have been modelled with facet surfaces.

#### Thorax

The multibody structure of the finite element model is almost the same as the ellipsoid model except that the potentiometer branch has been added.

The ribs are modelled with shell elements with one layer of solid elements at the inner side representing the damping material. At the front the ribs are connected to the bib shell elements and the bib is connected to the sternum. The sternum is modelled with solid elements. The spine box is modelled as a rigid body and represented by facet surfaces. The potentiometer components are modelled in the same way as the spine box. The sternum and rib stops are modelled with solid elements. A small facet plane was added to the sternum to improve the contact with the sternum stops.

### Abdomen

The abdomen has been modelled using tetrahedron elements and is not supported to a rigid body. Instead, the abdomen is free to move in any direction, restricted only by contact with internal dummy components.

### Pelvis

All metal parts of the pelvis are modelled as rigid bodies. The geometry is represented by facet surfaces.

### Jacket

The jacket of the Hybrid III 3-year-old consist of the complete skin surface of the torso. This means that the skin part of the pelvis is part of the jacket. Generally the jacket contains two layers of solid hexahedron elements over the complete outer surface. The thick parts in the pelvis and the two parts in the shoulders are modelled using tetrahedron elements. The jacket is not supported to any rigid body. The motion of the jacket is only restricted by contact with internal dummy components.

## CONTACTS BETWEEN DUMMY COMPONENTS

For both models, ellipsoid and finite element, contact is defined between head and thorax.

## 20.2 Model validation

The dummy model is developed and validated for frontal (OOP) loading using tests as described below. Although the model is not validated for side impact (OOP) loading, acceptable results have been obtained by some users for this condition as well. Parameters which are expected to have only a small effect on OOP results are obtained by scaling down the Hybrid III 50$^{th}$ percentile dummy model (see Chapter 36).

### Component tests

Test programmes were carried out for the thorax, the head and the neck, because those parts are considered to be most important for OOP. The initial conditions in the impact tests were chosen such that the dynamic behaviour of the dummy components is comparable as in a full-scale OOP test. The component tests used for development of the models are summarised in Table 20.1. Validation results are given in Figure 20.2 to Figure 20.5.

Table 20.1: Component tests for Hybrid III 3YO child dummy models.

| Component | Test description | specifications | | Model Ellipsoid | FE |
|---|---|---|---|---|---|
| Head | Drop tests | Different orientations 2.6 m/s | impacting - chin<br>- nose<br>- forehead | | x<br>x<br>x |
| Neck | Head and neck on sled | extension<br>flexion | 30 – 45g ; 5 – 8 m/s<br>24g ; 5 m/s | x<br>x | x<br>x |
| Neck+Head | Rigid impacts on head, bottom of neck supported | Impact mass<br>velocity<br>impact locations | 3.4 kg<br>3 – 6 m/s<br>- horizontal on forehead<br>- horizontal on nose<br>- horizontal on mouth<br>- uppercut on chin<br>- downward on forehead<br>- oblique/lateral on cheek | x<br>x<br>x<br>x<br>x<br>x<br>x<br>x | x<br>x<br>x<br>x<br>x<br>x<br>x<br>x |
| Clavicles | | Scaled from Hybrid III 50$^{th}$ percentile dummy model | | | |
| Shoulders | | Scaled from Hybrid III 50$^{th}$ percentile dummy model | | | |
| Elbows | | Scaled from Hybrid III 50$^{th}$ percentile dummy model | | | |
| Wrists | | Scaled from Hybrid III 50$^{th}$ percentile dummy model | | | |
| Thorax | Rigid impacts on isolated ribcage (ribs and sternum) | Impact mass: | 4 kg | x | |
| | | | 4.9 – 5.4 kg | | x |
| | | impact velocity: | 2.5 – 5.1 m/s | x | |
| | | | 2.6 – 5.4 m/s | | x |
| | | Impact locations: | - sternum only | x | |
| | | | - rib local | x | |
| | | | - ribcage | x | |
| | | | - ribs only | | x |
| | | variations: | - with and without jacket | x | x |
| | | | - impactor size and shape | x | x |
| | | | - frontal and oblique loading | x | x |

*Continued on the next page*

20

*Table 20.1 cont.*

| Component | Test description | specifications | Model Ellipsoid | FE |
|---|---|---|---|---|
| Abdomen Insert | | Scaled from Hybrid III 50th percentile dummy model | | |
| Lumbar Spine | Lumbar spine and thorax on sled | 24 – 32g;<br>4 – 6 m/s | x<br>x | |
| Hip joints | | Scaled from Hybrid III 50th percentile dummy model | | |
| Knees | | Scaled from Hybrid III 50th percentile dummy model | | |
| Ankles | | Scaled from Hybrid III 50th percentile dummy model | | |
| Surface compliance | | Calibrated using component tests or scaled from Hybrid III 50th percentile dummy model | x | x |

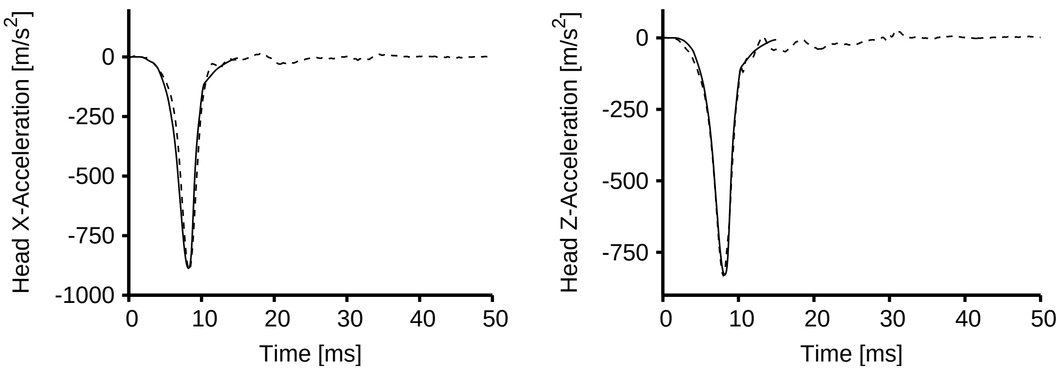


Figure 20.2: HIII3YO Head drop tests results (chin impact, 2.6m/s); experiment (— — —) and finite element model (———).

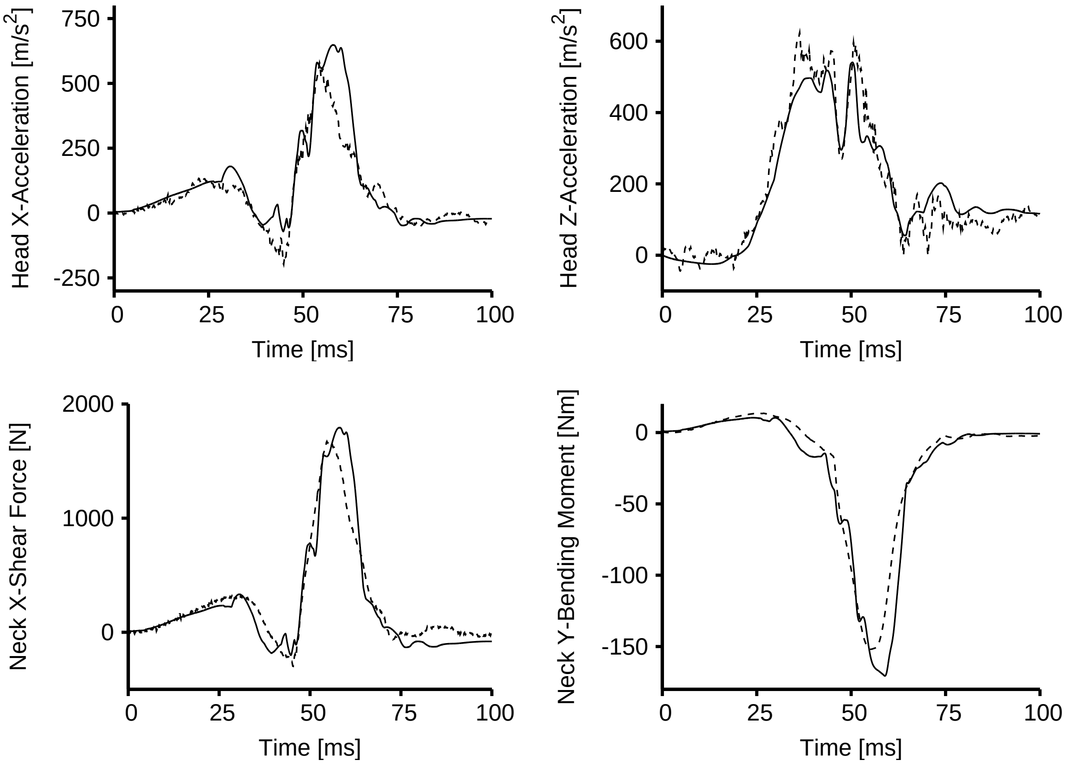


Figure 20.3: HIII3YO Head-Neck assembly sled tests results; Extension: 6.5m/s, 42g; experiment (— — —) and finite element model (———).



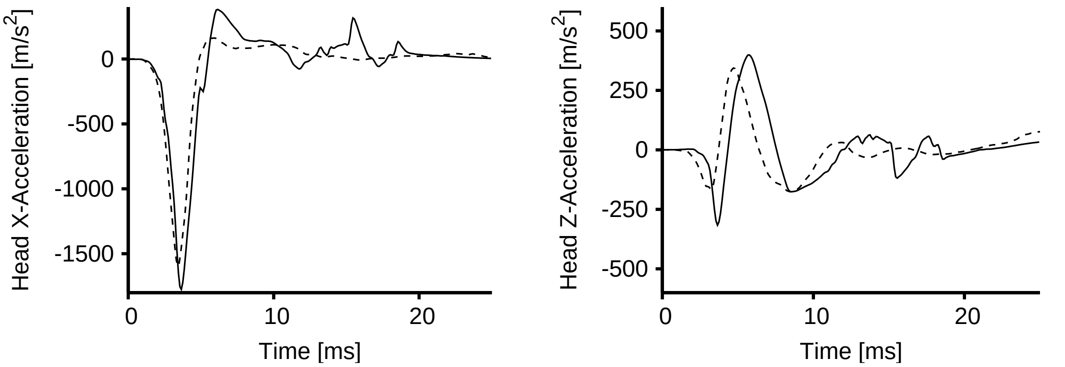


Figure 20.4: HIII3YO Head impact tests results (impact on mouth; 3.4kg impactor); experiment (— — —) and finite element model (———).

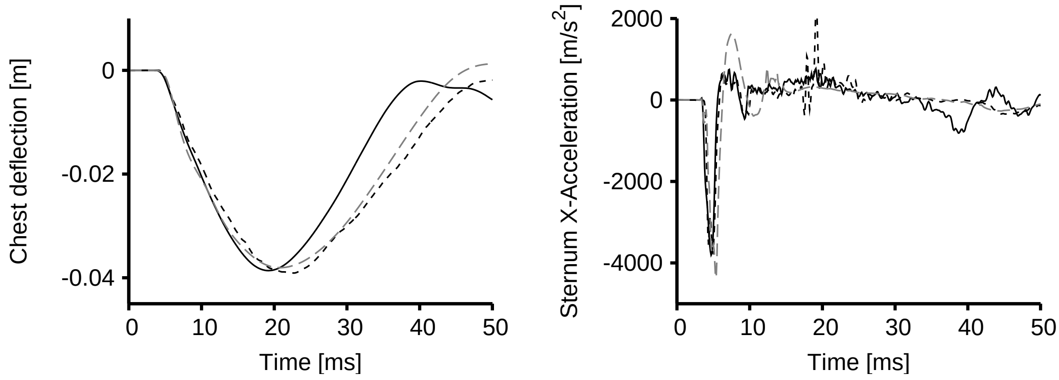


Figure 20.5: HIII3YO thorax impact tests results (impact on sternum; 4.9kg impactor, 4.4m/s); experiment (– – –), ellipsoid model (— —) and finite element model (———).

### Full dummy tests

The tests with the complete dummy used for development and validation of the models are summarised in Table 20.2. Some validation results are given in Figure 20.6. Several full-scale airbag validations have been done by users to check the model accuracy and robustness.

Table 20.2: Full dummy tests for Hybrid III 3 YO dummy models.

| Test description | specification impactor velocity (m/s) | mass (kg) | shape | Model Ellipsoid | FE |
|---|---|---|---|---|---|
| free sitting dummy hit by rigid guided impactor | | | | x | x |
| impactor locations: | | | | | |
| - forehead | 7 | 3.4 | small disc | x | x |
| - mouth | 7 | 3.4 | small disc | x | x |
| - thorax, mid | 6,7 | 1.7 | small disc | x | x |
| | 4,6 | 4.35 | large disc | x | x |
| - thorax, mid, shifted lateral | 6 | 1.7 | small disc | x | x |
| - thorax, upper | 6 | 1.7 | small disc | x | x |
| - thorax, oblique | 4 | 4.35 | large disc | x | x |
| - abdomen | 5 | 4.35 | large disc | x | x |
| thorax certification pendulum test | | | | x | |

20

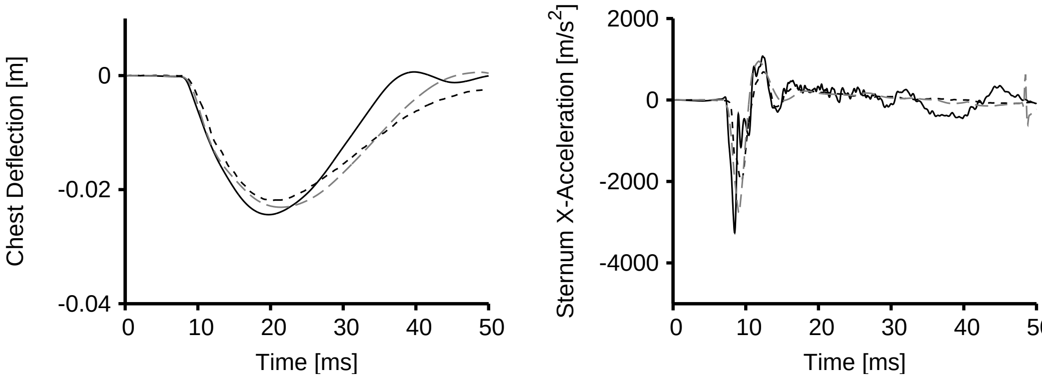


Figure 20.6: HIII3YO Full dummy thorax impact test validation results (large impactor, 4.35kg, 4 m/s); experiment (- - -), ellipsoid model (— —) and finite element model (——).

20

## 20.3 User instructions

### Timestep

Table 20.3: Recommended timestep for the Hybrid III 3YO dummy models.

| Model | timestep (s) |
|---|---|
| Ellipsoid | $\leq 1.0 \cdot 10^{-4}$ |
| Finite Element | $\leq 1.0 \cdot 10^{-6}$ |

### Dummy positioning

Table 20.4: Positioning joints of the Hybrid III 3YO dummy models.

| Joint Description | Identifier | Degree of freedom[a] | | | | | | Comment |
|---|---|---|---|---|---|---|---|---|
| Complete dummy | Dummy_jnt | R1<br>D1 | roll right<br>forward | R2<br>D2 | pitch down<br>leftward | R3<br>D3 | yaw left<br>upward | |
| Neck element | NeckPivotLow_jnt | R1 | | R2 | | R3 | | only for equilibrium state |
| | NeckPivotMid_jnt | R2<br>D1 | | | | | | |
| | NeckPivotUp_jnt | R1 | | R2 | | R3 | | |
| Left shoulder | ShoulderL_jnt | R1 | roll right | R2 | pitch down | R3 | yaw left | |
| Right shoulder | ShoulderR_jnt | R1 | roll right | R2 | pitch down | R3 | yaw left | |
| Left elbow | ElbowL_jnt | R1 | always zero | R2 | pitch down | | | |
| Right elbow | ElbowR_jnt | R1 | always zero | R2 | pitch down | | | |
| Lumbar spine[b] | LumbarSpine_jnt | R1<br>D1 | | R2<br>D2 | | R3<br>D3 | | only for equilibrium state |
| Left hip | HipL_jnt | R1 | pitch down | R2 | roll right | R3 | yaw left | |
| Right hip | HipR_jnt | R1 | pitch down | R2 | roll right | R3 | yaw left | |
| Left knee | KneeL_jnt | R1 | pitch down | | | | | |
| Right knee | KneeR_jnt | R1 | pitch down | | | | | |
| Left ankle | AnkleL_jnt | R1 | always zero | R2 | always zero | R3 | pitch down | |
| Right ankle | AnkleR_jnt | R1 | always zero | R2 | always zero | R3 | pitch down | |

[a] Positive translation or rotation given in global co-ordinate system while dummy is in reference position (see Figure 1.2).
[b] It is recommended not to change the initial position of the lumbar spine joint of the finite element model, otherwise initial penetrations may occur between jacket and thorax components.

### Dummy contacts

20

Table 20.5: Available groups to define contact between the Hybrid III 3YO components and environment.

| **Contact Description** | **Identifier**[a],[b] | **Ellipsoid model**[a] | **Finite element model**[a] |
|---|---|---|---|
| Head[c] | Head_*ctg* | Head_ell<br>Face_ell | Elements and nodes |
| Neck[c] | Neck_*ctg* | NeckUp_ell<br>NeckLow_ell | Elements and nodes |
| Left upper arm | ArmUpL_*ctg* | ArmUpL-ell | Elements and nodes[d] |
| Right upper arm | ArmUpR_*ctg* | ArmUpR_ell | Elements and nodes[d] |
| Left lower arm and hand | ArmLowL_*ctg* | ArmLowL_ell<br>HandL_ell | Elements and nodes[d] |
| Right lower arm and hand | ArmLowR_*ctg* | ArmLowR_ell<br>HandR_ell | Elements and nodes[d] |
| Thorax | Thorax_*ctg* | Collar_ell<br>ChestUpL/R_ell<br>ShoulderL/R_ell[c]<br>RibUpL/R_ell[c]<br>RibMidL/R_ell[c]<br>RibLowL/R_ell[c]<br>Sternum_ell[c]<br>ThoracicBackPlate_ell<br>LumbarSpineLow_ell<br>LumbarSpineUp_ell | N/A |
| Abdomen[c] | Abdomen_*ctg* | AbdomenLow_ell<br>AbdomenMid_ell<br>AbdomenUp_ell | N/A |
| Pelvis | Pelvis_*ctg* | Pelvis_ell<br>HipL/R_ell | N/A |
| Thorax and pelvis | Jacket_*ctg* | N/A | Elements and nodes |
| Left femur and knee | FemurKneeL_*ctg* | FemurL_ell<br>KneeL_ell | Elements and nodes[d] |
| Right femur and knee | FemurKneeR_*ctg* | FemurR_ell<br>KneeR_ell | Elements and nodes[d] |
| Left femur | FemurL_*ctg* | FemurL_ell | N/A |
| Right femur | FemurR_*ctg* | FemurR_ell | |
| Left knee | KneeL_*ctg* | KneeL_ell | N/A |
| Right knee | KneeR_*ctg* | KneeR_ell | |
| Left tibia | TibiaL_*ctg* | TibiaL_ell | Elements and nodes[d] |
| Right tibia | TibiaR_*ctg* | TibiaR_ell | Elements and nodes[d] |
| Left foot | FootL_*ctg* | N/A | Elements and nodes[d] |
| Right foot | FootR_*ctg* | | Elements and nodes[d] |
| Left shoe | ShoeL_*ctg* | ShoeHeelL_ell<br>ShoeL_ell | N/A |
| Right shoe | ShoeR_*ctg* | ShoeHeelR_ell<br>ShoeR_ell | |

[a] *ctg*=contactgroup, for all the ellipsoid and finite element models ctg is replaced by gmb (group_multibody) and gfe (group_finite element), respectively.

[b] L=Left; R=Right.

[c] Elastic contact characteristics are predefined for the ellipsoid model.

[d] Elastic contact characteristics are predefined for the facet surfaces.

## Output

Table 20.6: Hybrid III 3YO output signals.

| Sensor | Identifier | Signal resultant | x | direction[a] | y | direction[a] | z | direction[a] | Filter |
|---|---|---|---|---|---|---|---|---|---|
| Head | | | | | | | | | |
| CG accelerometer | HeadCG_acc | ar | a1 | forward | a2 | lateral | a3 | vertical | CFC1000 |
| | HeadBack_acc | ar | a1 | forward | a2 | lateral | a3 | vertical | CFC1000 |
| | HeadANG_acc | ar | a1 | forward | a2 | lateral | a3 | vertical | CFC1000 |
| Neck | | | | | | | | | |
| Upper load cell | NeckUp_lce_F | fr | f1 | shear | f2 | shear | f3 | axial | CFC1000 CFC600 |
| | NeckUp_lce_T | tr | t1 | roll | t2 | pitch | t3 | jaw | CFC600 |
| Lower load cell | NeckLow_lce_F | fr | f1 | shear | f2 | shear | f3 | axial | CFC1000 |
| | NeckLow_lce_T | tr | t1 | roll | t2 | pitch | t3 | jaw | CFC600 |
| Shoulder | | | | | | | | | |
| Left load cell | ShoulderL_lce_F | fr | f1 | shear | | | f3 | shear | CFC1000 |
| Right load cell | ShoulderR_lce_F | fr | f1 | shear | | | f3 | shear | CFC1000 |
| Thorax | | | | | | | | | |
| accelerometer | ThoraxT1_acc | ar | a1 | forward | a2 | lateral | a3 | vertical | CFC180 |
| | ThoraxT4_acc | ar | a1 | forward | a2 | lateral | a3 | vertical | CFC1000 |
| | ThoraxT12_acc | ar | a1 | forward | a2 | lateral | a3 | vertical | CFC180 |
| | ThoraxLow_acc | ar | a1 | forward | a2 | lateral | a3 | vertical | CFC180 |
| Chest deflection | ChestDeflection_dis | dr | d1 | displacement | | | | | CFC600 |
| | ChestDefl_dis_CFC180 | dr | d1 | displacement | | | | | CFC180 |
| | ChestDeflection_vel_CFC180 | vr | v1 | velocity | | | | | CFC180 |
| sternum accelerometer | SternumUp_acc | ar | a1 | forward | | | | | |
| | SternumLow_acc | ar | a1 | forward | | | | | |
| Lumbar Spine | | | | | | | | | |
| Lower load cell | LumbarSpineLow_lce_F | fr | f1 | shear | f2 | shear | f3 | axial | CFC1000 |
| | LumbarSpineLow_lce_T | tr | t1 | roll | t2 | pitch | t3 | jaw | CFC600 |
| Hip load cell | HipCupL_lce_F | fr | f1 | shear | f2 | shear | f3 | axial | CFC1000 |
| | HipCupR_lce_T | fr | f1 | shear | f2 | shear | f3 | axial | CFC1000 |

[a] Positive direction given according to SAE J211/1.

20

Table 20.7: Injury criteria defined for the Hybrid III 3YO.

| Injury criteria | Identifier | Filter |
|---|---|---|
| Head | | |
| HIC (15) | | |
| HIC (36) | HIC15_inj | CFC1000 |
| | HIC36_inj | CFC1000 |
| Neck | | |
| FNIC | | |
| tension | FNICtension_inj | CFC1000 (force) |
| shear | FNICshear_inj | CFC1000 (force) |
| bending | FNICbending_inj | CFC1000 (force) |
| | | CFC600 (moment) |
| NIJ | | |
| tension-extension | NTE_inj | CFC600 (force) |
| | | CFC600 (moment) |
| tension-flexion | NTF_inj | CFC600 (force) |
| | | CFC600 (moment) |
| compression-extension | NCE_inj | CFC600 (force) |
| | | CFC600 (moment) |
| compression-flexion | NCF_inj | CFC600 (force) |
| | | CFC600 (moment) |
| Thorax | | |
| 3ms | T3MS_inj | CFC1000 |
| VC | VC_inj_CFC180 | CFC180 |
| | VC_inj_CFC600 | CFC600 |
| Chest Deflection | ChestDef_CFC180_inj | CFC180 |

# 21 CRABI Child Dummy

The CRABI (Child Restraint AirBag Interaction) 12 month old dummy is used to evaluate aggressiveness of a deploying airbag to an out-of-position child of 12 months' age. The dummy has recently been included in FMVSS 208 and is the recommended dummy to represent a 12 month old child in the ISO "Out-of-Position" test procedures.

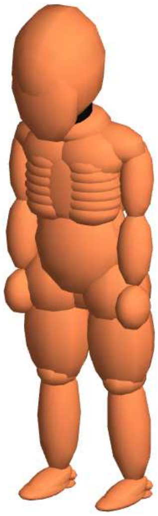

Figure 21.1: Ellipsoid CRABI 12 month old dummy model.

## 21.1 Model description

An ellipsoid model of the CRABI 12 month old dummy is available. The input is given in the files:

| | |
|---|---|
| Ellipsoid model: | d_crb12mel_usr.xml<br>d_crb12mel_inc.xml |

To run the model, the following licenses are required:

| | |
|---|---|
| Ellipsoid model: | MADYMO/Solver (Multibody)<br>MADYMO/Dummy Models/Child |

Figure 21.1 shows the model in the reference position. The ellipsoid model consists of 32 bodies.

**ELLIPSOID MODEL**

The model of the CRABI 12 month old dummy has been obtained by scaling down the standing Hybrid III 50th percentile dummy model (see Chapter 5). Therefore, the description of the ellipsoid model can be found in Section 5.1. Geometry measurements on the physical dummy and existing information about mass distribution, have been used as anthropometry source.

**CONTACTS BETWEEN DUMMY COMPONENTS**

For the ellipsoid model contact is defined between the head and thorax.

## 21.2 Model validation

No tests have been performed for validation of this version of the model.

## 21.3 User instructions

### Timestep

Table 21.1: Recommended timestep for the CRABI dummy model.

| **Model** | **timestep (s)** |
|---|---|
| Ellipsoid | $\leq 2.5 \cdot 10^{-5}$ |

### Dummy positioning

Table 21.2: Positioning joints of the CRABI dummy model.

| **Joint Description** | **Identifier** | **Degree of freedom**[a] | | | **Comment** |
|---|---|---|---|---|---|
| Complete dummy | Dummy_jnt | R1 roll right<br>D1 forward | R2 pitch down<br>D2 leftward | R3 yaw left<br>D3 upward | |
| Neck element | NeckPivotLow_jnt<br>NeckPivotUp_jnt<br>NeckBracket_jnt | R1<br>R1<br>R1 | R2<br>R2 | R3<br>R3 | only for equilibrium state |
| Left shoulder | ShoulderL_jnt | R1 pitch down | R2 roll right | | |
| Right shoulder | ShoulderR_jnt | R1 pitch down | R2 roll right | | |
| Left elbow | ElbowL_jnt | R1 yaw left | R2 pitch down | | |
| Right elbow | ElbowR_jnt | R1 yaw left | R2 pitch down | | |
| Left wrist | WristL_jnt | R1 yaw left | R2 roll right | | |
| Right wrist | WristR_jnt | R1 yaw left | R2 roll right | | |
| Lumbar spine | LumbarSpine_jnt | R1<br>R1 | R2<br>R2 | R3<br>R3 | only for equilibrium state |
| Left hip | HipL_jnt | R1 yaw left | R2 pitch up | R3 roll right | |
| Right hip | HipR_jnt | R1 yaw left | R2 pitch up | R3 roll right | |
| Left knee | KneeL_jnt | R1 pitch down | | | |
| Right knee | KneeR_jnt | R1 pitch down | | | |
| Left ankle | AnkleL_jnt | R1 always zero | R2 always zero | R3 pitch down | |
| Right ankle | AnkleR_jnt | R1 always zero | R2 always zero | R3 pitch down | |

[a] Positive translation or rotation given in global co-ordinate system while dummy is in reference position (see Figure 1.2).

Table 21.3: Available groups to define contact between the CRABI components and environment.

| Contact Description | Identifier[(a)] | Ellipsoid model[(b)] |
|---|---|---|
| Head | Head_*ctg* | Head_ell<br>Face_ell |
| Neck | Neck_*ctg* | Neck_ell<br>NoddingPlate_ell |
| Left upper arm | ArmUpL_*ctg* | ArmUpL_ell |
| Right upper arm | ArmUpR_*ctg* | ArmUpR_ell |
| Left lower arm and hand | ArmLowL_*ctg* | ArmLowL_ell<br>HandL_ell |
| Right lower arm and hand | ArmLowR_*ctg* | ArmLowR_ell<br>HandR_ell |
| Thorax | Thorax_*ctg* | Collar_ell<br>ChestUpL/R_ell<br>ShoulderL/R_ell<br>RibPart⟨*i*⟩L/R_ell, for i=1 to 6<br>Sternum_ell<br>ThoracicBackPlate_ell<br>LumbarSpineLow_ell<br>LumbarSpineUp_ell |
| Abdomen | Abdomen_*ctg* | AbdomenLow_ell<br>AbdomenMid_ell<br>AbdomenUp_ell |
| Pelvis | Pelvis_*ctg* | Pelvis_ell HipL/R_ell |
| Left femur and knee | FemurKneeL_*ctg* | FemurL_ell<br>KneeL_ell |
| Right femur and knee | FemurKneeR_*ctg* | FemurR_ell<br>KneeR_ell |
| Left tibia | TibiaL_*ctg* | TibiaL_ell |
| Right tibia | TibiaR_*ctg* | TibiaR_ell |
| Left shoe | ShoeL_*ctg* | FootL_ell<br>HeelL_ell<br>ShoeHeelL_ell<br>ShoeL_ell |
| Right shoe | ShoeR_*ctg* | FootR_ell<br>HeelR_ell<br>ShoeHeelR_ell<br>ShoeR_ell |

[(a)] *ctg* = contactgroup, ctg is replaced by gmb (group_multibody).
[(b)] L=Left; R=Right.

## Output

Table 21.4: CRABI output signals.

| **Sensor** | **Identifier** | **Signal** | | | | | | | **Filter** |
|---|---|---|---|---|---|---|---|---|---|
| | | **resul-tant** | **x** | **direc-tion**[a] | **y** | **direc-tion**[a] | **z** | **direc-tion**[a] | |
| Head | | | | | | | | | |
| CG accelerometer[b] | Head_acc | ar | a1 | forward | a2 | lateral | a3 | vertical | CFC1000 |
| Neck | | | | | | | | | |
| Upper load cell | NeckUp_lce_F | fr | f1 | shear | f2 | shear | f3 | axial | CFC1000 |
| | | | | | | pitch | | | CFC600 |
| | NeckUp_lce_T | tr | t1 | roll | t2 | | t3 | yaw | CFC600 |
| Lower load cell | NeckLow_lce_F | fr | f1 | shear | f2 | shear | f3 | axial | CFC1000 |
| | NeckLow_lce_T | tr | t1 | roll | t2 | pitch | t3 | yaw | CFC600 |
| Thorax | | | | | | | | | |
| accelerometer | Thorax_acc | ar | a1 | forward | a2 | lateral | a3 | vertical | CFC180 |
| Chest deflection | ChestDeflection_dis | dr | d1 | displace-ment | | | | | CFC600 |
| | ChestDefl_dis_ CFC180 | dr | d1 | displace-ment | | | | | CFC180 |
| | ChestDeflection_vel_ CFC600 | vr | v1 | velocity | | | | | CFC600 |
| Lumbar Spine | | | | | | | | | |
| Upper load cell | LumbarSpineUp_lce_F | fr | f1 | shear | f2 | shear | f3 | axial | CFC1000 |
| | LumbarSpineUp_lce_T | tr | t1 | roll | t2 | pitch | t3 | yaw | CFC1000 |
| Lower load cell | LumbarSpineLow_lce_F | fr | f1 | shear | f2 | shear | f3 | axial | CFC1000 |
| | LumbarSpineLow_lce_T | tr | t1 | roll | t2 | pitch | t3 | yaw | CFC1000 |
| Femur | | | | | | | | | |
| Left load cell | FemurL_lce_F | fr | f1 | shear | f2 | shear | f3 | axial | CFC600 |
| | FemurL_lce_T | tr | t1 | roll | t2 | pitch | t3 | yaw | CFC600 |
| Right load cell | FemurR_lce_F | fr | f1 | shear | f2 | shear | f3 | axial | CFC600 |
| | FemurR_lce_T | tr | t1 | roll | t2 | pitch | t3 | yaw | CFC600 |
| Tibia | | | | | | | | | |
| Upper load cell | TibiaUpL_lce_F | fr | f1 | shear | f2 | shear | f3 | axial | CFC600 |
| | TibiaUpL_lce_T | tr | t1 | roll | t2 | pitch | t3 | jaw | CFC600 |
| | TibiaUpR_lce_F | fr | f1 | shear | f2 | shear | f3 | axial | CFC600 |
| | TibiaUpR_lce_T | tr | t1 | roll | t2 | pitch | t3 | jaw | CFC600 |
| Lower load cell | TibiaLowL_lce_F | fr | f1 | shear | f2 | shear | f3 | axial | CFC600 |
| | TibiaLowL_lce_T | tr | t1 | roll | t2 | pitch | t3 | jaw | CFC600 |
| | TibiaLowR_lce_F | fr | f1 | shear | f2 | shear | f3 | axial | CFC600 |
| | TibiaLowR_lce_T | tr | t1 | roll | t2 | pitch | t3 | jaw | CFC600 |

[a] Positive direction given according to SAE J211/1.

Table 21.5: Injury criteria defined for the CRABI components.

| **Injury criteria** | **Identifier** | **Filter** |
|---|---|---|
| Head | | |

*Continued on the next page*

*Table 21.5 cont.*

| Injury criteria | Identifier | Filter |
|---|---|---|
| HIC (15) | HIC15_inj | CFC1000 |
| HIC (36) | HIC36_inj | CFC1000 |
| Neck | | |
| FNIC | | |
| tension | FNICtension_inj | CFC1000 (force) |
| shear | FNICshear_inj | CFC1000 (force) |
| bending | FNICbending_inj | CFC1000 (force)<br>CFC600 (moment) |
| NIJ | | |
| tension-extension | NTE_inj | CFC600 (force)<br>CFC600 (moment) |
| tension-flexion | NTF_inj | CFC600 (force)<br>CFC600 (moment) |
| compression-extension | NCE_inj | CFC600 (force)<br>CFC600 (moment) |
| compression-flexion | NCF_inj | CFC600 (force)<br>CFC600 (moment) |
| Thorax | | |
| 3ms | T3MS_inj | CFC180 |
| CTI | CTI_inj | CFC180 (acceleration)<br>CFC600 (deflection) |
| VC | VC_inj_CFC180<br>VC_inj_CFC600 | CFC180<br>CFC600 |
| Femur | | |
| FFC | | |
| Left | FFCL_inj | CFC600 |
| Right | FFCR_inj | CFC600 |
| Tibia | | |
| TCFC | | |
| Left | TIUpL_inj<br>TILowL_inj | CFC600<br>CFC1000 |
| Right | TIUpR_inj<br>TILowR_inj | CFC600<br>CFC1000 |

# 22 Q0 Child Dummy

In 1993, an ad-hoc child dummy working group, consisting of CRS manufacturers, research institutes and test-houses in Europe started the development of the Q-series of child dummies as successor to the P-series. The 0-year-old version, Q0, is now available for use in i-Size child restraint assessments. The MADYMO dummy model is based on the technical drawings and hardware measurements.

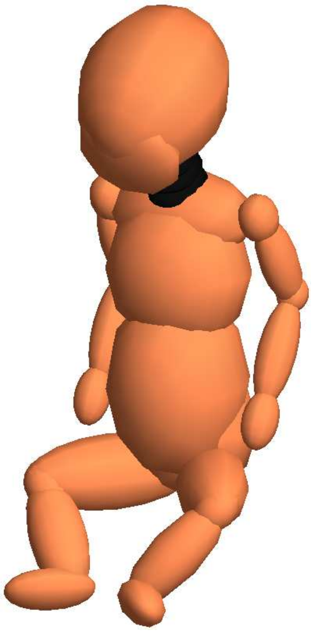

Figure 22.1: Ellipsoid model of the Q0 child dummy.

## 22.1 Model description

An ellipsoid model of the Q0 child dummy is available. The input is given in the files:

| | |
|---|---|
| Ellipsoid model: | d_q00yel_usr.xml<br>d_q00yel_inc.xml |

To run the model, the following licenses are required:

| | |
|---|---|
| Ellipsoid model: | MADYMO/Solver (Multibody)<br>MADYMO/Dummy Models/Child/Q Child 00 |

Figure 22.1 shows the Q0 model in the reference position. The model consists of 38 bodies and 38 joints.

**ELLIPSOID MODEL**

**Head**

The head geometry is described by two ellipsoids, one for the head and one for the face. The upper neck load cell is modelled separately and attached rigidly to the head with a bracket joint. The accelerometer mount is also represented and attached to the upper neck load cell with a bracket joint.

**Neck**

The outer surface of the neck segment is described by four ellipsoids, which define the contact group. The neck is modelled with a triple-joint restraint, applied to a cylindrical joint with a universal joint either side. The triple joint restraint enables to model the cross-interactions between the tension, shear, bending and torsion deformation modes in the neck.

**Shoulders and arms**

The motion of the shoulder relative to the thoracic spine is modelled with a revolute joint. The deformation (bending) of each flexible polyurethane arm is modelled with four spherical joints along the arm. Those joints are not meant for initial positioning.



**Thorax**

The thorax comprises the thoracic spine and torso flesh. Rigid bodies are included for the spinebox, the torso top plate and the thoracic spine bottom plate. The torso flesh is modelled by two ellipsoids, the clavicles region and the main thorax part, transferring load respectively to the torso top plate and the thoracic spine.

**Lumbar Spine and Abdomen**

The lumbar spine is exactly the same component as the neck, but turned upside down around the Y-axis. The large abdomen flesh covers the lumbar spine and transfers the load to the upper lumbar part. The lower lumbar part is rigidly attached to the pelvis bone body.

**Pelvis**

The outer surface of the pelvis flesh is connected to the pelvis bone.

### Hips and legs

The motion of the hip relative to the pelvis bone is modelled with a revolute joint. The deformation (bending) of each flexible polyurethane leg is modelled with one spherical joint at the knee. This joint is not meant for initial positioning.

### Suit

The additional mass of the suit of the Q0 child dummy is divided and added to that of the clavicles flesh, torso flesh, abdomen flesh and pelvis flesh bodies.

## CONTACTS BETWEEN DUMMY COMPONENTS

Internal contacts are pre-defined between the torso and arms, the arms and legs, and the left and right lower legs. Relative forward and lateral bending of the torso with respect to the pelvis is limited thanks to flexion restraints added between the thoracic spine and upper lumbar spine bodies, and between the lower lumbar spine and pelvis bodies.

## 22.2 Model validation

The dummy model was developed and validated using component tests and tests on the complete dummy.

### Component tests

The component tests used for development and validation of the models are summarised in Table 22.1.

Table 22.1: Component tests for Q0 child dummy model.

| Component | Test Description | Specifications | | Model Ellipsoid |
|---|---|---|---|---|
| Head | Head frontal drop test | Height, angle | 0.130m, 28° | x |
| | Head frontal drop test | Height, angle | 0.376m, 45° | x |
| | Head lateral drop test | Height, angle | 0.130m, 35° | x |
| Neck | Pendulum test, forward flexion | Velocity | 3.20m/s | x |
| | Pendulum test, forward extension | Velocity | 3.20m/s | x |
| | Pendulum test, lateral bending | Velocity | 3.23m/s | x |
| | Sled test, forward flexion | Velocity | 4.12m/s | x |
| Thorax | Frontal impactor test | Velocity | 3.20m/s | x |

### Full dummy tests

The full dummy tests used for the development and the validation are summarised in Table 22.2.

Table 22.2: Full dummy tests for Q0 dummy model.

| Test Description | Specifications | | Model Ellipsoid |
|---|---|---|---|
| Frontal thorax impactor test | Velocity | 4.00m/s | x |
| Lateral thorax impactor test | Velocity | 4.00m/s | x |
| Rearward facing CRS sled test | Velocity | 13.4m/s | x |
| Lateral CRS sled test with door impact | Velocity | 6.94m/s | x |

## 22.3 User instructions

### Timestep

Table 22.3: Recommended timestep for the Q0 dummy model.

| Model | timestep (s) |
|---|---|
| Ellipsoid | $\leq 1.0 \cdot 10^{-5}$ |

### Dummy positioning

Table 22.4: Positioning joints of the Q0 dummy model.

| Joint Description | Identifier | Degree of freedom[a] | | | | | | Comment |
|---|---|---|---|---|---|---|---|---|
| Complete dummy | Dummy_jnt | R1<br>D1 | roll right<br>forward | R2<br>D2 | pitch down<br>leftward | R3<br>D3 | yaw left<br>upward | |
| Neck | NeckUp_jnt<br>NeckMid_jnt<br>NeckLow_jnt | R1<br>D1<br>R1 | roll right<br>upward<br>pitch up | R2<br>R1<br>R2 | pitch up<br>yaw left<br>roll right | | | only for equilibrium state |
| Left shoulder | ShoulderL_jnt | R1 | pitch down | | | | | |
| Right shoulder | ShoulderR_jnt | R1 | pitch down | | | | | |
| Lumbar Spine | LumbarSpineUp_jnt<br>LumbarSpineMid_jnt<br>LumbarSpineLow_jnt | R1<br>D1<br>R1 | roll left<br>upward<br>pitch down | R2<br>R1<br>R2 | pitch down<br>yaw left<br>roll left | | | only for equilibrium state |
| Left hip | HipL_jnt | R1 | pitch down | | | | | |
| Right hip | HipR_jnt | R1 | pitch down | | | | | |

[a] Positive translation or rotation given in global co-ordinate system while dummy is in reference position.

22

### Dummy contacts

Table 22.5 below describes the Q0 contact groups available in the model and recommended for the definition of contacts between the dummy and the environment, in a CRS application. In addition, a Dummy_gmb contact group is available wherein all contact surfaces (those for which a characteristic is defined) are included. The Dummy_gmb group has not been used for dummy model calibration or validation.

Table 22.5: Pre-defined Q0 dummy contact groups.

| Contact Description | Identifier[a],[b] | Ellipsoids in group[b] |
|---|---|---|
| Head | Head_gmb | Head_ell<br>Face_ell |
| Neck | Neck_gmb | NeckMouldLow_ell<br>NeckMouldUp_ell<br>NeckMouldBottomPlate_ell<br>NeckMouldTopPlate_ell |
| Left arm | ArmL_gmb | ShoulderL_ell<br>ArmUpL_ell<br>ElbowL_ell<br>ArmLowL_ell<br>HandL_ell |
| Right arm | ArmR_gmb | ShoulderR_ell<br>ArmUpR_ell<br>ElbowR_ell<br>ArmLowR_ell<br>HandR_ell |
| Thorax | Thorax_gmb | Clavicles_ell<br>Thorax_ell |
| Abdomen | Abdomen_gmb | Abdomen_ell |
| Pelvis | Pelvis_gmb | Pelvis_ell |
| Left upper leg | UpperLegL_gmb | UpperLegL_ell |
| Left lower leg | LowerLegL_gmb | KneeL_ell<br>LowerLegL_ell<br>FootL_ell |
| Right upper leg | UpperLegR_gmb | UpperLegR_ell |
| Right lower leg | LowerLegR_gmb | KneeR_ell<br>LowerLegR_ell<br>FootR_ell |

[a] gmb=group_multibody.
[b] L=Left; R=Right.

22

## Output

Below in Table 22.6 all available Q0 child dummy output signals are shown. ISO-MME output can also be generated for the Q0 child dummy. Output requests for signals in ISO-MME format are pre-defined in the CONTROL_OUTPUT element in the user file.

Table 22.6: Q0 output signals

| Sensor | Identifier | Signal | | | | | | | Filter |
|---|---|---|---|---|---|---|---|---|---|
| | | resul-tant | x | direc-tion[(a)] | y | direc-tion[(a)] | z | direction[(a)] | |
| Head | | | | | | | | | |
| CG accelerometer[(b)] | Head_CFC1000_acc | ar | a1 | forward | a2 | rightward | a3 | downward | CFC1000 |
| Neck | | | | | | | | | |
| Upper load cell | NeckUpLC_CFC600_lce_F | fr | f1 | shear | f2 | shear | f3 | axial | CFC600 |
| | NeckUpLC_CFC600_lce_T | tr | t1 | roll | t2 | pitch | t3 | yaw | CFC600 |
| Thorax | | | | | | | | | |
| Accelerometer[(b)] | Thorax_CFC1000_acc | ar | a1 | forward | a2 | rightward | a3 | downward | CFC1000 |
| | Thorax_CFC180_acc | ar | a1 | forward | a2 | rightward | a3 | downward | CFC180 |
| Pelvis | | | | | | | | | |
| Accelerometer[(b)] | Pelvis_CFC1000_acc | ar | a1 | forward | a2 | rightward | a3 | downward | CFC1000 |

[(a)] Positive direction given according to SAE J211/1.

[(b)] The calculated acceleration is corrected in the x, y and z direction for a prescribed fictitious acceleration field to get correct values (see Theory manual).

22

In Table 22.7 all predefined injury criteria for the Q0 model are listed.

Table 22.7: Predefined injury criteria for the Q0 model.

| Component | Injury criteria | Filter |
|---|---|---|
| Head | HIC15_inj | CFC1000 |
| | HIC36_inj | CFC1000 |
| | Head_CFC1000_AccR_3MS_inj | CFC1000 |
| | Head_CFC1000_AccR_peak_inj | CFC1000 |
| Neck | NeckUp_CFC600_My_peak_inj | CFC600 |
| | NeckUp_CFC600_Tension_peak_inj | CFC600 |
| Thorax | Thorax_CFC1000_AccR_3MS_inj | CFC1000 |
| | Thorax_CFC1000_AccR_peak_inj | CFC1000 |
| | Thorax_CFC1000_AccZabs_3MS_inj | CFC1000 |
| | Thorax_CFC180_AccR_3MS_inj | CFC180 |
| | Thorax_CFC180_AccR_peak_inj | CFC180 |
| | Thorax_CFC180_AccZabs_3MS_inj | CFC180 |
| Pelvis | Pelvis_CFC1000_AccR_3MS_inj | CFC1000 |
| | Pelvis_CFC1000_AccR_peak_inj | CFC1000 |

In addition to the output signals and injury criteria given in Table 22.6 and Table 22.7, the head containment criterion can be best verified by the user in a simulation where the boundary planes are modelled and included in a contact definition with the dummy head.

# 23 Q1 Child Dummy

In 1993, an ad-hoc child dummy working group, consisting of CRS manufacturers, research institutes and test-houses in Europe started the development of the Q-series of child dummies as successor to the P-series. The 1-year-old version, Q1, is now available for use in i-Size child restraint assessments. The MADYMO dummy model is based on the Q6 modelling architecture, and has been scaled based on anthropometrical scaling rules and hardware measurements.

Figure 23.1: Ellipsoid model of the Q1 child dummy.

## 23.1 Model description

An ellipsoid model of the Q1 child dummy is available. The input is given in the files:

| | |
|---|---|
| Ellipsoid model: | d_q01yel_usr.xml<br>d_q01yel_inc.xml |

To run the model, the following licenses are required:

| | |
|---|---|
| Ellipsoid model: | MADYMO/Solver (Multibody)<br>MADYMO/Dummy Models/Child/Q Child 01 |

Figure 23.1 shows the Q1 model in the reference position. The model consists of 68 bodies.

**ELLIPSOID MODEL**

**Head**

The head is connected to the upper neck load cell by a bracket joint. The head geometry is described by two ellipsoids, one for the head and one for the face.

**Neck**

The neck is modelled with a triple-joint restraint, applied to a cylindrical joint with a universal joint either side. The outer surface of the neck segment is described by five ellipsoids, which define the contact group.

**Shoulders and Clavicles**

The shoulder and clavicle area is a flexible assembly connecting the arms to the spinebox and providing a load path to the ribcage. The motion of the shoulder relative to the spinebox is modelled in the MADYMO model with a translational joint, and the flexibility of the clavicle piece from the shoulder to the sternum attachment is modelled with a revolute-translational joint on each side. Each wing of the clavicles is attached to the sternum by a point restraint.

**Ribcage**

23

The ribcage of the Q1 consists of a thin flexible shell. It can deform under both lateral and frontal loading. To implement such properties, the Q1 ribcage model is comprised of five bodies on each side, joined at the front by a body for the sternum, and at rear the spinebox. The ribs are joined by revolute joints, creating a flexible loop representing the ribcage. Joint restraints determine the bending stiffness, and point and Cardan restraints are used to connect the frontmost rib bodies to the sternum. The bending and contact stiffness characteristics were calculated from thorax validation tests.

**Lumbar Spine and Abdomen**

As with the neck, the lumbar spine is represented by a triple-joint restraint, with a bracket joint used to measure forces and moments in the lower lumbar load cell. The abdomen consists of three ellipsoids, the upper and middle abdomen transferring load to the lumbar and the lower to the pelvis.

### Pelvis

Four ellipsoids characterise the contact surfaces of the pelvis: two representing the lower and rear pelvis that come into contact with a child seat, and two representing the pelvis wings for belt contact and side impact analyses.

## CONTACTS BETWEEN DUMMY COMPONENTS

Contacts are defined between the head and the thorax; the head and the legs; the thorax and arms; the abdomen and arms; the left and right arms; the left and right legs.

## 23.2 Model validation

The dummy model was developed and validated using component tests and tests on the complete dummy.

### Component tests

The component tests used for development and validation of the models are summarised in Table 23.1.

Table 23.1: Component tests for Q1 child dummy model.

| Component | Test description | specifications | | Model Ellipsoid |
|---|---|---|---|---|
| Head | Head frontal drop test | Starting height | 0.13 m | x |
| | Head lateral drop test | Starting height | 0.13 m | x |
| Neck | Forward bending pendulum | Velocity | 3.9m/s | x |
| | Lateral bending pendulum | Velocity | 3.9m/s | x |
| Lumbar | Forward bending pendulum | Velocity | 4.4m/s | x |
| | Lateral bending pendulum | Velocity | 4.4m/s | x |
| Thorax | Frontal pendulum test | Velocity | 4.3 m/s | x |
| | Lateral pendulum test | Velocity | 4.3 m/s | x |

### Full dummy tests

The full dummy tests used for the development and the validation are summarised in Table 23.2.

Table 23.2: Full dummy tests for Q1 dummy model.

| Test Description | Specifications | | Model Ellipsoid |
|---|---|---|---|
| Frontal CRS sled test | Velocity | 60 km/h, 53 km/h, 47 km/h | x |
| Lateral CRS sled test | Velocity | 50 km/h | x |

## 23.3 User instructions

### Timestep

Table 23.3: Recommended timestep for the Q1 dummy model.

| Model | timestep (s) |
|---|---|
| Ellipsoid | $\leq 1.0 \cdot 10^{-5}$ |

### Dummy positioning

Table 23.4: Positioning joints of the Q1 dummy model.

| Joint Description | Identifier | Degree of freedom[a] | | | | | | Comment |
|---|---|---|---|---|---|---|---|---|
| Complete dummy | Dummy_jnt | R1<br>D1 | roll right<br>forward | R2<br>D2 | pitch down<br>leftward | R3<br>D3 | yaw left<br>upward | |
| Neck element | NeckUp_jnt<br>NeckMid_jnt<br>NeckLow_jnt | R1<br>D1<br>R1 | roll right<br>upward<br>pitch up | R2<br>R1<br>R2 | pitch up<br>yaw left<br>roll right | | | only for equilibrium state |
| Left shoulder | ShoulderL_jnt | R1 | roll right | R2 | pitch down | R3 | yaw left | |
| Right shoulder | ShoulderR_jnt | R1 | roll right | R2 | pitch down | R3 | yaw left | |
| Left elbow | ElbowL_jnt | R1 | pitch down | | | | | |
| Right elbow | ElbowR_jnt | R1 | pitch down | | | | | |
| Lumbar Spine element | LumbarSpineUp_jnt<br>LumbarSpineMid_jnt<br>LumbarSpineLow_jnt | R1<br>D1<br>R1 | roll right<br>upward<br>pitch up | R2<br>R1<br>R2 | pitch up<br>yaw left<br>roll right | | | only for equilibrium state |
| Left hip | HipL_jnt | R1 | roll right | R2 | pitch down | R3 | yaw left | |
| Right hip | HipR_jnt | R1 | roll right | R2 | pitch down | R3 | yaw left | |
| Left knee | KneeL_jnt | R1 | pitch down | | | | | |
| Right knee | KneeR_jnt | R1 | pitch down | | | | | |

[a] Positive translation or rotation given in global co-ordinate system while dummy is in reference position

23

### Dummy contacts

Table 23.5 describes the Q1 contact groups available in the model and recommended for the definition of contacts between the dummy and the environment, in a CRS application. In addition, a Dummy_gmb contact group is available wherein all contact surfaces (those for which a characteristic is defined) are included. The Dummy_gmb group has not been used for dummy model calibration or validation.

Table 23.5: Available groups to define contact between the Q1 components and environment.

| **Contact Description** | **Identifier**[(a)],[(b)] | **Ellipsoid model**[(b)] |
|---|---|---|
| Head | Head_gmb | Head_ell<br>Face_ell |
| Neck | Neck_gmb | NeckUpperDisk_ell<br>NeckLowerDisk_ell<br>NeckUp_ell |
| Shoulders | SuitShoulder_gmb | SuitBackL_ell<br>SuitBackR_ell<br>SuitFrontL_ell<br>SuitFrontR_ell<br>SuitFrontSideL_ell<br>SuitFrontSideR_ell |
| Left upper arm | ArmUpL_gmb | ArmUpL_ell<br>ElbowL_ell<br>ShoulderL_ell |
| Left lower arm | ArmLowL_gmb | ArmLowL_ell<br>HandL_ell |
| Right upper arm | ArmUpR_gmb | ArmUpR_ell<br>ElbowR_ell<br>ShoulderR_ell |
| Right lower arm | ArmLowR_gmb | ArmLowR_ell<br>HandR_ell |
| Clavicles | Clavicles_gmb[(c)] | ClaviclePart(1-4)L/R_ell |
| Ribcage | Ribcage_gmb | Rib(1-5)L/R_ell<br>Sternum_ell |
| Back | Back_gmb | ThoracicSpineNeck_ell<br>ThoracicSpineBody_ell |
| Abdomen | Abdomen_gmb | AbdomenUp_ell<br>AbdomenMid_ell<br>AbdomenLow_ell |
| Pelvis | Pelvis_gmb | Pelvis_ell<br>PelvisBack_ell<br>PelvisSideL/R_ell |
| Left upper leg | LegUpL_gmb | LegUpPart(1-3)L_ell |
| Right upper leg | LegUpR_gmb | LegUpPart(1-3)R_ell |
| Left lower leg | LegLowL_gmb | KneeL_ell<br>LegLowPart(1-2)L_ell<br>FootL_ell |

*Continued on the next page*

*Table 23.5 cont.*

| Contact Description | Identifier[a],[b] | Ellipsoid model[b] |
|---|---|---|
| Right lower leg | LegLowR_gmb | KneeR_ell<br>LegLowPart(1-2)R_ell<br>FootR_ell |

[a] gmb=group_multibody.
[b] L=Left; R=Right.
[c] although composed of internal parts, this group should be included in any contact definition with shoulder belts.

## Output

Table 23.6: Q1 output signals

| Sensor | Identifier | Signal | | | | | | | Filter |
|---|---|---|---|---|---|---|---|---|---|
| | | resul-tant | x | direc-tion[a] | y | direc-tion[a] | z | direc-tion[a] | |
| Head | | | | | | | | | |
| CG accelero-meter[b] | Head_CFC1000_acc | ar | a1 | forward | a2 | lateral | a3 | vertical | CFC1000 |
| Neck | | | | | | | | | |
| Upper load cell | NeckUpLC_CFC600_lce_F<br>NeckUpLC_CFC600_lce_T | fr<br>tr | f1<br>t1 | shear<br>roll | f2<br>t2 | shear<br>pitch | f3<br>t3 | axial<br>yaw | CFC600<br>CFC600 |
| Thorax | | | | | | | | | |
| Accelero-meter[b] | Thorax_CFC1000_acc<br>Thorax_CFC180_acc | ar | a1 | forward | a2 | lateral | a3 | vertical | CFC1000<br>CFC180 |
| deflection | | | | | | | | | |
| Sternum | ChestDefFront_CFC180_Dis<br>ChestDefFront_CFC600_Dis | | d1 | displace-ment | | | | | CFC180<br>CFC600 |
| Left Lateral | ChestDefLatL_CFC180_Dis<br>ChestDefLatL_CFC600_Dis | | d1 | displace-ment | | | | | CFC180<br>CFC600 |
| Right Lateral | ChestDefLatR_CFC180_Dis<br>ChestDefLatR_CFC600_Dis | | d1 | displace-ment | | | | | CFC180<br>CFC600 |
| Lumbar Spine | | | | | | | | | |
| Lower load cell | LumbarLowLC_CFC600_lce_F<br>LumbarLowLC_CFC600_lce_T | fr<br>tr | f1<br>t1 | shear<br>roll | f2<br>t2 | shear<br>pitch | f3<br>t3 | axial<br>yaw | CFC600<br>CFC600 |
| Pelvis | | | | | | | | | |
| Accelero-meter[b] | Pelvis_CFC1000_acc | ar | a1 | forward | a2 | lateral | a3 | vertical | CFC1000 |

[a] Positive direction given according to SAE J211/1.
[b] The calculated acceleration is corrected in the x, y and z direction for a prescribed fictitious acceleration field to get correct values (see Theory manual).



In Table 23.7 all predefined injury criteria for the Q1 model are listed.

Table 23.7: Predefined injury criteria for the Q1 model.

| Component | Injury criteria | Filter |
|---|---|---|
| Head | HIC15_inj<br>HIC36_inj<br>Head_CFC1000_AccR_3MS_inj<br>Head_CFC1000_AccR_peak_inj | CFC1000<br>CFC1000<br>CFC1000<br>CFC1000 |
| Neck | NeckUp_CFC600_My_peak_inj<br>NeckUp_CFC600_Tension_peak_inj | CFC600<br>CFC600 |

*Continued on the next page*

*Table 23.7 cont.*

| Component | Injury criteria | Filter |
|---|---|---|
| Thorax | Thorax_CFC1000_AccR_3MS_inj | CFC1000 |
| | Thorax_CFC1000_AccR_peak_inj | CFC1000 |
| | Thorax_CFC1000_AccZabs_3MS_inj | CFC1000 |
| | Thorax_CFC180_AccR_3MS_inj | CFC180 |
| | Thorax_CFC180_AccR_peak_inj | CFC180 |
| | Thorax_CFC180_AccZabs_3MS_inj | CFC180 |
| | ChestDefFront_CFC180_peak_inj | CFC180 |
| | ChestDefFront_CFC600_peak_inj | CFC600 |
| | ChestDefLatL_CFC180_peak_inj | CFC180 |
| | ChestDefLatL_CFC600_peak_inj | CFC600 |
| | ChestDefLatR_CFC180_peak_inj | CFC180 |
| | ChestDefLatR_CFC600_peak_inj | CFC600 |
| Pelvis | Pelvis_CFC1000_AccR_3MS_inj | CFC1000 |
| | Pelvis_CFC1000_AccR_peak_inj | CFC1000 |

In addition to the output signals and injury criteria given in Table 23.6 and Table 23.7, the head containment criterion can be best verified by the user in a simulation where the boundary planes are modelled and included in a contact definition with the dummy head.

# 24 Q1.5 Child Dummy

In 1993, an ad-hoc child dummy working group, consisting of CRS manufacturers, research institutes and test-houses in Europe started the development of the Q-series of child dummies as successor to the P-series. The 1.5-year-old version, is now available for use in i-Size child restraint assessments. The model has been developed based on Q1 MADYMO dummy model being scaled up to size and mass of the Q1.5 dummy (based on anthropometrical scaling rules and hardware measurements).

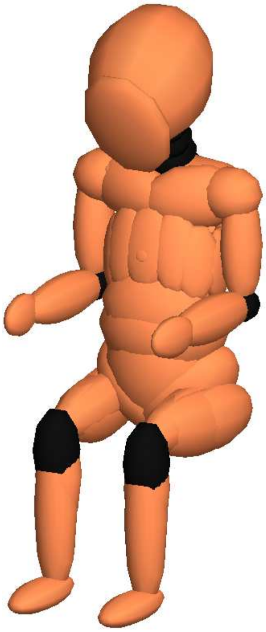

Figure 24.1: Ellipsoid model of the Q1.5 child dummy.

## 24.1 Model description

An ellipsoid model of the Q1.5 child dummy is available. The input is given in the files:

| | |
|---|---|
| Ellipsoid model: | d_q32yel_usr.xml<br>d_q32yel_inc.xml |

To run the model, the following licenses are required:

| | |
|---|---|
| Ellipsoid model: | MADYMO/Solver (Multibody)<br>MADYMO/Dummy Models/Q Child 1.5 Fc |

Figure 24.1 shows the Q1.5 model in the reference position. The model consists of 68 bodies.

**ELLIPSOID MODEL**

**Head**

The head is connected to the upper neck load cell by a bracket joint. The head geometry is described by two ellipsoids, one for the head and one for the face.

**Neck**

The neck is modelled with a triple-joint restraint, applied to a cylindrical joint with a universal joint either side. The outer surface of the neck segment is described by five ellipsoids, which define the contact group.

**Shoulders and Clavicles**

The shoulder and clavicle area is a flexible assembly connecting the arms to the spinebox and providing a load path to the ribcage. The motion of the shoulder relative to the spinebox is modelled in the MADYMO model with a translational joint, and the flexibility of the clavicle piece from the shoulder to the sternum attachment is modelled with a revolute-translational joint on each side. Each wing of the clavicles is attached to the sternum by a point restraint.

**Ribcage**

The ribcage of the Q1.5 consists of a thin flexible shell. It can deform under both lateral and frontal loading. To implement such properties, the Q1.5 ribcage model is comprised of five bodies on each side, joined at the front by a body for the sternum, and at rear the spinebox. The ribs are joined by revolute joints, creating a flexible loop representing the ribcage. Joint restraints determine the bending stiffness, and point and Cardan restraints are used to connect the frontmost rib bodies to the sternum. The bending and contact stiffness characteristics were calculated from thorax validation tests.

24

**Lumbar Spine and Abdomen**

As with the neck, the lumbar spine is represented by a triple-joint restraint, with a bracket joint used to measure forces and moments in the lower lumbar load cell. The abdomen consists of three ellipsoids, the upper and middle abdomen transferring load to the lumbar and the lower to the pelvis.

### Pelvis

Four ellipsoids characterise the contact surfaces of the pelvis: two representing the lower and rear pelvis that come into contact with a child seat, and two representing the pelvis wings for belt contact and side impact analyses.

## CONTACTS BETWEEN DUMMY COMPONENTS

Contacts are defined between the head and the thorax; the head and the legs; the thorax and arms; the abdomen and arms; the left and right arms; the left and right legs.

## 24.2 Model validation

The dummy model was developed and validated using component tests and tests on the complete dummy.

### Component tests

The component tests used for development and validation of the models are summarised in Table 24.1.

Table 24.1: Component tests for Q1.5 child dummy model.

| Component | Test description | specifications | | Model Ellipsoid |
|---|---|---|---|---|
| Head | Head frontal drop test | Starting height | 0.13 m | x |
| | Head lateral drop test | Starting height | 0.13 m | x |
| Neck | Forward bending pendulum | Velocity | 3.9m/s | x |
| | Lateral bending pendulum | Velocity | 3.9m/s | x |
| Lumbar | Forward bending pendulum | Velocity | 4.4m/s | x |
| | Lateral bending pendulum | Velocity | 4.4m/s | x |
| Thorax | Frontal pendulum test | Velocity | 4.3 m/s | x |
| | Lateral pendulum test | Velocity | 4.3 m/s | x |

### Full dummy tests

The full dummy tests used for the development and the validation are summarised in Table 24.2.

Table 24.2: Full dummy tests for Q1.5 dummy model.

| Test Description | Specifications | | Model Ellipsoid |
|---|---|---|---|
| Frontal CRS sled test | Velocity | 60 km/h, 53 km/h, 47 km/h | x |
| Lateral CRS sled test | Velocity | 50 km/h | x |

24

## 24.3 User instructions

### Timestep

Table 24.3: Recommended timestep for the Q1.5 dummy model.

| Model | timestep (s) |
|---|---|
| Ellipsoid | $\leq 1.0 \cdot 10^{-5}$ |

### Dummy positioning

Table 24.4: Positioning joints of the Q1.5 dummy model.

| Joint Description | Identifier | Degree of freedom[(a)] | | | | | | Comment |
|---|---|---|---|---|---|---|---|---|
| Complete dummy | Dummy_jnt | R1<br>D1 | roll right<br>forward | R2<br>D2 | pitch down<br>leftward | R3<br>D3 | yaw left<br>upward | |
| Neck element | NeckUp_jnt<br>NeckMid_jnt<br>NeckLow_jnt | R1<br>D1<br>R1 | roll right<br>upward<br>pitch up | R2<br>R1<br>R2 | pitch up<br>yaw left<br>roll right | | | only for equilibrium state |
| Left shoulder | ShoulderL_jnt | R1 | roll right | R2 | pitch down | R3 | yaw left | |
| Right shoulder | ShoulderR_jnt | R1 | roll right | R2 | pitch down | R3 | yaw left | |
| Left elbow | ElbowL_jnt | R1 | pitch down | | | | | |
| Right elbow | ElbowR_jnt | R1 | pitch down | | | | | |
| Lumbar Spine element | LumbarSpineUp_jnt<br>LumbarSpineMid_jnt<br>LumbarSpineLow_jnt | R1<br>D1<br>R1 | roll right<br>upward<br>pitch up | R2<br>R1<br>R2 | pitch up<br>yaw left<br>roll right | | | only for equilibrium state |
| Left hip | HipL_jnt | R1 | roll right | R2 | pitch down | R3 | yaw left | |
| Right hip | HipR_jnt | R1 | roll right | R2 | pitch down | R3 | yaw left | |
| Left knee | KneeL_jnt | R1 | pitch down | | | | | |
| Right knee | KneeR_jnt | R1 | pitch down | | | | | |

[(a)] Positive translation or rotation given in global co-ordinate system while dummy is in reference position

24

### Dummy contacts

Table 24.5 describes the Q1.5 contact groups available in the model and recommended for the definition of contacts between the dummy and the environment, in a CRS application. In addition, a Dummy_gmb contact group is available wherein all contact surfaces (those for which a characteristic is defined) are included. The Dummy_gmb group has not been used for dummy model calibration or validation.

Table 24.5: Available groups to define contact between the Q1.5 components and environment.

| **Contact Description** | **Identifier**[a],[b] | **Ellipsoid model**[b] |
|---|---|---|
| Head | Head_gmb | Head_ell<br>Face_ell |
| Neck | Neck_gmb | NeckUpperDisk_ell<br>NeckLowerDisk_ell<br>NeckUp_ell |
| Shoulders | SuitShoulder_gmb | SuitBackL_ell<br>SuitBackR_ell<br>SuitFrontL_ell<br>SuitFrontR_ell<br>SuitFrontSideL_ell<br>SuitFrontSideR_ell |
| Left upper arm | ArmUpL_gmb | ArmUpL_ell<br>ElbowL_ell<br>ShoulderL_ell |
| Left lower arm | ArmLowL_gmb | ArmLowL_ell<br>HandL_ell |
| Right upper arm | ArmUpR_gmb | ArmUpR_ell<br>ElbowR_ell<br>ShoulderR_ell |
| Right lower arm | ArmLowR_gmb | ArmLowR_ell<br>HandR_ell |
| Clavicles | Clavicles_gmb[c] | ClaviclePart(1-4)L/R_ell |
| Ribcage | Ribcage_gmb | Rib(1-5)L/R_ell<br>Sternum_ell |
| Back | Back_gmb | ThoracicSpineNeck_ell<br>ThoracicSpineBody_ell |
| Abdomen | Abdomen_gmb | AbdomenUp_ell<br>AbdomenMid_ell<br>AbdomenLow_ell |
| Pelvis | Pelvis_gmb | Pelvis_ell<br>PelvisBack_ell<br>PelvisSideL/R_ell |
| Left upper leg | LegUpL_gmb | LegUpPart(1-3)L_ell |
| Right upper leg | LegUpR_gmb | LegUpPart(1-3)R_ell |
| Left lower leg | LegLowL_gmb | KneeL_ell<br>LegLowPart(1-2)L_ell<br>FootL_ell |

*Continued on the next page*

*Table 24.5 cont.*

| Contact Description | Identifier[a],[b] | Ellipsoid model[b] |
|---|---|---|
| Right lower leg | LegLowR_gmb | KneeR_ell<br>LegLowPart(1-2)R_ell<br>FootR_ell |

[a] gmb=group_multibody.
[b] L=Left; R=Right.
[c] although composed of internal parts, this group should be included in any contact definition with shoulder belts.

24

## Output

Table 24.6: Q1.5 output signals

| Sensor | Identifier | Signal | | | | | | | Filter |
|---|---|---|---|---|---|---|---|---|---|
| | | resul-tant | x | direc-tion[a] | y | direc-tion[a] | z | direc-tion[a] | |
| Head | | | | | | | | | |
| CG accelero-meter[b] | Head_CFC1000_acc | ar | a1 | forward | a2 | lateral | a3 | vertical | CFC1000 |
| Neck | | | | | | | | | |
| Upper load cell | NeckUpLC_CFC600_lce_F | fr | f1 | shear | f2 | shear | f3 | axial | CFC600 |
| | NeckUpLC_CFC600_lce_T | tr | t1 | roll | t2 | pitch | t3 | yaw | CFC600 |
| Thorax | | | | | | | | | |
| Accelero-meter[b] | Thorax_CFC1000_acc | ar | a1 | forward | a2 | lateral | a3 | vertical | CFC1000 |
| | Thorax_CFC180_acc | | | | | | | | CFC180 |
| deflection | | | | | | | | | |
| Sternum | ChestDefFront_CFC180_Dis | | d1 | displace-ment | | | | | CFC180 |
| | ChestDefFront_CFC600_Dis | | | | | | | | CFC600 |
| Left Lateral | ChestDefLatL_CFC180_Dis | | d1 | displace-ment | | | | | CFC180 |
| | ChestDefLatL_CFC600_Dis | | | | | | | | CFC600 |
| Right Lateral | ChestDefLatR_CFC180_Dis | | d1 | displace-ment | | | | | CFC180 |
| | ChestDefLatR_CFC600_Dis | | | | | | | | CFC600 |
| Lumbar Spine | | | | | | | | | |
| Lower load cell | LumbarLowLC_CFC600_lce_F | fr | f1 | shear | f2 | shear | f3 | axial | CFC600 |
| | LumbarLowLC_CFC600_lce_T | tr | t1 | roll | t2 | pitch | t3 | yaw | CFC600 |
| Pelvis | | | | | | | | | |
| Accelero-meter[b] | Pelvis_CFC1000_acc | ar | a1 | forward | a2 | lateral | a3 | vertical | CFC1000 |

[a] Positive direction given according to SAE J211/1.
[b] The calculated acceleration is corrected in the x, y and z direction for a prescribed fictitious acceleration field to get correct values (see Theory manual).

In Table 24.7 all predefined injury criteria for the Q1.5 model are listed.



Table 24.7: Predefined injury criteria for the Q1.5 model.

| Component | Injury criteria | Filter |
|---|---|---|
| Head | HIC15_inj | CFC1000 |
| | HIC36_inj | CFC1000 |
| | Head_CFC1000_AccR_3MS_inj | CFC1000 |
| | Head_CFC1000_AccR_peak_inj | CFC1000 |
| Neck | NeckUp_CFC600_My_peak_inj | CFC600 |
| | NeckUp_CFC600_Tension_peak_inj | CFC600 |

*Continued on the next page*

*Table 24.7 cont.*

| Component | Injury criteria | Filter |
|---|---|---|
| Thorax | Thorax_CFC1000_AccR_3MS_inj | CFC1000 |
| | Thorax_CFC1000_AccR_peak_inj | CFC1000 |
| | Thorax_CFC1000_AccZabs_3MS_inj | CFC1000 |
| | Thorax_CFC180_AccR_3MS_inj | CFC180 |
| | Thorax_CFC180_AccR_peak_inj | CFC180 |
| | Thorax_CFC180_AccZabs_3MS_inj | CFC180 |
| | ChestDefFront_CFC180_peak_inj | CFC180 |
| | ChestDefFront_CFC600_peak_inj | CFC600 |
| | ChestDefLatL_CFC180_peak_inj | CFC180 |
| | ChestDefLatL_CFC600_peak_inj | CFC600 |
| | ChestDefLatR_CFC180_peak_inj | CFC180 |
| | ChestDefLatR_CFC600_peak_inj | CFC600 |
| Pelvis | Pelvis_CFC1000_AccR_3MS_inj | CFC1000 |
| | Pelvis_CFC1000_AccR_peak_inj | CFC1000 |

In addition to the output signals and injury criteria given in Table 24.6 and Table 24.7, the head containment criterion can be best verified by the user in a simulation where the boundary planes are modelled and included in a contact definition with the dummy head.

# 25 Q3 Child Dummy

In 1993, an ad-hoc child dummy working group, consisting of CRS manufacturers, research institutes and test-houses in Europe started the development of the Q-series of child dummies as successor to the P-series. The 3-year-old version, Q3, is the first dummy of the Q-series. The MADYMO dummy model architecture is mostly based on that of the Q6, and the detailed geometry was created from 3D-scan output and technical drawings.

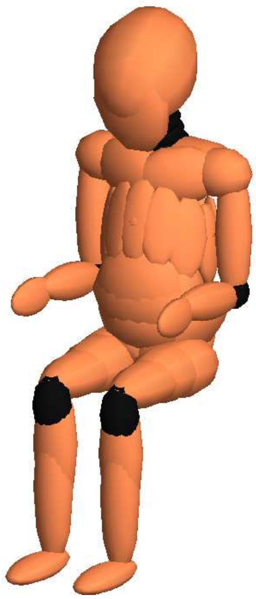

Figure 25.1: Ellipsoid model of the Q3 child dummy.

## 25.1 Model description

An ellipsoid model of the Q3 child dummy is available. The input is given in the files:

| | |
|---|---|
| Ellipsoid model: | d_q03yel_usr.xml |
| | d_q03yel_inc.xml |

To run the model, the following licenses are required:

| | |
|---|---|
| Ellipsoid model: | MADYMO/Solver (Multibody) |
| | MADYMO/Dummy Models/Q Child 3.0 Fc |

Figure 25.1 shows the Q3 model in the reference position. The model consist of 72 bodies.

**ELLIPSOID MODEL**

**Head**

The head geometry is described by two ellipsoids, one for the head and one for the face. The contact properties of the head ellipsoids have been obtained from head drop tests. The head is connected to the upper neck load cell by a bracket joint.

**Neck**

The neck is modelled with a succession of 4 joints: translational, universal, spherical and universal again, from the bottom to the top of the neck. They allow forward and lateral bending of the neck over 3 rotation points, as well as torsion and compression/extension.

**Shoulders and Clavicles**

The shoulder and clavicle area is a flexible assembly connecting the arms to the spinebox and providing a load path to the ribcage. The motion of the shoulder relative to the spinebox is modelled in the MADYMO model with a translational joint, and the flexibility of the clavicle piece from the shoulder to the sternum attachment is modelled with a revolute-translational joint on each side. Each wing of the clavicles is attached to the sternum by a point restraint.

**Ribcage**

The ribcage of the Q3 consists of a thin flexible shell. It can deform under both lateral and frontal loading. To implement such properties, the Q3 ribcage model is comprised of five bodies on each side, joined at the front by a body for the sternum, and at rear the spinebox. The ribs are joined by revolute joints, creating a flexible loop representing the ribcage. Joint restraints determine the bending stiffness, and point and Cardan restraints are used to connect the frontmost rib bodies to the sternum. The bending and contact stiffness characteristics were calculated from thorax validation tests.



**Lumbar Spine and Abdomen**

The lumbar spine is modelled with a triple-joint restraint, applied to a cylindrical joint with a universal joint either side. It is connected to the thoracic spine by a bracket joint. Between the lumbar spine and the pelvis another bracket joint is used to model the lower lumbar load cell. The abdomen consists of four ellipsoids, the upper, middle and back abdomen ellipsoids transfer loads to the lumbar spine and the lower abdomen ellipsoid transfers loads to the pelvis.

### Pelvis

Four ellipsoids characterise the contact surfaces of the pelvis: two representing the lower and rear pelvis that come into contact with a child seat, and two representing the pelvis wings for belt contact and side impact analyses.

## CONTACTS BETWEEN DUMMY COMPONENTS

Contacts are defined between the head and the thorax; the head and the legs; the arms and the legs; the thorax and the arms; the abdomen and the arms; the left and right arms; the left and right legs.

## 25.2 Model validation

The dummy model was developed and validated using component tests and tests on the complete dummy.

### Component tests

The component tests used for development and validation of the models are summarised in Table 25.1.

Table 25.1: Component tests for Q3 child dummy model.

| Component | Test Description | Specifications | | Model Ellipsoid |
|---|---|---|---|---|
| Head | Head frontal drop test | Height, angle | 0.130m, 28° | x |
| | Head lateral drop test | Height, angle | 0.130m, 35° | x |
| Neck | Pendulum test, frontal | Velocity | 3.9m/s, 2.7m/s, 5.4m/s | x |
| | Pendulum test, lateral | Velocity | 3.9m/s, 2.6m/s, 5.5m/s | x |
| Lumbar Spine | Pendulum test, frontal | Velocity | 4.4m/s, 3.5m/s, 5.5m/s | x |
| | Pendulum test, lateral | Velocity | 4.4m/s, 3.6m/s, 5.5m/s | x |
| Thorax | Impactor test, frontal | Velocity | 4.3 m/s, 4.2m/s, 3.0m/s | x |
| | Impactor test, lateral | Velocity | 4.3 m/s, 4.2m/s, 3.1m/s | x |

### Full dummy tests

The full dummy tests used for the development and the validation are summarised in Table 25.2.

Table 25.2: Full tests for Q3 child dummy model.

| Test Description | Specifications | | Model Ellipsoid |
|---|---|---|---|
| Frontal sled test | Velocity | 50km/h | x |
| Frontal CRS sled test | Velocity | 40km/h, 50km/h | x |
| Lateral CRS sled test with door impact | Velocity | 25km/h | x |
| Lateral CRS sled test | Velocity | 41km/h | x |

## 25.3 User instructions

### Timestep

Table 25.3: Recommended timestep for the Q3 dummy model.

| Model | timestep (s) |
|---|---|
| Ellipsoid | $\leq 1.0 \cdot 10^{-5}$ |

### Dummy positioning

Table 25.4: Positioning joints of the Q3 model.

| Joint Description | Identifier | Degree of freedom[a] | | | | | | Comment |
|---|---|---|---|---|---|---|---|---|
| Complete dummy | Dummy_jnt | R1 | roll right | R2 | pitch down | R3 | yaw left | |
| | | D1 | forward | D2 | leftward | D3 | upward | |
| Neck element | NeckUp_jnt | R1 | roll right | R2 | pitch up | | | only for equilibrium state |
| | NeckMid_jnt | R1 | yaw left | R2 | pitch up | R3 | roll right | |
| | NeckLow_jnt | R1 | pitch up | R2 | roll right | | | |
| | NeckTran_jnt | D1 | upward | | | | | |
| Left shoulder | ShoulderL_jnt | R1 | roll right | R2 | pitch down | R3 | yaw left | |
| Right shoulder | ShoulderR_jnt | R1 | roll right | R2 | pitch down | R3 | yaw left | |
| Left elbow | ElbowL_jnt | R1 | pitch down | | | | | |
| Right elbow | ElbowR_jnt | R1 | pitch down | | | | | |
| Lumbar Spine element | LumbarSpineUp_jnt | R1 | roll right | R2 | pitch up | | | only for equilibrium state |
| | LumbarSpineMid_jnt | D1 | upward | R1 | yaw left | | | |
| | LumbarSpineLow_jnt | R1 | pitch up | R2 | roll right | | | |
| Left hip | HipL_jnt | R1 | roll right | R2 | pitch down | R3 | yaw left | |
| Right hip | HipR_jnt | R1 | roll right | R2 | pitch down | R3 | yaw left | |
| Left knee | KneeL_jnt | R1 | pitch down | | | | | |
| Right knee | KneeR_jnt | R1 | pitch down | | | | | |

[a] Positive translation or rotation given in global co-ordinate system while dummy is in reference position.

### Dummy contacts

Table 25.5 below describes the Q3 contact groups available in the model and recommended for the definition of contacts between the dummy and the environment, in a CRS application. In addition, a Dummy_gmb contact group is available wherein all contact surfaces (those for which a characteristic is defined) are included. The Dummy_gmb group has not been used for dummy model calibration or validation.

Table 25.5: Pre-defined Q3 dummy contact groups.

| Contact Description | Identifier[(a)],[(b)] | Ellipsoid model[(b)] |
|---|---|---|
| Head | Head_gmb | Head_ell<br>Face_ell |
| Neck | Neck_gmb | NeckLowDisk_ell<br>NeckLow_ell<br>NeckLowerDisk_ell<br>NeckUp_ell<br>NeckUpperDisk_ell |
| Lower Neck LC | NeckLowLC_gmb | NeckLowLCbody_ell<br>NeckLowLCtop_ell |
| Back | Back_gmb | ThoracicSpineBracket_ell<br>ThoracicSpineBody_ell<br>ThoracicSpineNeck_ell |
| Ribcage | Ribcage_gmb | Rib(1-5)L/R_ell<br>Sternum_ell |
| Clavicles | Clavicles_gmb[(c)] | ClaviclePart(1-4)L/R_ell |
| Left upper arm | ArmUpL_gmb | ArmUpL_ell<br>ElbowL_ell<br>ShoulderL_ell |
| Left lower arm | ArmLowL_gmb | ArmLowL_ell<br>HandL_ell |
| Right upper arm | ArmUpR_gmb | ArmUpR_ell<br>ElbowR_ell<br>ShoulderR_ell |
| Right lower arm | ArmLowR_gmb | ArmLowR_ell<br>HandR_ell |
| Lumbar Spine | Lumbarspine_gmb | LumbarSpineBracketUp_ell<br>LumbarSpineLow_ell<br>LumbarSpineLowerDisk_ell<br>LumbarSpineUp_ell<br>LumbarSpineUpperDisk_ell |
| Pelvis | Pelvis_gmb | PelvisSideL/R_ell<br>Pelvis_ell<br>PelvisBack_ell |

*Continued on the next page*

*Table 25.5 cont.*

| Contact Description | Identifier[(a)],[(b)] | Ellipsoid model[(b)] |
|---|---|---|
| Abdomen | Abdomen_gmb | AbdomenLow_ell<br>AbdomenMid_ell<br>AbdomenUp_ell<br>AbdomenBack_ell |
| Left upper leg | LegUpL_gmb | LegUpPart(1-3)L_ell |
| Right upper leg | LegUpR_gmb | LegUpPart(1-3)R_ell |
| Left lower leg | LegLowL_gmb | KneeL_ell<br>LegLowPart(1-2)L_ell<br>FootL_ell |
| Right lower leg | LegLowR_gmb | KneeR_ell<br>LegLowPart(1-2)R_ell<br>FootR_ell |
| Upper Torso | SuitShoulder_gmb | SuitBackL/R_ell<br>SuitFrontL/R_ell<br>SuitFrontSideL/R_ell |

[(a)] gmb=group_multibody.
[(b)] L=Left; R=Right.
[(c)] although composed of internal parts, this group should be included in any contact definition with shoulder belts.

25

## Output

Below in Table 25.6 all available Q3 child dummy output signals are shown. ISO-MME output can also be generated for the Q3 child dummy. Output requests for signals in ISO-MME format are pre-defined in the CONTROL_OUTPUT element in the user file.

Table 25.6: Q3 output signals

| Sensor | Identifier | Signal | | | | | | | Filter |
|---|---|---|---|---|---|---|---|---|---|
| | | resultant | x | direction[a] | y | direction[a] | z | direction[a] | |
| Head | | | | | | | | | |
| CG accelerometer[b] | Head_CFC1000_acc | ar | a1 | forward | a2 | lateral | a3 | vertical | CFC1000 |
| Neck | | | | | | | | | |
| Upper LC | NeckUpLC_CFC600_lce_F | fr | f1 | shear | f2 | shear | f3 | axial | CFC600 |
| | NeckUpLC_CFC600_lce_T | tr | t1 | roll | t2 | pitch | t3 | yaw | CFC600 |
| Lower LC | NeckLowLC_CFC600_lce_F | fr | f1 | shear | f2 | shear | f3 | axial | CFC600 |
| | NeckLowLC_CFC600_lce_T | tr | t1 | roll | t2 | pitch | t3 | yaw | CFC600 |
| Thorax | | | | | | | | | |
| Accelerometer[b] | Thorax_CFC1000_acc | ar | a1 | forward | a2 | lateral | a3 | vertical | CFC1000 |
| | Thorax_CFC180_acc | ar | a1 | forward | a2 | lateral | a3 | vertical | CFC180 |
| Chest deflection | ChestDefFront_CFC600_Dis | | d1 | frontal | | | | | CFC600 |
| | ChestDefFront_CFC180_Dis | | d1 | frontal | | | | | CFC180 |
| | ChestDefLatL_CFC600_Dis | | d1 | lateral | | | | | CFC600 |
| | ChestDefLatL_CFC180_Dis | | d1 | lateral | | | | | CFC180 |
| | ChestDefLatR_CFC600_Dis | | d1 | lateral | | | | | CFC600 |
| | ChestDefLatR_CFC180_Dis | | d1 | lateral | | | | | CFC180 |
| Lumbar Spine | | | | | | | | | |
| Lower LC | LumbarLowLC_CFC600_lce_F | fr | f1 | shear | f2 | shear | f3 | axial | CFC600 |
| | LumbarLowLC_CFC600_lce_T | tr | t1 | roll | t2 | pitch | t3 | yaw | CFC600 |
| Pelvis | | | | | | | | | |
| Accelerometer[b] | Pelvis_CFC1000_acc | ar | a1 | forward | a2 | lateral | a3 | vertical | CFC1000 |

[a] Positive direction given according to SAE J211/1.
[b] The calculated acceleration is corrected in the x, y and z direction for a prescribed fictitious acceleration field to get correct values (see Theory manual).

In Table 25.7 all predefined injury criteria for the Q3 model are listed.

Table 25.7: Predefined injury criteria for the Q3 model.

| Component | Injury criteria | Filter |
|---|---|---|
| Head | HIC15_inj | CFC1000 |
| | HIC36_inj | CFC1000 |
| | Head_CFC1000_AccR_3MS_inj | CFC1000 |
| | Head_CFC1000_AccR_peak_inj | CFC1000 |

*Continued on the next page*

*Table 25.7 cont.*

| Component | Injury criteria | Filter |
|---|---|---|
| Neck | NeckUp_CFC600_My_peak_inj | CFC600 |
| | NeckUp_CFC600_Tension_peak_inj | CFC600 |
| Thorax | Thorax_CFC1000_AccR_3MS_inj | CFC1000 |
| | Thorax_CFC1000_AccR_peak_inj | CFC1000 |
| | Thorax_CFC1000_AccZabs_3MS_inj | CFC1000 |
| | Thorax_CFC180_AccR_3MS_inj | CFC180 |
| | Thorax_CFC180_AccR_peak_inj | CFC180 |
| | Thorax_CFC180_AccZabs_3MS_inj | CFC180 |
| | ChestDefFront_CFC180_peak_inj | CFC180 |
| | ChestDefFront_CFC600_peak_inj | CFC600 |
| | ChestDefLatL_CFC180_peak_inj | CFC180 |
| | ChestDefLatL_CFC600_peak_inj | CFC600 |
| | ChestDefLatR_CFC180_peak_inj | CFC180 |
| | ChestDefLatR_CFC600_peak_inj | CFC600 |
| Pelvis | Pelvis_CFC1000_AccR_3MS_inj | CFC1000 |
| | Pelvis_CFC1000_AccR_peak_inj | CFC1000 |

In addition to the output signals and injury criteria given in Table 25.6 and Table 25.7, the head containment criterion can be best verified by the user in a simulation where the boundary planes are modelled and included in a contact definition with the dummy head.

25

# 26 Q6 Child Dummy

The Q6 dummy is expected to be introduced into the EuroNCAP test protocol in 2015. TASS developed therefore an ellipsoid Q (Quality) version of the Q6 child dummy to answer the need for a fast, robust and well-validated model.

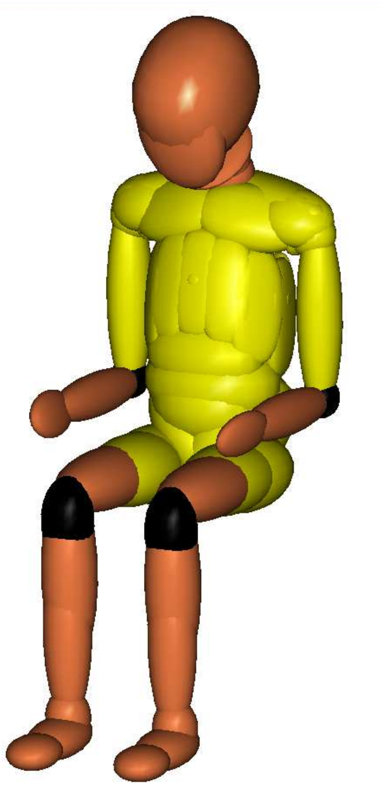

Figure 26.1: The Q6 ellipsoid child dummy model

The quality of the model, in terms of response correlation with validation test signals, has been determined by an objective rating method. For more information on this subject, the user is referred to the model quality report.

## 26.1 Model description

A quality rated ellipsoid model of the Q6 child dummy is available. The input is given in the files:

| | |
|---|---|
| Ellipsoid model: | d_q06yel_usr.xml<br>d_q06yel_inc.xml |

To run this model, the following licenses are required:

| | |
|---|---|
| Ellipsoid model: | MADYMO/Solver (Multibody)<br>MADYMO/Dummy Models/Child |

Figure 26.1 shows the Q6 ellipsoid model in the reference position.

**ELLIPSOID MODEL**

The geometry is represented by higher order ellipsoids that cover perfectly the 3D laser scan the hardware dummy. Masses, centres of gravity and moments of inertia were applied or calculated on the basis of hardware component mass measurements and 3D CAD drawings.

**Head**

The head is represented by two ellipsoids that cover the hardware geometry well enough to model contact with the environment in an accurate way. The contact properties of the head ellipsoids have been obtained from the head certification tests.

**Neck**

The neck of the Q6 is modelled using one triple joint (succession of one universal, one cylindral and another universal joint) completed by a triple joint restraint.

**Thorax**

The ribcage deformation is modelled thanks to a succession of revolute joints. Compression and bending of the ribcage in both frontal and lateral directions is therefore possible. The clavicle is also modelled as a flexible component for a good model performance and kinematics. The contact characteristics and bending stiffnesses of the ribcage have been obtained from the thorax certification tests and rigid sled tests with belt interaction.



**Lumbar spine**

The lumbar spine is, like the neck, modelled using one triple joint completed by a triple joint restraint.

**Pelvis and Abdomen**

The abdomen and pelvis are connected to each other. Part of the load on the abdomen is also transfered to the lumbar spine. The contact characteristics of the abdomen are obtained from impact tests.

**Arms and Legs**

Each arm is modelled using three bodies: upper arm, lower arm and hand. The motion of the elbow is modelled with a revolute joint; although there is no other mechanical joint present in the lower arm of the hardware dummy, the model uses a spherical joint to model the possible deformation of the wrist. Each leg is modelled using four bodies: upper leg, lower leg, foot and toes. The motion of the knee is modelled with a revolute joint; although there is no other mechanical joint present in the lower leg of the hardware dummy, the model uses spherical joints to model the possible deformations of the ankle and the foot. The arms resp. legs are connected to the thorax resp. pelvis with spherical joints.

## 26.2 User instructions

### Timestep

Table 26.1: Recommended timestep for the Q6 ellipsoid model.

| Model | timestep (s) |
|---|---|
| Ellipsoid | $\leq 1.0 \cdot 10^{-5}$ |

### Dummy positioning

Table 26.2: Positioning joints for the Q6 model.

| Joint Description | Identifier | Degree of freedom[a] | | | | | |
|---|---|---|---|---|---|---|---|
| Complete dummy | Dummy_jnt | D1 | forward | D2 | leftward | D3 | upward |
| | | R1 | roll right | R2 | pitch down | R3 | yaw left |
| Neck Up[b] | NeckUp_jnt | R1 | roll right | R2 | pitch up | | |
| Neck Mid[b] | NeckMid_jnt | D1 | upward | | | | |
| | | R1 | yaw left | | | | |
| Neck Low[b] | NeckLow_jnt | R1 | pitch up | R2 | roll right | | |
| Left Shoulder | ShoulderL_jnt | R1 | roll right | R2 | pitch down | R3 | yaw left |
| Right Shoulder | ShoulderR_jnt | R1 | roll right | R2 | pitch down | R3 | yaw left |
| Left Elbow | ElbowL_jnt | R1 | pitch down | | | | |
| Right Elbow | ElbowR_jnt | R1 | pitch down | | | | |
| Lumbar Up[b] | LumbarSpineUp_jnt | R1 | roll right | R2 | pitch up | | |
| Lumbar Mid[b] | LumbarSpineMid_jnt | D1 | upward | | | | |
| | | R1 | yaw left | | | | |
| Lumbar Low[b] | LumbarSpineLow_jnt | R1 | pitch up | R2 | roll right | | |
| Left hip | HipL_jnt | R1 | roll right | R2 | pitch down | R3 | yaw left |
| Right hip | HipR_jnt | R1 | roll right | R2 | pitch down | R3 | yaw left |
| Left knee | KneeL_jnt | R1 | pitch down | | | | |
| Right knee | KneeR_jnt | R1 | pitch down | | | | |

[a] Positive translation or rotation given in global coordinate system, with dummy in reference position (see Figure 26.1).
[b] ONLY FOR EQUILIBRIUM

26

### Dummy contacts

When defining contacts between the dummy model and its environment, only the contact groups defined in Table 26.3 need to be used.

Table 26.3: Predefined groups to define contact between the Q6 model components and their environment.

| Contacting Zone | Dummy Contact Group | For contact with |
|---|---|---|
| Head | Head_gmb | CRS (headrest) |
| Neck | Neck_gmb<br>NeckUpLC_gmb<br>NeckShield_gmb | Shoulder belt<br>Shoulder belt<br>Shoulder belt |
| Thorax | Ribcage_gmb<br>Clavicles_gmb | CRS (sides) and Shoulder belt<br>Shoulder belt |
| Back | Back_gmb<br>Lumbarspine_gmb | CRS (back)<br>CRS (back) |
| Lower Torso | Abdomen_gmb<br>Pelvis_gmb | CRS (sides) and Shoulder belt<br>CRS (seat and sides) and Lap belt |
| Arms | ArmUpL_gmb ArmLowL_gmb<br>ArmUpR_gmb ArmLowR_gmb | CRS (sides)<br>CRS (sides) |
| Legs | LegUpL_gmb LegUpR_gmb<br>LegLowL_gmb LegLowR_gmb | CRS (seat and sides) and Lap belt<br>Car bench |

It is advised to use orthotropic friction in all contacts between dummy and belt. The friction coefficients to use in the first and second direction are 0.3 and 0.7 respectively. Additionally a penetration-dependent multiplication function can be specified in the contact between shoulder belt and neck shield to mimic belt pocketing effects and to prevent the belt to slip off the shoulder.

Inter-component contacts have also been defined as shown in Table 26.4.

Table 26.4: Predefined inter-component contacts

| Contact Name | Master | Slave |
|---|---|---|
| ArmsThorax_cnt | ArmUpL_gmb ArmUpR_gmb | Ribcage_gmb |
| ArmsLegs_cnt | LegUpL_gmb LegUpR_gmb | ArmLowL_gmb ArmLowR_gmb |
| HeadLegs_cnt | Head_gmb | LegLowL_gmb LegLowR_gmb<br>LegUpL_gmb LegUpR_gmb |
| LegLeg_cnt | LegLowL_gmb LegUpL_gmb | LegLowR_gmb LegUpR_gmb |
| ArmsAbdomen_cnt | ArmLowL_gmb ArmLowR_gmb | Abdomen_gmb Pelvis_gmb |
| HeadThorax_cnt | Head_gmb | Clavicles_gmb Ribcage_gmb |



## Output

In Table 26.5 all predefined output definitions for the Q6 ellipsoid model are listed. When a signal is filtered the filter class is included in the name of the signal for more clarity.

Table 26.5: Predefined output signals for the Q6 model.

| **Sensor** | **Identifier** | **Signal** resultant | x | direction[a] | y | direction[a] | z | direction[a] | **Filter** |
|---|---|---|---|---|---|---|---|---|---|
| Head | | | | | | | | | |
| Head acc | Head_CFC1000_acc | ar | a1 | forward | a2 | right | a3 | down | CFC1000 |
| Neck | | | | | | | | | |
| Upper LC | NeckUpLC_CFC600_lce_F | | f1 | shear | f2 | shear | f3 | axial | CFC600 |
| | NeckUpLC_CFC600_lce_T | | t1 | roll | t2 | pitch | t3 | yaw | CFC600 |
| Lower LC | NeckLowLC_CFC600_lce_F | | f1 | shear | f2 | shear | f3 | axial | CFC600 |
| | NeckLowLC_CFC600_lce_T | | t1 | roll | t2 | pitch | t3 | yaw | CFC600 |
| Thorax | | | | | | | | | |
| Thorax acc | Thorax_CFC1000_acc | ar | a1 | forward | a2 | right | a3 | down | CFC1000 |
| | Thorax_CFC180_acc | ar | a1 | forward | a2 | right | a3 | down | CFC180 |
| Chest Deflection | ChestDefFront_CFC600_Dis | | d1 | frontal | | | | | CFC600 |
| | ChestDefFront_CFC180_Dis | | d1 | frontal | | | | | CFC180 |
| | ChestDefLatL_CFC600_Dis | | d1 | lateral | | | | | CFC600 |
| | ChestDefLatL_CFC180_Dis | | d1 | lateral | | | | | CFC180 |
| | ChestDefLatR_CFC600_Dis | | d1 | lateral | | | | | CFC600 |
| | ChestDefLatR_CFC180_Dis | | d1 | lateral | | | | | CFC180 |
| Lumbar | | | | | | | | | |
| Lumbar LC | LumbarLowLC_CFC600_lce_F | | f1 | shear | f2 | shear | f3 | axial | CFC600 |
| | LumbarLowLC_CFC600_lce_T | | t1 | roll | t2 | pitch | t3 | yaw | CFC600 |
| Pelvis | | | | | | | | | |
| Pelvis acc | Pelvis_CFC1000_acc | ar | a1 | forward | a2 | right | a3 | down | CFC1000 |

[a] Positive direction given according to SAE J211/1.

In Table 26.6 all predefined injury criteria for the Q6 model are listed.

Table 26.6: Predefined injury criteria for the Q6 model.

| **Component** | **Injury criteria** | **Filter** |
|---|---|---|
| Head | HIC15_inj | CFC1000 |
| | HIC36_inj | CFC1000 |
| | Head_CFC1000_AccR_3MS_inj | CFC1000 |
| | Head_CFC1000_AccR_peak_inj | CFC1000 |
| Neck | NeckUp_CFC600_My_peak_inj | CFC600 |
| | NeckUp_CFC600_Tension_peak_inj | CFC600 |
| Thorax | Thorax_CFC1000_AccR_3MS_inj | CFC1000 |
| | Thorax_CFC1000_AccR_peak_inj | CFC1000 |
| | Thorax_CFC1000_AccZabs_3MS_inj | CFC1000 |
| | Thorax_CFC180_AccR_3MS_inj | CFC180 |
| | Thorax_CFC180_AccR_peak_inj | CFC180 |
| | Thorax_CFC180_AccZabs_3MS_inj | CFC180 |

*Continued on the next page*

*Table 26.6 cont.*

| Component | Injury criteria | Filter |
|---|---|---|
| | ChestDefFront_CFC180_peak_inj | CFC180 |
| | ChestDefFront_CFC600_peak_inj | CFC600 |
| | ChestDefLatL_CFC180_peak_inj | CFC180 |
| | ChestDefLatL_CFC600_peak_inj | CFC600 |
| | ChestDefLatR_CFC180_peak_inj | CFC180 |
| | ChestDefLatR_CFC600_peak_inj | CFC600 |
| Pelvis | Pelvis_CFC1000_AccR_3MS_inj | CFC1000 |
| | Pelvis_CFC1000_AccR_peak_inj | CFC1000 |

# 27 Q10 Child Dummy

The Q10 dummy will be included into the EuroNCAP test protocol in 2016. TASS International therefore developed an ellipsoid version of the Q10 child dummy to answer the need for a fast, robust and validated model.

Figure 27.1: The Q10 ellipsoid child dummy model

## 27.1 Model description

An ellipsoid model of the Q10 child dummy is available. The input is given in the files:

| | |
|---|---|
| Ellipsoid model: | d_q10yel_usr.xml |
| | d_q10yel_inc.xml |

To run this model, the following licenses are required:

| | |
|---|---|
| Ellipsoid model: | MADYMO/Solver (Multibody) |
| | MADYMO/Dummy Models/Child |

Figure 27.1 shows the Q10 ellipsoid model in the reference position.

**ELLIPSOID MODEL**

The Q10 model design is based on data from CASPER and EPOCh sources and from official Q10 hardware documentation. All dummy model dimensions and masses are in line with the Q10 hardware dummy requirements.

**Head**

The head is represented by two ellipsoids that cover the hardware geometry well enough to model contact with the environment in an accurate way. The contact properties of the head ellipsoids have been obtained from the head certification tests.

**Neck**

The neck of the Q10 is modelled using one triple joint (succession of one universal, one cylindrical and another universal joint) completed by a triple joint restraint.

**Thorax**

The ribcage deformation is modelled using a succession of revolute joints. Compression and bending of the ribcage in both frontal and lateral directions is therefore possible. The ribcage is attached to the spinebox by means of a spherical joint, making it possible for the chest to slightly bend downwards as well. The clavicles are also modelled as flexible components for good performance and kinematics. The contact characteristics and bending stiffnesses of the ribcage have been obtained from thorax certification tests.

**Lumbar spine**

The lumbar spine is, like the neck, modelled using one triple joint completed by a triple joint restraint.



**Pelvis and Abdomen**

The abdomen and pelvis are connected to each other. Part of the load on the abdomen is also transferred to the lumbar spine. The pelvis design was obtained from the WorldSID 50th percentile model.

### Arms and Legs

Each arm is modelled using two bodies (an upper and a lower one), while the femurs are divided into four bodies in order to model the femoral load cells.

The arms resp. legs are connected to the thorax resp. pelvis with spherical joints. The elbow and knee joints are revolute joints.

## 27.2 User instructions

### Timestep

Table 27.1: Recommended timestep for the Q10 ellipsoid model.

| Model | timestep (s) |
|---|---|
| Ellipsoid | $\leq 1.0 \cdot 10^{-5}$ |

### Dummy positioning

Table 27.2: Positioning joints for the Q10 model.

| Joint Description | Identifier | Degree of freedom[a] | | |
|---|---|---|---|---|
| Complete dummy | Dummy_jnt | D1 forward | D2 leftward | D3 upward |
| | | R1 roll right | R2 pitch down | R3 yaw left |
| Neck Up[b] | NeckUp_jnt | R1 roll right | R2 pitch up | |
| Neck Mid[b] | NeckMid_jnt | D1 upward | | |
| | | R1 yaw left | | |
| Neck Low[b] | NeckLow_jnt | R1 pitch up | R2 roll right | |
| Left Shoulder | ShoulderL_jnt | R1 roll right | R2 pitch down | R3 yaw left |
| Right Shoulder | ShoulderR_jnt | R1 roll right | R2 pitch down | R3 yaw left |
| Left Elbow | ElbowL_jnt | R1 pitch down | | |
| Right Elbow | ElbowR_jnt | R1 pitch down | | |
| Lumbar Up[b] | LumbarSpineUp_jnt | R1 roll right | R2 pitch up | |
| Lumbar Mid[b] | LumbarSpineMid_jnt | D1 upward | | |
| | | R1 yaw left | | |
| Lumbar Low[b] | LumbarSpineLow_jnt | R1 pitch up | R2 roll right | |
| Left hip | HipL_jnt | R1 roll right | R2 pitch down | R3 yaw left |
| Right hip | HipR_jnt | R1 roll right | R2 pitch down | R3 yaw left |
| Left knee | KneeL_jnt | R1 pitch down | | |
| Right knee | KneeR_jnt | R1 pitch down | | |

[a] Positive translation or rotation given in global coordinate system, with dummy in reference position (see Figure 27.1).
[b] ONLY FOR EQUILIBRIUM



### Dummy contacts

When defining contacts between the dummy model and its environment, only the contact groups defined in Table 27.3 need to be used.

Table 27.3: Predefined groups to define contact between the Q10 model components and their environment.

| Area | Contact Group | Ellipsoids |
|---|---|---|
| Head | Head_gmb | Head_ell Face_ell |
| Neck | NeckUpLC_gmb | NeckUpLCbody_ell NeckUpLCtop_ell |
| | Neck_gmb | NeckUp_ell NeckLowerDisk_ell NeckUpperDisk_ell NeckLow_ell NeckLowDisk_ell NeckUpDisk_ell |
| | NeckLow_gmb | NeckLowLCbody_ell NeckLowLCtop_ell |
| Thorax | Ribcage_gmb | Rib[1-5][L l R]_ell Sternum_ell |
| | Clavicles_gmb | ClaviclePart[1-4][L l R]_ell |
| Back | Back_gmb | ThoracicSpineBody_ell ThoracicSpineNeck_ell ThoracicSpineNeckLow_ell |
| | Lumbarspine_gmb | LumbarSpineBracketUp_ell LumbarSpineLow_ell LumbarSpineUp_ell LumbarSpineUpperDisk_ell LumbarSpineLowerDisk_ell |
| Lower Torso | Abdomen_gmb | AbdomenLow_ell AbdomenMid_ell AbdomenUp_ell AbdomenBack_ell |
| | Pelvis_gmb | Pelvis[L l R]_ell PelvisBack_ell PelvisSide[L l R]_ell |
| Arms | ArmUp[L l R]_gmb | ArmUp[L l R]_ell Elbow[L l R]_ell Shoulder[L l R]_ell |
| | ArmLow[L l R]_gmb | ArmLow[L l R]_ell Hand[L l R]_ell |
| Legs | LegUp[L l R]_gmb | LegUpPart[1-3][L l R]_ell |
| | LegLow[L l R]_gmb | Knee[L l R]_ell LegLowPart[1-2][L l R]_ell Foot[L l R]_ell |
| Neck Shield | NeckShield_gmb | NeckShieldUp_ell NeckShieldUpper_ell NeckShieldLower_ell NeckShieldLower2_ell NeckShieldFront[L l R]_ell NeckShieldFrontSide[L l R]_ell NeckShieldBack[L l R]_ell |

It is advised to use orthotropic friction in all contacts between dummy and belt. The friction coefficients to use in the first and second direction are 0.2 and 0.5 respectively.

Inter-component contacts have also been defined as shown in Table 27.4.

Table 27.4: Predefined inter-component contacts

| Contact Name | Master | Slave |
|---|---|---|
| ArmsThorax_cnt | ArmUpL_gmb ArmUpR_gmb | Ribcage_gmb |
| ArmsLegs_cnt | LegUpL_gmb LegUpR_gmb | ArmLowL_gmb ArmLowR_gmb |
| HeadLegs_cnt | Head_gmb | LegLowL_gmb LegLowR_gmb LegUpL_gmb LegUpR_gmb |
| LegLeg_cnt | LegLowL_gmb LegUpL_gmb | LegLowR_gmb LegUpR_gmb |
| ArmsAbdomen_cnt | ArmLowL_gmb ArmLowR_gmb | Abdomen_gmb Pelvis_gmb |
| HeadThorax_cnt | Head_gmb | Clavicles_gmb Ribcage_gmb |
| HeadNeckShield_cnt | Head_gmb | NeckShield_gmb |

### Output

In Table 27.5 all predefined output definitions for the Q10 ellipsoid model are listed. When a signal is filtered the filter class is included in the name of the signal for more clarity.

Table 27.5: Predefined output signals for the Q10 model.

| Sensor | Identifier | Signal resul-tant | x | direc-tion[a] | y | direc-tion[a] | z | direc-tion[a] | Filter |
|---|---|---|---|---|---|---|---|---|---|
| Head | | | | | | | | | |
| Head acc | Head_CFC1000_acc | ar | a1 | forward | a2 | right | a3 | down | CFC1000 |
| Head avl | Head_CFC60_avl | vr | v1 | roll | v2 | pitch | v3 | yaw | CFC60 |
| Neck | | | | | | | | | |
| Upper LC | NeckUpLC_CFC600_lce_F | | f1 | shear | f2 | shear | f3 | axial | CFC600 |
| | NeckUpLC_CFC600_lce_T | | t1 | roll | t2 | pitch | t3 | yaw | CFC600 |
| Lower LC | NeckLowLC_CFC600_lce_F | | f1 | shear | f2 | shear | f3 | axial | CFC600 |
| | NeckLowLC_CFC600_lce_T | | t1 | roll | t2 | pitch | t3 | yaw | CFC600 |
| Thorax | | | | | | | | | |
| Thorax acc | Thorax_CFC1000_acc | ar | a1 | forward | a2 | right | a3 | down | CFC1000 |
| | Thorax_CFC180_acc | ar | a1 | forward | a2 | right | a3 | down | CFC180 |
| Chest Deflection | ChestDefFrontUp_CFC600_Dis | | d1 | frontal | | | | | CFC600 |
| | ChestDefFrontUp_CFC180_Dis | | d1 | frontal | | | | | CFC180 |
| | ChestDefFrontLow_CFC600_Dis | | d1 | frontal | | | | | CFC600 |
| | ChestDefFrontLow_CFC180_Dis | | d1 | frontal | | | | | CFC180 |
| | ChestDefLatUpL_CFC600_Dis | | d1 | lateral | | | | | CFC600 |
| | ChestDefLatUpL_CFC180_Dis | | d1 | lateral | | | | | CFC180 |
| | ChestDefLatLowL_CFC600_Dis | | d1 | lateral | | | | | CFC600 |
| | ChestDefLatLowL_CFC180_Dis | | d1 | lateral | | | | | CFC180 |
| | ChestDefLatUpR_CFC600_Dis | | d1 | lateral | | | | | CFC600 |
| | ChestDefLatUpR_CFC180_Dis | | d1 | lateral | | | | | CFC180 |
| | ChestDefLatLowR_CFC600_Dis | | d1 | lateral | | | | | CFC600 |
| | ChestDefLatLowR_CFC180_Dis | | d1 | lateral | | | | | CFC180 |
| Lumbar | | | | | | | | | |
| Lumbar LC | LumbarLowLC_CFC600_lce_F | | f1 | shear | f2 | shear | f3 | axial | CFC600 |
| | LumbarLowLC_CFC600_lce_T | | t1 | roll | t2 | pitch | t3 | yaw | CFC600 |
| Pelvis | | | | | | | | | |
| Pelvis acc | Pelvis_CFC1000_acc | ar | a1 | forward | a2 | right | a3 | down | CFC1000 |
| Pelvis avl | Pelvis_CFC60_avl | vr | v1 | roll | v2 | pitch | v3 | yaw | CFC60 |
| Pubic LC | Pubic_CFC600_lce_F | | f1 | shear | f2 | axial | f3 | shear | CFC600 |
| | Pubic_CFC600_lce_T | | t1 | roll | t2 | torsion | t3 | yaw | CFC600 |
| SacroIliac Wing LCs | SacroIliacLCL_CFC600_lce_F | | f1 | shear | f2 | axial | f3 | shear | CFC600 |
| | SacroIliacLCL_CFC600_lce_T | | t1 | roll | t2 | torsion | t3 | yaw | CFC600 |
| | SacroIliacLCR_CFC600_lce_F | | f1 | shear | f2 | axial | f3 | shear | CFC600 |
| | SacroIliacLCR_CFC600_lce_T | | t1 | roll | t2 | torsion | t3 | yaw | CFC600 |
| Femurs | | | | | | | | | |
| Femur LCs | FemurL_CFC600_lce_F | | f1 | shear | f2 | shear | f3 | axial | CFC600 |
| | FemurL_CFC600_lce_T | | t1 | roll | t2 | pitch | t3 | yaw | CFC600 |
| | FemurR_CFC600_lce_F | | f1 | shear | f2 | shear | f3 | axial | CFC600 |
| | FemurR_CFC600_lce_T | | t1 | roll | t2 | pitch | t3 | yaw | CFC600 |

[a] Positive direction given according to SAE J211/1.

In Table 27.6 all predefined injury criteria for the Q10 model are listed.

Table 27.6: Predefined injury criteria for the Q10 model.

| Component | Injury criteria | Filter |
|---|---|---|
| Head | HIC15_inj | CFC1000 |
| | HIC36_inj | CFC1000 |
| | Head_CFC1000_AccR_3MS_inj | CFC1000 |
| | Head_CFC1000_AccR_peak_inj | CFC1000 |
| Neck | NeckUp_CFC600_My_peak_inj | CFC600 |
| | NeckUp_CFC600_Tension_peak_inj | CFC600 |
| Thorax | Thorax_CFC1000_AccR_3MS_inj | CFC1000 |
| | Thorax_CFC1000_AccR_peak_inj | CFC1000 |
| | Thorax_CFC1000_AccZabs_3MS_inj | CFC1000 |
| | Thorax_CFC180_AccR_3MS_inj | CFC180 |
| | Thorax_CFC180_AccR_peak_inj | CFC180 |
| | Thorax_CFC180_AccZabs_3MS_inj | CFC180 |
| | ChestDefFrontUp_CFC180_peak_inj | CFC180 |
| | ChestDefFrontUp_CFC600_peak_inj | CFC600 |
| | ChestDefFrontLow_CFC180_peak_inj | CFC180 |
| | ChestDefFrontLow_CFC600_peak_inj | CFC600 |
| | ChestDefLatUpL_CFC180_peak_inj | CFC180 |
| | ChestDefLatUpL_CFC600_peak_inj | CFC600 |
| | ChestDefLatLowL_CFC180_peak_inj | CFC180 |
| | ChestDefLatLowL_CFC600_peak_inj | CFC600 |
| | ChestDefLatUpR_CFC180_peak_inj | CFC180 |
| | ChestDefLatUpR_CFC600_peak_inj | CFC600 |
| | ChestDefLatLowR_CFC180_peak_inj | CFC180 |
| | ChestDefLatLowR_CFC600_peak_inj | CFC600 |
| Pelvis | Pelvis_CFC1000_AccR_3MS_inj | CFC1000 |
| | Pelvis_CFC1000_AccR_peak_inj | CFC1000 |

# 28 TNO P Child Dummies (P3/4, P3, P6, P10 and P1 1/2)

The first TNO child dummies were developed in the late seventies for the evaluation of restraining devices for children in vehicles. The development was initiated by the work of an ECE-committee that was drafting a regulation for child restraint systems. The work resulted in ECE-Regulation 44, "Uniform provisions concerning the approval of restraining devices for child occupants of power driven vehicles" which came into force in 1982. The regulation initially described 4 dummies: the $P^3/_4$ , P3, P6 and P10 dummies representing children of respectively 9 months, 3, 6 and 10 years. In 1988 a simple dummy representing a new-born child, called P0 was added. In 1995 the $P1^1/_2$ (18 months) dummy was added which is now also specified for ECE-R44.

## 28.1 Model description

**TNO $P^3/_4$ , $P1^1/_2$ , P3, P6 and P10 models**

An ellipsoid model of the TNO $P^3/_4$ , $P1^1/_2$ , P3, P6 and P10 dummy models are available. The input is given in the files:

| | |
|---|---|
| TNO $P^3/_4$ Ellipsoid model: | d_tnop34el_usr.xml<br>d_tnop34el_inc.xml |
| TNO $P1^1/_2$ Ellipsoid model: | d_tnop32el_usr.xml<br>d_tnop32el_inc.xml |
| TNO P3 Ellipsoid model: | d_tnop03el_usr.xml<br>d_tnop03el_inc.xml |
| TNO P6 Ellipsoid model: | d_tnop06el_usr.xml<br>d_tnop06el_inc.xml |
| TNO P10 Ellipsoid model: | d_tnop10el_usr.xml<br>d_tnop10el_inc.xml |

To run these models, the following licenses are required:

| | |
|---|---|
| Ellipsoid models: | MADYMO/Solver (Multibody)<br>MADYMO/Dummy Models/Child |

Figure 28.1 shows the $P^3/_4$ , P3, P6 and P10 models in reference position. The basic set-up of these four models is identical. Every model consists of 15 bodies. In Figure 28.2 the $P1^1/_2$ model is shown in reference position. The basic set-up of the $P1^1/_2$ model is somewhat more complicated than that of the other P dummy models. The $P1^1/_2$ model consists of 23 bodies.

Most inertia properties of the bodies are based on measurements. Some inertia parameters of minor importance of the P6 and P10 were derived by scaling those of the $P^3/_4$ .

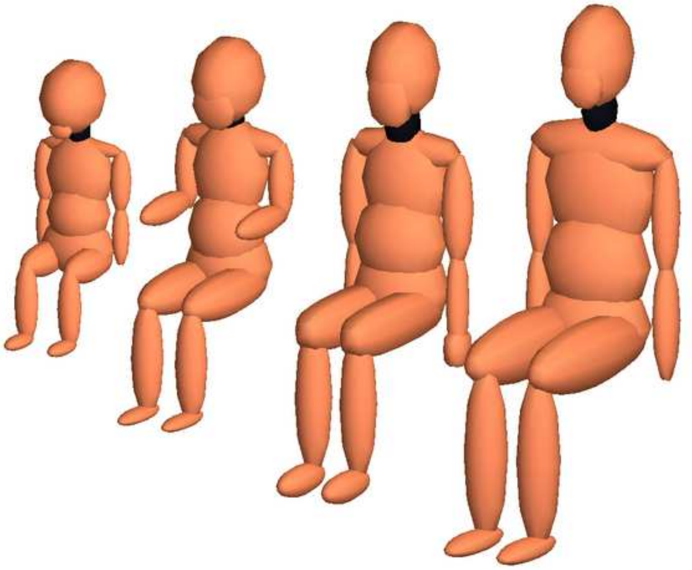

Figure 28.1: Ellipsoid TNO child dummy models, $P^3/_4$ , P3, P6 and P10.

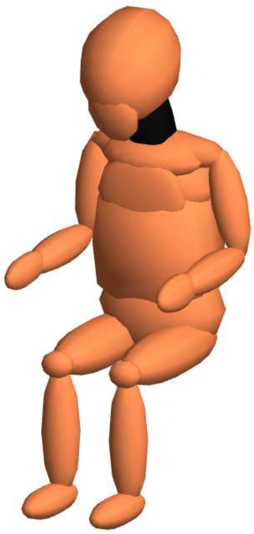

Figure 28.2: Ellipsoid TNO $P1^1/_2$ child dummy model.

## ELLIPSOID MODEL

### Hands and wrists

Only for the P1$^1/_2$ dummy model, hands have been defined as separate bodies and the wrists are bracket joints.

### Thorax

The thorax of the P$^3/_4$ , P3, P6 and P10 dummy models are described by one body.

For the P1$^1/_2$ dummy model, the sternum is a separate body describing the frontal area of the thorax. This body is included to describe chest deflections. A sensor for chest deflection is not available for the actual dummy, but this body is relevant for simulating contact interactions and belt interactions.

### Feet and ankle

Only for the P1$^1/_2$ dummy model, feet have been defined as separate bodies and the ankles are bracket joints.

### Joint properties

Joint characteristics for the hip, knee, shoulder, elbow and head-atlas block attachment are based on measurements of the joint free range of motion. Joint stops are set at 500Nm/rad. In addition, friction torques have been specified for these joints in agreement with the calibration prescribed in ECE regulation 44. The elastic joint characteristics for both neck joints and both lumbar spine joints have been obtained from static bending measurements on the P$^3/_4$ and P1$^1/_2$ dummies. The characteristics for the P3, P6 and P10 were derived by scaling those of the P$^3/_4$ . The damping coefficients for neck and lumbar spine have been tuned using tests with the complete dummies.

## CONTACTS BETWEEN DUMMY COMPONENTS

For the P1$^1/_2$ model contact is defined between head and thorax. For the P3 model contact is defined between head and thorax, chest and abdomen, abdomen and pelvis, head and arms, arms and legs. For the P10 model contact is defined between face and neck and between left and right foot.

## 28.2 Model validation

The models have been validated for frontal impact. In addition the P6 model has been validated for lateral loading. In this lateral validation the lower arms were removed and the upper arms were taped to the upper torso. Furthermore the P1$^1/_2$ and P10 models have been validated for rearward loading.

Some validation results for the P3 in frontal impact are given in Figure 28.3 and Figure 28.4. The head kinematics and accelerations are well predicted. The validation results for the upper torso acceleration are not so accurate. This is presumably due to the complex interaction between belt and seat during the experiment. The validation results for frontal impact for the P1$^1/_2$ model are given in Figure 28.5.

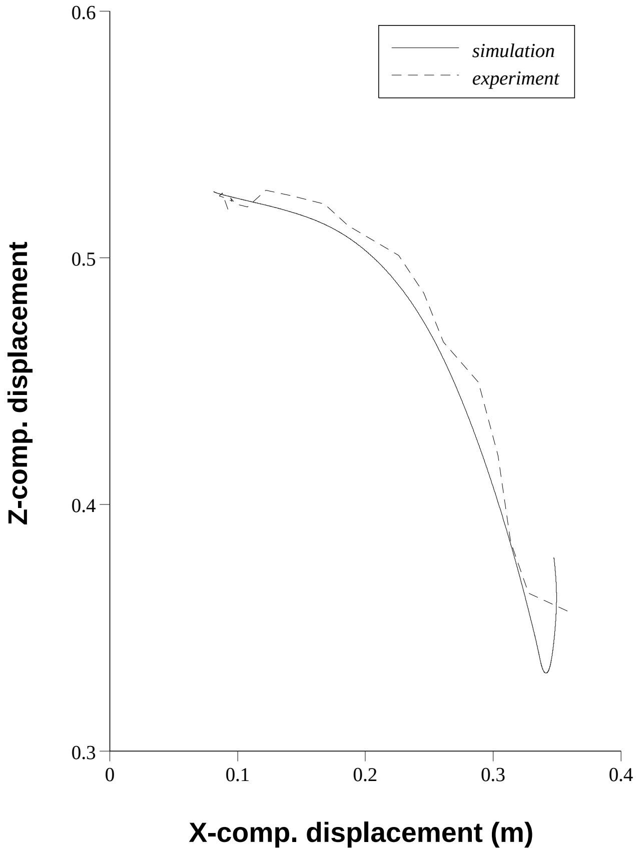


Figure 28.3: TNO P3 validation results; head trajectory.

28

**SLED TEST with P3 in FF-childseat**

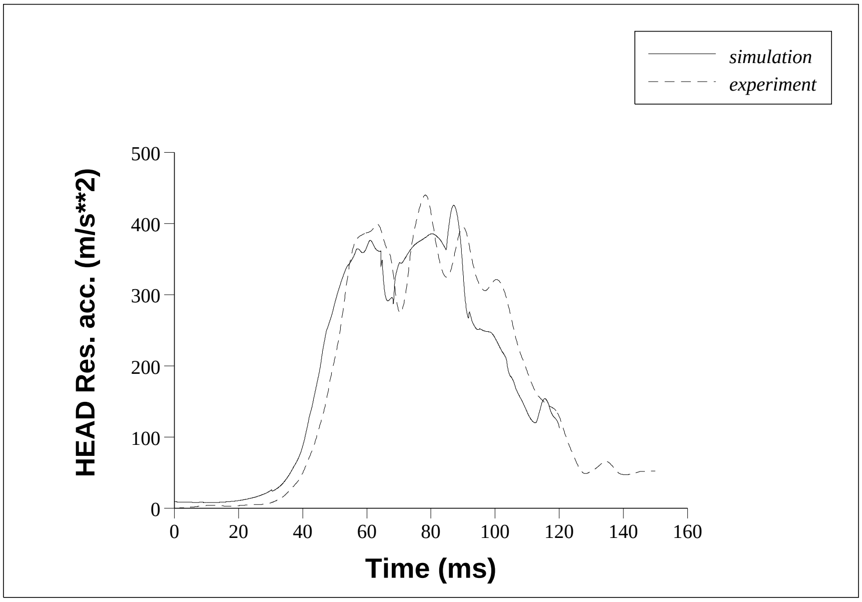


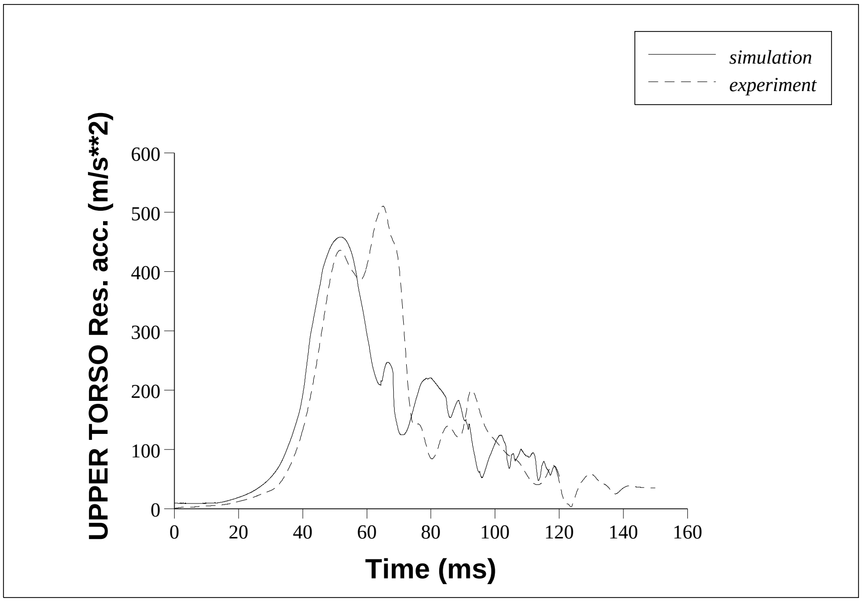


28

Figure 28.4: TNO P3 validation results.

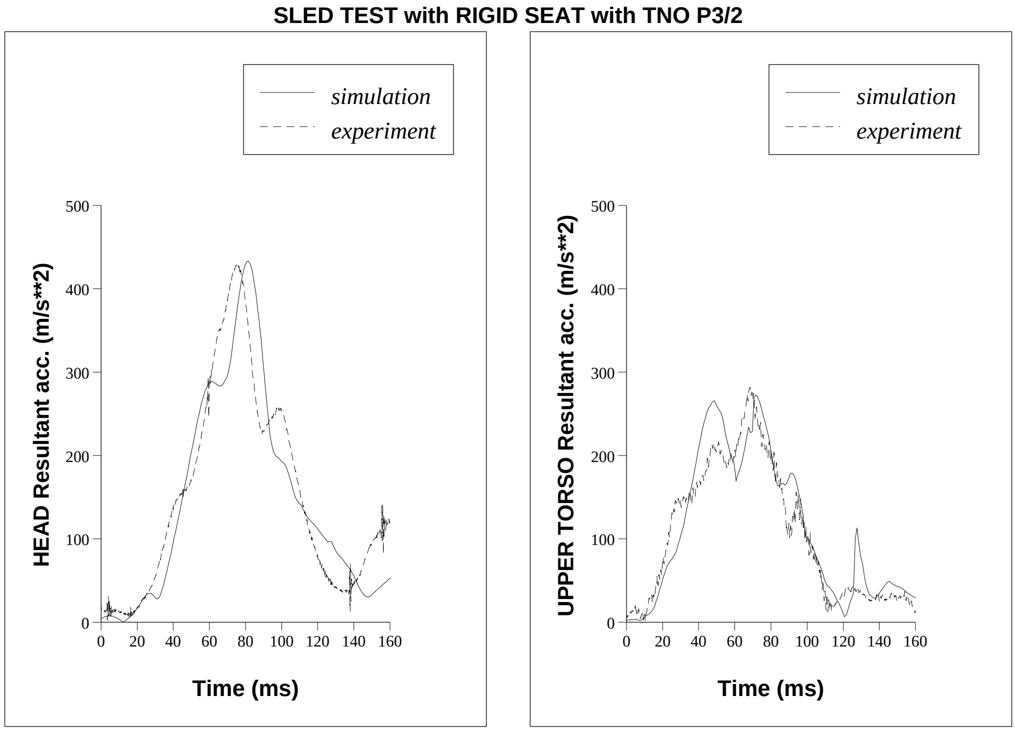


Figure 28.5: TNO P$1^1/_2$ model validation results.

## 28.3 User instructions

### Timestep

Table 28.1: Recommended timestep for the TNO-P dummy models.

| Model | timestep (s) |
|---|---|
| Ellipsoid | $\leq 5.0 \cdot 10^{-5}$ |

### Chin-chest contact

During forward flexion of the neck, the chin can contact the upper torso and the neck. This limits the head rotation and affects the head and upper torso accelerations. It is therefore recommended to implement such a contact in forward loading conditions. Chin-neck contact has been specified already in the P10 model. A contact interaction between chin and sternum is implemented in the P1$^1/_2$ model.

### Conventional belt interaction

Belt contact points have been defined on the P$^3/_4$ for a four-point belt.

Table 28.2: P$^3/_4$ attachment points for a conventional four-point belt.

| Attachment point<br>point 1 (POINT_REF_1) | point 2 (POINT_REF_2) |
|---|---|
| defined by user (seat) | ShoulderRSegment22_pnt |
| ShoulderRSegment31_pnt | defined by user (buckle system) |
| defined by user (seat) | ShoulderLSegment22_pnt |
| ShoulderLSegment31_pnt | defined by user (buckle system) |
| defined by user (buckle system) | HipSegment12_pnt |
| HipSegment21_pnt | defined by user (seat) |
| defined by user (seat) | HipSegment42_pnt |
| HipSegment51_pnt | defined by user (buckle system) |

28

The belt is thus considered in four sections. The two belt points on the dummy in each section are coincident and must be joined by tying.

The P1$^1/_2$ model has been validated with belt restraints. It was found that the belt properties had to be tuned (softened) considerably to account for belt intrusion of the dummy flesh.

It is recommended to attach shoulder belts first to the upper torso and then to the sternum body. This results in realistic load sharing between the shoulder area and the sternum area (see also the example of the adult Hybrid III models).

**Output**

Standard output signals of the dummies are the upper torso and head accelerations. Linear acceleration sensors have been included into the models. For the $P1^1/_2$ and P10, also pelvis acceleration signals are used and a linear acceleration sensor has been specified at the appropriate position.

In addition upper neck load transducers are available for the $P^3/_4$ , $P1^1/_2$ and P3 dummies and load transducers are available for the lower lumbar spine and lower neck of the $P1^1/_2$ .

The injury parameters HIC for the head resultant acceleration and the 3MS maximum for the upper torso resultant acceleration are generated.

For the $P1^1/_2$ and P3 the following specific EuroNCAP injury criteria are defined: peak of head resultant acceleration, head resultant acceleration 3MS, head vertical acceleration 3MS (absolute value of the negative part) -$P1^1/_2$ only-, absolute value of the chest vertical acceleration 3MS.

# 29 Active Human Model

The MADYMO facet active human model (AHM) is currently available in one body size, a mid-size male model representing the 50th percentile male model population. It is available in a sitting and a standing position (see Figure 29.1). The sitting and the standing version of the facet active human model are identical except for the initial joint rotations and the skin mesh of the pelvis and knee areas.

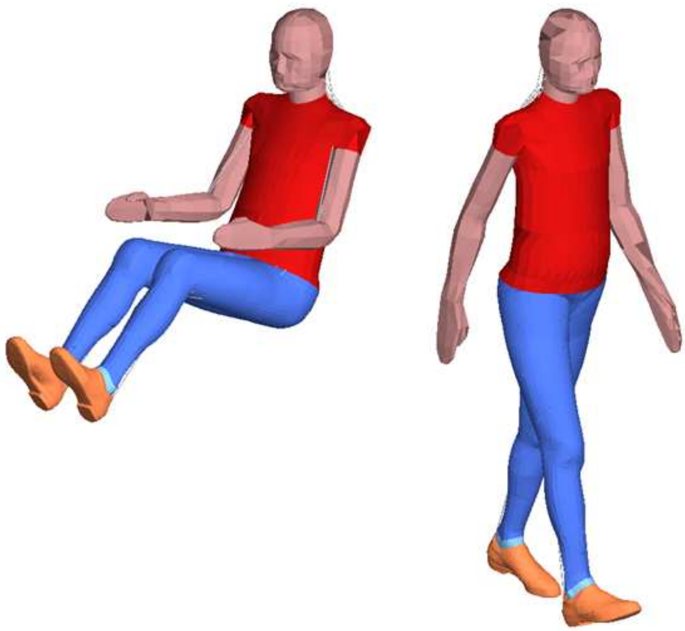

Figure 29.1: AHM facet model.

## 29.1 Model description

Facet models of the Active Human model are available. The input is given in the files:

| | |
|---|---|
| Facet model: | h_act50fc_sitting_usr.xml<br>h_act50fc_sitting_inc.xml<br>h_act50fc_standing_usr.xml<br>h_act50fc_standing_inc.xml |

To run this model, the following licenses are required:

| | |
|---|---|
| Facet model : | MADYMO/Solver (Multibody)<br>MADYMO/HumanActive |

Figure 29.1 shows the model in the reference position.

The facet active human model is based on earlier released human body models - the ellipsoid mid-size male pedestrian model, the facet mid-size male occupant model, controllers to stabilise the spine, the facet detailed leg model, the facet neck model, a controller to stabilise the neck model, a detailed facet arm model and a shoe model. Posture controllers were also implemented; these can be activated and deactivated.

Where references are made to literature, a complete reference list can be found in the human models manual.

### FACET MODEL

#### Anthropometry

The anthropometry of the adult facet occupant models was obtained from the database of the RAMSIS software package (RAMSIS 1997). The 1984 Western European population aged 18 to 70 years was used. For the facet mid-size male active human model, simply medium typologies were selected for height, weight and sitting height. In Table 29.1 the resulting anthropometry of the facet active human model is described.

Table 29.1: Anthropometry of the Active Human model.

| Parameter | value |
|---|---|
| Standing height (m) | 1.76 |
| Sitting height (m) | 0.92 |
| Weight (kg) | 75.3 |

The mass distribution of the facet active human models is based on the RAMSIS database. Rotational inertia values were derived by integration over the segment volume, where for each segment a homogeneous density was assumed. The neck rotational inertia was slightly increased to allow larger timesteps for the MADYMO calculations.



#### Configuration

The active human model consists of 190 bodies (182 rigid bodies and 8 flexible bodies). The first branch connects the head and vertebral bodies to the pelvis. Two branches connect the shoes and the bodies of the left and right leg to the pelvis. Separate branches connect the patella, toes and other bodies in the foot. Two branches connect the fingers and the bodies of the arm to the spine. The thumb is connected to the mid-hand joint on a separate branch from the fingers. The thorax and the abdomen each consist of 4 flexible bodies that divide the thorax and abdomen in horizontal slices. Attached to each slice at the left and right side and at the front, bodies have been placed for attachment of force models. The thorax and abdomen bodies are divided over 3 branches (front, left and right) for each slice.

**Head and neck**

The neck model was based on the facet neck model. In this neck model the surface geometries of the vertebrae and skull of this model were obtained from a digitised 50th percentile PMHS from the European project HUMOS, and modified using a study of the curvature of the neck.

The head and the cervical vertebrae (C1-C7) are represented by rigid bodies. The outer surfaces of the skull and the vertebrae consist of facets.

The intervertebral discs are modelled by point restraints and cardan restraints, based on stiffness data from literature (see Human Models Manual).

The articular facet joints and contacts between the spinous processes are modelled by point restraints with resistance in compression only. The contacts between skull (OC) and C1 and between C1 and C2 (dens) are modelled by an FE-FE contact with a stress-penetration characteristic. The OC of C1-skull and the dens contact area of C1-C2 have a detailed mesh in order to have a convex-concave smooth contact area. Ligaments surrounding the dens and the joint capsules offer resistance in tension and shear and are modelled with kelvin restraints.

The nuchal ligaments are each modelled by Kelvin restraints. The stiffness of the upper neck ligaments were increased from experimental values in order to avoid unrealistic large motions of the upper neck in flexion and extension.

The facet neck model includes 68 pairs (left/right) of muscle elements. These are used for passive resistance and for the hip controller, described in more detail in the section below relating to active behaviour control. Each muscle element is divided into segments which are supported on the relevant vertebrae by intermediate sliding points, enabling the muscles to curve around the vertebrae. These sliding points are located on the points of intersection of the muscle's initial line of action and the xy-plane of the intermediate vertebrae. Figure 29.2 all the muscles and ligaments in the facet neck model.

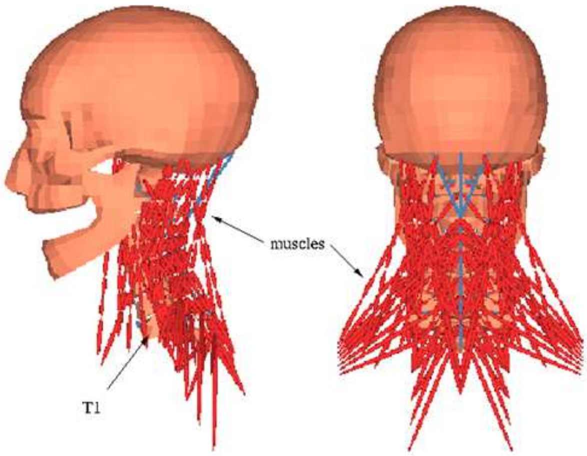


Figure 29.2: AHM head and neck model, including bones and muscles, excluding skin

**Spine**

The lumbar and thoracic spine were modelled to give a biofidelic response under a wide range of loading conditions. The vertebrae were modelled by rigid bodies connected by free joints and lumped restraint models in 3 rotational and 3 longitudinal directions (RESTRAINT.SIX_DOF). These joint resistance models describe the global dynamic response of the intervertebral discs, ligaments and effects of muscular resistance. The physical locations of the lumbar and thoracic vertebrae are each given by a single ellipsoid. The neutral position of the spine represents the spinal curvature of an erect standing person.

**Thorax and abdomen**

In an impact loading case the human thorax and abdomen can deform in a complex 3D manner due to both contact forces and spinal deformations. This has been modelled using flexible bodies, which efficiently describe 3D deformations with only a few degrees of freedom. The flexible bodies describe global deformations, while the contact algorithm captures local deformation. The resulting capability to model torso deformation has been validated against experimental data.

The thorax and the abdomen each consist of 4 flexible bodies. The flexible bodies divide the thorax and abdomen in horizontal slices, as is shown in Figure 29.3. The geometry of each flexible body is determined by the position of its skin nodes. A point mass has been assigned to each node.

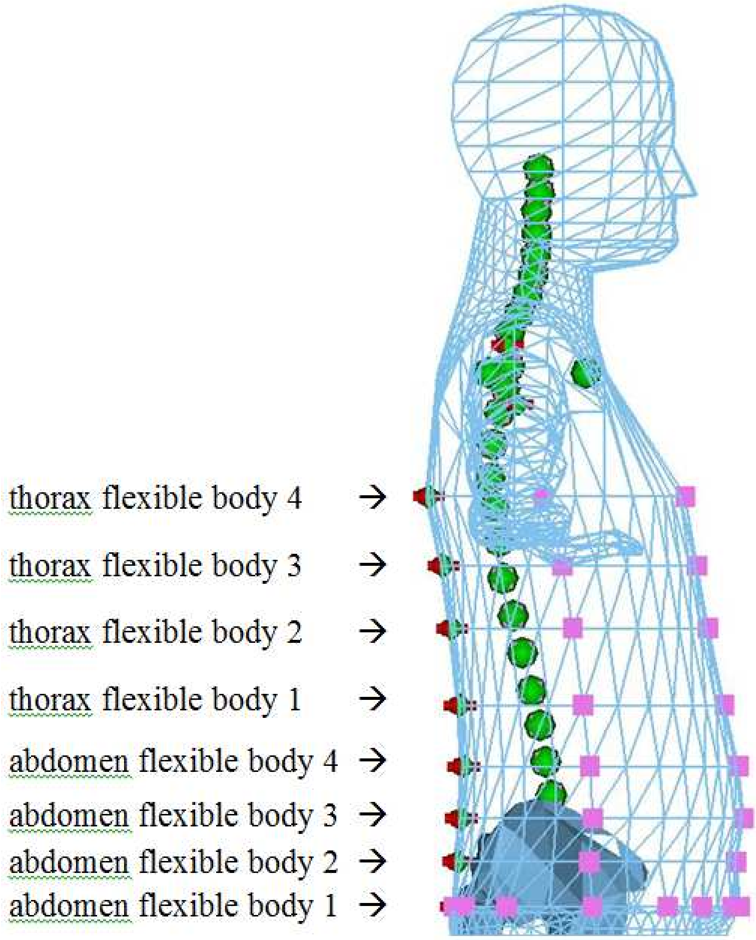


Figure 29.3: Right section view of the AHM with arrows highlighting flexible bodies and rigid bodies shown as green dots

The flexible bodies are each connected to the closest rigid vertebral body of the spine. Each flexible body is able to deform in 3 predefined deformation modes: 1 frontal mode and 2 lateral modes (left and right). The modes were determined analytically as linear functions of the coordinates of the nodes. The frontal mode contains both x- and y-displacements, the lateral modes only contain y-displacements. The input options for the flexible bodies only allow linear stiffness and damping, which is not sufficient for describing the demonstrated non-linear behaviour of the torso in impact. Therefore, point restraints were added to model the frontal and lateral stiffness and damping of the flexible bodies, and the stiffness and damping in all modes were set to negligibly low values (setting these values to zero is not allowed in MADYMO).

For attachment of the point restraints rigid bodies were added: 1 frontal, 1 left and 1 right of each flexible body. These rigid bodies are connected to the skin nodes of the flexible body. The point restraints at the frontal bodies and the lateral bodies only contribute to loading in the x-direction and y-direction, respectively. Coupling between frontal and lateral deformation is taken into account by the frontal deformation mode.

Vertical point restraints were added between the rigid bodies of each flexible body. These point restraints do not only have a z-component, but also have a small x- or y- component for frontal and lateral stiffness respectively. This was done in order to obtain a more realistic skin deformation. The two lowest flexible bodies also model the iliac wings. Since no biomechanical data was available the resistance for frontal loading of these two lowest flexible bodies, the stiffness is based on a model of the Hybrid III 50th percentile dummy.

**Shoulders and arms**

The shoulder and arms are based on a shoulder-arm model developed in the EU project APROSYS. The skeleton of the shoulders and arms are modelled with rigid bodies for each bone (clavicle, scapula, humerus, ulna, radius). The clavicles are each connected to the sternum with a free joint, which besides the rotations allows for some translations to represent clavicle and sternum deformation. The acromio-clavicular (clavicle-scapula) and gleno-humeral (scapula-humerus) joints are spherical joints, allowing three rotations. The elbow and radio-ulnar (lower arm rotation) joints are both modelled with revolute joints with only one degree of freedom. The wrist is modelled with a universal joint with two degrees of freedom. The hand is modelled by a 3-segment thumb and a 3-segment combined fingers. The joints of thumbs and fingers are locked, making the hands rigid during simulation - however the initial positioning is adjustable. In all joints in the arms (except the hands) restraints are applied to model the range of motion and the resistance.

In the human body, the scapulae contact the thorax. Active muscle force is needed to maintain this contact and to stabilise the shoulder girdle. These complex interactions between shoulder and thorax have been modelled by a set of passive restraint models. The scapula is supported on the spine by point restraints to T1 and T7. Thus, the load transfer from shoulder to spine has been modelled by the skeletal connection (scapula-clavicle-sternum-ribs-spine) and by these additional restraint models.

The main muscles in the arm are also included in the model. These are used for passive resistance and for the elbow controller, described in more detail in the section below relating to active behaviour control. The geometry of the scapula, clavicle, humerus, ulna and radius is represented by a facet surface. The arm model is shown in Figure 29.4.

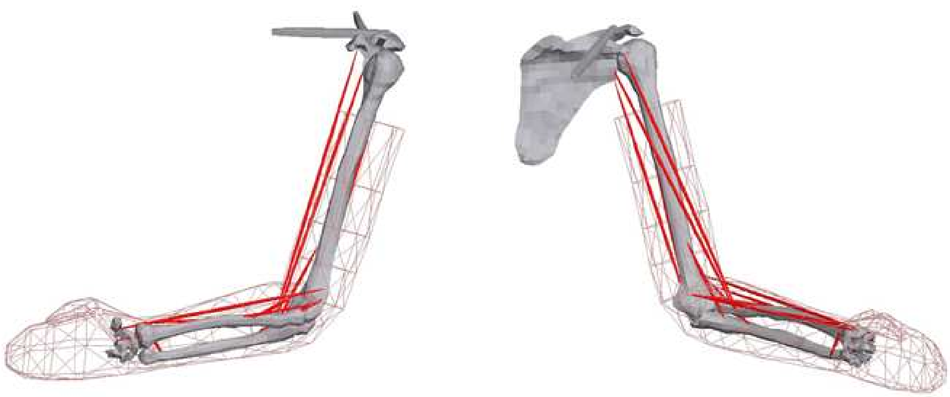

Figure 29.4: The left shoulder/arm model, including bones and muscles. Arm skin shown in wireframe

29

### Legs

The hip joints, connecting the pelvis to the legs, are modelled by spherical joints with cardan restraints. The knee joints, connecting the upper leg to the lower leg, are modelled by free joints restrained with point and cardan restraints. In this way, the knee can move in all degrees of freedom allowing knee shear, which is common in car-pedestrian impact, to be predicted. The ankles, connecting the lower legs to the feet, are modelled by spherical joints with cardan restraints. The feet are modelled in detail - all the feet bones and the joints between these bones are included. However, the joints in the feet are locked, since they do not affect the kinematics of the human in most scenarios when there are shoes around the feet.

In pedestrian impacts, bending and fracture of the leg bones affect the kinematics of the pedestrian. To account for this in both the femur and tibia/fibula, spherical joints were implemented in order to model bending and fracture. Cardan restraints were added at all these joints to capture the bending stiffness of femur and tibia/fibula. The stiffness is assumed to be equal throughout each long bone; the same characteristics are therefore used for all cardan restraints within one bone.

In car-pedestrian collisions fracture most often occurs in the lower leg. Therefore, only one fracture joint was implemented at the middle of the femur and three fracture joints at the tibia/fibula leg joints. All fracture joints are spherical joints that are initially locked until a predefined fracture trigger signal exceeds the fracture tolerance level. The implemented fracture levels for the upper and lower leg are based on 50% injury risk, see Table 29.2. These levels can be adapted in the model for studying a specific population group, e.g. elderly people, provided that the tolerance levels are known for the group. This can be done by changing the values for the DEFINE elements in the user file ([Femur | Tibia]Fract[Force | Torque]Lat).

Table 29.2: Fracture levels for the upper and lower leg, based on 50% injury risk

| Model Part | Torque (Nm) | Reference | Shear Force (N) | Reference |
|---|---|---|---|---|
| Mid-size male | | | | |
| Upper Leg | 430 | EEVC WG17 | 6000 | Based on EEVC WG17 |
| Lower Leg | 285 | Nyquist et al. (1985) | 4000 | Yang et al. (2000) |

In total 43 muscle elements have been modelled in the leg. These are used for passive resistance and for the hip and knee controller, described in more detail in the section below relating to active behaviour control. The set of muscles used in the model has been derived from literature. Eleven ligaments have been implemented in the ankle joint and foot; these are needed to stabilise the ankle joint. The geometry of the pelvis, femur, tibia, patella and fibula was scaled from measured values to fit the existing outer geometry, represented by a facet surface. As no fibula bodies are included, the fibula mesh is attached to the tibia. The leg model is shown in Figure 29.5.

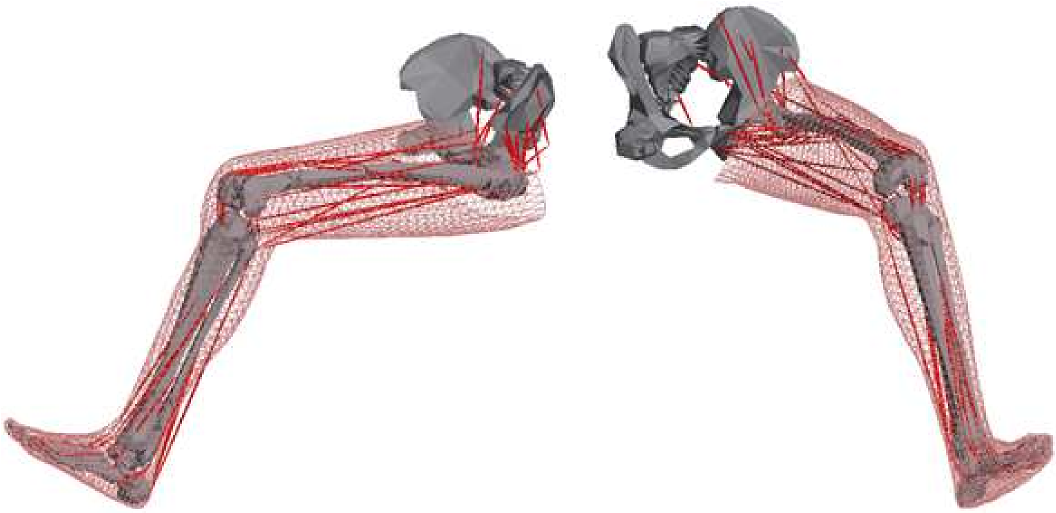

Figure 29.5: The (left) leg/foot model, including bones and muscles. Leg skin shown in wireframe

### Shoes

The shoes each consist of a rigid body with a facet surface supported to it. The shoes are each connected to a foot by a free joint. The feet fit in the shoes and the interaction between feet and shoes is represented with a cardan restraint and two point restraints. It represents the movement of the feet with respect to the shoes.

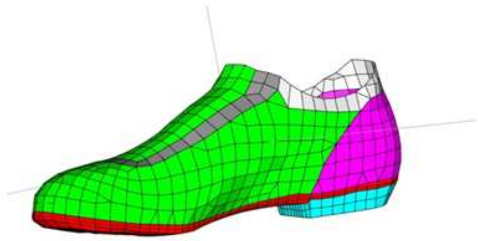

Figure 29.6: Right shoe of the AHM

### Skin and bones

The outer surface of the facet occupant model (skin) is described by a mesh of triangular elements defined as a null material. The skin is divided into several sections that are supported on the nearest bodies. In the thorax and abdomen area the skin is supported on flexible bodies. Different parts of the skin have different contact characteristics, based on the validation dataset. For the legs, pelvis, arms and neck the bones are also included. Similarly to the skin, the geometry of these bones is described by a mesh of elements defined as a null material. The skin and bones are both used in contact groups.

## CONTACTS BETWEEN DUMMY COMPONENTS

The contacts between dummy components defined can be found in Table 29.3

Table 29.3: Intercomponent contacts for the Active Human models.

| Model Type | Contact | Master Surface | Slave Surface |
|---|---|---|---|
| facet | Body_Head_cnt | BodyNoHeadArmsInternalCnt_gfe | HeadInternalCnt_gfe |
| | Body_ArmL_cnt | BodyNoArmsInternalCnt_gfe<br>ArmR_gfe | ArmL_gfe |
| | Body_ArmR_cnt | BodyNoArmsInternalCnt_gfe<br>ArmL_gfe | ArmR_gfe |
| | LegR_LegL_cnt | skinFootR_InternalCnt_gfe<br>skinLegR_InternalCnt_gfe | bonesLegL_InternalCnt_gfe<br>skinFootL_InternalCnt_gfe<br>skinLegL_InternalCnt_gfe |
| | LegL_LegR_cnt | skinFootL_InternalCnt_gfe<br>skinLegL_InternalCnt_gfe | bonesLegR_InternalCnt_gfe<br>skinFootR_InternalCnt_gfe<br>skinLegR_InternalCnt_gfe |
| | LegR_to_ShoeL_cnt | LegR_gfe | ShoeL_gfe |
| | LegL_to_ShoeR_cnt | LegL_gfe | ShoeR_gfe |
| | ShoeR_to_ShoeL_cnt | ShoeR_InternalCnt_gfe<br>SoleR_InternalCnt_gfe | ShoeL_InternalCnt_gfe<br>SoleL_InternalCnt_gfe |
| | ShoeL_to_ShoeR_cnt | ShoeL_InternalCnt_gfe<br>SoleL_InternalCnt_gfe | ShoeR_InternalCnt_gfe<br>SoleR_InternalCnt_gfe |
| | SkullOC_C1_cnt | Skull_gfe | C1_gfe |
| | C2dens_C1_cnt | C1_gfe | C2dens_gfe |

### Active behaviour control

The active human model contains controllers for the neck, spine, elbows and hips. These controllers will by default try to maintain the initial position under the influences of external loading. However, by means of a target angle function per degree of freedom, some controlled movements (voluntary or reflex) can be simulated. For the neck, co-contraction is included for simulating the stiffening effect of bracing. All controllers in the active human model are based on the scheme shown in Figure 29.7. This basic scheme is explained below, followed by more details for each body part and any deviations from the basic setup.

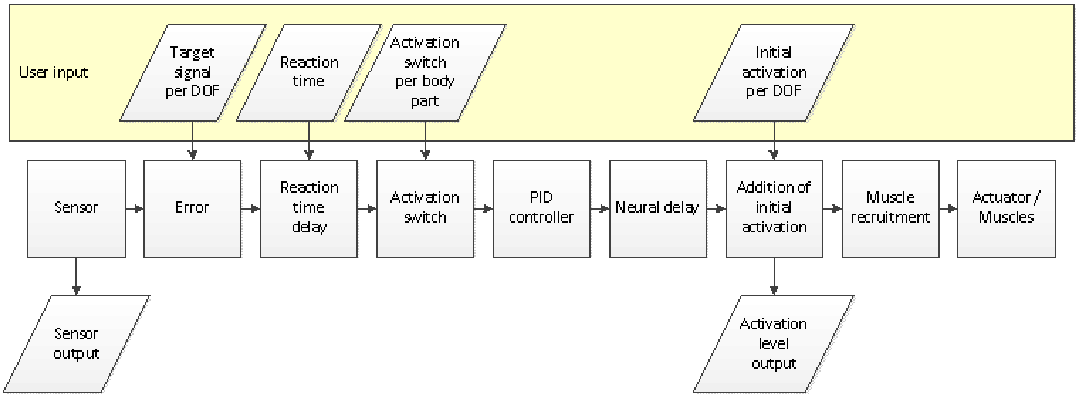


Figure 29.7: Basic controller scheme, with user input (top), main controller flow (mid) and available output (bottom).

The basic controller scheme starts with the sensors. For each degree of freedom that is controlled, a sensor is defined to measure the motion. Furthermore, a target signal, which by default is 0, can be defined by the user to simulate voluntary movement to stabilise the model in the initial position. The control error is then calculated as the difference between the sensor and target signals.

The next step is the reaction time. Here, the reaction time represents the time it takes for the human brain to start responding to any new event. This includes the time needed for the sensing, transfer of the signal to the brain and processing there. This cannot be included in the model as a pure time delay, as this would cause the controller to respond to events which occurred in the past. For example, in a crash scenario with a duration of 100 ms and a reaction time of 200 ms, 100 ms after the crash is over the controllers would make the model move based on control errors found during the crash, which is considered unrealistic. This would also make the model unstable. Therefore, the reaction time is implemented such that:

- Control errors related to pure stabilising behaviour, without any new events, causes a direct response
- New events only cause a response with a delay of the reaction time.

A new event is defined as any external load causing a control error that is larger than the maximum error occurring in the simulation up to the current time step. New events are automatically detected: if the error remains below the maximum the signal is transferred directly, but if the error is above, it is limited to the maximum during the reaction time before it increases further. An example with arbitrary input is shown in Figure 29.8.

29

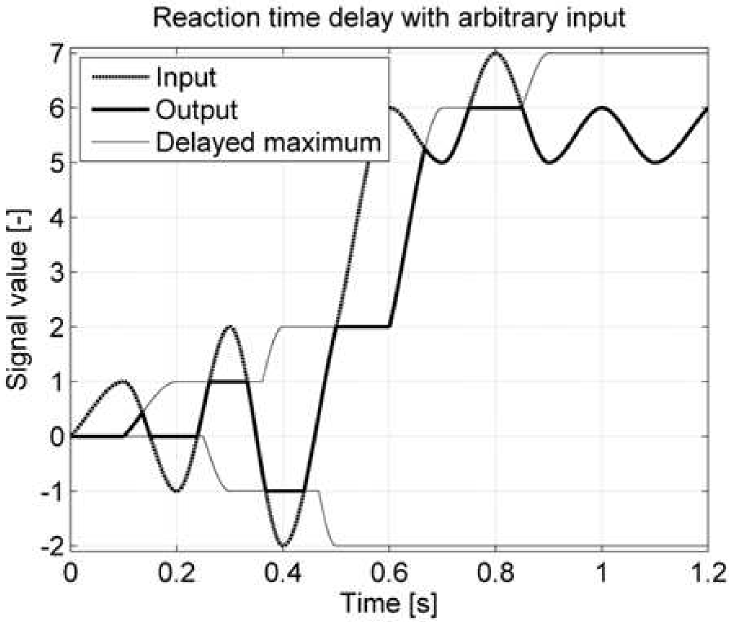


Figure 29.8: Example of the effect of the reaction times on the signal output of the controllers. The output signal is limited by the delayed (reaction time) maximum of the input.

For each body part (neck, spine, elbow, hip) the active behaviour can be switched on or off. This is done by multiplying the control signal by the activation parameter, where '0' results in no active behaviour, and '1' results in active behaviour (posture maintenance). The PID controller aims to reduce the error by calculating a correcting load. The P-action changes the controller action based on the present error. The I-action makes sure the controller will reduce the error to zero by integrating past errors. To damp out oscillations and reduce future errors the D-action increases the controller action if the error is increasing and decreases if the error is decreasing. After the PID-controller, a neural delay is implemented. The neural delay represents the time it takes for the signal transfer from the brain to the muscle and the time it takes for the muscle to convert the signal into a force. This neural delay is defined as:

$$d(output)/dt = (input/output)/\tau_{delay\_time} \tag{29.1}$$

For the controllers on the neck muscles $\tau_{delay\_time}$ is set to 40 ms, for the spine controllers to 70 ms, for controllers on the muscles in the arms to 70 ms and for the controllers on the muscles in the legs to 100 ms. The neural delay exhibits frequency-dependency, so lower-frequency signals are transferred better than signals with higher frequencies, and the delay decreases with increasing frequencies. This is shown in Figure 29.9, where for a step function and for a swept sine as input, the output of the neural delay is shown.

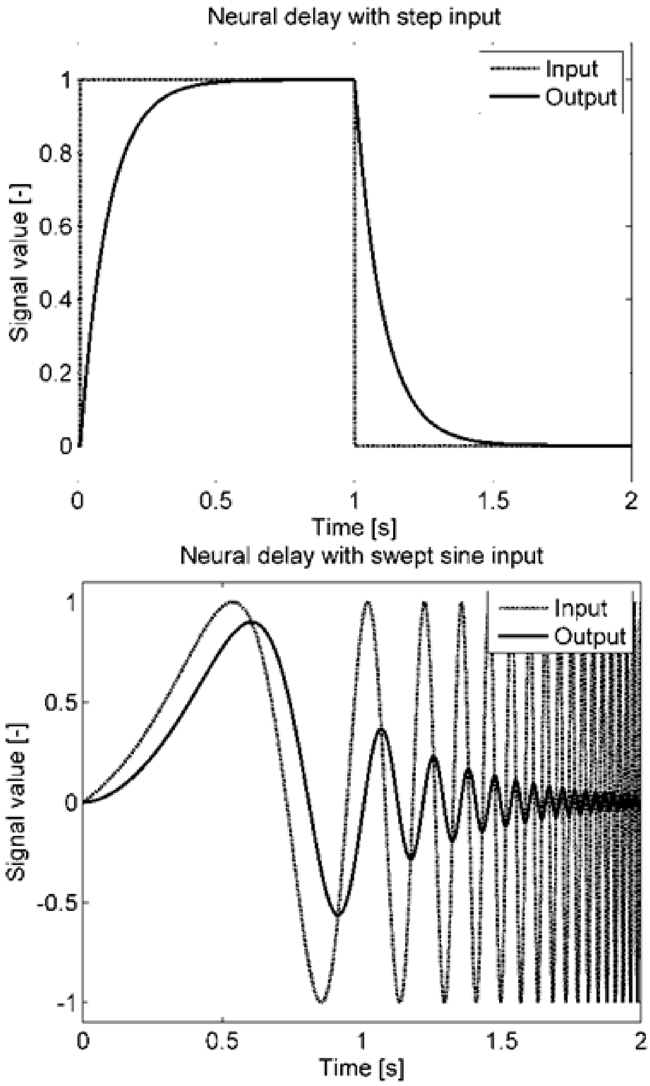


Figure 29.9: Frequency dependent behaviour of the neural delay for a step function (left) and swept sine(right).

In order to have a simulation in initial equilibrium, controller initialisation is required. To achieve this, a user-defined initial activation level has been implemented, which is added to the controller signal. The required values for the initialisation can be taken from the output of a settling simulation in which the model is run with only gravity applied to find an equilibrium. Finally, the signal from the controller, being one signal per degree of freedom, is converted to a signal for each actuator. This is done by means of a recruitment table with a constant factor for each degree of freedom and for each actuator, obtaining a weighted combination of the different degrees of freedom. The converted signals are then used as input for the actuators, which can either be muscles or multi-body actuators.

The neck controller acts in three degrees of freedom, being the three rotations of the head.

For each degree of freedom the neck controller follows the basic scheme as explained above. Depending on the user settings, the head rotations are calculated either relative to the reference space, to keep the head upright, or relative to T1, to keep the neck straight. As the vestibular system is in the head, usually a human will aim to keep its head upright. However, for large rotations of the body, as in e.g. a pedestrian impact, a strategy which keeps the neck straight is considered more realistic. Hence the user can select whether the head angles are calculated relative to the reference space or relative to T1. The muscle recruitment table for the neck is taken from literature and balanced, which means that an error in one degree of freedom results in a torque in only that degree of freedom. Besides the control on the three degrees of freedom of the head, neck co-contraction is also implemented. This refers to the simultaneous tension of all muscles without any resultant torque. Co-contraction will always be present to some extent, and is possibly higher if a person is tensed. In the active human model the co-contraction level is defined by the initial input as a relative value (0-1) of the maximum possible muscle activation. After application of the reaction time and the neural delay, the co-contraction level is included in the calculation of the muscle recruitment. The co-contraction is balanced for any pitch angle. As a constant co-contraction ratio is usually used, the delays can be switched off with the user settings, to avoid the co-contraction having to build up from zero during the first part of the simulation.

The controllers on the left and right hip each act in three degrees of freedom, being the three rotations of the hip joint, flexion-extension, medial-lateral rotation, and abduction-adduction. For each degree of freedom the hip controller follows the basic scheme as explained above. The muscle recruitment table for the hip is set up such that, for a specific degree of freedom, the muscles that have most effect in that degree of freedom are activated the most.

The controllers on the left and right knee each act on one degree of freedom per side, being knee flexion-extension. For flexion-extension the knee controller follows the basic controller scheme as explained above. The muscle recruitment for the knee divides the muscles in a group of flexors and extensors and activates all muscles in each group to the same extent.

The controllers on the left and right arm each act in only one degree of freedom per side, being elbow flexion-extension. For flexion-extension the elbow controller follows the basic controller scheme explained above. The muscle recruitment for the elbow divides the muscles into a group of flexors and a group of extensors and activates all muscles in one group equally.

The spine controller acts in three degrees of freedom per vertebra for each of the 5 lumbar and 12 thoracic vertebrae, so 17 vertebrae in total. For each vertebra, sensors are defined to measure the angle of the vertebra relative to the sacrum (pelvis). For the spine no target functions are defined. Hence, the rotation error for the spine is equal to the sensor output. Regarding the reaction time, activation switch, PID-controller and neural delay, the spine controller follows the basic scheme as explained above. The activation signal for each vertebra is then applied to that vertebra as well as to the vertebrae below, such that the spine is in a stable position. Finally, the initial activation levels are added to the activation signal (as in the basic scheme) and the signal is used in the actuators. For the spine, no muscles are included because of the complexity of the musculature of the thorax. Instead, multi-body actuators are used to directly apply a torque between two successive vertebrae.

## 29.2 Model Validation

The facet mid-size male AHM has been validated extensively for various loading conditions. Two categories of tests were conducted: volunteer tests for low-severity loading and post mortem human substitute (PMHS) tests for higher-severity loading. The blunt impact and segment tests, sled and vehicle tests and the vibration tests are detailed below.

### Blunt impact and segment tests

Blunt impact and segment tests used for the validation of the facet active human model are summarised in Table 29.4

Table 29.4: Blunt impact and segment tests used for validation of the Active Human model.

| Segment | Description | Test object | Specifications |
|---|---|---|---|
| Head | 2 frontal impact | PMHS | 2.0, 5.5 m/s |
| Shoulder | 2 lateral impact | PMHS | 4.5, 5.5 m/s |
| Thorax | 9 frontal impact | PMHS | 3.4 - 9.9 m/s |
| | 2 lateral impact | PMHS | 3.3, 5.9 m/s |
| | 1 frontal impact | Volunteer | 1.83 m/s |
| Abdomen | 3 frontal impact | PMHS | 6.9 - 9.4 m/s |
| | 2 rigid drop tests on armrest | PMHS | 4.4, 6.3 m/s |
| | 3 oblique impact | PMHS | 4.8 - 9.4 m/s |
| Pelvis | 4 lateral impact | PMHS | 3.6 - 9.8 m/s |
| Leg | 4 lateral impact | PMHS | 15.0, 20.0 m/s |

### Sled and vehicle tests

Sled and vehicle tests used for the validation of the full body behaviour of the facet active human model are summarised in Table 29.5

Table 29.5: Sled and vehicle tests used for validation of the Active Human model.

| Direction | Description | Test object | Specifications |
|---|---|---|---|
| Frontal | Rigid seat on sled | Volunteer | 15 g peak |
| | Car seat in car | Volunteer | Braking (<1 g) |
| Lateral | Rigid seat on sled | Volunteer | 7 g peak |
| | Rigid seat on sled | PMHS | 6.3, 8.7 m/s |
| | Car seat on sled | Volunteer | -2.5 - 4.0g |
| | Pedestrian impact | PMHS | 25 - 39 km/h |
| | Remote-controlled test vehicle | Volunteer | Braking (0.5 g) |
| Rear | Rigid seat on sled | Volunteer | 3.6 g peak |
| | Rigid seat on sled | PMHS | 9 - 12 g peak |
| Vertical | Rigid seat on sled | Volunteer | 6, 10 g |
| Rollover | Car seat on sled | Volunteer | Rotation |

### Vibration tests

Vibration tests used for the validation of the full body behaviour of the facet active human model are summarised in Table 29.6

Table 29.6: Vibration tests used for validation of the Active Human model.

| Direction | Description | Test object | Specifications |
|---|---|---|---|
| Vertical | Rigid seat sled | Volunteer | 0.5 - 15 Hz, 0.4 g peak |
| Frontal | Rigid seat sled | Volunteer | 0.35 - 4.05 Hz, 0.5 g peak |

## 29.3 User instructions

### Timestep

Table 29.7: Recommended time step for the Active Human model.

| Model | timestep (s) |
|---|---|
| Facet sitting mid-size male | $\leq 1 \cdot 10^{-5}$ |
| Facet standing mid-size male | $\leq 1 \cdot 10^{-5}$ |

### Dummy positioning

The sitting and standing model have different predefined initial conditions in order to be closer to the initial conditions found in common applications. The standing model is in an erect standing position with an S-curvature in the spine, while the sitting model is in a relaxed seating position with a C-curvature in the spine. From literature, the initial vertebral joint rotations of the sitting facet active human model can be taken to be as given in Table 29.9.

Table 29.8: Positioning joints of the Active Human model.

| Joint Description | Identifier | Degree of freedom[a] | | | Comment |
|---|---|---|---|---|---|
| Complete human | Dummy_jnt | D1 forward<br>R1 roll right | D2 leftward<br>R2 pitch down | D3 upward<br>R3 yaw left | |
| Lumbar intervertebral joint | L5_jnt | D1 forward<br>R1 roll right | D2 leftward<br>R2 pitch down | D3 upward<br>R3 yaw left | [b] |
| | L4_jnt | D1 forward<br>R1 roll right | D2 leftward<br>R2 pitch down | D3 upward<br>R3 yaw left | [b] |
| | L3_jnt | D1 forward<br>R1 roll right | D2 leftward<br>R2 pitch down | D3 upward<br>R3 yaw left | [b] |
| | L2_jnt | D1 forward<br>R1 roll right | D2 leftward<br>R2 pitch down | D3 upward<br>R3 yaw left | [b] |
| | L1_jnt | D1 forward<br>R1 roll right | D2 leftward<br>R2 pitch down | D3 upward<br>R3 yaw left | [b] |
| Thoracic intervertebral joint | T12_jnt | D1 forward<br>R1 roll right | D2 leftward<br>R2 pitch down | D3 upward<br>R3 yaw left | [b] |
| | T11_jnt | D1 forward<br>R1 roll right | D2 leftward<br>R2 pitch down | D3 upward<br>R3 yaw left | [b] |
| | T10_jnt | D1 forward<br>R1 roll right | D2 leftward<br>R2 pitch down | D3 upward<br>R3 yaw left | [b] |
| | T9_jnt | D1 forward<br>R1 roll right | D2 leftward<br>R2 pitch down | D3 upward<br>R3 yaw left | [b] |
| | T8_jnt | D1 forward<br>R1 roll right | D2 leftward<br>R2 pitch down | D3 upward<br>R3 yaw left | [b] |
| | T7_jnt | D1 forward<br>R1 roll right | D2 leftward<br>R2 pitch down | D3 upward<br>R3 yaw left | [b] |
| | T6_jnt | D1 forward<br>R1 roll right | D2 leftward<br>R2 pitch down | D3 upward<br>R3 yaw left | [b] |

*Continued on the next page*

*Table 29.8 cont.*

| Joint Description | Identifier | Degree of freedom[a] | | | Comment |
|---|---|---|---|---|---|
| | T5_jnt | D1 forward<br>R1 roll right | D2 leftward<br>R2 pitch down | D3 upward<br>R3 yaw left | [b] |
| | T4_jnt | D1 forward<br>R1 roll right | D2 leftward<br>R2 pitch down | D3 upward<br>R3 yaw left | [b] |
| | T3_jnt | D1 forward<br>R1 roll right | D2 leftward<br>R2 pitch down | D3 upward<br>R3 yaw left | [b] |
| | T2_jnt | D1 forward<br>R1 roll right | D2 leftward<br>R2 pitch down | D3 upward<br>R3 yaw left | [b] |
| | T1_jnt | D1 forward<br>R1 roll right | D2 leftward<br>R2 pitch down | D3 upward<br>R3 yaw left | [b] |
| Cervical intervertebral joint | T12_jnt | D1 forward<br>R1 roll right | D2 leftward<br>R2 pitch down | D3 upward<br>R3 yaw left | [b] |
| | C7_jnt | D1 forward<br>R1 roll right | D2 leftward<br>R2 pitch down | D3 upward<br>R3 yaw left | [b] |
| | C6_jnt | D1 forward<br>R1 roll right | D2 leftward<br>R2 pitch down | D3 upward<br>R3 yaw left | [b] |
| | C5_jnt | D1 forward<br>R1 roll right | D2 leftward<br>R2 pitch down | D3 upward<br>R3 yaw left | [b] |
| | C4_jnt | D1 forward<br>R1 roll right | D2 leftward<br>R2 pitch down | D3 upward<br>R3 yaw left | [b] |
| | C3_jnt | D1 forward<br>R1 roll right | D2 leftward<br>R2 pitch down | D3 upward<br>R3 yaw left | [b] |
| | C2_jnt | D1 forward<br>R1 roll right | D2 leftward<br>R2 pitch down | D3 upward<br>R3 yaw left | [b] |
| Atlanto-axial joint | C1_jnt | D1 forward<br>R1 roll right | D2 leftward<br>R2 pitch down | D3 upward<br>R3 yaw left | [b] |
| Atlanto-occipital joint | HeadOC_jnt | D1 forward<br>R1 roll right | D2 leftward<br>R2 pitch down | D3 upward<br>R3 yaw left | [b] |
| Sternum joint | SternumUp_jnt | D1 forward<br>R1 roll right | D2 leftward<br>R2 pitch down | D3 upward<br>R3 yaw left | [b] |
| Left sterno-clavicular joint | SternoClavicularL_jnt | D1 backward<br>R1 roll left | D2 leftward<br>R2 pitch down | D3 downward<br>R3 yaw right | [b] |
| Right sterno-clavicular joint | SternoClavicularR_jnt | D1 forward<br>R1 roll right | D2 leftward<br>R2 pitch down | D3 upward<br>R3 yaw left | [b] |
| Left acromio-clavicular joint | AcromioClavicularL_jnt | R1 roll left | R2 pitch down | R3 yaw right | [b] |
| Right acromio-clavicular joint | AcromioClavicularR_jnt | R1 roll right | R2 pitch down | R3 yaw left | [b] |
| Left glenohumeral joint (shoulder) | GlenohumeralL_jnt | R1 Adduction (roll left) | D2 Flexion (yaw right) | D3 Lateral rotation (pitch up) | |
| Right glenohumeral joint (shoulder) | GlenohumeralR_jnt | R1 Adduction (roll right) | D2 Flexion (yaw left) | D3 Lateral rotation (pitch up) | |
| Left elbow | ElbowL_jnt | R1 Flexion (yaw right) | | | |
| Right elbow | ElbowR_jnt | R1 Flexion (yaw left) | | | |

*Continued on the next page*

*Table 29.8 cont.*

| Joint Description | Identifier | Degree of freedom[a] | | | | | | Comment |
|---|---|---|---|---|---|---|---|---|
| Left radio-ulnar joint | RadioUlnarisL_jnt | R1 | Supination (pitch down) | | | | | |
| Right radio-ulnar joint | RadioUlnarisR_jnt | R1 | Supination (pitch down) | | | | | |
| Left wrist | WristL_jnt | R1 | Flexion (roll left) | R2 | Adduction (yaw right) | | | |
| Right wrist | WristR_jnt | R1 | Flexion (roll right) | R2 | Adduction (yaw left) | | | |
| Left fingers | FingerUp/Mid/LowL_jnt | R1 | Flexion (roll left) | | | | | [c] |
| Right fingers | FingerUp/Mid/LowR_jnt | R1 | Flexion (roll right) | | | | | [c] |
| Left thumb | ThumbUp/Mid/LowL_jnt | R1 | Flexion (roll left) | | | | | [c] |
| Right thumb | ThumbUp/Mid/LowR_jnt | R1 | Flexion (roll right) | | | | | [c] |
| Left hip | HipL_jnt | R1 | Extension (pitch down) | R2 | Adduction (roll left) | R3 | Lateral rotation (yaw left) | |
| Right hip | HipR_jnt | R1 | Extension (pitch down) | R2 | Adduction (roll right) | R3 | Lateral rotation (yaw right) | |
| Left knee | KneeL_jnt | R1 | Adduction (roll left) | D2 | Flexion (pitch down) | D3 | Medial rotation (yaw right) | |
| Right knee | KneeR_jnt | R1 | Adduction (roll right) | D2 | Flexion (pitch down) | D3 | Medial rotation (yaw left) | |
| Left ankle | AnkleL_jnt | R1 | Lateral rotation (yaw left) | R2 | Plantarflexion (pitch down) | R3 | Inversion (roll left) | |
| Right ankle | AnkleTorsionR_jnt | R1 | Lateral rotation (yaw right) | R2 | Plantarflexion (pitch down) | R3 | Inversion (roll right) | |
| Left shoe joint | ShoeL_jnt | D1<br>R1 | forward<br>roll right | D2<br>R2 | leftward<br>pitch down | D3<br>R3 | upward<br>yaw left | [b] |
| Right shoe joint | ShoeR_jnt | D1<br>R1 | forward<br>roll right | D2<br>R2 | leftward<br>pitch down | D3<br>R3 | upward<br>yaw left | [b] |

[a] Positive translation or rotation given in global co-ordinate system while dummy is in reference position (see Figure 1.2).

[b] In principle only for equilibrium state, however it might be necessary to rotate joints to position neck and head correctly.

[c] Included in a DISABLE block in the user file

Table 29.9: Vertebral joint rotations in a relaxed seating position according to Davidsson *et al* (1998).

| Joint | R1 | R2 | R3 |
|---|---|---|---|
| L5_jnt | 0.0 | 0.1021 | 0.0 |
| L4_jnt | 0.0 | 0.0821 | 0.0 |

*Continued on the next page*

*Table 29.9 cont.*

| Joint | R1 | R2 | R3 |
|---|---|---|---|
| L3_jnt | 0.0 | 0.0348 | 0.0 |
| L2_jnt | 0.0 | 0.0348 | 0.0 |
| L1_jnt | 0.0 | 0.0348 | 0.0 |
| T12_jnt | 0.0 | 0.0346 | 0.0 |
| T11_jnt | 0.0 | 0.0346 | 0.0 |
| T10_jnt | 0.0 | 0.0346 | 0.0 |
| T9_jnt | 0.0 | 0.0346 | 0.0 |
| T8_jnt | 0.0 | 0.0346 | 0.0 |
| T7_jnt | 0.0 | 0.0346 | 0.0 |
| T6_jnt | 0.0 | 0.0346 | 0.0 |
| T5_jnt | 0.0 | 0.0346 | 0.0 |
| T4_jnt | 0.0 | 0.0146 | 0.0 |
| T3_jnt | 0.0 | 0.0146 | 0.0 |
| T2_jnt | 0.0 | 0.0146 | 0.0 |
| T1_jnt | 0.0 | 0.0146 | 0.0 |
| C7_jnt | 0.0 | 0.0 | 0.0 |
| C6_jnt | 0.0 | 0.0 | 0.0 |
| C5_jnt | 0.0 | 0.0 | 0.0 |
| C4_jnt | 0.0 | 0.0 | 0.0 |
| C3_jnt | 0.0 | 0.0 | 0.0 |
| C2_jnt | 0.0 | 0.0 | 0.0 |
| C1_jnt | 0.0 | 0.0 | 0.0 |
| HeadOC_jnt | 0.0 | 0.0 | 0.0 |

Positioning of the facet active human model, using a pre-simulation to obtain an equilibrium, can be done in three steps:

1. The facet active human model is positioned manually as described above, using the Human_attachment and INITIAL.JOINT_POS elements in the user file. The human model can best be positioned just above the seat with its pelvis in the correct horizontal position.

2. A pre-simulation is performed in which the facet active human model is put into the seat using a gravitational field only (acceleration field of -9.81 $m/s^2$ in the z-direction). The run time for positioning the facet active human model needs to be sufficient for the model to find equilibrium (typically about 0.5 to 1 s). All active behaviour should be switched on (DEFINE's set to 1) in order to maintain an upright seating position. In order to export the initial posture and activation levels for a load case simulation, the output needs to be defined for all positioning joints (OUTPUT_JOINT_DOF) and all activation level operators (OUTPUT_CONTROL_SYSTEM). All joints for which the initial positions are not defined in the user file should be locked. The state of the flexible bodies in the thorax and the abdomen should be set to rigid. To facilitate these steps, in the user file a DISABLE element is included which contains all xml-elements required to define the output and to lock the non-positioning joints and flexible bodies. Depending on the application, some additional joints could be locked (e.g. the wrists and radio-ulnar joints to keep the arms in the desired position) or point-restraints can be added to keep e.g. the hands on a steering wheel.

3. The output from the final time step in the JNTPOS file of the pre-simulation can then be copied to the positioning elements (INITIAL.JOINT_POS) of the impact simulation file. For this the Import-INITIAL.JOINT_POS tool or the Active Human Initialiser tool in XMADgic can be used. In the impact simulation, the joints and bodies that were locked/rigid for the settling should be set to free/deformable again, any additional point-restraints should be removed and

the belt fitted around the positioned human model using e.g. the XMADgic belt fitting tool. To have the controllers start at the levels reached during the settling, the activation levels in the last timestep of the *.control file of the settling should be used to define the initial activation levels in the model, as described in the section below relating to active behaviour control. Users of XMADgic (7.6.1 and higher) can use the built-in Active Human Initialiser tool to import both joint positioning and initial activation levels.

### Dummy contacts

Table 29.10: Available groups to define contact between the Active Human components and environment.

| **Contact Description** | **Identifier**[a] | **Facet model** |
|---|---|---|
| Full Human | HumanBody_gfe | Elements and nodes |
| Full Human w/o arms | BodyNoArms_gfe | Elements and nodes |
| Full Human w/o head | BodyNoHead_gfe | Elements and nodes |
| Head | Head_gfe | Elements and nodes |
| Neck | Neck_gfe | Elements and nodes |
| Thorax | Thorax_gfe | Elements and nodes |
| Pelvis | Pelvis_gfe | Elements and nodes |
| Iliac wings[b] | IliacWings_gfe | Elements and nodes |
| Complete left arm | ArmL_gfe | Elements and nodes |
| Complete right arm | ArmR_gfe | Elements and nodes |
| Bones of left shoulder and upper arm [c] | ShoulderBonesL_gfe | Elements and nodes |
| Bones of left shoulder and upper arm [c] | ShoulderBonesR_gfe | Elements and nodes |
| Upper left arm | Upper_ArmL_gfe | Elements and nodes |
| Upper right arm | Upper_ArmR_gfe | Elements and nodes |
| Lower left arm (incl. hand) | Lower_ArmL_gfe | Elements and nodes |
| Lower right arm (incl. hand) | Lower_ArmR_gfe | Elements and nodes |
| Complete left leg | LegL_gfe | Elements and nodes |
| Complete right leg | LegR_gfe | Elements and nodes |
| Upper left leg | Upper_LegL_gfe | Elements and nodes |
| Upper right leg | Upper_LegR_gfe | Elements and nodes |
| Lower left leg (incl. hand) | Lower_LegL_gfe | Elements and nodes |
| Lower right leg (incl. hand) | Lower_LegR_gfe | Elements and nodes |
| Left Shoe | ShoeL_gfe | Elements and nodes |
| Right Shoe | ShoeR_gfe | Elements and nodes |

[a] L = Left; R = Right

[b] To be used in the lapbelt contact predefined in the user file

[c] To be used in the shoulderbelt contact predefined in the user file

### FE belt positioning and contact definition

In the sitting model, contacts have been predefined for belts and placed in a DISABLE block. If a belt is added to the model, these contacts should be enabled and the references to the belt groups (as SLAVE_SURFACE) should be updated. Characteristic-based contacts are predefined between the belts and BodyNoArms_gfe. These are the main contact between the human and the belt. In order to prevent unrealistically deep penetrations of the belt into the human body, surface-to-surface contacts with edge-contact have been predefined between the belts and the skeleton. The main advantage of using the group BodyNoArms_gfe is that, once the contacts with the belt are defined, the XMADgic beltfitting tool will automatically detect this group for the belt fitting and the belt can be fitted without interference of the arms. In most applications the belts will not contact the arms, so that omitting these from the contact is no problem. Depending on the position of the human model and the belt anchor points, the XMADgic beltfitting tool might incorrectly fit the shoulderbelt underneath the legs. This then can be resolved by selecting Thorax_gfe in the beltfitting tool. If the arms need to be included in the belt contact, use of the HumanBody_gfe contact group is recommended. In this case the user should either select the group BodyNoArms_gfe during belt fitting, or disable the initial conditions of the Glenohumeral[LR]_jnt and Elbow[LR]_jnt during belt fitting to keep the arms to the side. Disabling these initial conditions during belt fitting is also required when using XMADgic versions 7.4 or earlier.

### Output

The output signals and injury criteria for the Active Human are given below.

A selection of the most commonly-used output signals is supplied in the user file. It is important to bear in mind that many injury criteria available in the model have been developed for the assessment of injury risk based on the performance of the ATDs, and the injury risk may not directly correlate when calculated using the active human model output. Similarly, the chest deflection signal ChestDeflection_dis is an approximation to the corresponding hybrid-III output.

Table 29.11: Active Human output signals.

| Sensor | Identifier | Signal | | | | | | | Filter |
|---|---|---|---|---|---|---|---|---|---|
| | | resultant | x | direction[a] | y | direction[a] | z | direction[a] | |
| Head | | | | | | | | | |
| CG acceleration | HeadCG_acc | ar | a1 | forward | a2 | lateral | a3 | vertical | CFC1000 |
| OC acceleration | HeadOC_acc | ar | a1 | forward | a2 | lateral | a3 | vertical | CFC1000 |
| CG displacement | HeadCG_dis | dr | d1 | forward | d2 | lateral | d3 | vertical | CFC180 |
| OC displacement | HeadOC_dis | dr | d1 | forward | d2 | lateral | d3 | vertical | CFC1000 |
| CG position | HeadCG_pos | dr | d1 | forward | d2 | lateral | d3 | vertical | CFC180 |
| angular acc. | Head_aac | ar | a1 | roll right | a2 | pitch down | a3 | yaw left | CFC1000 |
| angular disp. | Head_ang | apos | r1 | roll right | r2 | pitch down | r3 | yaw left | CFC1000 |
| CG velocity | HeadCG_vel | vr | v1 | forward | v2 | lateral | v3 | vertical | CFC180 |
| OC force | HeadOC_lce_F[b] | fr | f1 | forward | f2 | lateral | f3 | vertical | CFC1000 |
| OC torque | HeadOC_lce_T[b] | tr | t1 | roll right | t2 | pitch down | t3 | yaw left | CFC600 |

*Continued on the next page*

*Table 29.11 cont.*

| Sensor | Identifier | Signal | | | | | | | Filter |
|---|---|---|---|---|---|---|---|---|---|
| | | resultant | x | direction[a] | y | direction[a] | z | direction[a] | |
| Head-T1 | | | | | | | | | |
| CG-T1 relative displacement | HeadCG_T1_dis | dr | d1 | forward | d2 | lateral | d3 | vertical | CFC600 |
| OC-T1 relative displacement | HeadOC_T1_dis | dr | d1 | forward | d2 | lateral | d3 | vertical | CFC600 |
| relative angle | Head_T1_ang | apos | r1 | roll right | r2 | pitch down | r3 | yaw left | CFC1000 |
| Neck | | | | | | | | | |
| C1 acceleration | C1_acc_CFC60 | ar | a1 | forward | a2 | lateral | a3 | vertical | CFC60 |
| Upper neck force | NeckUp_lce_F[b] | fr | f1 | forward | f2 | lateral | f3 | vertical | CFC1000 |
| | NeckUp_lce_F_CFC600[b] | | | | | | | | CFC600 |
| Upper neck torque | NeckUp_lce_T[b] | tr | t1 | roll right | t2 | pitch down | t3 | yaw left | CFC600 |
| *Cn* force[c] | *Cn*_lce_F[b] | fr | f1 | forward | f2 | lateral | f3 | vertical | CFC1000 |
| *Cn* torque[c] | *Cn*_lce_T[b] | tr | t1 | roll right | t2 | pitch down | t3 | yaw left | CFC600 |

*Continued on the next page*

*Table 29.11 cont.*

| Sensor | Identifier | Signal resultant | x | direction[a] | y | direction[a] | z | direction[a] | Filter |
|---|---|---|---|---|---|---|---|---|---|
| Thorax | | | | | | | | | |
| T1 acceleration | T1_acc | ar | a1 | forward | a2 | lateral | a3 | vertical | CFC1000 |
| | T1_acc_CFC60 | | | | | | | | CFC60 |
| T1 displacement | T1_dis | dr | d1 | forward | d2 | lateral | d3 | vertical | CFC1000 |
| T1 position | T1_pos | dr | d1 | forward | d2 | lateral | d3 | vertical | CFC180 |
| T1 angular acc. | T1_aac | ar | a1 | roll right | a2 | pitch down | a3 | yaw left | CFC1000 |
| T1 angular disp. | T1_ang | apos | r1 | roll right | r2 | pitch down | r3 | yaw left | CFC1000 |
| Thorax (T8) acc. | Thorax_acc | ar | a1 | forward | a2 | lateral | a3 | vertical | CFC180 |
| T12 acceleration | T12_acc | ar | a1 | forward | a2 | lateral | a3 | vertical | CFC180 |
| Chest compression | ChestDeflection_dis[f] | dr | d1 | forward | | | | | CFC600 |
| | ChestDefl_dis_CFC180 [f] | dr | d1 | forward | | | | | CFC180 |
| Chest compression velocity | ChestDeflection_vel_CFC600[f] | vr | v1 | forward | | | | | CFC600 |
| | ChestDeflection_vel_CFC180[f] | vr | v1 | forward | | | | | CFC180 |
| | ChestDeflection_vel_CFC60[f] | vr | v1 | forward | | | | | CFC60 |
| Sternum acc. | Sternum_acc | ar | a1 | forward | a2 | lateral | a3 | vertical | CFC1000 |
| | Sternum_acc_CFC180 | | | | | | | | CFC180 |
| Sternal rib *n* acc. wrt spine | Thorax*n*Front_acc_CFC180 | ar | a1 | forward | a2 | lateral | a3 | vertical | CFC180 |
| L/R rib *n* acc. wrt spine | Thorax*n*[L/R]_acc_CFC180 | ar | a1 | forward | a2 | lateral | a3 | vertical | CFC180 |
| Sternum disp./vel. wrt T1 | Sternum_T1_dvl | dr | d1 | forward | d2 | lateral | d3 | vertical | CFC600 |
| Sternal rib *n* dist./vel. wrt spine | Ribs*n*_Spine_dvl[g] | dr | d1 | forward | d2 | lateral | d3 | vertical | CFC180 |
| L/R rib *n* dist./vel. wrt spine | Rib*n*[L/R]_Spine_dvl[g] | dr | d1 | forward | d2 | lateral | d3 | vertical | CFC180 |
| Sternal rib *n* deflection | Ribs*n*_Spine_dis[g] | dr | d1 | forward | d2 | lateral | d3 | vertical | CFC600 |
| L/R rib *n* deflection | Rib*n*[L/R]_Spine_dis[g] | dr | d1 | forward | d2 | lateral | d3 | vertical | CFC600 |
| T*n* force[d] | T*n*_lce_F[b] | fr | f1 | forward | f2 | lateral | f3 | vertical | CFC1000 |
| T*n* torque[d] | T*n*_lce_T[b] | tr | t1 | roll right | t2 | pitch down | t3 | yaw left | CFC600 |
| L*n* force[e] | L*n*_lce_F[b] | fr | f1 | forward | f2 | lateral | f3 | vertical | CFC1000 |
| L*n* torque[e] | L*n*_lce_T[b] | tr | t1 | roll right | t2 | pitch down | t3 | yaw left | CFC600 |
| Pelvis | | | | | | | | | |
| Pelvis acceleration | Pelvis_acc | ar | d1 | forward | a2 | lateral | a3 | vertical | CFC1000 |
| Pelvis position | Pelvis_pos | dr | f1 | forward | d2 | lateral | d3 | vertical | CFC180 |
| Left/right hip force | Hip[L/R]_lce_F[b] | fr | | forward | f2 | lateral | f3 | vertical | CFC600 |
| Femurs (left/right) | | | | | | | | | |
| Femur acceleration | Femur*n*[L/R]_acc[h] | ar | a1 | forward | a2 | lateral | a3 | vertical | CFC1000 |
| Femur force | Femur[L/R]_lce_F[b] | fr | f1 | forward | f2 | lateral | f3 | vertical | CFC600 |
| Femur torque | Femur[L/R]_lce_T[b] | tr | t1 | roll right | t2 | pitch down | t3 | yaw left | CFC600 |

*Continued on the next page*

*Table 29.11 cont.*

| Sensor | Identifier | Signal | | | | | | | Filter |
|---|---|---|---|---|---|---|---|---|---|
| | | resul-tant | x | direc-tion[a] | y | direc-tion[a] | z | direc-tion[a] | |
| Knees (left/right) | | | | | | | | | |
| Knee position | Knee[L/R]_pos | dr | d1 | forward | d2 | lateral | d3 | vertical | CFC180 |
| Knee shear/compress. | Knee[L/R]_dis | dr | d1 | forward | d2 | lateral | d3 | vertical | CFC180 |
| Knee bending/torsion | Knee[L/R]_ang | apos | r1 | flexion | r2 | lateral bending | r3 | torsion | CFC1000 |
| Lower legs (left/right) | | | | | | | | | |
| Tibia acc. | Tibia*n*[L/R]_acc[h] | ar | a1 | forward | a2 | lateral | a3 | vertical | CFC1000 |
| Ankle position | Ankle[L/R]_pos | dr | d1 | forward | d2 | lateral | d3 | vertical | CFC180 |
| Upper tibia force | TibiaUp[L/R]_lce_F[b] | fr | f1 | forward | f2 | lateral | f3 | vertical | CFC600 |
| Upper tibia torque | TibiaUp[L/R]_lce_T[b] | tr | t1 | roll right | t2 | pitch down | t3 | yaw left | CFC600 |
| Mid-tibia force | TibiaMid[L/R]_lce_F[b] | fr | f1 | forward | f2 | lateral | f3 | vertical | CFC600 |
| Mid-tibia torque | TibiaMid[L/R]_lce_T[b] | tr | t1 | roll right | t2 | pitch down | t3 | yaw left | CFC600 |
| Lower tibia force | TibiaLow[L/R]_lce_F[b] | fr | f1 | forward | f2 | lateral | f3 | vertical | CFC600 |
| Lower tibia torque | TibiaLow[L/R]_lce_T[b] | tr | t1 | roll right | t2 | pitch down | t3 | yaw left | CFC600 |
| Foot acc. | Foot[L/R]_acc | ar | a1 | forward | a2 | lateral | a3 | vertical | CFC1000 |

[a] Positive direction given according to SAE J211/1

[b] These output signals are used for calculation of the load cell output and for injury criteria. The force output can be found in the RTF file and the torque output in the RTT file. It is not recommended to use these signals, but instead the load cell output listed below

[c] n = 1 to 7, neck vertebrae from upper to lower

[d] n = 1 to 12, thoracic vertebrae from upper to lower

[e] n = 1 to 5, lumbar vertebrae from upper to lower

[f] Analogous to Hybrid-III output

[g] n = 1 to 4, from lower to upper

[h] n=1 to 4, from proximal to distal

Table 29.12: Active Human load cell output.

| Sensor | Identifier[a] | Signal | | | | | | | Filter |
|---|---|---|---|---|---|---|---|---|---|
| | | resul-tant | x | direc-tion[b] | y | direc-tion[b] | z | direc-tion[b] | |
| Upper neck force | NeckUp_F*dir*_lce | fr | f1 | forward | f2 | lateral | f3 | vertical | CFC1000 |
| Upper neck torque | NeckUp_M*dir*_lce | tr | t1 | roll right | t2 | pitch down | t3 | yaw left | CFC600 |
| Head OC force | HeadOC_F*dir*_lce | fr | f1 | forward | f2 | lateral | f3 | vertical | CFC1000 |
| Head OC torque | HeadOC_M*dir*_lce | tr | t1 | roll right | t2 | pitch down | t3 | yaw left | CFC600 |
| Cervical spine force | C*n*_F*dir*_lce[c] | fr | f1 | forward | f2 | lateral | f3 | vertical | CFC1000 |
| Cervical spine torque | C*n*_M*dir*_lce[c] | tr | t1 | roll right | t2 | pitch down | t3 | yaw left | CFC600 |

*Continued on the next page*

Table 29.12 cont.

| Sensor | Identifier[a] | Signal resultant | x | direction[b] | y | direction[b] | z | direction[b] | Filter |
|---|---|---|---|---|---|---|---|---|---|
| Thoracic spine force | Tn_Fdir_lce[d] | fr | f1 | forward | f2 | lateral | f3 | vertical | CFC1000 |
| Thoracic spine torque | Tn_Mdir_lce[d] | tr | t1 | roll right | t2 | pitch down | t3 | yaw left | CFC600 |
| Lumbar spine force | Ln_Fdir_lce[e] | fr | f1 | forward | f2 | lateral | f3 | vertical | CFC1000 |
| Lumbar spine torque | Ln_Mdir_lce[e] | tr | t1 | roll right | t2 | pitch down | t3 | yaw left | CFC600 |
| Hip force | Hip[L/R]_Fdir_lce | fr | f1 | lateral | f2 | frontal | f3 | vertical | CFC600 |
| Femur force | Femur[L/R]_Fdir_lce | fr | f1 | forward | f2 | lateral | f3 | vertical | CFC600 |
| Femur torque | Femur[L/R]_Mdir_lce | tr | t1 | roll right | t2 | pitch down | t3 | yaw left | CFC600 |
| Upper tibia force | TibiaUp[L/R]_Fdir_lce | fr | f1 | forward | f2 | lateral | f3 | vertical | CFC600 |
| Upper tibia torque | TibiaUp[L/R]_Mdir_lce | tr | t1 | roll right | t2 | pitch down | t3 | yaw left | CFC600 |
| Mid tibia force | TibiaMid[L/R]_Fdir_lce | fr | f1 | forward | f2 | lateral | f3 | vertical | CFC600 |
| Mid tibia torque | TibiaMid[L/R]_Mdir_lce | tr | t1 | roll right | t2 | pitch down | t3 | yaw left | CFC600 |
| Lower tibia force | TibiaLow[L/R]_Fdir_lce | fr | f1 | forward | f2 | lateral | f3 | vertical | CFC600 |
| Lower tibia torque | TibiaLow[L/R]_Mdir_lce | tr | t1 | roll right | t2 | pitch down | t3 | yaw left | CFC600 |

[a] *dir* is direction x, y or z

[b] Positive direction given according to SAE J211/1

[c] n = 1 to 7, neck vertebrae from upper to lower

[d] n = 1 to 12, thoracic vertebrae from upper to lower

[e] n = 1 to 5, lumbar vertebrae from upper to lower

The following sensor output is defined in a DISABLE block in the user file. The block can be enabled in order to give the output required for settling runs.

Table 29.13: Active Human sensor/controller output (in control file).

| Sensor | Identifier | Type | Filter |
|---|---|---|---|
| Head roll angle | Head_RX_control | Operator | None |
| Head pitch angle | Head_RY_control | Operator | None |
| Head yaw angle | Head_RZ_control | Operator | None |
| Tn forward bending angle | Tn_RYfwd_sen[a] | Sensor | None |
| Tn lateral bending angle | Tn_RXlat_sen[a] | Sensor | None |
| Tn torsion angle | Tn_RZtor_sen[a] | Sensor | None |
| Ln forward bending angle | Ln_RYfwd_sen[b] | Sensor | None |
| Ln lateral bending angle | Ln_RXlat_sen[b] | Sensor | None |
| Ln torsion angle | Ln_RZtor_sen[b] | Sensor | None |
| Hip flexion angle | Hip[L/R]_flexion_sen | Sensor | None |
| Hip abduction angle | Hip[L/R]_abduction_sen | Sensor | None |
| Hip axial rotation angle | Hip[L/R]_rotation_sen | Sensor | None |

*Continued on the next page*

29

*Table 29.13 cont.*

| Sensor | Identifier | Type | Filter |
|---|---|---|---|
| Elbow flexion angle | Elbow[L/R]_sen | Sensor | None |
| Radio-ulnar rotation angle | RU[L/R]_sen | Sensor | None |
| Knee extension angle | Knee[L/R]_extension_sen | Sensor | None |
| Head roll activation level | Head_Roll_act | Operator | None |
| Head pitch activation level | Head_Pitch_act | Operator | None |
| Head yaw activation level | Head_Yaw_act | Operator | None |
| T*n* forward bending activation level | T*n*_RYfwd_act[a] | Operator | None |
| T*n* lateral bending activation level | T*n*_RXlat_act[a] | Operator | None |
| T*n* torsion activation level | T*n*_RZtor_act[a] | Operator | None |
| L*n* forward bending activation level | L*n*_RYfwd_act[b] | Operator | None |
| L*n* lateral bending activation level | L*n*_RXlat_act[b] | Operator | None |
| L*n* torsion activation level | L*n*_RZtor_act[b] | Operator | None |
| Hip flexion activation level | Hip[L/R]_flexion_act | Operator | None |
| Hip abduction activation level | Hip[L/R]_abduction_act | Operator | None |
| Hip axial rotation activation level | Hip[L/R]_rotation_act | Operator | None |
| Elbow flexion activation level | Elbow[L/R]_act | Operator | None |
| Radio-ulnar rotation activation level | RU[L/R]_act | Operator | None |
| Knee extension activation level | Knee[L/R]_extension_act | Sensor | None |

[a] n = 1 to 12, thoracic vertebrae from upper to lower
[b] n = 1 to 5, lumbar vertebrae from upper to lower

## Injury

Table 29.14: Injury criteria defined for the Active Human.

| Injury criteria | Identifier | Filter |
|---|---|---|
| Head | | |
| HIC (15) | HIC15_inj | CFC1000 |
| HIC (36) | HIC36_inj | CFC1000 |
| 3ms (cum) | H3MS_inj[e] | CFC1000 |
| 3ms (cont) | Con3MS_HeadCG_inj | CFC1000 |
| Max. res. acceleration | HaccRpeak_inj[e] | CFC1000 |
| Neck | | |
| max Tension | NecktensZpeak_inj | |
| max Compression | NeckcompZpeak_inj | |
| MOC | | |
| lateral | MOCx_inj | CFC600 (force and moment) |
| frontal | MOCy_inj | CFC600 (force and moment) |
| | MOCy_CFC1000_inj | CFC1000/CFC600 (force/moment) |
| FNIC | | |
| tension | FNICtension_inj | CFC1000 |
| shear | FNICshear_inj | CFC1000 |
| bending | FNICbending_inj | CFC1000/CFC600 (force/moment) |
| NIC Rearward | NIC_rearward_C1T1_inj | CFC60 |

*Continued on the next page*

Table 29.14 cont.

| Injury criteria | Identifier | Filter |
|---|---|---|
| NIJ | | |
| tension-extension | NTE_inj | CFC600 (force and moment) |
| tension-flexion | NTF_inj | CFC600 (force and moment) |
| compression-extension | NCE_inj | CFC600 (force and moment) |
| compression-flexion | NCF_inj | CFC600 (force and moment) |
| tension-extension | NTE_CFC1000_inj[e] | CFC1000/CFC600 (force/moment)[a] |
| tension-flexion | NTF_CFC1000_inj[e] | CFC1000/CFC600 (force/moment)[a] |
| compression-extension | NCE_CFC1000_inj[e] | CFC1000/CFC600 (force/moment)[a] |
| compression-flexion | NCF_CFC1000_inj[e] | CFC1000/CFC600 (force/moment)[a] |
| NKM | | |
| flexion-anterior | NFA_inj | CFC600 (force and moment) |
| extension-anterior | NEA_inj | CFC600 (force and moment) |
| flexion-posterior | NFP_inj | CFC600 (force and moment) |
| extension-posterior | NEP_inj | CFC600 (force and moment) |
| Thorax | | |
| 3ms (cumulative) | | |
| Thorax | T3MS_inj | CFC180 |
| T1 | Cum3MS_T1_inj | CFC1000 |
| T12 | Cum3MS_T12_inj | CFC1000 |
| Sternum | Cum3MS_Sternum_inj | CFC1000 |
| | Cum3MS_Sternum_CFC180_inj | CFC180 |
| 3ms (contiguous) | | |
| T1 | Con3MS_T1_inj | CFC1000 |
| T12 | Con3MS_T12_inj | CFC1000 |
| Sternum | Con3MS_Sternum_inj | CFC1000 |
| | Con3MS_Sternum_CFC180_inj | CFC180 |
| Combined Thoracic Index | | |
| Thorax | CTI_inj | CFC180/CFC600 (acc./disp/) |
| Upper sternum | CTISternum_inj | CFC180/CFC600 (acc./disp/) |
| Centre rib layer $n$[b] | CTIRibs$n$_inj | CFC180/CFC600 (acc./disp/) |
| left/right rib layer $n$[c] | CTIRib$n$[L/R]_inj | CFC180/CFC600 (acc./disp/) |
| VC | | |
| VC | VC_inj_CFC180 | CFC180 |
| | VC_inj_CFC600 | CFC600 |
| Centre rib layer $n$[b] | VCRibs$n$_inj | CFC180 |
| left/right rib layer $n$[c] | VCRib$n$[L/R]_inj | CFC180 |
| Pelvis | | |
| 3ms (cumulative) | Cum3MS_Pelvis_inj | CFC1000 |
| 3ms (contiguous) | Con3MS_Pelvis_inj | CFC1000 |
| Femurs | | |
| Femur force criterion | FFC[L/R]_inj | CFC600 |
| Peak compression | Femur[L/R]compZpeak_inj | |
| Knee slider peak displacement | kneeslider[L/R]_inj | CFC180 |
| Tibia | | |
| TI | TIUp[L/R]_inj[d,e] | CFC600 |
| | TILow[L/R]_inj[d,e] | CFC600 |
| TCFC | TCFCUp[L/R]_inj | CFC600 |
| | TCFCLow[L/R]_inj | CFC600 |

Continued on the next page

*Table 29.14 cont.*

| Injury criteria | Identifier | Filter |
|---|---|---|
| Feet | | |
| Peak acceleration | Foot[L/R]accRpeak_inj$^{(e,f)}$ | CFC1000 |

[(a)] NIJ injury output with other filtering than CFC600 will generate a warning in the reprint file in MADYMO release 7.2 and older.

[(b)] n = 2 to 4, from lower to upper

[(c)] n = 1 to 4, from lower to upper

[(d)] The same injury is also written to *_adjusted_inj - this is for use with the MADYMO Protocol Rating tool. The eccentricity of the joint in the Active Human model is 0, and so the results are identical to the non='adjusted' values

[(e)] Analogous to Hybrid-III output

[(f)] The result of the 2-D acceleration vector (in ZX-plane) will be given as the maximum value

### Active behaviour control

The facet active human model allows active behaviour modelling. Sensors in the model measure the human positions, and based on their readings, control systems determine the activation levels of various active elements in the model (muscles and actuators). The behaviour of the controllers can be adapted in the user file by changing the following parameters and functions inside the SYSTEM.MODEL:

- Activation parameters (5 DEFINEs in GROUP_DEFINE)
- Neck controller parameters (5 DEFINEs in GROUP_DEFINE)
- Neck co-contraction with time (1 FUNCTION.XY)
- target angle time histories (15 FUNCTION.XYs)
- initial activation levels (66 SIGNAL.CONSTANTs in CONTROL_SYSTEM)

For each active body part, a DEFINE is present in the user file which can be used to switch the active behaviour on (VALUE=1, default) or off (VALUE=0). For all volunteer tests in the validation of the active human model these DEFINEs are set to 1, while for all cadaver tests they are set to 0. The DEFINEs are:

- NeckActivation_def (3 DOF)
- SpineActivation_def (17x3 DOF)
- HipActivation_def (2x3 DOF)
- ElbowActivation_def (2x1 DOF)
- KneeActivation_def (2x1 DOF)



The following DEFINEs are specifically for the neck controller:

- HeadRef_def [0 | 1]: Selects whether the head rotation is calculated relative to the reference space (value=0) or relative to T1 (value=1). If head control is assumed to be based mainly on vestibular input (balance), HeadRef_def should be set to 0 to keep the head upright. This is the default for the sitting model. If head control is assumed to be based mainly on proprioceptive input (muscle elongations), HeadRef_def should be set to 1 to keep the neck straight. This is the default for the standing model, as in pedestrian, bicycle or motorcycle accidents the head cannot be kept upright due to large body rotations, in which case keeping the neck straight is assumed to be more realistic.

- NeckCCR_def [0, 1]: This is the neck co-contraction ratio. It can vary between 0 (no co-contraction, default) and 1 (full co-contraction, with maximum activation of the flexor muscles). Use this DEFINE if a constant co-contraction level is used. For a variable co-contraction level, use the FUNCTION described below.

- VarNeckCCR_def [0 | 1]: This DEFINE enables (value=1) / disables (value=0, default) the delays for the neck co-contraction. If a constant co-contraction is used, no delays are required for co-contraction. If a delay is defined, for the first part of the simulation (during the time of the delay) the co-contraction will be zero. The delays can be disabled in order to have the co-contraction active during the whole simulation. If a variable co-contraction is used (FUNCTION described below), the delays may be activated by setting the value of VarNeckCCR_def to 1.

- ReactionTime_def [0, ∞]: This is the reaction time in seconds (default 0.1s), the time it takes for the controllers to respond to new events. It is not for stabilization under constant loading. The response time is different per situation; it can be a reflex time triggered by the onset of an acceleration (at e.g. the pelvis) or a reaction to an coming event. Reported motor reflex delays in literature range from 10 to 120 ms. Reaction times depend on the situation and on the person involved.

- DelayEnable_def [0, 1]: This DEFINE enables (value=1, default) / disables (value=0) the delays for all controllers. For a settling simulation, the equilibrium state should be reached within the shortest possible time and hence delays should be disabled.

The FUNCTION Neck_CCR_fun can be used to define a variable co-contraction, e.g. to simulate an increasing co-contraction as a result of a fright response. This function uses the NeckCCR_def DEFINE value by default. To make the co-contraction variable, this FUNCTION can be adjusted by the user. Note that in that case the VarNeckCCR_def DEFINE should be set to 1.

For all degrees of freedom of the neck, elbow, hip and knee, a FUNCTION *_target_fun is defined in the user file. Default, these are constant zero, to have the controller work towards the initial conditions. If a variable target is desired (e.g. voluntary or reflex motion), these functions can be adjusted. The function value is the angle relative to the initial conditions. For a smooth motion the functions should therefore start at zero.

A CONTROL_SYSTEM is included in the user file with a SIGNAL.CONSTANT defining the initial activation level for each controlled degree of freedom. If a settling run is performed with the controllers active, they will have some activation level in the final equilibrium state - these are available in the output. To include these in the final simulation, SIGNAL.CONSTANTs can be used. The conversion of the output data to model input can be done manually, or by means of the Active Human Initialiser tool, found in XMADgic (versions 7.6.1 and higher).

# 30 FMVSS 201 featureless Hybrid III Headform

A featureless Hybrid III headform as specified in FMVSS 201[1] has been developed to assess the protection offered to occupants by the interior of a vehicle when head contact occurs. This "free motion" headform is also proposed for the evaluation of head impact protection in side impacts according to the new EEVC procedures. The model of this headform is described in Section 30.1.



[1]Federal Motor Vehicle Safety Standard 201: Occupant protection in interior impact, Federal Register, Vol. 62, No. 67, April 8, 1997.

## 30.1 Model description

A finite element model of the FMVSS 201 featureless Hybrid III headform is available. The input is given in the files:

| | |
|---|---|
| Finite element model: | d_fmhffe_usr.xml<br>d_fmhffe_inc.xml |

To run these models, the following licenses are required:

| | |
|---|---|
| Finite element model: | MADYMO/Solver (Multibody)<br>MADYMO/Solver (FEM)<br>MADYMO/Dummy Models/Subsystems |

Figure 30.1 shows the model in the reference position. The finite element model consists of a single body and a finite element skin.

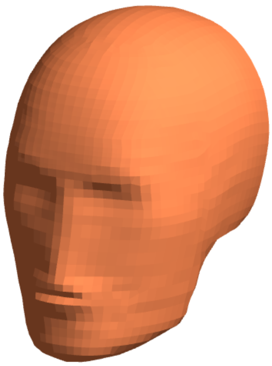

Figure 30.1: Finite element model of the FMVSS 201 featureless Hybrid III headform.

**FINITE ELEMENT MODEL**

A finite element model is attached to a single rigid body. The finite element model contains shell and solid elements. The shell elements describe the metal skull and mounting plate and the outer surface of the head. The nodes from the metal skull and mounting plate elements are rigidly attached to the single rigid body using supported nodes. The outer surface is used as the contact surface of the headform. The solid elements (SOLID1) describe the vinyl rubber skin. Two layers of SOLID1 elements were used through the thickness of the skin. To account for the fact that the aluminium casting of the head is not modelled fully, the single rigid body is given inertial properties so that the complete model has the correct total mass and rotational inertial properties. A cross section of the mesh is shown in Figure 30.2.

The vinyl rubber material is modelled using a linear visco-elastic material model. The visco-elastic material allows the model to represent the energy dissipation in the rubber at varying speeds.

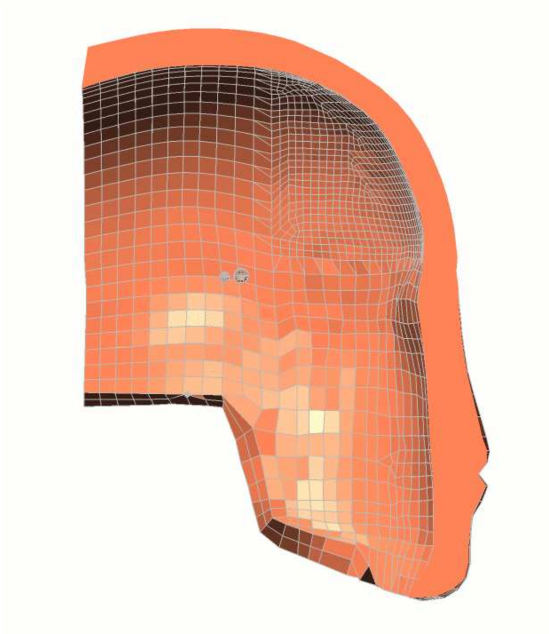

Figure 30.2: Cross section of mesh with ellipsoids at C.G. (upper) and Occipital Condyle (lower).

## 30.2 Model validation

The finite element model isvalidated for two different drop tests (impact speed of 2.7 and 4.0 m/s) on rigid plates. The validation results are shown in Figure 30.3. The test data is taken from Chou et al.[1]

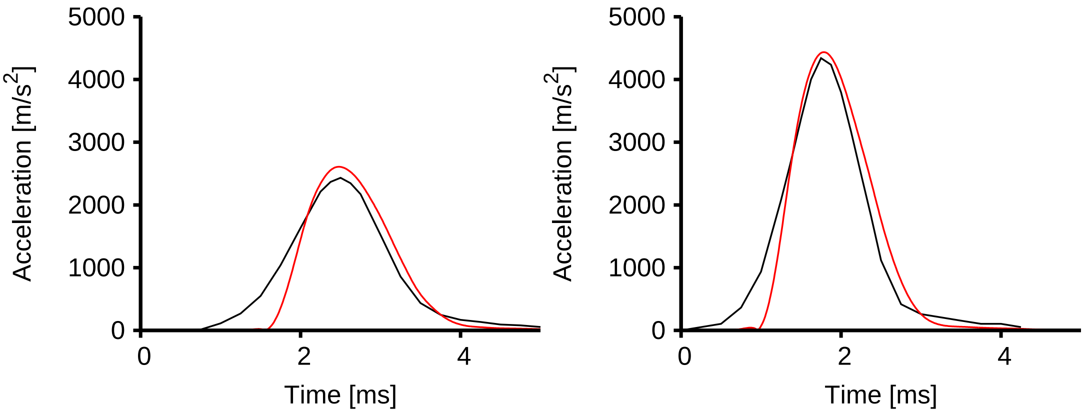


Figure 30.3: 2.7m/s (left) and 4.0m/s (right) rigid impact validation results.



[1]Chou C.C., Zhao Y., Huang Y., Lim G.G., (1996), "Development and validation of a deformable featureless headform model using LS-DYNA3D". ESV-1996. ESV paper 96-S8-O-08.

## 30.3 User instructions

### Timestep

Table 30.1: Recommended timestep for the FMVSS 201 headform models.

| Model | timestep (s) |
|---|---|
| Finite element | $\leq 2.0 \cdot 10^{-6}$ |

### Headform positioning

To position the headform (i.e. the occipital condyle point) in inertial space, the Headform_attachment (CRD_OBJECT) and Headform_attachment_ori (ORIENTATION.SUCCESSIVE_ROT) elements must be used. Next, the headform impact velocity can be applied through initialisation of the headform_jnt by putting the initial velocity in the attribute V1 under INITIAL.JOINT_VEL. Varying or finetuning the headform position wrt its impact point also can be done through initialisation of the headform_jnt: by using the attributes D1, D2 and D3 under INITIAL.JOINT_POS.

Table 30.2: Positioning joints of the headform impactor models.

| Joint Description | Identifier | Degree of freedom[a] | | | | | |
|---|---|---|---|---|---|---|---|
| Headform | Headform_attachment | pos[1] | global x-position | pos[2] | global y-position | pos[3] | global z-position |
| Headform | Headform_attachment_ori | R1 | roll right | R2 | pitch down | R3 | yaw left |
| Headform | Headform_jnt | D1<br>V1 | forward<br>impact velocity | D2 | leftward | D3 | upward |

[a] Positive translation or rotation given in global co-ordinate system while headform is in reference position.

### Headform contacts

The headform models have a single predefined contact group that the user can refer to when defining contact with the impacted structure.

For contacts with rigid objects or objects of which the compliance is modelled with FE material models other than NULL or RIGID, the contact definition can refer directly to the predefined headform skin compliance (CONTACT_TYPE=MASTER/SLAVE). If the compliance of the impacted FE object is also represented by a contact characteristic, the two contact characteristics can be combined by using CONTACT_TYPE=COMBINED.

Table 30.3: Available groups to define contact between the headform impactor model and the environment.

| Contact Description | Identifier | FE model |
|---|---|---|
| Headform skin | Headform_gfe | Elements and nodes |

## Headform output

Table 30.4: FMVSS 201 headform output signals.

| Sensor | Identifier | Signal | | | | | | | Filter |
|---|---|---|---|---|---|---|---|---|---|
| | | resultant | x | direction[(a)] | y | direction[(a)] | z | direction[(a)] | |
| Head | | | | | | | | | |
| CG accelerometer | HeadCG_acc | ar | a1 | forward | a2 | lateral | a3 | vertical | CFC1000 |
| CG velocity | HeadCG_vel | vr | v1 | forward | v2 | lateral | v3 | vertical | CFC1000 |
| CG displacement | HeadCG_dis | dr | d1 | forward | d2 | lateral | d3 | vertical | CFC1000 |

[(a)] Positive direction given according to SAE J211/1.

The output signal HeadCG_acc is used in the 36ms HIC calculation. The HIC output must then be converted to the HIC(d) injury parameter specified by FMVSS 201. The following formula should be used:

$$\mathrm{HIC}(d) = 0.75446 \cdot \mathrm{HIC} + 166.4$$

30

# 31 FMVSS 226 Ejection Mitigation featureless Headform

The FMVSS 226 ejection mitigation featureless headform impactor was developed to enable an occupant protection effectiveness evaluation of ejection mitigation countermeasure solutions. It follows the requirements of the voluntary test procedure defined by NHTSA Final Rule document, issued on January 19$^{th}$ 2011 (Docket No. NHTSA-2011-0004-0001).

The impactor consists of an aluminium skull covered with vinyl skin, and steel skull cap accommodating the accelerometer mount. The headform face is featureless to simplify the contact interaction. The total weight of the headform and the moving impactor is 18 kg, which represents the effective mass of shoulders and the head.

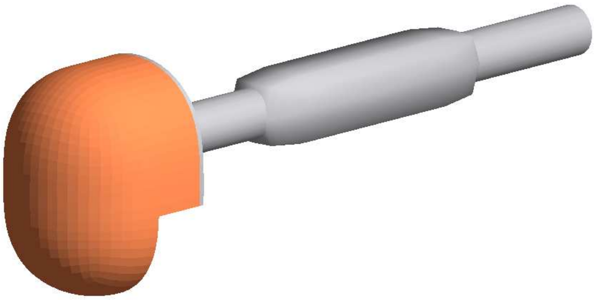

Figure 31.1: The FMVSS 226 featureless headform model in reference position.

## 31.1 Model description

The finite element model of the FMVSS 226 featureless headform is available. The input is given in the files:

| | |
|---|---|
| Finite element model: | d_emhffe_usr.xml<br>d_emhffe_inc.xml |

To run this model, the following licenses are required:

| | |
|---|---|
| Finite element model: | MADYMO/Solver (Multibody)<br>MADYMO/Dummy Models/Subsystems |

### COMPLETE HEADFORM MODEL

The model is a combination of FE and multibody parts. The headform model consists of a single body representing head skull and a finite element skin. The impactor consists of two rigid bodies and appropriate MB geometrical representation.

#### Finite element headform model

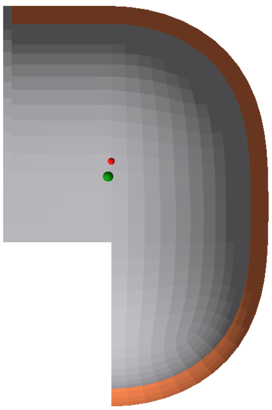

Figure 31.2: Cross section of mesh with ellipsoids at C.G. (green) and accelerometer A.I.P. (red)

The finite element model, composed of both shell and solid elements, is attached to a single rigid body. The shell elements describe the metal skull and the mounting plate. The metal skull and mounting plate are rigidly attached to the rigid body using supported nodes. The solid elements represent the vinyl rubber skin. Two layers of elements were used throughout the thickness. The vinyl rubber material is modelled using a linear visco-elastic material model. The solid elements are covered by shell elements from the outside, which are used as the contact surface of the headform. A cross section of the mesh is shown in Figure 31.2.

Taking into account the fact that the aluminium skull is not represented by deformable FE, the rigid body is given inertial properties, so that the complete model has the correct total mass and inertia properties. The headform model is connected to the probe to allow adjustments of the headform angle along the probe longitudinal axis.

**Multibody impactor model**

The impactor consists of two rigid bodies representing the impactor base and the impactor probe, connected between each other by the translational joint. The probe geometry is represented by a cylinder and an ellipsoid.

## 31.2 Model validation

The finite element model has been validated in the certification pendulum test (at 1.2 m/s impact velocity), as specified in the "18kg Ejection Mitigation Featureless Headform P/N ATD-7304" technical product sheet. The certification results are shown in Figure 31.3.

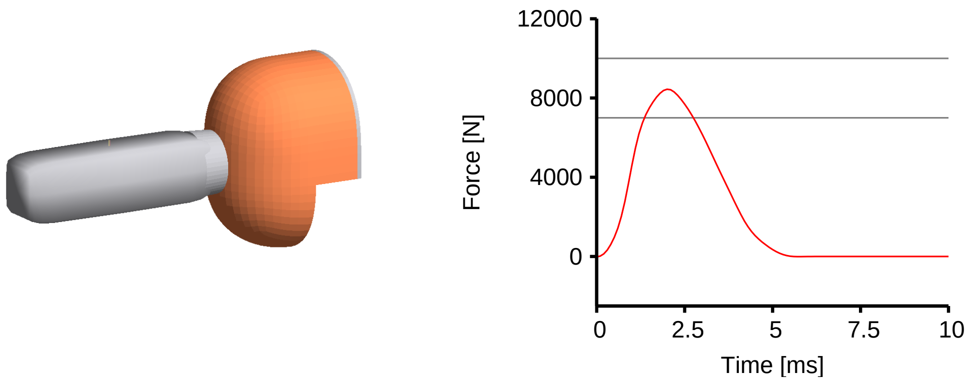


Figure 31.3: Certification test configuration (left) and test results (right).

The robustness of the model has been checked on several rigid wall tests. It has been tested up to 29 km/h (8.1 m/s) impact speed, that is higher than a maximum protocol velocity.

## 31.3 User instructions

### Timestep

Table 31.1: Recommended timestep for the FMVSS 226 headform model.

| Model | timestep (s) |
|---|---|
| Finite element | $\leq 1.0 \cdot 10^{-6}$ |

### Headform positioning

The positioning for complete headform impactor is presented in Table 31.2. The headform can be rotated with respect to the probe allowing the adjustment of its angle (Vertical, 45 deg and Horizontal) to comply with Final Rule FMVSS 226 "Ejection Mitigation" (docket NHTSA-2011-0004) document.

Table 31.2: Positioning joints of the FMVSS 226 headform model.

| Joint Description | Identifier | Degree of freedom | | | | | | Comment |
|---|---|---|---|---|---|---|---|---|
| Impactor positioning | ImpactorBase_jnt | D1 | global x-position | D2 | global y-position | D3 | global z-position | (a) |
| | | R1 | pitch down | R2 | roll right | R3 | yaw left | |
| Initial probe shift and velocity | Probe_jnt | D1 | forward | | | | | (b) |
| | | V1 | impact velocity | | | | | |
| Headform angle | Headform_jnt | R1 | roll right | | | | | (b) |

(a) Positive translation or rotation given in global coordinate system while headform is in reference position.

(b) Positive translation or rotation given along the probe longitudinal axis.

### Headform contacts

The headform model has a predefined contact group that the user can refer to when defining contact with the impacted structure.

In general, the headform surface should be chosen as the master group in contact definitions. This is also the way in which the contacts were defined in the headform model validation test suite. Since the headform skin is a deformable FE model, it is recommended to use NODE_TO_SURFACE or SURFACE_TO_SURFACE contact method with PENALTY or ADAPTIVE force definition. In case the interacting structure is a deformable facet surface type of model with CHARACTERISTIC.CONTACT defined, CONTACT_METHOD.NODE_TO_SURFACE_CHAR is recommended.

Table 31.3: Available groups to define contact between the FMVSS 226 headform model and the environment.

| Contact Description | Identifier | FE model |
|---|---|---|
| Headform | Headform_gfe | Elements and nodes |

### Headform output

In the Table 31.4 all predefined output definitions for the ejection mitigation headform model are listed.

Table 31.4: FMVSS 226 headform output signals.

| Sensor | Identifier | Signal | | | | | | | Filter |
|---|---|---|---|---|---|---|---|---|---|
| | | resultant | x | direction[a] | y | direction[a] | z | direction[a] | |
| Headform and Probe | | | | | | | | | |
| CG accelerometer | Headform_acc | ar | a1 | lateral | a2 | longitudinal | a3 | vertical | CFC1000 |
| velocity | Probe_vel | | | | v2 | longitudinal | | | CFC180 |
| displacement | Probe_dis | | | | d2 | longitudinal | | | CFC180 |

[a] Positive direction given according to SAE J211/1 and NHTSA specification.

Table 31.5: Injury criteria defined for the FMVSS 226 headform.

| Injury criteria | Identifier | Filter |
|---|---|---|
| Headform and Probe | | |
| HIC (36) | HIC36_inj | |
| Impactor displacement | ImpactorDisp_inj | |

# 32 Pedestrian Subsystem Impactors

The pedestrian subsystem impactors represent parts of the human body and are used to assess the impact behaviour of specific regions of a vehicle. Within the framework of the European Enhanced Vehicle-safety Committee Working Groups 10 and 17, pedestrian subsystem impactors and test methods for the evaluation of pedestrian protection by vehicles have been developed. The EEVC WG17 impactors available are an adult headform impactor of 4.8kg, a child headform impactor of 2.5kg, a complete legform impactor and an upper legform impactor.

As a result of discussions with the European automobile industry, another headform impactor has been developed in addition to the EEVC child and adult headform impactors. This ACEA headform impactor has a mass of 3.5kg.

Currently, the EuroNCAP pedestrian impact test protocol uses the pedestrian subsystem impactors to assess the pedestrian injury risk for new car models. European directive 2003/102/EC, dealing with pedestrian protection, also prescribes the use of the EEVC and ACEA impactors for pedestrian injury risk assessment.

The headform impactor models are described in Section 32.1.1. In Section 32.1.2 the complete legform impactor models are described and the upper legform impactor model is described in Section 32.1.3.

## 32.1 Model description

To run the pedestrian impactor models, the following licenses are required:

| | |
|---|---|
| Ellipsoid models: | MADYMO/Solver (Multibody)<br>MADYMO/Dummy Models/Subsystems |
| Finite element models: | MADYMO/Solver (Multibody)<br>MADYMO/Solver (FEM)<br>MADYMO/Dummy Models/Subsystems |

### 32.1.1 Headform impactors

The headform impactors consist of an aluminium sphere covered by a moulded skin. Inside the aluminium sphere an instrumentation cavity provides room for a tri-axial accelerometer or three uni-axial accelerometers. The headform impactors are used to assess the injury risks following pedestrian head impacts on the bonnet and the leading edge of a vehicle.

Five hardware headform impactors exist: the *EEVC Working Group* 17 4.8 kg adult headform, the *EEVC Working Group* 17 2.5 kg child headform, the *ACEA* 3.5 kg headform, the *JARI* 4.5 kg adult headform and the *JARI* 3.5 kg child headform.

The following headform impactor models are available:

| | |
|---|---|
| – EEVC WG17 4.8 kg, finite element | d_adhffe_usr.xml, d_adhffe_inc.xml |
| – EEVC WG17 2.5 kg, finite element | d_chhffe_usr.xml, d_chhffe_inc.xml |
| – ACEA 3.5 kg, finite element | d_aceahffe_usr.xml, d_aceahffe_inc.xml |
| – JARI 4.5 kg, FE | d_jariadhffe_usr.xml, d_jariadhffe_inc.xml |
| – JARI 3.5 kg, FE | d_jarichhffe_usr.xml, d_jarichhffe_inc.xml |

See the finite element models of the pedestrian headform impactors in Figure 32.1 and Figure 32.2.

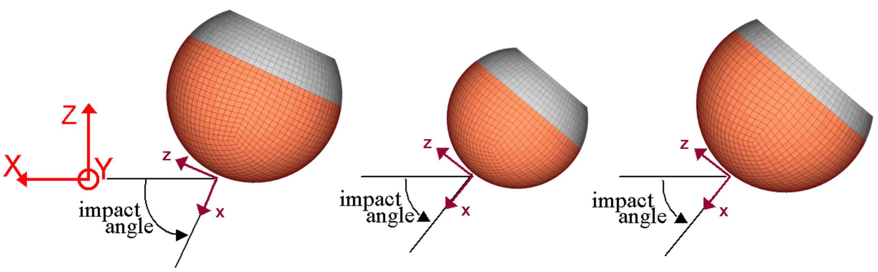


Figure 32.1: EEVC WG17 adult (left), child (centre) and ACEA (right) headforms.

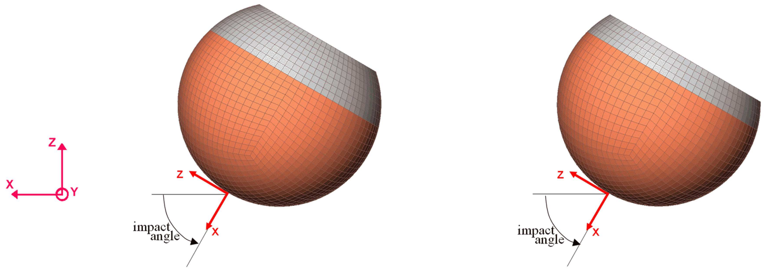


Figure 32.2: JARI adult (left) and JARI child (right)

**FE MODEL**

In the FE headform impactor models the aluminium inner skull is represented by a rigid body and a facet surface mesh, while the rubber skin is modelled as a deformable, solid element FE mesh. The total FE headform inertia properties are the combination of the rigid body and the FE inertia properties. The FE model skins are modelled with SOLID8 elements using a full-integration formulation.

For all headform models, the x-axis of the body local co-ordinate system is aligned along the longitudinal axis (which is also the direction of propulsion), pointing from the centre of the headform to the front side of the headform. The headform origin (origin of the headform joint child co-ordinate system) is situated 1 mm in front of the outer surface of the skin, on the longitudinal axis of the headform. The accelerometer co-ordinate system is aligned to the body local co-ordinate system. In its reference position (defined in the user file) the headform origin is located in the origin of the global co-ordinate system and the headform has been given a pitch angle (around the y-axis) that corresponds with the angle defined in related pedestrian safety test protocols.

### 32.1.2 Complete legform impactor

The complete legform consists of two foam-covered steel segments, representing the femur (upper leg) and the tibia (lower leg). These segments are joined by a deformable knee joint represented by two plastic-deformable steel ligaments. Deformation of these ligaments represents lateral knee bending. Knee shear is represented by a steel shear spring located inside the femur steel tube. The legform models represent the legform with shear damper as developed by the Transport Research Laboratory (TRL). The available complete legform impactor models are shown in Figure 32.3. The following legform models are available:

| | |
|---|---|
| – Ellipsoid model | d_legfel_usr.xml, d_legfel_inc.xml |
| – Finite Element model | d_legffe_usr.xml, d_legffe_inc.xml |

Figure 32.3: Complete legform impactor models: ellipsoid model (left) and FE model (right).

**ELLIPSOID MODEL**

The basis of the legform models is formed by a chain of three rigid bodies. These bodies represent respectively the femur steel and foam, (part of) the shear spring and the tibia steel and foam. The bodies Femur_bod and ShearSpring_bod are connected with a translational joint (ShearSpring_jnt) to represent the shear displacement in shear spring. The bodies ShearSpring_bod and Tibia_bod are connected with a revolute joint (Knee_jnt) that represents the deformable knee ligaments.

A joint restraint on the shear spring translational joint is used to model the shear spring stiffness and the end stops for the shear displacements when steel-to-steel contact occurs between shear spring end and inner femur tube. The effect of the damper is included in this joint restraint model with a constant damping coefficient. A second joint restraint, working on the knee revolute joint, is included to model the bending stiffness of the knee ligaments. Hysteresis is included in the loading characteristic in order to model the plasticity of the ligament deformation. Both the shear spring and the knee bending characteristic are directly derived from the static legform certification corridors as defined by EEVC-WG17. The force-deflection curves correspond to loading curves in the middle of the static shear and bending certification corridors. A point restraint between Femur_bod and Tibia_bod is included to represent flesh and skin influence on the shear behaviour.

The outer legform surface is represented by two separate cylinders: one for the femur and one for the tibia region. The foam and skin compliance is lumped in a predefined force-based contact characteristic that includes hysteresis. For simulations in which the bumper system is modelled with ellipsoids, hysteresis of the bumper ellipsoids can be modelled with any hysteresis model as long as the loading and unloading curve are strictly increasing and include zero force for zero penetration. The characteristics of the legform and bumper can then be combined using CONTACT_FORCE_CHAR with CONTACT_TYPE = COMBINED. Purely for visualisation, the damper assembly on the back- or non-impact side of the legform impactor is also represented with a cylinder. The ellipsoid legform model geometry as well as the rigid body inertia properties are defined such that all the EEVC-WG17 design specifications are met.

The ShearSpring joint displacements and the Knee joint deflection angle are used as output to represent the measured legform knee shear displacement and knee bending angle. The tibia acceleration measurement is represented by linear acceleration output at the appropriate location on the tibia body.

**FE MODEL**

The multi-body chain (bodies, joint and joint restraints) forming the core of the FE model is identical to that of the ellipsoid model. However, in the FE model the foam and skin that cover the steel tubes are modelled explicitly, with SOLID8 finite element meshes. MATERIAL.FOAM is used to model the foam and skin material properties. Strain rate dependency has been included using the Johnson-Cook model. Purely for visualisation, the damper assembly on the back- or non-impact side of the legform impactor is represented with a cylinder. The FE legform model geometry as well as the combined rigid body and finite element inertia properties, are defined such that all the EEVC-WG17 design specifications are met.

The outer surfaces of the steel femur and tibia tubes are modelled with fully supported MEM4 meshes with MATERIAL.NULL (facet surfaces). The foam to steel load transfer is modelled with a contact definition using CONTACT.FE_FE. The legform impactor output definitions are included in the same way as in the ellipsoid model.

### 32.1.3 Upper legform impactor

The upper legform impactor is used to test the bonnet leading edge. The upper legform consists of a rigid support frame at the non impacted side and a front member tube at the impacted side. The support frame and the front member tube are connected at the ends through load cell assemblies. The front member tube is covered with foam and a rubber skin. Strain is measured on the rear of the front member tube at three positions. A propulsion shaft, which is effectively part of the impactor during impact, is connected to the support frame by a torque-limiting joint. In this joint, the friction torque is set to a minimum of 650 Nm to protect the guidance components. The upper legform mass depends upon the general shape of the front of the car and is specified in the proposed regulation. Extra weights can be mounted on the back of the support frame.

A finite element upper legform impactor model is available.This model describes the upper legform impactor as developed by TRL.

– Finite Element model d_uplffe_usr.xml, d_uplffe_inc.xml

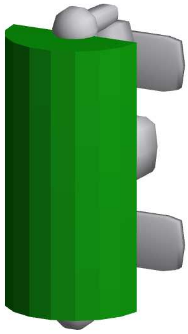

Figure 32.4: Finite Element model of the EEVC upper legform.

**FE MODEL**

The upper legform consists of six bodies and one FE model. The tree structure co-ordinate system is oriented such that x is forward (the impact direction), y is leftward and z is upward. The origin is situated 50 mm in negative x direction from the torque limiting joint (see Figure 32.4).

The external geometry of the model at the impact side is described by SOLID8 elements using reduced element integration. Geometry was retrieved from the proposed regulation and measurements on a physical upper legform. The outer diameter of the mesh is equal to 153 mm and the length in longitudinal direction of the mesh is equal to 300 mm. The external geometry of the database at the non-impacted side is described by ellipsoids.

The mass of the foam and rubber is equal to the upper bound of the mass specified by the proposed regulation. The mass of the other components in front of the loadcell assemblies (excluding the foam and skin) is chosen equal to the mass specified by the proposed regulation.

The default total mass of the legform database is equal to 12 kg. The total mass of the impactor depends upon the general shape of the front of the car. The user has to adapt the mass of the extra weights in the database to agree with the test procedure. The mass of the propulsion shaft is equal to 3.8 kg but can be different depending on the propulsion system.

The total mass can be specified in the user file, using the DEFINE element 'Impactor_mass'. MADYMO will calculate the appropriate masses for the weight adjustment bodies based on this.

The impacted side of the legform is modelled with one FE model. The foam and skin is modelled with 4 element layers of SOLID8 elements (using reduced integration) and the impactor tube with SHELL4 elements. The FOAM material model is used to describe the material behaviour of foam and skin. The inner layer of SOLID8 elements shares nodes with the SHELL4 elements. The end nodes of the impactor tube are connected to the adapter bodies.

## 32.2 Model validation

The headform impactor models have been validated based on the headform certification impact tests and headform drop tests. The certification test results are given in Figure 32.5.The complete legform impactor models have been validated using the EEVC and ACEA dynamic certification tests. The upper legform impactor model has been validated using the EEVC dynamic certification test.

Table 32.1: Tests used for validation of the pedestrian subsystem impactor models.

| **Test** | **Test** | **Model** | |
|---|---|---|---|
| **description** | **specification impact mass, impact velocity** | **ell** | **FE** |
| EEVC WG17 child headform drop test | 2.2 m/s | | x |
| EEVC WG17 child headform certification impact test | 1.0 kg, 7.0 m/s | | x |
| EEVC adult headform drop test | 2.7 m/s | | x |
| EEVC adult headform certification impact test | 1.0 kg, 10.0 m/s | | x |
| ACEA headform drop test | 2.7 m/s | | x |
| ACEA headform certification impact test | 1.0 kg, 7.0 m/s | | x |
| Complete legform EEVC certification impact | 9.0 kg, 7.5 m/s | x | x |
| Complete legform ACEA certification impact | 16.0 kg, 7.5 m/s | x | x |
| Upper legform certification impact | 3.0 kg, 7.1 m/s | | x |

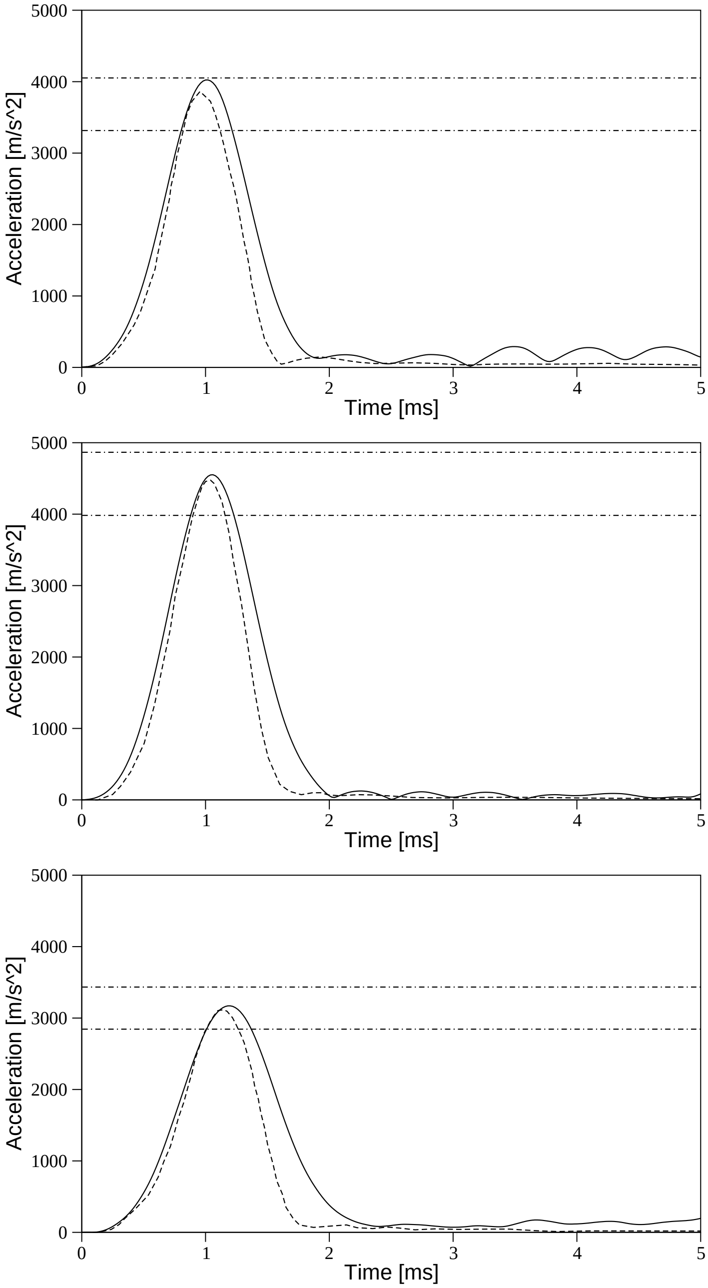


Figure 32.5: Certification test responses of the FE headform impactor models: EEVC WG17 adult (top), child (middle) and ACEA (bottom), experiment (— — —), certification corridors (—·—) and FE model (———).

## 32.3 User instructions

### 32.3.1 Headform impactors

**Timestep**

Table 32.2: Recommended timestep for the headform impactor models.

| Model | timestep (s) |
|---|---|
| Finite element | $\leq 1 \cdot 10^{-6}$ |

**Headform positioning**

The headform origin (the headform joint child coordinate system) is located 1mm in front of the outer skin surface on its longitudinal (propulsion) axis. In reference position, the headform origin is located in the origin of reference space. The headform orientations are predefined such that the headform impact angles with respect to the horizontal plane are in correspondence with those defined in the pedestrian test protocols.

When using SAE-based vehicle model orientations, the headform impactors can be positioned by filling in the global co-ordinates of the cross-point of the bonnet surface and the propulsion axis of the headform, in the POS attribute of the CRDSYS_OBJECT element named Headform_Attachment. This attribute defines the global x, y and z-coordinates of the parent joint coordinate system of the headform joint. Next, the attribute D1 in the INITIAL.JOINT_POS element of the Headform_jnt can be used to shift the headform backward from this cross-point until there is no initial penetration any-more between bonnet and impactor. The attributes D2 and D3 could be used to define variations from the exact target impact location.

If the user wants to change the headform impact angle with respect to the horizontal plane, he can do so in the element ORIENTATION.SUCCESSIVE_ROTATION named Headform_Orientation_ori by changing the angle defined in the R1 attribute.

The attribute V1 under INITIAL.JOINT_VEL is used to apply the impact velocity of the headform impactors.

Table 32.3: Positioning joints of the headform impactor models.

| Joint Description | Identifier | Degree of freedom [a] |
|---|---|---|
| Headform joint | Headform_Orientation_ori | R1 pitch down |
| | Headform_Attachment | POS[1] global x-position of headform origin<br>POS[2] global y-position of headform origin<br>POS[3] global z-position of headform origin |
| | Headform_jnt | D1 forward D2 leftward D3 upward<br>V1 impact velocity |

[a] Positive translation or rotation given in global co-ordinate system while headform is in reference position (see Figure 32.1).

## Headform contacts

Table 32.4: Available groups to define contact between the headform impactor models and their environment.

| Contact Description | Identifier | FE model |
|---|---|---|
| Headform skin | Headform_gfe | outer skin surface elements and nodes |

## Output

Table 32.5: Output signals defined for the headform impactor models.

| Sensor | Identifier | Signal | | | | | | | Filter |
|---|---|---|---|---|---|---|---|---|---|
| | | resultant | x | direction | y | direction | z | direction | |
| Headform | Headform_acc | ar | | | | | | | CFC1000 |

Table 32.6: Injury criteria defined for the headform impactor models.

| Sensor | Identifier | Filter |
|---|---|---|
| Headform | | |
| HIC (15) | HIC15_inj | CFC1000 |

### 32.3.2 Complete legform impactor

#### Timestep

Table 32.7: Recommended timestep for the complete legform impactor models.

| Model | timestep (s) |
|---|---|
| Ellipsoid | $\leq 1 \cdot 10^{-4}$ |
| Finite element | $\leq 1 \cdot 10^{-6}$ |

#### Legform positioning

The complete legform impactor can be positioned with respect to its environment by initialising the Legform_jnt.

The positioning point of reference is 1mm in front of the impact side of the lower edge of the tibia. In its reference position, this point is positioned at the origin of reference space. The reference orientation is such that the legform stands in upright position, with the upper end of the femur pointing in +z direction and the impact vector pointing in +x direction.

When using SAE-based vehicle model orientations, the user can simply fill in the global x- and y-co-ordinates of the desired impact point on the bumper model as INITIAL_JOINT_DOF input values for respectively D1 and D2. The global z-co-ordinate corresponding to ground level should be filled in for D3. No re-orientation of the legform is needed when using SAE-based vehicle model orientations. The attribute V1 under INITIAL.JOINT_VEL is to be used to apply the initial impact velocity of the legform impactor.

Table 32.8: Positioning joints of the complete legform impactor models.

| Joint Description | Identifier | Degree of freedom [a] | | | | | |
|---|---|---|---|---|---|---|---|
| Legform | Legform_Orientation_ori | R1 | roll right | R2 | pitch down | R3 | yaw left |
| | Legform_jnt | D1<br>V1 | forward<br>impact velocity | D2 | leftward | D3 | upward |

[a] Positive translation or rotation given in global co-ordinate system while headform is in reference position (see Figure 32.1).

#### Legform contacts

For the ellipsoid model separate contact groups are included for the femur and the tibia region. It is important to note that these groups contain multibody cylinders, which are always considered infinite in contact definitions. Users should beware of possible undesired side-effects of these cylinders in contact when designing their conceptual MB vehicle front end models. For this reason, it is advised for the ellipsoid model to use the separate tibia and femur contact groups rather than the single contact group defined for the whole ellipsoid legform model. For the finite element models the single contact group for the complete legform skin is to be used.

Table 32.9: Available groups to define contact between the legform impactor and its environment.

| Contact Description | Identifier[(a)] | Ellipsoid model | FE model |
|---|---|---|---|
| Legform skin | LegformSkin_*ctg* | Femur_cyl<br>Tibia_cyl | Elements and nodes |
| Femur skin | FemurSkin_*ctg* | Femur_cyl | |
| Tibia skin | TibiaSkin_*ctg* | Tibia_cyl | |

[(a)] *ctg* refers to contact group, for the ellipsoid models ctg is replaced by gmb (group_multibody) and for the facet and FE model by gfe (group_finite element).

### Legform function scaling parameters

For the legform impactor models, some hardware parameters have been made scalable through FUNC_MOD elements in the user-files. The scalable parameters are the shear spring shear stiffness, the knee ligament bending stiffness, and the confor foam compression stiffness. For the first two of these parameters, only Y-scaling is allowed and a valid scaling range is given that ensures the model to comply with the legform static certification requirement corridors for bending and shear stiffness. For these parameters, a Y-scale value of 1.0 (no scaling applied) corresponds to mid-corridor curves for the static certifications. Scalability of the confor foam compression loading curve has been included because of the known limitations of hardware legform reproducability due to the confor foam sensitivity to testing temperature and humidity. The user can choose whether to use X- and Y-scale factors to tune his model to, for instance, the latest hardware certification responses of the legform impactor used in his project. More information on the scalable parameters and their validity ranges is given in Table 32.10.

Table 32.10: Parameters available for function scaling in the complete legform impactor models.

| Parameter Description | Base function | X-scaling range | Y-scaling range |
|---|---|---|---|
| Confor foam stiffness | LegformCntLoa_fun (ell)<br>CF45Loa_fun (FE) | to meet dynamic certification requirements: depends on the other scale factors used | to meet dynamic certification requirements: depends on the other scale factors used |
| Spring shear stiffness | SpringShearLoa_fun | | to meet static shear certification requirements:<br>0.88 <Y_SCALE< 1.12 |
| Knee bending stiffness | LigamentBendingLoa_fun | | to meet static bending certification requirements:<br>0.90 <Y_SCALE< 1.10 |

### Output

The shear spring displacement and knee bending potmeters are represented by joint kinematics output (OUPUT_JOINT_DOF). The responses can be found in the joint positions output file (*.jps). Note that the knee bending angle output is defined in radians instead of degrees.

Table 32.11: Output signals of the complete legform models.

| Sensor | Identifier | Signal | | | | | | | Filter |
|---|---|---|---|---|---|---|---|---|---|
| | | resul-tant | x | direction | y | direction | z | direction | |
| Knee | ShearSpring_dis | dof1 | | | | | | | |
| | KneeBending_ang | dof1 | | | | | | | |
| Tibia | Tibia_acc | | a1 | forward | | | | | CFC180 |

### 32.3.3 Upper legform impactor

**Upper legform positioning**

To place the upper legform in an environment, the position of the legform is specified in the element INITIAL.JOINT_POS, in the joint "Impactor_guidance". The orientation of the upper legform is specified in the associated element ORIENTATION.SUCCESSIVE_ROT . In the model, the impact velocity is specified as V1-value in the element INITIAL.JOINT_VEL of the joint "Impactor_guidance".

**Output**

Constraint forces are generated of which the body x-component forces represent the lower and upper load cell forces.

The bending moments have to be calculated from the Y-strains in three elements. Output is generated from these elements. The centre of these elements coincides with the centre of the strain gauges. The bending moments have to be calculated by:

$$\mathrm{Moment} = 1.19 \cdot 10^6 \cdot \mathrm{Y} - \mathrm{strain}$$

This gives an optimal fit of experimental data. The value in the equation is a little bit larger than the constant resulting from analytical equations. Possible reasons for this difference can be uncertainties such as the material properties, geometry and the end supports of the impactor tube. The friction load and the joint rotation of the torque limiting joint is generated to check if the torque limit was reached.

# 33 ECE-R12 body block

The body block is used in ECE regulation 12. The regulation deals with steering wheel system approval with regard to driver protection in the event of a frontal impact.

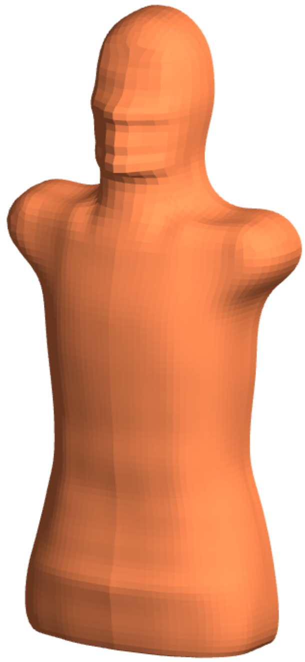

Figure 33.1: Body block facet model.

## 33.1 Model description

A facet model of the body block is available. The model is defined in the following files:

| | |
|---|---|
| Facet model: | d_bblockfc_usr.xml<br>d_bblockfc_inc.xml |

To run these models, the following licenses are required:

| | |
|---|---|
| Facet model: | MADYMO/Solver (Multibody)<br>MADYMO/Dummy Models/Subsystems |

Figure 33.1 shows the model in the reference position. The facet model consists of one body and a single facet surface representing the body block geometry.

**FACET MODEL**

The facet surface representing the body block geometry was derived from an actual body block. Higher order ellipsoids are defined to visually represent the wooden base and backing structure attached to the plywood back plate. The plywood back plate itself is included in the facet surface. Two contact characteristic are included, one representing the compliance of the body block for blunt object impacts and a second one that includes a stiffening correction for more focal impacts, where the deforming body block area is much larger than the actual area in contact.

Centre of gravity (CG) and moments of inertia properties are implemented according to SAE J944 JUN80 specifications. ($CG = 21.7\text{in} = 55.12\text{cm}$ from top of head, $I_{yy}$ through $CG = 20\text{lbf} \cdot \text{in} \cdot \text{s}^2 = 23\text{kgf} \cdot \text{cm} \cdot \text{s}^2 = 2.26\text{kg} \cdot \text{m}^2$).

## 33.2 Model validation

The model has been calibrated based on three dynamic impact tests.

In two of these tests, the body block hits a rigidly supported steel 'D' section tube (100mm diameter) at approximately 6.0ms$^{-1}$. The location of impact is at the CG height on the body block for the first test and approximately 100mm below the CG height for the second test. The contact characteristic representing the body block surface compliance for blunt object impacts was calibrated to these two tests such that the simulated support reaction forces (in both X and Z direction) correlate with the measured data.

In the third impact test, the body block hits the edge of a rigidly supported, plywood steering wheel shaped half disk (disk diameter 450mm, edge radius 15mm) at approximately 6.7ms$^{-1}$. The location of impact is at the CG height on the body block. The contact characteristic representing the body block surface compliance for focal impacts was calibrated to this test, such that the simulated support reaction force (in X direction) correlates with the measured data. The contact characteristic for focal impact uses the same stiffness and damping functions as the one for blunt impact, but the total stiffness is scaled up to account for the larger ratio between the actual deforming body block surface and surface that is really in contact with 'focal' objects.

It should be noted that the body block acceleration (which was also measured in the third impact test) was found to correlate less accurately. This is because of the partly decoupled inertial behaviour of the rubber/foam impact shape and the wooden base of the body block during impact (in spite of the two being taped together). This decoupled behaviour is not represented in the facet body block model, which therefore can not accurately predict the reaction forces and the body block accelerations at the same time. The body block contact characteristics have been calibrated based on the support reaction forces, which are the more important test response signals, since the ECE R12 specification for the body block impact test is based on the steering column reaction force applied to the body block.

A quasi-static simulation has been performed to ensure that the facet body block model complies with the specifications for compliance of the body block as stated in ECE-12 regulation, Issue 1, page 22. In this test a 100mm square steel tube is pushed against the body block on a point 475mm down from its top. The loading force is measured until 12.7mm compression of the body block occurs. The tests with the body block used for calibration and validation of the models are summarised in Table 33.1. Results of the dynamic tests are shown in the figures following this table.

Table 33.1: Full dummy tests for Hybrid III 50$^{th}$ percentile dummy model.

| **Test description** | **specification impact velocity (m/s)** |
|---|---|
| Impact on rigid 'D' section tube, body block CG at impact height | 6.0 |
| Impact on rigid 'D' section tube, body block CG 100 mm above impact height | 6.0 |
| Impact on rigid steering wheel shape, body block CG at impact height | 6.7 |
| ECE-12 certification test (quasi static test) | — |

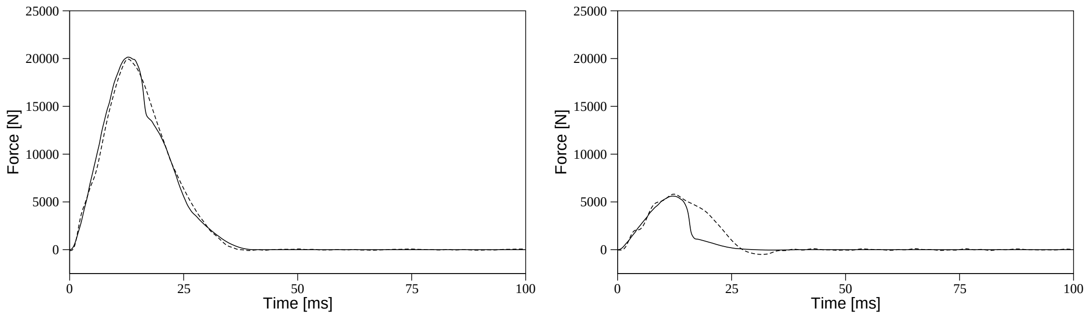


Figure 33.2: Validation results: steel D-tube impact test at CG height. Support reaction forces in longitudinal (left) and vertical direction (right). Plots show experiment (— — —) versus simulation (———).

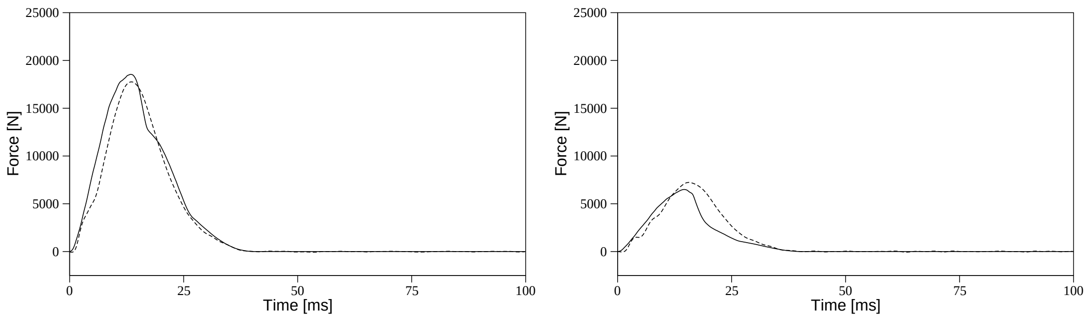


Figure 33.3: Validation results: steel D-tube impact test 100 mm below CG height. Support reaction forces in longitudonal (left) and vertical direction (right). Plots show experiment (— — —) versus simulation (———).

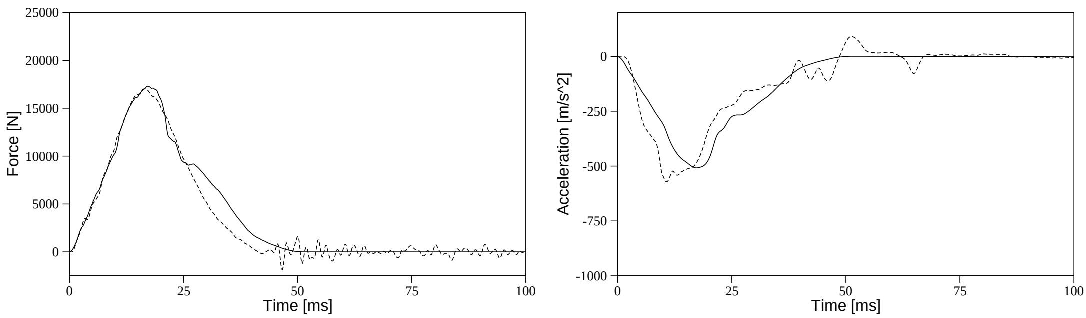


Figure 33.4: Validation results: plywood "steering wheel" impact test at CG height. Support reaction force (left) and body block acceleration (right), both in longitudinal direction. Plots show experiment (— — —) versus simulation (———).

## 33.3 User instructions

### Timestep

Table 33.2: Recommended timestep for the body block model.

| Model | timestep (s) |
|---|---|
| Facet | $\leq 1.0 \cdot 10^{-4}$ |

### Dummy positioning

For positioning the body block in inertial space, the Dummy_Attachment and Dummy_Attachment_ori elements can best be used. The reference positioning point on the body block is located at the backside of the plywood back plate, at the height of the so called reference line, which is located 11 mm above the bottom and 287 mm below the CG of the body block (see Figure 33.1).

After positioning the body block in reference space, the propulsion velocity can be given through the attribute V1 in the INITIAL.JOINT_VEL element for the BodyBlock_jnt. If the user wants to position the body block initially right in front of the steering wheel (e.g. in order to save computation time), the vertical velocity just before impact should be defined through the attribute V3.

If the user wants to have initial body block to steering wheel contact at $t = 0$ms and the simulation to start a few ms earlier, the attributes of the INITIAL.JOINT_POS element for the BodyBlock_jnt could be used to define the initial distance between steering wheel and body block impact points. These attributes could then also be used to define small variations from to 'nominal' body block impact position and orientation.

Table 33.3: Positioning joints of the body block model.

| Joint Description | Identifier | Degree of freedom[(a)] | | | | | |
|---|---|---|---|---|---|---|---|
| Body Block | Dummy _Attachment | pos[1] | forward | pos[2] | leftward | pos[3] | upward |
| | Dummy _Attachment_ori | R1 | yaw left | R2 | pitch down | | |
| Body Block | BodyBlock_jnt | R1 | roll right | R2 | pitch down | R3 | yaw left |
| | | D1 | forward | D2 | leftward | D3 | upward |
| | | V1 | forward | | | V3 | upward |

[(a)] Positive translation or rotation given in global co-ordinate system while body block is in reference position (see Figure 33.1).

### Dummy contacts

For contact definition between the body block and the impacted object, two contact groups have been defined. Both represent the complete body block surface, however they refer to different contact characteristics that represent the body block surface compliance. The group "BodyBlockBlunt_gfe" is meant to be used for contacts with blunt objects, so that the real contact surface is not very much smaller than the actual deforming body block surface. This contact group can be used for contact definitions between the body block and the hub of the steering wheel. The group "BodyBlockFocal_gfe" is meant to be used for contacts with objects with a relatively small contact surface, so that during penetration into the body block the real contact surface becomes significantly smaller than the actual deforming body block surface. This contact group can be used for contact definitions between the body block and the rim of the steering wheel.

It is advised to use the body block itself as the master surface. As there will be quite large nodal penetrations, the surface with the smallest radius of curvature should be chosen as the slave surface to ensure the penetration to be measured perpendicular to the flatter surface. In body block applications rim of the steering wheel will be the surface with the smaller radius of curvature.

Table 33.4: Available groups to define contact between the body block and environment.

| **Contact Description** | **Identifier**[(a)] | **Facet model** |
|---|---|---|
| Body block | BodyBlockBlunt_gfe | All elements and nodes |
| | BodyBlockFocal_gfe | All elements and nodes |

### Output

Although the body block does not contain any standard instrumentation, the acceleration of the body block is predefined as output. This accelerometer is located on the back side of the backplate of the bodyblock, at the height of the bodyblock centre of gravity. Note that this output is not listed for actual output request under CONTROL_OUTPUT in the user file.

Table 33.5: Body block output signals.

| **Sensor** | **Identifier** | **Signal** | | | | | | | **Filter** |
|---|---|---|---|---|---|---|---|---|---|
| | | **resul-tant** | **x** | **direction** | **y** | **direction** | **z** | **direction** | |
| Body block | BodyBlockCG_acc | ar | ax | forward | ay | right-ward | az | down-ward | CFC180 |

# 34 H-Point Manikin

Two of the main design objectives for car interior are comfort and safety. Both comfort and safety of a car seat are determined by the position that the occupant takes in the seat. Car and seat manufacturers use the SAE J826 3D H-point manikin to measure seat and package related reference points to design, audit and benchmark seats. This manual describes the numerical representation of this H-point manikin in MADYMO.

Figure 34.1: The MADYMO H-point manikin model.

## 34.1 Model description

The MADYMO model name and input file name of the H-point manikin model are:

d_hpmanfc_usr.xml
d_hpmanfc_inc.xml

### 34.1.1 Geometry

The H-point manikin model consists of a back plate, a pelvis plate, the back bone, masses in the backrest, the angle measurement structure, hip masses, thigh masses, T-bar and the lower extremities represented by the knees, lower legs, the ankles and the feet. See Figure 34.1 for an overview of the H-point manikin model. All components visible in Figure 34.1 have been modelled using finite element (FE) and articulations between these parts have been defined using multi-body components.

A laser scanner has been used to digitise the geometry of the H-point. The shape of each part has been scanned individually and converted to surfaces. Afterwards, all parts have been connected together. In the SAE J826 H-point manikin, two mass components can be added to the lower legs. In the H-point manikin model, these masses have been represented by separate rigid bodies.

The standard form of the SAE J826 H-point manikin represents a 50$^{th}$ percentile Hybrid III. The total mass of the MADYMO H-point manikin model is 75kg. As in the SAE J826 H-point manikin, the mass of the model can be easily adapted towards a 5th or 95th percentile Hybrid III dummy by removing the discs in the back and/or pelvis or adding masses to the pelvis plate (see also Section 34.1.3 for the weight distribution).

### 34.1.2 FE components

Since none of the components of the H-point manikin model will deform in determination of the H-point, all FE components have been modelled by a rigid material model (MATERIAL.RIGID) as well as to save CPU time. The mesh definition is essential for an accurate description of the contact surfaces. Smaller element sizes may give a more precise surface but also results in larger CPU times. In order to find an optimum between accuracy and CPU time, the element size for the pelvis and back plate is set to 12mm. Table 34.1 shows of each part the element type and if relevant, the thickness.

Table 34.1: Overview of the element and material types used for the FE components.

| Part | Element Type | Material type | Thickness |
|---|---|---|---|
| Hip_angle | Shells | Rigid | 6.3mm |
| H_point_mass_props | Shells | Rigid | Right: 2.4 mm<br>Left: 3.6 mm |
| Hip_mass | Solids | Rigid | |
| Pelvis_mass | Solids | Rigid | |
| Pelvis_bracket | Shells | Rigid | 2.1mm |

*Continued on the next page*

*Table 34.1 cont.*

| Part | Element Type | Material type | Thickness |
|---|---|---|---|
| Pelvis_mass_locations | Solids | Rigid | |
| Pelvis_push_nob | Solids | Rigid | |
| Pelvis_re-enforce_plate | Shells | Rigid | 3.1mm |
| Pelvis_plate | Shells | Rigid | 3.4mm |
| Backbone | Shells | Rigid | 2.4mm |
| Back_plate | Shells | Rigid | 3.3mm |
| Mass_backrest | Solids | Rigid | |
| Spike | Shells | Rigid | 3.4mm |
| Backrest_angle_measurement | Solids | Rigid | |
| T-bar | Solids | Rigid | |
| Knee_angles | Shells | Rigid | 3.3mm |
| Lower_legs | Solids | Rigid | |
| Foot_angles | Solids | Rigid | |
| Feet | Solids | Rigid | |

### 34.1.3 Multi-body components

The articulation between the various structures (hips, knees and ankles) are modelled by kinematic joints, which enable a robust and efficient simulation of anatomically correct kinematics. Additional bodies are defined and supported to the FE structures. The bodies are given low masses and inertia, so that they hardly influence the kinematics of the FE structure. Revolute joints have been applied to represent the hips, the knees and the ankles. Further, translational joints have been defined for adjustment of the upper and lower leg length and the distance between the left and right knee.

### 34.1.4 Settings

The settings for the H-point manikin are based on SAE J826 and ISO 6549. This means that the back angle is set to 25° . Further settings are:

- the thigh length (i.e. the distance from H-point to knee): 432mm
- tibia length (i.e. the distance from knee to ankle): 417mm
- distance between the knees: 239mm

In the H-point manikin model, the joints for the T-bar; knees and ankles are locked in the initial position. Also the H-point joint is locked, all other joints are not restricted. In some applications, the amount of computations van be reduced by locking the backbone. In this case, it is recommended to check if the accuracy in H-point prediction is not affected by locking of this joint.

### 34.1.5 Positioning

For positioning the H-point manikin model into a seat model, it is recommended to follow the instruction described in SAE J826 and ISO 6549 as much as possible. This means:

- Position the pelvis plate parallel to the seat cushion; the distance should be as small as possible (about 2 to 3mm).
- Position the back plate, which has an angle of 25° in relation to vertical, as close as possible to the seat.
- Adjust the seat back such that it is parallel to the back plate of the H-point manikin model.
- The positioning of the feet is identical to the back plate and pelvis plate, parallel to the floor surface and about 2 to 3mm above it.
- Define a gravitational field and allow the H-point manikin model to settle into the seat until an equilibrium has been reached between H-point manikin model and seat model.

Note that the back angle of the H-point manikin model should be still 25° after the settling. This can be checked by investigating whether the device for backrest angle measurement is in horizontal position (pre-set at 25° ).

## 34.2 Model validation

The above described technique for determination of the H-point by numerical simulations has been validated by two experiments: the first validation is based on experiments with the H-point manikin on a foam block (see Section 34.2.1), the second validation is based on experiments with the H-point manikin on a real seat (see Section 34.2.2).

### 34.2.1 Foam block experiments

In the experiments, the H-point was determined after settling of the H-point manikin on a foam block. The dimension of the foam block were 380 x 380 x 100mm, its density was 55kg/m$^3$. In the experiments, the back and feet were not supported. The back of the H-point manikin was locked at 5.5° . Figure 34.2 shows the experimental conditions.

Figure 34.2: The experimental set-up of the H-point measurement of a block foam (left) and the numerical simulation of the experiments with the H-point manikin model (right).

In the simulations, the experimental conditions were copied from the experiments. In Figure 34.2 the numerical condition is depicted. Comparison of the numerical results with the experimental results showed, the described numerical techniques allow a accurate prediction of the H-point. The differences between experiment and simulation were: $\Delta x = 0.4mm$ and $\Delta z = 0.5mm$.

### 34.2.2 Real seat experiments

A second validation was performed with the H-point manikin model based on experiments with a real car seat. In MADYMO, a model of this seat has been developed. All components are represented in the model by a detailed geometric and mechanical description. Realistic properties, determined in separate experiments, have been defined for the foam. Figure 34.3 shows the H-point manikin model settled in the seat model.

The results of the numerically predicted H-point were reasonable in comparison with the experimental values. The value in horizontal direction deviated 6.2mm from the experiments, the value in vertical direction 8.4mm.

Figure 34.3: The H-point manikin model in a real car seat.

To save CPU time, all metal frame parts have been modelled rigid. Further, alpha damping has been defined for the seat and the H-point manikin model to more quickly reach equilibrium between H-point manikin model and the seat. Also the foam density has been increased by a factor of 10. It has to be noted, that in each case it has to be checked whether these assumptions influence the prediction of the H-point. In the above described condition, the influence was negligible.

## 34.3 User instructions

### 34.3.1 Integration method and time step

The recommended integration method and minimum integration time step for the FE pelvis model is given in Table 34.2. Note that the integration time step used by MADYMO in the simulation is dependent on stiffness, density and size of the elements (Courant criterion, see MADYMO Theory Manual) and so in case of H-point prediction more probably dependent of the seat model than on the H-point manikin model.

Table 34.2: Recommended integration method and time step for the H-point manikin model.

| Model | Integration method | Time step (s) |
|---|---|---|
| H-point manikin model | EULER | $< 1.0 \cdot 10^{-5}$ |

### 34.3.2 H-point manikin model positioning

In order to position of the complete H-point manikin model with respect to its environment, the Hpoint_jnt in the INITIAL.JOINT_POS has to be used. The orientations of the translational (D) and rotational (R) degrees of freedom of the H-point manikin model are given in Table 34.3. The joint translations and rotations are defined as shown in Figure 34.4.

Table 34.3: Positioning joints of the H-point manikin model.

| Parameter | | D1/R1 | D2/R2 | D3/R3 |
|---|---|---|---|---|
| Complete model | HPoint_jnt | X/Roll right | Y/Pitch down | Z/Yaw left |
| Knee left | KneeL_jnt | Y | | |
| Knee left | LegLowL_jnt | Pitch down | | |
| Lowerleg left | Ankle_jnt | Z | | |
| Ankle Left | FootL_jnt | Pitch down | | |
| Knee right | JneeR_jnt | Y | | |
| Knee right | LegLowR_jnt | Pitch down | | |
| Lowerleg right | AnkleR_jnt | Z | | |
| Ankle right | FootR_jnt | Pitch down | | |
| T-bar | Tbar_jnt | X | | |
| Backbone | Backbone_jnt | Pitch down | | |

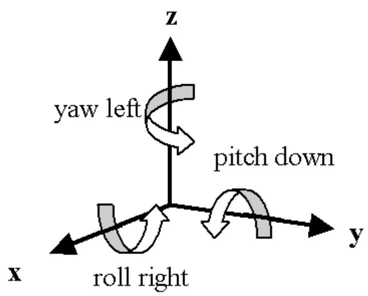


Figure 34.4: Definition of joint translations and rotations of the H-point manikin model.

### 34.3.3 Mass settings

The default set-up of the H-point manikin model represents the mass of 50th percentile Hybrid III. The model can be adapted to the mass of a $5^{th}$ and $95^{th}$ Hybrid III by varying the parameters varPelvisMass and varHipMass in CONTROL_ANALYSIS.TIME/DEFINE as prescribed in Table 34.4.

Table 34.4: Prescribed parameter values in H-point manikin model.

| Parameter | varPelvisMass | varHipMass |
|---|---|---|
| 5th % Hybrid III | 4600 | 3300 |
| 50th % Hybrid III | 7300 | 9000 |
| 95th % Hybrid III | 14000 | 14000 |

### 34.3.4 Contacts

Various groups have been defined in the include file for contact definition with a seat or the ground. They are listed in Table 34.5.

Table 34.5: Predefined groups for contact definition

| Description | Identifier |
|---|---|
| Back Plate | BackPlate |
| Pelvis Plate | PelvisPlate |
| Left Foot | FootL |
| Right Foot | FootR |

### 34.3.5 Output

For definition of the output of the H-point with respect to the inertial space or a point on a seat, it is recommended to use OUTPUT_BODY_REL (Table 34.6).

Table 34.6: Predefined output.

| Signal | Identifier | D1/R1 | D2/R2 | D3/R3 | Filter |
|---|---|---|---|---|---|
| H-point w.r.t. IS | H-point_rds | x | y | z | CFC1000 |

# 35 TNO-10 Dummy

The TNO-10 was developed as a loading device for the evaluation of a belt restraining device in a simulated frontal crash situation. The dummy represents a 50th percentile male adult in general size and weight distribution without lower arms and with only one lower leg.

The dummy can be used as a test device in tests according to the ECE-regulation no. 16 "Uniform provision concerning the approval of safety belts and restraint systems for adult occupants of power driven vehicles" and in tests according to the EEC directive 82/319.

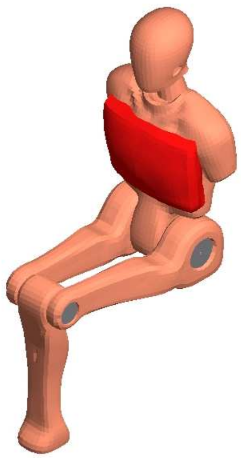

Figure 35.1: TNO-10 dummy model in sitting position.

## 35.1 Model description

The input of the TNO-10 facet model is given in the files:

| | |
|---|---|
| Facet model: | d_tno10fc_usr.xml<br>d_tno10fc_inc.xml |

To run this model, the following licenses are required:

| | |
|---|---|
| Facet model: | MADYMO/Solver (Multibody)<br>MADYMO/Dummy Models/Frontal |

Figure 35.1 shows the facet model in the reference position. The facet model consists of 8 bodies.

**FACET MODEL**

**Geometry and inertia**

Dummy geometry and joint positions are based on scan data and Principal dimensions.

The dummy component masses are based on hardware measurements. Centre of gravity and moment of inertias are derived from scan data geometry. The required standard weight of the dummy is 75.5 kg according to ECE-regulation no. 16. In order to tune the dummy to its total mass, hip correction masses have been introduced as well as the torso-back correction masses. If more than 3 hip correction masses are used then the torso-back correction masses should be used as well. The number of torso-back correction masses used should always be even, in order to obtain symmetrical mass distribution. Torso-back tuning masses up to 6 kg are supplied with the dummy (see user model file).

**Head and Neck**

The neck of the dummy is modeled with three joints, respectively for the head, the atlas and the neck and bodies for the head, the atlas and the neck. Two of the joints are spherical with six dof restraints. A revolute joint is used for modeling the nodding of the head.

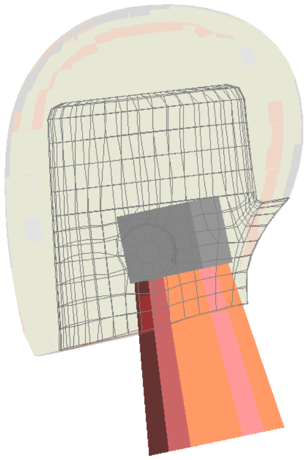

Figure 35.2: TNO-10 neck model.

**Torso and Legs**

The torso of the hardware dummy is made of one piece which can rotate about the horizontal axis through the H point. The torso is quite flexible so motion of one part of the torso with respect to another part of the torso is possible. For this flexibility a spherical joint with a six dof restraint is used for the connection of the lower and the upper torso.

A bracket joint is used to model the connection between upper torso and chest cushion.

The lower torso is connected to the upper legs by means of a revolute joint.

## CONTACTS BETWEEN DUMMY COMPONENTS

Contacts are defined between the head and chest cushion and the head and the thorax. The following dummy to dummy contacts have been defined:

- Head to cushion
- Head to thorax

## 35.2 Model validation

The TNO-10 model is developed and validated for frontal impact. Validation results are obtained for lower and upper torso displacement. Some validation results for the TNO-10 dummy in frontal impact are given in Figure 35.3.

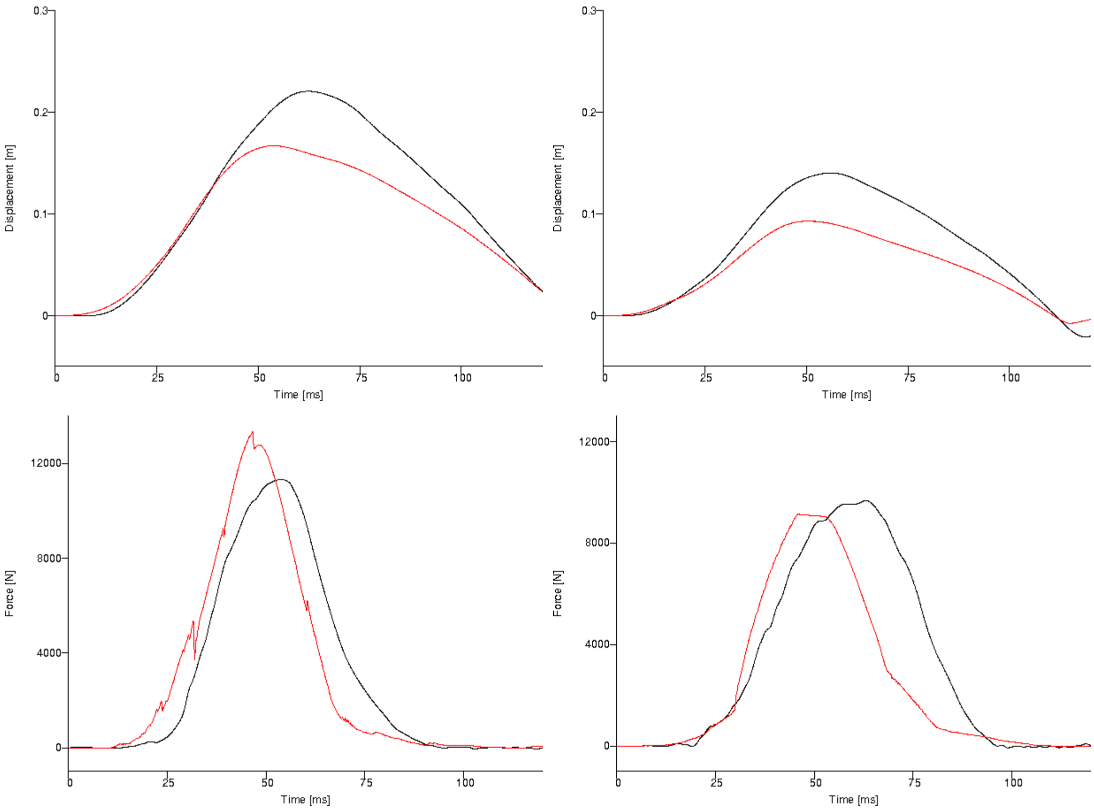


Figure 35.3: Validation results of the TNO-10 dummy sled test; experiment (black), facet model (red). Clockwise from top left: Upper torso displacement, lower torso displacement, buckle force, lap belt force.

## 35.3 User instructions

General instructions for the use of the TNO-10 dummy can be found in Chapter 1 of the Madymo Model Manual.

### Timestep

Table 35.1: Recommended timestep for the TNO-10 dummy model.

| Model | timestep (s) |
|---|---|
| Facet | $\leq 1 \cdot 10^{-5}$ |

### Dummy positioning

Table 35.2: Positioning joints of the TNO-10 facet dummy model.

| Joint Description | Identifier | Degree of freedom[a] | | | | | | Comment |
|---|---|---|---|---|---|---|---|---|
| Complete dummy | Dummy_jnt | D1<br>R1 | forward<br>roll right | D2<br>R2 | leftward<br>pitch down | D3<br>R3 | upward<br>yaw left | |
| Head | Head_jnt | R1 | pitch down | | | | | |
| Atlas | Atlas_jnt | R1 | yaw left | R2 | pitch down | R3 | roll left | |
| Neck | Neck_jnt | R1 | yaw left | R2 | pitch down | R3 | roll left | |
| Upper Leg | Hip_jnt | R1 | pitch down | | | | | |
| Lower Leg | Knee_jnt | R1 | pitch down | | | | | |

[a] Positive translation or rotation given in global coordinate system while dummy is in reference position.

### Additional masses

The ECE-16 test protocol describes the use of additional masses in the TNO-10 hardware dummy. These ballast weights have been included in the MADYMO model user file, and can be activated to simulate a dummy with a non-standard weight profile. The dummy's user file contains DISABLE blocks which can be enabled in order to add or remove the ballast weights as required.

### Dummy contacts

In general, the dummy surface should be chosen as the master group in contact definitions. With the dummy surfaces as master the direction of the contact forces and torques is always controlled by the dummy model.

Table 35.3: Available groups to define contact between the TNO-10 components and environment.

| Contact Description | Identifier | Facet model |
|---|---|---|
| Head | Head_gfe | Closed outer head surface |
| Neck | Neck_gfe | Closed outer neck surface |
| Chest cushion | ChestCushion_gfe | Closed outer chest cushion surface |
| Torso | Torso_gfe | Closed outer thorax and pelvis surface |
| Upper legs | Thigh_gfe | Closed outer upper legs surface |
| Lower leg | LowerLeg_gfe | Closed outer lower leg surface |

## Output

Table 35.4: TNO-10 dummy model output signals.

| Sensor | Identifier | Signal | | | | | | | Filter |
|---|---|---|---|---|---|---|---|---|---|
| | | resultant | x | direction[b] | y | direction[b] | z | direction[b] | |
| Head[c] | HeadCG_acc | ar | A1 | forward | A2 | lateral | A3 | vertical | CFC1000 |
| Upper torso displacement | UpperTorso_dis[d] | dr | | Displacement | | | | | |
| | UpperTorso(L/R)_dis[d] | dr | | Displacement | | | | | |
| Lower torso displacement | LowerTorso_dis[d] | dr | | Displacement | | | | | |
| | LowerTorso(L/R)_dis[d] | dr | | Displacement | | | | | |

[b] Positive direction given according to SAEJ211/1.

[c] The calculated acceleration is corrected in the x direction for a prescribed fictitious acceleration field to get correct values.

[d] For both output definitions the POINT_OBJECT_2.MB should be changed with proper values depending on the initial positions of the dummy.

Attachment reference points for the lower and the upper torso displacement have been defined at the rear on the central line of the dummy (middle reference points) according to the ECE R16 regulation. Options for the left and the right attachment reference points for the lower and the upper torso displacement are also available and they have been defined with respect to the rear central line of the dummy as well. The attachment reference points for the upper and the lower torso displacement should be used in pairs either as the left or the middle (set as default in the current model) or the right reference points, depending on the type of test.

## 35.4 Example: sled test with belt restraint

This example features the TNO-10 dummy in a sitting position on a sled, restrained by a three point belt. The input of the facet model is given in the files:

| | |
|---|---|
| Facet model: | e_tno10fc.xml |
| | d_tno10fc_inc.xml |

Figure 35.4 shows the model set-up. In this example an FE belt is used.

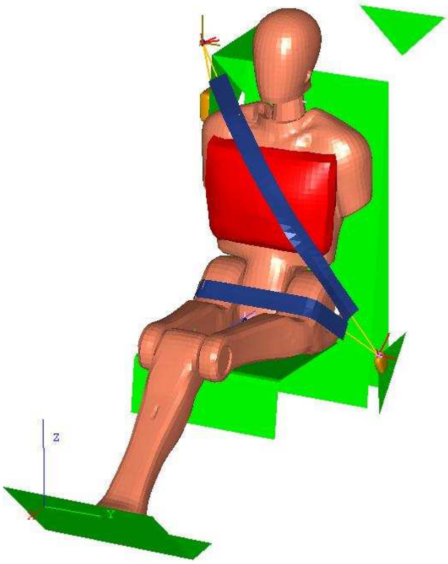


Figure 35.4: Model set-up for the TNO-10 dummy model.

**Environment**

The test environment consisted of a rigid seat, and foot plane mounted on a rigid sled. The dummy was placed in a realistic seating position. The acceleration pulses aproximate an ECE R16 mid-severity crash (50 km/h). The test environment is modelled with the facet surfaces for the facet model.

**Belt restraint system**

In the experiment the dummy was restrained by the three point belt restraint system. Elongation of the belt used in the experiment reads 8%. The belt system contains the load-limiter of 3.5 kN.The belt characteristics is given in Figure 35.5.

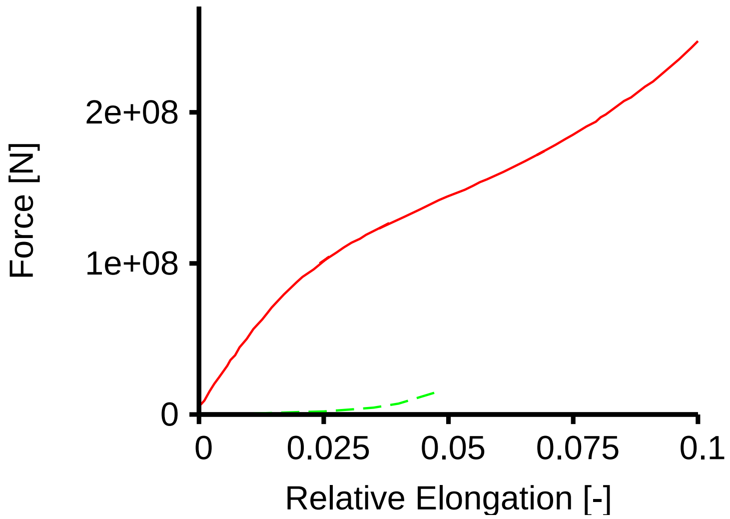


Figure 35.5: The belt characteristic for the TNO-10 dummy model; load (———), unload (– – –).

### Contact interactions

The dummy interacts with the rigid seat, the foot plane and the belt. All friction coefficients have been estimated. The facet dummy uses element-node contact interactions and are listed in Table 35.5.

Table 35.5: Contact interaction between dummy and sled for the facet model.

| **Model type** | **Contact surface** | |
|---|---|---|
| | **master** | **slave** |
| facet | Seat_Back_gfe<br>Seat_Back_gfe<br>Seat_Cush_gfe<br>SeatCush_gfe | Torso_gfe Thigh_gfe<br>LowerTorso_gfe<br>Thigh_gfe |
| | Sled_Floor_gfe | LowerLeg_gfe |
| | Neck_gfe<br>ChestCushion_gfe<br>Torso_gfe Thigh_gfe<br>Torso_gfe Thigh_gfe | SchoulderBelt_gfe<br>SchoulderBelt_gfe<br>SchoulderBelt_gfe<br>SchoulderBelt_gfe<br>LapBelt_gfe<br>LapBelt_gfe |

### Discussion

Good correlation results can be obtained for the facet model. In this example the dummy is seated on a rigid seat, as for ECE/R16 tests.

More realistic physical parameters can be used to improve the confidence in parameter variation studies.

# 36 Hybrid III 50th percentile Base Model

The Hybrid III 50$^{th}$ percentile male is the most widely applied dummy for the evaluation of automotive safety restraint systems in frontal crash testing. The size and weight of the dummy represent an "average" of the USA adult male population. It is accepted in several standards (FMVSS 208, ECE R.94) and used in global NCAP programmes.

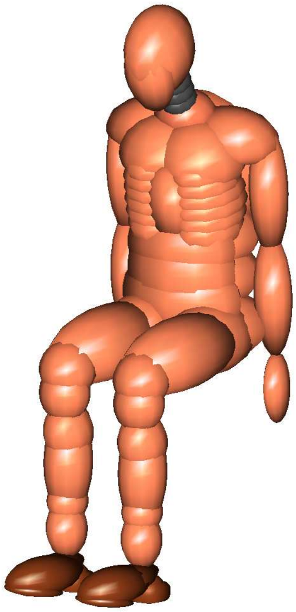

Figure 36.1: Hybrid III 50$^{th}$ percentile dummy ellipsoid model.

## 36.1 Model description

The standard ellipsoid model of the Hybrid III $50^{th}$ percentile male dummy is described here. Although this model had been replaced by a more advanced Q model, it is still used as a reference for several other dummy models and is therefore described in this Model Manual.

Figure 36.1 shows the model in the reference position. The ellipsoid model consists of 37 bodies.

The inertia properties in the model include the standard instrumentation consisting of the sternum deflection sensor and the acceleration sensors of the lower torso, the upper torso and the head. The inertia of the shirt and the shorts are not included into the model.

**ELLIPSOID MODEL**

**Neck**

The neck is represented by 5 kinematic joints located in the centres of the 4 rubber disks and on the rotation axis of the nodding joint (OC). The rubber disks are represented by spherical joints and the nodding joint by a revolute joint.

**Thorax/Ribs and sternum**

In the physical dummy, the sternal region of the thorax is rather compliant compared to the more lateral regions of the thorax. To include this difference in the model two bodies have been included in the model. The rib body represents the front of the rib cage (left and right) and the sternum body represents the compliant sternal region (centre). The sternum body is connected to the rib body with a translational joint allowing sternum compression. The rib body is connected to the upper torso body by means of a cardan-restraint combined with a point-restraint. These combined restraints describe the stiffness of the ribs.

The ellipsoids of the ribs are located at the actual rib positions, but the contours are adapted to include the size of the thorax jacket. For the jacket surface above the ribs two additional ellipsoids have been specified. These ellipsoids are connected to the rib body. However, it should be noted that in the real dummy, this upper area of the jacket is only indirectly supported by the rib cage and is very compliant.

**Lumbar spine**

To obtain a model for the lumbar spine a combination of a free joint and a protected joint resistance model is used. This protected joint resistance model describes the lumbar spine compliance in the model. The relations between rotations (bending & torsion) and displacements (compression & elongation and shear), and moments and forces were determined in a quasi-static manner and are specified in the protected model. The joint location has been chosen in the middle between the connection plates of the lumbar spine. The mass and inertia properties of the actual lumbar spine have been divided over both spine bodies. The upper spine body is connected to the upper torso by means of a bracket joint, similarly the lower spine body is connected to the lower torso. These bracket joints allow for the output of constraint loads at the upper and lower lumbar spine load cells.

In the complete physical dummy, lumbar spine deformation is not only resisted by the lumbar spine itself but also by contact interaction of the rib cage, the abdomen and the lower torso. This interaction is included in the models with three point-restraints. These point-restraints are referred to as "Abdomen vertical compression left/middle/ right".

**Abdomen**

The abdomen has been modelled as a separate body, which is connected to the lower torso with a translational joint. This body is included to describe the combined deformation of the abdomen and the lower torso flesh in response to lap belt loading.

The characteristics of the abdomen joint are based on experiments with a belt loading of abdomen and lower torso.

**Hip**

The hip model is a combination of a spherical joint and a protected joint resistance model. The hips are modelled with so called "modified femurs" allowing enlarged hip flexion. However, this model also provides a reasonable prediction for moderate loading of "unmodified femurs". Friction has been implemented for the hip joints with the Coulomb friction in RESTRAINT.JOINT elements in which both a constant friction and an additional load dependent friction were specified.

**Knees**

The knee has been modelled as a JOINT.REVO_TRAN joint describing flexion and the translational movement of the knee slider. It should be noted that the physical knee slider mechanism of the dummy has been criticised for being not very reproducible. Therefore a precise prediction of the knee slider movement is not to be expected.

**Ankles and feet**

The foot and ankle have been modelled, allowing about 45 degrees dorsiflexion, and include a rubber joint stop to reduce tibia load peaks. The geometry of the feet is described in detail by three ellipsoids. Contact loading functions for these ellipsoids were derived from static and dynamic component tests. The shoes are implemented as separate bodies. A free joint is specified between shoes and feet. This joint allows translation and rotation of the feet inside the shoes. Contact functions for the shoe soles are defined according to dynamic component tests.

**Contacts between dummy components**

Contacts are defined between the head and the thorax and between the thorax and the left and right upper legs.

## 36.2 Standard Output

### OUTPUT SIGNALS

Table 36.1: Typical output signals of the hybrid III $50^{th}$ percentile ellipsoid model.

| Sensor | Identifier | Signal resultant | x | direction[(a)] | y | direction[(a)] | z | direction[(a)] | Filter |
|---|---|---|---|---|---|---|---|---|---|
| Head | | | | | | | | | |
| CG accelerometer[(b)] | HeadCG_acc | ar | a1 | forward | a2 | lateral | a3 | vertical | CFC1000 |
| Neck | | | | | | | | | |
| Upper load cell | NeckUp_lce_F_CFC1000 | fr | f1 | shear | f2 | shear | f3 | axial | CFC1000 |
| | NeckUp_lce_F_CFC600 | | | | | | | | CFC600 |
| | NeckUp_lce_T | tr | t1 | roll | t2 | pitch | t3 | yaw | CFC600 |
| Lower load cell | NeckLow_lce_F | fr | f1 | shear | f2 | shear | f3 | axial | CFC1000 |
| | NeckLow_lce_T | tr | t1 | roll | t2 | pitch | t3 | yaw | CFC600 |
| Thorax | | | | | | | | | |
| accelerometer[(b)] | Thorax_acc | ar | a1 | forward | a2 | lateral | a3 | vertical | CFC180 |
| deflection Chest | ChestDeflection_dis | dr | d1 | displacement | | | | | CFC600 |
| | ChestDefl_dis_CFC180 | dr | d1 | displacement | | | | | CFC180 |
| | ChestDeflection_vel_CFC600 | vr | v1 | velocity | | | | | CFC600 |
| | ChestDeflection_vel_CFC180 | vr | v1 | velocity | | | | | CFC180 |
| Lumbar Spine | | | | | | | | | |
| Upper load cell | LumbarSpineUp_lce_F | fr | f1 | shear | f2 | shear | f3 | axial | CFC1000 |
| | LumbarSpineUp_lce_T | tr | t1 | roll | t2 | pitch | t3 | yaw | CFC1000 |
| Lower load cell | LumbarSpineLow_lce_F | fr | f1 | shear | f2 | shear | f3 | axial | CFC1000 |
| | LumbarSpineLow_lce_T | tr | t1 | roll | t2 | pitch | t3 | yaw | CFC1000 |
| Pelvis | | | | | | | | | |
| Accelerometer | Pelvis_acc | ar | a1 | forward | a2 | lateral | a3 | vertical | CFC1000 |
| Femur | | | | | | | | | |
| Left load cell | FemurL_lce_F FemurL_lce_T | fr | f1 | shear | f2 | shear | f3 | axial | CFC600 |
| | | tr | t1 | roll | t2 | pitch | t3 | yaw | CFC600 |
| Right load cell | FemurR_lce_F FemurR_lce_T | fr | f1 | shear | f2 | shear | f3 | axial | CFC600 |
| | | tr | t1 | roll | t2 | pitch | t3 | yaw | CFC600 |
| Tibia | | | | | | | | | |
| Left Upper load cell | TibiaUpL_lce_F TibiaUpL_lce_T | fr | f1 | shear | f2 | shear | | | CFC600 |
| | | tr | t1 | roll | t2 | pitch | | | CFC600 |
| Right Upper load cell | TibiaUpR_lce_F | fr | f1 | shear | f2 | shear | | | CFC600 |
| | TibiaUpR_lce_T | tr | t1 | roll | t2 | pitch | | | CFC600 |
| Left Lower load cell | TibiaLowL_lce_F | fr | f1 | shear | f2 | shear | f3 | axial | CFC600 |
| | TibiaLowL_lce_T | tr | t1 | roll | t2 | pitch | | | CFC600 |
| Right Lower load cell | TibiaLowR_lce_F | fr | f1 | shear | f2 | shear | f3 | axial | CFC600 |
| | TibiaLowR_lce_T | tr | t1 | roll | t2 | pitch | | | CFC600 |

*Continued on the next page*

*Table 36.1 cont.*

| Sensor | Identifier | Signal | | | | | | | Filter |
|---|---|---|---|---|---|---|---|---|---|
| | | resul-tant | x | direc-tion[a] | y | direc-tion[a] | z | direc-tion[a] | |
| Knee | | | | | | | | | |
| Left Knee | KneeL_pos | joint position dof1: rotation, dof2: displacement | | | | | | | none |
| Right Knee | KneeR_pos | joint position dof1: rotation, dof2: displacement | | | | | | | none |

[a] Positive direction given according to SAE J211/1.

[b] The calculated acceleration is corrected in the x direction for a prescribed fictitious acceleration field to get correct values (see Theory manual).

## INJURY CRITERIA

Table 36.2: Typical injury criteria defined for the Hybrid III 50$^{th}$ percentile .

| Injury criteria | Identifier | Filter |
|---|---|---|
| Head | | |
| HIC (15) | HIC15_inj | |
| HIC (36) | HIC36_inj | |
| Neck | | |
| FNIC | | |
| tension | FNICtension_inj | CFC1000 |
| shear | FNICshear_inj | CFC1000 |
| bending | FNICbending_inj | CFC600 |
| NIJ | | |
| tension-extension | NTE_inj | CFC600 (force)<br>CFC600 (moment) |
| tension-flexion | NTF_inj | CFC600 (force)<br>CFC600 (moment) |
| compression-extension | NCE_inj | CFC600 (force)<br>CFC600 (moment) |
| compression-flexion | NCF_inj | CFC600 (force)<br>CFC600 (moment) |
| Thorax | T3MS_inj | |
| 3ms (cumulative) | | |
| CTI | CTI_inj | |
| VC | VC_inj_CFC180<br>VC_inj_CFC600 | CFC180 (deflection)<br>CFC600 (deflection) |
| Femurs | | |
| FFC | | |
| Left | FFCL_inj | CFC600 |
| Right | FFCR_inj | CFC600 |
| Tibia | | |
| TI | | |
| Upper left | TIUpL_inj | CFC600 |
| Upper right | TIUpR_inj | CFC600 |
| Lower Left | TILowL_inj | CFC600 |
| Lower right | TILowR_inj | CFC600 |

*Continued on the next page*

*Table 36.2 cont.*

| Injury criteria | Identifier | Filter |
|---|---|---|
| TCFC | | |
| Upper left | TCFCUpL_inj | CFC600 |
| Upper right | TCFCUpR_inj | CFC600 |
| Lower left | TCFCLowL_inj | CFC600 |
| Lower right | TCFCLowR_inj | CFC600 |